Synthesis, Fractionation, Characterisation and Toxicity of Naphthenic Acids from Complex Mixtures

By

David Jones

A Thesis submitted to Plymouth University in partial fulfilment for the degree of

Doctor of Philosophy

School of Geography, Earth and Environmental Science

Faculty of Science and Technology

April 2013

For Beatrice Belgrave-Jones

One equal temper of heroic hearts,
Made weak by time and fate, but strong in will
To strive, to seek, to find, and not to yield.
Ullyses., Alfred Lord Tennyson

Abstract

Amongst the polar organic compounds occurring in unrefined and refined crude oils and the associated polluted production waters, complex mixtures of acids, known historically as naphthenic acids (NAs), have achieved prominence. This is particularly because NAs have been designated a toxicant class of concern in the oil sands process-affected water (OSPW) that has accumulated in vast quantities following exploitation of the oil sands of Northern Alberta, Canada in recent years. However, though there have been calls for NAs to be added to pollutant inventories, at the initiation of the current study, little knowledge existed of the exact composition of refined or unrefined NAs.

The overall aim of the current study was therefore to identify individual NAs in refined (commercial) and unrefined (e.g. oil sands process-derived) complex mixtures of acids and then to assess the toxicity of any identified NAs. Individual NAs were tentatively identified by interpretation of the electron ionisation mass spectra of methyl ester derivatives, following comprehensive multidimensional gas chromatography-mass spectrometry (GCxGC-MS).

Reference acids were then either purchased, or more commonly, where they were not commercially-available, synthesised, mainly by micro-hydrogenation methods, for co-chromatography and comparison of mass spectra of methyl esters with those of unknowns. The synthetic NAs, purified to >97% were then subjected to

toxicological assessments using the Microtox™ assay. In all, 34 compounds were obtained pure enough for testing. Microtox results revealed that the toxicity endpoint (50% Inhibition Concentration, IC_{50}) was between 0.004 and 0.7 mM. Exponential and other correlations were noted between carbon number and toxicity in several of the structural groups of acids assayed, which may be beneficial for predictions of toxicity of non-synthesised acids. Although *n*-hexanoic acid (IC_{50} 0.7 mM) had the lowest toxicity, adamantane-type acids were the least toxic as a group overall. Conversely, the decahydronaphthalene (decalin)-type acids had the largest range of toxicities (IC_{50} 0.004 to 0.3 mM) and the most toxic acid assayed was 3-decalin-1-yl-propanoic acid. According to USEPA guidelines many individual acids can be said to show low to medium toxicity.

Since the acids in commercial and unrefined NAs occur in complex mixtures, an attempt was also made to assess mixture toxicity. Mixtures of individual structural groups of acids (e.g. acyclic isoprenoid acids, *n*-acids) and a mixture of all 34 acids were assessed. Apart from the adamantane sub-group of acids, all of the mixtures showed toxicities lower than the sum of the parts when calculated using equations for Concentration Addition and Model Deviation Ratios (simply the predicted IC_{50}/Observed IC_{50}). A hypothesis that achievement of a critical micelle concentration is

required to produce toxicity was proposed to explain the lower than expected results.

Some of the mass spectra of NA present in the commercial and unrefined mixtures were inconsistent with those of any of the alicyclic acids synthesised or purchased. These were hypothesised to be aromatic acids. Fractionation experiments of the NA mixtures using silver ion thin layer chromatography and solid phase extraction (Ag^+TLC and Ag^+SPE) were carried out in order to provide further evidence for aromatic acids. Ag^+TLC allowed separation of a methylated NA mixture from OSPW into three distinct fractions; Ag^+SPE resulted in eleven fractions, through the use of a wider range of solvents and differential solvent ratios. Analysis of the fractions by GC-MS revealed that each fraction was largely still made up of unresolved acids (as esters), although one or two fractions revealed some resolved acids. Use of averaged mass spectra and mass chromatography on each fraction revealed further resolved chromatographic peaks and associated interpretable mass spectra. Each of eight of the eleven sub-fractions were examined by GC-MS, in some cases by GCxGC-MS, and all by infrared spectroscopy, ultraviolet visible spectrophotometry and elemental analysis. A number of structures were proposed for the aromatic acids, including those with sulphur-containing moieties. It was noted that far from being minor components, aromatic acids comprised *ca*.25-40% of the OSPW acid extracts.

Table of Contents

Figures and Tables

Figures

Chapter 1

Chapter 5

Appendix B

Tables

Chapter 4

Chapter 5

Appendix A

Acknowledgements

In August 2005 I left my job to enrol at university to read for a BSc in Environmental Science, I had no idea at the time that seven and a half years later I would be completing my Ph.D. Throughout these seven (often difficult) years my wife, Bea Belgrave-Jones, has stood beside me, encouraged me and loved me, in fact without her this whole adventure would never have begun. It's been a long time since that chat in that café in Tintagel!

For this reason I dedicate this thesis to her.

I would like to also thank my supervisors, (Professor Steve Rowland, Dr Anthony Lewis and Dr Alan Scarlett) for all the help and advice that has been so freely given over the years. In that vein I also have to thank Dr Charles West who, although not an official supervisor, has often acted as such and has on many occasions stopped to help me through difficult problems. I would also like to extend thanks to all of the staff and PhD students within the Petroleum and Environmental Geochemistry Group (PEGG) and the wider Biogeochemistry Centre at Plymouth University. Obviously it would be remiss not to mention the help and advice provided by the Davy Laboratory 5th Floor Technicians, the two Andy's (Arnold and Tonkin) Clare and Ian. At some point I'll return all that glassware I 'borrowed'.

They say that the road to a PhD is a lonely one. In this respect I have been lucky to have excellent friends and family. My parents, who

always supported me and were (are) always proud of me and my sisters, brothers in law and nieces who always provided amusement, not always intentional, to take my mind off my studies. My grandfather, who died before I started the PhD, showed me that giving up is not an option and if you want something bad enough then you should fight for it.

I have also been blessed to have good friends who will drink with me, laugh with me and support me. My friends, who play music in various bands with me, have been a constant source of amusement and have enabled a necessary release from the pressures of completing my PhD. The Landlord, staff and regulars at the Nowhere Inn, a home from home of sorts and a safe haven on a night out, plus the best pint of Guinness this side of Ireland. Plus those who noticed the struggle and were there to chat and put aside their own problems to help me in mine. In particular Toni, who has had her ear bent on many occasions when all she wanted was a drink with friends, for this I am very grateful (and apologetic).

These last three and a half years have not been without stress and hardship but they have also provided some of the most satisfying moments in my life.

Dave Jones

06/04/13

Authors Declaration

At no time during the registration for the degree of Doctor of Philosophy has the author been registered for any other University award without prior agreement of the Graduate Committee.

This study was financed with aid of a studentship from Plymouth University and was carried out within the Petroleum and Environmental Geochemistry research Group on Plymouth University campus.

A programme of advanced study was undertaken which included advanced training in chemical and toxicological techniques, completion of the General Teaching Associate course and completion of other relevant courses such as IT, Professional Writing and Applying for Research Funding.

A full list of the thirteen publications (including links to the full text of three first authorship papers) and seven research conferences where this work was presented either as an oral or poster presentation is included in Appendix D at the back of this thesis.

Word Count of main body of thesis:
67500

Signed……..

Date……..

L

Chapter 1 Introduction

1. Naphthenic Acids: Toxic Mixtures of Water-soluble Organic Compounds in Petroleum and Process Waters from Petroleum Industry Operations

Petroleum derived fossil fuels, whether conventionally drilled or unconventionally mined (such as the bituminous products of the oil sands developments of Athabasca, northern Alberta, Canada), whilst consisting predominantly of hydrocarbons, also comprise compounds which are classed as 'water soluble' non-hydrocarbons (e.g. Lo et al., 2006). These fractions include, amongst others, poorly characterised, relatively water-soluble compounds known by the general term naphthenic acids (NA) (Quagraine et al., 2005b). When oil waste is disposed of, such water-soluble fractions are present in the largely aqueous discharges of oil production platforms (so-called Produced Water; PW) or the process-affected waters of oil sands operations (so-called Oil Sands Process Affected Water; OSPW) (Hsu et al., 1999; Whitby et al., 2010) . Both PW and OSPW are associated with a number of toxicological and hormonal effects in a variety of organisms and cell-based assays and may be of environmental importance (Clemente and Fedorak, 2005; Colavecchia et al., 2004; Headley and McMartin, 2004; MacKinnon and Boerger, 1986; Thomas et al., 2009). However, the relationship between toxicity and chemical structure is virtually unknown for many of these compounds since

the compounds exist in complex mixtures and are very poorly characterised.

1.1 Petroleum and commercial NA

The term ‘naphthenic acids’ appears to have been first coined by Markowninoff and Oglobin (Markownikoff and Oglobin, 1883). Over a century later, it was accepted by the International Union of Pure and Applied Chemistry (IUPAC) as an agreed term for the carboxylic acids found in petroleum (IUPAC, 1997; Smith, 2006). However, despite decades of research, very few of the individual acids in NA from petroleum were ever identified until the present study was conducted.

For example, scientists working for the famous American Petroleum Institute Project 6, spent years attempting to isolate individual acids, initially from an alkali wash provided by the Humble Oil and Refining Company and later from a Signal Hill Crude oil supplied by the McMillan Petroleum Company from their Long Beach Refinery, with only limited success (reviewed by Lochte and Littman, 1955). Later, von Braun and Cason and co-workers (Cason and Khodair, 1966; Cason and Liauw, 1965; Von Braun, 1931) laboriously isolated acids fractions from a San Joachim Valley naphthenic-type Californian crude oil, characterised the isolates by UV- Visible absorption spectroscopy and later gas chromatography-mass spectroscopy and then synthesised the putative isolated acids, often producing acids which were not identical to those isolated, despite years of work (Cason and Khodair, 1966, 1967a, b; Cason and Liauw, 1965) (Figure 1.1) By 1975 the number of acids

identified in petroleum NA was still less than 20 (Seifert, 1975; Figure 1.2) Brient et al. (1995) summarised the structures of some NA in a much cited review, but many were purely conjectural, even by this date (Figure 1.1) (Chapter 2). Brient et al., (1995) summarised the consensus view, in the petroleum industry and related fields that NA can generally be thought of as acyclic, mono- or polycyclic monocarboxylic acids and at least partly, alkyl substituted. They considered that the carboxylic acid group might be attached directly to the cyclic moiety or attached through a side chain, with those NA with an ethanoate side chain (viz: alkylcycloacetic acids) possibly one of the common groups (Headley and McMartin, 2004; Smith, 2006); Figure 1.: Chapter 2).

The degree of undersaturation of the individual NA is usually denoted by the z term in the formula ($C_nH_{2n+z}O_2$) where z is a zero or negative even integer, which therefore denotes the loss of hydrogen due to double bond or ring formation (usually, but only by convention, NA have been considered not to possess double bonds, such that z then reflects the degree of cyclicity. For example, *z* may equal zero (acyclic acids), -2 (monocyclic (and/or strictly monounsaturated)), -4 (bicyclic (and/or strictly diunsaturated)) and so on (e.g. Han et al., 2008).

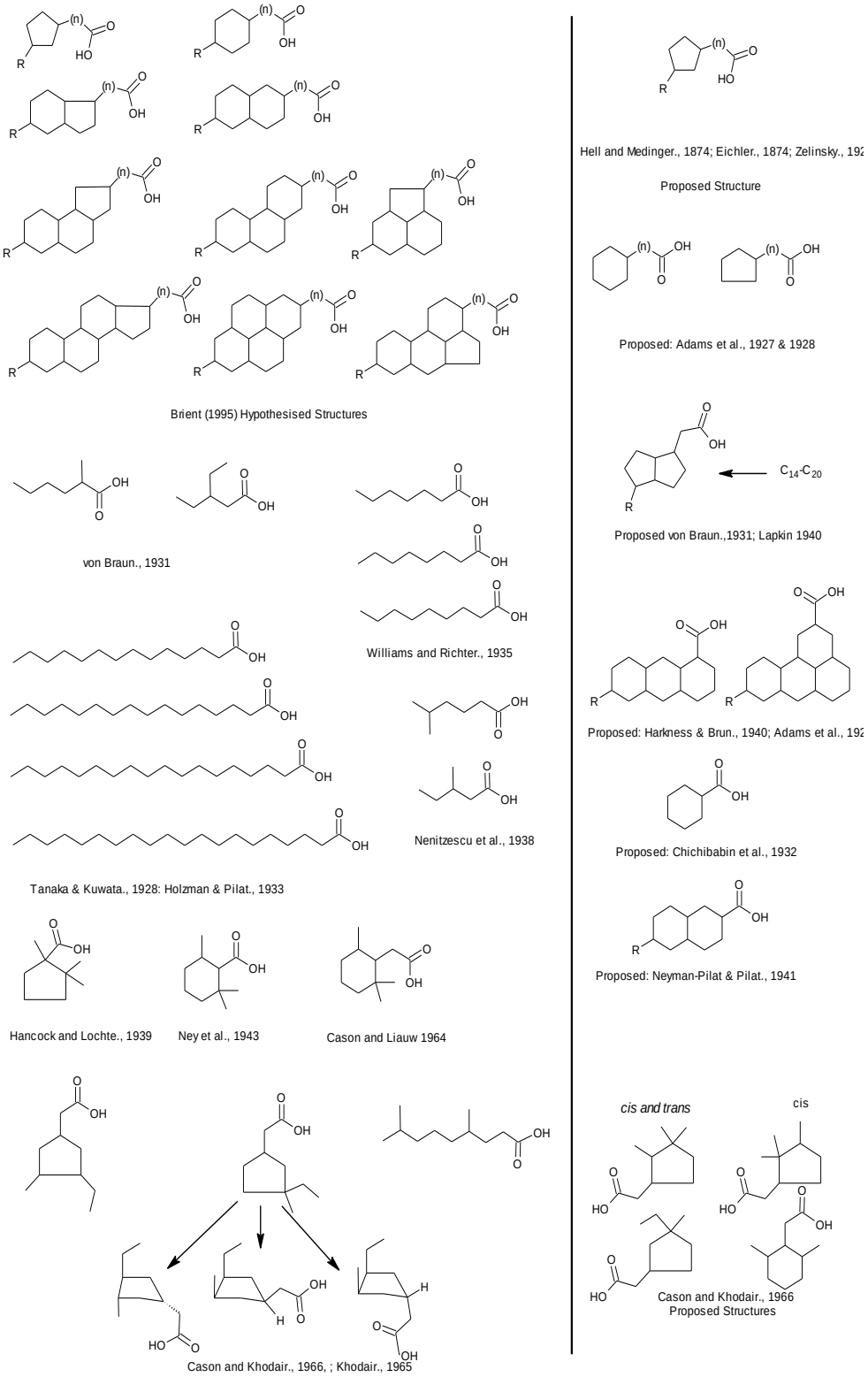

Figure 1.1. Proposed and Identified petroleum acid structures, dates previous to 1955 reviewed by Lochte and Littman (1955); arrows denote isomeric structures.

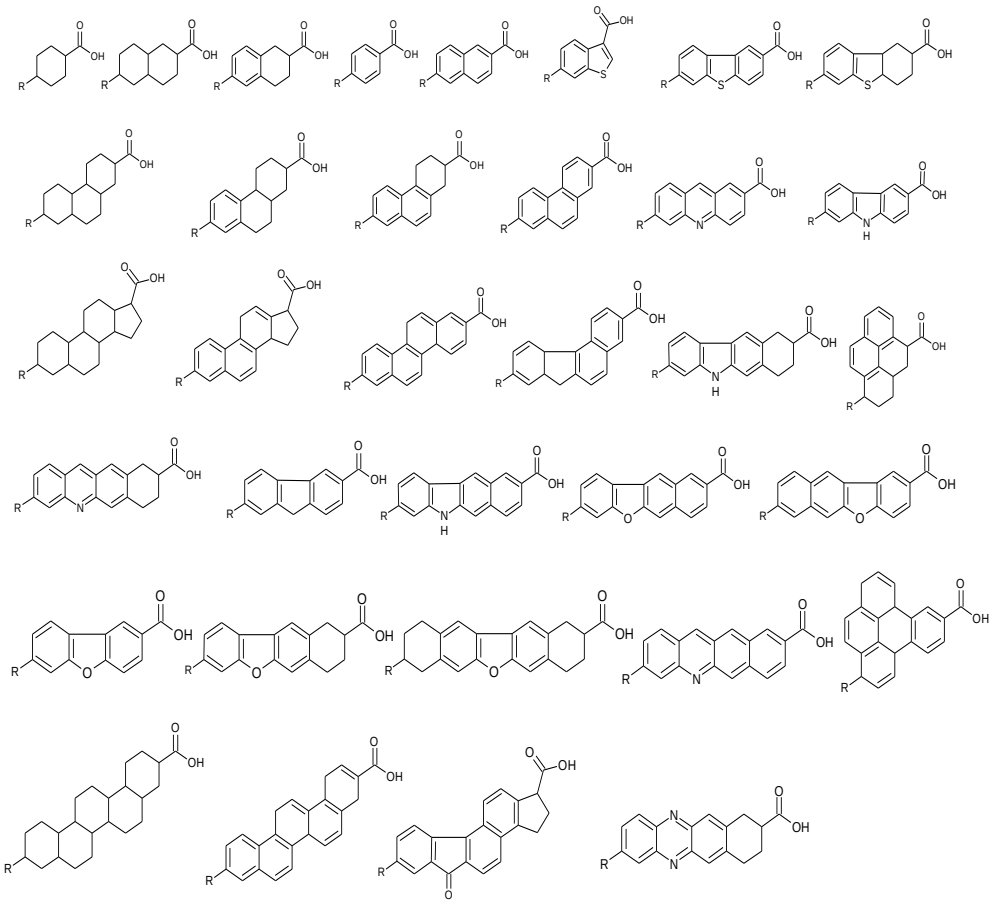

Proposed: Seifert and Teeter., 1970 a&b
Possible structures confirmed with UV Vis NMR and mass spectroscopy
From Midway Sunset 31E Californian Crude Oil

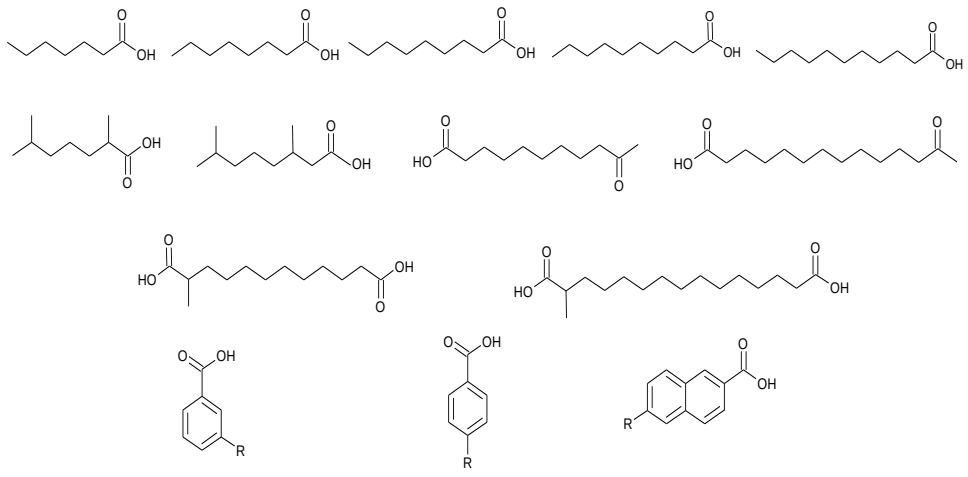

Proposed and Identified: Haug et al., 1970
Using mass spectroscopy
From the Colorado Green River Formation Shale Oil

Figure 1.2. Proposed and identified structures of petroleum acids from Seifert and Teeter (1970 a and b) and Haug et al., (1970)

The concentration of NA in petroleum is highly dependent on the source of the oil, typically ranging from between 0 and 3% by weight (Clemente and Fedorak, 2005; Seifert and Howells, 1969; Tissot and Welte, 1984). The concentration is often referred to by the Total Acid Number (TAN) which is arrived at by titration of the carboxylic acid groups with potassium hydroxide by standardised potentiometric method or colour indicating methods . Highly acidic petroleum is known from, for example, Rumania, Russia, China and the North Sea (Quagraine et al., 2005b). These oils are particularly high in NA content with concentrations as high as ~3% by weight compared to most U.S. oils, which have NA concentrations of generally ~0.1-0.3% by weight. However, some Californian petroleums have acid concentrations of ~4%. High TAN contents usually decrease the value of crude petroleum but isolation and sale of the NA may allow some recovery of these losses. For example, when petroleum is refined by distillation, NA occur in a wide variety of fractions with abundance increasing with boiling point to a maximum in the gas fraction (~325^{o}C). However the kerosene/ jet fuel (b.p. 125-300^{o}C and gas oil/diesel fractions (b.p. 180-350^{o}C) (A.P.I., 2003, 2005) are the usual sources for commercial Naphthenic acids, with the acid number decreasing in heavier fractions (i.e. 255 mg KOH g^{-1} for kerosene to 170 mg KOH g^{-1} from diesel to 120 mg KOH g^{-1} from heavy fuel oil (Brient et al., 1995). A short discussion on the production of commercial Naphthenic acids is given by Brient et al., 1995.

The main commercial applications of NA, once isolated, are in the generation of metal salts (Figure 1.3). The largest applications for the metal salts are copper naphthenates which have been used as a biocide for wood preservation for ~100 years. The most common copper Naphthenate on the market is a Danish product Cuprinol (Name derived from ‘copper in oil’) (Freeman and Memphis, 1992). Copper (and zinc) naphthenates are known to control fungi, wood decay and the formation of moulds.

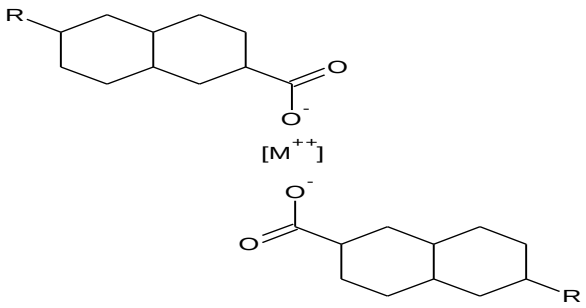

Figure 1. 3. Hypothetical structure of a metal naphthenate where R equals an alkyl side chain and [M^{++}] represents the metal ion.

The main use for metal naphthenates however, has been as catalysts to accelerate the drying of oil based paints (Table 1.1); the metal ions have a specific task within the drying process and are generally used in conjunction with other metal naphthenates. However the introduction of clean air acts in the USA and Europe has caused the lessening of these products in use as driers, as they can leach volatile organic compounds (Brient et al., 1995).

Cobalt naphthenate has been extensively used as an adhesion promoter for the steel cords in radial tyres and as an additive (as a cobalt soap) to restrict the damage to tyres upon sudden deflation. Metal naphthenates are also used in the adhesion of aggregates to asphalt as textile preservatives and as fuel additives (Table 1.1). Aluminium naphthenate is a gelling agent, and was used during World War II and in the Vietnam war, when it became an important ingredient in the incendiary, Napalm (Naphthenic and Palmitic acids) (Brient et al., 1995; Conley, 1996).

Table 1.1. Industrial applications for metal naphthenates (adapted from Brient et al., 1995)

Name	Applications
copper naphthenates	wood and textile preservative, catalyst
zinc naphthenates	wood and textile preservative, lubricant, wetting agent
cobalt naphthenates	paint drier, tyres, ink drier, catalyst, Natural rubber
manganese naphthenates	paint drier, catalyst, fuel additive
lead naphthenates	paint drier, wetting agent, lubricant additive
calcium naphthenates	paint drier, catalyst, lube additive
iron naphthenates	paint drier, fuel additive, catalyst
zirconium naphthenates	paint drier, electro-photographic developer
cerium naphthenates	paint drier, catalyst, fuel additive
vanadium naphthenates	paint drier, catalyst, corrosion inhibitor
sodium naphthenates	emulsifier, ore flotation, leather
potassium naphthenates	emulsifier, plant growth modifier
aluminium naphthenates	gelling agent, pigment wetting, asphalt additive

(Information from Barnes et al., 2005; Bhuvaneswary and Thachil, 2008; Brient et al., 1995; Freeman and Memphis, 1992)

Other derivatives, such as esters, amides and imidazolines have been used as adhesion promoters and bitumen emulsifiers. Esters have been reported as replacements for phthalates, as additives and lubricants for fuels and for aiding oil recovery. Glycol esters have recently found use in leather tanning. Naphthenic acid alcohol derivatives (from a reduction of the carboxylic acid group to an ester) are useful as surfactants, solvents and lubricants (Brient et al., 1995).

These commercial applications of NA and the discharge of NA in PW from conventional oil platforms (e.g. Thomas et al., 2009), represent vectors for the possible introduction of NA into the wider environment. However, relatively few studies of the distribution or possible effects of the NA seem to have been made until recently, and even to date the number of studies is small.

Sauer et al. (1997) fractionated 14 different PW samples to evaluate the potential toxic components. It was found that the acidic organic fraction (containing naphthenic acids) of a coastal Californian oil had toxicity similar to that of the un-fractionated PW, but that of a Louisianan oil only exhibited slight toxicity after a 48hr mortality test to the Mysid Shrimp *Mysidopsis bahia*. However, the toxicity results are given in a % form from a non stated concentration comparable with existing PW, without an explanation of whether the authors are referring to the PW concentrations in the lab or in the environment near to the sampling points, so it is difficult to assess whether PW (or the organic acid extract of PW) is a threat to marine species from this work alone (Sauer et al., 1997).

Lee and Neff (2011)) briefly mentioned naphthenic acids in their work 'Produced Water'. Comparing concentrations of NA in PW of North American oils from the Gulf of Mexico, and California (up to 7160 mg L^{-1} organic acids) and four different Norwegian oils (up to 761 mg L^{-1} organic acid). No toxicological information was given apart from a reference to research published by Thomas et al., (2009).

The latter authors (Thomas et al., 2009), carried out an effects directed analysis on the estrogenic and androgenic effects of PW in the North Sea. They reported that fractions containing an unresolved gas chromatographic ‘hump’ of NA were responsible for some of the hormonal effects (Section 1.3; Table 1.2).

Tollefsen et al. (2012)) studied the toxicity of commercial NA mixtures from three different suppliers, to Rainbow trout liver cells and noted major toxicological differences between the mixtures. However, no compositional studies were reported for the NA. Several other studies of the toxicity of commercial NA mixtures have been conducted in attempts to understand more about the toxicity of the acids in OSPW; these are therefore reviewed later herein in the latter context (*vide infra*). Few, if any of these, reported any detailed compositional information for the acids in the commercial mixtures.

However, very recently, partly as a result of findings made in the present study (*vide infra*), compositional information has been produced for one sample of commercial NA (Rowland et al., 2011d; West et al., 2011). These studies have allowed some of the individual acids and some other components of one commercial NA mixture to be assigned.

1.1.1 Commercial Petroleum Acids

Through use of a multidimensional comprehensive GC-MS method Rowland and co-workers workers analysed a commercial acid mixture. Using co-chromatography of synthesised or purchased acids to identify

numerous acids. Straight chain (normal or '*n*') acids had previously been identified in the acid extracts of crude oils (e.g. Holzmann and Pilat, 1933) and within a Colorado Green River Shale oil (e.g. Haug et al., 1971) but had not been identified within a concentrated sample of 'naphthenic acids' (commercial or otherwise). Rowland et al., 2011c were able to identify *n*-acids ranging from octanoic to octadecanoic within the commercial NA sample which also contained numerous methyl-branched acids and acyclic isoprenoid acids.

The commercial sample was also found to contain cyclohexyl acids, both methyl branched and otherwise along with several bicyclic decahydronapthalene acids. Similar mass spectra to the National Institute for Standards and Technology (NIST) library spectra for perhydroindane acids were also noted, but these remain tentative assignments. The assignment of the cyclic acids agrees with the general view that naphthenic acids have large proportions of cyclic moieties existing within the complex mixtures. Although most of the co-chromatographed acids in this study were purchased from commercial suppliers, some had to be synthesised in house herein (Chapter 2).

Also of interest in the commercial NA sample was the separation from the alicyclic fraction of a small amount of aromatic acids (Rowland et al., 2011). This was especially evident when a polar first dimension GC column was used along with an apolar second dimension column whilst the other identified acids had been analysed with an apolar primary GC column and a polar GC secondary column (Rowland et al., 2011 c).

Numerous mono-aromatic acids were positively identified (with both branched alkyl substituents and otherwise) (Rowland et al 2011).

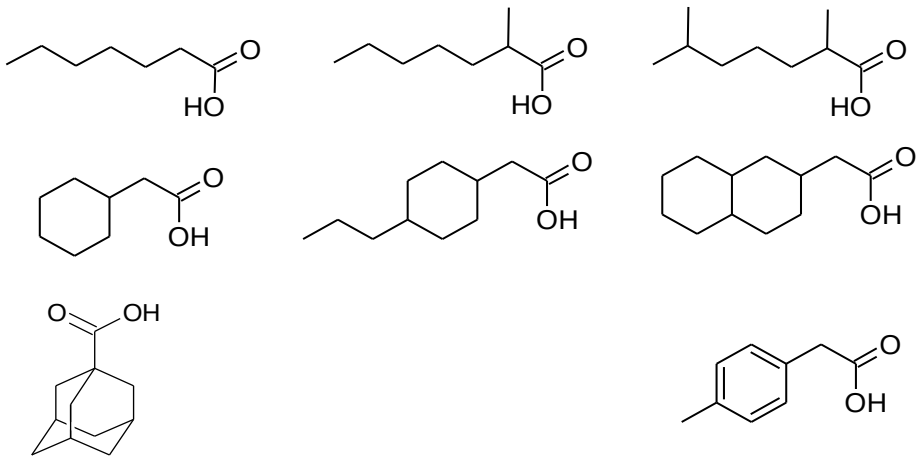

Figure 1.4. Structural groups of carboxylic acids identified by Rowland et al (2011) within a sample of a petroleum commercial mixture (Rowland et al., 2011c).

Also separated by the reversed phase column set were a series of alkylated phenols (West et al., 2011) which are known toxicants that can have estrogenic and androgenic effects on a range of species (Thomas et al., 2009 and references therein) and which have been shown to have individual acute toxicities about four orders of magnitude greater than naphthenic acids of similar molecular weights (Choi et al., 2004; Jones et al., 2011). The concentration of phenols (alongside other possibly unknown impurities) could affect the results of toxicity assays on commercial NAs which have been erroneously assumed by most workers to contain only acids (discussed by West et al., 2011).

1.1.2. Acid extracts from Oil Sands Process Water

Utilising multidimensional comprehensive GC-MS for analysis of a sample of the acid extracts from a Syncrude tailings pond OSPW Rowland et al.,

were able to identify a series of tricyclic adamantane-type diamondoid acids. Through co-chromatography of authentic standards both adamantane-1-carboxylic acid and 3-ethyl-adamantane-1-carboxylic acid were identified in the complex OSPW acid extract (Rowland et al., 2011b). Using the mass spectral knowledge gleaned from this confirmation of tricyclic acids other, tentative, identifications were able to be made. In all mass spectra for ten carboxylic and ethanoic adamantane acids were assigned to individual acid structures.

In the same sample of OSPW acid extract tetra and penta diamondoid acids were identified (Rowland et al., 2011b). Co-chromatography of diamantane penta cyclic diamondoid acids allowed a positive identification of diamantane-1-carboxylic acid and diamantane-3-carboxylic acid. Diamantane-4-carboxylic acid was postulated to exist but no trace of diamantane-2-carboxylic acid could be found. By use of the mass spectral information a number of tentative identifications were able to be made. Both methyl and dimethyl diamantane acids were postulated to exist within the sample of OSPW acid extract as are the ‘ring opened’ tetra cyclic species of diamantane acid (Rowland et al., 2011b). The positive identification of both the adamantane and diamantane species represents the first species of individual naphthenic acids to have a firm assignment of structure.

In conclusion, much still needs to be understood about the composition and toxic effects (if any) of the individual NA in acids derived from

petroleum and sold commercially and indeed, of NA in petroleum and PW. Recent identifications, including those made as part of the present study (e.g. (Rowland et al., 2011a-d; West et al., 2011) have allowed studies herein of the toxicity of individual acids and mixtures of relevant petroleum NA, probably for the first time (Chapters 2, 3, 4; partly published as Jones et al., 2011).

1.2 Oil Sands 'NA'

The largest area of oil sands development exists in the Athabasca region of north eastern Canada (Figure 1.4) which, in 2007, produced an average of $1.13x10^6$ barrels of oil per day (Frank et al., 2008). The 'oil' in the sands occurs as a bituminous deposit thought to have been laid down in a deltaic or fluviatile environment along the rim of a sedimentary basin (Schramm et al., 2000) which migrated, in response to pressure, concentration and gravitational gradients until the Clearwater shale prevented any further movement from its present position in the McMurray formation in the Athabasca region of Alberta, Canada (Czarnecki et al., 2005; Figure 1.6).

The McMurray formation has a number of distinct deposits showing evidence that it was once a drainage basin that was flooded by the encroachment of a shallow sea on many occasions. Geological deposits suggest that the bulk of the sediment is from estuarine conditions with layers of these deposits disrupted through marine or fluvial deposits (Schramm et al., 2000 & Czarnecki et at 2005).

Athabasca oil sands are made up from a mixture of bitumen, quartz, water and clays and are said to be ‘water wet’ oil sands (Figure 1.5) which enhances the ability to extract the oils from the sands as opposed to the ‘oil wet’ oil sands prevalent in Utah, New Mexico or California (Czarnecki et al., 2005).

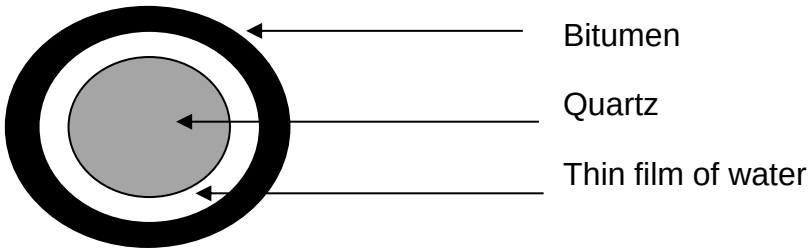

Figure 1.5. A representation of a ‘water wet’ oil sand where a grain of quartz is coated with a thin film (10 nm) of water which separates the bitumen from the quartz (adapted from Schramm et al., 2000 & Czarnecki et at 2005).

Essentially it is thought that each grain of quartz is coated by a thin layer of water (up to 10 Nanometres thick) which would mean that the bitumen is not in direct contact with the quartz. This thin layer of water allows extraction of the bitumen through the Clark Caustic Hot Water Extraction Method (Schramm et al 2000). The ‘water wet’ nature of these oil sands is considered a reasonable position by most authors (notably Schramm et al., 2000; Schramm et al., 2003 & Czarnecki et at 2005) although it has also been postulated that the water exists in an emulsified state with the bitumen and it is this which coats the quartz (Zajik et al., 1981).

There is postulation that the bitumen available today exists due to degradation *in situ*, i.e. after the migration, by a combination of evaporation, diffusion, oxidation and bacterial degradation. These factors would have been able to degrade the lighter oil components and leave heavily degraded bitumen in place (Schramm et al., 2000). Organic acids present in the Athabasca Oil Sands are thought to represent 1-2% by weight of the unrefined oil sands bitumen. However, it has been calculated that NA in the processed waters only make up ~0.1-0.2% by weight, or approximately 10% of the total organic acid content found in the bitumen (Schramm et al., 2000).

Oil sands processing typically employs the Clark Caustic Hot Water Extraction Method where the oil sands are slurried with water in large rotating drums. This process allows dispersal of large 'lumps' of oil sands into smaller pieces. In order to remove the bitumen from the sand, air, heated to 80^{o}C, is introduced, so that the bitumen is aerated to approximately 30% v/v gas. At this point, NaOH is added to raise the pH which has the effect of producing natural surfactants such as sodium naphthenates (Figure 1.3; (Quagraine et al., 2005 b) that aid the detachment of the bitumen from the sand. The amounts of oil sand/water/NaOH are typically in proportions (according to mass) of 1/0.4/0.0012, equalling approximately 40% water and 0.12% NaOH. This slurry is then transported to primary flotation tanks where the aerated bitumen is able to separate from the slurry (Schramm et al., 2000). A more

detailed discussion of oil sands processing is given by Schramm et al., (2000).

As a result of this processing, vast quantities of alkaline, saline water (OSPW) accumulate and are stored in tailings ponds and after recycling, eventually in so-called End Pit lakes or settling ponds (e.g. Headley & McMartin., 2004; Frank et al., 2009 and references therein). An estimation made in 2005 asserted that ~one billion m^3 of OSPW will have accumulated into the settling ponds by 2025 (Figure 1.4.) (Quagraine et al., 2005b). This OSPW is a major concern to the oil companies operating in northern Alberta as the OSPW will eventually have to be reclaimed and, due to the zero tolerance non release agreement (Frank et al., 2009), no OSPW can be discharged (deliberately or accidentally) into the environment surrounding the oil sands developments, primarily due to the toxicity of undiluted or somewhat diluted OSPW to many organisms (e.g. fish, birds, algae and plants) (Headley and McMartin., 2004; Peters et al., 2007; Kavanagh et al., 2011).

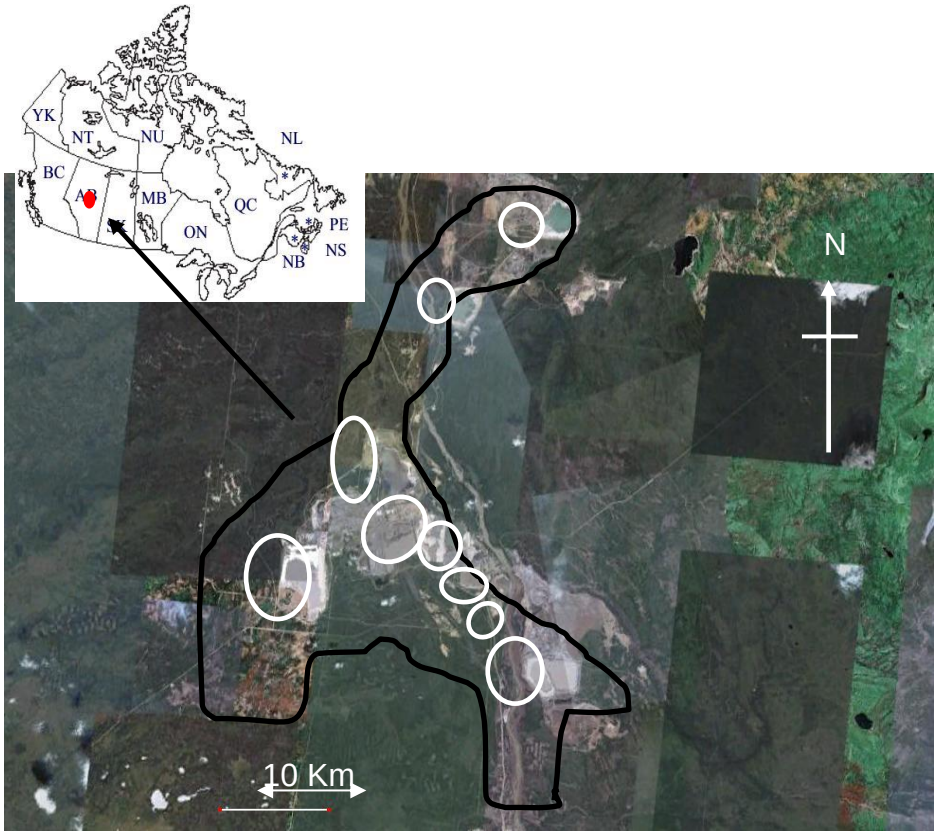

Figure 1.6. An Athabasca Oil Sands development (ringed by black line); showing geographical position in Alberta, Canada and position of settling ponds (ringed in white); image from Google Earth™ 2010**.**

NA are said to exist in OSPW at concentrations ranging from 20-150 mg L^{-1} (Hagen et al., 2012; Holowenko et al., 2001; Headley et al., 2009 and references therein). Holowenko et al., (2001) outlined the NA quantification method commonly used to obtain such concentration data (based upon the Syncrude oil company's standard analytical method) which was published in 1995 (Holowenko et al., 2001). By acidifying a filtered tailings sample to pH 2.5 and extracting with DCM, the sample was analysed via Fourier Transform infrared spectroscopy (FTIR) and the intensity of the carbonyl stretching frequencies recorded. Within the oil sand acid extracts there are both carboxylic monomer type acids as well as hydrogen bonded dimers

(Scott et al., 2008). Both have slightly different wavelength absorbance values (the monomer absorbs at 1740-1750 cm^{-1} and the dimer absorbs at 1700-1715 cm^{-1}).

The FT-IR spectrometer was calibrated using a commercial sample of naphthenic acids (Holowenko and co-workers utilised a Kodak preparation) and the peak heights at 1743 cm^{-1} (for the monomer) and 1706 cm^{-1} (for the dimer) were analysed. FTIR spectra of corresponding acid monomers and dimers in the OSPW have absorptions at approximately these two values (Holowenko et al., 2001; Scott et al., 2008). The peak heights of the standard NA samples at these wavelengths were then summed and plotted as NA concentration vs combined peak heights. The peak heights from the extracted oil sands were simply compared to commercial acid calibration curve for quantification (Holowenko et al., 2001).

The above method is briefly mentioned by Schramm et al., (2000). However this account refers to unpublished work by Mackinnon in 1990, which may well relate to an earlier method reported equally briefly, by Mackinnon and Boerger (1986), itself apparently based on an unpublished consultancy report by Zenon Environmental Inc. made for Syncrude Ltd. The latter report is said to be available from the Athabasca University library (http://library.athabascau.ca/) but all attempts to retrieve it have failed (personal communication, S.J.Rowland, Plymouth University 2012).

Mackinnon and Boerger (1986) compared the FTIR peaks at the absorbance wavelengths for the above carbonyl frequencies from a DCM extracted sample of Syncrude tailings pond water which had been either pH extracted or additionally had been dialysed to provide a diasylate with a molecular weight cut off at 2000 Daltons. These were then compared to the spectrum of an unknown (thought likely to be the Kodak commercial NA) commercial standard. It was noted that the sample with the molecular weight cut off had an extremely similar FTIR profile to that of the commercial standard with a prominent peak at a wavelength of 1707 cm^{-1}; very similar to that reported by Holowenko (2001) for the dimer NA species.

Scott et al., (2008) compared the FT-IR quantification methods recommended by Syncrude with a GC-MS method formulated by Merlin et al., (2007). For this study 18 water samples from various locations throughout Alberta were collected and analysed for NA content, these locations included tailings ponds, river and Steam Assisted Gravity Drainage sites (SAGD) (a method by which parallel wells are drilled into the oil sands and steam is injected to reduce the viscosity of the bitumen which then flows from the injector well to a second, lower, well for collection of the bitumen and co-produced water from the condensed steam).

In the GC-MS method, the NA were extracted from 1 L water samples by acidification to pH 2 by HCl after which 150 g of NaCl was added and the water was extracted with 3x 60 mL of chloroform. Authentic 9-fluorene-

carboxylic acid was added as an internal standard. The acids were then extracted from the chloroform with an alkaline solution (pH 11.6) which was subsequently acidified to pH 2 and extracted with DCM The acids extracted for FTIR analysis were removed from the water in a similar way.

For calibration of their FTIR method, Scott et al. (2008) used a Merichem commercial NA mixture as it had already been shown that use of different commercial mixtures in calibrations can give differential results (Rowland et al., 2011c; Scott et al., 2005; Scott et al., 2008a). An assumption was made that quantifying the concentrations of the $C_{13}H_{22}O_2^-$ isomers in the commercial mixture would be representative of not just the same isomer classes in the oil sand, but all of the isomer classes; this despite earlier evidence that commercial mixtures contained different compound classes in different concentrations to that of the oil sands (Garcia-Garcia et al., 2011; Headley and McMartin, 2004). Other assumptions were that the commercial mixture is representative of the NA being analysed; that solvent extraction efficiency is high; that the derivitisation methods being used have the same efficiency throughout both the standards and the samples and are effective against all compounds within the mixtures; and that the response of the detector is the same for all compounds being analysed (Scott et al., 2008).

When measuring concentrations of NA in river samples it was found that the FTIR method consistently measured higher concentrations than the GC-MS method (Scott et al., 2008). However, the median percentage recovery for GC-MS method was better (105%: range 105-180%) than the

FTIR method (49%: range 30-210%). In all but one case the GC-MS method measured lower NA concentrations in the tailings pond and the SAGD sites than did the FTIR method, which gave a range of concentrations between 11 and 110 mg L^{-1} (Scott et al., 2008), consistent with earlier findings using the Kodak commercial mixture as a calibration standard (e.g. Schramm et al., 2000; Holowenko et al., 2001).

It seems then, that for quantification of NA in OSPW, the superior method is FTIR, though recoveries up to 210% could explain why higher concentrations were noted in these samples compared to the GC-MS method (which had the better median recoveries). The assumption of similarity between commercial NA used as calibrants and OSPW NA is a concern. It was calculated that the $C_{13}H_{22}O_2^-$ isomers made up 8% of the Merichem commercial NA mixture so it was assumed that a recovery of either less than or greater than 8% in the GC-MS method for the same isomers was a failing of the method, not an indication of differing concentrations between commercial standards and OSPW acid extracts.

Although there is literature detailing acids in petroleum derived fossil fuels, and measurements by FTIR and GC-MS of NA concentrations in OSPW as discussed above, identification of the individual acids in OSPW remained elusive until the present and related studies were conducted (e.g. Rowland et al., 2011a).

Since similarities were observed between the FTIR spectrum of an un-named commercial NA mixture (although subsequent studies are based on

the Kodak P2388 standard (e.g. Holowenko et al., 2001)) and the spectrum of a DCM acid extract of processed water from a number of Syncrude oil sands tailings ponds in an early study (Mackinnon and Boerger., 1986), numerous subsequent workers chose to refer to the acids of OSPW as ‘Naphthenic acids’ (e.g. Headley et al., 2002; Lai et al., 1996; Lo et al., 2006 and many others). Although numerous differences in the toxicity and biodegradability of OSPW acids and commercial NA were noted (Scott et al., 2005), it was not until (Grewer et al., 2010) pointed out the differences more emphatically, that the term NA began to be less used or qualified for the acids of OSPW (Garcia-Garcia et al., 2011; Grewer et al., 2010; Kannel and Gan, 2012). Most workers seemed to have ignored the fact that over 50 years earlier, Knoterus (1957) had pointed out that the term naphthenic acids was “not very appropriate”, even for petroleum acids.

Methods for the classification and determination of OSPW acids have included GC-MS and GC-HRMS of derivatives (Holowenko et al., 2002; Scott et al., 2008; Thomas et al., 2009), liquid chromatography- mass spectrometry (LC-MS) (e.g. Bataineh et al., 2006) and, as discussed above, FTIR (Clemente and Fedorak, 2005). However, these methods usually only allow at best, determination of groups of acids, since the mixtures are so complex, as revealed by the unresolved chromatographic profiles of most methods (e.g. Figure 1.7).

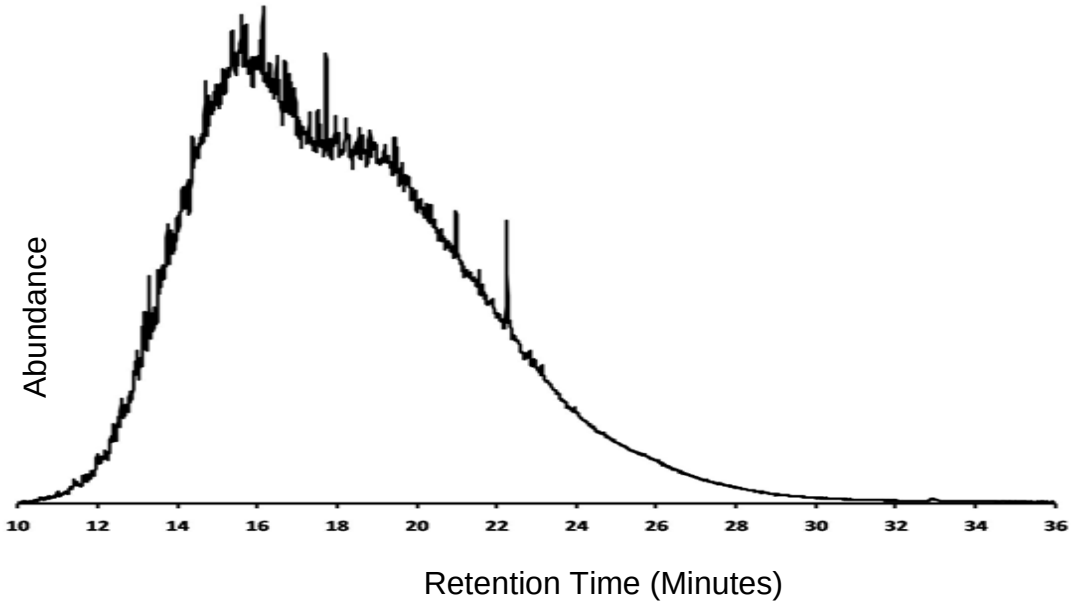

Figure 1.7. Chromatogram of the methyl esters of an acid extract from a Syncrude OSPW revealing a large unresolved 'hump' of compounds (adapted from Rowland et al., 2011e.)

Liquid Chromatography Quadrupole multistage Mass Spectrometry (LCQ-MS_n (Grbović et al., 2012), comprehensive two dimensional gas chromatography mass spectrometry (GCxGC-MS) (Hao et al., 2005) and FTICRMS (e.g. Barrow et al., 2010) (see below) have all been used to try to characterise individual acids in OSPW, but have met with only limited success (Hao et al., 2005; Shepherd et al., 2010). Literature detailing 'characterisation' of the acids is in abundance; an internet search conducted at the time of writing, revealed that over 4000 scholarly articles had been published detailing research into putative 'identification' of the acids (if acids in both the oil sands and crude oil matrices are included). However the data from these methods revealed only the 'z' and carbon numbers of the individual acids, not the structures.

Applications of so-called two-dimensional or multi-dimensional comprehensive GCxGC-MS have allowed the resolution of other unresolved complex mixtures, such as crude oil aromatic hydrocarbons (Booth et al., 2008; Booth et al., 2007) but more polar fractions, such as NA had either not been analysed, or the spectra have not been interpreted (Hao et al., 2005). However, as part of the present study, Rowland and colleagues (including the present author) published a number of articles detailing methods for the identification of individual acids in OSPW acid extracts from two oil sands industries (Rowland et al., 2011a-d; 2012). Rowland et al., used a novel instrument utilising a Zoex manufactured cryogenic modulator attached to a modified Agilent GC attached to an Almsco Time of Flight Mass Spectrometer which, produced electron ionisation mass spectra with clear fragment and molecular ions in many cases, due purportedly to improvements in mass spectrometer flight tube design and electronics (http://www.almsco.com/Products/Benchtof.aspx). This enabled the researchers to interpret the spectra and suggest structures for some individual acids, as methyl esters (e.g. Rowland et al., 2011a,b). A key part of these studies and related studies of a commercial NA mixture (Rowland et al., 2011c,d; West et al., 2011) was the use of purchased or synthesised methyl esters of the acids to confirm the assignments. Many of the syntheses are described herein (*vida infra*, Chapter 2). A number of the acids identified in OSPW by the methods are shown in Figure 1.4. One disadvantage of the GCxGC-MS method is the need for derivatisation of

the OSPW acids to esters (Rowland et al. used formation of methyl esters by heating with boron trifluoride-methanol complex) in order to preserve the GC column life and to improve the chromatographic properties of the acids. It is well known that production of methyl esters in this way is kinetically slow (Shepherd et al., 2010) such that some acids are not efficiently esterified, and that a variety of side reactions may also take place, such as dehydration of hydroxy species. It is also well known that some compounds are not amenable to the conditions found in hot GC injection systems (Zaikin and Halket, 2009)

In fact, prior to the present study (*vide infra*, Chapter 5), there was still much debate about whether the acid extracts of the OSPW contain hydroxy acids (Headley et al., 2011) aromatic acids (Kavanagh et al., 2009; Rowland et al., 2011; Jones et al., 2012) or phenols (Grewer et al., 2010; Hargesheimer et al., 1984; Laredo et al., 2004; West et al., 2011). A way of overcoming characterisation difficulties is to use a high resolution, accurate mass solution. Barrow et al. (2004) showed that Fourier Transform Ion Cyclotron Resonance Mass Spectrometry (FT-iCR/MS) was a useful tool in the characterisation of empirical mass and z group species within commercial PAs and in a sample of Syncrude OSPW. Barrow and colleagues were able to determine the masses of ions to within 0.5 ppm, highlighting two distinct ions in the Acros commercial acid at m/z 213.185999 and m/z 297.279946 and in the Fluka sample at m/z 209.154766 and 297.279946 enabling an determination of the mass errors and showing that this method is able to differentiate between isotopic

isomers (or isotopomers). It is noted that a number of determined masses had reported mass errors (the difference between the observed mass and a theoretical mass) of less than the weight of an electron. Determined masses of the two commercial samples were said to be 87 and 93% accurate to 1ppm for the Acros and Fluka commercial NA samples and 76% of the acids detected in the Syncrude OSPW extract. The three samples differed in z group abundance with the Acros having an abundance the z=-0 group, relative abundances were in the order of z=-0>z=-4.z=-2>z=-6 whilst the Fluka was more abundant in the z=-4 species (relative concentrations were z=-4>z=-2>z=-6). The Syncrude sample had z group abundances in the order of z=-4>z=-6, the authors also note the surprising abundance of the z=-12 group exhibited within the OSPW sample. The Syncrude OSPW sample had a lower percentage of determined masses accurate to 1ppm. This is because this sample was externally calibrated against the Acros FTICR-MS data and will have a lower mass accuracy for this reason (Barrow et al., 2004)

Bataineh et al., (2006) detected oxidised NA through use of a HPLC/QTOF-MS analysis on NA within a sample of Syncrude tailings pond water (TPW) before and after microbial degradation. The authors describe a method for direct liquid chromatographic separation of NA, using six model NA and three model hydroxylated NA compounds for method development. A Merichem commercial NA and NA extracted by a liquid-liquid extraction method (described by Clemente et al., (2004)); and a solid phase extraction method (refined from Headley et al., (2002)).

HPLC/QTOF-MS results were compared to results from GC-MS and GC-HRMS analysis (method based on Holowenko et al., 2002). Microbial degradation was performed on both the Merichem and the TPW using methods set out by Scott et al., (2005). Initial NA concentrations were 100 mg L^{-1} for the Merichem and ~50 mg L^{-1} for the TPW, though it is not stated how the TPW concentrations were determined.

Mass accuracy was determined by utilisation of the model compounds this was reduced from <20 ppm to <10 ppm by correction of instrumental drift through use of a reference solution with two perfluoroalkylcarboxylates at m/z 162.9824 and 262.9760 respectively. Using mass accuracy in conjunction with retention times allowed an accurate confirmation of NA empirical formulas.

Characterisation of the Merichem showed that the NA profiles from the HPLC/QTOF-MS method were somewhat similar to previously produced GC-MS data (Clemente et al., 2004). The ions with the greatest intensity were the z=-2 series, which were equivalent to 41% of the total mixture. There were no NA determined in either the GC-MS method or the HPLC method that were greater than C_{20}. However the GC-MS method did detect ions corresponding to C_5-C_7 that were undetected by the HPLC/QTOF-MS. Substantial differences were noted in the TPW comparison with GC-MS data being more complex in Nature than the HPLC data. The z-=-4 group were most abundant according to the HPLC data (36%) compared to 17% detected by the GC-MS method. The most abundant group in the GC-MS

data was z=0 (21%). Bataineh and colleagues also highlight the absence of the so-called $C22^{+}$ cluster (Holowenko et al., 2002 and Section 1.31 this chapter) stating that this cluster is more likely explained by double derivitisation of hydroxy-NA.

Biotransformation products, such as hydroxyl-NA, were determined by comparison with three model compounds; this was able to confirm the presence of hydroxyl and di-hydroxy-NA, though no ‘z’ group classification could be determined with any degree of accuracy.

When analysing the microbial degradation product it was noted that no significant degradation occurred in the TPW, confirming the microbial recalcitrance of these compounds. However significant biotransformation was noted in the Merichem commercial mixture. The authors note that the biodegradation was dependant on ‘z’ number and (to a lesser extent) carbon number and suggest that the most recalcitrant fractions included the compounds that were more highly branched. Bataineh et al., (2006) go on to state that no oxidised products were detected in the biotransformed Merichem acids, meaning that the presence of hydroxyl-NA in TPW remained a mystery, though it was postulated, at the time of publication, that microbial degradation was the most likely route.

Han et al., (2009) used a HPLC high resolution mass spectrometer (HPLC/HRMS) with a mass resolution of ~100000 to assess in situ biodegradation of OSPW. Following up on previous work (Han et al., 2008) where it was noted that a 50% biodegradation of OSPW samples took

from 44-240 days to occur, potentially due to a higher degree of alkyl branching, Han and colleagues examined field aged Syncrude OSPW for several potential biomarkers of microbial degradation. Examining OSPW from the Mildred Lake settling basin (MLSB) and from dyke water seepage (DWS), potential markers included the presence of oxidised PAs noted by Bataineh et al., (2006). Han noted that both mono and di-oxidised PAs were potential components of the OSPW (O_3 and O_4 species respectively) with mono carboxylic NA having z numbers of -4 to -8 and di-carboxylic NA with z numbers of -6 to -12. This was different from examined ore extracts which showed the potential presence of a mono-oxidised NA with a -12 z number. It was noted that the sample that contained the largest concentrations of oxidised NA compared to non oxidised NA was the oldest, which (the authors state) was suggestive of a slow biodegradation via hydroxylated intermediates. Though it is mentioned that oxidised NA may well be more recalcitrant to biodegradation so their relative concentration would increase as non-oxidised parent NA are mineralised. (Martin et al., 2010) followed this work with a 98 day biodegradation study on ozonised NA, and found that within the non-ozonised fraction, ~59% of a mass spectrometer response could be attributed to oxidised NAs; the total response from oxidised NAs decreased by 30% after the 98 day study.

Headley et al. (2010) detailed the FT-ICR/MS analysis of run-off from mature fine tailings ponds of OSPW. They discovered that whilst oxygen species (O_2-O_4) were>90% prevalent, there was also an up to 10%

presence of oxygenated sulphur species. Whilst determining the oxygen species, the authors stated that the O_4 species were dominant over the O_2 species in every sample, suggesting to them that di-carboxylic acids were predominant. However this dominance of di-carboxylic acids is based on the assumption that all measured species respond in the same way to negative-ion electro-spray ionisation (ESI). The authors do note that differences in response factors are to be expected based on the ability of compounds to form deprotonated molecules. Di-carboxylic acids are more likely to deprotonate than mono carboxylic acids as there are two available acidic hydrogen atoms, plus oxygenated sulphur species with higher pK_a values are less likely to deprotonate than lower pK_a acids (Headley et al., 2010).

Headley et al. (2011b)investigated a 'fingerprinting' technique for distinguishing polar organics from the OSPW and those derived Naturally from the weathering of the oil sands. They investigated a range of different classes as (they state) NA with general formula $C_nH_{2n+z}O_2$ may only make up a small fraction of the OSPW acids and that toxicity is usually associated with total organics not only the NA. This is a distinct departure from the statements of much previous, including very recent, research (Section 1.3 and references therein). Previous research focused on the toxicity of NA and tended to ignore the presence of other polar organics. Using FT-ICR/MS Headley et al., (2011) differentiated between samples using the presence of sulphur and nitrogen-containing species and recommended this technique to assess whether leakage from tailing ponds

into the Natural environment is occurring. However it is apparent, because of the geographical position of the oil sands deposits and the siting of the tailing ponds, that a certain amount of mixing of Naturally-eroded oil sands NA and OSPW NA must occur, especially during the spring thaw when the erosion power of rivers is maximised in the region (Headley et al., 2011b).

In a separate publication Headley et al. (2011a)) investigated the effects of salt on the analysis of NA mixtures with FTICR-MS. It was noted that significant differences were apparent for the interactions of sodium ions with OSPW acid extracts. There was an enhancement of the z=-4 species in the presence of sodium and salting out effects were observed for the O_1, O_3, O_4, O_2S and O_3S species. It is thought that these salting out effects will limit the bioavailability of NA in aquatic systems (Headley et al., 2011a)

Data from synchronous fluorescence spectrometry (SFS) suggested that the acid extractable fraction from numerous OSPW contained aromatic moieties (Kavanagh et al., 2009)). As part of a study conducted herein (*vide infra*, Chapter 5) acid OSPW extracts were fractionated using argentation thin layer chromatography (Ag^+TLC; Rowland et al., 2011c) and later, argentation solid phase extraction (Ag^+SPE) to provide evidence for a major occurrence of aromatic acids in OSPW (Chapter 5; Jones et al., 2012)

1.3 Toxicity of Naphthenic acids

1.3.1 Commercial Mixtures and Acid Extracts of OSPW

There is a zero release policy of OSPW in force in Athabasca (Scott et al., 2008b) primarily because of the reported 20-150 mg L^{-1} concentrations of the NA which are said to be amongst the components of OSPW that exhibit the largest acute toxicity (Headley and McMartin, 2004). Mackinnon and Boerger (1986), for instance, described two treatments for detoxifying the tailing ponds, using the Microtox™ assay amongst others, to quantify the toxicity. They concluded that it is the polar acidic fraction of the tailing ponds, which include naphthenic acids, that is the most toxic component of the OSPW (Mackinnon and Boerger., 1986). Rogers et al. (2002) stated that naphthenic acids in the OSPW represent the main toxic concern for aquatic organisms (Rogers et al., 2002). Nero et al., (2006) stated that NA are thought to be the primary cause of histopathological alterations in the gills and livers of fish (Nero et al., 2006). Young et al., (2008) in their study on estimating the concentrations of NA in fish stated that is the NA pose the highest risk to aquatic biota because they regularly exist at lethal concentrations (Young et al., 2008). In a recent review by Kannel and Gan., (2012) the authors stated that OSPW is toxic *because* (emphasis added) of the presence of the polar organic carboxylic acids, known as naphthenic acids (Kannel and Gan., 2012). Numerous authors also mention that the toxicity of the NA accounts for the OSPW toxicity but in general most refer back to previous work such as that of Mackinnon and Boerger (e.g. Scott et al., 2008; Grewer et al., 2010)

One of the most popular assays for measuring the acute toxicity of NA is the Microtox™ bioluminescence test (SDI Europe, Hampshire, UK) (Table 1.2). This assay tests the response of the marine bacterium *Vibrio fischerii* (*Beijerinck*, 1889) to a toxicant by measuring the output of bioluminescence, reduction of which is proportional to the effect of the toxicant (Clemente and Fedorak, 2005). The Microtox™ test works on a non-specific narcosis, or baseline toxicity (Leftley, 2000), where the compound in question reacts with proteins in the cell membrane but does not gain access to the inner parts of the cell. This interaction can affect the fluidity, thickness and surface tension of the cell membrane and can result in cell death (Cronin and Schultz, 1997; Schultz, 1989; Veith and Broderius, 1990) Narcosis is thought to be linked to structure, hydrophobicity and the size and weight of a molecule. Hydrophobic molecules more easily penetrate the lipid bilayer in a cell membrane; the larger (and more hydrophobic) a compound is, the more damage to a cell membrane occurs (Frank et al., 2009)

Microtox™ is a useful screening assay as bioluminescence is also lessened by an interruption in electron transport, so results can be (carefully) extrapolated beyond the effects on *V. fischerii* (Leftley, 2000). Light production in *V. fischerii* is controlled by synthesis of a luciferase enzyme and requires a source of energy to create a luciferase-flavin complex, which comes from oxidation of an aldehyde substrate (Figure 1.8) (Leftley., 2000).

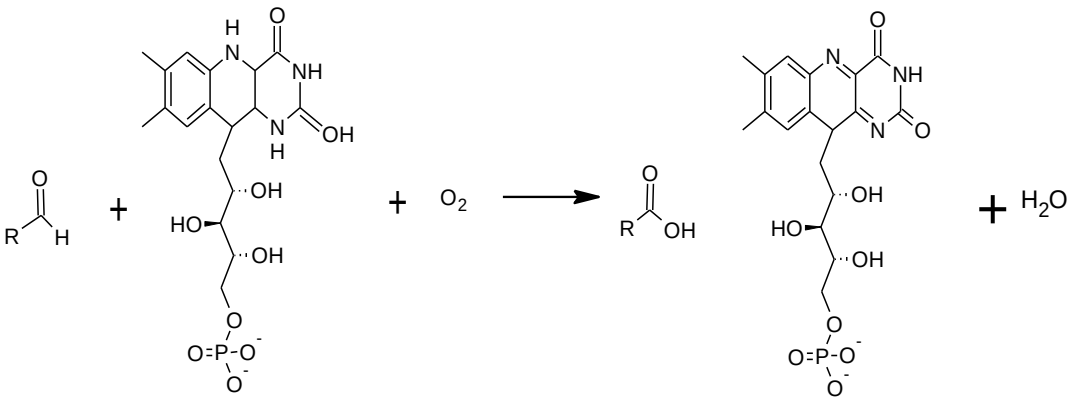

Figure 1.8. Oxidation of an aldehyde substrate by a luciferase-falvin complex

In aerobic bacteria, such as *V. fischerii*, the oxidation of an aldehyde substrate is connected to the electron transport chain via a FADH reductase (Figure 1.11) Any interference with the electron transport, through the introduction of a toxicant, will produce a toxic stress effect in the microbe and lessen the amount of light output (Leftley, 2000; Stewart, 1990). Other active sites affected by a toxicant introduced to the Microtox system include cell membranes, cell permeability, ribosomes and protein synthesis (Leftley, 2000). Many studies have based their entire toxicity data on this one test. Although useful it does not show if there is any potential for intracellular toxicity such as estrogenic or androgenic effects; nor does it show the effects on growth (or inhibition thereof) of an organism.

In general NA have been tested either as OSPW (an assumption is made that NA is responsible for the toxicity (Rogers et al., 2002)), whole NA complex mixtures, or on occasion, as distilled fractions of OSPW (Frank et al., 2009 ; Garcia-Garcia et al., 2010). Acid extracts derived from Oil Sands Process Affected Waters (OSPW) typically have an effective

concentration that has a 50% deleterious effect (IC_{50}) of ~30 mg L^{-1} to the Microtox™ test, whilst some commercial NA mixtures have a general toxicity of ~10 mg L^{-1} (Clemente and Fedorak, 2005; Clemente et al., 2004) i.e. the OSPW is less toxic. Because of the uncertainty of the chemical composition and unknown molecular weights of NA, IC50s are generally reported in units of mg L^{-1} rather than as molar values.

NA that occur in OSPW and in commercial mixtures generally have molecular weights of less than a thousand Daltons, which is reported to be the cut off size for a compound to enter a cell (Holowenko et al., 2002). This implies that all NA are potentially toxic and bio-available and hence the non-specific narcosis toxicity model would predict increasing deleterious effects correlated with increasing molecular weight. However, it has been reported that the higher molecular weight NA are generally less toxic than their smaller counterparts, which raises questions about current knowledge of the mechanisms of NA toxicity (Clemente and Fedorak, 2005; Frank et al., 2009).

NA have been estimated and detected in wild fish in the Athabasca region (Young et al., 2008) at concentrations of up to 2.8 mg kg^{-1}. Young et al. (2007) exposed rainbow trout to both a commercial preparation of NA (Merichem) and OSPW. Fish were either fed pellets impregnated with Merichem NA (some of which contained an undecanoic acid standard) or exposed directly to water containing 3 mg L^{-1} Merichem acids or a Syncrude pond water containing ~15 mg L^{-1} NA (measured by HPLC) .Testing was conducted at pH 7.6 for the Merichem acids and pH

8.4 for the OSPW. NA in fish extracts treated with a Merichem commercial NA were determined by GC-MS by determining the presence of the *m/z* 267 ion (which is indicative of NA esterified with a tertiary-butyl trimethylsilyl substituent). NA were detected in all three exposure mechanisms but no units detailing concentrations were given, the detection being based upon the presence of a chromatographic 'hump' between retention times of 15 and 20 minutes when searching for the fragment ion at *m/z* 267. No 'hump' was observed in fish not exposed to the NA or to OSPW. A number of fatty acids were observed in the total ion current (TIC) chromatogram. No chromatographic hump was observable in the TIC . The authors stated that the minimum detection limit for this method was 1 µg NA g^{-1} fish (Young et al., 2007).

Follow up work in 2008 (Young et al., 2008) allowed examination of the depuration of NA (95% depurated after 1 day) and the bioconcentration factors (~2 at pH 8.2). Exposure and extractions were similar to methods described previously (Young et al., 2007) although this experiment also included a number of fish from wild sources. As previously, GC-MS detection was based on the presence on an *m/z* 267 ion. However, it is apparent that this is based upon the M+57 ion from a tert-butyldimethylsilyl derivatised carboxylic acid of 13 carbons and a z number of -4 (a bicyclic acid). No authentic standard was available to test the assumption that bicyclic acids exist in the OSPW and in Merichem commercial NA. Whilst these acids have been recently identified in a commercial NA sample

(Rowland et al., 2011d) they have yet to be determined in OSPW acid extracts (Young et al., 2008).

When analysing wild the wild fish samples it was discovered that NA concentrations in samples taken from fish species taken from the Athabasca River were variable, ranging from 0.2-2.8 mg kg^{-1}. When samples were retaken from the same fish samples several months later it was discovered that the NA concentrations had changed considerably in each sample. This variability highlights an issue with the reproducibility of this method, yet the authors state that (at the time of publication) it is the only available method for determining NA concentrations in wild fish. Young and co-workers analysed nine fish samples (that exhibited initial concentrations of <1mg kg^{-1}) several months after initial analysis and found no difference in concentrations. This result seems to be justification of the method, yet the calculated detection limits are set at 1 mg kg^{-1} so all of these nine fish exhibited NA concentrations below the detection limits both in initial and subsequent analysis (Young et al., 2008).

It is also stated that the maximum concentrations of NA in wild fish is 2.8 mg kg^{-1} however this is only true of one repetition, two subsequent analysis of the same fish, which were stored after the initial analysis at -20^{o}C, exhibited concentrations at 6.7 mg kg^{-1} and 4.6 mg kg^{-1} respectively (mean 4.7 mg kg^{-1}; standard deviation1.9 mg kg^{-1}: RSD 40%). It is notable that the RSDs recorded for the in triplicate analysis of NA concentrations in wild fish range from 14-67%. Fish that did not display a chromatographic hump at a retention time of 15-20 minutes, corresponding to the m/z 267

ion were assumed to have a zero NA concentration. However one of these fish did show peaks which may correspond to unsaturated NA moieties. These peaks were ignored as the authors based their structural assumptions on the earlier work by Brient et al (1996) (Young et al., 2008).

It must be noted that fish exhibiting concentrations below the limits of detection (1 mg kg^{-1}) do so only for NAs corresponding to the *m/z* 267 ion. With the heterogeneity of NA displayed within a super complex mixture questions must be raised at the veracity of this method. Later work by Rowland et al (2011b) has shown that the bi-cyclic moiety that Young et al., (2008) state correspond to the *m/z* 267 ion has yet to be discovered within a Syncrude OSPW acid extract and whilst that does not preclude the presence of this particular acid group in other OSPW acid extracts it is an important point. That may have consequences for the analysis of wild fish samples and the determination of NA thereof.

The determined lethal concentrations to fish have been elucidated to lie between 4-75 mg NA L^{-1} (LC_{50}s) (Dokholyan and Magomedov, 1984; Nero et al., 2006) these concentrations seem to be species dependant (e.g. they differ for chum salmon, rainbow trout and Caspian round goby (*ibid*.)). However Dokholyan & Magomedov (1984) assayed the effects to fish from sodium naphthenates at an unspecified pH and from an unspecified source, with either an acute 96 h, or ten day assay or a chronic 60 day testing regime. They found that adult fish (sturgeon, roach and goby) were far less susceptible to the effects of sodium naphthenates compared to the

juvenile species assayed. They concluded that sodium naphthenates (and therefore NA) have differential effects depending on species and the age of the tested fish, with the most susceptible to a chronic 60 day exposure was the young chum salmon (LC_{50} 1.4 mg L^{-1}) and the least susceptible was the adult goby (LC_{50} 13.5 mg L^{-1}). The authors also established that sodium naphthenates have a lethal dose (LD_{50}) of 0.15 mg L^{-1} to the zooplankter *Nephargoides maeoticus*. This concentration is now the maximum allowable concentration in waters in Russia and has been suggested as the maximum concentration in other countries (Clemente and Fedorak, 2005; Quagraine et al., 2005a; Whitby et al., 2010). As the commercial NA that Dokholyan & Magomedov assayed were from an unspecified source and as the test pH was not mentioned, it will be impossible to reproduce Dokholyan & Magomedov's results with any level of accuracy or precision (Clemente and Fedorak, 2005).

Nero et al., (2006) measured the effects of salinity on NA toxicity to yellow perch. Assaying both an Acros commercial NA mixture and the acid extracts of an OSPW, Nero and co-workers investigated the modifying effects of salinity on the toxicity to these mixtures. NA concentrations were determined as above by use of the FTIR method detailed by Holowenko et al., (2001). NA were classified by mass spectrometry by carbon number and z value. The assays were conducted at pH 8.19 to 8.40 and a salinity of 0.1-1 PSU. Low mortality was observed in the control solutions and 100% mortality was observed in the highest test concentrations (3.6 mg L^{-1} commercial acid; 6.8 mg L^{-1} extracted OSPW). The addition of salt

reduced mortality by 40% for the commercial mixture and by 50% for the OSPW acid extracts. Commercial acids showed between 20 and 80% higher mortality than the OSPW acid extracts whether salt was added or not. It was found that NA and mixtures of NA and salt had high levels of histopathological effects in the gill, though there was no significant difference in liver pathology; there was evidence to suggest that the addition of salt led to differential effects. This result, plus the higher toxicity of the commercial acids led the authors to conclude that the difference in chemical composition was the cause of the differences in toxicity (a conclusion supported by the later research of Garcia-Garcia et al. 2011).

Selected authors describe the toxicity of NA, when utilising the Microtox™ assay, as a percentage volume/volume (% v/v) which translates low toxicity to 100% (v/v) and high toxicity to 0% (v/v) (e.g. Holowenko et al., 2002; Clemente & Fedorak., 2005). However it is rare when reporting in this manner that actual toxic concentrations in mg L^{-1} are reported and it is essential to examine the papers carefully to glean more useful data (in mg L^{-1}) from them. Holowenko (2002), for instance, reported on the presence of the so-called C_{22+} NA cluster in selected OSPW samples and the effects on toxicity. The so-called 'C_{22+} cluster' is essentially the sum of the compounds in each relative z grouping that have 22 (or greater) carbon atoms. Taking six Suncor samples and three Syncrude samples, Holowenko noted a difference in C_{22+} NA and a relative difference in toxicity. However, there was also a relative difference in concentrations of NA, with the highest concentration (68 mg L^{-1} NAs, 11% v/v EC_{20}) showing

the highest toxicity and the sample with the lowest concentration (24 mg L^{-1} NA, >100% v/v EC_{20}) showing the lowest toxicity.

The authors stated that they were unsure whether the toxicity was influenced by the concentrations of NA, the chemical structures of the NA, or both. It is likely that a NA with more than twenty two carbon atoms would be very poorly soluble at the relevant pH required for a Microtox™ assay, so an increase in concentrations of these larger molecules could well decrease the toxicity to the Microtox™ assay which is based upon the narcosis or baseline mode of action which relies upon an interaction with the cell membrane. However the toxicity test pH is not stated so it is not possible to make an exact determination. The presence of the C_{22+} cluster has since been questioned as Clemente et al., (2004) proposed that these NA were more likely to be artefacts of a double derivitisation of hydroxylated NA , this was (somewhat) shown to be correct by Bataineh et al., (2006) when analysing a TPW sample for the presence of hydroxyl NA after biodegradation.

Kamaluddin and Zwiazek, (2002) reported the affect of NA on Aspen trees, stating that concentrations of NA inhibit root water transport, gas exchange and leaf growth. Root hydraulic and stomatal conductance declined to ~43% of the control when exposed to concentrations of 150 and 300 mg NA L^{-1}. The 300 mg L^{-1} solution also affected net photosynthesis and leaf chlorophyll (~35% lower than control) (Kamaluddin and Zwiazek, 2002). However, these concentrations were above those found in the OSPW and

certainly far higher than found in the environment (Frank et al., 2009; Frank et al., 2008) so the environmental relevance of the study is questionable. The study states that Aspen trees would be at risk if the OSPW ever escaped into the Athabasca River, but the authors did not take into account that any NAs present would then be in a more dilute concentration.

Table 1.2. Selected published toxicology assays completed on Naphthenic acids and the oil sands process affected waters

Test Organism	Reference	Comments and Endpoints
Mammals		
Wistar Rats	Rogers *et al*., (2002)	Food consumption suppressed in rats given up to 300 mg kg^{-1} over 14 days. Liver weight increase, elevated blood amylase, lower hypocholesterolemia and excessive glycogen accumulation observed in rats given up to 60 mg kg^{-1} OSPW over 90 days. An assumption that the NAs are driving the toxicity is stated
Female Mice	Garcia-Garcia et al (2011)	Female mice orally exposed to the organic extracts of OSPW, subsequently analysed for NA concentrations (50 mg mL^{-1} NA) and to Merichem commercial NA. Mice exposed to 50 mg kg-1 and 100 mg kg-1 of both OSPW organic extract NA and Merichem NA. Discovered differential effects between the two mixtures with Merichem being the more toxic. Recommendation that commercial NA cannot be substituted for OSPW organic fraction NA (see Hagen *et al*., (2012) below).
Molluscs		
Oyster Embryos	Smith, (2006)	Tested a number of surrogate NAs including isomers of butylcyclohexylbutanoic acid and cholanic acid on oyster embryos. The subjectivity of the test is a concern as is the amount of MeOH used as a carrier solvent (see text). IC50 calculated at 0.1-0.5 mg L^{-1}.
Zooplankton		
Nepargoides maeoticus	Dokholyan and Magomedov, (1984)	Sodium Naphthenates from unspecified source. Zooplankton susceptible to concentrations >0.15 mg L^{-1}, this concentration is now the maximum allowable aquatic concentration (MAAC) in Russia and has been suggested as the MAAC elsewhere (Clemente and Fedorak, 2005; Quagraine et al., 2005b)..

Crustaceans		
Daphnia Magna	Frank *et al*., (2009 & 2010)	Frank et al (2009 & 2010) tested NA surrogates (4 mono acids and 4 di acids). IC50s for *D. magNA* ranged from 109 mg L^{-1} (cyclohexylpentanoic acid) to 1166 mg L^{-1} (hexanoic acid) in the mono acids and between 1344 mg L^{-1} (cyclohexylsuccinic acid) to 3223 mg L^{-1} (succinic acid) in the di acids.
	MacKinnon and Boerger, (1986)	see data for rainbow trout as same endpoints apply
Birds		
Tree Swallows	Gentes *et al*., (2007)	Nestlings exposed to 1.5mg NAs day^{-1} from 7-13 days of age. No effect on growth, Ethoxyresorufin-O-deethylation (EROD) activity, blood chemistry or organ weights. Slight change in extramedullary erythropoeisis in the liver. No reproductive or chronic study carried out.
Trees		

Aspen	Kamaluddin and Zwiazek., (2002)	Tested at non-relevant concentrations (see text). Roots exposed to NAs for 3-5 weeks. Hydraulic conductivity and gas exchange processes affected at concentrations up to 300 mg L^{-1}.
Fish		
Chum Salmon, roach, kutum, sturgeon, Caspian round gobi	Dokholyan and Magomedov., (1984)	Fish exposed to 12-100 mg L^{-1} sodium naphthenate. LD_{50} for chum salmon observed at 25 mg L^{-1}. 2 month old Roach, kutum and sturgeon LD_{50}s at 50 mg L^{-1}, and 2 year old roach and Caspian round Gobi LD_{50} at 75 mg L^{-1} (Clemente and Fedorak, 2005). NAs from unspecified source.
Fathead minnow	Kavanagh et al (2011)	Exposed fathead minnows to samples of aged OSPW containing >25 mg L^{-1} NA. Aged OSPW inhibited reproduction and reduced male sexual characteristics. Also lowered concentrations of testosterone and 11-ketotestosterone in male fish and concentrations of 17β-estradiol in females.
Yellow perch	Nero *et al*., (2006)	Effects of salinity on the toxicity of NAs tested. Gill and liver histopathological changes monitored after a three week exposure to a commercially available and oils sands produced NAs. LC_{100}s observed at 3.6 and 6.8 mg L^{-1} respectively. Exposure to a 25% solution resulted in reduced gill surface area and high levels of gill epithelial, mucous and chloride cell changes.
Yellow Perch and Japanese Medaka	Peters et al.,(2007)	Exposed yellow perch eggs and medaka embryos to Mildred lake settling basin surface (MLSB) water and a commercial sodium naphthenate standard. Eggs were fertilised and incubated to solutions of MLSB water ranging from 100- 0.16% and sodium naphthenate solutions of 20-1.25 mg L^{-1}. An increase in deformities and hatch length were observed as concentrations increased. MLSB was noted to be more toxic than the commercial standard.
Yellow Perch	Van den Heuvel et al., (2011)	Created two experimental ponds which were stocked with oil sands fine tailings capped with natural water and a lake in a watershed containing bitumen bearing clays. Both ponds were stocked with yellow perch caught in Mildred Lake. Two natural lakes were also sampled as a comparison. A reduction in testes size, testosterone and 11-ketotestosterone was noted in the capped fine tailings lake but not in the watershed lake. No changes in female fish were noted. Studied over 13 years toxicity was able to be correlated with increasing (and decreasing) NA concentrations within the lakes

Rainbow trout	MacKinnon and Boerger, (1986)	Tailings pond water shown to be acutely toxic to trout with a LC_{50} of 10% for surface tailing ponds water that had not been treated through acidification, This dropped to a LC_{50} of >100% (not acutely toxic after treatment and storage for 1 year. Does not state what the starting concentrations are so it is difficult to apply an mg L^{-1} endpoint to the data.
Goldfish	Hagen *et al*., (2012)	Acute and sub chronic toxicity of Naphthenic acid exposed Goldfish. Found that sub-chronic exposure (20 mg L^{-1}) reduces Goldfish's ability to fight infection from pathogenic microbial species. However acute exposure (one week) increases resistance to infection. States that this is the first time that this effect has been observed in Goldfish exposed to OSPW derived NAs. However the test medium was a commercial Merichem mixture so this statement is incorrect (see text and Garcia-Garcia (2011)).
Yeast		
YES & YAS Assays	Thomas *et al*., (2009)	Reports that petrogenic Naphthenic (pNAs) acids are weak estrogen receptor (ER) agonists that can account for 65% of the unknown ER agonist potency. pNAs also disrupt binding of the androgen receptors (AR) to the AR ligand receptor

Bacteria		
TetrahymeNA pyrformis	Seward and Schultz, (1999)	Tested 39 aliphatic carboxylic acids (mono, di and unsaturated) alongside 3 carboxylic acid sodium salts. Toxicity endpoints presented in *log*(IGC_{50}) in mM concentrations which describes the inhibition to growth. Carboxylic (mono, di and unsaturated) acids had *log*(IGC_{50})s of between -0.06 (0.87 mM) and 0.9 (7.94 mM). Sodium salts had *log*(IGC_{50})s of between -1.45 (0.03 mM) and -0.08 (0.83 mM).
Vibrio fisherii		*Little or no information in the method sections of these papers on how the NAs were prepared for testing.*
	MacKinnon and Boerger, (1986)	Found that untreated oil sands produced water (OSPW) had a 30% IC50, which decreased to >100% after one year's storage. Treated OSPW had an IC50 of >100% at time zero. See 'rainbow trout' and text for discussion on the method of reporting the data.
	Holowenko *et al*., (2002)	Tested process affected waters from 6 Suncor sites and found acute inhibition toxicity (IC_{50} and IC_{20}) of between 64 and 100% (IC_{50}) and 11 and 100% (IC_{20}). Though these results are highly dependent on the starting concentrations with the highest concentrations showing the highest toxicity. Noted a correlation between lower toxicity and the so called C22+ cluster (see text).
	Clemente *et al*., (2004)	Noted that toxicity decreased in commercial NA mixtures after biodegradation with a starting point for the Merichem mixture at an IC50 of 10% which moved to a non-toxic 100% over 45 days. Kodak salts were also analysed with similar results.
	Scott *et al*., (2008)	NAs from the OSPW produced from the Athabasca oil sands were ozonated for up to 130 hrs. Initial inhibition concentrations (IC_{20}s) of 23% v/v decreased after 11 minutes. OSPW became completely non-toxic after 50 minutes treatment.
	Frank *et al*.,	Assessment of distilled fractions from a NA mixture and noted that the lower molecular weight fraction was the most

	(2008)	toxic. With IC50s ranging from 41.9-64.9 mg L^{-1} (see text and Figure 2.5).
	Frank *et al*., (2009 & 2010)	Noted IC50s of between 0.07 mM and 19.12 mM for mono acids and 26.09 mM and 627.31 mM for di acids (see *D. magNA* and text).
	Mishra *et al.,* (2010)	Tested microwave treated OSPW and commercial mixtures. Toxicity dropped from an IC50 of 15.85% to 36.45% in the commercial mixture but an increase (22.92% to 19.77%) was noted in the OSPW. However this test was performed at pH 8.47. The Microtox™ parameters require testing between pH 6 and 8.
	Jones *et al*., (2011)	Tested individual 'Naphthenic acids' that were previously identified in OSPW and the Merichem commercial acid mixtures (Rowland et al., 2011b; Rowland et al., 2011d; Rowland et al., 2011e) (see Chapter 3 for a more in-depth analysis)

Frank et al (2008) reported differences in the toxicities of distilled fractions of OSPW acid fractions isolated by Kugelrohr distillation. Separate fractions were isolated by different boiling points. The OSPW was esterified via a diazomethane derivitisation method and distilled into fractions with different median molecular weights. Fractions were collected between 130^{o}C and >220^{o}C distillation temperature with measured toxicities (IC50) ranging from 41.9 mg L^{-1} (130^{o}C) to 64.9 mg L^{-1} (>220^{o}C). Frank and colleagues stated that these results were in agreement with the assumptions made by Holowenko et al., (2002) that the C_{22+} NA were less toxic than lower molecular weight NA and stated that the >220^{o}C (highest molecular weight fraction) was the least toxic, However most fractions had little (if any) statistical difference in toxicity and an anomalous (and unexplained) result was recorded in the 160^{o}C fraction. The >220^{o}C fraction has similar toxicity to the 130^{o}C fraction, the 220^{o}C fraction and the stock solution. If the median molecular weight values for the acids from MS data are used to convert the mg L^{-1} results to milli molar (mM) values there is very little difference in toxicity throughout (Figure 1.10) even amongst those fractions that are starred in Figure 1.9 which highlight the reported statistically different fractions from the stock solution (Frank et al., 2008).

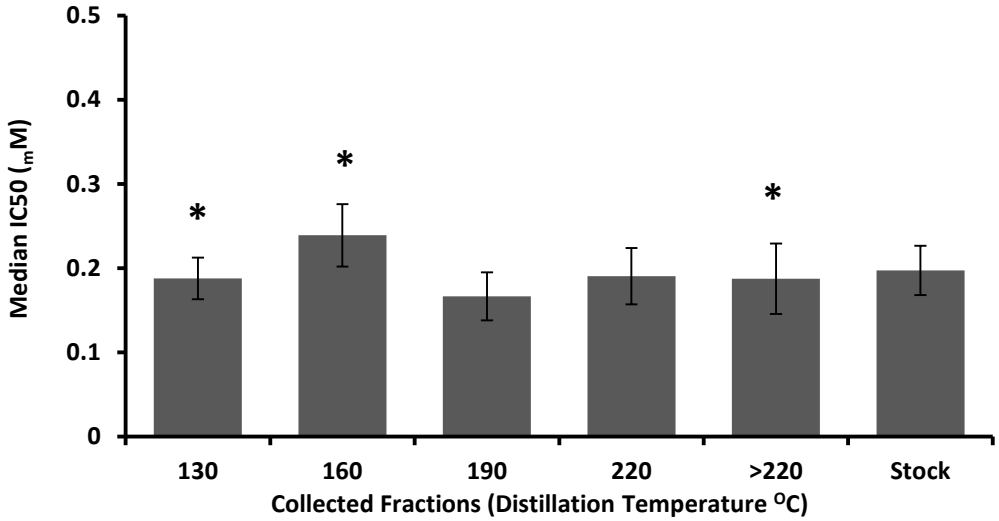

Figure 1.9. Microtox™ median IC_{50} values for distilled fractions of naphthenic acids, error bars are 95% confidence limits. Stars indicate fractions that are reported to be significantly different from that of the un-distilled stock solution (Adapted from Frank et al., 2008).

Other testing regimes have focused on the toxicity of OSPW after it has been biodegraded (Table 1.2). It was found (in general) that the toxicity of NA mixtures (commercial and from OSPW) decreased over time of exposure to live microbes. Methods for degrading the oil sands to test for lessening toxicity have included biodegradation, ozonation, acidification and microwave treatment (Clemente and Fedorak, 2005; Holowenko et al., 2002; MacKinnon and Boerger, 1986; Mishra et al., 2010b; Scott et al., 2008b).

Hagen et al., (2012) assayed the effects of NA complex mixtures on Goldfish. Their results showed that Goldfish exposed to 20 mg L^{-1} NA exhibited a differential host defence against pathogens between acute and sub-chronic assays. Goldfish exposed for one week (Acute) had an increased defence against the protozoan pathogen *Trynanosoma carassii.* However when exposed for 12 weeks (sub-chronic) the defences against *T. Carassii* lessened. It was also

discovered that Goldfish exposed to lesser concentrations (1 and 5 mg L^{-1}) remained unaffected.

However as NA only exist at such concentrations as 20 mg L^{-1} in the OSPW tailing ponds and the background levels in natural sources (such as the Athabasca river) are up to 1 mg L^{-1} (Hagen et al., 2012; Schramm et al., 2000; Whitby et al., 2010) such data are only relevant to fish that exist within the produced waters.

There are sometimes discrepancies between reported research results and what the authors claim the results show. Hagen et al. (2012) discuss the fact that Goldfish exposed to the acid extract of OSPW were sensitive to higher concentrations of NA but the research methods stated that the NA used in the study was a commercial (Merichem) NA mixture, not OSPW. This is despite previous research stating that commercial mixtures and OSPW extracts contain different compounds and have different toxic effects (Garcia-Garcia et al., 2011; Headley and McMartin, 2004; Rowland et al., 2011d; Rowland et al., 2011e)

Oddly, this latter research was based upon the previous research carried out by Garcia-Garcia et al. (2011) who assayed gene expression in mice exposed to both a commercial mixture of NA and the organic extract of OSPW (containing 50 mg mL^{-1} NA and concluded that:

"...*the results presented here indicate that commercial NA preparations are not the best model to study OSPW toxicity*..." (Garcia-Garcia et al., 2011).

Very few publications on NA consider the toxicity of NA other than those associated with the OSPW of the Canadian oil sands industry. As an exception,

Thomas et al., (2009) investigated the potential for NA to act as *in vitro* xeno oestrogens and anti androgens from concentrations found in oil produced water (PW) from North Sea oil wells. Using the Yeast cell Estrogen Screen (YES) and the Yeast cell Androgen Screen (YAS) receptor binding assays, it was found that petrogenic NA could account for ~65% of ER agonist potential and that NA can disrupt binding to the androgen receptor (Table 1.2).

1.3.2 Identified and Surrogate Individual Acids

Smith (2006) used the oyster embryo viability test to assess the toxicity of four butylcyclohexlybutanoic acids and cholanic acid and decahydro-2-Napthoic acid (DHPA). IC50 values for the butanoic acids ranged from 0.11-0.49 mg L^{-1} (0.002-0.0005 mM) whilst the cholanic acid and the DHNA had IC50s of 0.002 and <0.001 mg L^{-1} ($1.1x10^{-5}$ and $<3.3x10^{-6}$ mM respectively). The method of preparation of the toxicant mixtures was unclear but it seems a large quantity of MeOH (1.25%) was used as a carrier solvent which might in itself have a deleterious effect on the oyster embryos. The recommended use of carrier solvent in toxicology tests is a maximum of 0.01% (Hutchinson et al., 2006; OECD, 2000). Although the oyster embryo test is now a standard assay used by the UK Environment Agency, the endpoint of the test is subjective i.e. healthy embryos form a 'perfect D' shape and this is assessed by eye; therefore this assay is best performed by experienced operators. The IC_{50} from this test for the cholanic acid would very likely put this compound into a list of the most toxic known organic compounds when it is predicted to have an IC_{50} of 0.03 mM (0.9 mg L^{-1}) by the ECOSAR Predictive Toxicology model. This test would therefore need to be reproduced before acceptance (Smith, 2006).

Frank et al., (2009) investigated the effect of carboxylic acid content on toxicity to the bacterium *Vibrio Fischeri* using the Microtox™ assay. Using four mono carboxylic acids (*n*-hexanoic, cyclohexane carboxylic, decanoic and cyclohexanepentanoic acids) and four di-carboxylic acids (succinic, adipic, 1,4-cyclohexanedicarboxylic and cyclohexylsuccinic acid). Frank noted that the addition of an extra carboxylic acid reduced the toxicity significantly to both the Microtox™ assay and a Daphia magna 48 hour assay for all of the surrogate acids. It is notable that toxicity also increased with molecular weight. This was also noted in the study by Jones et al (2011). Frank et al., hint that a possible explanation is the lower hydrophobicity of the dicarboxylic acids, hence their observed lower toxicity. The authors note that because di-carboxylic acids can be produced via microbial transformation (Johnson et al., 2012a), that these acids are possible contributors to the lower acute toxicity of aged OSPW.

Rowland and co-workers briefly investigated the toxicity of the metabolites of microbial degraded NA discussed by Smith et al. (2008). Utilising the Microtox™ assay, four isomers of butylcyclohexylbutanoic acid and the degradation products (isomers of butylcyclohexylethanoic acid) were assayed. It was noted that the toxicities of the degradation products were lower than those of the parent compounds (Rowland et al., 2011a). It was noted that these isomers (or similar compounds) existed in a commercial NA mixture (Rowland et al., 2011c) but have yet to be positively identified in the sample of acid extracts of OSPW that has been extensively investigated (Rowland et al., 2011a).

Jones et al., (2011) utilised the Microtox™ assay to assess the toxicity endpoints to a range of individual NA that had been positively identified within the acid

extracts of OSPW and a Merichem commercial mixture. Acid compositional groups included *n*-acid, branched monocyclohexyl acids, branched mono aromatic acids and the tricyclic diamondoid adamantane acids. In all, over 35 acids were tested IC50s ranged between 0.7 mM (C_6 hexanoic acid) to 0.004 mM (C_{13} 3-(decahydronaphthalen-2-yl)pronanoic acid) and increased exponentially with increasing carbon number (Jones et al., 2011) (Chapter 3 provides an in-depth discussion).

Knowledge of the individual effects of these acids can also inform analysts of potential threats from mixtures of acids. This work also presented evidence that lower molecular weight NA increase in toxicity with increasing molecular weight up to a solubility cut-off point and postulated that the effects discussed by Holowenko et al., (2002) are also likely associated partly with a solubility limit.

Tollefsen et al., (2012) assessed the toxicity of three butylcyclohexylbutanoic acid isomers, three butylphenylbutanoic acid isomers and three commercial mixtures of NA. The butanoic acids were assayed individually, as a binary mixture (4-sec-butylphenyl butanoic acid and 4-n-butylphenyl butanoic acid) and as a total 6 component mixture on the metabolic inhibition and membrane integrity of trout hepatocytes. For the individual assays the IC_{50}s for metabolic inhibition ranged from 108-405 µM with the 4-*n*-butylcyclohexylbutanoic acid being the most toxic. For the cyclohexyl acids, toxicity was in the order of n>s>i which mirrored the previous research by Rowland et al., (2011a) although the individual assessments on the Microtox™ assay did show a somewhat higher susceptibility that the trout hepatocytes.

The aromatic moieties were less toxic than their saturated counterparts, with toxicities ranging from 230 µM for the *s* isomer to 405 µM for the *i* isomer. Again the sensitivity shown by the Microtox assay was higher. For the membrane integrity assay, IC_{50}s ranged from 188 – 656 µM, though in this case both the most toxic and the least toxic were cyclohexyl moieties (*n* and *i* respectively). Membrane integrity was affected at ~2x higher concentrations compared to metabolic inhibition.

When assessing the mixture toxicity an assumption of concentration addition as a mode of action (MOA) was made. Concentration addition assumes that each compound acts in the same manner and that toxicity is equal to the sum of its parts (European Commission Report on the Toxicity of Chemical Mixtures., 2011) and has been proposed as a probable MOA for Naphthenic acids (Frank et al., 2008). In order to assess whether concentration addition (CA) was occurring two simple equations were utilised (Equations 1 & 2).

$$ECx_{mix} = \left(\sum_{i=1}^{n} (p_i / ECx_i) \right)^{-1}$$

Equation 1

$$E_{mix} = 1 - \prod_{i=1}^{n} (1 - E_i)$$

Equation 2

Where $EC_{x(mix)}$ is the predicted, total concentration of the mixture that produces X% effect; Pi is the relative fraction of component i in the mixture and ECxi is the concentration of a substance i provoking a certain effect when applied alone. Equation 2 is applied to assess independent action (IA), where toxicity is less than the sum of its parts and an assumption of dissimilar action is made. The MOA was determined by using a model deviation ratio (MDR) which is the predicted concentration divided by the actual concentration. A MDR of 1 indicates that CA is occurring, though a factor of 2 is applied as this is within expected interlaboratory/interexperiment deviation. On the whole the results for the total six component mixture and the binary mixtures indicated that CA was the most likely MOA with all of the results lying within the applied deviation factor for CA. When applying the IA equation a number of MDRs lay outside of the deviation.

When assessing these results with the commercial mixtures it was noted that there was a variability of toxicity in the commercial mixtures that made it difficult to compare them. Although one commercial mixture was comparable to the toxicity of the synthetic acids, two were more toxic. Such differences in toxicities may be explained by the heterogeneity of the commercial mixtures and the possible presence of non NA compounds such as polyaromatic hydrocarbons and alkylated phenols (e.g. West et al., 2011).

The MDR is not widely used by researchers investigating the toxicity of mixtures. It is generally utilised as a test of whether the mixture toxicity can be described effectively as acting with a concentration addition MOA. The 2x deviation factor was first described by Deneer (2000) in his review of mixture toxicity of pesticides in aquatic media. Although the author states that it may not be appropriate to

apply to all data sets it does give a safety factor as synergistic results can be applied erroneously (Drescher and Boedeker, 1995).

NA have been extensively assayed for toxicity, both as individual compounds and within mixtures (either commercial petroleum, OSPW acid extracts or as un-extracted OSPW) only recently have structural properties been definitively elucidated so that MOAs and toxic effects of these super-complex mixtures can be determined with a degree of certainty (Chapters 3 and 4, this work).

1.4 Remediation of OSPW acids

1.4.1 Bioremediation and Biodegradation

One of the origins of carboxylic acids, in petroleum and oil sands bitumen, is via aerobic and anaerobic biodegradation of petroleum hydrocarbons (Aitken et al., 2004; Head et al., 2003; Singer and Finnerty, 1984) by bacterial species such as *Candida sp. Streptomyces sp.* and *Athrobacter sp*., usually through α, ω and β oxidation pathways (Figures 1.6 – 1.9). In aerobic biodegradation, alkanes are metabolised to alcohols, which are subsequently transformed through aldehydes and ketones, to mono and dicarboxylic acids (Figure 1.6) (Alexander, 1999; Quagraine et al., 2005a; Singer and Finnerty, 1984). Also *n*-alkane oxidation to acids has been observed in fungi (Walker and Cooney, 1973).

In order for prokaryotic species to be able to degrade acids, oxidation must occur. This oxidation usually takes the β-oxidation route. However, this route relies on co-enzyme A, which exists in the mitochondria (Figure 1.10) and this pathway is only available to eukaryotic species. Prokaryotes must therefore

utilise a different means to ‘activate’ fatty acids for degradation and metabolisation.

An issue encountered by prokaryotes is the presence of an inner and an outer cell membrane. To overcome this *Escherichia coli (E.Coli)* utilises two specialist proteins, the *fadL* (a fatty acid transporter for the outer membrane) and *fadR* (a transcriptional regulator for *fad* genes). It has been postulated that prokaryotes utilise two distinct acyl co-enzyme A dehydrogenases, a long chain and a short chain, mutations of which result in differential patterns of acyl-COA actions. *β*-oxidation in prokaryotes is enabled by an electron transferring flavoprotien (ETF) (somewhat similar to the mitochondrial protein in eukaryotic species) which transfers electrons into the electron transport chain via the Flavin Adenine Dinucleotide (FAD) cofactor (Kunau et al., 1995) (Figure 1.11).

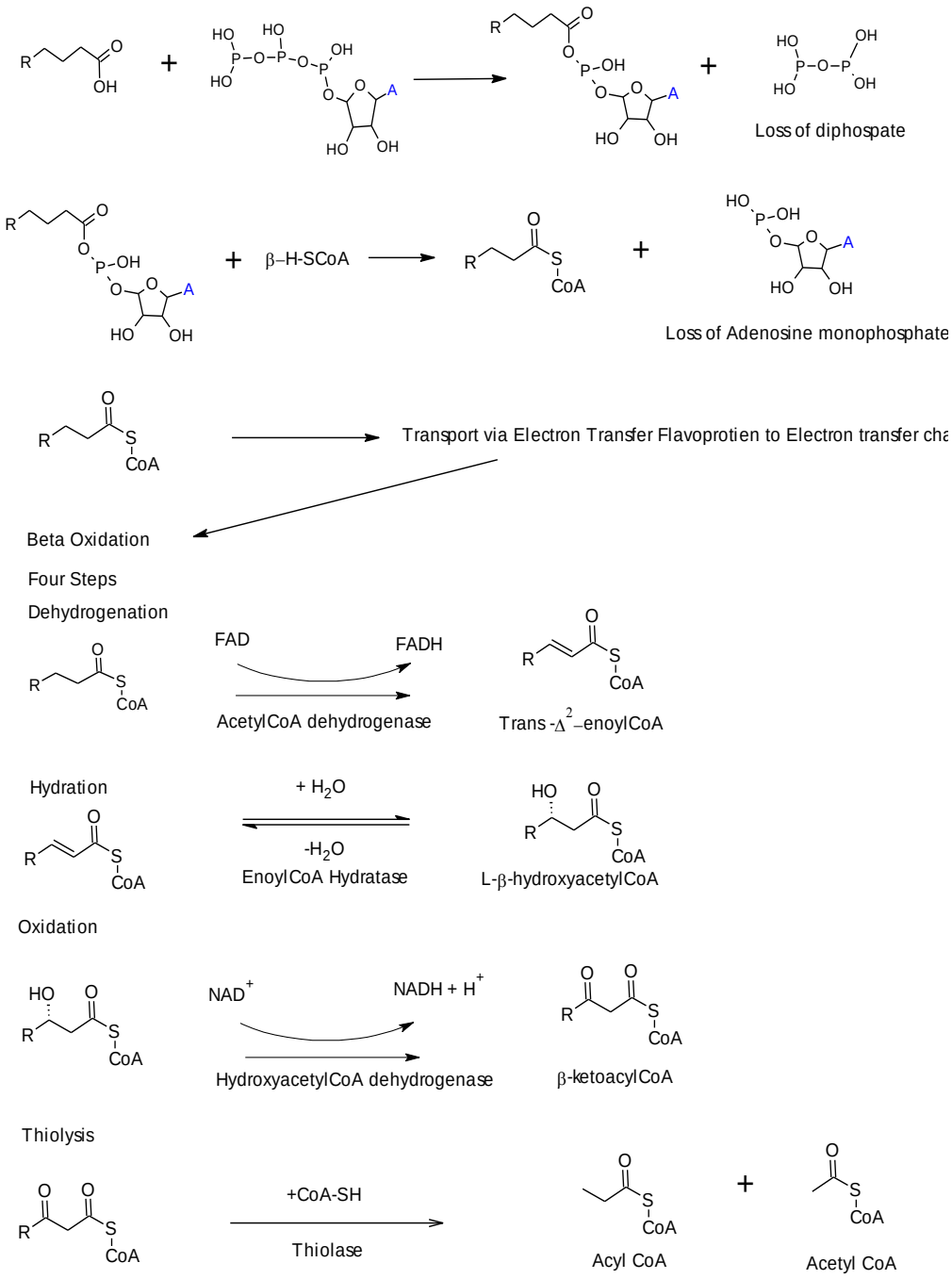

Figure 1.10. β-oxidation pathway of fatty acids, including activation by adenosine triphosphate (Kunau et al., 1995). Prokaryotic species activate fatty acids in the inner cellular membrane. FAD-FADH is shown in Figure 1.11.

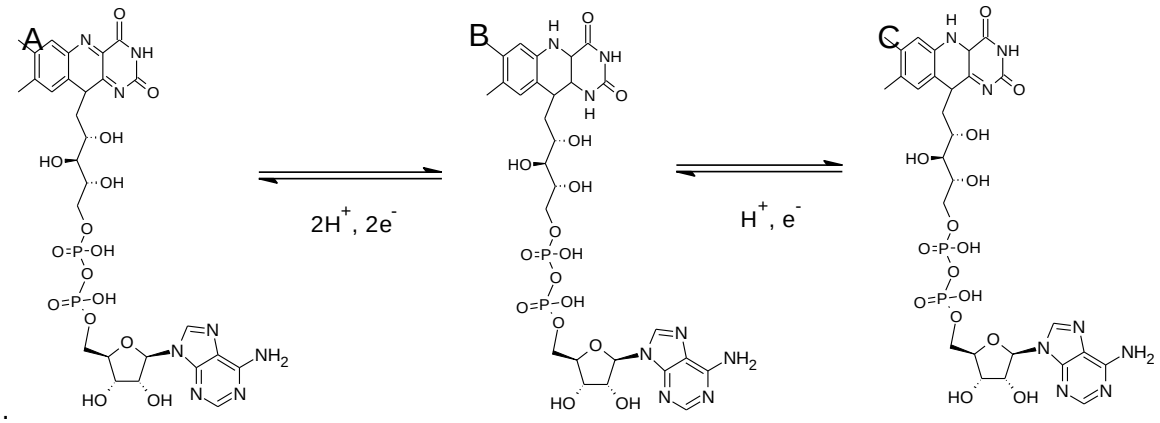

Figure 1.11. Flavin adenine dinucleotide (A) cofactor (FAD), and its reduction to $FADH_2$ (B) and FADH (C).

However, most petroleum derived acids include cyclic moieties which in certain cases can hinder β–oxidation . Certain bacteria (e.g. *Alcaligenes sp*.) utilise a combination of ***α*** and ***β*** oxidation to overcome this inhibition (Figure 1.12) (Whitby., 2010).

Successful completion of alicyclic ring cleavage via β–oxidation can also depends on the number of carbon atoms in an alkyl chain. It has been noted that alicyclic acids with an even carbon numbered alkyl chain are more recalcitrant to biodegradation and therefore may accumulate more readily in the environment than alicyclic acids that have odd numbered alkyl chains (Quagraine et al., 2005a; Whitby 2010). Whereas Johnson et al., (2012a and b) have shown that cyclohexylbutanoic acids with butyl side chains are biodegraded through the β–oxidation route to an ethanoic moiety. It was also noted that the butyl side chain was able to be oxidised to a second carboxyl group. Johnson and colleagues noted that whilst exposed to a single strain (*Pseudomonas putida KT2440)* that the *n*-butyl side chain moiety was able to be metabolised after 14 days of a 49 day exposure but that a more recalcitrant *t*-butyl moiety was unable

to be metabolised after the full 49 days. It was also noted that an increase in concentration of the *n*-butyl isomer retarded the degradation of this moiety, possibly explained by potentially increasing toxicity to the bacterial strain (Johnson et al., 2012a; Johnson et al., 2012b).

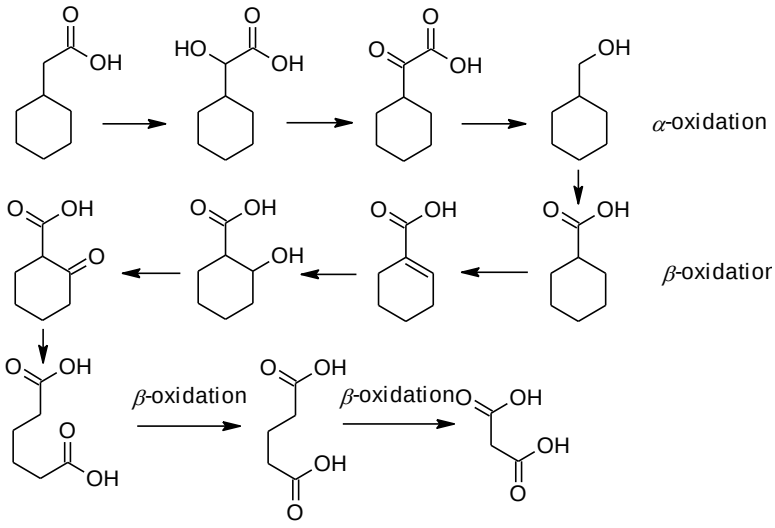

Figure 1.12 Proposed oxidation pathways (combined α + β) for the aerobic biotransformation of cyclohexylethanoic acid by the bacterium Alcaligenes sp**.** (Modified from Quagraine et al., 2005a; Whitby et al., 2010)

Another proposed metabolisation pathway for cyclohexyl type carboxylic acids is aromatisation. This pathway was first described by Blakley (1974) and involves a *para*-hydroxylation attack on the cyclohexyl ring which creates a *p*-hydroxybenzoic acid as an aromatic intermediate. The hydroxyl group is then reduced to a keto group, which can then be transformed to a second carboxylic acid to allow β-oxidation to take its course (Blakley, 1974; Blakley and Papish, 1982; Whitby et al., 2010).

However Quagraine et al., (2005a) reported that oxidation of cyclohexane to hexa-1, 6-dicarboxylic acid occurs through a Baeyer Villiger step which inserts a oxygen into the cyclohexyl ring creating an oxocycloheptane which is then cleaved by lactone hydrolase to form hexa-1, 6-dicarboxylic acid. Quagraine et al. state that most reports focus on the mixed culture approach as the only effective way to degrade cyclohexyl rings, leading to β-oxidation, whilst reiterating that effective oxidation generally occurs through this route only when a side chain has an odd number of carbon atoms (Quagraine et al., 2005a). Although the authors acknowledge the presence of the combined α and β oxidation routes utilised by a small number of bacterial strains that are able to degrade *even* numbered side chains (Quagraine et al 2005a; Whitby., 2010; Figure 1.8)

It is important to note that although numerous proposed oxidation pathways create final substrates that include dicarboxylic acids (Johnson et al., 2011; 2012), to date the only evidence for the presence of di-acids in OSPW is work by Frank et al (2009) and Headley and Barrow (e.g Headley et al., 2010; Section 1.2 this chapter). Frank et al. utilised Nuclear Magnetic Resonance (^{1}H NMR) spectroscopy to assess the content of a methylated acid extract of OSPW and noted that di-carboxylic species were likely present. Previous to this research NA had been considered to be mono-carboxylic, by methylating fractions collected by Kugelrohr Fractionation (discussed Section 1.3.1) and analysing through ^{1}H NMR Frank and colleagues noted that the ratio of methyl ester hydrogen atoms to other aliphatic hydrogen atoms steadily increased within each fraction relative to higher MW. Frank states that the increased ratio is indicative of higher carboxylic

acid content within NAs of higher MW. Further evidence was also found with an analysis of the chemical shifts of hydrogen atoms within alkyl and cyclo-alkane groups and chemical shifts of hydrogen atoms attached to a carbon atom adjacent to carbonyl carbon atoms. The increase in hydrogen atoms that fitted these criteria in relation to MW added weight to the evidence for di-carboxylic acids. In order to rule out an artificially enhanced result from the presence of an alcohol analysis by FTIR was carried out, there was a negligible amount of alcohol present because of the lack of O-H stretching in the wavelength band 3200-3400 cm^{-1} due to methylation. There was, however, an increasing amount of signal intensity in the C-H stretching wavelength band (2850-2960 cm^{-1}).This was noted as higher MW fractions were analysed due to a larger amount of methyl esters, potentially due to extra carboxylic acids, on the higher MW more cyclic compounds. Frank et al (2009) noted that the presence of di-carboxylic acids would likely reduce the overall acute toxicity as an extra carboxylic moiety would reduce the hydrophobicity of the compound thus lessening the toxicity.

In order to reduce the toxicity of petroleum-derived acids (either petroleum acids, commercially derived NA or acids extracted from OSPW), single strains and communities of microbes have been exposed to individual acids or to complex mixtures. Generally it has been noted that following biodegradation, acids are less toxic and it has been postulated that the reasons lie with the removal of the more bio-available lower molecular weight compounds (Clemente et al., 2004). However it must be noted that the toxicity assays utilised are generally ‘acute’ assays such as the Microtox™ assay, so the reduction in toxicity would more likely be due to a reduction in solubility (Jones et al., 2011). If compounds that

remain after biodegradation have the potential to have a greater sub-lethal toxic effects (e.g. estrogenic effects (Scarlett et al., 2012)). It is possible that the removal of the lower molecular weight compounds may well increase recalcitrance and enhance toxicity to certain chronic end-points (Quagraine et al., 2005a).

1.4.2 Photo-remediation

Photo-remediation of petroleum derived acids has also been subject to research as a way to lessen the toxicity of the NA and therefore the OSPW perhaps to allow some form of release or at least, reduction of the large quantities of tailings pond water currently being stored in Canada. Photo-remediation relies on the process of photolysis which is where chromophores (light absorbing molecules) are chemically changed as a consequence of exposure to UV/VIS radiation. Light absorbing molecules can be either the target organic compound or a catalyst which can then transfer energy to the target compound (direct and indirect photolysis respectively) (Headley & McMartin., 2004). In a review by Headley and McMartin (2004) it was suggested that due to photolysis generally being limited to the top few millimetres of natural surface waters (depending on several factors including colour and turbidity), it is unlikely that OSPW acid extracts will readily degrade naturally by this route (Headley & McMartin., 2004). It is perhaps unsurprising, therefore, that literature detailing *direct* photolysis of NA is limited with only (seemingly) McMartin et al., (2004) dealing with the issue.

McMartin et al (2004) carried out a study on mixtures and individual compounds to determine the effectiveness of UV/VIS radiation sources for reducing the concentrations and receptor binding efficacy. The authors stated that neither the

concentrations nor the receptor binding activity was reduced over a period of 7-10 days. However it was noted that compositional changes had occurred. These changes could not be assessed by the analytical methods available at the time so there was no way of knowing if the changes that occurred had made the tested materials (two commercial mixtures, a OSPW acid extract and six surrogate acids) more susceptible to biodegradation. The authors also discussed (briefly) the importance of humic acids as photosensitisers, photoinhibiters and as a source of $OH^{\bullet}$ radicals. McMartin et al., (2004) went on to state that photolysis can be an effective measure against 'selected' naphthenic acids. Although it seems that the most effective wavelength is 254nm with the other tested wavelengths performing at less than optimal efficiency (McMartin et al., 2004).

Most literature on photolysis involves the use of TiO_2 as a catalyst. One of the most recent studies (Mishra et al., 2010a) based its hypothesis on the 'effectiveness' statement of McMartin et al., (2004). Mishra et al., were able to degrade a Fluka commercial NA and a OSPW acid extract (in the presence of TiO_2) under laboratory conditions using UV 254 nm lighting.

The authors stated that OSPW extracts degraded at a higher rate than the commercial acids, ascribing this to the presence of 'NA-Like' acids (i.e. dicarboxylic and aromatic acids) which are said to be more susceptible to photolysis. Determination of compounds before and after photolysis was performed by low resolution electron spray ionisation mass spectrometry, which the authors admit is prone to false positive detections and misclassifications, and by comparison of z number distributions.

Mishra et al., (2010a) tested the toxicity of the 'before' and 'after' photoexposure products by the Microtox™ assay and stated that there was a lessening of toxicity from 15% to >90% in both the Fluka and the acid extracts. However the reference point is not stated (i.e.15% of what?) and concentrations in mg L^{-1} were not stated or discussed. It is also interesting that the OSPW extract in de-ionised water was tested at pH 9.69 before treatment and pH 7.66 after treatment, which raises doubts as to the veracity of this test as *Vibrio fischeri* (the bacterium utilised in the Microtox™ assay) has an optimum performance between pH 6 and 8 and it is likely that the stated high toxicity in the 'before' treatment is due to a pH effect rather than to the presence of Naphthenic acids. The test for toxicity on OSPW acid extract in river water was also performed outside of the Microtox™ test specified parameters (pH 8.86 and pH 8.31 respectively) and showed only a moderate toxicity to begin with (20%->90% respectively). However this again is impossible to assess as no concentrations are stated.

1.4.3. Ozonation of OSPW Acid Extracts

Ozonation is the process of adding ozone to the acid extracts of OSPW. Because ozone is an unstable species it can readily react with organic compounds, creating hydroxy acids and keto acids, (Mahato and Banerjee, 1985; Mahato and Mukherjee, 1984) which are then able to be bio-degraded through the processes listed in section 1.3.1.

Research on the ozonation of the OSPW acid extracts has generally been hailed as a success (Anderson et al., 2011; He et al., 2011; Martin et al., 2010). However, a paper by Martin et al., (2010) stated that although ozonation reduced the acid content to a few residual NA, the toxicity (to Microtox™) was not reduced

and it required significant biodegradation to reduce the toxicity of the NA. This raises the question: does ozonation really reduce the NA content, do researchers know what compounds they are starting with or conversely what compounds they end up with; or does ozonation create a series of more toxic compounds within the acid extract complex mixtures? Moreover, Microtox assays were made at pH 10 for the Merichem commercial mixture so pH effects were likely outweighing the toxic effects of the acids.

In order to answer the former questions, He et al.,(2011) tested the products of ozonation using an assay of estrogenicity. They found that ozonation did not attenuate the estrogenic or androgenic effects of OSPW, though they did state that OSPW (interestingly not the acid extracts) could produce estrogenic or anti-androgenic effects through receptor mediated pathways. Although the authors reported no significant differences between ozonated and non-ozonated samples, they stated that ozonation could mitigate estrogenic effects from OSPW.

Scott et al., (2008) seemed to be the pioneers of this technique when applied to OSPW acid extracts. A decrease of greater than 95% NA concentration was noted after a 130 minute ozonation and the concentrations of higher molecular weight NA were severely lessened. The researchers also noted a decrease in toxicity after 50 minutes ozonation of OSPW.

Research by Anderson et al., (2011) also noted an attenuation of toxic effects from ozonation. Two separate batches of OSPW were treated with 30 and 80 mg L^{-1} of ozone (O_3) respectively to examine the effects on the midge *Chironomus*

dilutus. Compared to untreated OSPW, emergence and pupation was significantly greater, with 71% less pupation from the OSPW compared to the OSPW treated with 80 mg L^{-1} ozone. The authors state that the organic fractions within OSPW cause toxicity, and that ozonation attenuates the toxic effect.

1.5 Predictive Toxicology and Quantitative Structure Activity Relationships

In order to assess the toxicity of a compound or a mixture thereof it is often useful to apply a predictive computer model. Often known as quantitative structure activity relationships (QSARs) these models assume that each chemical (either singly or within a mixture) act in a similar fashion due to similarities in structure. Many QSARs have been developed (e.g. El-Alawi et al., 2002; Russom et al., 1997; Seward and Schultz, 1999) and it is beyond the scope of this chapter to conduct a full review. However, a few studies will serve to illustrate the approach. A number of these QSARs have been applied to hydrophobic compounds, many of which induce Narcosis which has a MOA of disturbing the cellular membrane (Donkin et al., 1989 and references therein; Könemann, 1980). A few have focused on the effects of petroleum derived pollutants on a number of endpoints. As organic compounds from petroleum have been relatively successfully assessed via QSARs (e.g Donkin et al., 1989) it is perhaps unsurprising that Naphthenic or petroleum acids are beginning to be assessed in the same manner.

A number of QSAR studies have postulated that the Log K_{ow} and the pK_a values of acidic compounds are important parameters to be assessed and can be useful in predicting the mechanism of action of a given compound. Schultz (1987) assessed the toxicity of 21 organic compounds using two separate QSARs, one

assessing the potential for polar Narcosis and the other assessing the potential for uncoupling of oxidative phosphorylation (a metabolic pathway that releases energy by the oxidation of nutrients to produce adenosine triphosphate). Schultz discovered that pK_a values were a good discriminator of the MOA and a decent basis for selecting the correct model for each individual phenol. It was noted that phenols with pK_a values of <6.5 were correctly modelled using the uncoupling of oxidative phosphorylation QSAR. This potentially raises a question mark over the assumption of a narcotic mode of action for petroleum acids or naphthenic acids which have pK_as of ~4.5 (Scarlett et al., 2012).

Zhao et al. (1996) assessed the toxicity of 20 organic acids or bases using a QSAR based upon Log K_{ow} and pK_a in order to assess ionised and non-ionised forms. In order to assess the QSAR these compounds were also assessed on the Microtox™ assay, a 24 hr *Daphnia magna* assay and a 48hr mortality test to *Cyprinus carpiol* (carp) at different pH values.

It was noted that the Microtox assay was more sensitive to these acids than both the carp and *Daphnia* assays. This was postulated to be due to the difference in species; the bacterium in the Microtox™ assay being a unicellular organism was said to be susceptible to both the ionised and the non-ionised forms of the acids and bases, whereas the other two test species had a greater propensity to obstruct the ionised forms, thus lessening the toxic effects. It was noted that the QSARs were able to predict the toxicity to each organism to a relatively good degree and each test species was able to have a particular QSAR applied to it.

Seward and Schultz (1999) utilised a QSAR to assess toxicity of mono carboxylic acid, di-carboxylic acid, unsaturated carboxylic acid and carboxylic acid sodium salt moieties for possibly the first time. A parallel 40 hr population density assay using the freshwater ciliate *Tetrahymena pyriformi* was made. It was found that QSARs could be ultilised with confidence on all but the unsaturated carboxylic acids, using Log K_{ow} as a single descriptor.

Frank et al., (2010) and Jones et al., (2011) used the freely available US EPA predictive model ECOSAR model as a predictor of toxicity towards 8 surrogate NA ((Frank et al., 2010)) and 35 NA respectively (the latter identified within the acid extract of the OSPW or a commercial NA mixture (Jones et al., 2011 and Chapter 3)).

Frank and colleagues suggested that the ECOSAR model had potential to serve as a prioritisation tool for identification of NA with higher potential toxicities by comparing the ECOSAR predicted results to results gleaned from a 48 hr *D. magna* assay and a 15 minute Microtox™ assay (Frank et al., 2010). The Microtox™ assay comparison gave results that were within one order of magnitude of the ECOSAR QSAR results, with the exception of succinic acid where the toxicity was underestimated by the model.

Jones et al., (2011) utilised ECOSAR to identify potential candidates for toxicity testing on the Microtox™ assay. Although >45 acids were chosen, only 35 were found to be soluble enough for testing (Chapter 3). Jones and colleagues found that the ECOSAR test performed adequately but when direct comparisons were

made, differential trends (exponential, linear etc.) were evident depending on acid structural class (Chapter 3 and orally presented to SETAC Milan 2011).

Scarlett et al (2012) utilised ADMET Predictor™ software (Simulations Plus, California, USA) to assess environmental and human toxicity endpoints to a range of previously identified and tentatively identified NA (54 in total) plus six alkylphenols. The authors also assayed a number of tricyclic acids via the CALUX® nuclear receptor reporter gene bioassay for estrogenic, androgenic, and aryl-hydrocarbon receptor transactivation to compare with the modelling of ER activity.

Scarlett and colleagues found that the most toxic compounds (predicted by ADMET) were mono-aromatic polycyclic acids. Some of these were also predicted to be the most carcinogenic to rats and mice, to possess estrogenic and androgenic activity and to have a potential to affect human reproductive processes. Mono-aromatic polycyclic acids have recently been postulated to exist within the acid extracts of the OSPW (Rowland et al., 2011d) so the prediction of toxic effects such as these is interesting. Other compounds modelled to be toxic included the pentacyclic diamantane acids which were predicted to exhibit androgenic activity and be able to act as substrates for the cytochrome P450 enzyme CYP3A4. The model was validated by assaying tricyclic acids with the CALUX ER alpha bioassay. As predicted by ADMET, the tricyclic acids exhibited no effect to the bioassay (Scarlett et al., 2012).

Predictive models and QSARs cannot adequately take the place of toxicity testing but they can serve as a signpost directing the researcher towards the

most toxic compounds and can remove the need for unnecessary, often costly and time consuming, synthesis and toxicological testing .

1.6 Aims and Objectives of Research

The aims of the present research were:

- On the basis of new identifications of acids as a result of progress with multi-dimensional comprehensive GCxGC-MS made herein and in related studies (e.g. Rowland et al., 2011a-c), to synthesise and characterise a range of previously unavailable individual carboxylic acids (Chapter 2).
- To use the above acids to confirm or refute, by GCxGC-MS co-chromatography and mass spectral comparisons, the presence of the acids within OSPW acid extract complex mixtures (Chapter 2 and Rowland et al., 2011a-d).
- To assess whether the synthesised acids are toxic, either individually or within mixtures, in the Microtox screening bioassay (Chapters 3, 4 and Jones et al., 2011).
- To further fractionate the complex mixtures of acids in an OSPW acid extract by argentation chromatography and to analyse these fractions via elemental analysis, FTIR, ultraviolet spectrophotometry,GC MS and GCxGC-MS using multiple combinations of GC phases (Chapter 5; Jones et al ., 2013; Jones et al., 2012 and Rowland et al 2011d).

Chapter 2

Synthesis of 'Model' Naphthenic Acids through Catalytic Hydrogenation

2.1. Catalytic Hydrogenation

Recent advances in analytical techniques have allowed researchers to identify individual compounds that exist within an OSPW acid extract complex mixture (Chapter 1; Rowland et al., 2011 a-d). The two dimensional gas chromatography time of flight mass spectrometry (GCxGC MS) method that the latter researchers have used ideally requires the use of samples of authentic acids to co-chromatograph with the unknowns and also to allow a comparison of mass spectral data of unknowns with those of authentic compounds. The individual authentic compounds, mixtures and the OSPW acid extract mixtures can then be used for toxicological studies. However, for a number of the identified compounds, no commercially available authentic compound is available. It is therefore necessary to synthesise these compounds to high purity. This approach to determination and characterisation of petroleum acids has precedent in previous research into naphthenic acids.

2.1.1 Literature Review

The strategy of the research detailed herein was heavily influenced by previous research dating back to 1874. A number of petroleum acids that have their synthesis detailed here have been either postulated or determined in crude oils at some point over the last ~130 years and as paraffinic and asphaltic (bituminous) type oils have been shown to have similar acidic compounds (Seifert, 1975) it

could be hypothesised that these structures would be present within the Oil Sands Process Affected Water (OSPW) acid extracts. Although a number of acids were later synthesised after the postulations of Rowland and colleagues from GCxGC MS of unknowns (Rowland et al., 2011a-e: Rowland et al., 2012; and Chapter 5) the basic premise of the existence of petroleum acids in OSPW lays heavily on the earlier research. A short review of this previous work is therefore pertinent.

2.1.2 Determination and Characterisation of Petroleum Acids

There has been much debate over the origins of petroleum acids. Although certain researchers were convinced that the acids could be produced during the refinery process a common view was that petroleum acids were precursors to petroleum hydrocarbons. The refinery process hypothesis was abandoned after research by von Braun (1931), Pilat and Rayman (1932) and von Braun and Wittmeyer (1934) in which it was noted that acid extracts before and after refinery processes were essentially the same, indicating that the acids must be in place before the petroleum is refined (Lochte and Littman, 1955).

The ‘precursor to hydrocarbon’ hypothesis gained prominence in the early 1900s with work by Neuberg (1906), Engler (1913), Tanaka and Kuwata (1929) and Petrov and Ivanov (1932) who suggested that petroleum acids and hydrocarbons all had a similar origin in long chain fatty acids, with Tanaka and Kuwata (1929) suggesting that the fatty acids were themselves sourced from shark or whale oils. Neuberg concluded that the acids were formed underground not only from fats and oils but also from proteins that had been affected by bacterial action and

Engler suggesting that cracking and cyclisation could explain the source of the known naphthenic acids.

The theory that hydrocarbons were the precursors of the petroleum acids was discounted due to the unlikelihood of enough oxygen existing in situ to create the acids whilst diagenesis and other extensive changes were occurring or the likelihood of other oxidative agents existing in such conditions (Lochte and Littman, 1955). However, work by Head and Larter (2004) and da Cruz et al., (2011) suggests that anaerobic processes are able to oxidise hydrocarbons in deep, oxygen depleted, reservoirs to produce petroleum acids either alone or in a co-operative process with aerobic bacteria (Head and Larter, 2004; da Cruz et al., 2011).

In fact evidence suggests that the different types of acid prevalent in crude oils can have a number of different origins (e.g. Siefert, 1975). For instance, it is likely that acyclic isoprenoid acids are present from the degradation of the phytol side chain of chlorophyll (Figure 2.1) and from large polycyclic tetra-carboxylic C_{80}-C_{82} acids present in the lipid membranes in Archea (Figure 2.7) (Sutton et al., 2010).

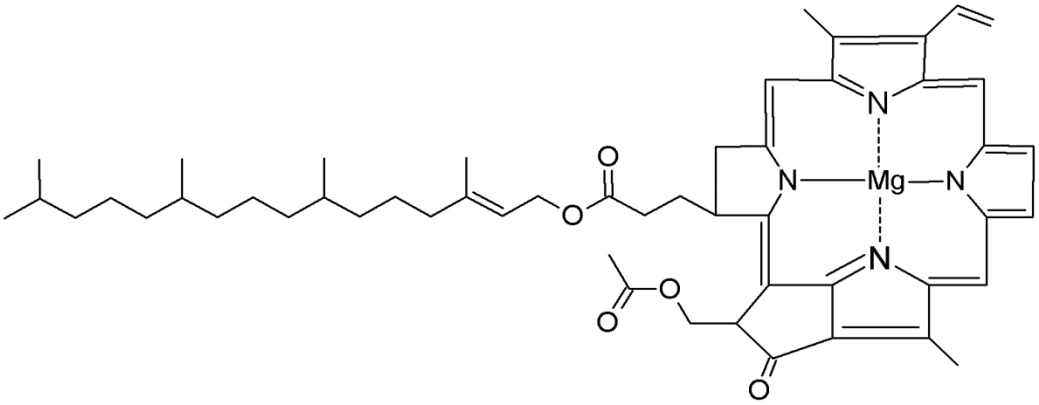

Figure 2.1. Structure of chlorophyll showing the isoprenoid phytol side chain

It has been postulated that certain steroidal acids can be traced back to bile acids (Seifert, 1975) with cholic, desoxycholic and phocaecholic acids all presenting a steroidal acid structure (Figure 2.2 A, B and C) however Seifert also points out that algae, plants and yeast all possess chemical structures that are potentially able to be oxidised to a 5-α-steroid acid (Figure 2.2 D, E and F)

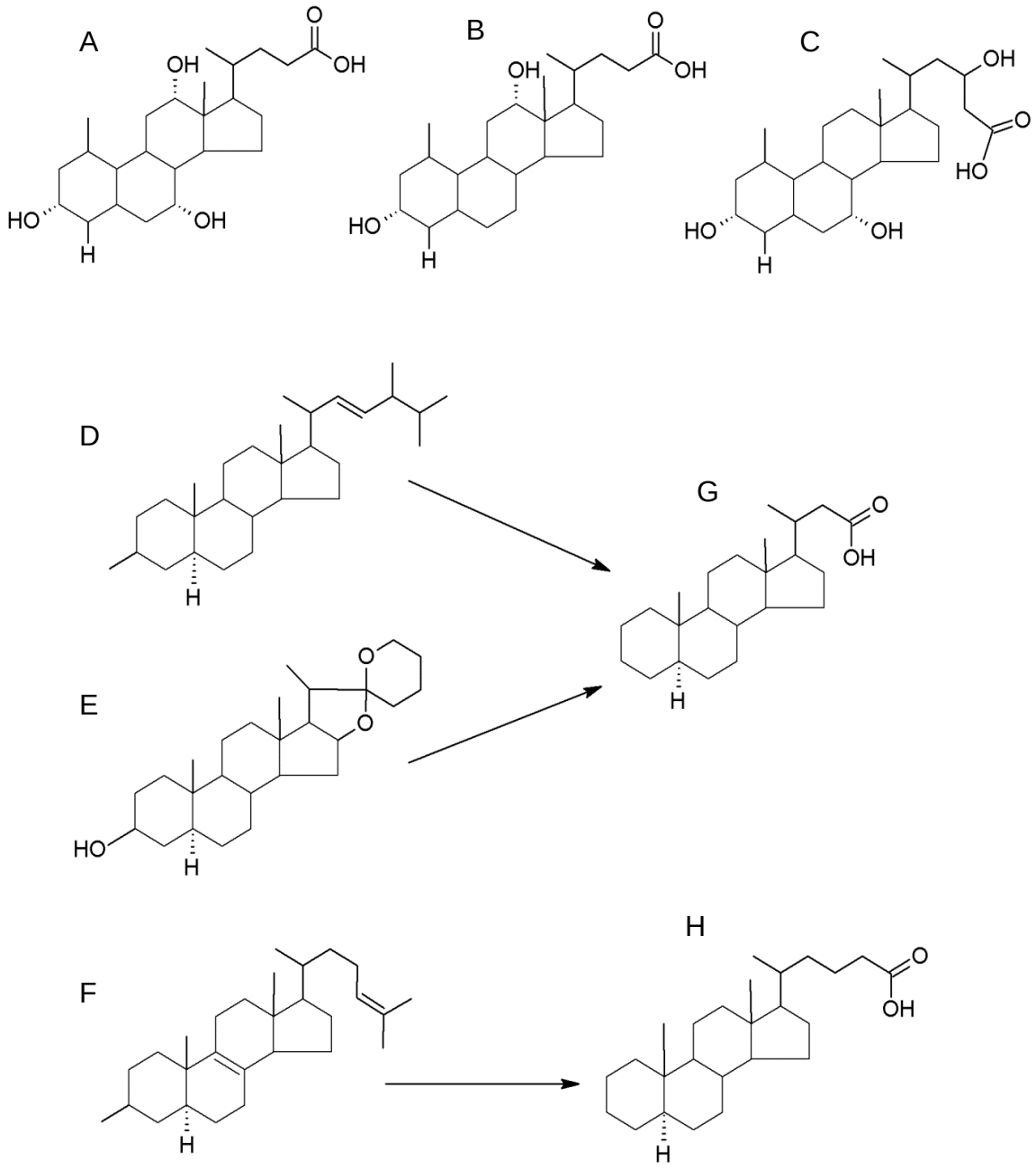

Figure 2.2. Structures of (A) cholic, (B) desoxycholic and (C) phocaecholic bile acids, plus chemical structures present in (D) algae, (E) plants and (F) yeast thought to be able to oxidise to (G & H) 5-α-steroid acids

Steroidal type acids are also likely to be carboxylated through beta-oxidation

(Chapter 1, Section 1.4, Figure 1.11) of cholesterol like compounds, which is

itself bio-synthesised from squalene, a triterpene present in all biota (Personal Communication, Steve Rowland) (Figure 2.3).

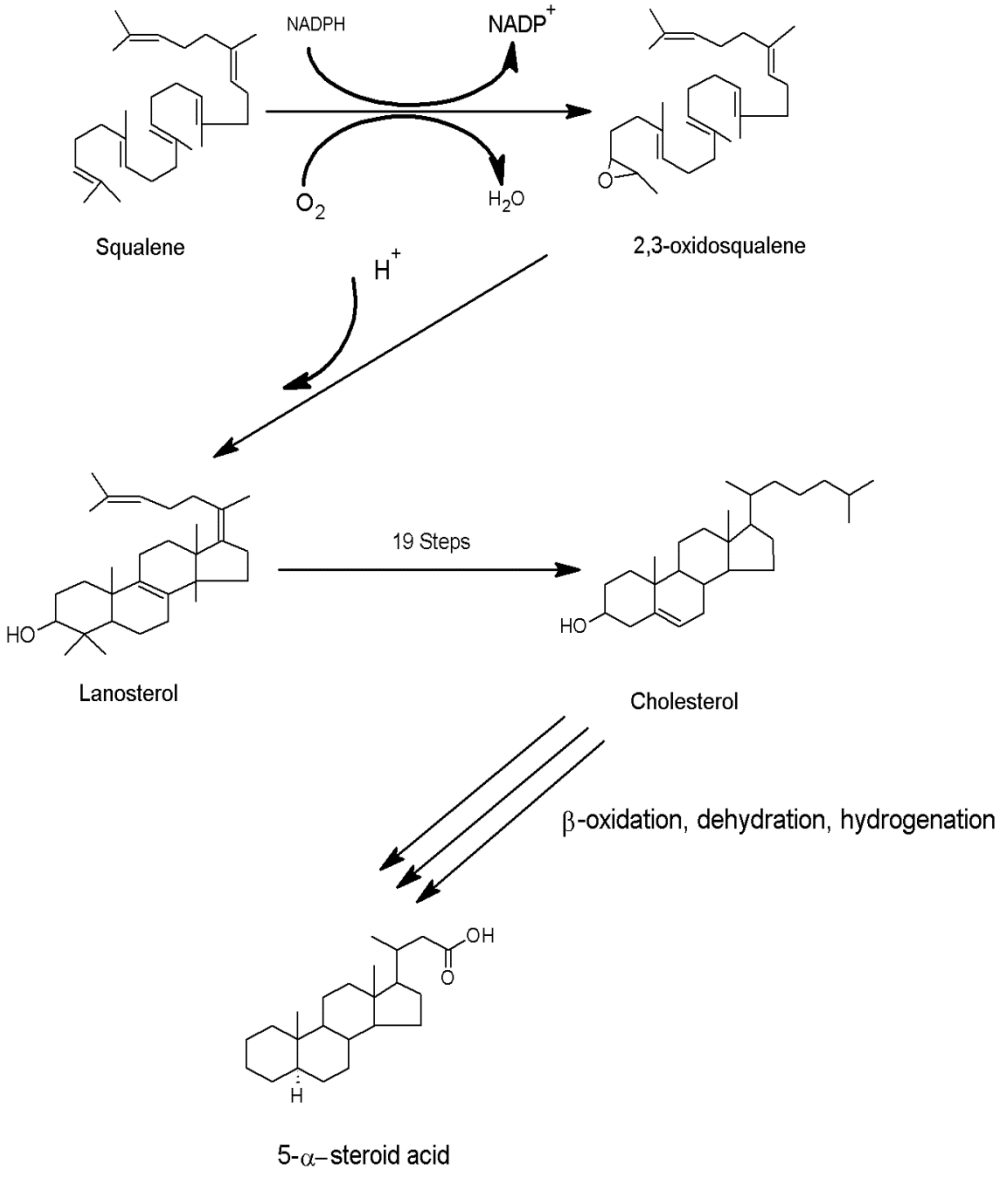

Figure 2.3. Biosynthesis of a 5-α-steroid acid from squalene

Seifert (1975) reviews work discussing the origin of petroleum acids up to the early 1970's. Although the author has little to say about *n*-acids, mentioning that they are thought to derive from biological remnants, he discusses in detail the

origins of isoprenoid, mono and polycyclic and mono and poly aromatic acids. An interesting feature of the review (and of Seifert's work in general) is the similarity of the structures of the petroleum based acids to the structures of known petroleum hydrocarbons. This implies that there is a relationship between the petroleum acids and the petroleum hydrocarbons.

The nature of petroleum acids was first researched in the 1870s and culminated in what is often quoted as the first treatise on the subject (Hell and Medinger, 1874; reviewed by Lochte and Littman, 1955). Hell and Medinger took samples of Romanian oil petroleum acids that yielded the molecular formula $C_{10}H_{19}COOH$. It was suspected that this formula corresponded to acids which belonged to a mainly homologous group because the compounds were unable to be converted to crystalline salts. It was concluded that the acids were generally cyclic as none of the molecules showed the properties associated with unsaturated compounds. It is interesting that the molecular formula postulated by Hell and Medinger is that of some of the monocylic acids now known in petroleum (Lochte and Littman, 1955). The work Hell and Medinger and that of Eichler (1874) who worked on acids from the Baku oil fields eventually led Markownikoff to recognise the compounds as carboxylic acids and assign the name 'naphthenic acid' to these compounds for the first time (Eichler, 1874; Markownikoff and Oglobin, 1883).

It was often, at this time and subsequently, assumed that 'naphthenic acids' contained only acyclic, cyclopentyl and cyclohexyl moieties originating from the natural hydrogenation of compounds within oil fields (Lochte and Littmann, 1955). However certain authors postulated that since coal tar contained plenty of aromatic compounds, it was logical that the acids should also contain these

aromatic moieties. This view was particularly popular with Aschan (1892). However work by Zelinsky (1924), with a newly developed catalytic hydrogenation technique, discovered that little or no hydrogen was evolved when indirect reduction of naphthenic acids was carried out. This suggested that aromatic acids were not present in appreciable quantities (Zelinsky, 1924; Lochte and Littman, 1955). It was as a direct result of Zelinsky's 1924 work that cyclopentane rather than the cyclohexane moiety was considered predominant, with assumptions being made that the naphthenic acids consisted almost solely of compounds containing this structure. This view was held up to and including 1955 when Lochte and Littman published their comprehensive review and indeed was prevalent in the 1990s (e.g. Brient et al., 1995).

Work on naphthenic acids remained popular throughout the 1880s where it was noted that different oils from diverse global areas (e.g. Middle East, America and Russia) contained different concentrations of acids. It also became apparent that different oils from similar geographical regions also contained different acid concentrations (e.g. Texas versus Baku) (Lochte and Littman, 1955). The reasons for these differences remained elusive but an assumption, postulated by von Braun (1938), was made about a correlation between oils high in naphthenic acids and oils high in naphthenes (as one was assumed to derive from the other). Von Braun's assumption was based upon work by Shipp (1936) which illustrated that paraffinic based oils were (in general) low in naphthenic aids, whilst asphalt based oils are generally high in naphthenic acid content (Shipp, 1936) However it was also shown that not all asphaltic based oils have high naphthenic acid contents and that oils derived from adjacent oil fields have widely differing

naphthenic acid contents (Lochte and Littman, 1955). The early work (1874-1955) carried out on petroleum acids are extensively reviewed by Lochte and Littman (1955) in their seminal work ‘The Petroleum Acids and Bases’.

The prevailing view that ‘naphthenic acids’ contain predominantly cyclopentyl and cyclohexyl carboxylic acids had been challenged as early as 1957 when Knoterus discovered aromatic carboxylic acids existing within the petroleum (Knoterus, 1957; reviewed by Seifert, 1975. Working with a hypothesis suggested from the earlier work of Muller and von Pilat (1936) who considered the presence of aromatic moieties within the acid mixture, Knoterus separated the naphthenic acid fractions from Venezuelan Crude Oil and after esterification with methanol reduced them to the corresponding hydrocarbons.

Using chromatography, infrared and UV analysis, thermal diffusion and dehydrogenation techniques Knoterus was able to deduce that both mono and di-aromatic moieties (at least) existed within the naphthenic acids. A percentage weight of between 58 and 68% saturates and between 21 and 26% mono and di aromatics was deduced, the remainder being made up with dibenzothiopenes and resins. Knoterus concludes that the term naphthenic acids is inappropriate as it refers to the cyclopentyl and cyclohexyl acids previously isolated and ignores the presence of aromatic acids. Knoterus states that it would be better to refer to the carboxylic acid fraction as petroleum acids (Knoterus, 1957). However it appears to have been convenient for authors to sideline Knoterus’ research and class aromatic acids as non-naphthenic acids rather than a general nomenclature of petroleum acids (e.g. Headley et al., 2009; Toor et al., 2012).

Throughout the 1960s and 1970s research on the naphthenic and petroleum acids continued through the work of both Seifert and Cason (and co-workers). These researchers worked extensively on the petroleum acid problem and both authors extended the knowledge of the structural classes within petroleum and naphthenic acids.

Cason and colleagues, working in the mid to late 1960s, were able to elucidate structural information of individual acids within Californian petroleum (Cason and Liauw, 1964; Cason and Kodar, 1966a & b; Cason and Kodar, 1967). Prior to 1964 only a small amount of structural information was available to researchers with acyclic and monocyclic acid structures being determined by workers such as Lochte and Littman (reviewed in Lochte and Littmann, 1955). However only acids containing less than 10 carbons had elucidated structures, the issue of the C_{10} to C_{20} structures (the most abundant range) remained (Chapter 1, Section 1.1 Figures 1.1 A and B).

Cason and co-workers had previously been able to isolate a number of $>C_{10}$ acyclic isoprenoids (e.g. Cason and Graham, 1965). Through use of fractional distillation, gas chromatography and amide crystallisation, Cason was able to characterise the structure of a C_{11} cyclic isoprenoid, monocyclic ethanoic acid (*trans*-2,2,6-trimethylcyclohexylethanoic acid) (Figure 2.4).

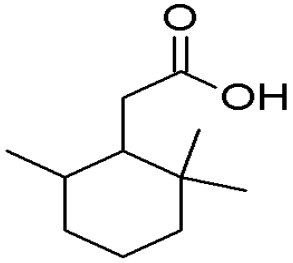

Figure 2.4. Structure of 2,2,6-trimethylcyclohexylethanoic acid, isolated by Cason and co-workers in the 1960s

Continuation of this work led to the elucidation of numerous compounds including C_{11} isoprenoid acids and cycloalkylethanoic acids ,including methyl cyclopentane and methyl cyclohexane moieties (Chapter 1, Figure 1.1) (Cason and Liauw, 1964; Cason and Kodar, 1966a & b; Cason and Kodar, 1967).

Alicyclic isoprenoid acids were also determined in a Green River Shale oil by Haug et al., (1970). Who also determined structures of normal, straight chain acids, α-methyl branched straight chain acids, naphthoic and non-aromatic bicyclic acids, branched monocyclic and branched mono-aromatic acids (Chapter 1, Figure 1.1) (Haug et al., 1970).

However it is work by Seifert and co-workers that has (arguably) led to the greatest advances in characterisation and determination of acid structures in crude oils. Seifert first isolated ‘interfacially active’ carboxylic acids and phenols from a Californian crude oil (Siefert and Howells, 1969). A number of phenolic structures are postulated in this paper but it is the later work that is of most interest to this review (Chapter 1, Figure 1.1).

Using a newly developed comprehensive approach Seifert et al., (1969) were able to identify a number of structural classes in a sample of the acid extracts of Californian crude oil. By converting the crude oil derived carboxylic acids to their corresponding hydrocarbons the researchers were able to identify classes of acids that had not previously been reported (Siefert et al, 1969). These structural classes included polycyclic and monoaromatic polycyclic acids. Further work on this enabled Seifert and Teeter (1970) to determine fluorene and tetrahydrophenanthrene type acids, alongside trimethylnaphthalenes, tetralins and indanes (Seifert and Teeter, 1970a & b). This work and the work of others not included here was reviewed by Seifert (1975) (Seifert, 1975 and references therein).

Working on the Alberta Oil Sands, Cyr and Strausz (1983) were able to determine the structures of certain tricyclic terpenoid acids. Using the methyl esters of a sample of Athabasca bitumen treated with diazomethane, it was revealed that at least four tricyclic terpenoid acids were present (C_{20}, C_{21} compounds and two C_{24} isomers) (Figure 2.5).

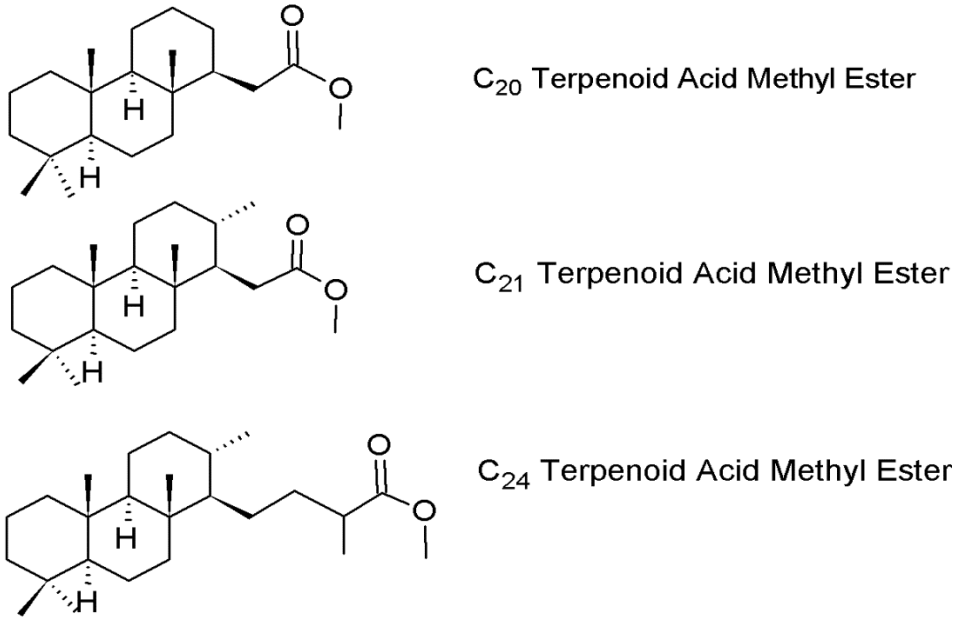

Figure 2.5. Determined C_{20}, C_{21} and C_{24} terpenoid acids found in Athabasca Oil sands.

The concentrations were later determined to include terpenoid acid isomers between C_{20} and C_{26}. It was noticed by Cyr and Strauss (1983) that the C_{21} and C_{24} isomers were make up at least 75% of the mixture. It was also noted that the carboxy group was attached to an alkyl side chain rather than the 'C' ring (Cyr and Straus, 1983).

The work by Cyr and Strauss was followed up with a study on the attempted synthesis of the identified C_{20} terpenoid acid (Figure 2.5A). Kaufman et al., (1988) utilised a number of synthesis routes before being able to synthesise the C_{20} terpenoid to a purity that when analysed with GC-MS confirmed the presence of this structure within the oil sands acid extracts (Kaufman et al., 1988).

It is noteworthy that in the 1960s and 1970s research into petroleum acids was limited to a few researchers (e.g Seifert and Cason). In the 1980s to the early 1990s interest in naphthenic or petroleum acids was rekindled. As the global price in oil went up so development of oil sands and other non-conventional

sources became economically viable, hence research into the so called naphthenic acids was stimulated. It is well known that naphthenic acids are able to complex with metal ions (e.g. calcium) creating naphthenates with far reaching consequences in pipeline oil flow as these naphthenates can be deposited as solids and cause flow-assurance issues. There is plenty of literature available which details the issues of the phenomena now referred to as 'calcium naphthenate deposition' (e.g Sutton et al., 2010; Malpolelo et al., 2011 and references therein). Although a detailed discussion of this problem is outside of the scope of this review, it has become clear in recent years that certain high molecular weight naphthenic acids (the so called 'ARN' C_{80} tetraprotic acids (Figure 2.6)) are instrumental in the deposition process (e.g. Lutnaes et al., 2006). ARN acids are thought to originate from the membrane lipids of the Archaea organisms and are generally thought to have between 80 and 82 carbon atoms (Figure 2.6).

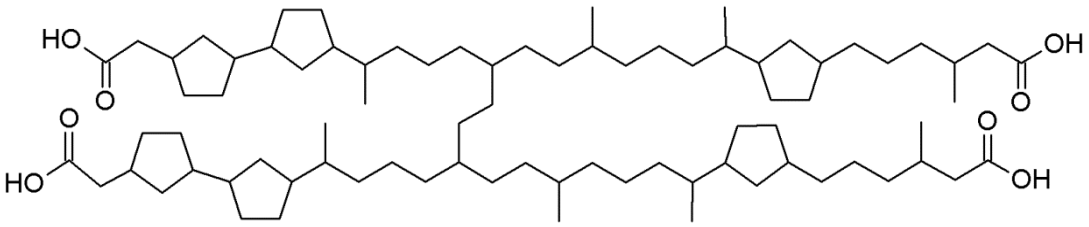

Figure 2.6. Structure of one regioisomer of a six ring tetraprotic C80 'ARN' acid**,** molecular formula $C_{80}H_{142}0_8$.

Recent work on the oil sands derived naphthenic acids has relied heavily on ion cyclotron mass spectral analysis and Fourier Transform Infra-Red Spectroscopy to determine the molecular weights and potential empirical formulas of compounds existing within the naphthenic acid complex mixtures (e.g. Bataineh

et al., 2006; Barrow et al., 2010). These empirical formulas can be then used to calculate the relevant '*Z*' number of each compound (Section 1.1, Chapter 1) thus characterising these acids into structural groupings.

However ongoing work by Rowland and colleagues has been able to elucidate structural information on many of the compound classes via use of novel two dimensional gas chromatography time of flight mass spectrometry (e.g. Rowland et al., 2011a). This worked relied heavily on the synthesis of saturated acids by the catalytic hydrogenation of authentic aromatic acids (Figure 2.7)

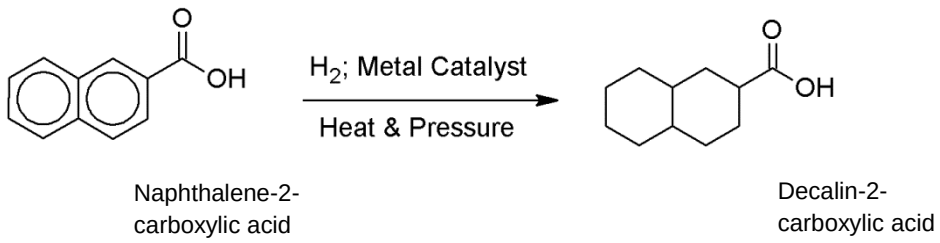

Figure 2.7. General reaction scheme for the conversion of naphthalene-2-carboxylic acid to decalin-2-carboxylic acid isomers by catalytic hydrogenation.

2.1.3. Catalytic Hydrogenation

Catalytic hydrogenation of aromatic compounds was first shown to be effective when Sabatier and Senderens were able to reduce phenol and aniline to their saturated counterparts (cyclohexanol and cyclohexanamine; Figure 2.8) by passing the vapour of these organic molecules with hydrogen over a hot finely divided nickel catalyst (Sabatier and Senderens, 1904).

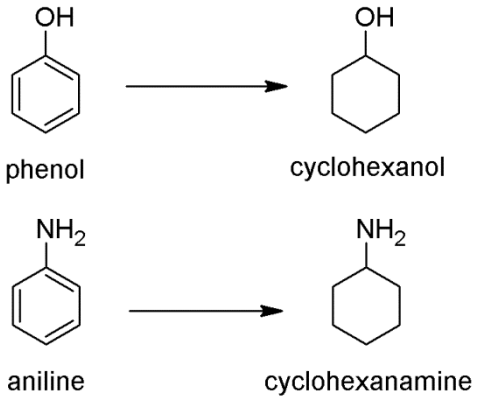

Figure 2.8. Reduction of phenol and aniline to their saturated counterparts

Another 10 years had passed before Sabatier was able to hydrogenate benzene to a cyclohexane using a metal catalyst (Sabatier and Espil, 1914). This work relied heavily on Sabatier's original discovery of metal based catalytic hydrogenation in 1899 (Sabatier and Senderens, 1899) a discovery which merited the award of a Nobel Prize (awarded jointly with Victor Grignard in 1912). Hydrogenation with use of a platinum catalyst was first noted by Debus (1863) when hydrocyanic acid was transformed to methylamine; however aromatic compounds are far more stable so take more energy to transform into their saturated counterparts. Although Sabatier was successfully able to convert benzene to cyclohexane his efforts to convert naphthalene to decahydronaphthalene were only partially successful with the formation of tetrahydronaphthalene.

Aromatic compounds are chemically stable and a lot of energy is required to break the pi (π) bonds that create the double bonded structure (for benzene it is ca 150 kJ mol^{-1}) and replace it with sigma (σ) bonded hydrogen (Figure 2.9). The stability of aromatic compound derives from an overlap of the molecular π orbitals which create a de-localised electron cloud above and below the structure. This

stability, coupled with the amount of energy required to break and create bonds, means that hydrogenating aromatic compounds to fully saturated moieties can be difficult and time consuming.

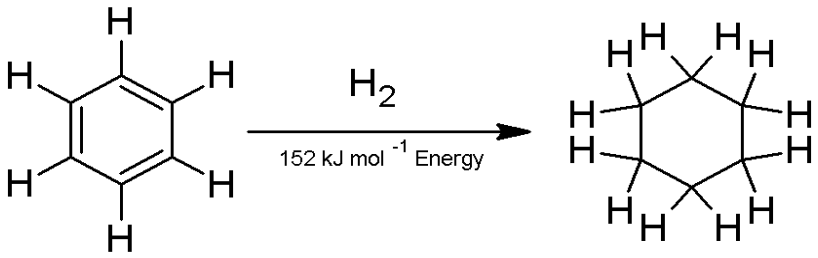

Figure 2.9. General reaction scheme of benzene to cyclohexane due to hydrogenation, showing amount of energy required to convert one mole of benzene**.**

It has been noted that the process of hydrogenating aromatic compounds usually proceeds with the additional hydrogen atoms being bound onto one side of the aromatic compound. Linstead et al., (1942) postulated that this was due to a catalytic hindrance and that the aromatic compound must interact with the catalyst, essentially lying flat on the surface of the metal for hydrogenation to be able to take place. This process predominantly produces *cis* isomers, although the authors note that *trans* isomers can be produced if the hydrogenation process is protracted. It was also mentioned that hydrogenation experiments with non-planar diaromatic compounds were unlikely to proceed to completion as only one ring could interact with the catalyst, whilst the other ring is able to interfere with the process, causing a hindrance to complete saturation. However, work by Siegel and Smith (1960a & b) on the catalytic hydrogenation of cyclohexenes

showed that the production of predominant *cis* isomers on complete saturation ranged from 69% to 80% with the remainder being *trans* isomers. This was confirmed by Sauvage et al.,(1960) who showed that the percentage of *cis* isomers could be as low as 38% and as high as 83% depending on the compound used and the steric selectivity of the compound when interacting with the catalyst.

In aromatic compounds that contain more than one ring, hydrogenation occurs via successive reversible steps. Equilibrium constants have been calculated for each of these steps and it has been found that the equilibrium constant is higher for the first stage of the hydrogenation process (hydrogenation of the first ring) than for successive steps. However it has also been determined that more moles of hydrogen are required to hydrogenate the final ring (leading to complete saturation). Therefore hydrogenation of the first ring in a di-aromatic compound is less thermodynamically favoured than complete saturation (Stanislaus and Cooper, 1994).

The process of catalytic hydrogenation over the so called group VIII metals occurs when the aromatic compound is associatively adsorbed as a π-complex where the π electrons in the aromatic species combine with the empty π-orbitals of the group VIII metals. It has also been noted that during the catalytic hydrogenation of benzene, cyclohexene derivatives desorb from the π-complex before further hydrogenation (Stanislaus and Cooper, 1994). However cyclohexadienes do not seem to desorb from the complex as it is postulated that they are too strongly adsorbed for desorption to occur. Rates of absorption of the

carbon atoms making up a benzene ring seem to be dependent on temperature. At a temperature range of 120-200^{o}C there is a threefold increase in the carbon to metal bonds when using nickel as a catalyst. Relative activity for benzene-cyclohexane on group VIII metals revealed a sequence gradient of activity (at 117^{o}C) of Pt>Pd>Ir>Ru>Rh (Moyes and Wells. 1973). So it seems that a Pt based catalyst has the greater chance of fully converting an aromatic compound to an alicyclic. It is also noted that the reaction between Pt and benzene is greater than that between Ni and benzene at temperatures below 100^{o}C. This is rapidly reversed when higher temperatures are used (Moyes and Wells, 1973). However it must be noted that these metals exist within groups VIII, IX and X on the periodic table and the most useful hydrogenation metals (Pt, Rh and Pd) are more correctly classed as platinum type metals.

It seems then that catalytic hydrogenation of aromatic compounds is fraught with difficulties when attempted at low temperatures and low pressures. In the present study the ability to hydrogenate certain mono and diaromatic acids to the pure alicyclic analogues was considered essential in order to produce pure ‘model’ naphthenic acids for identification and toxicological purposes.

2.2. Methods and Materials

2.2.1 Materials

A Mini Clave 150 mL reaction chamber was obtained from Buchii (Oldham UK). Solvents (hexane and methanol) were purchased from Rathburn (Walkerburn, Scotland, UK) and Fisher (Loughborough UK) and were HPLC grade or better. Platinum oxide catalyst and authentic acids standards were supplied by Sigma-Aldrich (Gillingham, UK). Grade 5, 150 mL filter papers were supplied by Whatman and vials were supplied by either Fisher or Sigma-Aldrich. H-Cube® and all attendant catalysts and supplies were sourced from ThalesNano (Budapest, Hungary). Derivatisation catalysts (10% boron trifluoride methanol complex (BF_3-MeOH and N,O-bis(trimethylsilyl)trifluoroacetamide + trimethylchlorosilane (BSTFA+ 1 % TMCS)) were supplied through Sigma Aldrich as were pyridine and phosphoryl chloride. Other authentic compounds were supplied by Sigma Aldrich, Fluka (a subsidiary of Sigma Aldrich), Acros Organics (Geel, Belgium) and Chiron (Trondheim, Norway). Mixtures were magnetically stirred with a Stuart Scientific Magnetic Stirrer. All glassware was soaked in Decon90 for 24 hours and rinsed thoroughly in deionised water before being dried at 110^{o}C for 24 hours.

2.2.2 Initial Hydrogenation Method

Typically 100 mg sample of an authentic aromatic acid standard was dissolved in 100 mL of a suitable solvent hexane or methanol (MeOH) and transferred to a three necked round bottom flask (RBF). Adam's catalyst (PtO_2-H_2O; 20-40mg) was added to the solution. A condenser tube fitted with a pressure gauge was attached to the middle neck and a Pasteur pipette was added to one of the

remaining necks of the RBF. The third neck was sealed with a glass stopper and all joints were sealed with liberal application of Para-film®. Hydrogen was bubbled through the Pasteur pipette and into the mixture at ~8 psi. The mixture was agitated by constant magnetic stirring for 7-8 hours. The solution was filtered through a Whatman Number 5 15 cm filter into a single neck RBF. This was reduced using a rotary evaporator and transferred to a pre weighed 7 mL vial. The compound was derivatised and analysed by the methods detailed below (Section 2.6, 2.7 and 2.8)

2.2.3 Buchii Reaction Chamber

Typically a 100 mg sample of an authentic aromatic acid was dissolved in 100 mL of MeOH in the 150mL reaction chamber of the Buchii Mini Clave Reaction Chamber; 20-40 mg of Adam's catalyst was added to the solution. The reaction chamber was placed into the Mini Clave and the lid was sealed. N_2 gas was added to the headspace to purge the reaction chamber of air and H_2 gas was bubbled through the solution at a constant rate under 0.5-1 bar of pressure. The solution was agitated by use of a magnetic stirrer. The reaction was allowed to proceed for 7 hours and was checked periodically to assess that the stirring of the solution, the pressure and the introduction of H_2 gas remained constant. After 7 hours of hydrogenation the reaction chamber was removed and the solution was filtered through a 150 mm grade 5 Whatman filter into a 250 mL RBF. The filter paper was then rinsed thoroughly in clean water and dried before discarding to prevent spontaneous combustion.

The solvent was evaporated on a Buchii rotor evaporator whilst being heated in a Buchii water bath at 45^{o}C and then transferred to a pre weighed and pre-rinsed 7

mL vial in 1 mL of MeOH. This solvent evaporated to dryness under a steady stream of N_2 whilst being heated to 37^{o}C and the vial was reweighed. A 1 mL aliquot of MeOH was added to the vial and a 1 mg aliquot was removed and refluxed with the BF_3-MeOH complex for 30 minutes at 70^{o}C. This was extracted three times with water and hexane and the hexane fraction dried over anhydrous sodium sulphate. A calculated amount was added to a GC vial and made up to 1 mL to create a 0.05 mg mL^{-1} solution. This was analysed on an Agilent Gas Chromatograph Mass Selective Detector (GC-MS) (Section 2.8).

2.2.4 ThalesNano H-Cube®

The ThalesNano H-Cube® system is a flow-through hydrogenator connected to a HPLC pump. The solution to be hydrogenated is passed through the pump and the hydrogenator at a constant rate and passed, under a given temperature and pressure (up to 100 bar and 100^{o}C) over a packed metal catalyst cartridge (CatCart®). Hydrogen is generated from de-ionised water by electrolysis, precluding the use of a hydrogen cylinder and a fume hood as the H-Cube® can be set up as a bench top device. Two tubes lead from reservoirs of solvent into the HPLC pump and a switch system can be employed to ensure no air is taken into the H-Cube® (Figure 2.10).

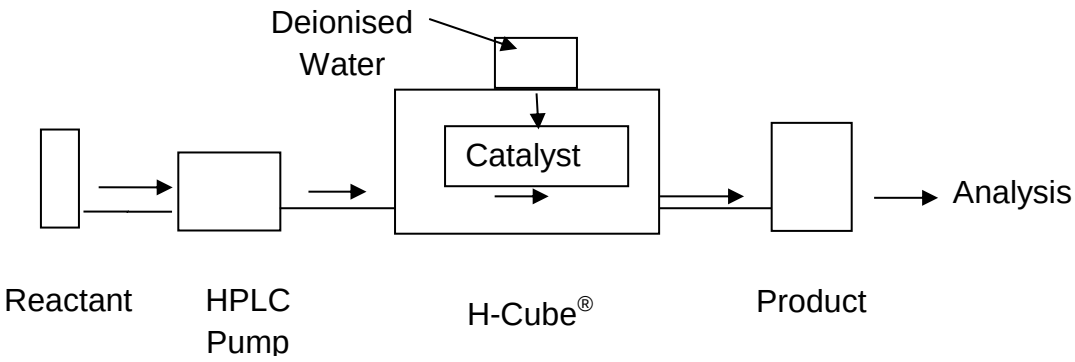

Figure 2.10. Box schematic of the H-Cube® catalytic hydrogenator. Arrows depict direction of flow

A 100mg sample of an authentic acid was dissolved in MeOH to give a <0.5 molar solution. The deionised water reservoir was topped up and the tubes that connect to the HPLC pump were immersed in vessels containing clean MeOH. The HPLC pump was flushed to ensure that no air entered the H-Cube® whilst in use. As Adam's catalyst was not available as an H-Cube CatCart® cartridge a 5% rhodium over carbon (5% Rh/C) catalyst was added to the system and the catalyst holder was fastened to finger tightness. The HPLC pump was set to a flow rate of 1 mL min^{-1} and clean MeOH was flushed through the system at this flow rate at 0 bar and $0^{o}C$. The pressure and temperature were then increased by increments of 20 bar and $20^{0}C$ until the required pressure and temperature were achieved (generally 80 bar and $80^{o}C$). Fittings that could allow air into the system were constantly checked throughout this process. Once the pressure and temperature had stabilised the solution containing the aromatic acid to be hydrogenated was allowed to flush through the system. Retention time through the H-Cube® were generally ~5 minutes elutions are discarded before collection of subsequent aliquots in a clean RBF; a 1 mL aliquot was removed for analysis by GC MSD. The RBF was stoppered and kept in the dark until analysis was

complete. If complete saturation had not occurred the solution was passed through the H-Cube® again. A complete flush of clean solvent for 20 was conducted between experiments to ensure no contamination occured.

2.2.5 Dehydration Method

Dehydration was achieved by the methods of Rinehart and Perkins (1963) as modified by West (2008). Briefly: Roughly 50 mg of an alcohol (e.g. 2-hydroxybicyclo [3,2,1] octane-6-carboxylic acid) was dissolved in dry pyridine and cooled to 0-5^{o}C in ice. Phosphoryl chloride ($POCl_3$) was slowly added whilst magnetically stirred. The mixture was allowed to stand for 8 hours after which the mixture was added to ice water slurry. The mixture was extracted three times with hexane and washed twice with hydrochloric acid (HCl) and once with water to remove the pyridine (as a hydrochloride salt) and to extract the crude alkene. A small amount was removed (1.5 mg) for boron-trifluoride in methanol (BF_3 MeOH) derivatisation and the remaining amount was taken for hydrogenation via the H-Cube® (Figure 2.2).

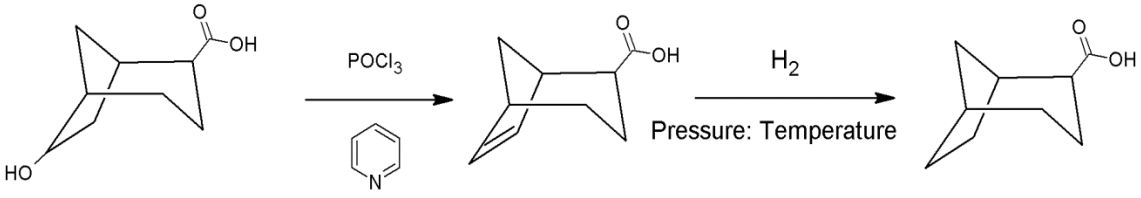

Figure 2.11. Schematic for the dehydration and hydrogenation of a bicyclic alcohol carboxylic acid

2.2.6 Boron-trifuoride in Methanol Derivatisation Method

Between 1-10 mg of the sample acid was added to 2 mL of BF_3-MeOH in a glass vial and heated at 70^{o}C for at least 30 minutes. After removal from the heat the

vial was allowed to cool and 1 mL of water and 1 mL of hexane was added. The sample was mixed via autovortex and allowed to settle into two distinct phases. The upper layer was removed into a separate vial and more hexane was added, mixed and removed. The extraction was completed between 3 and 5 times and the hexane dried over anhydrous sodium sulphate. Once dry the hexane was carefully removed to a pre-weighed vial and reduced to dryness under a steady stream of N_2. This was re-eluted with the addition of 1 mL of clean hexane and a calculated amount was added to a GC vial and made up to 1 mL to create a ~0.01 mg/mL solution. This was analysed with GC-MS (section 2.8).

2.2.7 BSTFA + TMCS Derivatisation Method

A small amount of sample was added to excess BSTFA- 1% TMCS and heated at 70^{o}C for 30 minutes. The mixture was allowed to cool (diluted if necessary) and analysed on GC-MS.

2.2.8 GC-MS Method

For GC-MS, extracts were analysed using an Agilent GC-MSD (Agilent Technologies, Wilmington, DE, USA). This comprised a 7890A gas chromatograph fitted with a 7683B Series autosampler and a 5975A quadrupole mass selective detector. The column was a HP-5MS fused silica capillary column (30 m x 0.25 mm i.d x 0.25 μm film thickness). The carrier gas was helium at a constant flow of 1.0 mL min^{-1}. A 1.0 μL sample was injected into a 300°C splitless injector. The oven temperature was programmed from 40 to 300^{o}C at 10 °C min^{-1} and held for 10 min.

2.3. Results and Discussion

Catalytic hydrogenation of a variety of acids was achieved using a Buchii reaction chamber, a H-Cube® hydrogenator or by an amalgamation of the two. All of these compounds were hydrogenated in their free acid state before being esterified with BF_3-MeOH, or occasionally with BSTFA+TMCS.

2.3.1. Synthesis of *cis-/trans*-4-hexylcyclohexylethanoic acid

Although a few monocyclic 'naphthenic acids' were identified long ago (e.g. Lochte and Littman, 1955, Seifert, 1975; Figure 1.1, Chapter 1) relatively few have been identified in petroleum acids and OSPW until the present and associated studies (e.g. Cyr and Straus, 1986; Rowland et al., 2011). Furthermore, only limited examples are available from commercial sources. Therefore an initial attempt was made to synthesise a mixture of cis-/trans-4-hexylcyclohexylethanoic acid by catalytic hydrogenation of 4-hexylphenylethanoic acid (Figure 2.12).

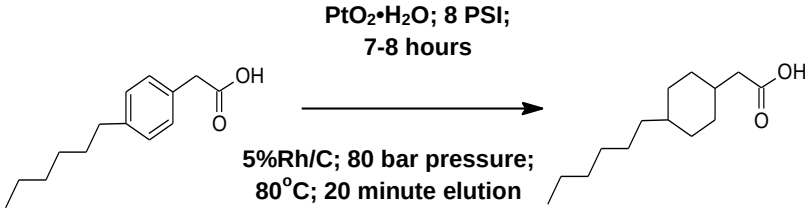

Figure 2.12. Reaction scheme for the catalytic hydrogenation of the reactant (4-n-hexylphenylethanoic acid) to the product, (cis-/trans-4-hexylcyclohexylethanoic acid); revealing Buchii reaction chamber (above arrow) and H-Cube® (below arrow) catalytic hydrogenation conditions.

The latter acid, purchased from a commercial source (Sigma-Aldrich, stated purity >99%) was converted to the trimethyl silyl (TMS) esters and examined by GC-MS (Figure 2.13A). A single chromatographic peak was observed at 17.40 minutes. Analysis of the mass spectrum (Figure 2.13B) reveals a molecular ion ($M^{+\bullet}$) at *m/z* 292 indicative of the TMS esters of 4-*n*-hexylphenylethanoic acid. Significant fragment ions are revealed at *m/z* 277 (loss of the methyl groups) m/z 248 (potential cleavage of a propane from the hexyl side chain), *m/z* 206 and 221(also indicative of cleavage on the hexyl side chain); *m/z* 175 which indicates cleavage of a carboxy trimethyl silyl group and the base ion at *m/z* 73 which is a characteristic ion associated with TMS esters.

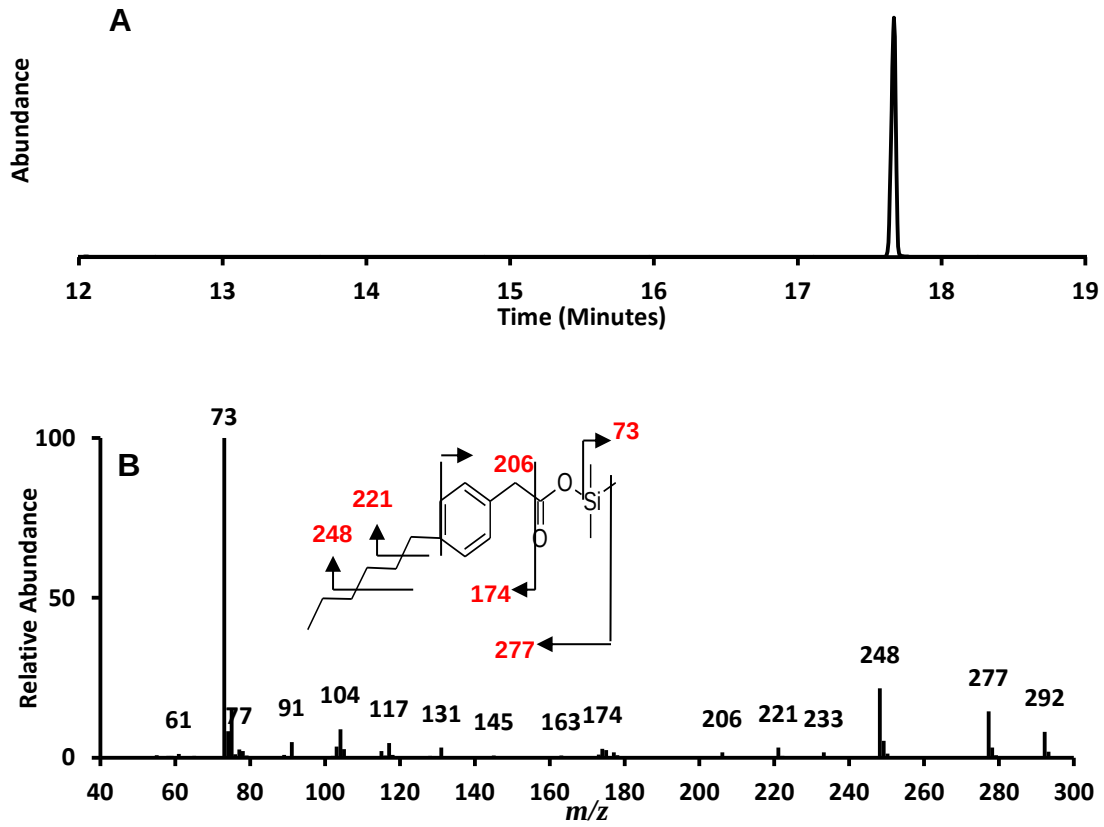

Figure 2.13. (A) Total ion current chromatogram of TMS esters of 4-n-hexylphenylethanoic acid. (B) Mass spectrum of component displayed at RT17.40 minutes**.** GC Conditions: Column HP-5MS 30 m x 0.25 mm i.d x 0.25 μm film thickness; Solvent delay 6 minutes; oven programme 40-300^{o}C at 10^{o}C min^{-1}, hold 10 min; injector 300^{o}C);MS conditions: Source 230^{o}C, ionisation energy 70 eV, mass range 50-550 Daltons.

Catalytic hydrogenation of the reactant was initially carried out using the method described in section 2.2. The product of the initial hydrogenation attempt was analysed by GC-MS. The chromatogram (Figure 2.14A) reveals one chromatographic peak at RT 17.37 min.

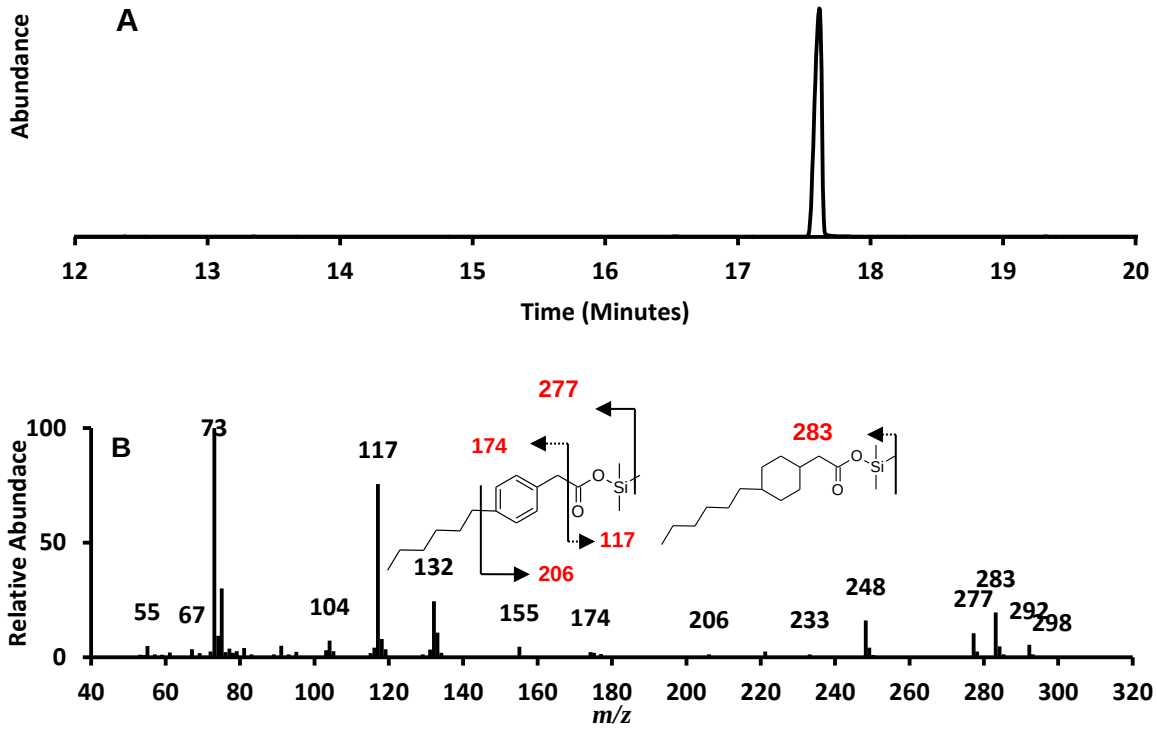

Figure 2.14. (A) Total ion current chromatogram of TMS esters of the attempted catalytic hydrogenation of 4-n-hexylphenylethanoic acid to cis-/trans-4-n-hexylphenylcyclohexylethanoic acid; (B) mass spectrum component at RT 17.37**.** GC-MS conditions as described in Figure 2.13.

Analysis of the mass spectrum revealed (Figure 2.14B) that $M^{+\bullet}$ for 4-n-hexylphenylethanoic acid TMS ester (*m/z* 292) and cis-/trans 4-n-hexylcyclohexylethanoic acid TMS ester (*m/z* 298) are both present. A strong *m/z* 283, indicating a loss of a methyl group from the cyclohexyl moiety is also revealed as is a fragment ion at *m/z* 277, characteristic of a loss of a methyl group from both the reactant and the product and indicating that the reactant did not fully saturate.

It was decided that derivatisation with BF_3-MeOH might split the single peak into both the reactant and the product. Esterification with BF_3-MeOH reveals two

distinct chromatographic peaks at RT 16.21 and RT 16.40 minutes (Figure 2.15A).

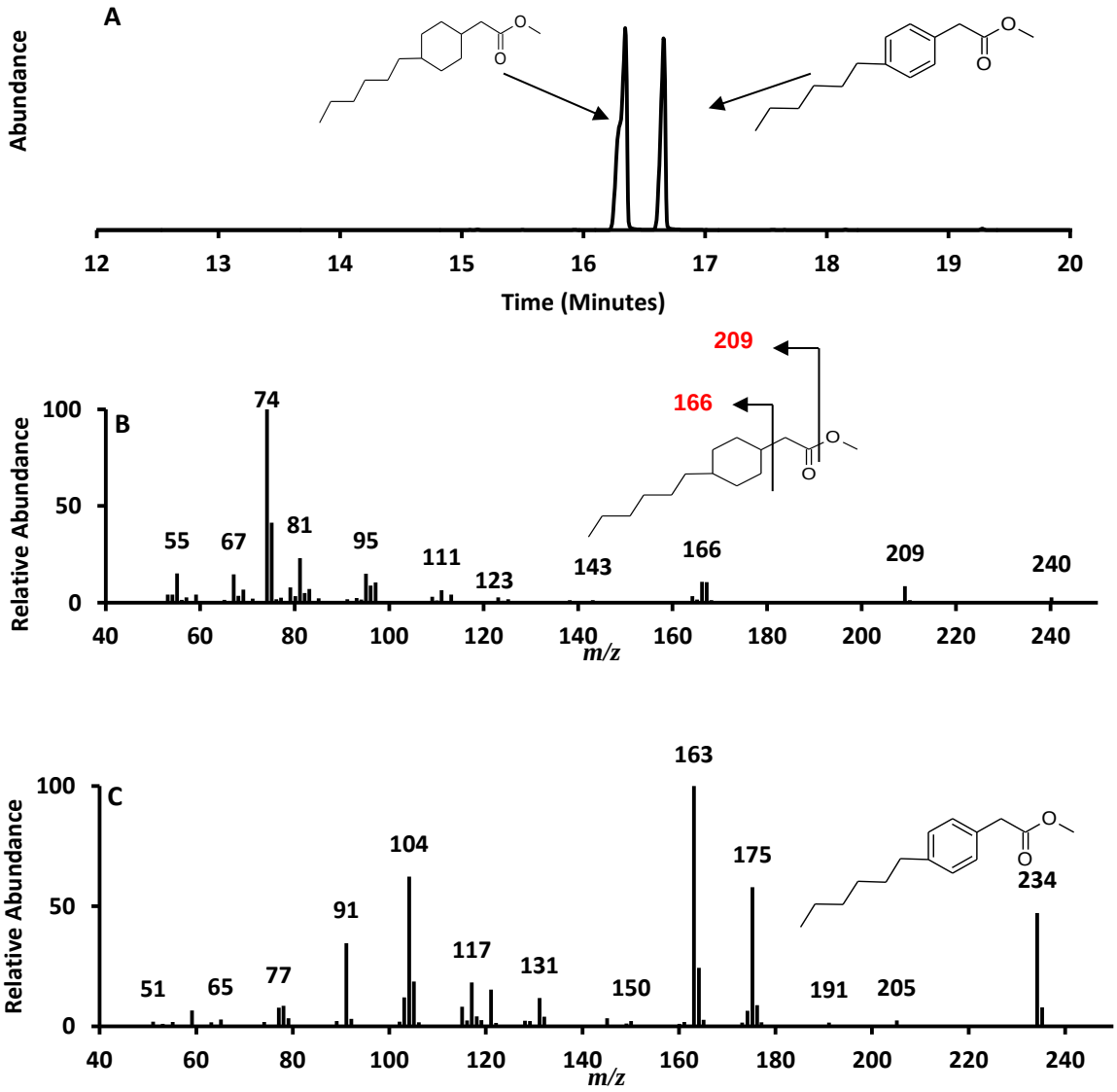

Figure 2.15. (A)Total ion current chromatogram of methyl esters of the catalytic hydrogenation products of 4-n-hexylphenylethanoic acid. (B) Mass spectrum of component displayed at RT16.21 minutes; (C) mass spectrum of the component displayed at RT 16.40. GC Conditions as previously in Figure 2.13.

Analysis of the mass spectra allows an assignment of *cis/trans*-4-*n*-hexylcyclohexyl ethanoic acid methyl ester for peak A (Figure 2.15B)($M^{+\bullet}$ *m/z* 240; *m/z* 209 indicating loss of a methoxy and *m/z* 166 indicating the loss on the ethanoate ion; and an assignment of 4-*n*-hexylphenyl ethanoic acid for peak B (Figure 2.15C) ($M^{+\bullet}$ *m/z* 234; *m/z* 175 indicating loss of a carboxylate ion). Peak A reveals an apparent 'shoulder' which may be indicative of the two isomers (*cis* and *trans*) co-eluting.

Roughly 58% of the reactant was driven to full saturation so it was necessary to re-hydrogenate the sample. It was decided that all subsequent hydrogenations would be carried out with the methods described in Section 2.2.3 and 2.2.4.

Catalytic hydrogenation of 4-*n*-hexylphenylethanoic acid continued with the H-Cube™ flow-through hydrogenator. The products were derivatised with the BF_3-MeOH esterification method and analysed with GC-MS (Figure 2.16).

Figure 2.16A reveals chromatographic peaks at RT 15.36, 15.38 and 15.59 minutes. Analysis of the mass spectra allows assignments of components to each peak. Peaks at RT 15.36 and 15.38 reveal ions that are indicative of the *cis/trans* isomers of 4-*n*-hexylcyclohexylethaonic acid methyl esters (Figure 2.16 B & C).

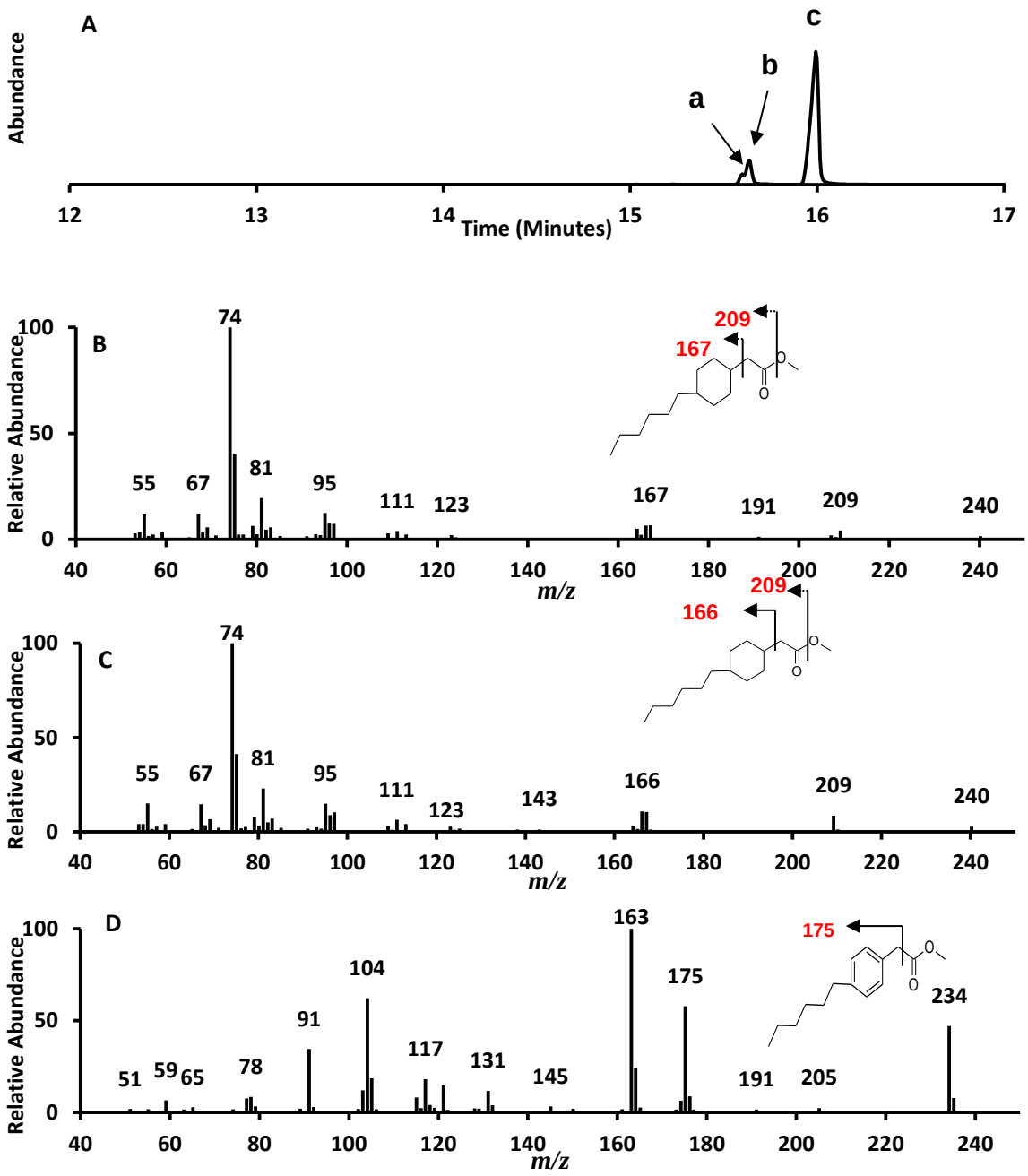

Figure 2.16. (A)Total ion current chromatogram of BF3-MeOH esters for the catalytic hydrogenation of 4-n-hexylphenylethanoic acid to cis-/trans-4-n-hexylphenylcyclohexylethanoic acids. (B) Mass spectrum of component at RT 15.36 minutes. (C) Mass spectrum of component at RT 15.38 minutes.(D) Mass spectrum of component at RT 15.59 minutes. GC-MS conditions as described in Figure 2.13.

Both mass spectra have $M^{+\bullet}$ at *m/z* 240 and an ion at *m/z* 209 indicating the loss of a methoxy ion (*m/z* 31). There is also a loss of *m/z* 73/74 for the ethanoate group. These ions have slightly different abundances in Figure 2.16 B&C as does the *m/z* 209 ion signifying that both isomers are represented in the chromatogram. As it is usual for the *trans* isomer to elute first (Rowland et al., 2011) RT 15.36 is assigned thus, with RT 15.38 assigned as the *cis* isomer and RT 15.59 as the un-converted authentic acid described in Figure 2.13.

Given the obvious poor yield of this experiment, the reaction was repeated three times (the original 20 mL re-eluted through the H-Cube® at 1 ml min^{-1}, 20 minutes per experiment, plus the initial 20 minutes, totalling 80 minutes overall) (Figure 2.17). The GC-MS analysis of the methylated product revealed that these subsequent experiments only produced a product totalling 36% of the total compounds in the sample (RT 15.36 and 15.38 minutes; Figure 2.17C). Retention times and mass spectral data are as detailed above as are peak to compound assignments.

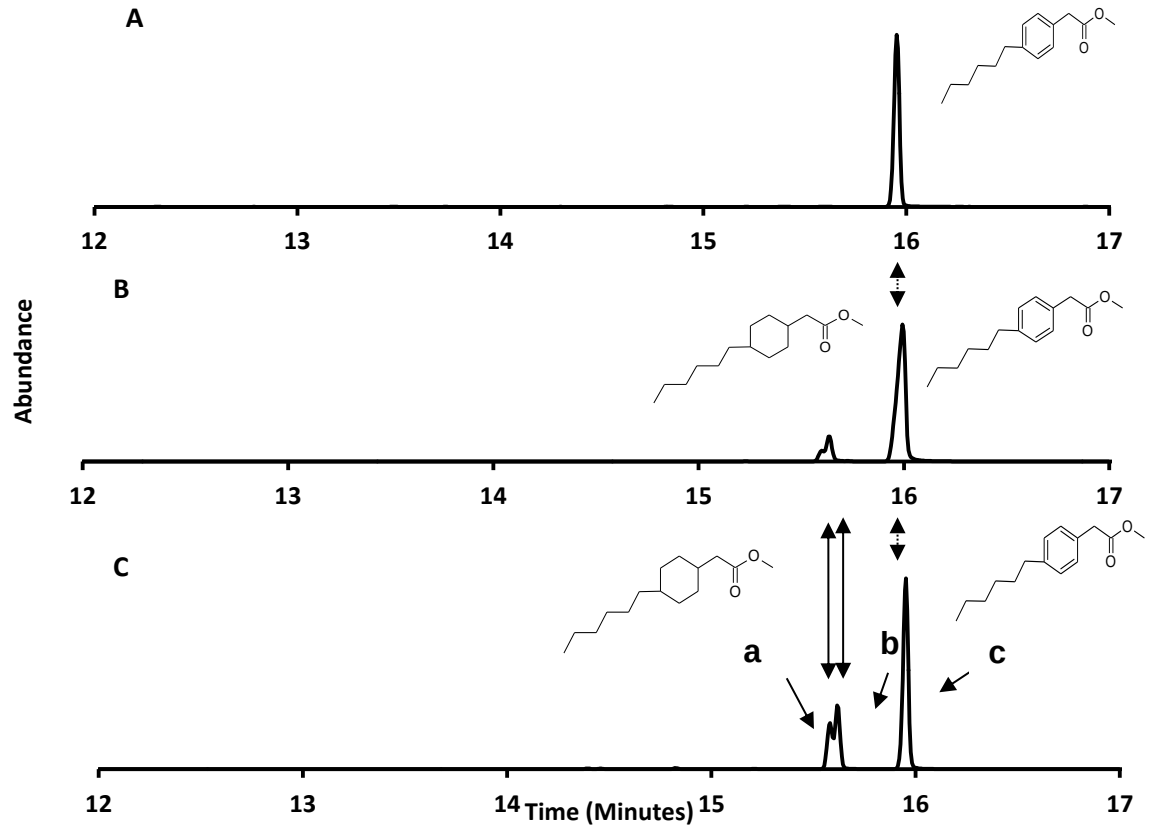

Figure 2.17. Total ion current chromatograms of BF_3-MeOH esters for (A) the authentic 4-n-hexylphenylethanoic acid; (B) initial H-Cube® catalytic hydrogenation of 4-n-hexylphenylethanoic acid mo cis/trans 4-n-hexylphenylcyclohexylethanoic acid plus (C) subsequent H-Cube® hydrogenations of 4-n-hexylphenylethanoic acid to cis-/trans 4-n-hexylphenylcyclohexylethanoic acid**.** GC-MS conditions as described in Figure 5.13

2.3.2. Synthesis of cis-/trans-4-methylcyclohexylethanoic acid

An authentic sample of 4-methylphenylethanoic acid was purchased from a commercial source (Sigma-Aldrich, stated purity >99%) and was converted to the methyl ester by heating (30 minutes 70^{o}C) with BF_3-MeOH and examined by GC-MS (Figure 2.18A), a single chromatographic peak was apparent at RT 10.04 minutes. The mass spectrum was consistent with the expected compound and comprised significant ions $M^{+\bullet}$ *m/z* 164; loss of a carboxylate ion at *m/z* 105 and

loss of an ethanoate ion at *m/z* 91 leaving a methylbenzene fragment (Figure 2.18B).

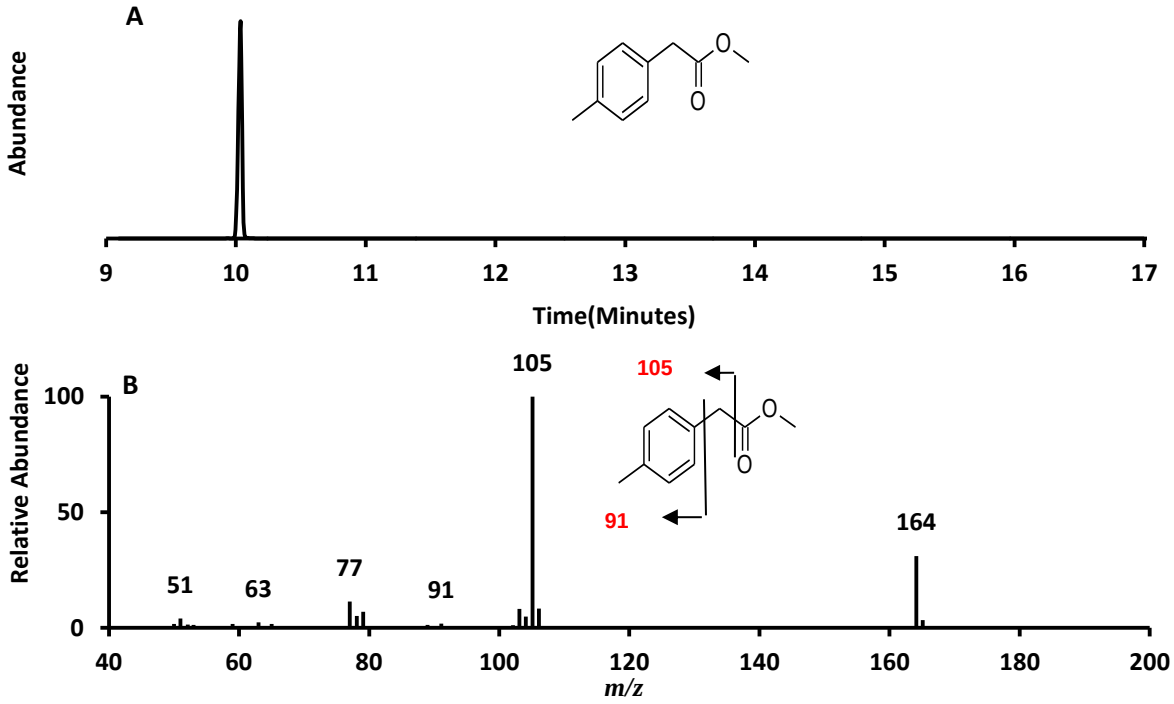

Figure 2.18. (A)Total ion current chromatogram of BF_3-MeOH esters for the authentic 4-methylphenylethanoic acid.(B) Mass spectra for the component at RT 10.04 minutes**.** GC-MS conditions as described in Figure 2.13.

Catalytic hydrogenation of 75 mg of the reactant (Figure 2.19) through the H-Cube® hydrogenator using 5% palladium hydroxide on carbon catalyst (Pd(OH)/C) was followed by derivatisation with BF_3-MeOH, the product was analysed with GC-MS (Figure 2.19).

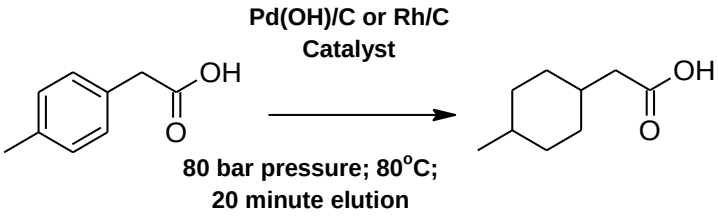

Figure 2.19. Reaction scheme for the catalytic hydrogenation of the reactant (4-methylphenylethanoic acid) to the product, (cis-/trans-4-methylcyclohexylethanoic acid); revealing H-Cube® catalytic hydrogenation conditions.

The chromatogram revealed two peaks (RT 9.25 and 10.04 minutes). Mass spectral analysis reveals the peak at RT 9.25 contains ions expected for the required product (Figure 2.20D).The $M^{+\bullet}$ at *m/z* 170 is six Daltons more than the reactant (*m/z* 164) and is indicative of the addition of 6 hydrogen atoms to the aromatic ring by catalytic hydrogenation; significant ions are revealed at *m/z* 139, *m/z* 111 and *m/z* 97 (loss of a methoxy, carboxylate and ethanoate ions respectively). The base ion (*m/z* 74) is also characteristic of a loss of an ethanoate group (Figure 2.20B). The $M^{+\bullet}$ of cis-/trans 4-methylcyclohexylethanoic acid (*m/z* 170) is not abundant enough to be seen in Figure 2.20C, Figure 2.20D depicts a close up of the *m/z* 170 region, showing an M+1 at *m/z* 171 (^{13}C abundance) and the loss of a methyl group at *m/z* 155. Figure 2.20D shows the mass spectrum for the component at RT 10.04 and is thus assigned as a 4-methylphenylethanoic acid methyl ester (described previously)

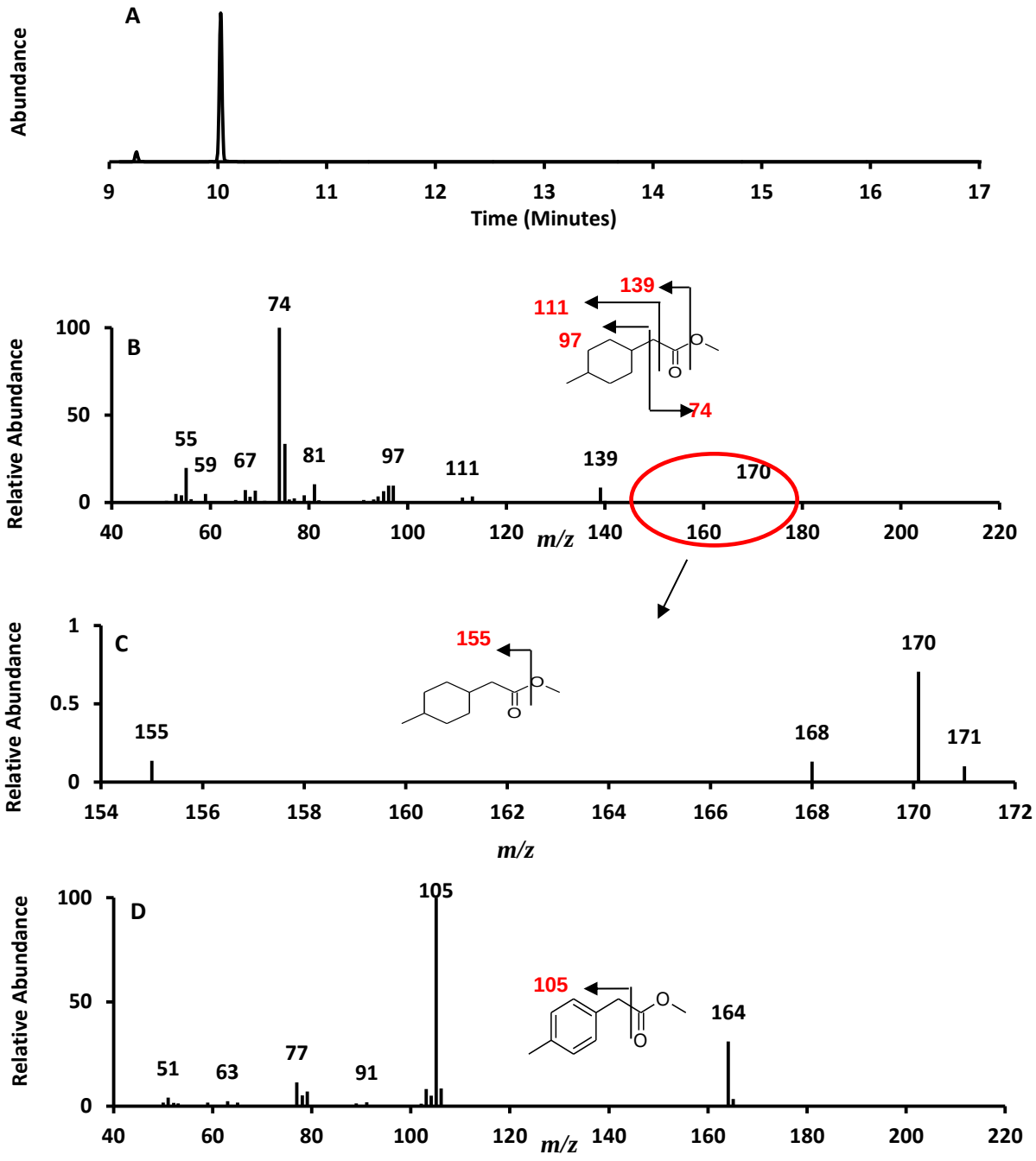

Figure 2.20. (A)Total ion chromatogram for the catalytic hydrogenation of 4-methylphenylethanoic aid methyl ester. (B) Mass spectrum for the component at RT 9.25 minutes. (C) Close up of the *m/z* 155-171 region of Figure 3.9C. (D)Mass spectrum for the component at RT 10.04 minutes**.** GC-MS conditions as described in Figure 2.13.

Given the obvious poor yield of this experiment, the reaction was repeated using 5% rhodium on carbon (Rh/C) catalyst (Figure 2.21A) and for a longer period of 40 minutes (2x 20 minute elution). GC-MS of the resultant product indicated complete hydrogenation of the reactant (peak at RT 9.25 minutes Figure 2.21A). The mass spectrum of the latter was identical to the mass spectra produced for palladium hydroxide experiment and displays fragment ions consistent with the required product (Figure 2.21B). From the initial 75mg of 4-methylphenylethanoic acid 38 mg (nominal weight due to addition of hydrogen) of pure *cis-/trans*-4-methylcyclohexylethanoic acid was recovered.

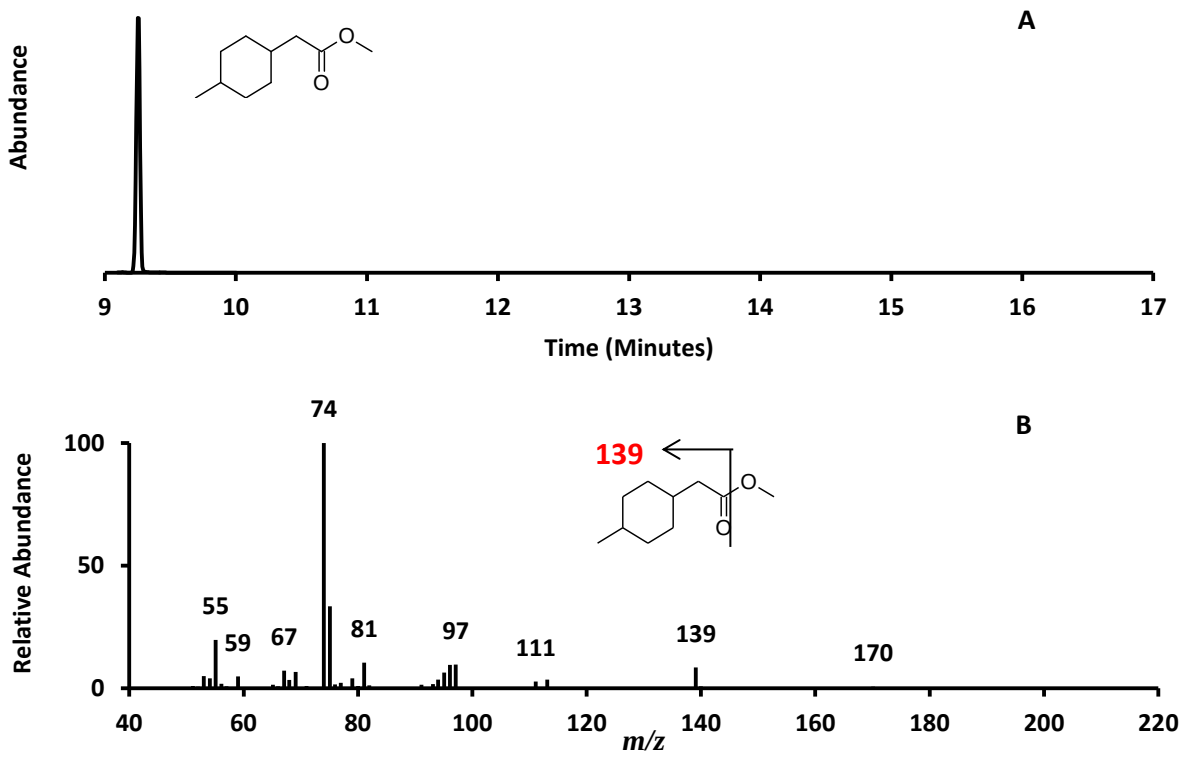

Figure 2.21. (A)Total ion chromatogram for the catalytic hydrogenation of 4-methylphenylethanoic aid methyl ester. (B) Mass spectrum for the component at RT 9.25 minutes**.** GC-MS conditions as described in Figure 2.13

2.3.3 Synthesis of cyclohexyl-6-hexanoic acid

An initial attempt was made to synthesise a mixture of cyclohexyl-6-hexanoic acid by hydrogenation of phenyl-6-hexanoic acid (Figure 2.22).

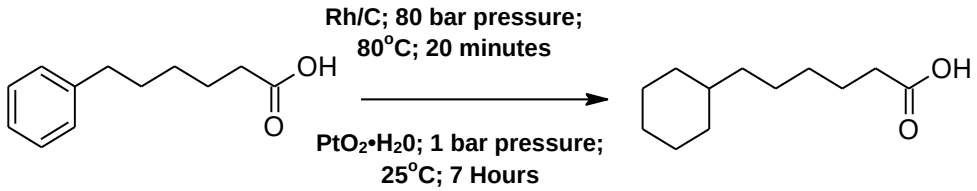

Figure 2.22. Reaction scheme for the catalytic hydrogenations of phenyl-6-hexanoic acid (the reactant) to the product (cyclohexyl-6-hexanoic acid) plus the H-Cube® (above arrow) and Buchii reaction chamber (below arrow) catalytic hydrogenation conditions.

Thus, the latter acid, purchased from a commercial source (Sigma-Aldrich, stated purity >99%; actual purity 98%) was converted to the methyl ester by heating at 70°C for 30 minutes with BF_3-methanol and examined by GC-MS (Figure 2.23A).

The chromatogram (Figure 2.23) shows a distinct peak at RT 14.02 minutes. The mass spectrum (Figure 2.23B) was consistent with the expected compound and comprised significant ions. The $M^{+\bullet}$ at *m/z* 206 is consistent with the molecular weight of pheny-6-hexanoic acid methyl ester, the fragment ion at *m/z* 174 indicates loss of methanol (*m/z* 32). The base ion at *m/z* 91 indicates benzylic cleavage with the loss of a pentanoate group (*m/z* 115) and *m/z* 130 indicates cleavage of the hexanoate group.

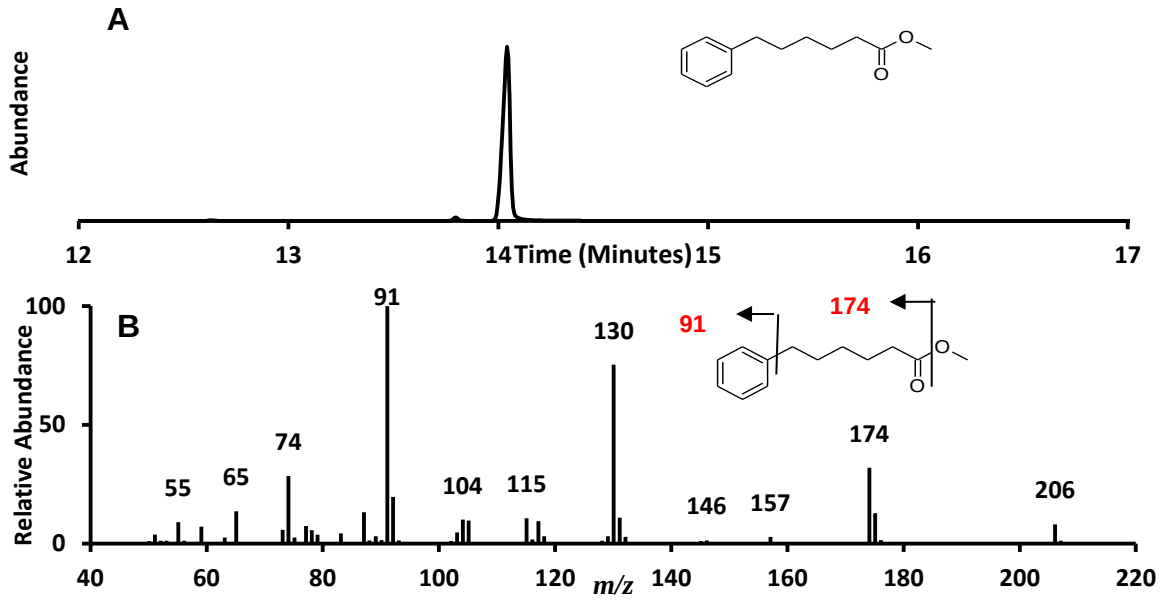

Figure 2.23. (A) Total ion current chromatogram of BF3-MeOH esters for the authentic phenyl-6-hexanoic acid. (B) Mass spectra for the component eluting at RT 14.02 minutes**.** GC-MS conditions as described in Figure 2.13.

Hydrogenation of phenyl-6-hexanoic acid was attempted on the H-Cube® (Rh/C catalyst 80 bar/80^{o}C/1 mL min^{-1}). This resulted in an incomplete reaction with 20.2% of the reactant (phenyl-6-hexanoic acid) remaining (total product and reactant recovered 48.2 mg; 96% recovery Table 2.?) (Figure 2.24A).

Two distinct peaks are displayed in the chromatogram (RT 13.50 and RT 14.02 minutes). Analysis of the mass spectra reveals that the peak at RT 13.50 has an $M^{+\bullet}$ at *m/z* 212, 6 Daltons greater than the reactant and consistent with the molecular weight of the product (cyclohexyl-6-hexanoic acid methyl ester). Significant ions exist at *m/z* 74 (cleavage of an ethanoate group) *m/z* 87 (propanoate group), *m/z* 129 (hexanoate group) and *m/z* 181(loss of methoxy) allowing an assignment of cyclohexyl-6-hexanoic acid methyl ester (Figure 2.23).

Analysis of the mass spectrum of the component at RT 14.02 reveals that it is identical to the reactant mass spectra described above (Figure 2.23B).

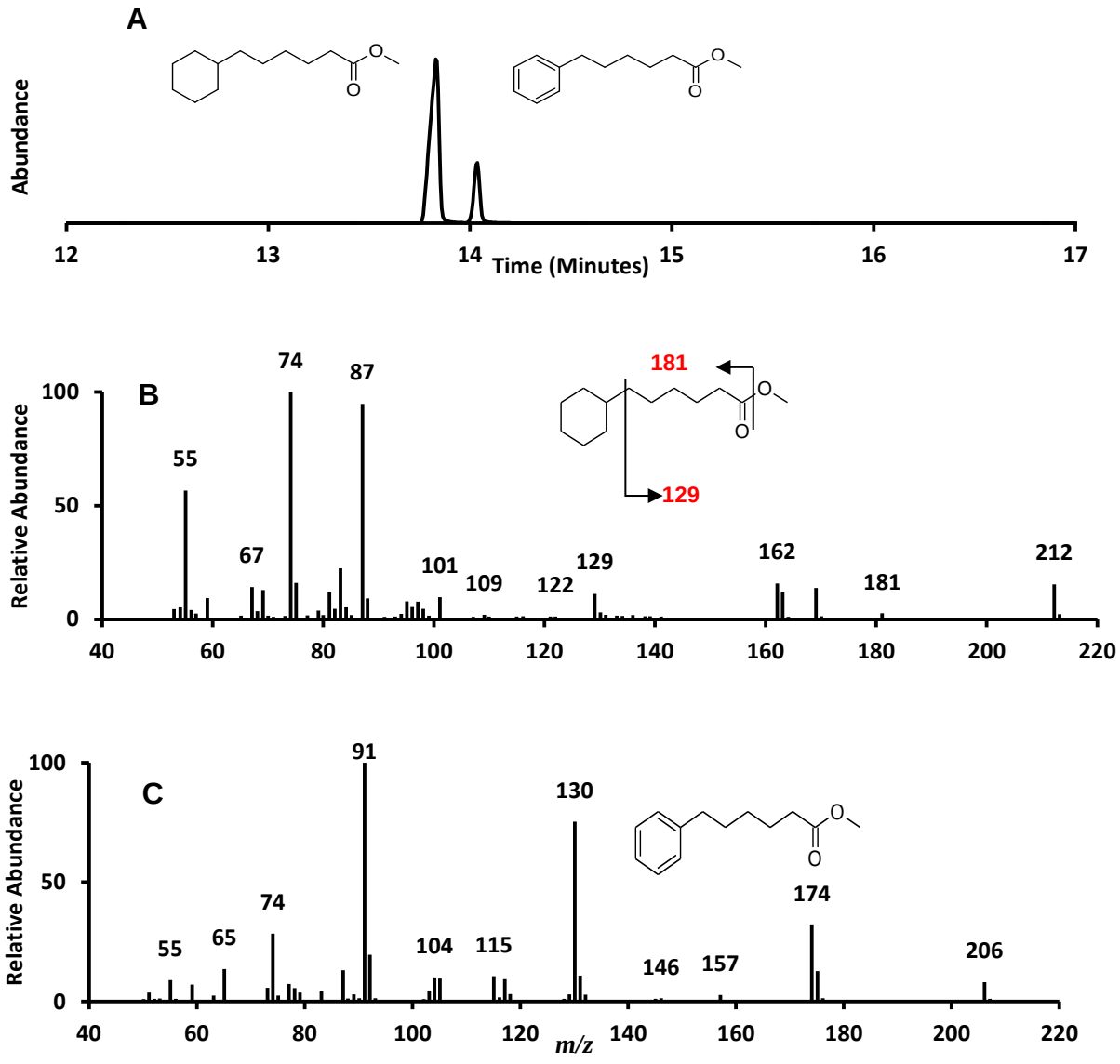

Figure 2.24. (A) Total ion current chromatogram of BF_3-MeOH esters for the catalytic hydrogenation products of phenyl-6-hexanoic acid. (B) Mass spectra for the component at RT 13.50 minutes**.** (C) Mass spectra for the component at RT 14.02 minutes. GC-MS conditions as described in Figure 2.13.

Due to restricted further availability of the H-Cube® at this time the experiment was completed using (the Buchii reaction chamber (PtO_2•H_2O (Adams) catalyst; 1 bar; 25°C, 7h) (Figure 2.24B). The products were esterified with BF_3-MeOH and analysed with GC-MS.

The Chromatogram reveals a single peak at RT 13.50 minutes (Figure 2.25A). Analysis of the mass spectrum (Figure 2.25B) reveals that it is identical to the previously described mass spectra assigned to the cyclohexyl-6-hexanoic acid methyl esters (Figure 2.25B)

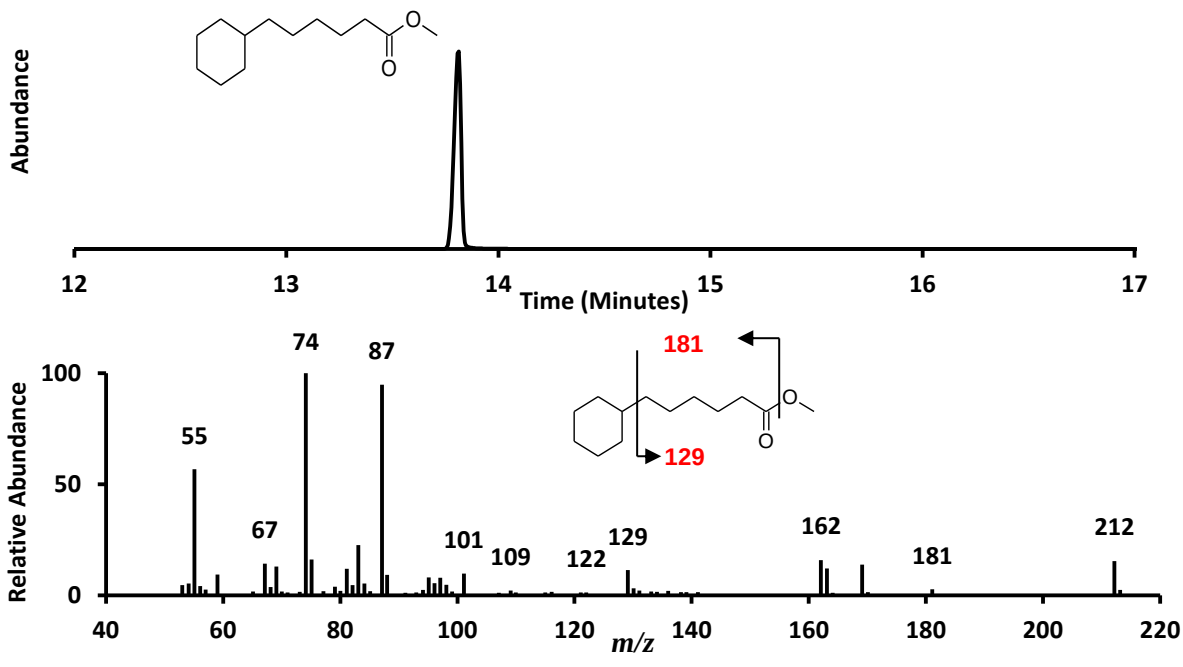

Figure 2.25. (A) Total ion current chromatogram of BF_3-MeOH esters for the catalytic hydrogenation products of phenyl-6-hexanoic acid. (B) Mass spectrum for the component at RT 13.50 minutes**.** GC-MS conditions as described in Figure 2.13.

2.3.4. Synthesis of cis-/trans 4-isopropylphenylethanoic acid

An initial attempt was made to synthesise a mixture of cis-/trans 4-isopropylphenylethanoic by hydrogenation of 4-isopropylphenylethanoic acid (Figure 2.26).

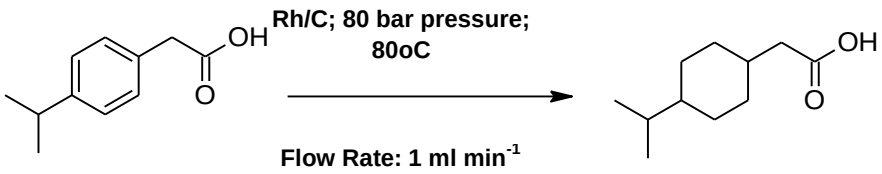

Figure 2.26. Reaction scheme for the catalytic hydrogenations of the reactant (4-isopropylphenylethanoic acid) to the product, (cis-/trans 4-isopropylcyclohexylethanoic acid); plus the H-Cube® catalytic hydrogenation conditions.

Thus, the latter acid, purchased from a commercial source (Sigma-Aldrich, stated purity >99%; actual purity 98%) was converted to the methyl ester by heating at 70^{o}C for 30 minutes with BF_3-methanol complex and examined by GC-MS (Figure 2.27).

The GC chromatogram (Figure 2.27A) displayed a single peak at RT 12.05 minutes. Analysis of the mass spectrum (Figure 2.27B) was consistent with the expected compound. The $M^{+\bullet}$ at *m/z* 192 is consistent with the products molecular weight, the base ion at *m/z* 177 indicates loss of a methyl group (*m/z* 15). The fragment ion at *m/z* 133 indicates the loss of the carboxylate group

(Figure 2.27B). The abundance of *m/z* 177 results from the loss of three methyl groups, two groups cleaved from the isopropyl side chain and one from the ester group.

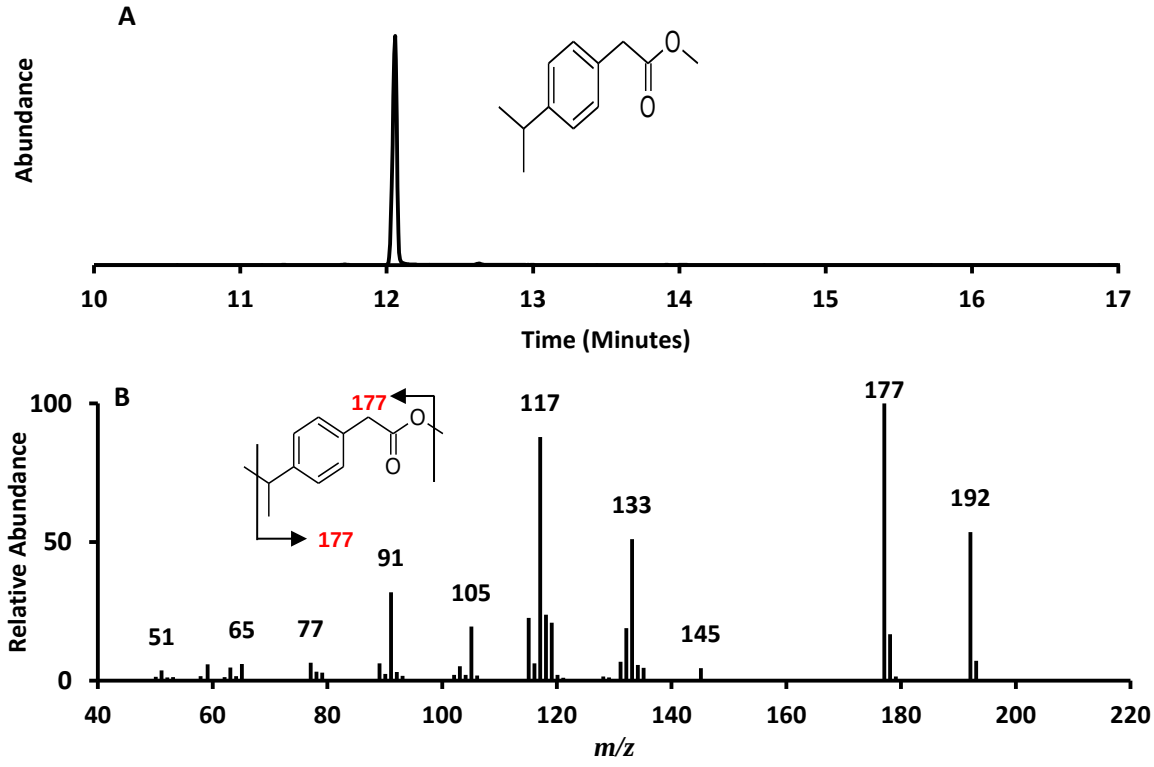

Figure 2.27. (A) Total ion current chromatogram of BF_3-MeOH esters for the authentic 4-isopropylphenylethanoic acid. (B) Mass spectra for the component at RT 12.05 minutes**.** GC-MS conditions as described in Figure 2.13.

The initial attempt at hydrogenation was carried out on the H-Cube® catalytic hydrogenator and the products derivatised with BF_3-MeOH. On examination of the GC chromatogram (Figure 2.28) it was apparent that only 15% of the reactant had been converted to the product. Analysis of the mass spectra for peaks eluting at RT 11.46 and 11.49 minutes (the cis-/trans isomers of the product)

show that the $M^{+\bullet}$ has increased by 6 Daltons (synonymous with the addition of 6 hydrogen atoms) to *m/z* 198. Ions at *m/z* 124 indicate loss of the alkanoate side chain, *m/z* 167 describes the loss of methanol and the ion at *m/z* 155 indicates loss of the isopropyl group. The peak at RT 11.46 has been assigned as the *trans* isomer due to the earlier elution.

Due to the low yield of hydrogenated product the experiment was repeated. The reactant was re-eluted through the H-Cube® on a further three occasions, however it was noted that at most only ~20% of the product was present in the final sample (Figure 2.28). It was postulated that this was because of steric hindrance caused by the structural properties of the isopropyl substituted group preventing the complete complexation of the π electrons attached to the aromatic ring and the 5% Rh/C catalyst thus hindering the reaction. Due to the potential hindrance the experiment was stopped at this point.

Analysis of the chromatograms (Figure 2.28A and B) and the mass spectra (Figure 2.28 C and D) reveal identical retention times and fragmentation patterns as detailed above.

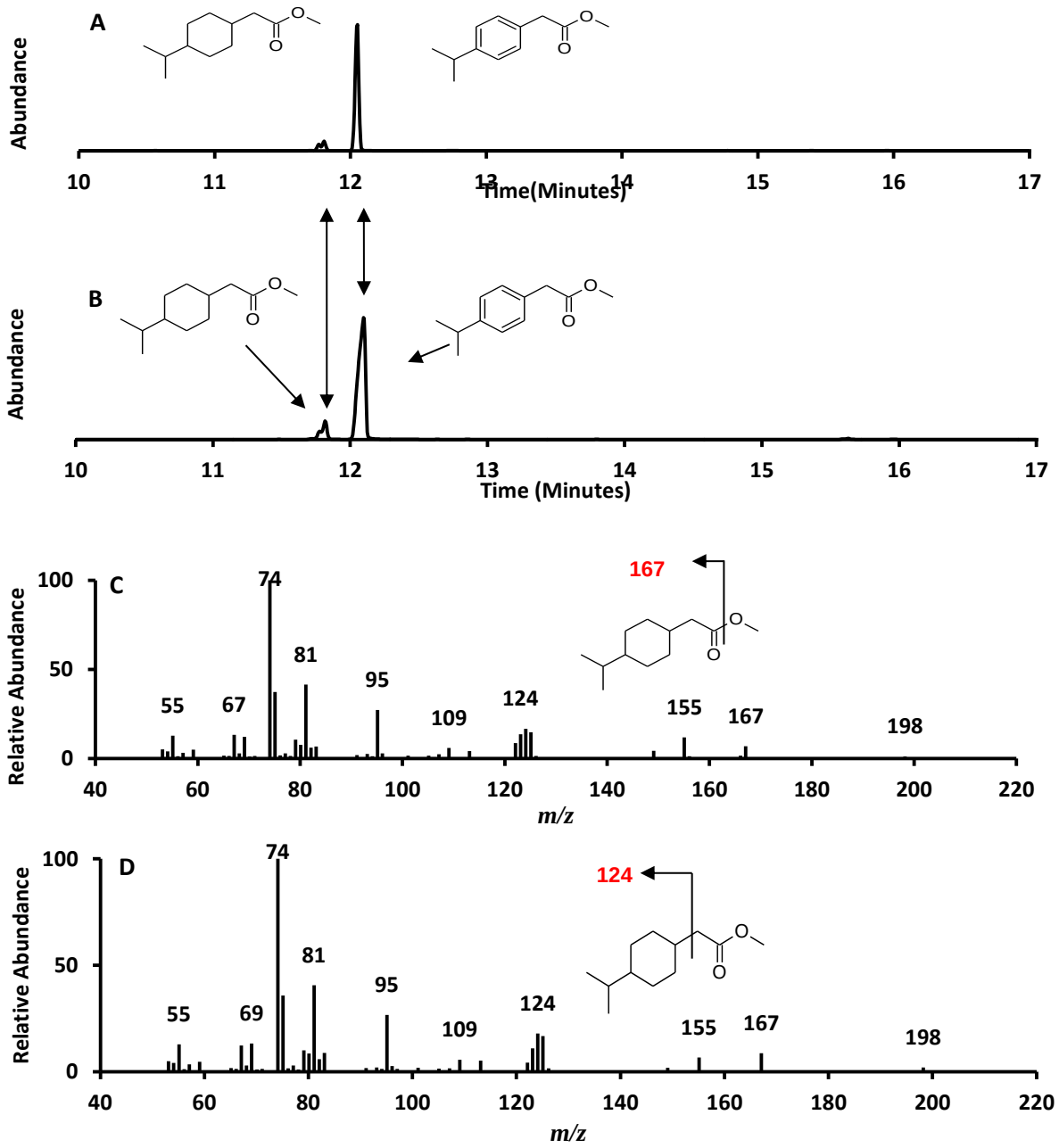

Figure 2.28 (A) Total ion current chromatogram of BF_3-MeOH methyl esters for initial hydrogenation of the reactant (4-isopropylphenylethanoic acid). (B) Product (cis-/trans 4-isoproylcyclohexylethanoic acid) for the subsequent H-Cube® elution's. (C) Mass spectrum for the component at RT 11.46 minutes (trans-4-isoproylcyclohexylethanoic acid). (D) Mass spectrum for the component at 11.49 minutes (cis-4-isoproylcyclohexylethanoic acid). GC-MS conditions as described in Figure 2.13.

The $M^{+\bullet}$ at *m/z* 198 in Figure 2.28C is not abundant enough to be clearly seen, this ion is shown in Figure 2.29 alongside other significant ions that have a poor abundance in Figure 2.28 (C and D) such as the M+1 ^{13}C abundance ion at *m/z* 199; loss of the methyl group at *m/z* 183; and a loss of H_2O at *m/z* 180.

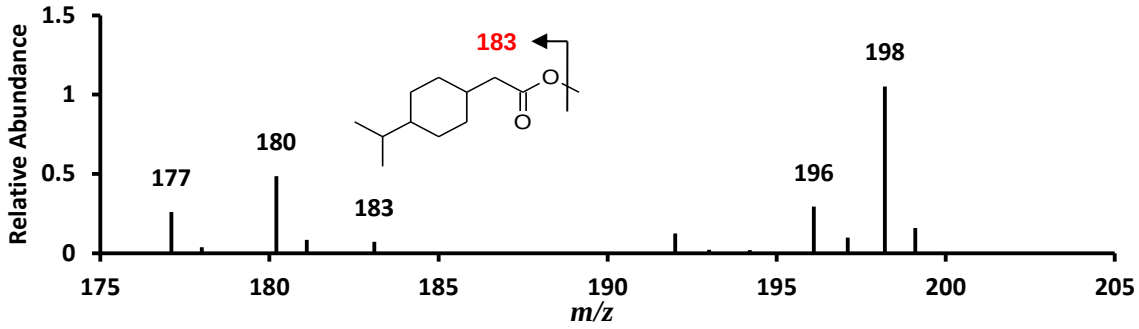

Figure 2.29. Close up of the *m/z* 198 region from the mass spectra for *trans*-4-isoproylcyclohexylethanoic acid.

2.3.5 Synthesis of *cis-/trans*-4'-n-pentylcyclohexylethanoic acid

The unpredictable nature of the catalytic hydrogenation observed with the preceding experiments, in which the H-Cube and particularly rhodium on carbon catalyst, was used with few reactions proceeding to complete saturation of the aromatic ring, suggested that investigation of hydrogenation with other catalysts might be worthwhile.

Therefore, 4-*n*-penylphenylethanoic acid was purchased from Sigma Aldrich (stated purity >99%) and converted to the methyl ester by heating at 70^{o}C for 30 minutes with BF_3-MeOH examined by GC-MS (Figure 3.16). The chromatogram (Figure 2.30A) displayed a single peak at RT 14.52 minutes. Analysis of the attendant mass spectra (Figure 2.29B) was consistent with the expected

compound. The $M^{+\bullet}$ at *m/z* 220 is consistent with the products molecular weight, the base ion at *m/z* 163 indicates loss of a butyl group from the alkyl side chain. The fragment ion at *m/z* 147 indicates the loss of the alkanoate group (Figure 2.30B). Figure 2.30C is a close up of the *m/z* 170-220 region in which ion abundance is too small to be displayed adequately in Figure 2.29B. This mass spectrum depicts the loss of a methyl group at *m/z* 205 and a methanol (M-32) at *m/z* 178.

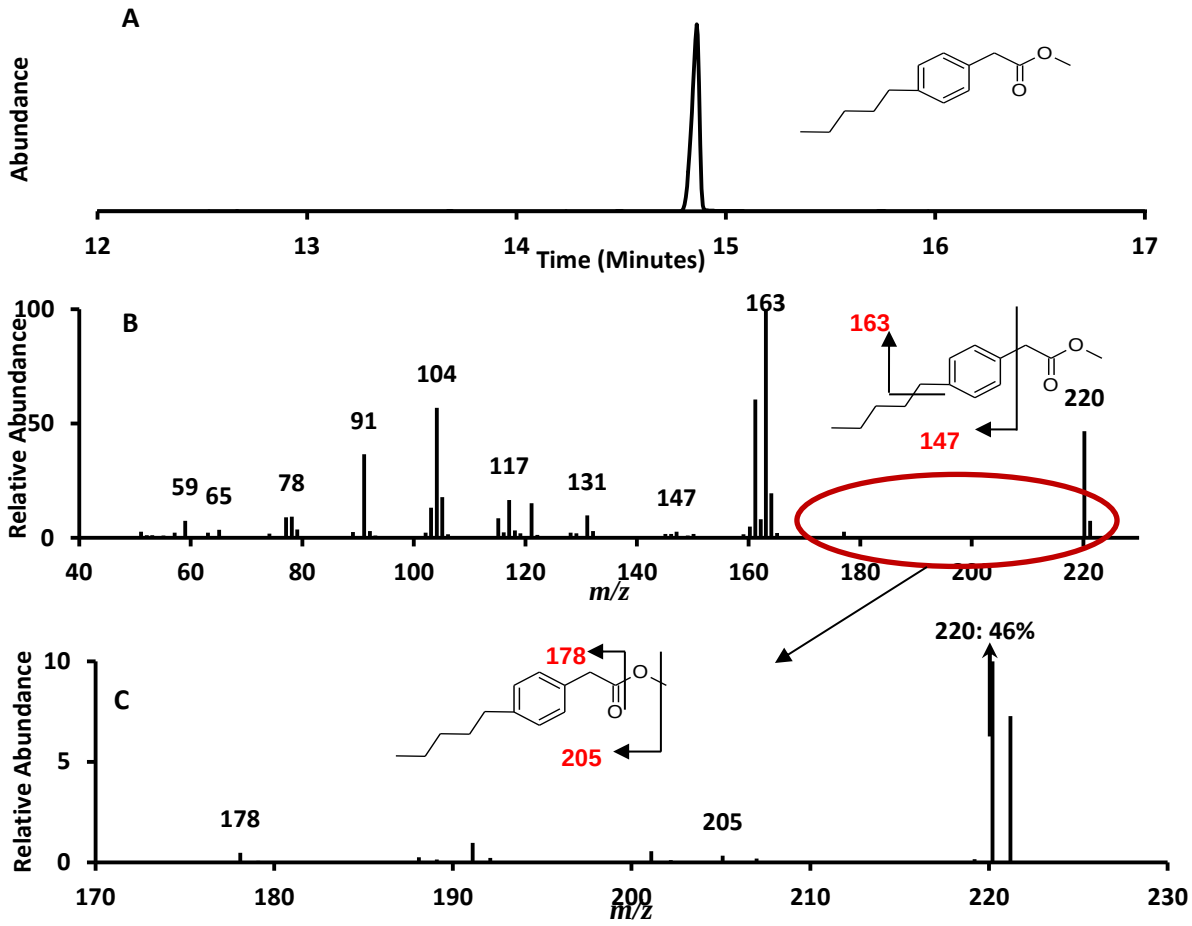

Figure 2.30. (A) Total ion current chromatogram of BF_3-MeOH esters for the authentic 4-n-pentylphenylethanoic acid; (B) mass spectra for the component at RT 14.52 minutes (C) mass spectra for the m/z 170-220 region of Figure 2.30B**.** GC-MS conditions as describedin Figure 2.13.

A sample of 4-*n*-pentylphenyl ethanoic acid was introduced to the H-Cube® (Figure 2.31) under the same conditions (80 bar and 80°C) with three separate catalysts (5% Rhodium over carbon (Rh/C) 5% Platinum over carbon (Pt/C) and 5% Palladium hydroxide over carbon (Pd (OH)/C)).

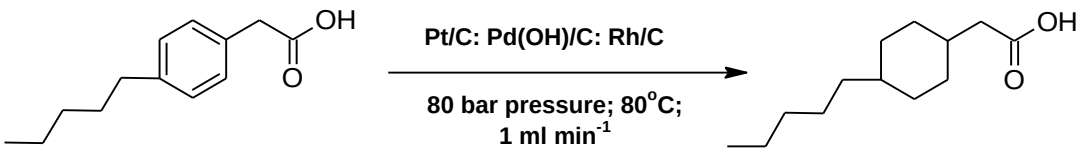

Figure 2.31. Reaction scheme for the catalytic hydrogenation of the reactant (4-n-pentylphenylethanoic acid) to the product (cis-/trans 4-n-pentycyclohexylethanoic acid)**;** plus the H-Cube® catalytic hydrogenation conditions

Figure 2.32 shows the chromatograms resulting from GC-MS examination of the methyl esters of the products from this experiment. It is shown that Pt/C (Figure 2.32A) did not hydrogenate the phenyl moiety at all whilst Pd(OH)/C (Figure 2.32B) only saturated 10% of the compound. However when Rh/C was used 96% of the phenyl moiety was driven to full saturation, a subsequent hydrogenation drove this reaction to >99% purity (Figure 2.32C&D).

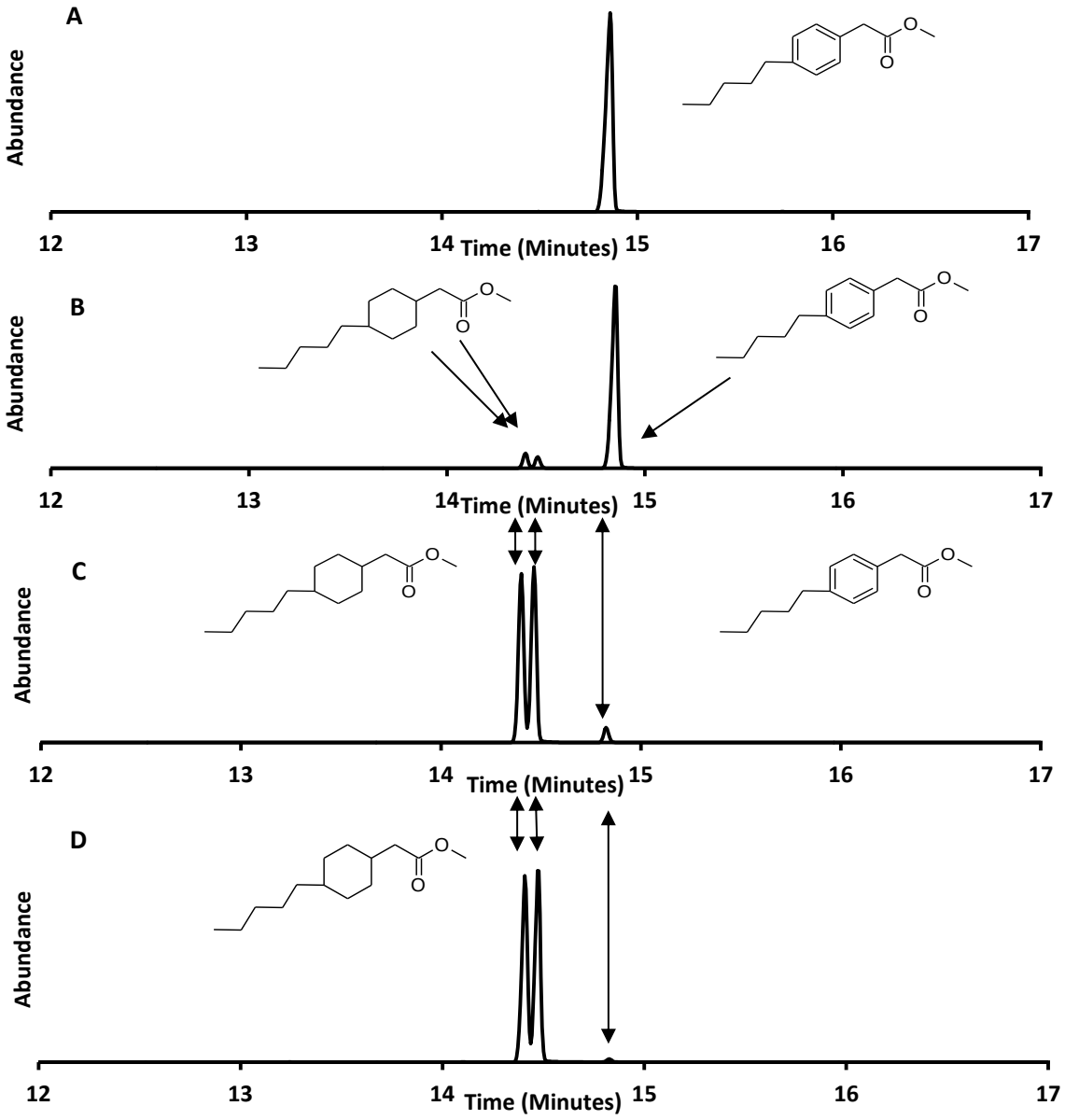

Figure 2.32. Total ion current chromatograms for the BF_3-MeOH methyl esters. (A) Hydrogenation attempt of 4-n-pentylphenylethanoic acid with Pt/C catalyst (peak RT 14.52 minutes). (B and C) Hydrogenation attempt with Pd(OH)/C and Rh/C catalysts respectively (peaks at RT 14.24 , 14.28 and 14 52 minutes). (D) Re-hydrogenation with Rh/C. GC-MS conditions as described in Figure 2.13.

As it is common for the *trans* isomer to elute first (Rowland et al., 2011d) the peak eluting at RT 14.24 minutes in Figure 2.32B has been assigned as the trans isomer and the peak eluting at 14.28 minutes has been assigned as the *cis* isomer.

Figure 2.33 shows the mass spectra connected to Figure 2.32; Figure 2.33A is assigned to the peak eluting at RT 14.52 and has been assigned as the reactant (4-n-pentylphenylethanoic acid methyl ester) and is described above. Figure 2.32B has been assigned as mass spectra of the *trans* isomer of 4-n-pentylcyclohexylethanoic acid (RT 14.24 minutes) and thus Figure 2.32C is assigned as the mass spectra of the *cis* isomer (RT 14.28 minutes).

The difference of 6 Daltons in the $M^{+\bullet}$ between Figure 2.32A and 2.32 B&C (*m/z* 220 and *m/z* 226 respectively) is consistent with the addition of 6 hydrogen atoms and significant ions are displayed in both mass spectra with the loss of the alkanoate side chain (*m/z* 152/153) and a methoxy group (*m/z* 195) apparent in both spectra.

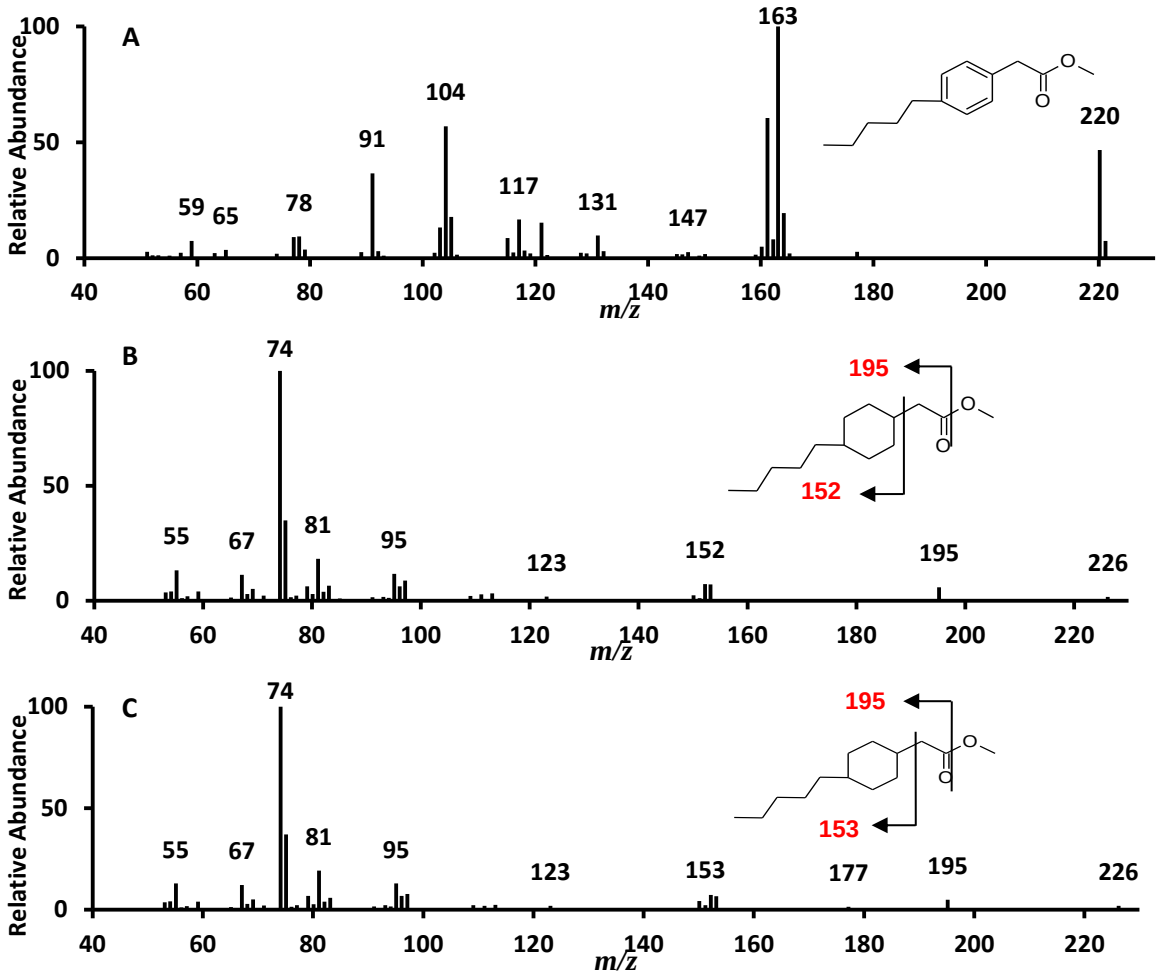

Figure 2.33. Mass spectra for (A) 4-n-pentylphenylethanoic acid; (B) trans 4-n-pentylcyclohexylethanoic acid; and (C) cis 4-n-pentylcyclohexylethanoic acid. GC-MS conditions as described in Figure 2.13.

2.3.6. Synthesis of cis-/trans 4-nonylphenylethanoic acid

This acid was synthesised in house for a previous study (unpublished data). A small amount was converted to the methyl ester by reacting with the BF_3-MeOH complex (70^{o}C; 30 minutes) and the results analysed by GC-MS (Figure 2.34A&B). The resulting chromatogram (Figure 2.34A) displayed a single peak at RT 19.01 minutes which was confirmed as 4-nonylphenylethanoic acid (purity >99%) by analysis of the mass spectra (Figure 2.34B&C).

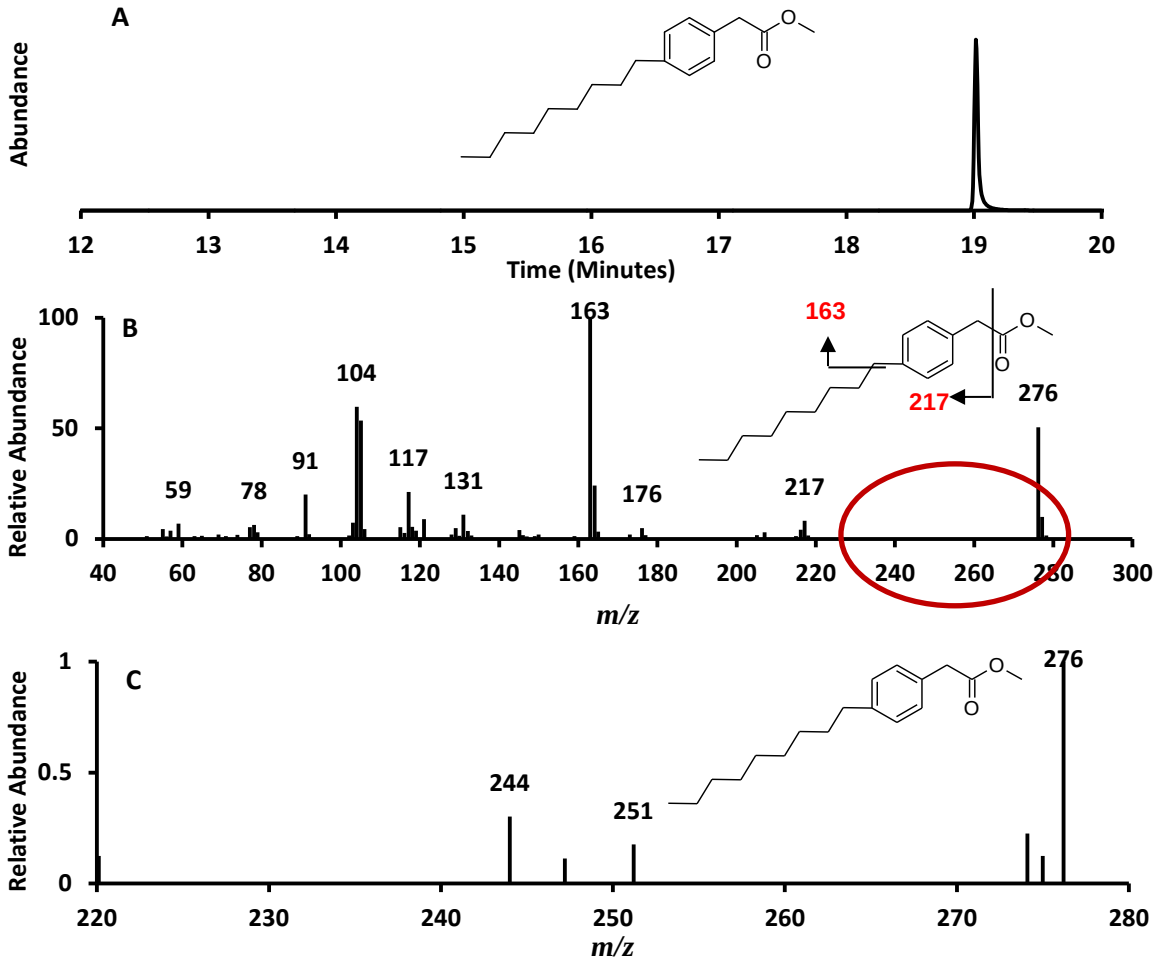

Figure 2.34. (A) Total ion current chromatogram of BF_3-MeOH esters for the synthesised 4-n-nonylphenylethanoic acid. (B) Mass spectrum for the methyl ester of 4-n-nonylphenylethanoic acid. (C) Mass spectrum for the *m/z* 220-280 region for the methyl ester of 4-n-nonylphenylethanoic acid**.** GC-MS conditions as described in Figure 2.13.

Figure 2.34B displays a $M^{+\bullet}$ of *m/z* 276 consistent with the molecular weight of 4-nonylphenylethanoic acid; significant fragment ions included *m/z* 217 indicating the loss of a carboxylate group and *m/z* 163 indicating cleavage of an octane from the nonyl side chain. Figure 2.34C shows a close up of the *m/z* 220-280 region of Figure 2.34B. It can be seen that there is a significant (though weak) fragment at *m/z* 244 indicating loss of a methanol group (M-32).

A 20 mg sample in 20 mL of MeOH of 4-nonylphenylethanoic acid was introduced to the H-Cube® for catalytic hydrogenation with a Rh/C catalyst at 80 bar pressure and 80°C (Figure 2.35).

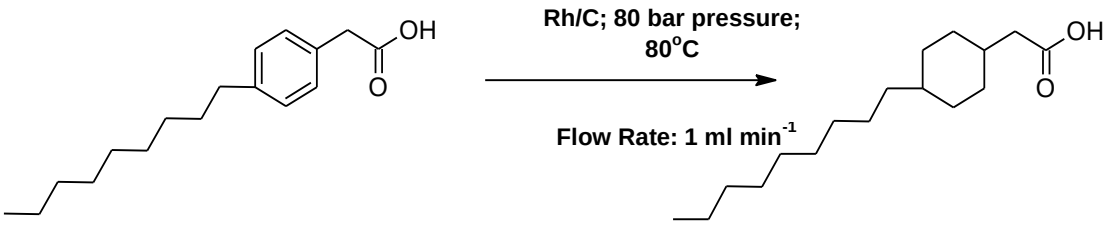

Figure 2.35. Depicting the reactant 4-n-nonylphenylethanoic acid; the product, cis-/trans 4-n-nonylcyclohexylethanoic acid plus the H-Cube® catalytic hydrogenation conditions

Only one attempt was made to convert the nonylphenylethanoic acid to the cyclohexyl moiety as there was a limited availability of the H-Cube® hydrogenator at that time and there were some concerns as to whether the resultant product would be soluble enough to assess on the Microtox™ assay (Chapter 3). It was decided that this compound would not be re-hydrogenated in the Buchii reaction chamber.

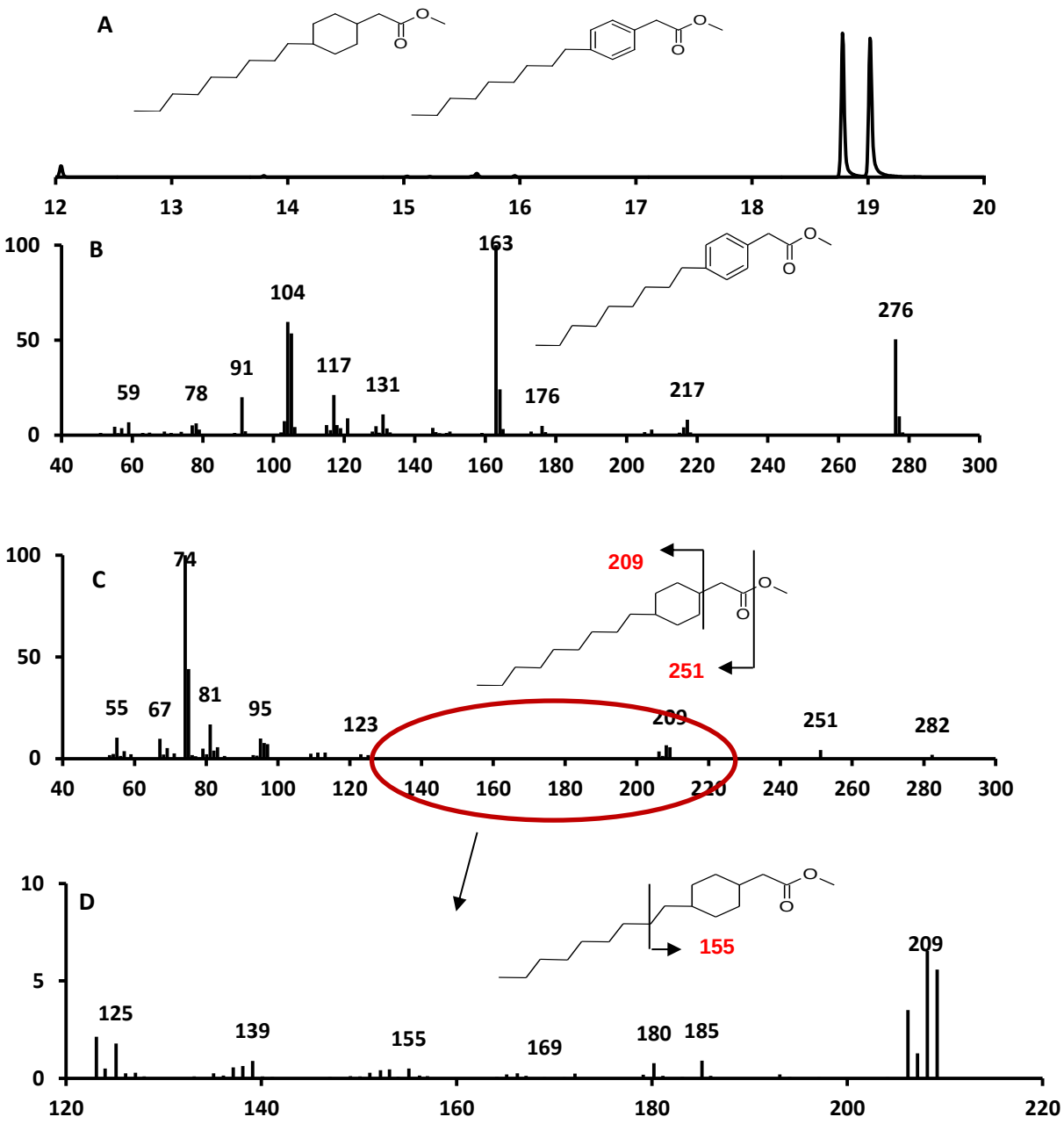

Figure 2.36. (A) Total ion current chromatogram of BF_3-MeOH esters for the reactant (4-n-nonylphenylethanoic acid) and the product (cis-/trans 4-n-nonylcyclohexylethanoic acid). (B) Mass spectrum for the compound eluting at RT18.47 Minutes. (C) Mass spectrum of the compound eluting at RT 19.01 Minutes. (C) Close up of the *m/z* 120-220 region in Figure 2.36B. GC-MS conditions as described in Figure 2.13.

Analysis of the BF_3-MeOH methyl esters of the product with GC-MS revealed that there are two distinct peaks apparent in the chromatogram (RT 18.47 and 19.01 respectively). Analysis of the mass spectra allowed peak 'a' in Figure 2.36A to be assigned as the desired product cis-/trans 4-n-nonylcyclohexylethanoic acid with a yield of 52% and peak b as the reactant (4-n-nonylphenylethanoic acid). The mass spectra for peak 'b' (Figure 2.36B) has been described previously. The spectra for Figure 2.36A was able to be assigned as cis-/trans 4-n-nonylcyclohexylethanoic acid due to the presence of significant ions.

The $M^{+\bullet}$ is 6 Daltons greater than that of the mass spectra of 4-n-nonylphenylethanoic acid, indicating the addition of 6 hydrogen atoms. Also present are fragment ions at m/z 251 (M-31) indicating loss of a methoxy group and m/z 209 indicating the loss of the alkanoate side chain. Analysis of Figure 2.34C allows a determination of ions too weak to be seen in Figure 2.36B. There is a weak fragment ion at m/z 169 indicating benzylic cleavage on the nonyl side chain and an ion at m/z 155 showing the cleavage of the nonyl side chain from the cyclohexyl ring.

2.3.7. Synthesis of cis-/trans 4-tertiarybutylcyclohexylethanoic acid

The acid of interest was synthesised for a previous study (Smith et al., 2008?) and had a stated purity of >99%. A sample of this acid was converted to the methyl esters by reacting with a BF_3-MeOH complex (70^{o}C; 30 minutes) and the resultant product was analysed by GC-MS for purity (Figure 2.37). Figure 2.35A shows one distinct peak (RT 12.55 minutes; purity >99%); analysis of the mass spectra reveals significant ions that are consistent with the methyl esters of 4-t-

butylphenylethanoic acid.

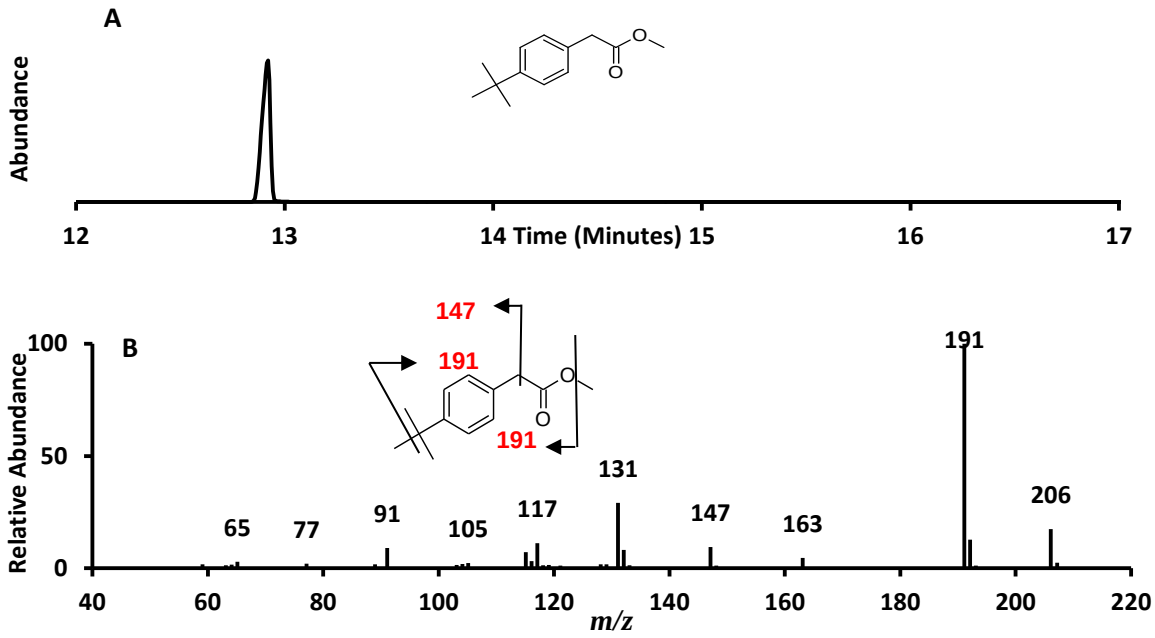

Figure 2.37. (A) Total ion current chromatogram of BF_3-MeOH esters for the synthesised 4-t-butylphenylethanoic acid. (B) Mass spectrum for the methyl ester of 4-t-butylphenylethanoic acid. GC-MS Conditions as described in Figure 2.13.

The $M^{+\bullet}$ is apparent at *m/z* 206 consistent with the molecular weight of 4-t-butylphenylethanoic acid. The base ion at *m/z* 191 (M-15) indicates loss of methyl groups from the ester and the butyl group; M-59 (*m/z* 147) shows cleavage of a carboxylate group and a weak ion at *m/z* 132 indicates loss of the alkanoate side chain.

Conversion of 4-t-butylphenylethanoic acid to cis-/trans 4-t-butylcyclohexylethanoic acid (Figure 2.38) was attempted for a collaborative study with an external laboratory. A sample (100 mg) was introduced to the H-Cube hydrogenator using a Rh/C catalyst at 80^{o}C; 80 bar pressure and a flow rate of 1 mL min^{-1}.

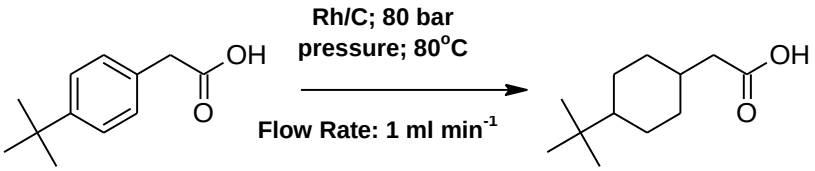

Figure 2.38. Depicting the reactant 4-t-butylphenylethanoic acid; the product, cis-/trans 4-t-butylcyclohexylethanoic acid plus the H-Cube® catalytic hydrogenation conditions.

Initial hydrogenation of 4-t-butylphenylethanoic acid with the H-Cube did not elicit any change. Analysis of the chromatogram (Figure 2.39A) shows one distinct peak at RT 12.55, the same RT as that displayed in Figure 2.37A and analysis of the mass spectrum (Figure 2.39D) confirmed that this peak could be assigned as the reactant (4-t-butylphenylethanoic acid). It was determined that the catalyst had been contaminated and was no longer able to affect the conversion of the reactant to the product.

The reaction was attempted again with a new catalyst and was analysed through GC-MS (Figure 2.39B). The chromatogram displays two peaks; peak ‘a’ (RT 12.39 minutes: 89% yield) was assigned as the product through analysis of the mass spectra (Figure 2.39E), peak ‘b’ was assigned as the reactant as it had the same retention time and mass spectral data as the synthetic standard analysed in Figure 2.37.

Analysis of Figure 2.39D revealed that the $M^{+\bullet}$ was 6 Daltons greater than the $M^{+\bullet}$ shown in Figure 2.39C. The mass spectra for the compound assigned as the product (cis-/trans 4-t-butylcyclohexylethanoic acid) also revealed significant ions

consistent with this product. M-15 (m/z 197) indicates loss of a methyl group and the ion at m/z 181 is consistent with cleavage of a methoxy group. There is a weak ion at m/z 155 which indicates cleavage of the butyl group from the cyclohexyl ring. The presence of m/z 81 also indicates the presence of a cyclohexyl ring. A yeld of 89% (Figure 2.39B) was deemed to be pure enough as the study was not for toxicological effects.

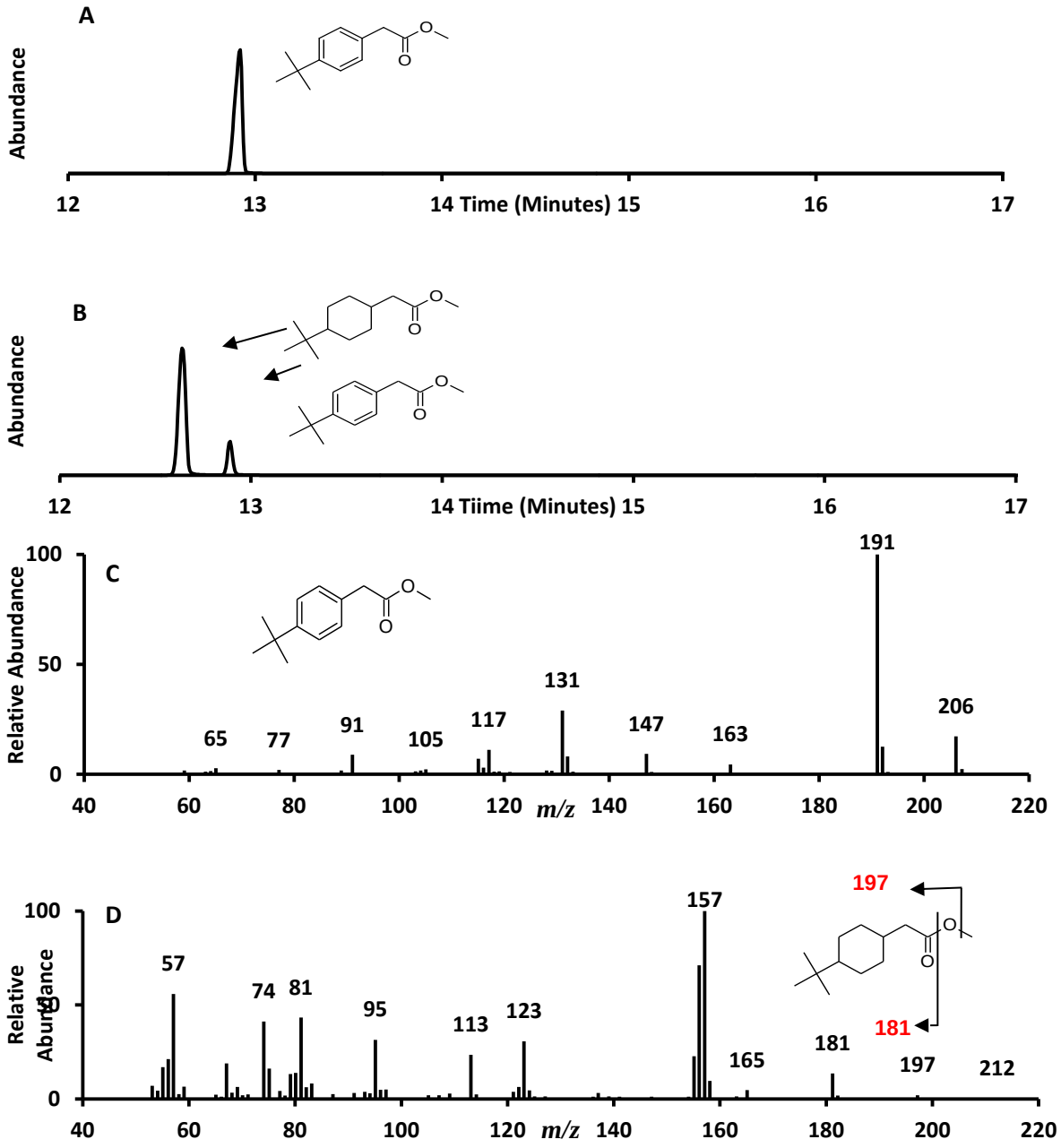

Figure 2.39 (A) Total ion current chromatogram of BF_3-MeOH esters for the intial hydrogenation of the synthesised 4-t-butylphenylethanoic acid. (B) Chromatogram for the final hydrogenation. (C) Mass spectrum for the methyl ester of 4-t-butylphenylethanoic acid. (D) Mass spectrum for 4-t-butylcyclohexylethanoic acid. GC-MS conditions as described in Figure 2.13.

2.3.8. Synthesis of cis-/trans 4-tertiarybutylcyclohexylbutanoic acid

An attempt was made to synthesise a mixture of cis-/trans 4-t-butylylphenylbutanoic by hydrogenation of 4-t-butylphenylbutanoic acid (Figure 2.40).

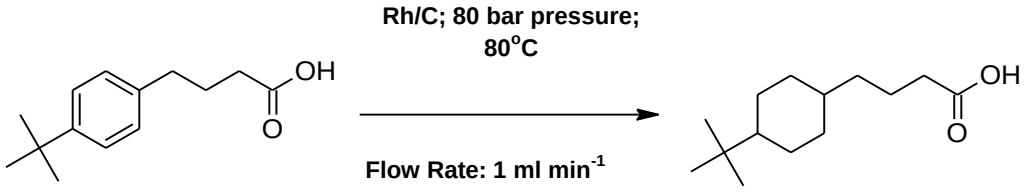

Figure 2.40. Depicting the reactant 4-t-butylphenylbutanoic acid; the product, cis-/trans 4-t-butylcyclohexylbutanoic acid plus the H-Cube® catalytic hydrogenation conditions.

A sample of 4-t-butylphenylbutanoic acid was synthesised for a previous study (Smith et al., 2008) and converted to methyl esters by reacting with a BF_3-MeOH complex for 30 minutes at 70°C (Figure 2.41). This sample was analysed by GC-MS (Figure 2.39); the chromatogram depicts one peak at RT 15.14 minutes and a smaller isomer peak (~1%) at RT14.43 minutes (Figure 2.41A) indicating the reactant was >99% pure.

Analysis of the mass spectra (Figure 2.41B) reveals significant ions consistent with the reactant are present. The $M^{+\bullet}$ is *m/z* 234 which matches the molecular weight of 4-t-butylphenylbutanoic acid; *m/z* 219 indicates loss of a methyl group and that this the base ion is due to the ability for this compound to lose methyl four separate methyl groups; one from the ester and three from the butyl side chain. A loss of an ethanoate group (M-74) is indicated by the *m/z* 160 ion and a weak *m/z* 133 is characteristic of a loss of the alkanoate side chain. A close up of

the *m/z* 160-210 region (Figure 2.41C) reveals a weak *m/z* 177 indicating cleavage of the butyl side chain from the phenyl moiety and an *m/z* 202 consistent with the loss of methanol.

Figure 2.41D is the mass spectrum from the isomer revealed by the small chromatographic peak at RT 14.43 minutes. Analysis revealed that significant ions are present ($M^{+\bullet}$ *m/z* 234); loss of methyl fragment (*m/z* 219); loss of methanol (*m/z* 202); cleavage of the butyl side chain (*m/z* 177); and loss of an ethanoate group and the alkanoate side chain (*m/z* 160 and *m/z* 133 respectively). .

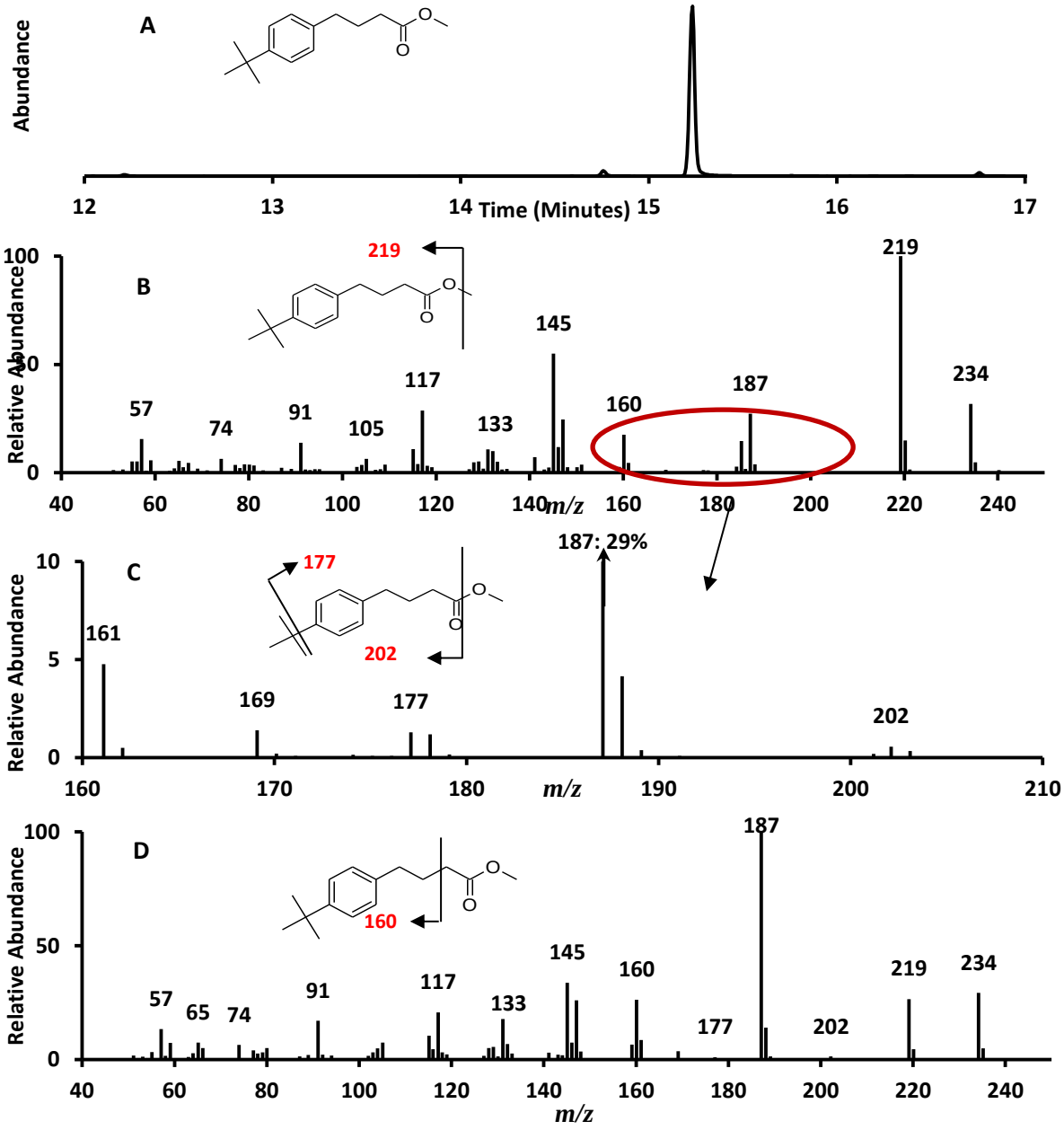

Figure 2.41 (A) Total ion current chromatogram of BF_3-MeOH esters for the synthesised 4-t-butylphenylbutanoic acid. (B) Mass spectrum for the methyl ester of 4-t-butylphenylethanoic acid (RT 15.14 Minutes) (C) Close up of the *m/z* 160-210 region in Figure 2.39B. (D) Mass spectrum for the methyl ester of the isomer of 4-t-butylphenylethanoic acid (RT 14.43 Minutes). GC-MS Conditions as described in Figure 2.13.

A 100 mg sample of the product (in 20 mL MeOH) was introduced to the H-Cube® where it was flowed at 1 mL min-1 over a Rh/C catalyst at 80 bar pressure and 80^{o}C. The resultant product was analysed by GC-MS. Figure 2.42 shows the chromatogram from this experiment and it can be seen that only one major peak at RT 15.14 minutes and a smaller peak at RT 14.43 minutes are apparent. These RT match the RTs of the reactant so it was deemed that the initial elution through the H-Cube® had no effect (Figure 2.42A). Three subsequent experiments were carried out and analysed with GC-MS. Figure 2.42B shows two distinct major peaks (RT 15.03 and 15.14) alongside the minor peak assigned as the reactants isomer. A yield of 28% of the product was noted after the second elution, however two more elutions could not increase the yield and it was hypothesised that some steric hindrance was occurring that was preventing a full conversion.

Mass spectral analysis of the peak at RT 15.03 and RT 15.43 allowed these peaks to be assigned as the product and the reactant respectively (4-t-butylcyclohexylbutanoic acid). Figure 2.42C depicts the mass spectra of the reactant which has been described previously. Figure 2.42D displays significant ions which are consistent with the product. An increase of 6 Daltons in the $M^{+\bullet}$ is characteristic of the addition of 6 hydrogen atoms at *m/z* 242. Loss of methanol (M-32) is indicated by the fragment ion at *m/z* 208 and a cleavage on the alkanoate side chain is consistent with the ions *m/z* 87 and *m/z* 152, loss of the butyl side chain is characterised by the ion at *m/z* 183 and 57 and *m/z* 81 is indicative of a cyclohexyl ring.

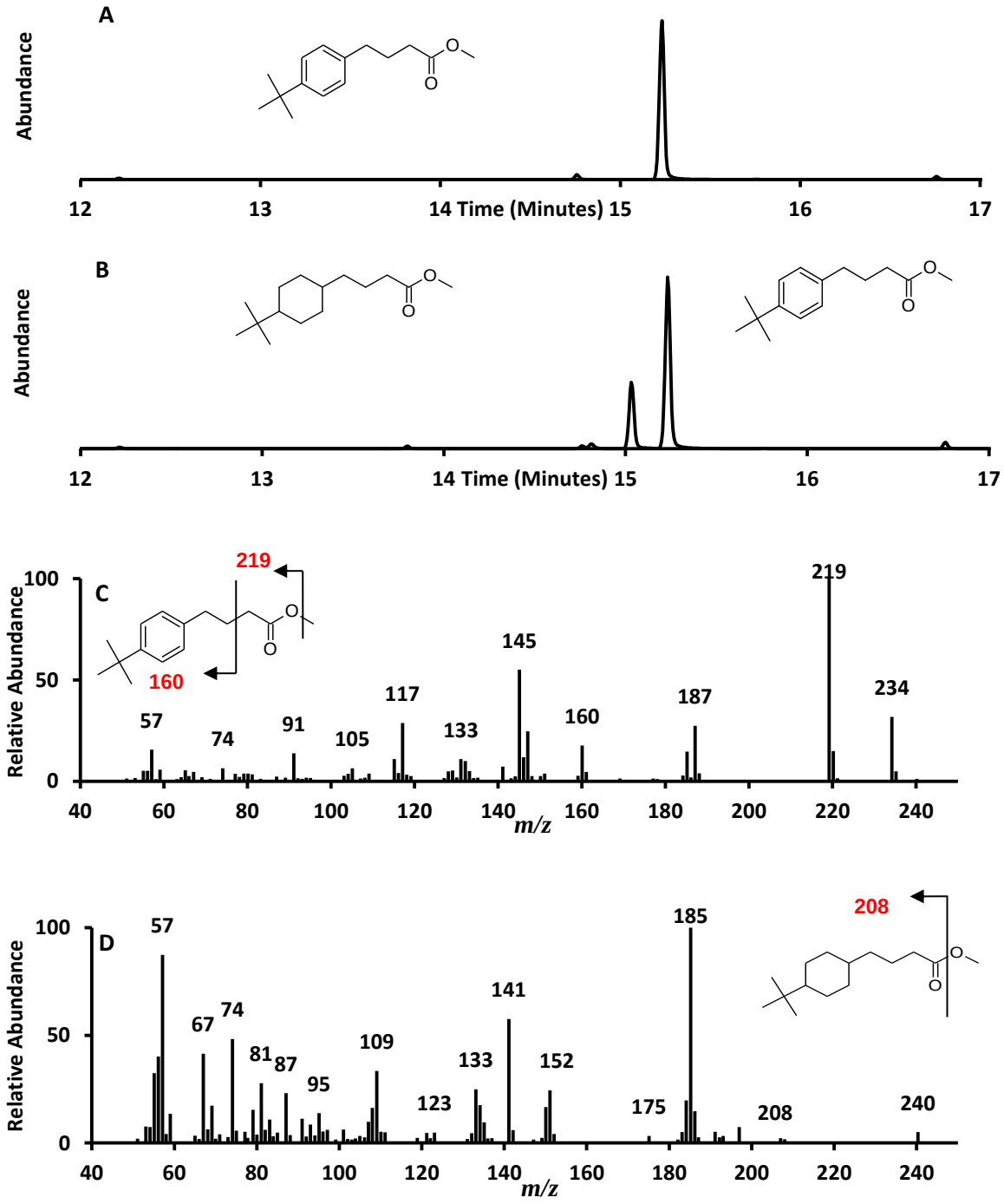

Figure 2.42(A) Total ion current chromatogram of BF_3-MeOH esters for the intial hydrogenation of the synthesised 4-t-butylphenylbutanoic acid. (B) Chromatogram for the subsequent hydrogenation attempt. (C) Mass spectrum for the methyl ester of 4-t-butylphenylbutanoic acid. (D) Mass spectrum for 4-t-butylcyclohexylbutanoic acid. GC-MS conditions were as described in Figure 2.13.

2.3.9. Synthesis of octahydro-1*H*-indene-2-carboxylic acid and 1-methyloctahydro-1*H*-indene-2-carboxylic acid

For purposes of identification within the commercial mixtures or the acid extracts of the oil sands process affected waters samples of indane-2-carboxylic acid and 1-methyl-1*H*-indene-2-carboxylic acid were hydrogenated with the H-Cube catalytic hydrogenator. A small sample of each was reacted with the BF_3-MeOH complex and analysed with GC-MS to assess purity (Figure 2.43).

Figure 2.43 (A) shows one distinct peak (RT 11.59 minutes) and a number of lesser peaks. However analysis showed that these lesser peaks arose from a slight contamination in the solvent so the reactant was assigned as >99% pure and later elutions proceeded with clean solvent. Analysis of the mass spectra (Figure 2.43B) showed significant ions that are characteristic of the reactant. The $M^{+\bullet}$ is assigned at *m/z* 176, corresponding to the molecular weight of indane-2-carboxylic acid methyl ester. Fragment ions are seen at *m/z* 161, 145 and 116 corresponding to loss of a methyl group, a methoxy group and the alkanoate group respectively. The fragments at *m/z* 102 and 91 indicate a cleavage of the cyclopentyl ring leaving methyl benzene (*m/z* 91) and a methyl 2-methylpropanoate (*m/z* 102) as major fragments. Smaller ion fragments (*m/z* 77, 65 and 51) alongside *m/z* 91 are indicative of benzylic cleavage and indicate loss of an ethyne (*m/z* 26) from the methyl benzene (*m/z* 91-65) and from a charged benzene ring ($C_6H_5^+$; *m/z* 77).

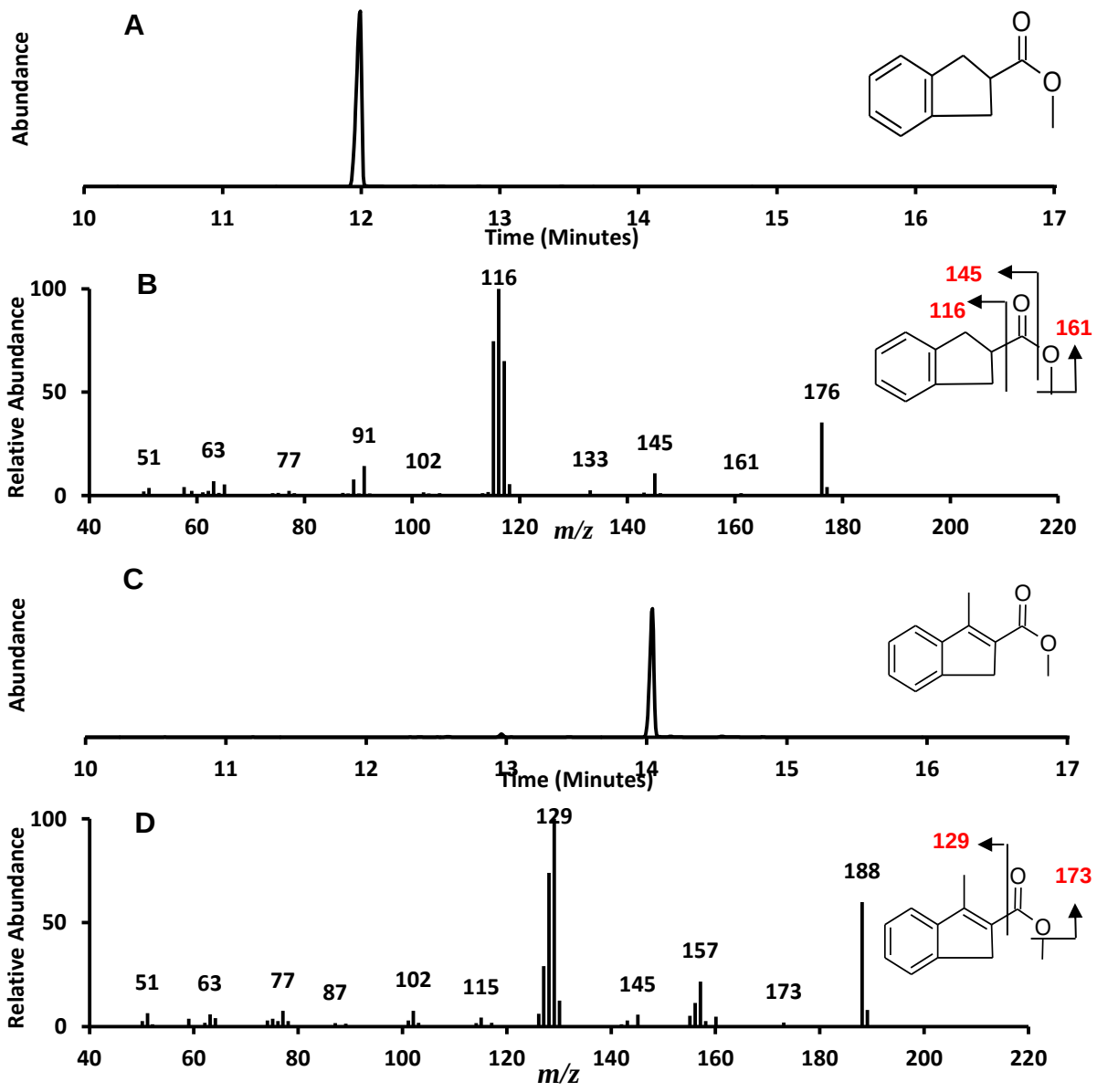

Figure 2.43. (A) Total ion current chromatogram of BF_3-MeOH esters for the authentic indane-2-carboxylic acid; (B) mass spectra for the methyl ester of indane-2-carboxylic; (C) Total ion current chromatogram of BF3-MeOH esters for the authentic 1-methyl-1H-indene-2-carboxylic acid (D) mass spectra for the methyl ester of 3-methyl-1H-indene-2-carboxylic acid. GC-MS Conditions as described in Figure 2.13.

Figure 2.43(C) also shows one distinct peak (RT 14.02 minutes >99% pure), analysis of the mass spectra (Figure 2.43D) reveals significant ions consistent with an assignment of 1-methylindene-2-carboxylic acid. The $M^{+\bullet}$ is assigned as *m/z* 188 consistent with the molecular weight of the reactant. Major fragment ions are noted at *m/z* 173, 157 and 129 (base ion) these ions correspond to the loss of the alkanoate side chain (*m/z* 60) a methoxy group (*m/z* 31) and a methyl group (*m/z* 15). The fragment at *m/z* 115 is consistent with the cleavage of the benzene ring leaving a methyl (2*Z*)-2-methylbut-2-enoate fragment. Ions consistent with a benzene ring (*m/z* 77 and 65) are also apparent.

An attempt was made to synthesise octahydro-1*H*-indene-2-carboxylic acid and 1-methyloctahydro-1*H*-indene-2-carboxylic acid utilising the H-Cube® (Figure 2.44A&B).

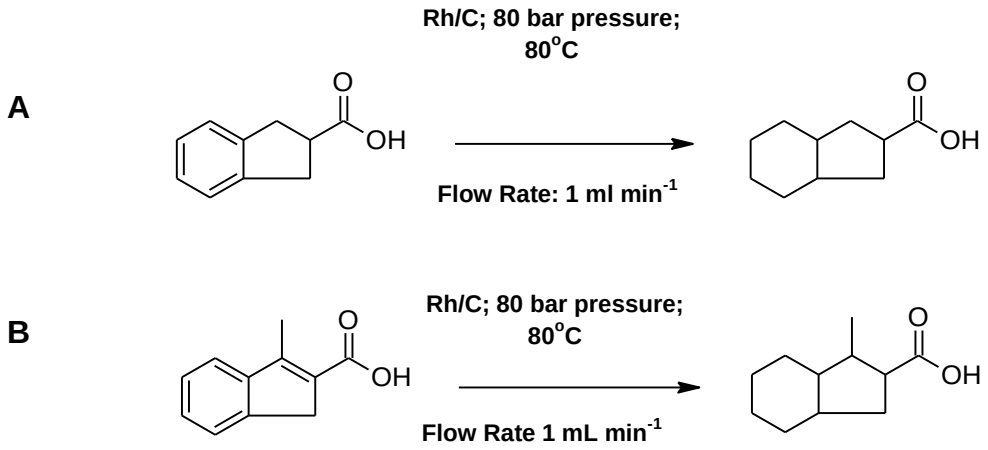

Figure 2.44. (A) Depicting the reactant indane-2-carboxylic acid; the product, octahydro-1H-indene-2-carboxylic acid; and (B) the reactant 1-methyl-1H-indene-2-carboxylic acid the product, 1-methyloctahydro-1H-indene-2-carboxylic acid plus the H-Cube® catalytic hydrogenation conditions.

A sample (100 mg in 20 mL MeOH) of each acid was eluted through the H-Cube® catalytic hydrogenator at 80^{o}C and 80 bar pressure at a flow rate of 1 mL min^{-1}. This elution was repeated before the products were reacted with BF_3-MeOH and analysed on a GC-MS (Figure 2.45).

Figure 2.45 shows five distinct peaks, peak E (RT 11.59 minutes) has the same retention time as the reactant and is assigned as such, this peak has a yield of 25% relative to the sum of all the peaks and shows that 75% of the reactant was converted to a product (Table 2.1). Analysis of the mass spectrum confirms the assignment of the reactant (Figure 2.46E), significant ions in the mass spectrum are $M^{+\bullet}$ *m/z* 176, a base ion at *m/z* 116 highlighting a loss of the alkanoate side chain and ions at *m/z* 161 and 145 for loss of methyl and methoxy respectively.

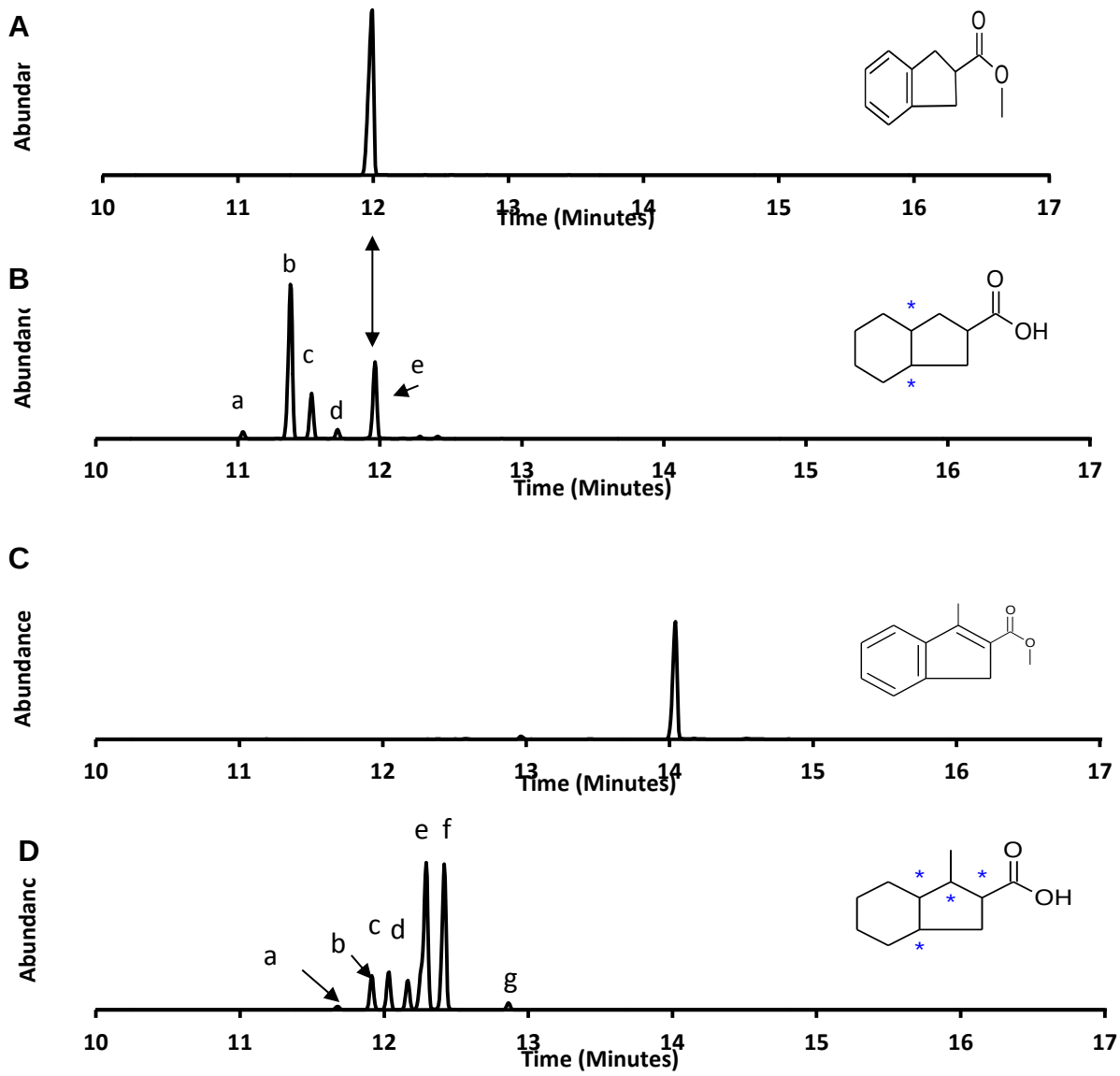

Figure 2.45. (A) Total ion current chromatogram of BF_3-MeOH esters for the reactant (authentic indane-2-carboxylic acid). (B) Total ion current chromatogram for the methyl esters of the catalytic hydrogenation products from chromatogram A. (C) Total ion current chromatogram of BF_3-MeOH esters for the reactant (authentic 1-methyl-1H-indene-2-carboxylic acid). (D) Total ion current chromatogram for the methyl esters of the catalytic hydrogenation products from chromatogram C; blue stars indicate stereo centres. GC-MS Conditions as described in Figure 2.13.

Table 2.1. Yield of chromatographic peaks from products of the catalytic hydrogenation of indane-2-carboxylic acid and 3-methyl-1*H*-indene-2-carboxylic acid

Indane-2-carboxylic acid Hydrogenation Products		3-methyl-1H-indene-2-carboxylic acid Hydrogenation Products	
Peak	% Yield	Peak	% Yield
A	2.15	A	0.89
B	54.83	B	7.39
C	14.51	C	8.53
D	3.00	D	6.70
E	25.51	E	41.35
		F	33.62
		G	1.53

Therefore peaks A-D in Figure 2.46B are assigned as products, analysis of the mass spectra for these peaks reveals that three of the peaks can be assigned as fully saturated octahydro--1*H*-indene-2-carboxylic acid (peaks A-C) and one peak can be potentially assigned as a partially saturated 2,3,3a,4,5,6-hexahydro-1*H*-indene-2-carboxylic acid (Peak D). Analysis of the mass spectra in Figure 2.46A-

C reveals a similar $M^{+\bullet}$ (*m/z* 182) which is consistent with the addition of six hydrogen atoms to the reactant and therefore increasing the molecular weight by 6 Daltons. However there are a few differences between Figure 2.46 A and C and Figure 2.46B. Both mass spectra for the chromatographic peaks A and C (Figure 2.46A and C) show low abundance in the fragment ions associated with the cleavage of the alkanoate side chain (*m/z* 150 and *m/z* 123) and base ions in the *m/z* 87 or 96 region. However the base ion in Figure 2.46A is *m/z* 96 with *m/z* 87 at a 90% relative abundance while the base ion in Figure 2.46C is m/z 87 with *m/z* 96 at 99% relative abundance.

These two ions (*m/z* 87 and 96) can be associated with the cleavage of the cyclopentyl ring leaving a methyl-cyclohexane fragment and a methylpropanoate fragment; *m/z* 81 and *m/z* 67 are indicative of cycloalkanes.

Figure 2.46B shows distinct differences. The $M^{+\bullet}$ is assigned as *m/z* 182 which is consistent with an octahydro-1*H*-indene-2-carboxylic acid however there the similarity with the other two isomers ends. The base ion in Figure 2.46B is *m/z* 81 (indicative of cycloalkanes) and the $M^{+\bullet}$ at *m/z* 182 is shown to be the second most abundant ion (relative abundance of 94%). Significant fragments are revealed at *m/z* 167 (loss of methyl) *m/z* 150 (loss of methanol) and *m/z* 123 (loss of the alkanoate side chain). A fragment at *m/z* 87 is also apparent signifying cleavage of the cyclopentyl ring to leave a methylpropanoate group. Figure 2.46D has been potentially assigned as a partially saturated 2,3,3a,4,5,6-hexahydro-1*H*-indene-2-carboxylic acid.

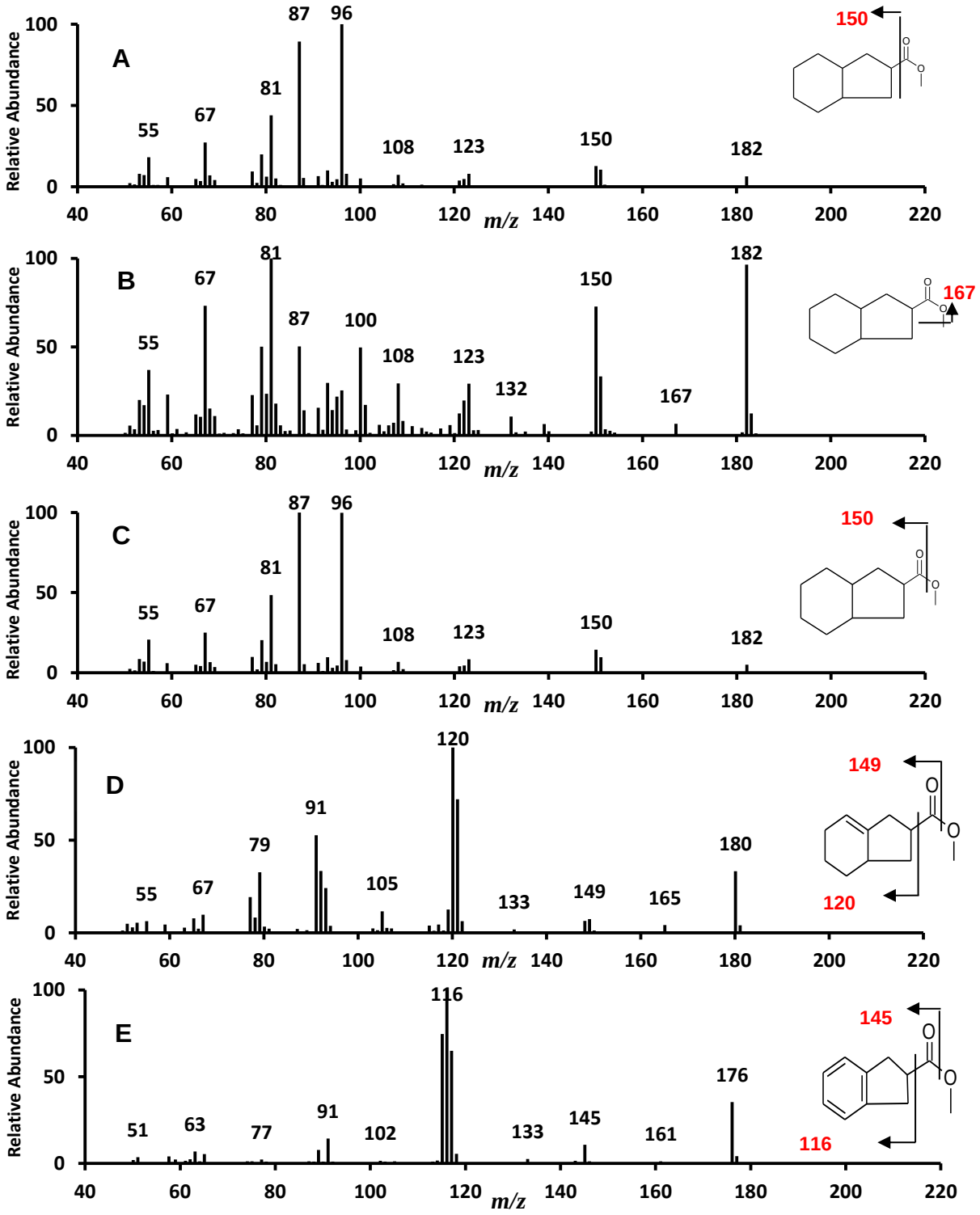

Figure 2.46. Mass spectrum (A, B & C) of stereo isomers of octahydro-1H-indene-2-carboxylic acid. (D) A postulated 2,3,3a,4,5,6-hexahydro-1H-indene-2-carboxylic acid. (E) Indane-2-carboxylic acid; MS conditions as described above in Figure 2.13.

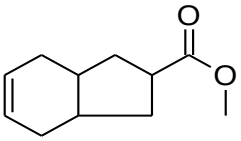

Figure 2.47. Structure of 2,3,3a,4,7,7a-hexahydro-1*H*-indene-2-carboxylic acid methyl ester.

The $M^{+\bullet}$ at *m/z* 180 indicates that only four hydrogen atoms have been added to the aromatic ring, however from this mass spectra it is difficult to deduce where the double bond lies within the cyclohexyl moiety, the spectra could easily describe 2,3,3a,4,7,7a-hexahydro-1*H*-indene-2-carboxylic acid (Figure 2.47).

Significant ions present in the mass spectra of Figure 2.46D are *m/z* 165, 149 and 120 indicating the groups that arise from loss of the alkanoate side chain; there are no ions apparent in the mass spectra which would allow an assignment for the positioning of the double bond. Figure 2.46E shows the mass spectrum of the peak assigned to the remaining reactant and is described above in Figure 2.43.

Figure 2.45D depicts a chromatogram for the products from the catalytic hydrogenation of 1-methyl-1*H*-indene-2-carboxylic acid. It can be seen that there are five distinct peaks (b-f) and two lesser peaks (a and g). Retention times of these peaks range from 11.38 minutes (peak a) to 12.52 minutes (peak g); comparison with the single chromatographic peak assigned to the reactant in Figure 2.45C (RT 14.02) suggests that all of the reactant has been converted to either fully saturated or partially saturated products. Analysis of the mass spectra will confirm this hypothesis.

Figure 2.48 (A-D) depicts the mass spectra for the chromatographic peaks (a-d) in Figure 2.45D. Figure 2.48E depicts a close up of the *m/z* 80-125 region in Figure 2.48C which allows a potential determination for the positioning of a double bond.

Analysis of the mass spectra reveals that Figure 2.48 A, B and D all possess a $M^{+\bullet}$ at *m/z* 196 which is consistent with an assignment of a fully saturated 1-methyloctahydro-1*H*-indene-2-carboxylic acid. Significant fragment ion are depicted in each of these mass spectra at *m/z* 181, 164 and 137 showing loss of a methyl group, a methanol and the alkanoate side chain, each of these ions are in differing abundances in their respective mass spectra indicating that these are stereo isomers. Ions present at *m/z* 87 and 110 indicate cleavage across the cyclopentyl ring creating a methyl propanoate fragment (*m/z* 87).

Analysis of Figure 2.48C reveals an $M^{+\bullet}$ at *m/z* 194 indicating that a partial saturation has occurred leaving one double bond somewhere within the structure. Significant ions reveal that the alkanoate side chain has fragmented from the structure with an ion at *m/z* 135 and that a methoxy group has also been cleaved revealing an ion at *m/z* 165. No clues are apparent from analysing this mass spectrum as to where the double bond lies.

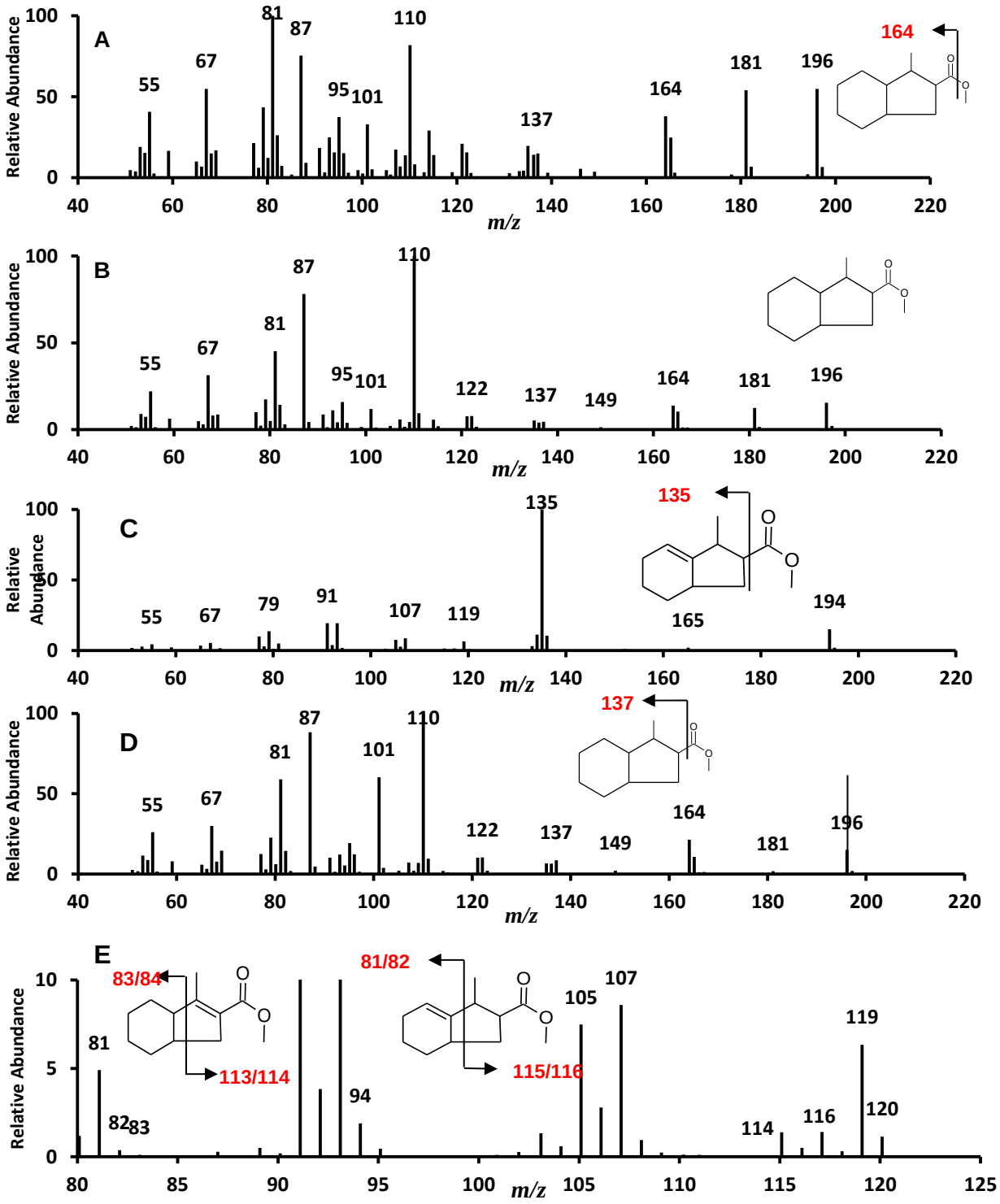

Figure 2.48. (A, B and D) Mass spectra of stereo isomers of 1-methyloctahydro-1H-indene-2-carboxylic acid methyl esters. (C) Partially saturated 1-methyl-2,3,3a,4,5,6-hexahydro-1H-indene-2-carboxylic acid methyl esters. (E) Close up of the m/z 80-125 region of 1-methyl-2,3,3a,4,5,6-hexahydro-1H-indene-2-carboxylic acid methyl esters.

The structure of the product shows that a single double bond is apparent in the cyclopentyl ring as well as the double bonds within the aromatic moiety so it is possible that the aromatic ring has saturated and left this double bond in place; however it is more likely that one double bond remains within the aromatic ring because of the stability of the benzene ring compared to the stability of a single double bond.

Analysis of Figure 2.48E reveals weak ions not able to be seen in Figure 2.48C. If the double bond lies within the cyclohexyl ring there should be fragment ions at *m/z* 81/82 and *m/z* 115/116, if the bond lies in the cyclopentyl ring these ions should be *m/z* 83/84 and *m/z* 113/114 (Figure 2.48E).

Analysis of the mass spectrum reveals a strong *m/z* 81 and a weak *m/z* 82 and 83 but no *m/z* 84, similarly whilst there is the presence of *m/z* 114, 115 and 116 there is no *m/z* 113 indicating that the double bond is more likely to remain within the cyclohexyl ring and has been removed from the cyclopentyl moiety. There are no ions which determine the position of the double bond apparent so the assignment of this mass spectra as describing a 1-methyl-2,3,3a,4,5,6-hexahydro-1*H*-indene-2-carboxylic acid molecule is somewhat speculative.

This analysis is similar for Figure 2.49C which has a similar mass spectra and assignment as Figure 2.48C. Similarities between these mass spectra and that of adamantane-1-carboxylic acid will be discussed below.

Analysis of the mass spectra attached to the remaining peaks (e-g) reveals that peak e (Figure 2.49A) can be assigned as a fourth stereo isomer of 1-methyloctahydro-1*H*-indene-2-carboxylic acid methyl esters. The $M^{+\bullet}$ at *m/z* 196

is consistent with the fully saturated moiety as are the alkanoate side chain fragments at *m/z* 181 (M-15 methyl group); *m/z* 164 (M-32 methanol) and *m/z* 137 (M-59 alkanoate side chain; and *m/z* 87 a methylpropanoate ion from cleavage of the cyclopentyl ring.

Analysis of Figure 2.49B suggests that this mass spectrum can be assigned as the partially saturated 1-methyl-2,3-dihydro-1*H*-indene-2-carboxylic acid. The $M^{+\bullet}$ is at *m/z* 190 consistent with the addition of two hydrogen atoms, thus more likely saturating the cyclopentyl ring, rather than partially saturating the aromatic ring. Significant ions are present at *m/z* 185 (loss of methyl) *m/z* 159 (loss of methoxy) and *m/z* 130 (loss of the alkanoate side chain). The ion at *m/z* 91 is attributed to a methyl benzene fragment and *m/z* 115 is potentially due to cleavage of the cyclopentyl ring leaving a methylbutanoate group.

The mass spectrum in Figure 2.49C is similar in aspect to that in Figure 2.48D and suggests a 1-methyl-2,3,3a,4,5,6-hexahydro-1*H*-indene-2-carboxylic acid methyl esters. The $M^{+\bullet}$ at *m/z* 194 is characteristic of the addition of 6 Daltons from the saturation of the cyclopentyl ring and partial saturation of the aromatic group, which is a more likely scenario that full saturation of the aromatic group due to this groups greater stability. Analysis of the mass spectrum reveals significant ions at *m/z* 179 (loss of methyl) *m/z* 163 (loss of methoxy and a base ion at m/z 135 (loss of the alkanoate side chain).

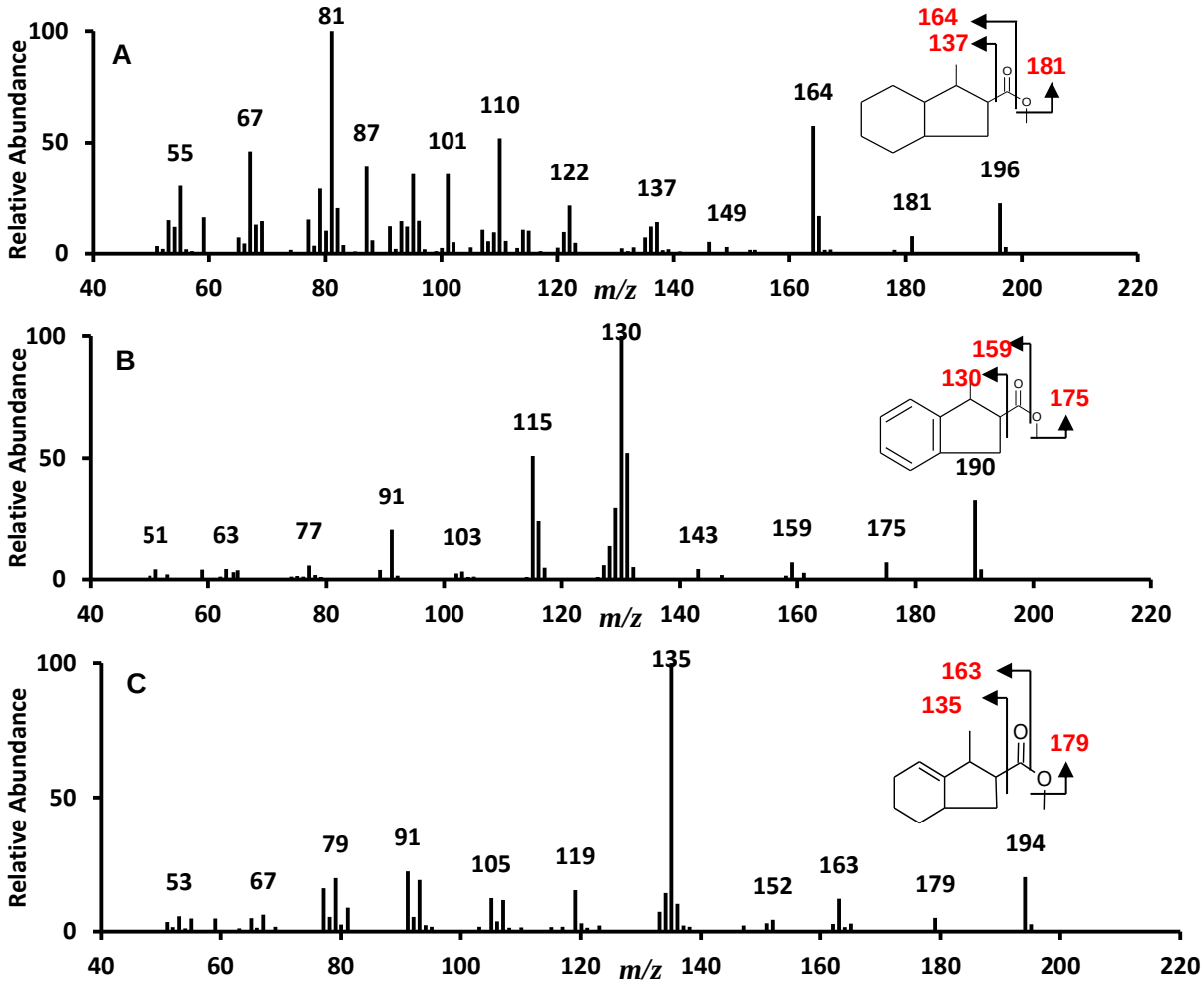

Figure 2.49. (A) Mass spectrum of a stereo isomers of 1-methyloctahydro-1H-indene-2-carboxylic acid methyl esters; (B) mass spectrum of partially saturated 1-methyl-2,3-dihydro-1H-indene-2-carboxylic acid methyl esters (C) partially saturated 1-methyl-2,3,3a,4,5,6-hexahydro-1H-indene-2-carboxylic acid methyl esters.

Analysis of the mass spectrum of 1-methyl-2,3,3a,4,5,6-hexahydro-1*H*-indene-2-carboxylic acid methyl esters displayed in Figures 2.48C and 2.49C reveals similar spectra to that of adamantane-1-carboxylic acid (Figure 2.50A). However close analysis of Figure 2.48A and the mass spectrum of 1-methyl-2,3,3a,4,5,6-hexahydro-1*H*-indene-2-carboxylic acid methyl ester (Figure 2.50B) reveals some

differences. In the adamantane spectrum there are no ions apparent between the $M^{+\bullet}$ at *m/z* 194 and the base ion (*m/z* 135; loss of the alkanoate side chain) and whilst there are similar smaller ions (notably *m/z* 67 and 79) it is apparent that these ions are also in a far lower abundance.

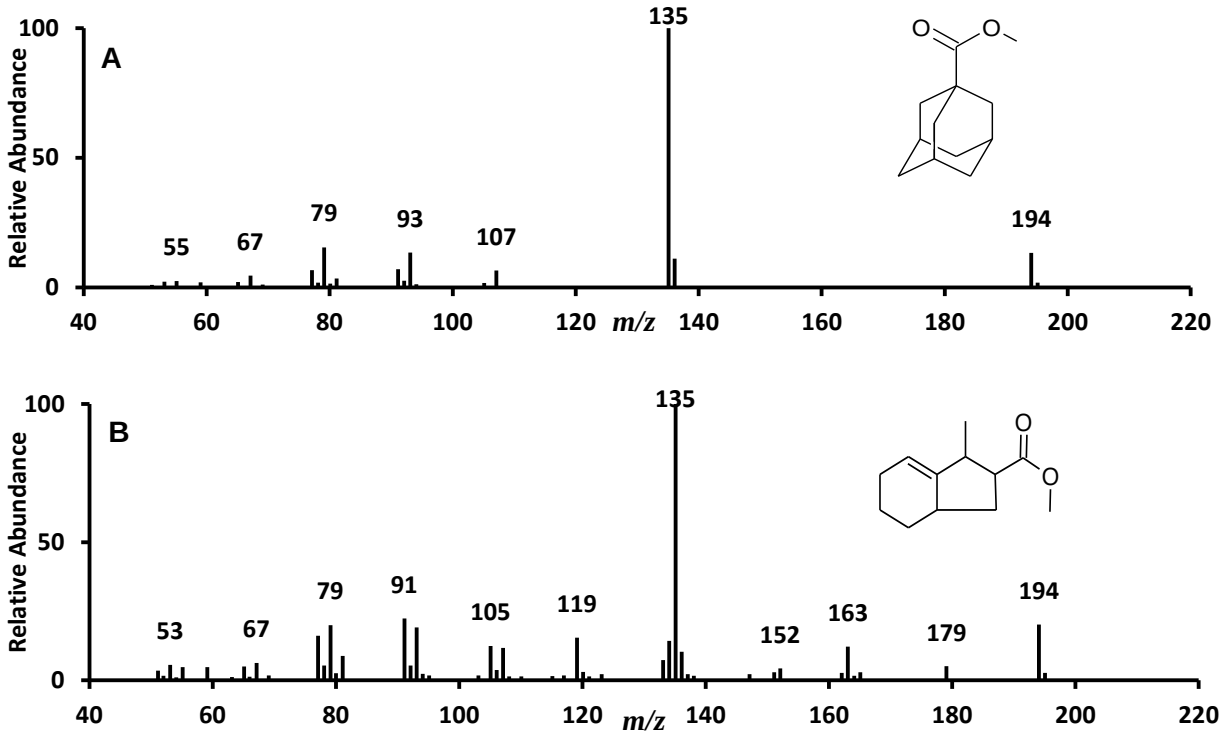

Figure 2.50. Comparison of mass spectra of (A) adamantane-1-carboxylic acid methyl esters and (B) 1-methyl-2,3,3a,4,5,6-hexahydro-1*H*-indene-2-carboxylic acid methyl ester

This comparison seems to confirm that the assignment of 1-methyl-2,3,3a,4,5,6-hexahydro-1*H*-indene-2-carboxylic acid methyl ester to the chromatographic peaks is correct. More evidence is provided by Figure 2.51 which compares the retention times of the seven peaks from the catalytic hydrogenation (in red) and the retention time of the methyl esters of an authentic adamantane-1-caboxylic

acid. It is notable that the adamantane peak does not co-elute with any of the hydrogenation products, and the nearest product peak is assigned to 1-methyl-2,3,3a,4,5,6-hexahydro-1*H*-indene-2-carboxylic acid methyl esters, a partially saturated species with an aromatic ring and an $M^{+\bullet}$ of *m/z* 190. Peaks assigned to isomers of 1-methyl-2,3,3a,4,5,6-hexahydro-1*H*-indene-2-carboxylic acid have retention times of 12.09 and 12.49 minutes whilst the peak assigned to adamantane-1-carboxylic acid methyl esters has a retention time of 12.29 minutes. Not assessing the retention times of the chromatographic peaks, in this case, could well have led to an incorrect assignment of the molecules that are responsible for the peaks.

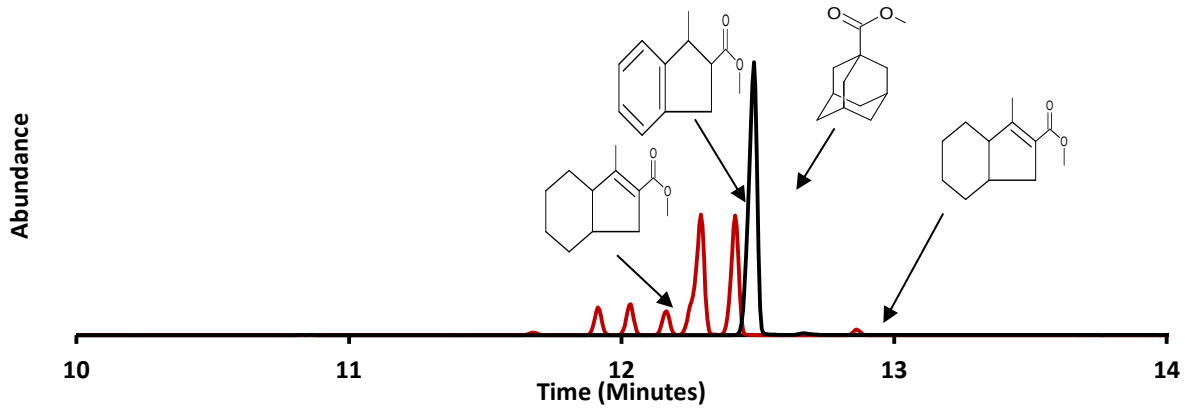

Figure 2.51. Comparison of chromatographic peak retention times for the methyl esters of the hydrogenated products of 1-methyl-1*H*-indene-2-carboxylic acid and adamantane-1-carboxylic acid methyl esters.

2.3.10. Synthesis of Decahydronaphthalene-1-carboxylic acid

Decahydronaphthalene-1-carboxylic acid methyl esters had recently been tentatively identified in a commercial mixture of naphthenic acids (Rowland et al., 2011b). In order to compare toxicity, mass spectra and two dimensional retention times a pure sample of this compound was required. In order to achieve this

authentic sample of naphthalene-1-carboxylic acid (Sigma Aldrich; stated purity >99%) was hydrogenated (Figure 2.52). Initially hydrogenated using the Buchii reaction chamber naphthalene-1-carboxylic acid was also hydrogenated utilising the H-Cube® catalytic hydrogenator.

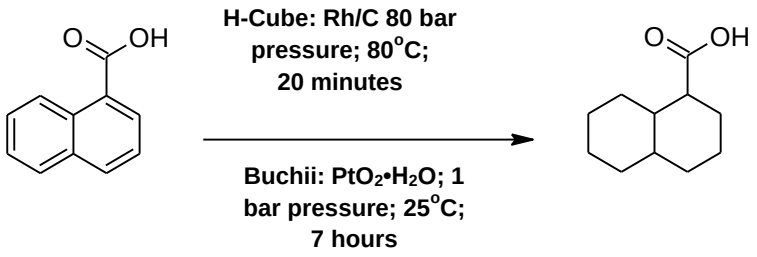

Figure 2.52. Reaction scheme for the catalytic hydrogenation of naphthalene-1-carboxylic acid (the reactant) to the product (decahydronaphthalene-1-carboxylic acid)**;** plus the catalytic hydrogenation conditions for both the H-Cube® (above arrow) and the Buchii reaction chamber (below arrow).

A sample of naphthalene-1-carboxylic acid was reacted with the BF_3-MeOH complex and assessed for purity on a GC-MS (Figure 2.53). There are two distinct peaks at RT 14.24 minutes (88% yield) and RT 14.37 (12% yield).

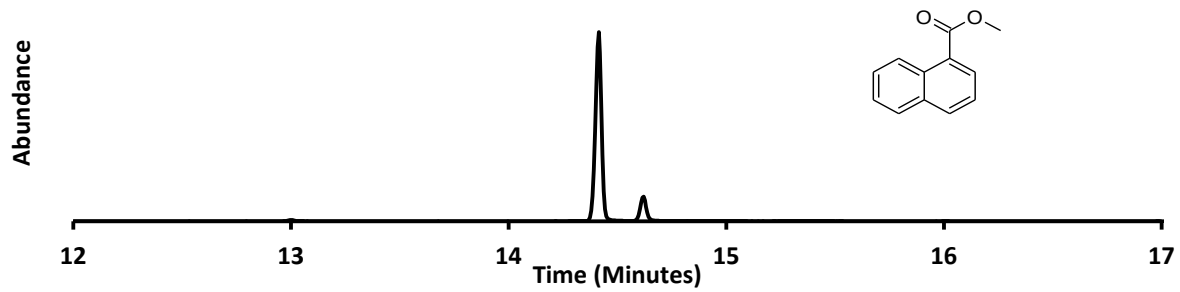

Figure 2.53. Chromatogram of the reactant naphthalene-1-carboxylic acid methyl ester; GC Conditions as described in Figure 2.13.

Analysis of the mass spectra (Figure 2.54) reveals that both chromatographic peaks displayed in Figure 2.53 have a very similar aspect. Both spectra display an $M^{+\bullet}$ at *m/z* 186 and fragment ions at *m/z* 155 (loss of methoxy M-31) and *m/z* 127 (M- 59 loss of an alkanoate side chain).

The mass spectrum displayed in Figure 2.54A) also has a weak fragment ion at *m/z* 171 (loss of a methyl group), both spectra have an ion at *m/z* 77 indicative of cleavage of a benzene ring. Both peaks suggest an assignment of a naphthalene carboxylic acid.

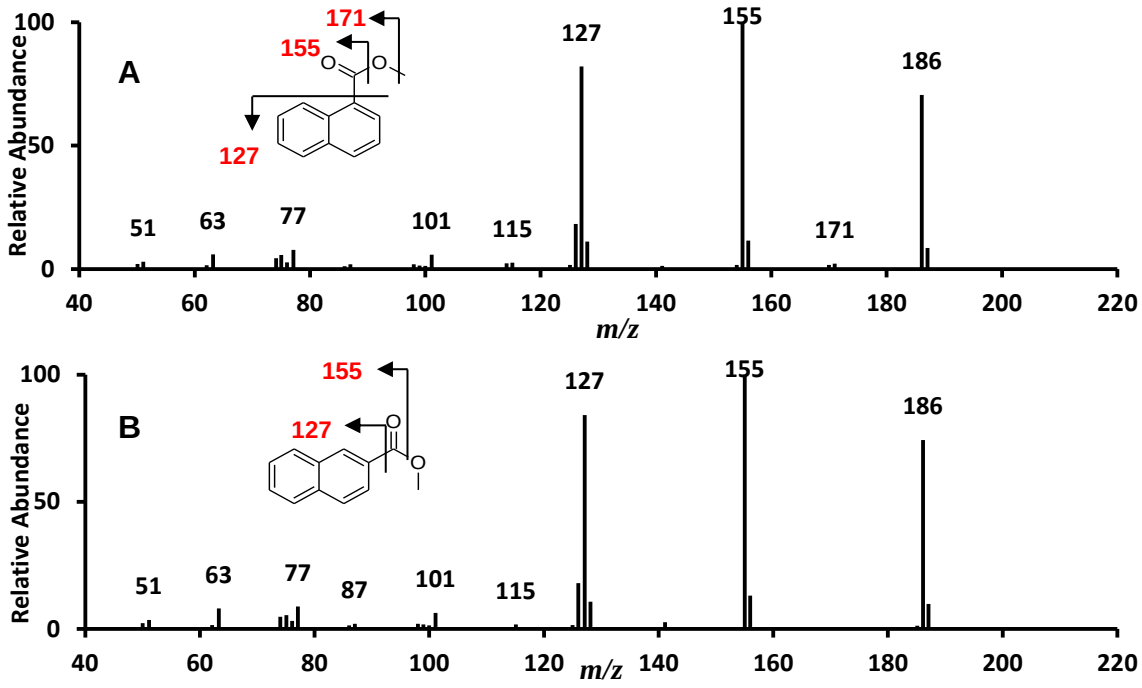

Figure 2.54. (A) Mass spectrum for the compound eluting at RT 14.24 minute. (B) Mass spectrum for the compound eluting at RT 14.37 minutes. MS conditions as described in Figure 2.13.

Comparisons with the RT of an authentic sample of naphthalene-2-carboxylic acid methyl esters (Sigma Aldrich; Stated purity >99%) (Figure 2.55 A and B) reveals that the peak eluting at 14.37 minutes is likely to be characteristic of a small amount of the '2' isomer as it has an identical RT and mass spectrum (Figure 2.64C).

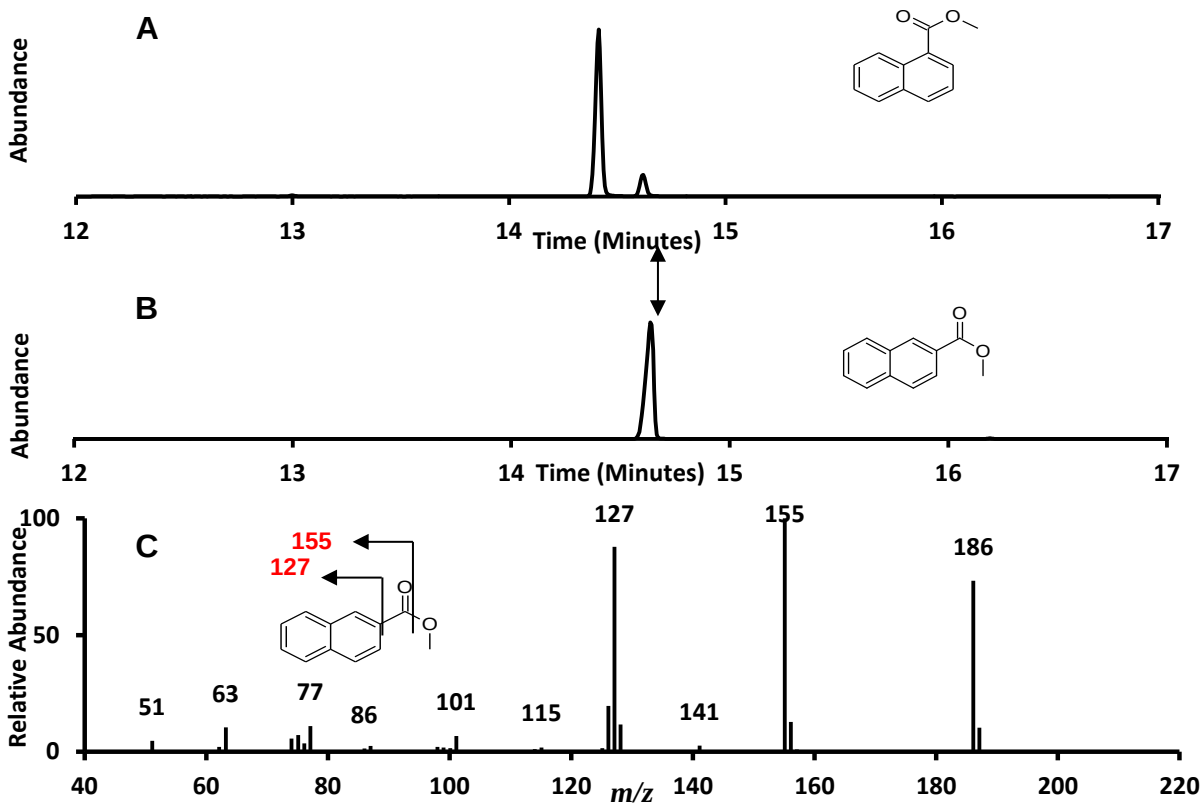

Figure 2.55. Comparison of chromatograms from (A) naphthalene-1-carboxylic acid; (B) naphthalene-2-carboxylic acid; and (C) mass spectrum of the compound eluting at 14.37 minutes, assigned as a naphthalene-2-carboxylic acid**;** GC-MS conditions as described in Figure 2.13.

Catalytic hydrogenation of a sample of naphthalene-1-carboxylic acid proceeded using the Buchii reaction chamber. The product was reacted with BF_3-MeOH and analysed by GC-MS. This experiment was re-done on three occasions (Figure 2.56).

Analysis of the chromatograms displayed in Figure 2.56 reveals that after 7 hours five distinct peaks were apparent (Figure 2.56B). Only one of these peaks (peak d) matched the retention time of the reactant peak assigned to naphthalene-1-

carboxylic acid. After 14 hours of hydrogenation none of the reactant was apparent in the chromatogram and after 21 hours only chromatograms assigned to the product was displayed.

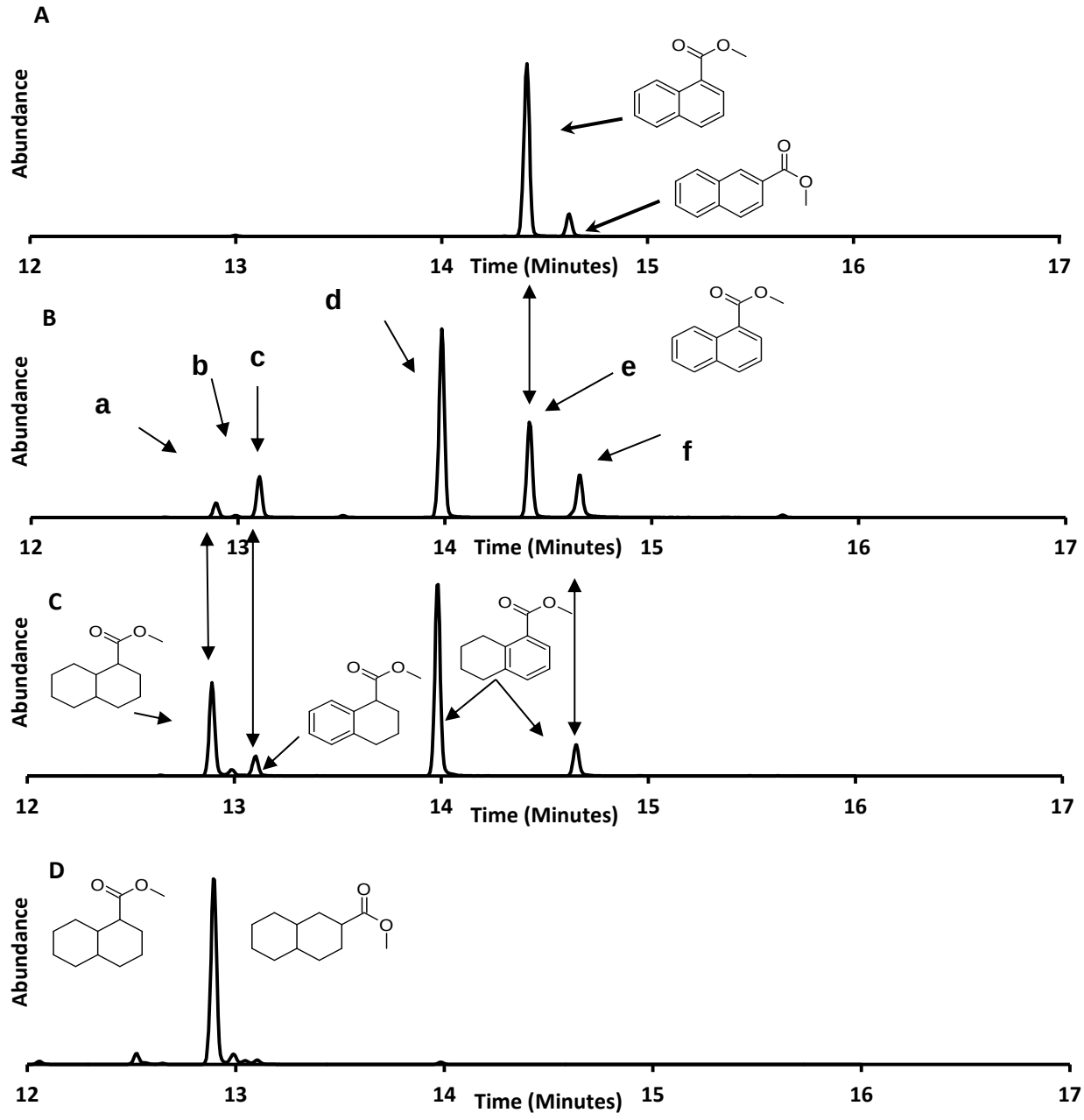

Figure 2.56. Chromatograms detailing changes across the three hydrogenation attempts with (A) displaying the original reactant chromatogram; (B) revealing the changes in the chromatogram after a 7 hour Buchii catalytic hydrogenation; (C) after 14 hours; and (D) after 21 hours**.** Assignments were confirmed by mass spectral analysis. GC conditions as described in Figure 2.13**.**

Figure 2.57*i* and *ii* display the chromatogram and mass spectra for the analysis of the 7 hour hydrogenation.

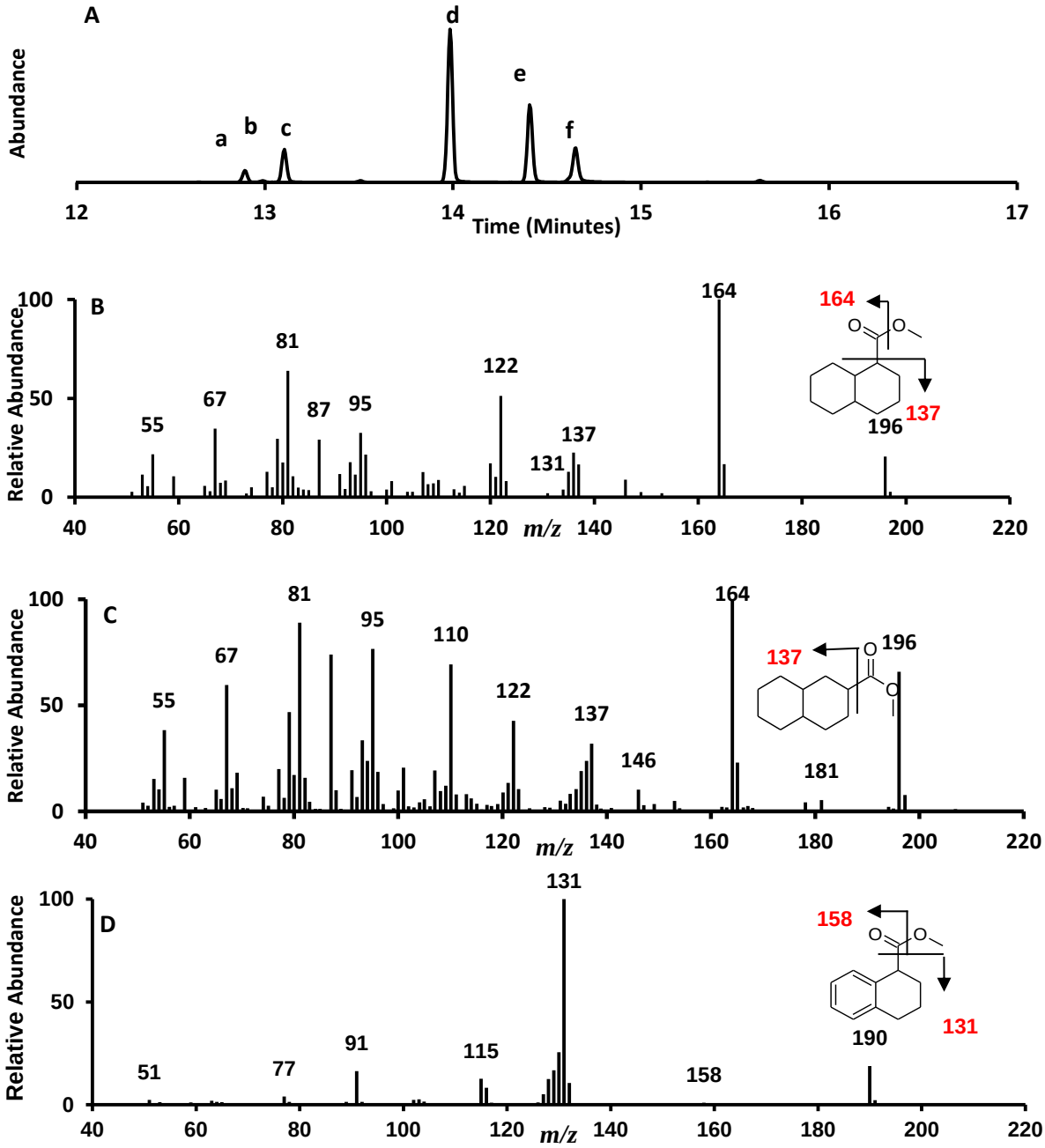

Figure 2.57i. Total ion current chromatogram (A) after a 7 hour catalytic hydrogenation of the reactant (naphthalene-1-carboxylic acid methyl ester). (B) Mass spectrum for compound eluting at RT 12.53.minutes. (C) Mass spectrum for compound eluting at RT 12.59 minutes. (D) Mass spectrum for compound eluting at RT 13.06 minutes**.** GC-MS conditions as described in Figure 2.13.

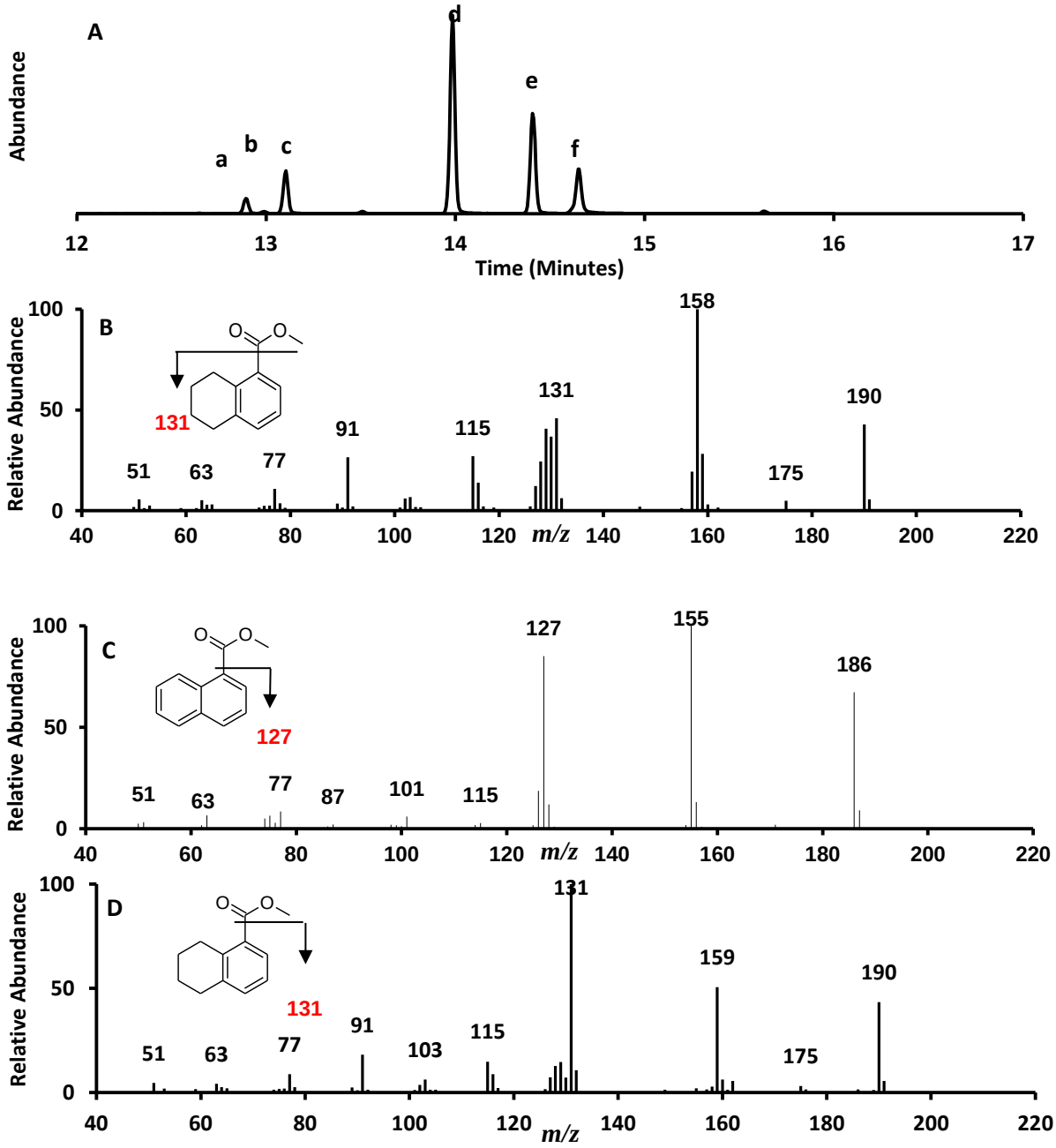

Figure 2.57ii. Total ion current chromatogram (A) after a 7 hour catalytic hydrogenation of the reactant. (B) Mass spectrum for compound eluting at RT 13.59 minutes. (C) Mass spectrum for compound eluting at RT 14.24 minutes. (D) Mass spectrum for compound eluting at RT 14.39 minutes. GC-MS conditions as described in Figure 2.13.

It can be seen that there are five distinct peaks in the chromatogram (peaks a and c-f) and one minor peak (peak b). Retention times and yields for these peaks are detailed in Table 2.2.

Analysis of the mass spectra confirms the tentative assignments of compounds to chromatographic peaks. Peak a (RT 12.53 minutes: Figure 2.57*i* B) is revealed to have an $M^{+\bullet}$ of *m/z* 196, consistent with the addition of ten hydrogen atoms in the hydrogenation process, significant ions reveal the cleavage of the alkanoate side chain (*m/z* 164 and *m/z* 137: methanol and carboxylic acid methyl ester cleavage respectively). The ion at *m/z* 122 could indicate cleavage across a cyclohexyl ring leaving an ethanoic acid methyl ester fragment (M-74). Peak b (RT 12.59 minutes: Figure 2.57*i* C) is also confirmed as a decahydronaphthalene moiety, though the mass spectrum differs noticeably from the earlier eluting peak. The $M^{+\bullet}$ at *m/z* 196 is characteristic of the addition of ten Daltons from the complete saturation of the reactant. Significant fragment ions exist at m/z 181 (loss of methyl); *m/z* 164 (loss of methanol) and *m/z* 137 (loss of the alkanoate side chain). Ions at *m/z* 81 and 67 indicate that a cyclohexyl ring is present, and the possibility of electron transfer occurring creating double bonds in the cleaved ring. If this is the case then the ion at *m/z* 110 can be assigned to a dimethylcyclohexyl containing one double bond. Differences in the two mass spectra assigned to decahydro species might be due to differences between the '1' and '2' carboxylic acid moieties as there was a small amount of naphthalene-2- carboxylic acid present in the reactant, it is natural to assume the presence of a small amount of the saturated '2' carboxylic acid product. The mass spectra in

Figure 2.57*i* C has been compared to the mass spectra in a pure decahydronaphthalene-2-carboxylic acid (Figure 2.55) and found to have distinct similarities, so the peak eluting at RT 12.59 minutes is assigned as the '2' isomer and the peak eluting at RT 12.53 minutes as the '1' isomer.

Peak c (RT 13.06 minutes: Figure 2.57*i* D) has been assigned as a partially saturated 1,2,3,4-tetrahydronaphthalene-1carboxylic acid. The $M^{+\bullet}$ at m/z 190 is consistent with the addition of four hydrogen atoms which would saturate one benzene ring yet leave the other intact. Comparison with the yields of the other partially saturated species shows that only a relatively small amount of this partially saturated product is present hinting towards this being a non-preferential hydrogenation product due to the steric hindrance caused by the presence of the carboxylic acid. Analysis of the $M^{+\bullet}$ of this mass spectra and that of 5,6,7,8-tetrahydronaphthalene-1-carboxylic acid methyl esters shows that the 1,2,3,4-tetrahydro species $M^{+\bullet}$ is not as abundant relative to the base ion (18% relative abundance compared to 41 and 42%) indicating that the 1,2,3,4-tetrahydro species is not as stable as the 5,6,7,8-tetrahydro moiety. Analysis of the significant fragment ions in Figure 2.57*i* D reveals that the characteristic ions from side chain cleavage are present (m/z 159 and 131) indicating loss of methoxy and the alkanoate side chain. The ion at m/z 77 indicates the presence of a benzene ring and m/z 115 indicates a cleavage across the cyclohexyl ring forming a pentanoic acid methyl ester.

Analysis of the mass spectrum in Figure 2.57*ii* reveals that peaks d and f (RT 13.59 and 14.39 minutes) can be assigned as the partially saturated 5,6,7,8-

tetrahydronaphthalene-1-carboxylic acid and the remaining peak can be assigned to the remaining unsaturated product (RT 14.24 minutes: naphthalene-1-carboxylic acid).

Figure 2.57*ii* B is revealed as the mass spectra for a 5,6,7,8-tetrahydronaphthalene-1-carboxylic acid methyl ester. The $M^{+\bullet}$ at 190 is consistent with the addition of 4 hydrogen atoms to one of the benzene rings, the relative abundance of the $M^{+\bullet}$ ion indicates that the saturation has occurred on the ring that is not connected to the carboxylic acid, rendering a more stable compound. Significant fragment ions indicate loss of a methyl group (*m/z* 175); a methanol (*m/z* 158, the base ion) and the alkanoate side chain (*m/z* 131). Ions at *m/z* 91, 77, 63 and 51 indicate the presence of a benzene ring. Although the mass spectra in Figure 2.57*ii* D indicate a similar structure with similar fragmentation patterns the base ion at *m/z* 131 indicates a different isomer. The mass spectra of napththalene-1-carboxylic acid methyl ester (Figure 2.57*i* C) have been discussed previously.

Chromatographic peaks and mass spectra present after 14 hours of hydrogenation have similar RTs, $M^{+\bullet}$ and fragmentation patterns. A noticeable difference is the lack of the peak assigned to the reactant which has now been saturated into fully and partially hydrogenated species. As the mass spectra are the same as displayed in Figure 2.57 (*i* and *ii*) they will not be described here again. Analysis of the chromatogram from the 21 hour catalytic hydrogenation (Figure 2.58) reveals that of the peaks assigned to the reactant or partially saturated species have now been converted to the fully saturated

decahydronaphthalene moieties. Close inspection reveals a peak at a RT of 13.06 minutes characteristic of a tetrahydronaphthalene species (described above), Table 2.2 reveals that this peak is 2.5% of the total yield leaving the decahydronaphthalene-1-carboxylic acid isomers at ~ 92% yield and the decahydronaphthalene-2-carboxylic acid isomer at ~ 5.5%.

Table 2.2. Retention times and percentage yields for the reactants and products determined during the synthesis of decahydronaphthalene-1-carboxylic acid.

		Yield (%)			
Assignment	RT	0	7	14	21
DHN-1-CA	12.32	0	0	0	4.92
DHN-1-CA	12.53	0	3.64	26.67	86.99
DHN-2-CA	12.59	0	0.57	2.03	5.59
THN-CA	13.06	0	10.26	6.02	2.50
THN-CA	13.59	0	46.95	55.57	0
NA-1-CA	14.24	88.28	24.62	0	0
NA-2-CA	14.37	11.71	0	0	0
THNA-CA	14.39	0	13.33	9.70	0

DHN-1-CA is decahydronaphthalene-1-carboxylic acid methyl esters; DHN-2-CA is decahydronaphthalene-1-carboxylic acid methyl esters; THN-CA is tetrahydronaphthalene-1-carboxylic acid methyl esters; NA-1-CA is naphthalene-1-carboxylic acid methyl ester; NA-2-CA is naphthalene-2-carboxylic acid methyl esters; RT is retention time.

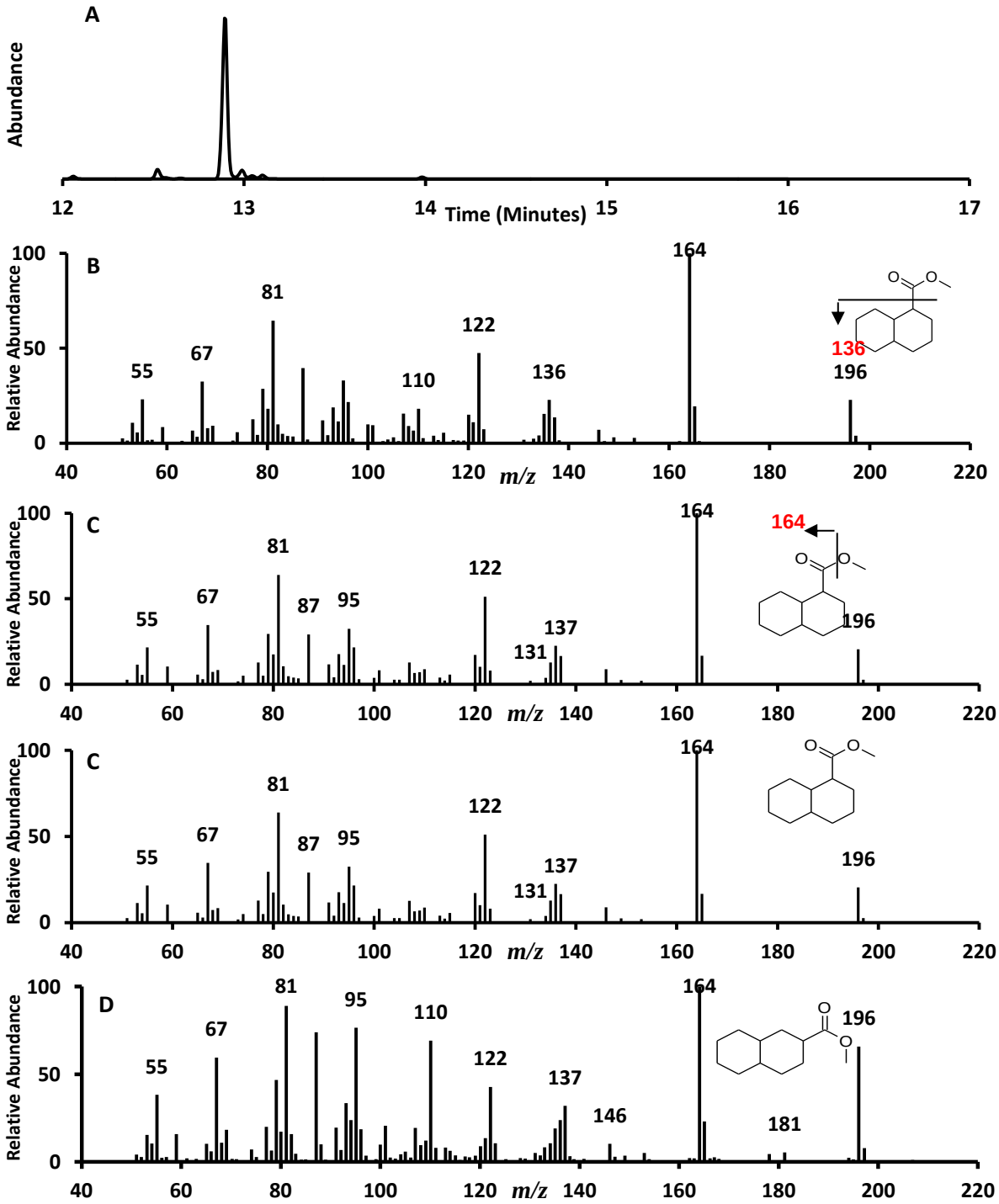

Figure 2.58. (A)Chromatogram 21 hour catalytic hydrogenation of naphthalene-1-carboxylic acid. (B) Mass spectrum for component at RT 12.32 minutes. (C) Mass spectrum for the component at 12.53 minutes. (D) Mass spectrum for component at RT 12.59 minutes. GC-MS conditions as described in Figure 2.13.

Analysis of the mass spectra for the peaks at RT 12.53 and 12.59 in Figure 2.58A are described above. The peak eluting at RT 12.32 minutes (mass spectrum Figure 2.58B) is assigned as a decahydronaphthalene-1-carboxylic acid as the mass spectrum is redolent of that shown in Figure 2.48C. The $M^{+\bullet}$ is the same at *m/z* 196 as are the other significant fragments ions at *m/z* 164 (loss of methanol) the only apparent difference in these two spectra is the relative abundance of *m/z* 136 and *m/z* 137 (loss of the alkanoate side chain). Figure 2.58 (D) is assigned to a small abundance of decahydronaphthalene-2-carboxylic acid methyl esters. Assignment was confirmed by mass spectral analysis, comparison of mass spectra from a previous experiment analysis and comparison of retention times (Table 2.3). It was noted that the mass spectrum produced for Figure 2.67D is identical to that produced in Figure 2.57*i* C, which was previously assigned as the '2' isomer.

Synthesis of decahydronaphthalene-1-carboxylic acid was also attempted on the H-Cube® catalytic hydrogenator (Figure 2.59). The compound was eluted though the H-Cube® at 1 mL min^{-1} at a pressure of 80 bar and a temperature of 80^{o}C, the catalyst was Rh/C. This compound was the first chemical to be assessed on the H-Cube® catalytic hydrogenator and achieved a full saturation after a 20 minute experiment.

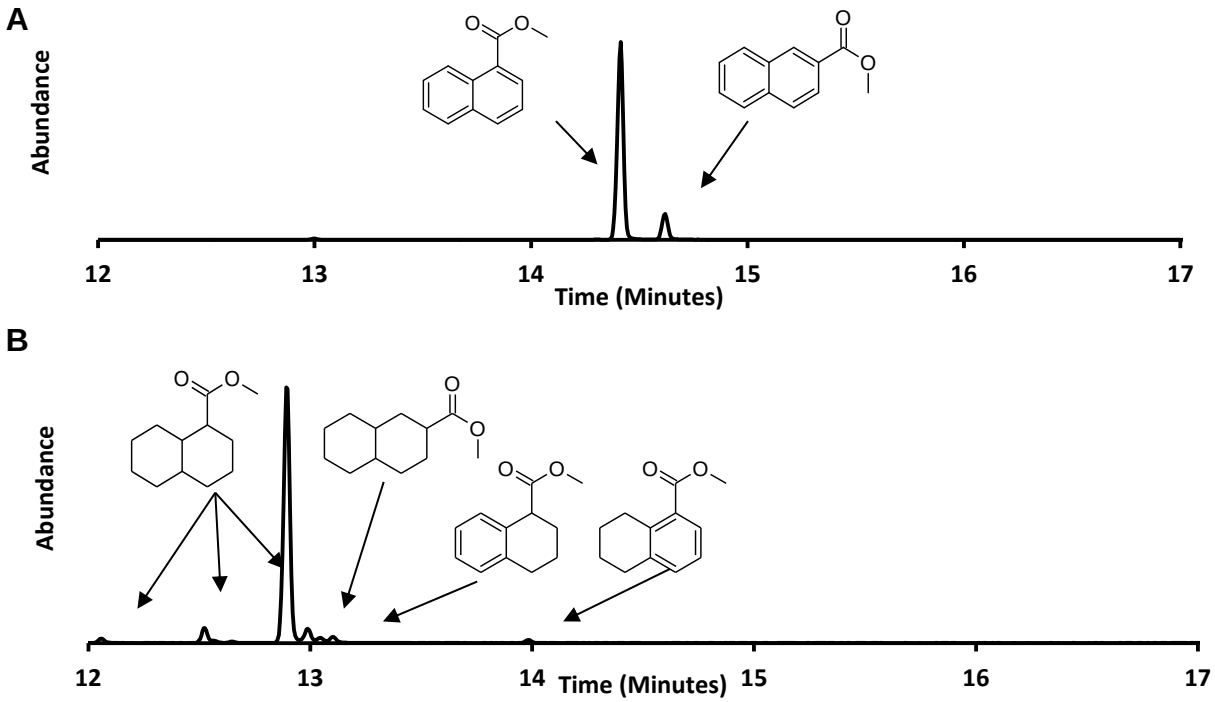

Figure 2.59. (A) Chromatogram from the H-Cube® catalytic hydrogenation of the reactant naphthalene-1-carboxylic acid methyl esters to the product (B) (decahydronaphthalene-1-carboxylic acid methyl esters**,** GC conditions as described previously.

Confirmation of chromatogram assignments in Figure 2.59 was made through analysis of mass spectra, comparison to the mass spectra produced from the previous Buchii reaction chamber experiments (Figure 2.57) and comparison of retention times (Table 2.2 and 2.3).

It was found that identical mass spectra and retention times to that revealed after the 21 hour Buchii experiment were produced (Figure 2.58; Table 2.3; discussed above). Table 2.3 shows that a yield of ~96% decahydronaphthalene carboxylic acid was produced with a 20 minute experiment compared to 21 hours in the Buchii reaction chamber, ~5% was assigned to the '2' position carboxylic acid, however this was deemed pure enough to assess toxicologically and

chromatographically on the two dimensional GC-MS to confirm mass spectra and retention times in a comparison with naphthenic acid 'super-complex' mixtures.

Table 2.3. Retention times and percentage yields for the reactants and products determined during the synthesis of decahydronaphthalene-1-carboxylic acid via the H-Cube® hydrogenator.

Assignment	RT(A)	RT(B)	Yield (B) (%)	Sum of Isomers (%)
DHN-1-CA		12.04	1.50	96.51
DHN-1-CA	12.32	12.32	4.80	
DHN-1-CA	12.53	12.53	84.76	
DHN-2-CA	12.59	12.59	5.45	
THN-CA	13.06	13.06	2.44	3.49
THN-CA	13.59	13.59	1.05	

RT(A) is retention times from the Buchii experiments; RT(B) is retention times from the H-Cube® experiments; assignment abbreviations are listed above (Table 2.3).

2.3.11. Synthesis of Decahydronaphthalene-2-Carboxylic Acid

A sample of naphthalene-2-carboxylic acid was reacted with BF_3-MeOH and assessed for purity on a GC-MS (Figure 2.60A). There is one distinct peak apparent at RT 14.37 minutes (>99% yield). Analysis of the mass spectrum (Figure 2.60B) confirmed the assignment of naphthalene-2-carboxylic acid methyl esters.

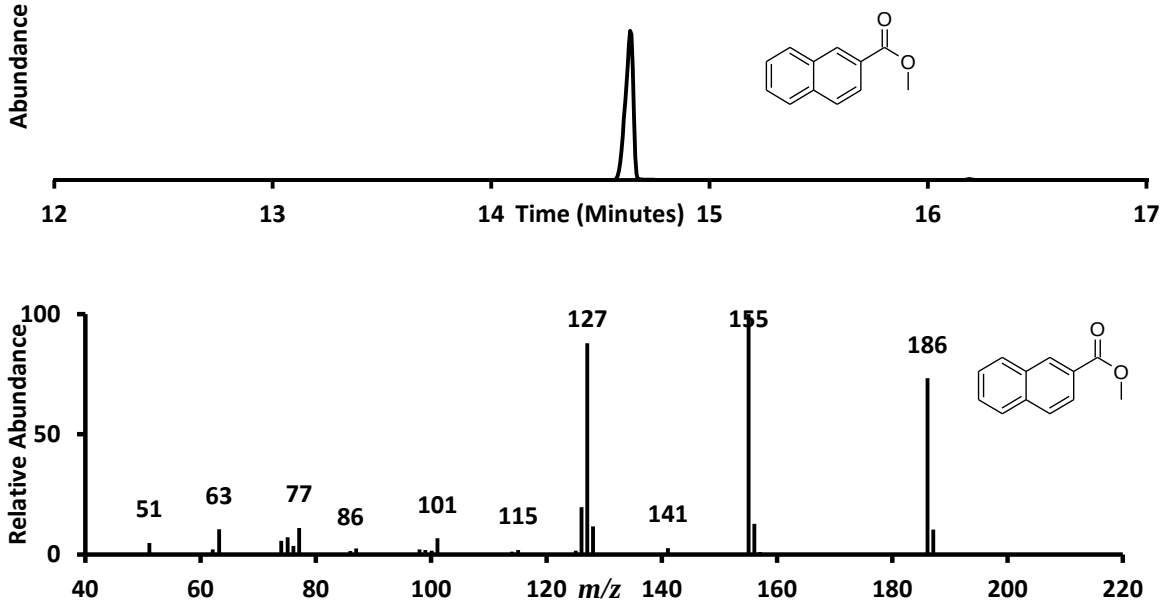

Figure 2.60. (A) Chromatogram of the methyl esters of naphthalene-2-carboxylic acid. (B) Mass spectrum for the component eluting at RT 14.37 minutes**.** GC-MS conditions as described in Figure 2.13

Analysis of the mass spectrum (Figure 2.60B) reveals a $M^{+\bullet}$ at *m/z* 186, consistent with the molecular weight of this compound. Significant fragment ions exist at *m/z* 155 and 127 indicating loss of a methoxy ion and the alkanoate side chain. The ion at *m/z* 77 indicates cleavage of a benzene ring.

A sample of the reactant was eluted through the H-Cube® catalytic hydrogenator at 80 bar pressure, 80°C, Rh/C catalyst, and 1 mL $minute^{-1}$ (Figure 2.61).

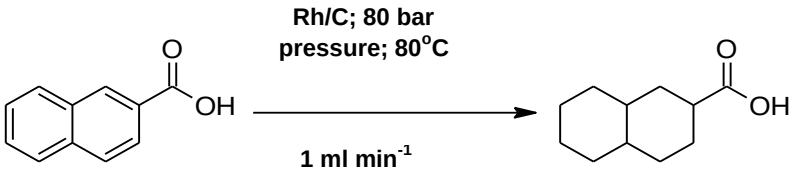

Figure 2.61. Reaction scheme for the catalytic hydrogenation of the reactant (naphthalene-2-carboxylic acid) to the product (decahydronaphthalene-2-carboxylic acid**)**; plus hydrogenation conditions.

A sample of the product was reacted with BF_3-MeOH and analysed with GC-MS. The chromatogram (Figure 2.62*i* A) revealed four distinct peaks (peaks b, c, e and f) and two lesser peaks (peaks a and d) with retention times ranging from 12.34 minutes to 14.37 minutes and yields ranging from ~1.6 to ~57% (detailed in Table 2.4). Analysis of the mass spectra was able to confirm compound assignments to particular chromatographic peaks.

Figure 2.62*i* B shows the mass spectra associated with peak 'a'. This has been assigned as an isomer of decahydronaphthalene-2-carboxylic acid methyl ester. The $M^{+\bullet}$ at *m/z* 196 is ten Daltons higher than the $M^{+\bullet}$ of the naphthalene moeity, consistent with the addition of ten hydrogen atoms. Significant fragment ions present are *m/z* 164 (loss of methanol) and *m/z* 136 (loss of the alkanoate side chain). The fragment ion at *m/z* 87 indicates cleavage of a propanoic acid methyl esters, *m/z* 81, *m/z* 95 and *m/z* 110 reveals the cleavage of a cyclohexyl, a methyl cylcohexyl and a dimethyl cyclohexyl moieties with the creation of a double bond from electron transfer, *m/z* 67 is also indicative of a cyclohexyl ring.

Figure 2.62*i* C and D (peaks 'b' and 'c') are also assigned as isomers of decahydronaphthalene-2-carboxylic acid. The $M^{+\bullet}$ in both spectra are revealed at *m/z* 196 and the significant ions are similar to the mass spectra detailed in Figure 2.50*i* B. An extra fragment ion at *m/z* 181 is apparent in Figure 2.50*i* C and D consistent with loss of a methyl group.

Figure 2.62*ii* details the mass spectra from the remaining three peaks (d-f). Figure 2.62*ii* B reveals a mass spectra with an apparent $M^{+\bullet}$ at *m/z* 194 consistent with an assignement of a partially saturated moiety containing a single double bond, potentially signalling the presence of a minor amount of 1,2,3,4,4a,5,6,7-octahydronaphthalene-2-carboxylic acid. Significant ions exist at *m/z* 162 and 134 (loss of methanol and the alkanoate side chain respectively), weak ions at *m/z* 81 and 87 indicate the presence of cyclohexene (formed through electron transfer) and propanoic acid methyl ester fragments, *m/z* 79 indicates presence of a cyclohexadiene, indicating that a cyclohexene was already present in the molecule as an electron transferred during cleavage creates the extra bond. The position of the double bond in the molecule shown in Figure 2.62*ii* B is purely arbitrary.

Figure 2.62*ii* C reveals the presence of an 1,2,3,4-tetrahydronaphthalene-2-carboxylic acid methyl ester. The $M^{+\bullet}$ is *m/z* 190 consistent with the addition of the four hydrogen atoms needed to create this molecule. Significant ions exist at *m/z* 158 and *m/z* 130 signifying cleavage of a methanol and the alkanoate side chain. A fragment at *m/z* 115 indicates cleavage of a butanoic acid methyl ester. Ions at *m/z* 91, 77, 65 and 51 indicate that benzene and methyl benzene have been cleaved from the molecule.

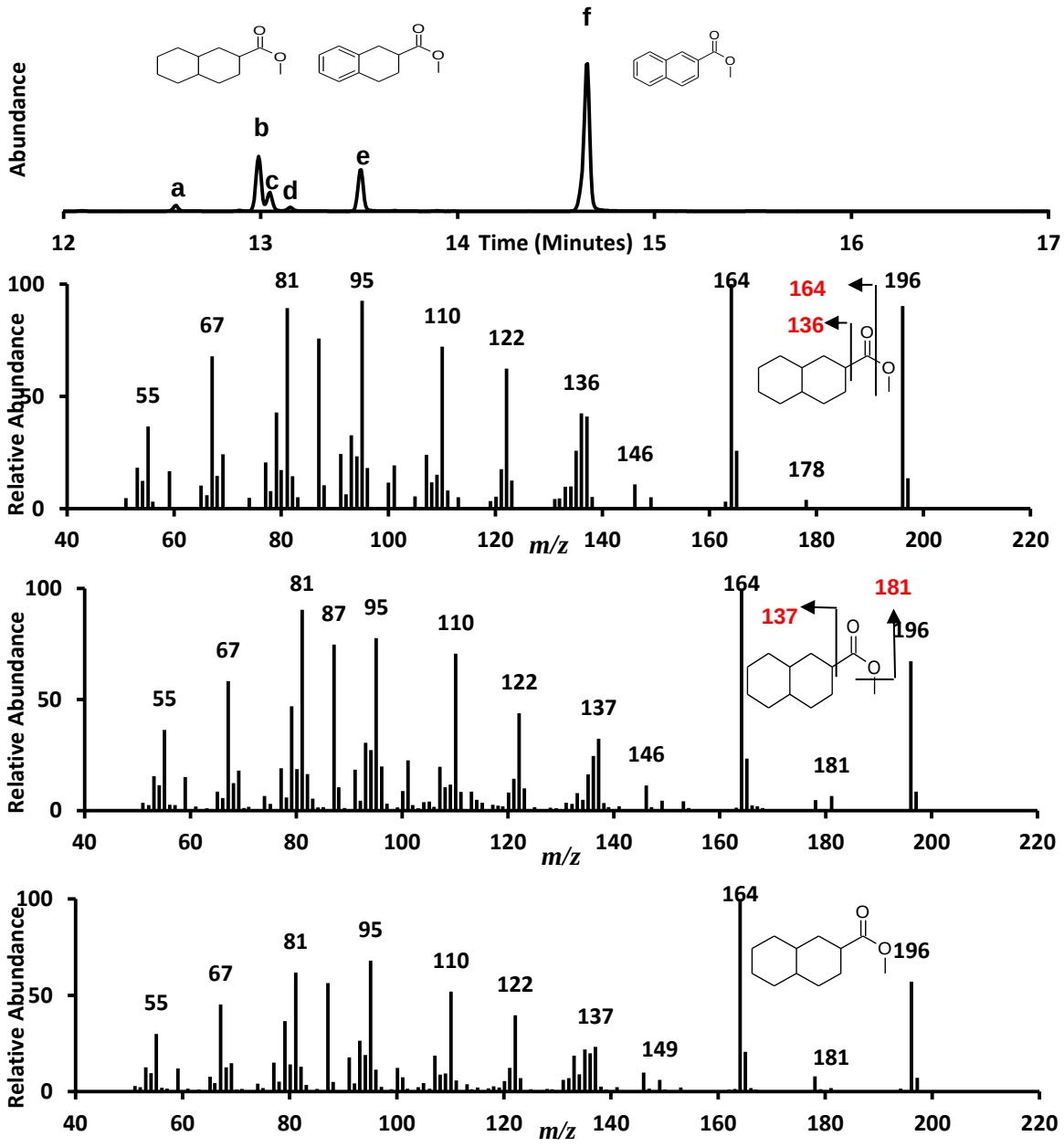

Figure 2.62i. (A) Chromatogram from the 20 minute elution of the reactant (naphthalene-2-carboxylic acid methyl ester). (B, C and D) Isomers of decahydronaphthalene-2-carboxylic acid methyl esters**.** GC-MS conditions as described in Figure 2.13.

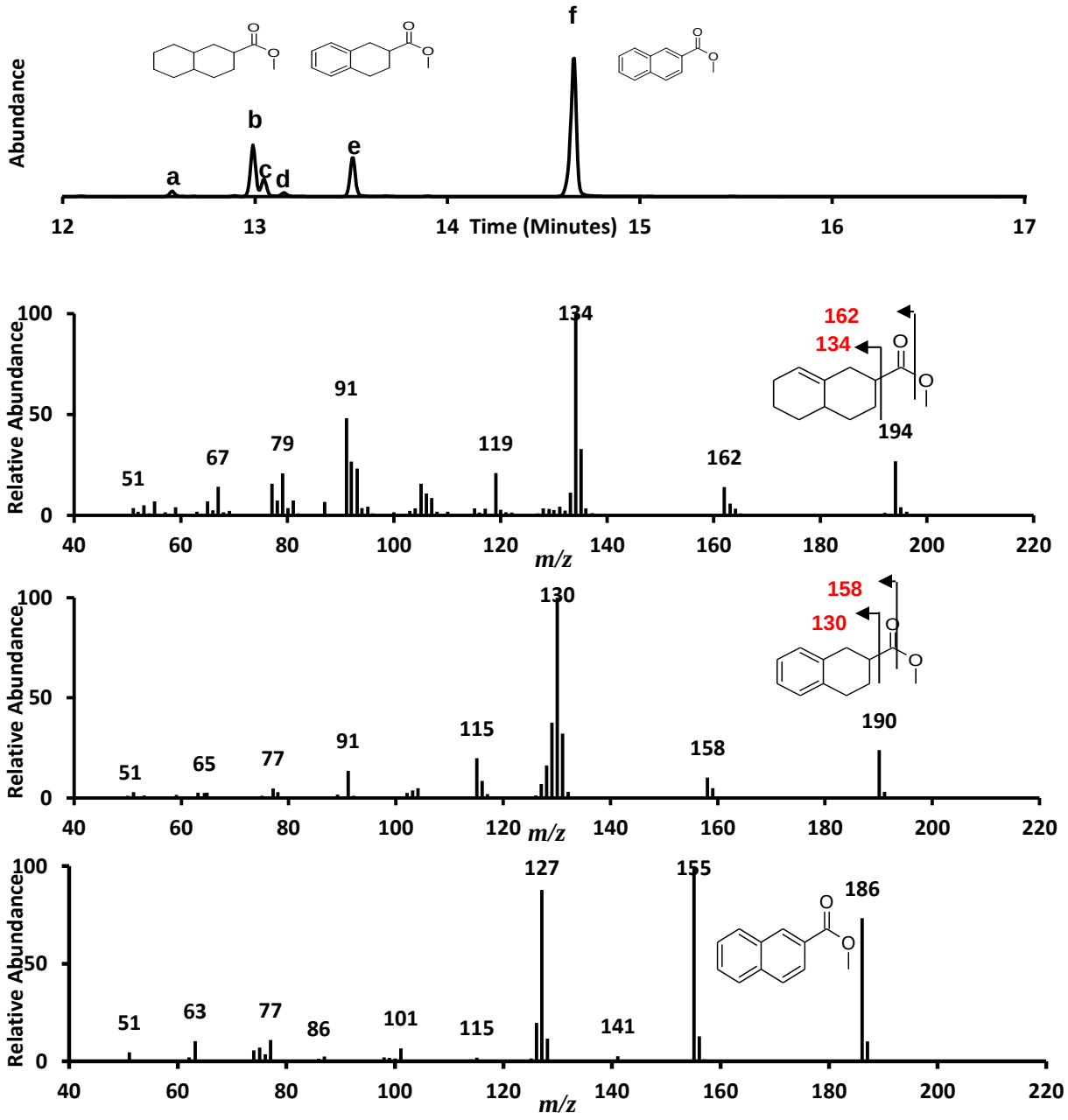

Figure 2.62ii (A) Chromatogram from the 20 minute elution of the reactant (naphthalene-2-carboxylic acid methyl ester) with (B) revealing a potential partially saturated 1,2,3,4,4a,5,6,7-octahydronaphthalene-2-carboxylic acid methyl ester; (C) 1,2,3,4-tetrahydronaphthalene-carboxylic acid methyl ester; and (D) the reactant naphthalene-2-carboxlylic acid methyl ester. GC-MS conditions as described in Figure 2.13.

This isomer is more likely as the $M^{+\bullet}$ has a relative abundance of ~20% similar to the 1,2,3,4-tetrahydronaphthalene-1-carboxylic acid methyl esters described previously, a 5,6,7,8-tetrahydrnaphthalene moiety would have a $M^{+\bullet}$ at ~40% relative abundance. Figure 2.62*ii* D shows the presence of the reactant (naphthalene-2-carboxylic acid) which is described above in Figure 2.60.

The products from the first, unsuccessful hydrogenation attempt were eluted through the H-Cube® for a second time, under the same conditions (Figure 2.63). The chromatogram (Figure 2.63A) shows three distinct peaks and a very minor peak with retention times ranging from 12.06-13.03 minutes, three of which matched retention times of decahydronaphthalene species present in the first elution (Figure 2.63; Table 2.4). These peaks were tentativley assigned as four isomers of decahydronaphthalene-2-carboxylic acid methyl esters. Analysis of the relative mass spectra will aid in the confirmation of these assignments. Analysis reveals an $M^{+\bullet}$ of m/z 196 in all four mass spectra (Figure 2.63B-E) this is consistent with the addition of ten hydrogen atoms to create a fully saturated decahydronaphthalene species. Significant fragment ions are *m/z* 164 (throughout the four mass spectra) indicating a loss of methanol; *m/z* 136 (Figure 2.63C) and *m/z* 137 (Figure 2.63 B,D and E) indicating loss of the alkanoate side chain; and *m/z* 181 (Figure 2.63 C-E) indicating loss of a methyl group. Other significant ions present thoughout are *m/z* 67 and 81 characteristic of a cyclohexane group, *m/z* 95 and *m/z* 110 indicate cleavage of a methyl cyclohexyl and a dimethylcyclohexyl groups respectively; and *m/z* 87 indicate cleavage of a propanoic acid methyl ester. Table 2.4 shows that it took two separate elutions

with the H-Cube to fully saturate the naphthalene moiety to a >99% pure decahydronaphthalene moiety.

Table 2.4. Retention time and percentage yield comparison between the first and second elutions of naphthalene-2-carboxylic acid on the H-Cube® catalytic hydrogenator.

					Sum Isomers (%)	
Assignment	RT(A)	RT(B)	Yield (A) (%)	Yield (B) (%)	1st Elution	2nd Elution
DHN-2-CA	0.00	12.06	0.00	0.70	26.83	100
DHN-2-CA	12.34	12.34	1.94	6.87		
DHN-2-CA	12.59	12.59	18.28	67.12		
DHN-2-CA	13.03	13.03	6.61	25.31		
THN-2-CA	13.09	13.09	1.64	0.00	15.92	0.00
THN-2-CA	13.31	13.31	14.28	0.00		
NA-2-CA	14.37	14.37	57.25	0.00	57.25	0.00

RT(A) and Yield (A) are retention times and yields from the first elution; RT (B) and yield (B) are retention times and yields from the second elution; assignment abbreviations are described above.

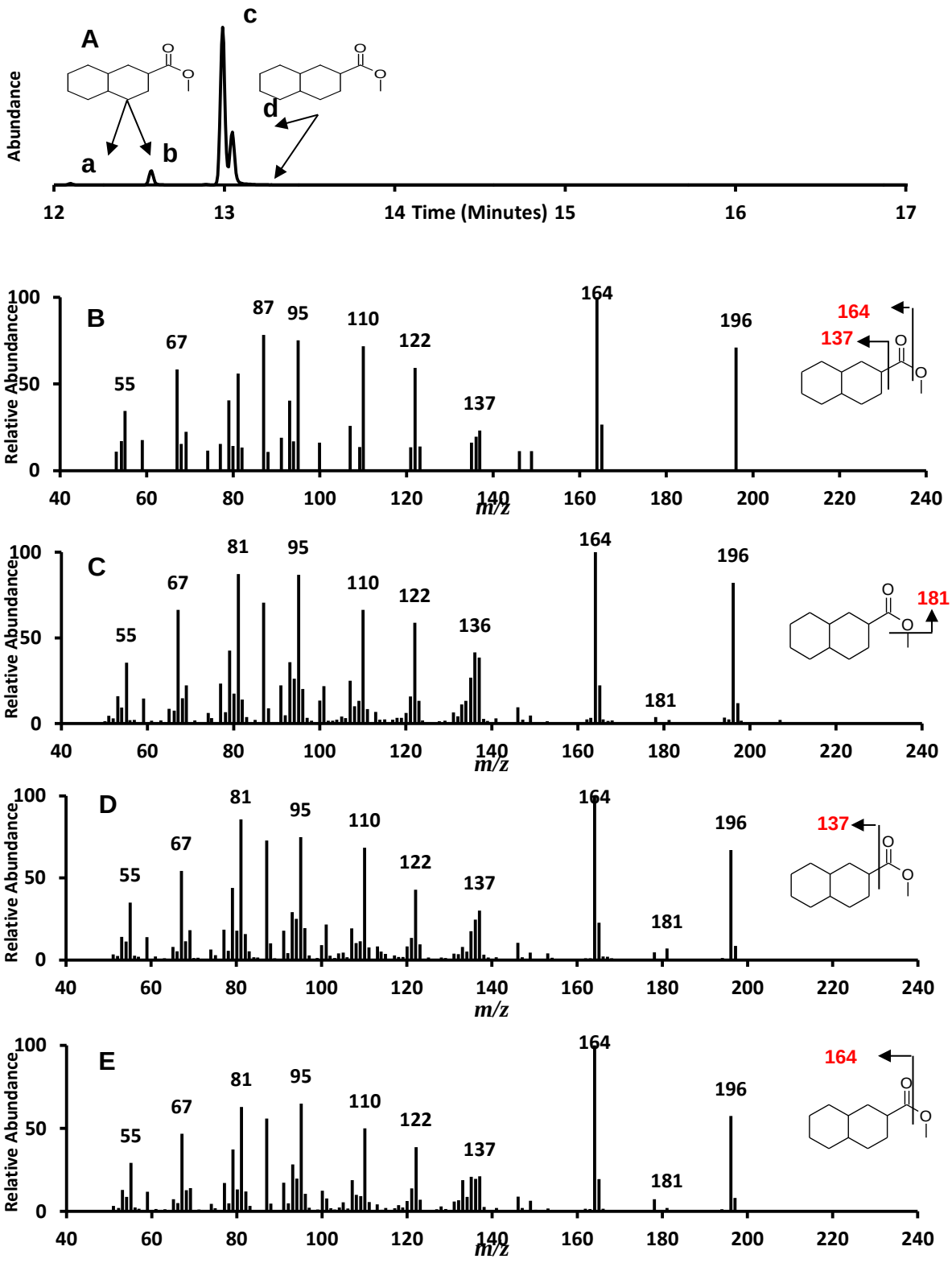

Figure 2.63. (A) Chromatogram from second (40 minute) elution through H-Cube® catalytic hydrogenator. (B-E) Isomers of decahydronaphthalene-2-carboxylic acid; GC-MS conditions as described in Figure 2.13.

2.3.12 Synthesis of Decahydronaphthalene-1-Ethanoic Acid

An authentic sample of the reactant, naphthalene-1-ethanoic acid (Sigma Aldrich; stated purity >99%), was reacted with the BF_3-MeOH complex and analysed with GC-MS to assess purity (Figure 2.64). The chromatogram reveals one distinct peak at 15.18 minutes (yield 97.7%) and a lesser peak at 15.30 minutes (yield 2.3%) (Figure 2.64A). Analysis of the mass spectra allows assignment of each peak to a compound. The mass spectra in Figure 2.64B reveals an $M^{+\bullet}$ of *m/z* 200 consistent with an assignment of naphthalene-1-ethanoic acid methyl ester and significant fragment ions are shown at *m/z* 141 (loss of carboxylate) and *m/z* 127 (loss of the alkanoate side chain; *m/z* 115 indicates a cleavage of a pentanoic acid methyl ester and *m/z* 91 indicates the presence of a methyl benzene fragment.

Analysis of Figure 2.64C reveals similar mass spectrum to that assigned as naphthalene-1-ethanoic acid. The $M^{+\bullet}$ and major fragments are the same (*m/z* 200, 141 and 127) though in this case a fragment ion is apparent at *m/z* 169, indicating the loss of a methoxy ion. It is apparent that there is another possibility for the $M^{+\bullet}$ at *m/z* 212 with a methyl fragment from this molecular ion at *m/z* 197 (M-15); it is likely that this mass spectra indicates a co-elution with a small amount of an unknown compound alongside a naphthalene ethanoic acid isomer. Comparison of retention times with a subsequent elution of naphthalene-2-ethanoic acid methyl acid (RT 15.30) confirms that this mass spectrum describes naphthalene-2-ethanoic acid methyl ester.

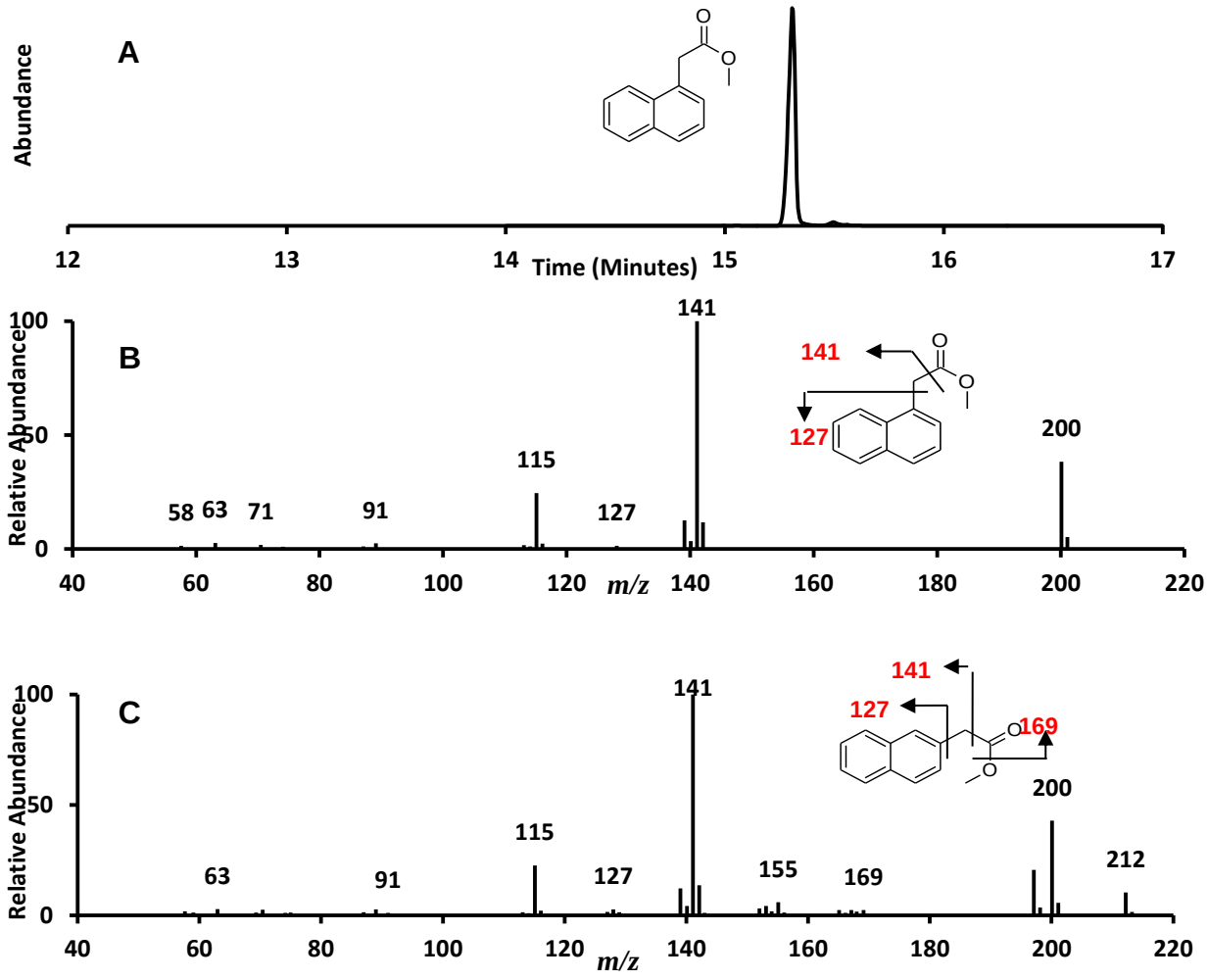

Figure 2.64. (A) Chromatogram of the methyl esters of naphthalene-1-ethanoic acid. (B) Mass spectrum the component eluting at RT 15.18 minutes. (C) Mass spectrum for the component eluting at 15.30 minutes. GC-MS conditions as described in Figure 2.13.

A sample of naphthalene-1-ethanoic acid was hydrogenated in both the Buchii reaction chamber and on the H-Cube® catalytic hydrogenator (Figure 2.65), samples for each experiment were reacted with BF_3-MeOH and analysed with GC-MS.

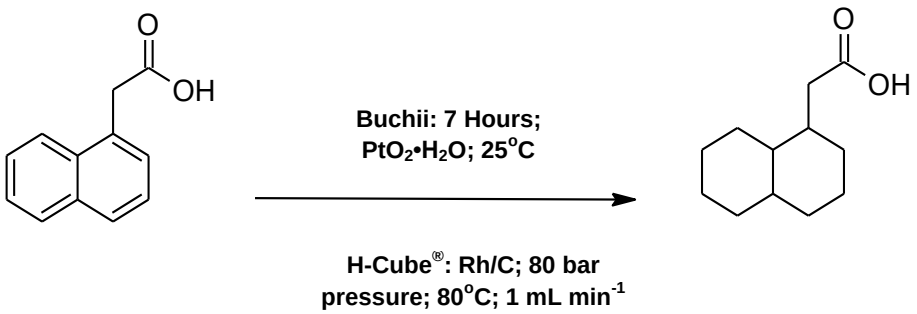

Figure 2.65. Reaction scheme for the catalytic hydrogenation of the reactant (naphthalene-1-ethanoic acid) to the product (decahydronaphthalene-1-ethanoic acid)**;** plus hydrogenation conditions.

Analysis of the chromatogram after the initial experiment (Figure 2.66A) reveals two large peaks (RT 14.58 and 15.18 minutes) and two lesser peaks (RT 14.26 and 14.04 minutes). The peak at 15.18 minutes has an identical RT to the reactant; the other peaks can therefore be assigned as partially or fully hydrogenated species.

Analysis of the mass spectra (Figure 2.66B-E) reveals that the small peak at 14.04 minutes has a $M^{+\bullet}$ of *m/z* 210 (Figure 2.64B), ten Daltons greater than the reactant which is consistent with the addition of ten hydrogen atoms, therefore this peak can be assigned to a small amount of the product (decahydronaphthalene-1-ethanoic acid). Significant fragment ions are *m/z* 179 (loss of a methoxy group); *m/z* 136 (loss of the alkanoate side chain); *m/z* 95 which indicates a methyl cyclohexyl fragment; and *m/z* 74 (ethanoic acid methyl ester fragment).

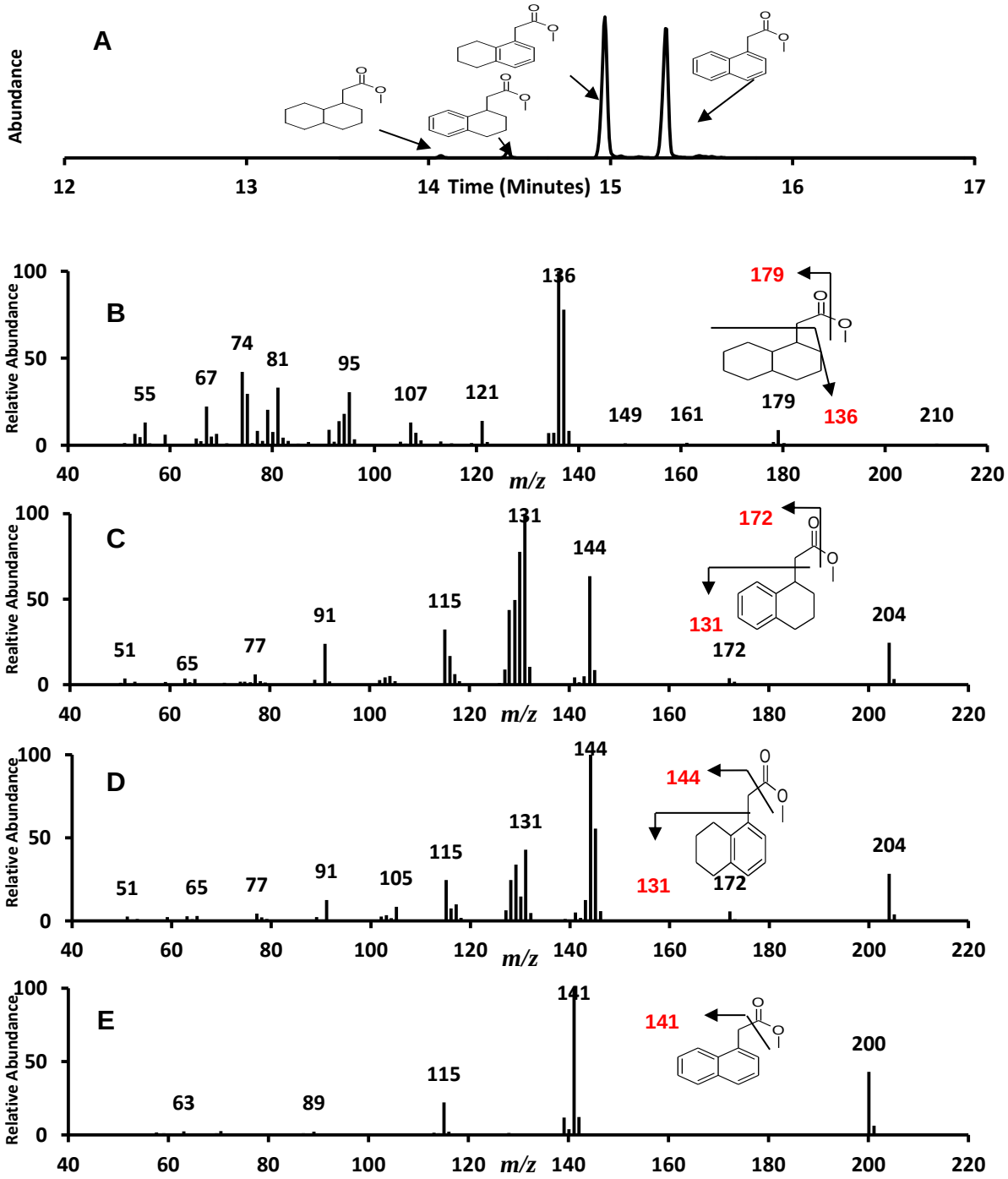

Figure 2.66. (A) Chromatogram from the initial 7 hour Buchii reactor chamber experiment. (B) Mass spectrum for component eluting at RT 14.04 minutes. (C) Mass spectrum for component eluting at 14.26 minutes. (D)Mass spectrum for component eluting at 14.58 minutes.(E) Mass spectrum for component eluting at 15.18 minutes**,** GC-MS conditions as described in Figure 2.13.

The mass spectra displayed in Figure 2.66C is assigned as a 1,2,3,4-tetrahydronaphthalene-1-ethanoic acid methyl ester. An $M^{+\bullet}$ of *m/z* 204 is consistent with the addition of the 4 hydrogen atoms required to saturate one of the aromatic rings. The relative abundance of the $M^{+\bullet}$ (23%) is near the optimum relative abundance for the 1,2,3,4-tetrahydro moiety of ~20%, it is also noted that compound has eluted immediately after the fully saturated species (RT 14.26 minutes) which is consistent with previously analysed chromatograms of the 1,2,3,4-tetrahydronaphthalenes (i.e. Figure 2.63*ii*). Significant fragment ions are apparent at *m/z* 172, 144 and 131 (base ion) detailing the fragments from the ethanoate side chain and *m/z* 91 indicating the presence of a methyl benzene fragment.

Figure 2.66D is the mass spectrum assigned to a 5,6,7,8- tetrahydronaphthalene-1-ethanoic acid methyl ester. Retention time (RT 14.58 minutes) notwithsatnding there are other precedents for assigning this mass spectra thus. An $M^{+\bullet}$ of *m/z* 204 is consistent with the addition of the 4 hydrogen atoms required to partially saturate this compound. Analysis of the significant fragment ions reveals that the base ion is positioned at *m/z* 144 (as opposed to m/z 131 for the 1,2,3,4-tetrahydro species), comparison with the tetrahydro species in Figure 2.47*i* and *ii* shows that the 1,2,3,4-tetrahydro species, eluting first, has a base ion equating with the alkanoate side chain (*m/z* 130) as does the 1,2,3,4-tetrahydro species in Figure 2.50, the 5,6,7,8-tetrahydro species has a base ion at *m/z* 158 equating with loss of methanol and the ion indicating loss of the alkanoate side chain is far less abundant. Other significant ions are at *m/z* 131 and *m/z* 115. Figure 2.66E is

assigned as a naphthalene-1-ethanoic acid methyl ester, the chromatogram and mass spectra have been described previously.

A subsequent attempt at catalytic hydrogenation (Figure 2.67B) reduced the amount of reactant present and increased both tetrahydro species. A small amount of decahydronaphthalene-ethanoic acid is also apparent. The mass spectra for the reactant and the tetrahydro moeities have been descibed previously, as has one isomer of the decahydronaphthalene. However, as Figure 2.67C shows, there are potentially a number of isomers of the decahydro species apparent.

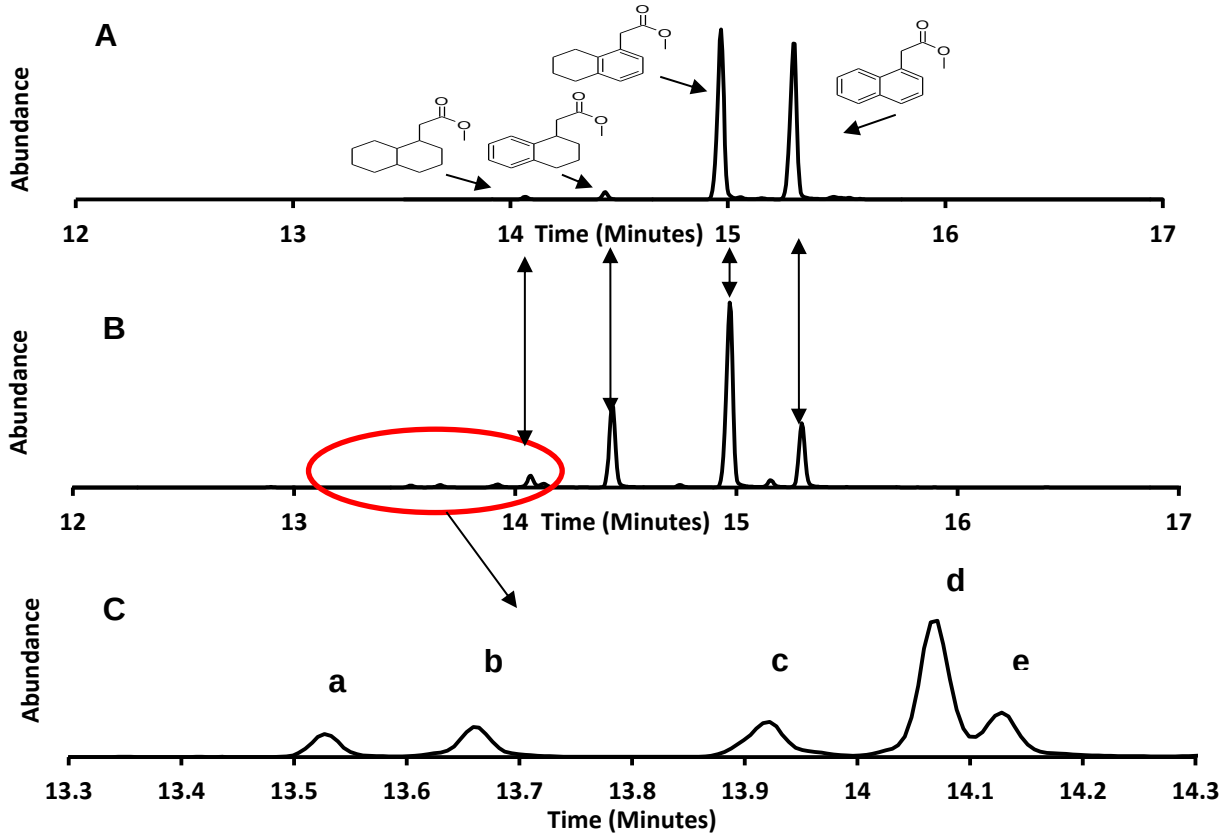

Figure 2.67. (A) Chromatogram from initial hydrogenation on Buchii Reaction Chamber. (B) Chromatogram from subsequent hydrogenation attempt.(C) Close up of 13.30-14.30 minute area of Figure 2.65B. GC conditions as described in Figure 2.13.

Analysis of the mass spectra (Figure 2.68) reveals that only three of the chromatographic peaks can be assigned to decahydro species (Figure 2.68C chromatographic peaks ‘a’,’c’ and ‘d’) whilst peaks ‘b’ and ‘e’ seem to fit an octahydro moeity.

Analysis of Figure 2.68A revealed no $M^{+\bullet}$ at m/z 210. There is an ion at m/z 207 (relative abundance 6.8%). This ion was discounted as the $M^{+\bullet}$ as not only is it an odd number which would hint at the presence of nitrogen (see ‘nitrogen rule’ Sparkman et al., 2011) but it is also the major ‘bleed’ ion from the siloxane coating of the chromatographic column and indicates the presence of a cyclic hexamethylcyclotrisiloxane (Sigma Aldrich., 2012: http://www.sigmaaldrich.com/analytical-chromatography/gas-chromatography/columns/slb-gc-capillary/low-bleed.html). Significant fragment ions at m/z 179 (M-31; loss of a methoxy group) and m/z 136 (M-74; loss of the alkanoate side chain) indicate that the molecular weight of the compound assigned to peak ‘a’ is 210 Daltons characteristic with the addition of 10 hydrogen atoms to the reactant to produce an isomer of decahydronaphthalene-1-ethanoic acid methyl ester.

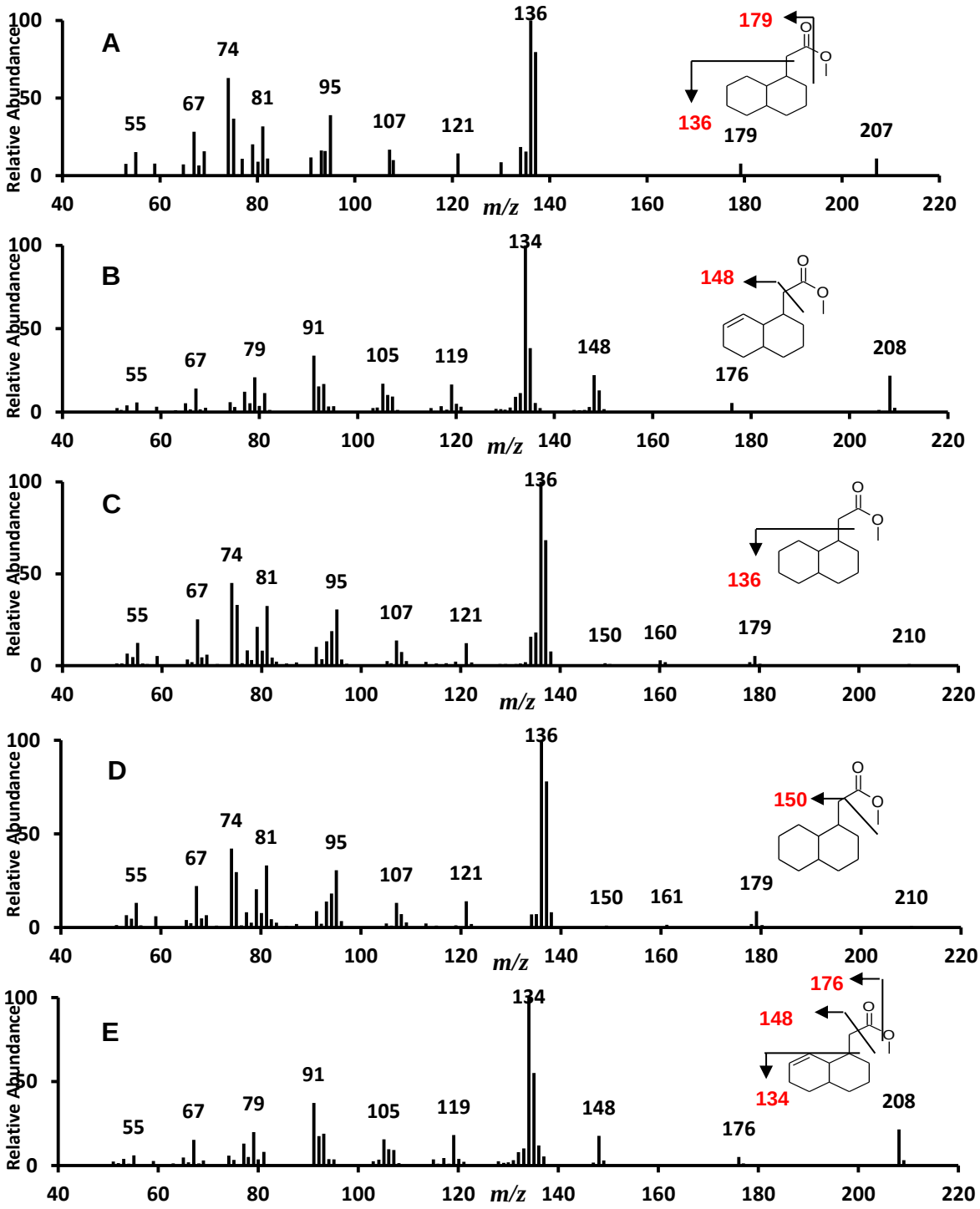

Figure 2.68. Mass spectra from chromatographic peaks a-e in Figure 2.67C. (A, C and D) Revealing a decahydronaphthalene-1-ethanaoic acid methyl ester. (B and E) Octahydronaphthalene-1-ethanoic acid methyl ester**.** MS conditions as described in Figure 2.13.

Analysis of Figures 2.68B and E reveals an $M^{+\bullet}$ of *m/z* 208 consistent with the addition of 8 hydrogen atoms and characteristic of octahydronaphthalene-1-ethanoic acid methyl esters. Significant fragment ions in both mass spectra are similar with peaks apparent at *m/z* 176, 148 and 134 indicative of alkanoate side chain cleavage.

Analysis of Figure 2.68C and D reveals that both mass spectra have an $M^{+\bullet}$ at *m/z* 210 consistent with the addition of 10 hydrogen atoms and indicative of isomers of decahydronaphthalene-1-ethanoic acid methyl esters. Significant fragment ions are revealed at *m/z* 179 (loss of methoxy), *m/z* 150 (loss of a carboxylate ion) and *m/z* 136 loss of the alkanoate side chain. This hydrogenation attempt was examined via GCxGC-MS and the mass spectra and 2D retention times were compared with unknown compounds eluting within a commercial mixture of naphthenic acids (Rowland et al., 2011d).

2.3.13 Synthesis of Decahydronaphthalene-2-ethanoic Acid

An attempt was made to synthesis decahydronaphthalene-2-ethanoic acid from an authentic naphthalene-2-ethanoic acid (Sigma Aldrich: Stated Purity >99%) through catalytic hydrogenation (Figure 2.69) using both the Buchii reaction chamber and the H-Cube® flow through hydrogenator.

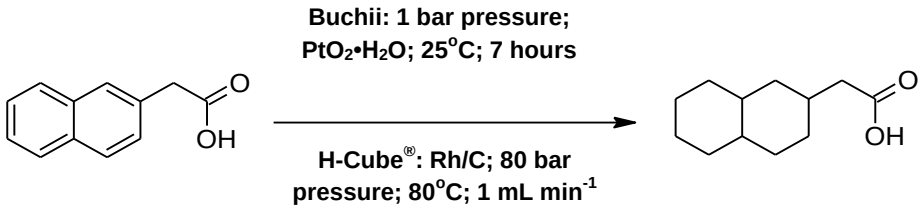

Figure 2.69. Reaction scheme for the catalytic hydrogenation of the reactant (naphthalene-2-ethanoic acid) to the product (decahydronaphthalene-2-ethanoic acid); plus catalytic hydrogenation conditions.

A small amount of reactant was esterified with BF_3-MeOH and analysed with GC-MS for purity (Figure 2.70). The chromatogram (Figure 2.70A) shows one distinct peak at RT 15.30 minutes giving a purity of >99%. Analysis of the mass spectra (Figure 2.70B) reveals an $M^{+\bullet}$ at *m/z* 200 consistent with a naphthalene-2-ethanoic acid methyl ester; significant ions are shown at *m/z* 141 characteristic with the loss of a carboxylate and at *m/z* 115 indicating a cleavage of a pentanoic acid methyl ester. No other ions are abundant enough to be revealed on Figure 2.70B, however a close up of the *m/z* 143-201 area (Figure 2.70C) reveals fragment ions at *m/z* 185 (loss of a methyl group) and at *m/z* 168 (loss of methanol). The $M^{+\bullet}$ and the fragment ions allow an assignment of naphthalene-2-ethanoic acid methyl ester.

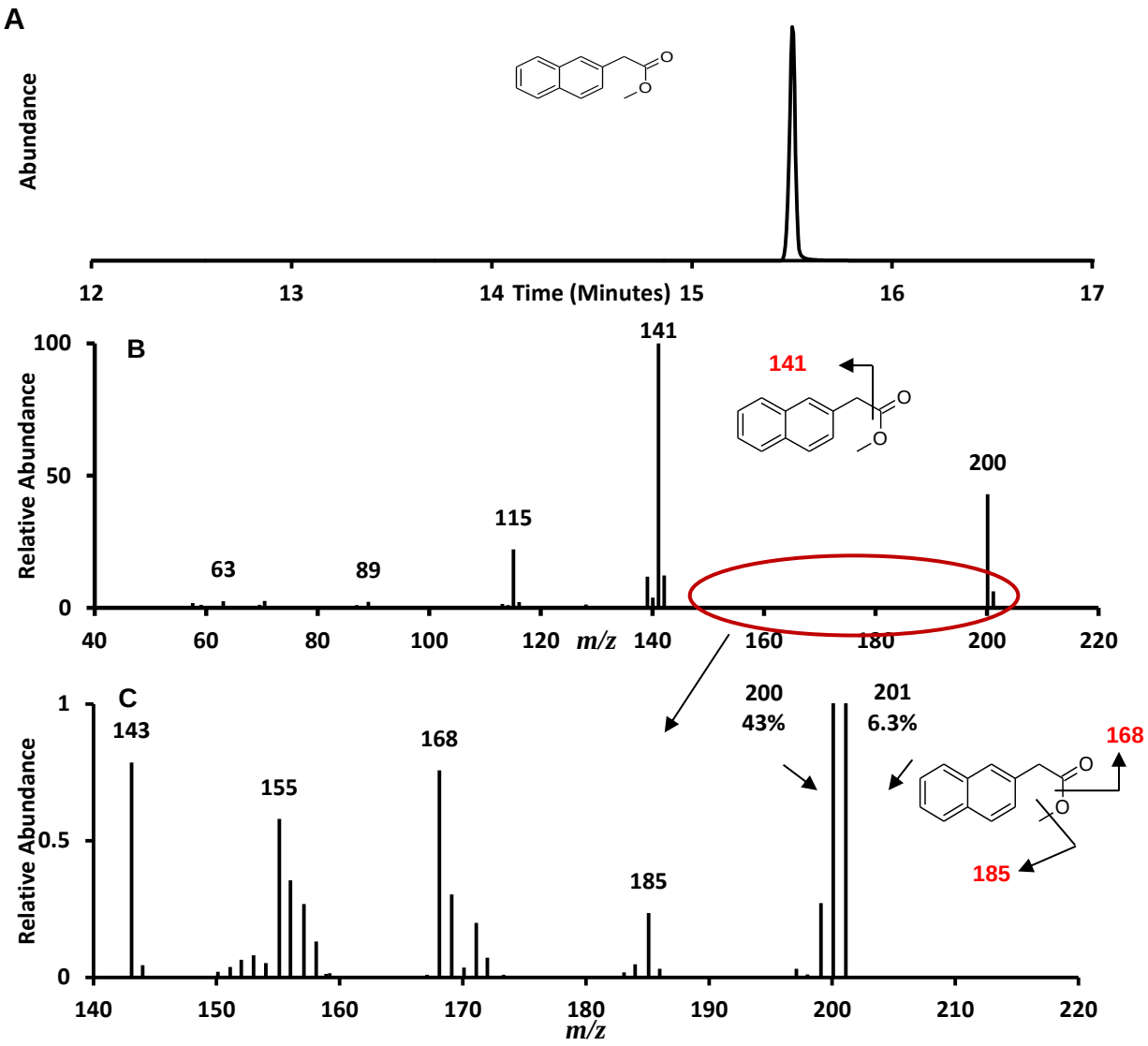

Figure 2.70. (A) Chromatogram of the methyl esters of naphthalene-2-ethanoic acid. (B) Mass spectrum of the component eluting at RT 15.30 minutes. (C) Close up of *m/z* 140-220 region of Figure 2.68B. GC-MS conditions as described in Figure 2.13.

A sample was hydrogenated using the Buchii reaction chamber, a sample of the product was derivatised with BF_3-MeOH and analysed with GC-MS (Figure 2.71B). This experiment was repeated for a further 7 hours (Figure 2.71C).

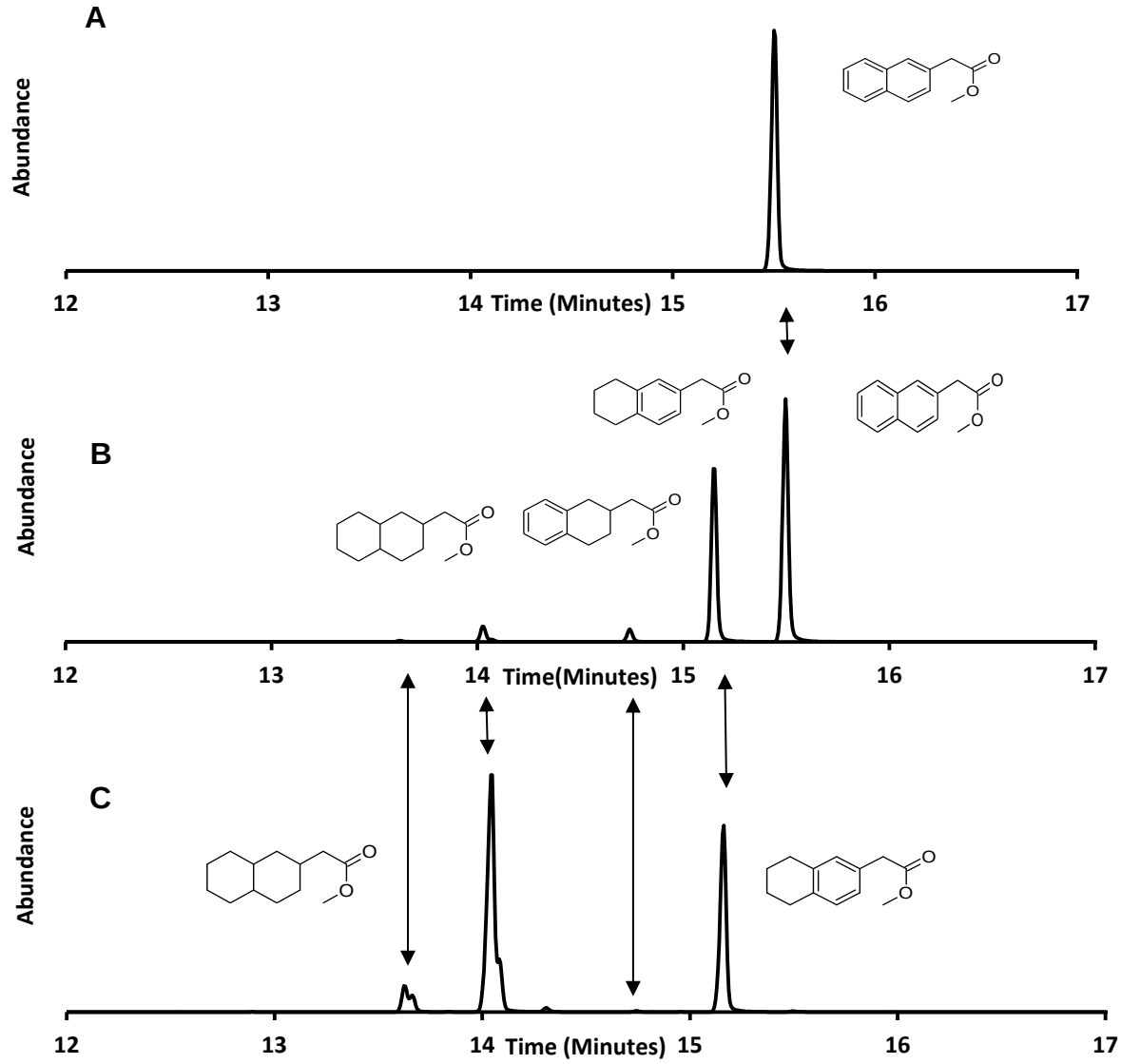

Figure 2.71. (A) Chromatogram of authentic naphthalene-2-ethanoic acid methyl ester. (B) Chromatogram after first hydrogenation attempt with the Bucii reaction chamber. (C) Chromatogram after second hydrogenation attempt with the Buchii reaction chamber**.** GC conditions as described in Figure 2.13.

Analysis of the chromatogram from the first attempt (Figure 2.71B) reveals two distinct chromatographic peaks (RT 15.09 and 15.30 minutes) and two lesser chromatographic peaks (RT 14.01 and 14.44 minutes). The peak at RT 15.30 is provisionally assigned as the reactant (naphthalene-2-ethanoic acid methyl ester) and the peaks at RT 14.44 and 15.19 are likely to be indicative of the tetrahydro species. The peak at RT 14.01 is tentatively assigned as a fully saturated decahydronaphthalene moiety. Analysis of the chromatogram from the second attempt reveals that all of the reactant has now been saturated, either partially or fully. There is a distinct peak at RT 15.19, tentatively assigned as the 5,6,7,8-tetrahydronaphthalene moiety as it matches the RT of the peak in Figure 2.71B that elutes nearest to the reactant. The compound represented by the peak at RT 14.44 is no longer apparent and the peak at RT 14.01 is revealed to be in the greatest abundance and is shown to represent two isomers of the decahydronaphthalene moiety (RT 14.01 and 14.05 minutes); there is a secondary dual chromatographic peak apparent at RT 13.37 and 13.39 minutes which is also tentatively assigned as representing two more decahydronaphthalene-2-ethanoic acid methyl ester isomers. Analysis of the mass spectra will confirm these assignments (Figure 2.72 and 2.73). Table 2.5 details percentage yields of each peak in Figure 2.71B and C.

Analysis of the mass spectra from the first hydrogenation attempt reveals that the tentative assignments from the chromatograms can be confirmed (Figure 2.72). The chromatographic peak at RT 14.01 minutes (peak ‘a’: Figure 2.72B) has a mass spectrum with an $M^{+\bullet}$ at m/z 210, this is consistent with the addition of ten hydrogen atoms to the reactant increasing the molecular weight by ten Daltons

and is therefore indicative of the presence of a decahydronaphthalene ethanoic acid methyl ester. The assignment of the '2' isomer can be made due to the differences in the mass spectral profile between Figure 2.72B and the '1' isomer mass spectrum shown in Figure 2.66.

Table 2.5. Percentage yields from the hydrogenation attempts of naphthalene-2-carboxylic acid using the Buchii reaction chamber.

					Sum Isomers (%)	
Assignment	RT(A)	RT(B)	Yield (A) (%)	Yield (B) (%)	1st Attempt	2nd Attempt
DHN-2-EA		13.37	0.00	4.15	3.40	65.36
DHN-2-EA		13.39	0.00	3.11		
DHN-2-EA	14.01	14.01	3.40	50.45		
DHN-2-EA		14.05	0.00	7.64		
THN-2-EA	14.44		2.88	0.00	41.42	34.64
THN-2-EA	15.09	15.09	38.54	34.64		
NA-2-EA	15.30		55.16	0.00	55.16	0.00

DHN-2-EA is decahydronaphthalene-2-ethanoic acid methyl esters; THN-EA is tetrahydronaphthalene-2-ethanoic acid methyl esters; NA-2-CA is naphthalene-2-carboxylic acid methyl esters; RT(A) is the retention time from the first attempt; RT(B) is the retention time from the second attempt

Significant ions in Figure 2.72B exist at *m/z* 74 (base ion); *m/z* 136 (loss of the ethanoate side chain) and *m/z* 179 (loss of a methoxy group); this is compared to the '1' isomer which has a base ion at *m/z* 136 (Figure 2.68).

Analysis of Figure 2.72C (peak 'b') reveals an $M^{+\bullet}$ at *m/z* 204 consistent with the addition of 4 hydrogen atoms to the reactant and characteristic with a tetrahydronaphthalene moiety. The assignment of a 1,2,3,4-tetrahydronaphthalene species is due to the chromatographic peak eluting just after the decahydronaphthalene moiety and the relative abundance of the $M^{+\bullet}$ (10%) which is smaller than the mass spectrum assigned to the 5,6,7,8-tetrahydronaphthalene species (Figure 2.71D: $M^{+\bullet}$ relative abundance ~40%) and hinting towards a less stable species of tetrahydronaphthalene. Significant fragment ions exist at *m/z* 172 (loss of methanol) *m/z* 130 (Base ion: loss of the alkanoate side chain) and *m/z* 77 ($C_6H_5^+$ benzene fragment).

Peak 'c' is assigned as a 5,6,7,8-tetrahydronaphthalene-2-ethanoic acid methyl ester. The mass spectrum (Figure 2.71D) reveals an $M^{+\bullet}$ at *m/z* 204 at ~40% relative abundance, consistent with an assignment of a 5,6,7,8-tetrahydronaphthalene ethanoic acid methyl ester. Significant fragment ions exist at *m/z* 131 indicating the loss of the ethanoate side chain and at *m/z* 145, indicative of a loss of a carboxylate fragment and is the base ion, this is consistent with an *m/z* 144 base ion for the similar '1' position 5,6,7,8-tetrahydronaphthalene ethanoic acid discussed in Figure 2.66.

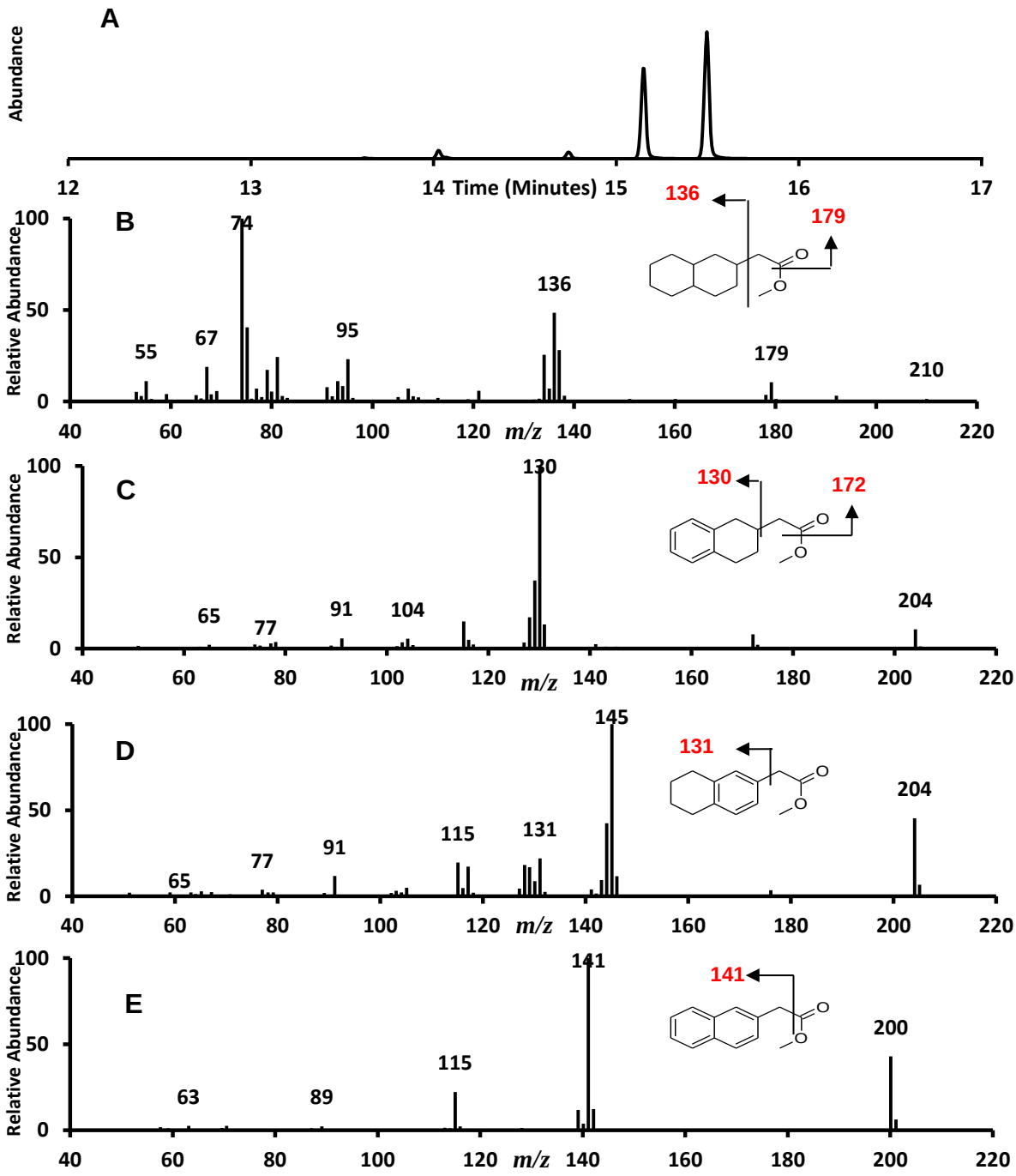

Figure 2.72. Chromatogram from first hydrogenation of naphthalene-2-ethanoic acid. (B) Mass spectrum for component eluting at RT 14.01minutes. (C) Mass spectrum for component eluting at RT 14.44 minutes. (D) Mass spectrum for component eluting at RT 15.09 minutes. (E) Mass spectrum for component eluting at RT 15.30 minutes. GC-MS conditions as described in Figure 2.31.

Peak ‘d’ (RT 15.30 minutes) is assigned to the reactant (naphthalene-2-ethanoic acid methyl ester) the mass spectra and retention time (RT 15.30 minutes) is identical to the mass spectra and chromatogram displayed in Figure 2.72 and has been discussed previously. Analysis of the mass spectrum from the second hydrogenation attempt reveals that the first four chromatographic peaks (Figure 2.72A peaks ‘a’-‘d’) can be assigned as isomers of decahydronaphthalene-2-ethanoic acid methyl esters; peak ‘e’ shares the same retention time and identical mass spectra to the 5,6,7,8-tetrahydronaphthalene-2-ethanoic acid methyl ester displayed in Figure 2.71D and has been discussed previously.

Analysis of the mass spectra for peaks ‘a’-‘d’ reveals that all four spectra are very similar. All four spectra have an $M^{+\bullet}$ at m/z 210 indicating that ten hydrogen atoms have added to the original reactant thus increasing the molecular weight by ten Daltons, this is consistent with the molecular weight of a decahydronaphthalene ethanoic acid species. Significant fragment ions are similar throughout. The base ion is revealed to be at m/z 74 throughout; similarly there is another fragment ion at m/z 136 which appears in all four spectra, which indicates the loss of the ethanoate side chain.

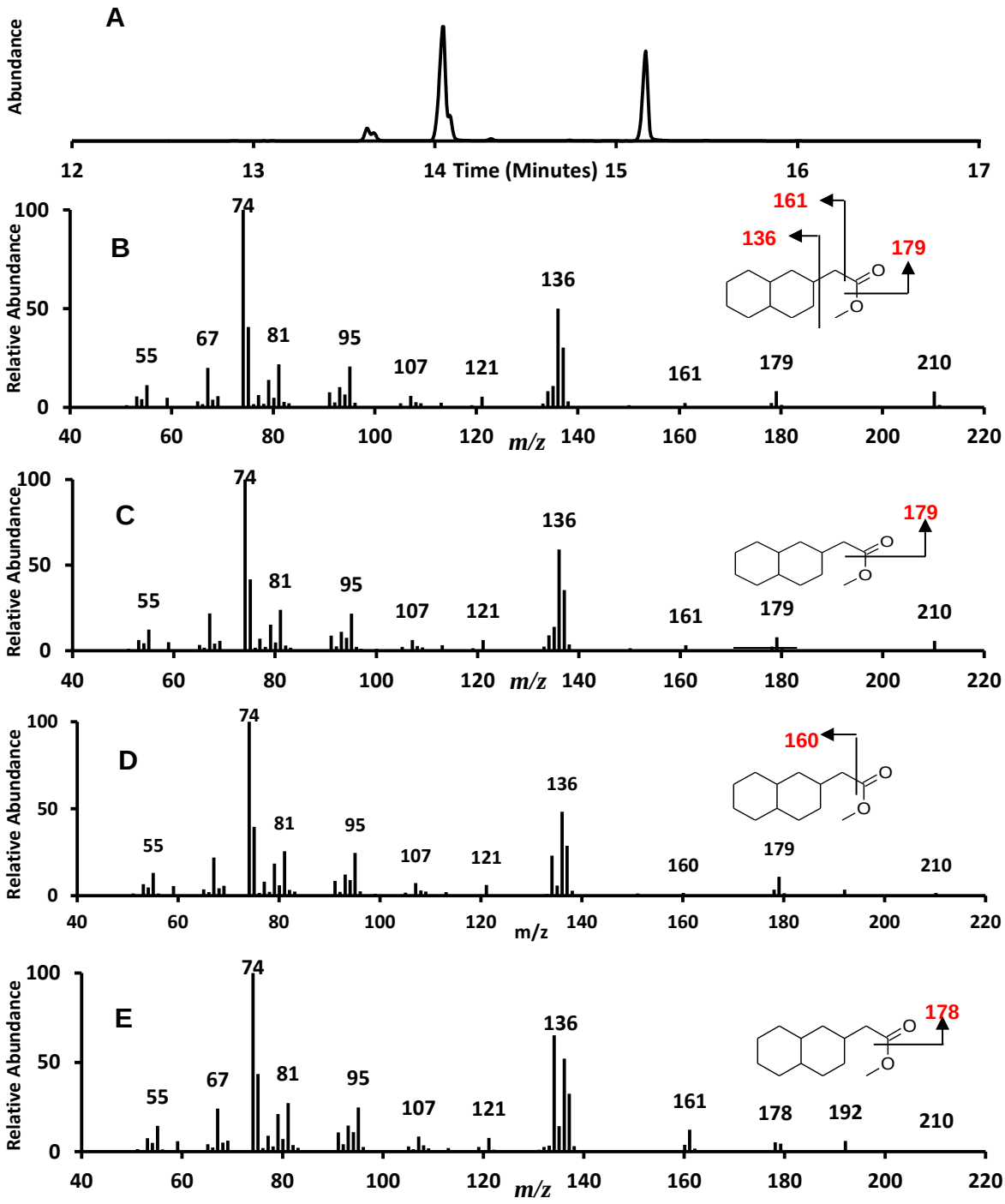

Figure 2.73. (A) Chromatogram from second catalytic hydrogenation attempt. (B-E) Mass spectra for isomers of decahydronaphthalene-2-ethanoic acid methyl esters. GC-MS conditions as described in Figure 2.13.

Peaks a-c (Figure 2.73B-D) show a fragment at m/z 179 indicating loss of a methoxy group, whilst peak ‘d’ (Figure 2.73E) has a more abundant fragment at m/z 178, indicating loss of methanol. Fragment ions at m/z 161 are revealed in the mass spectra representing peaks ‘a’, ‘b’ and ‘d’ (Figure 2.73B,C and E) indicating the loss of a carboxylate ion whilst this loss is indicated by the fragment at m/z 160 in the mass spectra representing peak ‘c’ (Figure 2.73D) indicating a difference in the position of the charge retention on the carboxylate fragments.

A fresh sample of the reactant was prepared for catalytic hydrogenation utilising the H-Cube® hydrogenator. A small aquilot was taken during the first attempt (Figure 2.74B) and analysed with GC-MS. This sample was re-eluted through the H-Cube on two subsequent occasions until all of the reactant had been converted to the product.

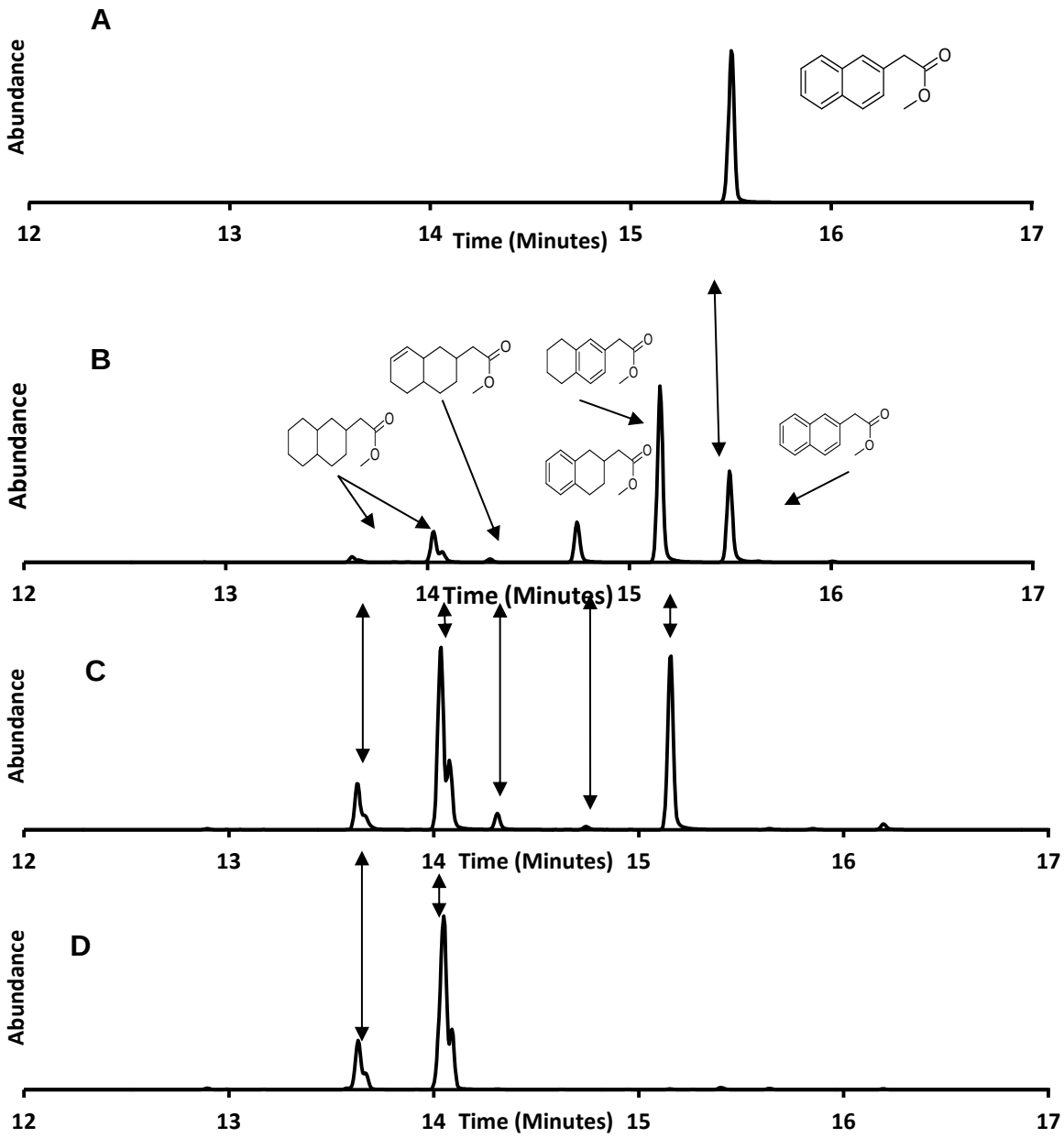

Figure 2.74. (A) Chromatogram of authentic naphthalene-2-ethanoic acid. (B) Chromatogram from first H-Cube® attempt with the reactant. (C) Chromatogram of the second H-Cube attempt.(D) Chromatogram from the third attempt. GC conditions as described in Figure 2.13.

Analysis of the chromatograms in Figure 2.74 reveals that partially and fully saturated products share identical retention times to the chromatograms in Figure

2.62, Table 2.6 details these similarities and also shows percentage yields for the reactant and each product. However at RT 14.18 is a small peak which is not apparent in the Buchii reaction experiments. Analysis of this mass spectrum (Figure 2.75) allows an assignment of an octahydronaphthalene-2-ethanoic acid methyl ester. The $M^{+\bullet}$ at m/z 208 is indicative of eight hydrogen atoms adding eight Daltons to the molecular weight, significant fragment ions exist at m/z 176, 148 and 134, these are characteristic of the loss of the alkanoate side chain and m/z 134 is indicative of an octahydronaphthalene fragment.

Table 2.6. Percentage yields from the hydrogenations attempts using the H-Cube® hydrogenator, showing a comparison of retention times with the Buchii reaction chamber experiments.

Assignment	RT Buchii	RT H-Cube	Yield A (%)	Yield B (%)	Yield C (%)
DHN-2-EA	13.37	13.37	1.54	6.17	6.37
DHN-2-EA	13.39	13.39	0.63	2.10	5.32
DHN-2-EA	14.01	14.01	8.29	24.27	75.79
DHN-2-EA	14.05	14.05	3.27	9.77	12.52
OHN-2-EA	0.00	14.18	1.05	3.52	0.00
THN-2-EA	14.44	14.44	11.29	7.00	0.00
THN-2-EA	15.09	15.09	48.20	47.18	0.00
NA-2-EA	15.30	15.30	25.73	0.00	0.00

Sum Isomers%

	Sum A	Sum B	Sum C
DHN-2-EA	13.73	42.31	100.00
DHN-2-EA			
DHN-2-EA			
DHN-2-EA			
OHN-2-EA	1.05	3.52	0.00
THN-2-EA	59.49	54.18	0.00
THN-2-EA			
NA-2-EA	25.73	0.00	0.00

Assignment abbreviations detailed in Table 2.6 apart from OHN-2-EA which is octahydronaphthalene-2-ethanoic acid methyl ester.

..

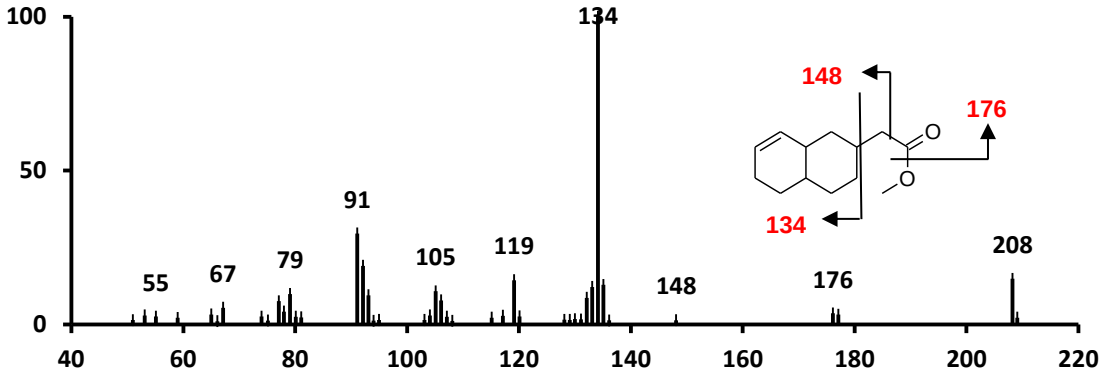

Figure 2.75. Mass spectra for the chromatographic peak at RT14.18 minutes revealing an octahydronaphthalene-2-ethanoic acid methyl ester; MS conditions as described in Figure 2.13.

2.3.14. Synthesis of Decahydronaphthalene-1-propanoic Acid

An attempt was made to synthesise decahydronaphthalene-1-propanoic acid through the catalytic hydrogenation of an authentic sample of naphthalene-1-propanoic acid (Figure 2.76) (Sigma Aldrich: Stated purity >99%). Initially hydrogenated with the H-Cube® flow through hydrogenator the experiment was completed by use of the Buchii reaction chamber.

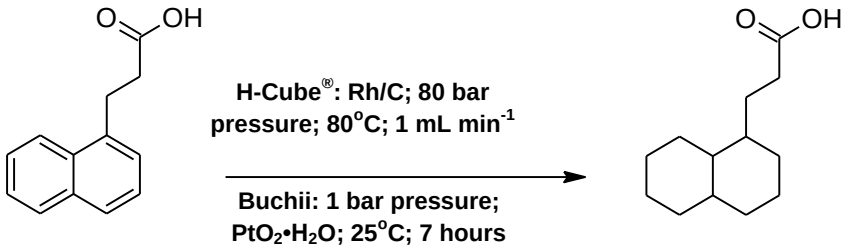

Figure 2.76. Reaction scheme for the catalytic hydrogenation of the reactant (naphthalene-1-propanoic acid) to the product (decahydronaphthalene-1-propnaoic acid)**;** plus hydrogenation reaction conditions for the H-Cube® (above arrow; and the Buchii reaction chamber (below arrow).

A small amount of the reactant was esterified with the BF_3-MeOH complex (30 minutes; 70^{o}C) and analysed with GC-MS to assess purity (Figure 2.77). Figure 2.77A reveals the chromatogram has one distinct peak at a retention time of RT 16.31 minutes and a much smaller peak at RT 16.12 minutes which makes up 1.2% of the chromatographic peaks thus dictating that the larger peak makes up >98% of the chromatogram. Mass spectral analysis reveals that the peak at RT 16.31 is naphthalene-1-propanoic acid methyl ester (Figure 2.77B); and the smaller peak is most likely to be a small amount of a partially saturated species, 5,6,7,8-tetrahydronaphthalene-1-propanoic acid methyl ester (Figure 2.77C). The $M^{+\bullet}$ at *m/z* 214 in Figure 2.77B is consistent with the molecular weight of a naphthalene-1-propanoic acid methyl ester.

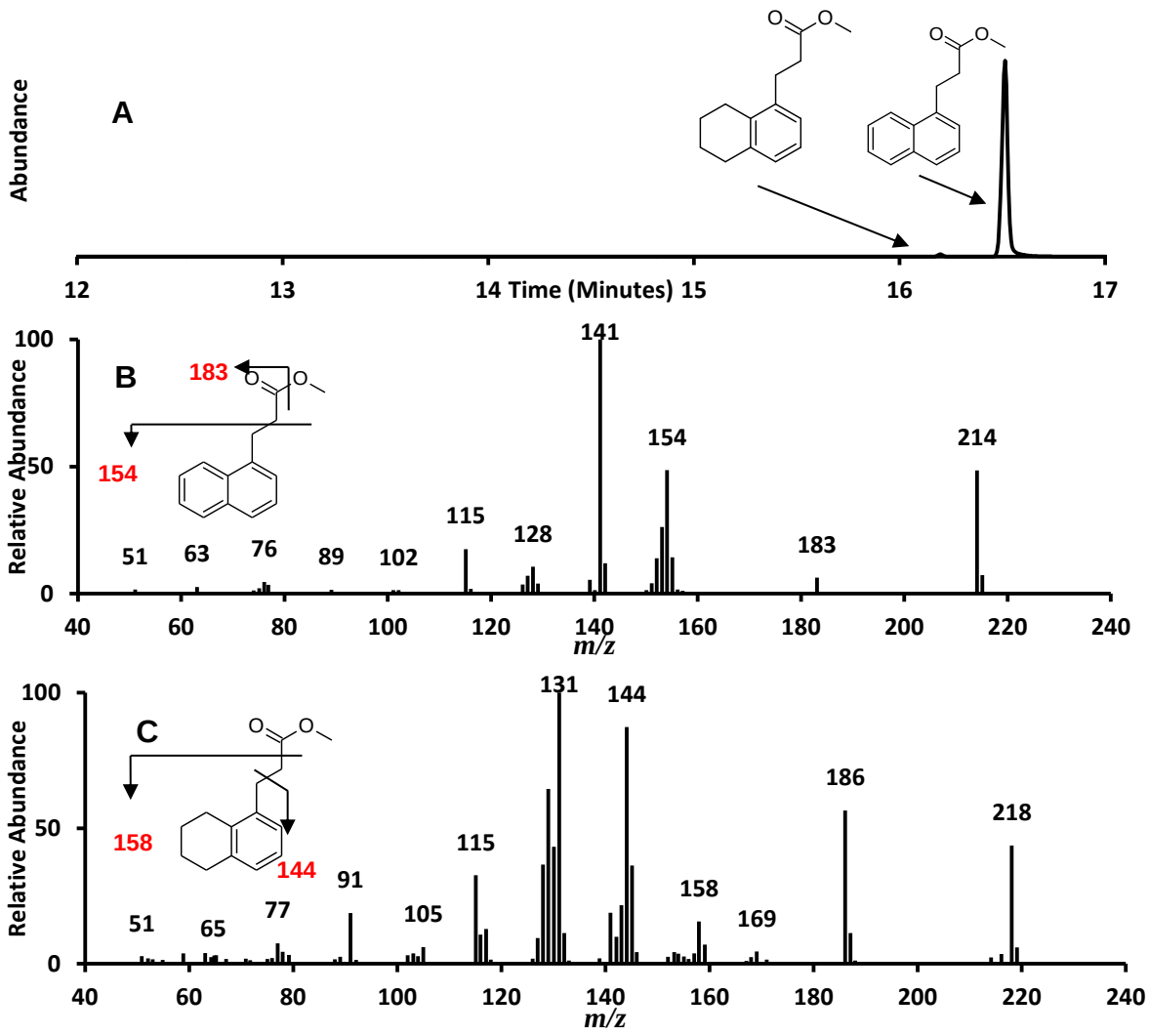

Figure 2.77. (A) Chromatogram of naphthalene-1-propanoic acid methyl esters; (B) mass spectra of component eluting at RT 16.31 minutes, assigned as naphthalene-1-propanoic acid methyl ester; (C) mass spectra of component eluting at RT 16.20 minutes, assigned as 5,6,7,8-tetrahydronaphthalene-1-propanoic acid methyl esters. GC-MS conditions as described in Figure 2.13.

Significant fragment ions are apparent at *m/z* 183 (loss of a methoxy group); *m/z* 154 (loss of a carboxylate ion); *m/z* 141 (loss of an ethanoate ion); and *m/z* 128 (loss of the alkanoate side chain. These fragment ions coupled with the $M^{+\bullet}$ allow an assignment of naphthalene-1-propanoic acid.

The $M^{+\bullet}$ at *m/z* 218 in Figure 2.77C is consistent with the addition of four hydrogen atoms, increasing the molecular weight by four Daltons. Significant fragment ions at *m/z* 186 (methanol ion); *m/z* 158 (carboxylate ion); *m/z* 144 (ethanoate ion); and *m/z* 131 (alkanoate side chain) allow a assignment of a tetrahydronaphthalene species. The relative abundance of the $M^{+\bullet}$ at *m/z* 218 (43%) and the GC elution close to the reactant hints towards a 5,6,7,8-tetrahydronaphthalene-1-propanoic acid methyl ester.

An initial attempt to hydrogenate the reactant with the H-Cube® flow through hydrogenator (Rh/C; 80^{o}C; 80 bar pressure; 1 mL min-^{1}) resulted in all of the reactant being converted to two isomers of tetrahydronaphthalene (1,2,3,4-tetrahydronaphthalene moiety; RT 15.50 minutes; 20%: 5,6,7,8-tetrahydronaphthalene moiety; RT 16.20 minutes; 80%: Figure 2.78B). A subsequent attempt had little effect and it was determined that a fresh catalyst was required (Figure 2.78C). A third attempt on the H-Cube® fully hydrogenated the bulk of the partially hydrogenated reactants with the 1,2,3,4-tetrahydro species being converted and the chromatographic peak representing the 5,6,7,8-tetrahydro species being reduced to 14% of the total peak area (Figure 2.78D). Distinct peaks at RT 14.57 minutes and 15.25 minutes plus smaller peak with and RT at 15.16 minutes (with an apparent shoulder at RT 15.13 minutes)

indicate that the sample consists mainly of the fully saturated decahydronaphthalene moiety.

Due to limited time availability with the H-Cube® the final attempt proceeded in the Buchii reaction chamber (Figure 2.78E). The chromatogram reveals that the naphthalene-1-propanoic acid reactant has been potentially converted to four isomers of decahydronaphthalene-1-propnaoic acid (RT's at 14.57, 15.13, 15.16 and 15.25 minutes) (Figure 2.78).

Analysis of the mass spectra connected to the chromatographic peaks will aid in the positive identification of these four isomers and the partially converted species apparent in Figure 2.78 B, C and D. Table 2.7 details the abundance of each peak and shows the progression of the hydrogenation attempts throughout.

The chromatographic peaks at RT 15.51 and 16.12 revealed in Figure 2.78B, C and D have identical mass spectra (Figure 2.79). Analysis of Figure 2.79 reveals that these two peaks can be assigned to a 1,2,3,4-tetrahydronaphthalene-1-propanoic acid methyl ester (RT 15.51; Figure 2.60A) and a 5,6,7,8-tetrahydronaphthalene-1-propanoic acid methyl ester (RT 16.12; Figure 2.78B). The assignment of the individual isomers can be made by analysis of the retention times (the 1,2,3,4-tetrahydronaphthalene isomer elutes earlier) and the abundance of the $M^{+\bullet}$ (Figure 2.79A $M^{+\bullet}$ abundance 19%; Figure 2.79B $M^{+\bullet}$ abundance 44%).

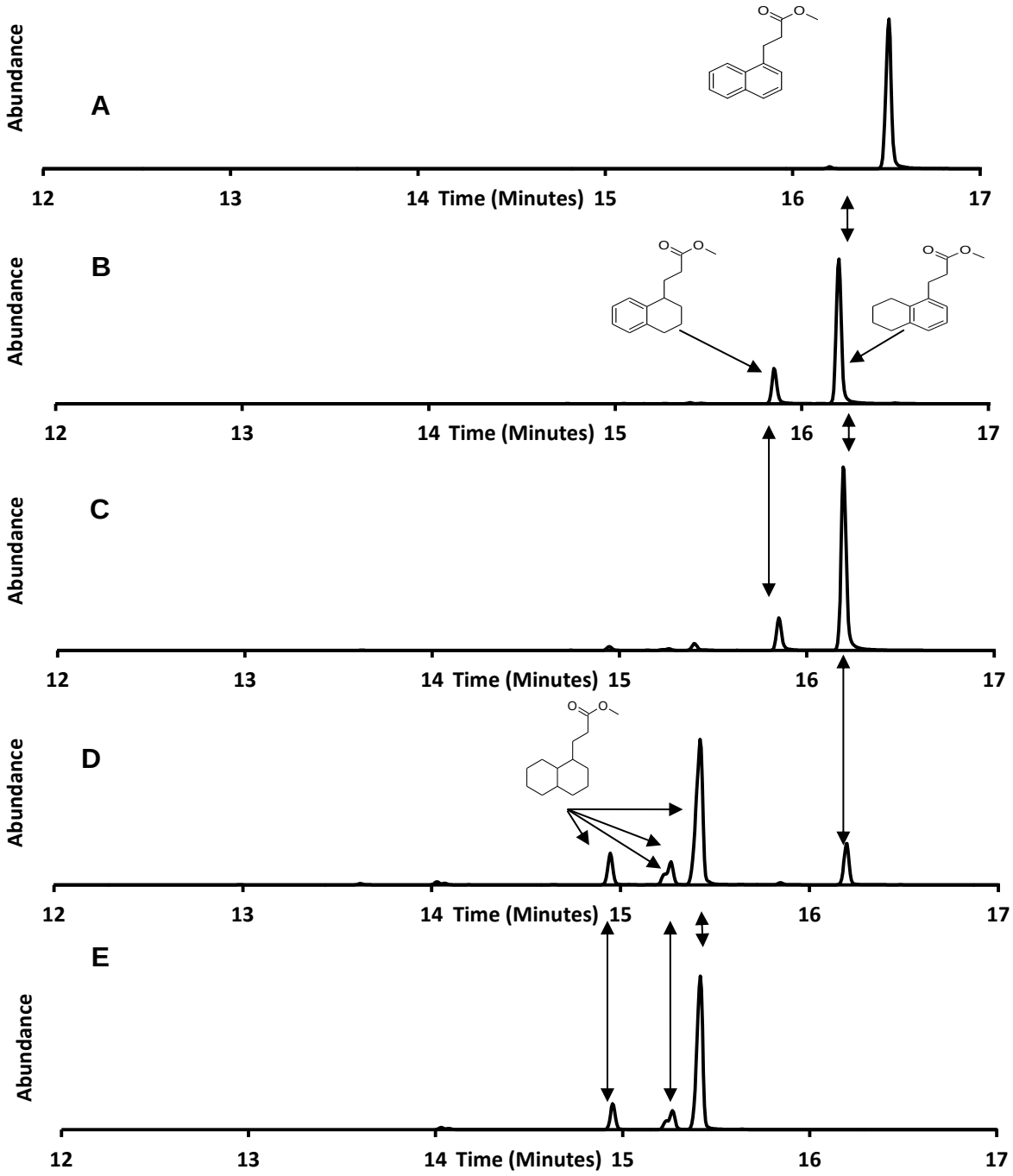

Figure 2.78. (A) Chromatogram of reactant, naphthalene-1-propanoic acid methyl ester. (B) Chromatogram from first hydrogenation attempt with the H-Cube®. (C) Chromatogram from the second H-Cube® attempt. (D) Chromatogram from the third H-Cube® attempt. (E) Chromatogram from the final attempt using the Buchii reaction chamber**,** GC conditions as described in Figure 2.13.

Table 2.7. Percentage yields from the hydrogenation attempts of naphthalene-1-propanoic acid

Assignment	RT	Reactant (%)	Attempt 1 (%)	Attempt 2 (%)	Attempt 3 (%)	Attempt 4 (%)
DNPA	14.57	0.00	0.00	1.58	10.75	11.31
DNPA	15.16	0.00	0.00	0.73	9.03	9.12
DNPA	15.24	0.00	0.00	2.97	64.72	79.57
TNPA	15.51	0.00	19.42	14.12	0.87	0.00
TNPA	16.12	1.21	79.88	80.60	14.62	0.00
NPA	16.31	98.79	0.70	0.00	0.00	0.00
		Sum Isomers				
DNPA	14.57	0.00	0.00	5.27	84.50	100.00
DNPA	15.16					
DNPA	15.24					
TNPA	15.51	1.21	99.30	94.73	15.50	0.00
TNPA	16.12					
NPA	16.31	98.79	0.70	0.00	0.00	0.00

DNPA is decahydronaphthalene-1-propanoic acid; TNPA is tetrahydronaphthalene-1-propanoic acid; NPA is naphthalene-1-propanoic acid; DNPA at RT 15.16 minutes details two isomers at RT 15.14 and 15.16

Both mass spectra reveal an $M^{+\bullet}$ at *m/z* 218 indicative of an addition of four hydrogen atoms to the reactants naphthalene moiety, thus increasing the molecular weight by four Daltons. Significant fragment ions exist in both Figure 2.79A and B; *m/z* 186, 158, 144 and 131 indicate the cleavage of a methanol group, a carboxylate group, an ethanoate group and the alkanoate side chain. The fragment at *m/z* 186 is more abundant in the 5,6,7,8-tetrahydronaphthalene moiety (Figure 2.79B), indicating that this fragment is more stable than the *m/z* 186 in Figure 2.79A. This pattern of fragment ions, coupled with the $M^{+\bullet}$ indicate that these two mass spectra are characteristic of tetrahydronaphthalene propanoic acid methyl ester isomers.

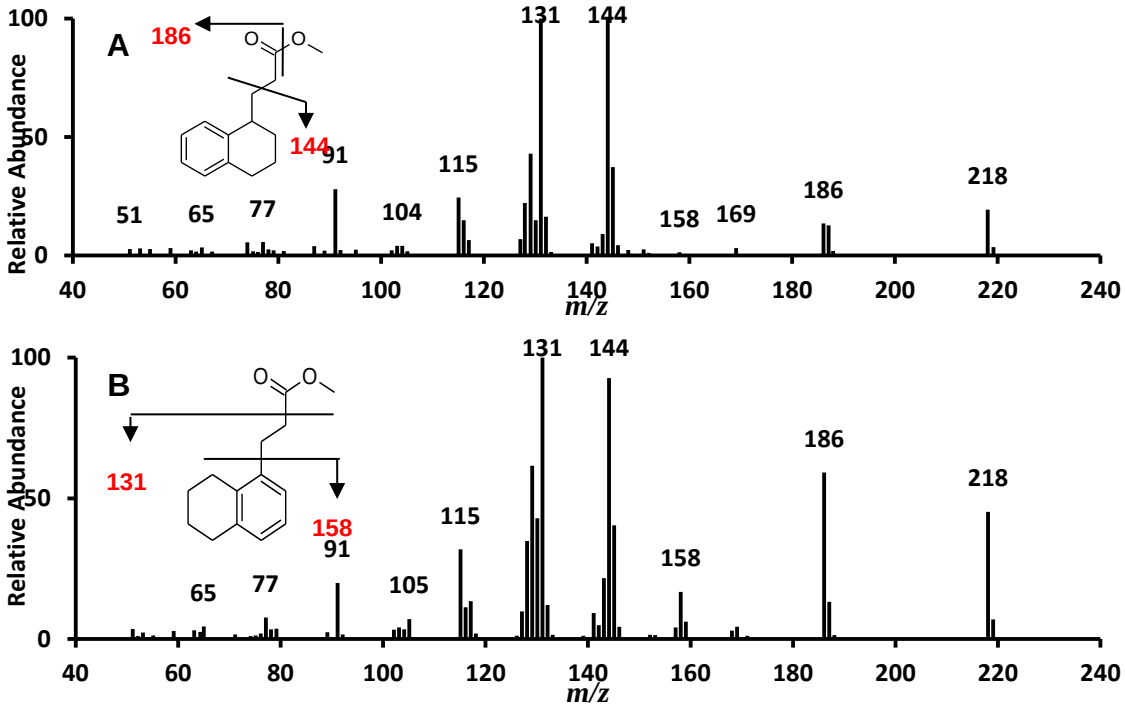

Figure 2.79. Mass spectra for chromatographic peaks detailed in Figure 2.66, revealing (A) mass spectrum for component eluting at at RT 15.51. (B) Mass spectrum for component eluting at RT 16.12. MS conditions as described in Figure 2.13.

Analysis of the mass spectra produced from the chromatographic peaks at RT 14.57, 15.16 (two peaks) and 15.24 (Figure 2.78D and E) reveals that there are four potential isomers of the decahydronaphthalene-1-propanoic acid methyl esters present (Figure 2.80; also detailed in Rowland et al., 2011d). All four isomers have an $M^{+\bullet}$ at m/z 224 consistent with the addition of ten hydrogen atoms to the reactant thus increasing the molecular weight by ten Daltons. Significant fragment ions are revealed at m/z 193 (loss of methoxy) and m/z 151 (base ion; loss of an ethanoate group) (Figure 2.80 A, B and D). However the mass spectra detailed in Figure 2.80C shows a base ion at m/z 148 with a slightly less abundant ion at m/z 151.

All mass spectra displayed show an ion at m/z 135 which is at odds with the loss of the alkanoate side chain which would leave an m/z 137 fragment. The fragmentation pattern coupled with the $M^{+\bullet}$ is consistent with decahydronaphthalene-1-propanoic acid methyl ester isomers

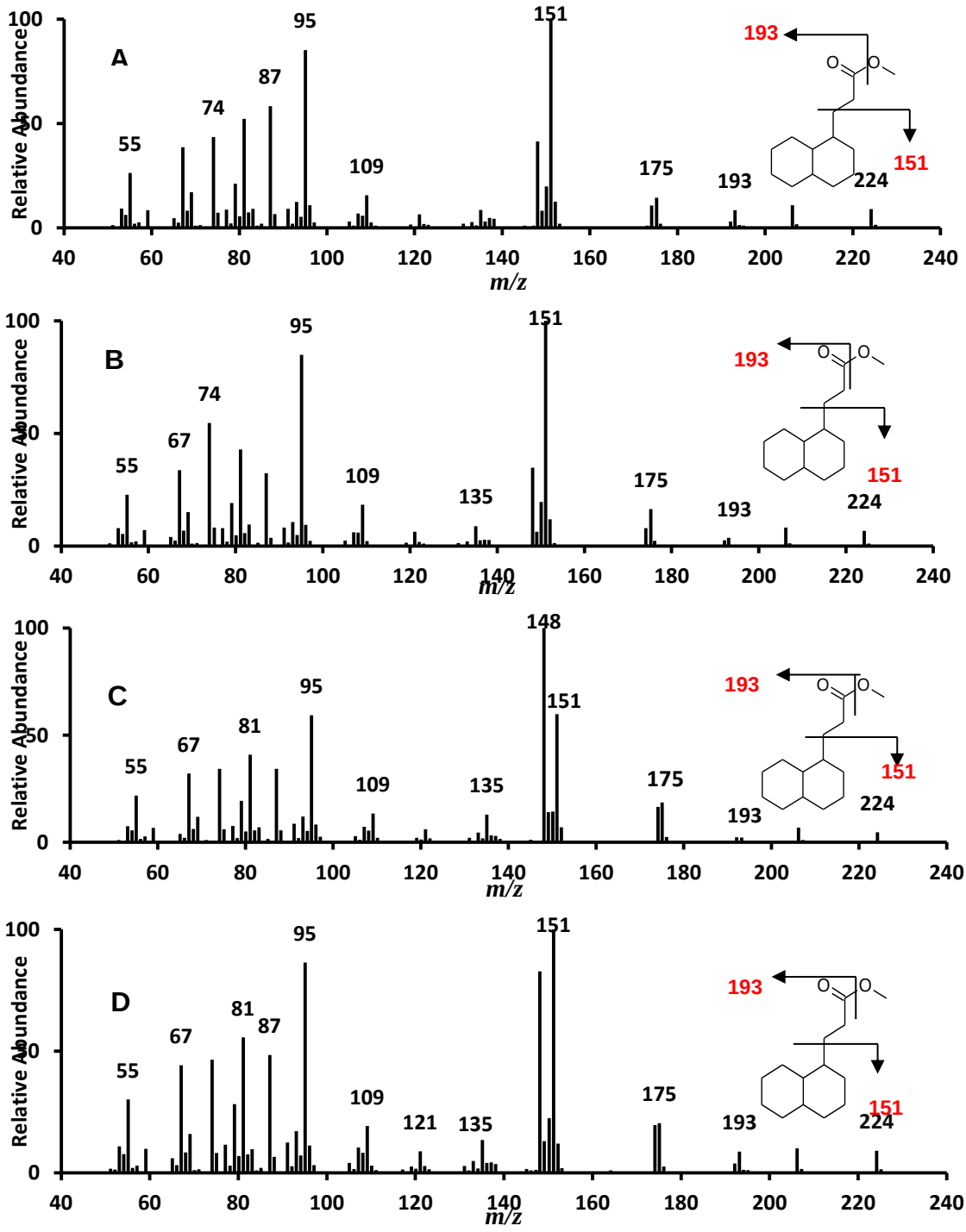

Figure 2.80. Mass spectra for isomers of decahydronaphthalene-1-propanoic acid methyl esters; displaying (A) mass spectrum for component eluting at RT 14.57; (B) mass spectrum for component eluting at RT 15.14; (C) mass spectrum for component eluting at RT 15.16; and (D) mass spectrum for component eluting at RT 15.24. MS conditions as described in Figure 2.13.

2.3.15. Synthesis of 4-methyl-decahydronaphthalene-1-carboxylic acid

An attempt was made to synthesis 4-methyldecahydronaphthalene-1-carboxylic acid through the catalytic hydrogenation of an authentic sample of 4-methylnaphthalene-1-carboxylic acid (Sigma Aldrich; stated purity >99%). The hydrogenation was attempted using the Buchii reaction chamber (25^{o}C, PtO_2•H_2O, 7 Hours) and the H-Cube® flow through hydrogenator (Rh/C, 80^{o}C, 80 bar pressure, 1 mL min^{-1}) (Figure 2.81)

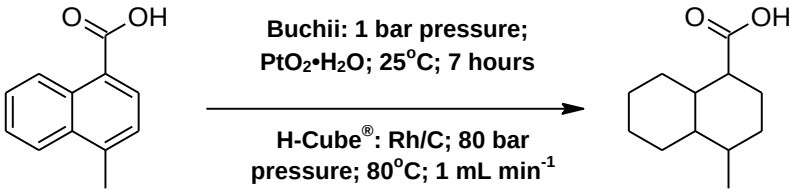

Figure 2.81. Catalytic hydrogenation of the reactant (4-methylnaphthalene-1-carboxylic acid) to the product (4-methyldecahydronaphthalene-1-carboxylic acid); plus hydrogenation conditions.

To confirm the purity of the reactant a small amount was esterified with the BF_3-MeOH complex and analysed with GC-MS. The resultant chromatogram reveals one distinct peak at a retention time of RT 16.01 minutes confirming that the analysed compound is >99% pure (Figure 2.82A). Analysis of the mass spectrum (Figure 2.82B) revealed an $M^{+\bullet}$ at *m/z* 200 consistent with a C_{13} di-aromatic acid methyl ester.

Significant fragment ions exist at *m/z* 185 (indicating the loss of a methyl group) and *m/z* 169 (base ion; indicating loss of methoxy). The fragment ion at *m/z* 141 indicates cleavage of the alkanoate side chain and is consistent with a methyl

naphthalene fragment. The fragmentation pattern and the $M^{+\bullet}$ are consistent with an assignment of a methylnanphthalene-1-carboxylic acid methyl ester.

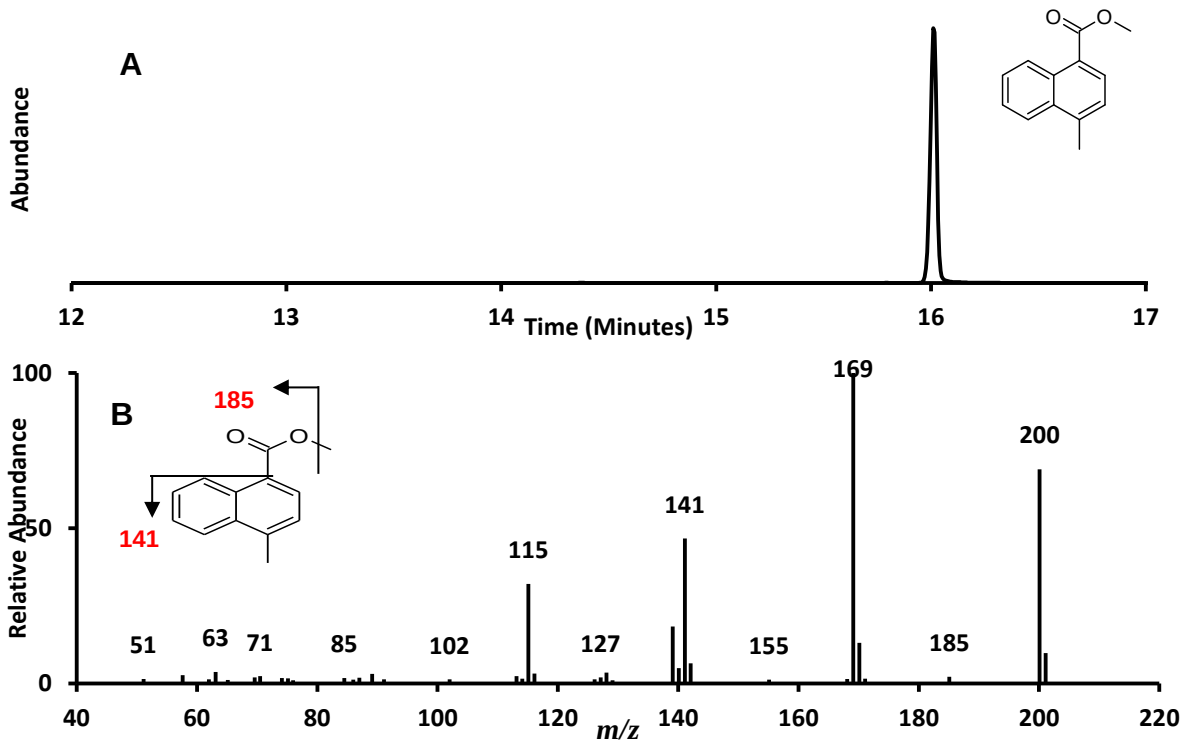

Figure 2.82. (A) Chromatogram of the methyl esters of 4-methylnaphthalene-1-carboxylic acid. (B) Mass spectrum for the component eluting at RT 16.01. GC-MS conditions as described in Figure 2.13.

An initial attempt to synthesis 4-methyldecahydronaphthalene-1-carboxylic acid was made using the Buchii reaction chamber (Figure 2.83). The chromatogram (Figure 2.82B) reveals that only a small amount of the reactant was converted to a possible tetrahydronaphthalene moiety (RT 15.38 minutes; 4.42%), the RT of the abundant peak is identical to that of the reactant (RT 16.01 minutes). Analysis of the mass spectra reveals that the chromatographic peak at RT 16.01 is identical to that displayed in Figure 2.82B and is thus assigned as the reactant, 4-methylnaphthalene-1-carboxylic acid methyl ester. Analysis of the mass

spectra from the chromatographic peak at RT 15.38 minutes (Figure 2.83A) reveals an $M^{+\bullet}$ at m/z 204, characteristic with the addition of four hydrogen atoms and consistent with a tetrahydronaphthalene moiety, the relative abundance of the $M^{+\bullet}$ (39%) indicates that this is likely to be a 4-methyl-5,6,7,8-tetrahydronaphthalene-1-carboxylic acid methyl ester. Significant fragment ions exist at m/z 189 (loss of a methyl group) m/z 172 (loss of methanol) and m/z 145 (loss of the alkanoate side chain) leaving a methyltetrahydronaphthalene fragment.

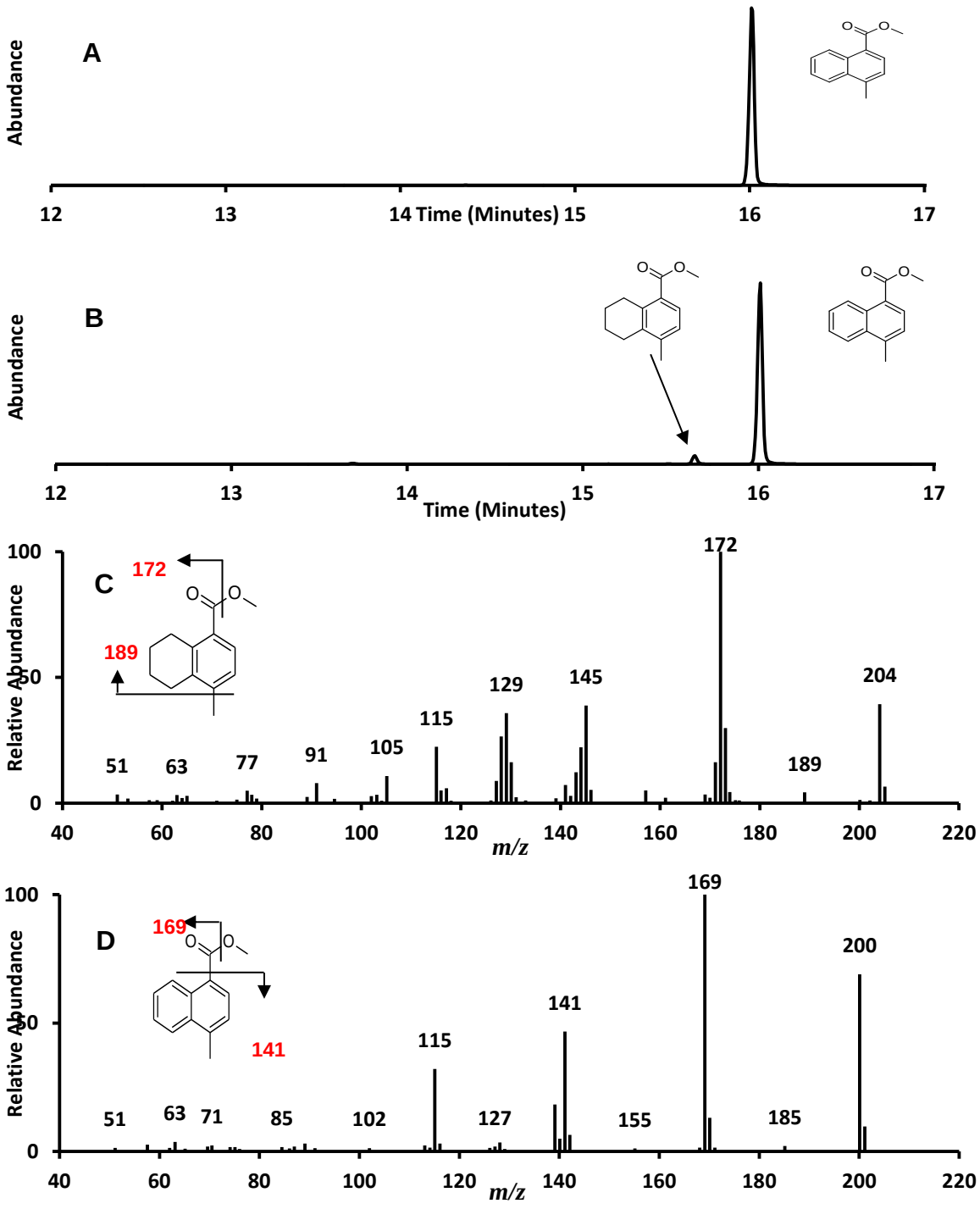

Figure 2.83. (A) Chromatogram of 4-methylnaphthalene-1-carboxylic acid. (B) Chromatogram of the initial catalytic hydrogenation attempt. (C) Mass spectrum of the component eluting at RT 15.38. (D) Mass spectrum for the component eluting at RT 16.01 minutes, GC-MS conditions as described in Figure 2.13.

Three subsequent attempts proceeded with the H-Cube® flow through hydrogenator. The first H-Cube attempt reduced the amount of reactant in the mixture and increased the 5,6,7,8-tetrahydrnaphthalene moiety (RT 15.38 minutes) to be the most abundant species (Figure 2.84B: Table 2.8). A small chromatographic peaks is apparent at RT 13.41 minutes this peak is tentatively assigned a 1,2,3,4-tetrahydronaphthalene species. Analysis of Figure 2.84C reveals that the chromatographic peak at RT 13.41 has increased in abundance and has a small secondary peak attached at RT 13.51, a subsequent hydrogenation attempt (Figure 2.84D) was able to remove all of the reactant but was not able to have a discernible effect on the tentatively assigned tetrahydronaphthalene species. Thus it is unlikely that any decahydronaphthalene moieties have been successfully synthesised; an analysis of the mass spectra attached to each chromatographic peak will be able to confirm these tentative assignments.

Table 2.8 and Figure 2.84D reveal that in the final attempt more reactant is converted to the 5,6,7,8-tetrahydronaphthalene moiety than the 1,2,3,4-tetrahydro species, this is likely due to the presence of the methyl group inhibiting the hydrogenation reaction and preventing the interaction with the metal catalyst, thus only allowing a small amount of the reactant to be converted to a 1,2,3,4-tetrahydronaphthalene moiety, it is also likely that this inhibition prevented the 4-methylnaphthalene-1-carboxylic acid being fully saturated to the desired decahydronaphthalene species (e.g. Freidlin et al., 1975).

Table 2.8. Percentage yields from the hydrogenation attempts of 4-methylnaphthalene-1-carboxylic acid

Assignment	RT (Min)	Attempt 1 %	Attempt 2 %	Attempt 3 %	Attempt 4 %
4-MTNCA	13.41	0.00	0.00	24.79	10.39
4-MTNCA	13.47	0.00	2.52	3.04	1.28
4-MTNCA	15.39	4.42	5.60	43.10	88.32
4-MNCA	16.01	95.58	91.88	29.07	0.00
		Sum Isomer (%)			
4-MTNCA	13.41	4.42	8.12	70.93	100.00
4-MTNCA	13.47				
4-MTNCA	15.39				
4-MNCA	16.01	95.58	91.88	29.07	0.00

4-MTNCA is 4-methyltetrahydronaphthalene-1-carboxylic acid methyl ester; 4-MNCA is 4-methylnaphthalene-1-carboxylic acid methyl ester.

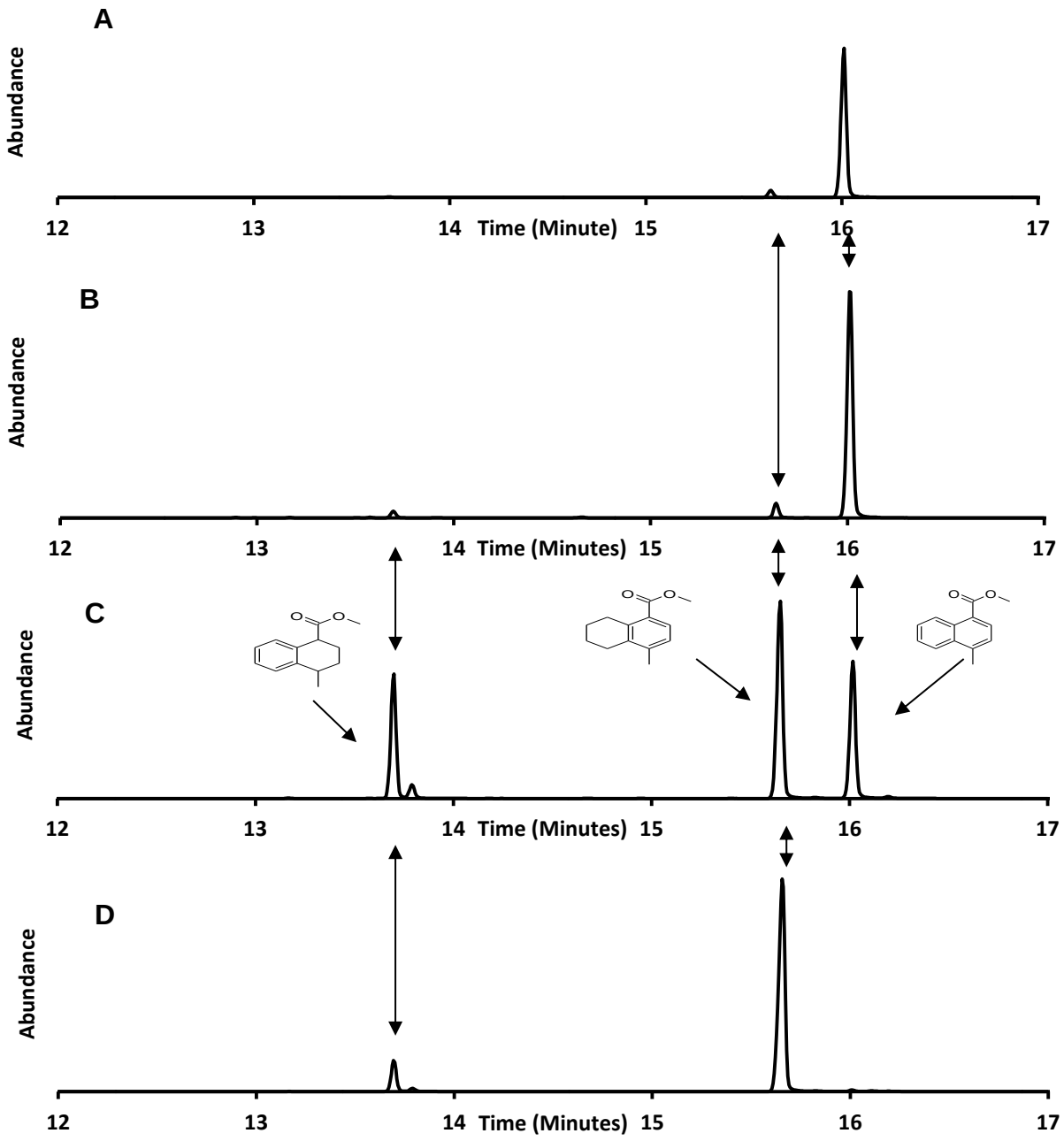

Figure 2.84. Chromatograms from the attempted catalytic hydrogenation of 4-methylnaphthalene-1-carboxylic acid utilising the H-Cube® flow through hydrogenator. With (A) showing the initial Buchii attempt; (B) the initial H-Cube® attempt; (C) the second attempt on the H-Cube®; and (D) the final attempt at hydrogenation, GC conditions as described in Figure 2.13.

Analysis of the mass spectra reveals that the chromatographic peaks at RT 16.01 and 15.39 are identical throughout and have been described previously (Figure 2.83). The mass spectra for the chromatographic peaks at RT 13.41 and 13.47 reveal that both can be classified as a partially hydrogenated species (Figure 2.85).

Both mass spectra exhibit an $M^{+\bullet}$ at m/z 204, characteristic with the addition of four hydrogen atoms during the hydrogenation process and consistent with a methyltetrahydronaphthalene-1-carboxylic acid methyl ester. Assignment of a 4-methyl-1,2,3,4-tertrahydronaphthalene species is due to the elution order of these compounds compared to the 5,6,7,8-tetrahydronaphthalene moiety (RT 13.41 and 13.47 compared to RT 15.39) and the relative abundance of the molecular ion (~20%). Both mass spectra reveal significant fragment ions at m/z 145 (base ion loss of the alkanoate side chain, leaving a methyl-tetrahydronaphthalene fragment) and a small fragment at m/z 189 (loss of a methyl group). Figure 2.85B also displays a minor fragment at m/z 172 indicating the loss of methanol. The elution order of these compounds, the fragmentation pattern, the relative abundance and the m/z of the $M^{+\bullet}$ allow a classification of 4-methyl-1,2,3,4-tetrahydronaphthalene-1-carboxylic acid methyl ester.

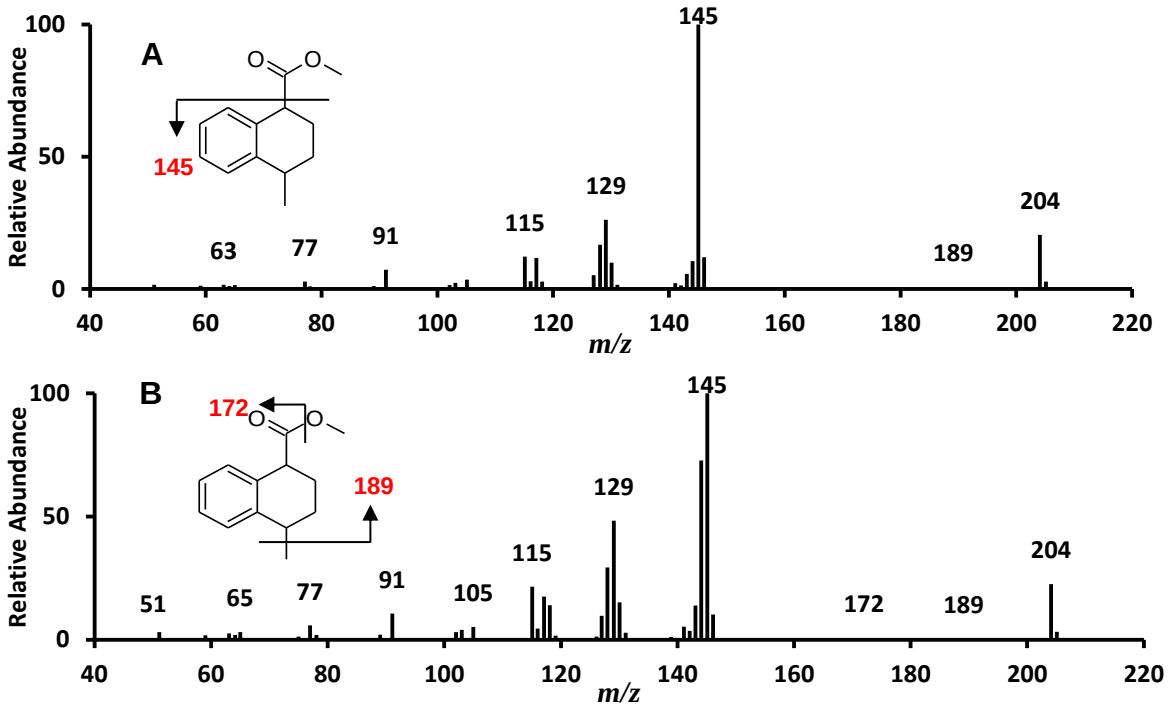

Figure 2.85. Mass spectra of two isomers of 4-methyl-1,2,3,4-tetrahydronaphthalene-1-carboxylic acid methyl esters eluting at (A) RT 13.41 minutes and (B) and RT13.47 minutes, MS conditions as described in Figure 2.13.

2.3.16 Infrared Spectroscopy of Naphthalene Type Compounds

Infra-red spectroscopy was utilised to assess the changes in the naphthalene to decahydronaphthalene hydrogenated acids. Figure 2.86 shows the changes in the infra-red spectra between naphthalene-1-carboxylic acid methyl ester and decahydronaphthalene-1-carboxylic acid methyl ester.

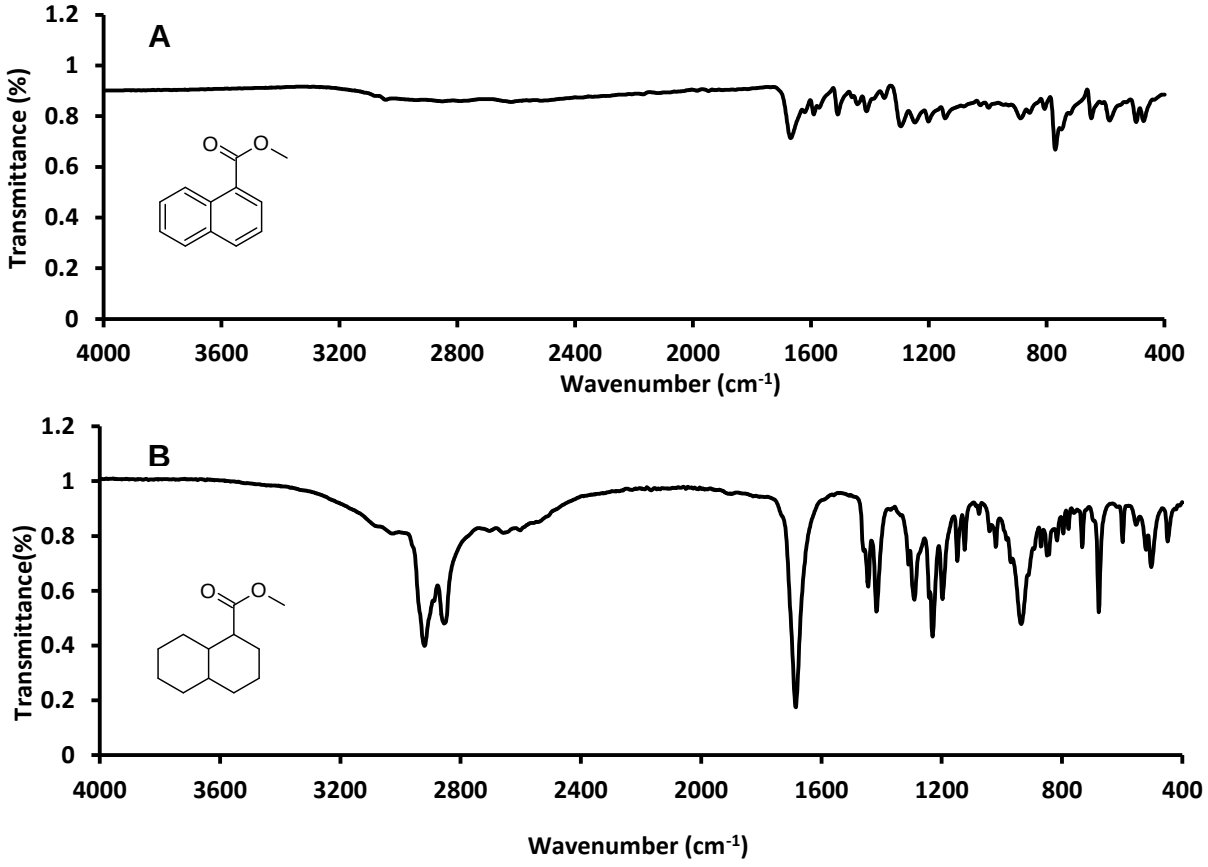

Figure 2.86. Infra red spectra of (A) naphthalene-1-carboxylic acid methyl ester; (B) decahydronaphthalene-1-carboxylic acid methyl ester**.**

The region detailing the vibration momentum or stretch of heteroatoms (C-H, O-H or N-H) between 2800-3000 wavenumber cm^{-1} displays the largest difference between the spectra. C-H bonds are far more abundant in spectrum B than

spectrum A, where they are largely absent. There is a wider C=O stretch in spectrum B compared to spectrum A (1600-1800 wavenumber cm^{-1}) and a C=O stretch in spectrum A which is absent from spectrum B (aromaticity region ~1580 wavenumber cm^{-1}).

Naphthalene-2-carboxylic acid methyl ester was also assessed with infra-red spectroscopy (Figure 2.87). The largest difference is displayed in the 2800-3000 Wavenumber cm-1 regions. This shows that there is an area of C-H saturation in spectrum (B) that is absent in spectrum (A). And a small stretch in the aromaticity region at ~1580 in spectrum (A) that is absent from spectrum (B).

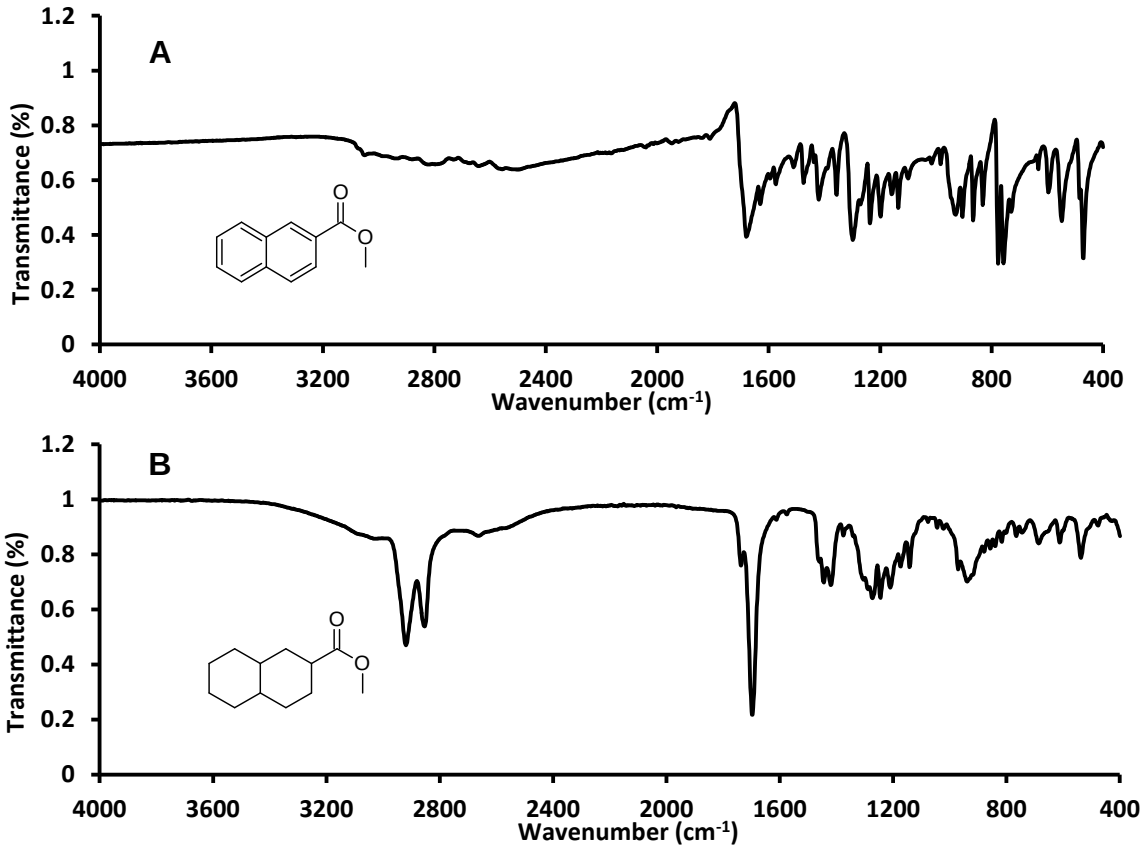

Figure 2.87. Infra-red spectra for (A) naphthalene-2-carboxylic acid methyl ester and (B) decahydronaphthalene-2-carboxylic acid methyl ester.

Figure 2.88 shows the spectra for both ethanoic acid moieties of naphthalene and their hydrogenation products.

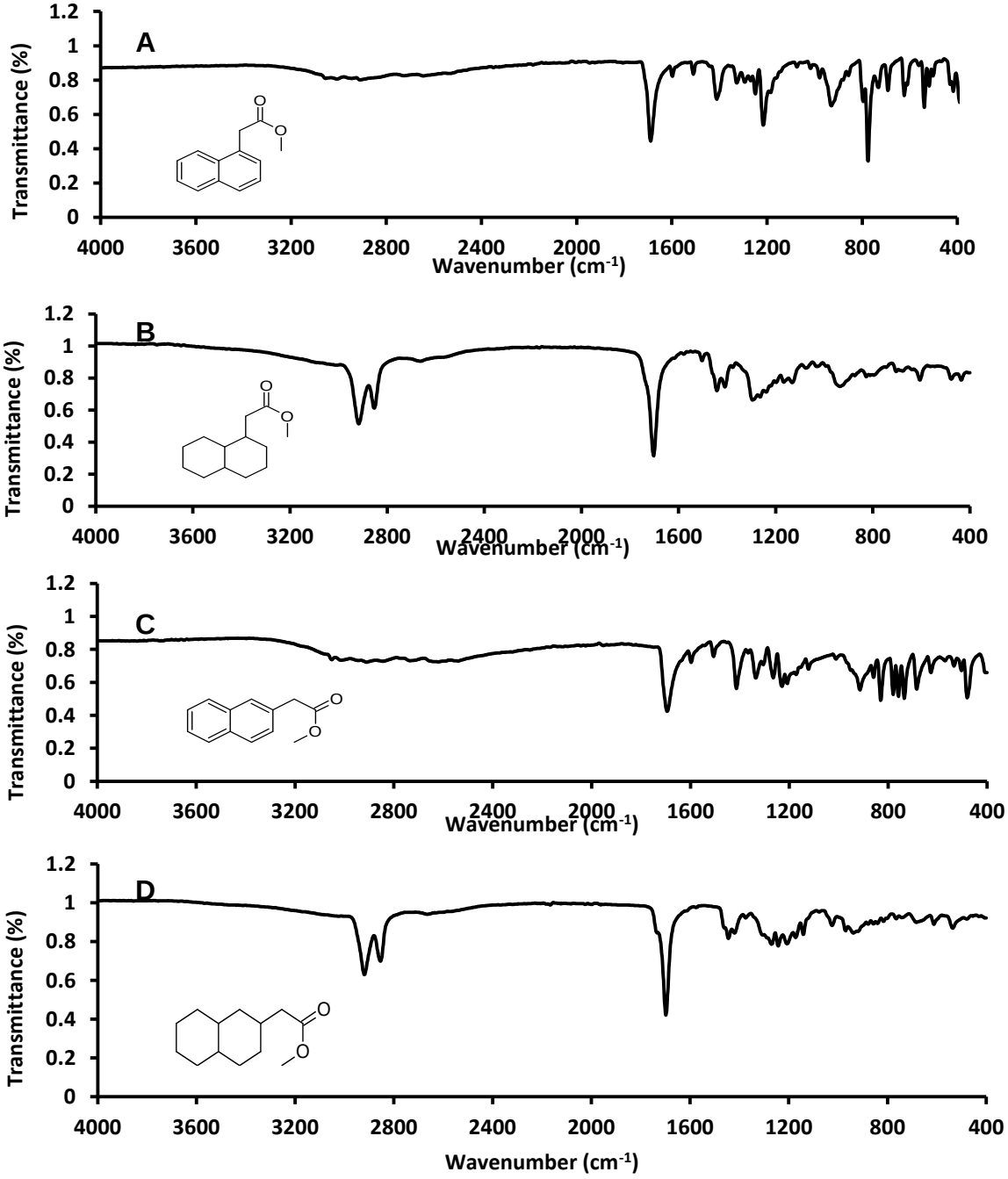

Figure 2.88. (A) Infra red spectra for naphthalene-1-ethanoic acid; (B) decahydronaphthalene-1-ethanoic acid methyl ester; (C) naphthalene-2-ethanoic acid methyl ester; and (D) decahydronaphthalene-2-ethanoic acid methyl ester.

Moving through the spectra it can be seen that the C-H stretch increases through spectrum ‘A’ and ‘C’ (the naphthalene moieties) where it is not present through to spectrum ‘B’ and ‘D’ (the decahydronaphthalene moieties) where there is a prominent stretch. Other features include the C=C stretch at ~1580 wavenumber cm^{-1} in spectra ‘A’ and ‘C’ that is not present in spectra ‘B’ and ‘D’.

Naphthalene-1-propanoic acid (Figure 2.89) shows a similar profile, though no spectra for the final product is available. There is a difference between the spectra at wavenumber cm^{-1} 2800 and 3000 indicating that there are C-H bonds in spectra (B) that are not present in spectra (A). In this case a stretch at ~1580 is present in both spectra indicating incomplete hydrogenation at this stage.

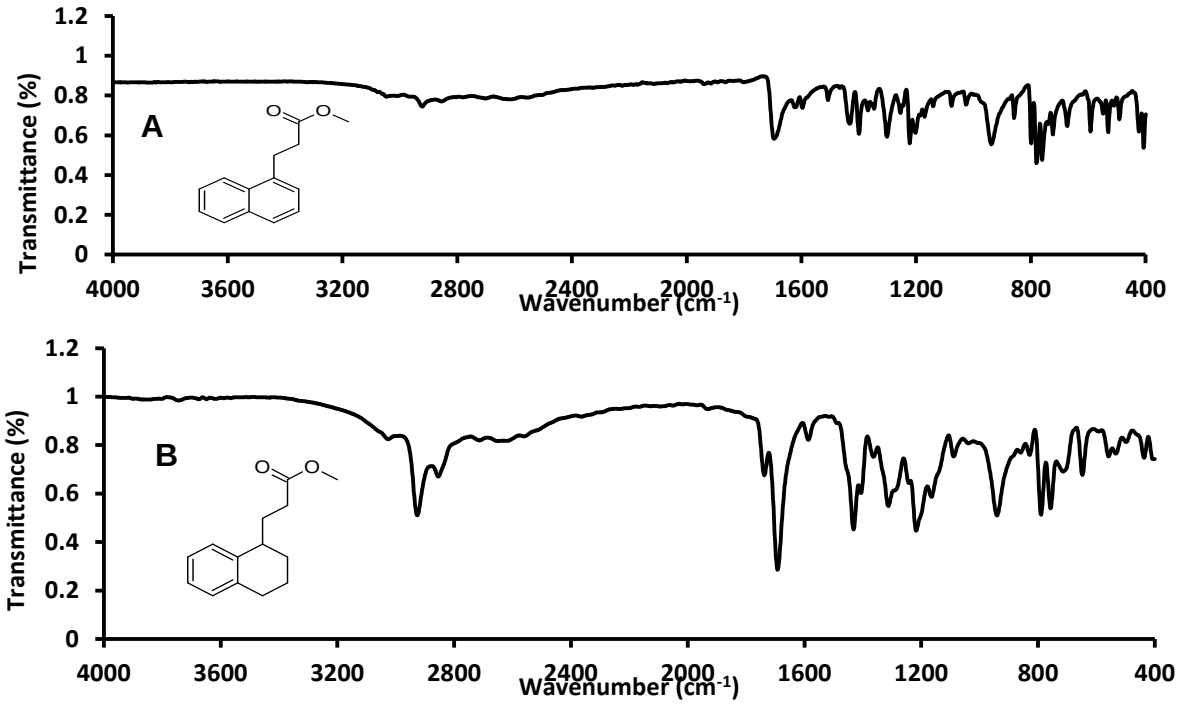

Figure 2.89. Infra-red spectra for (A) naphthalen-1-yl-propanoic acid methyl ester and (B) tetrahydronaphthalene-1-propanoic acid methyl ester**.**

For 4-methyl-naphthalene-1-carboxylic acid methyl esters (Figure 2.90) the spectra display the incomplete hydrogenation to a tetrahydronaphthalene moiety.

This is apparent by the smaller stretch at 2800-3000 wavenumber cm^{-1} and the presence of an aromatic at ~1580 Wavenumber cm^{-1}.

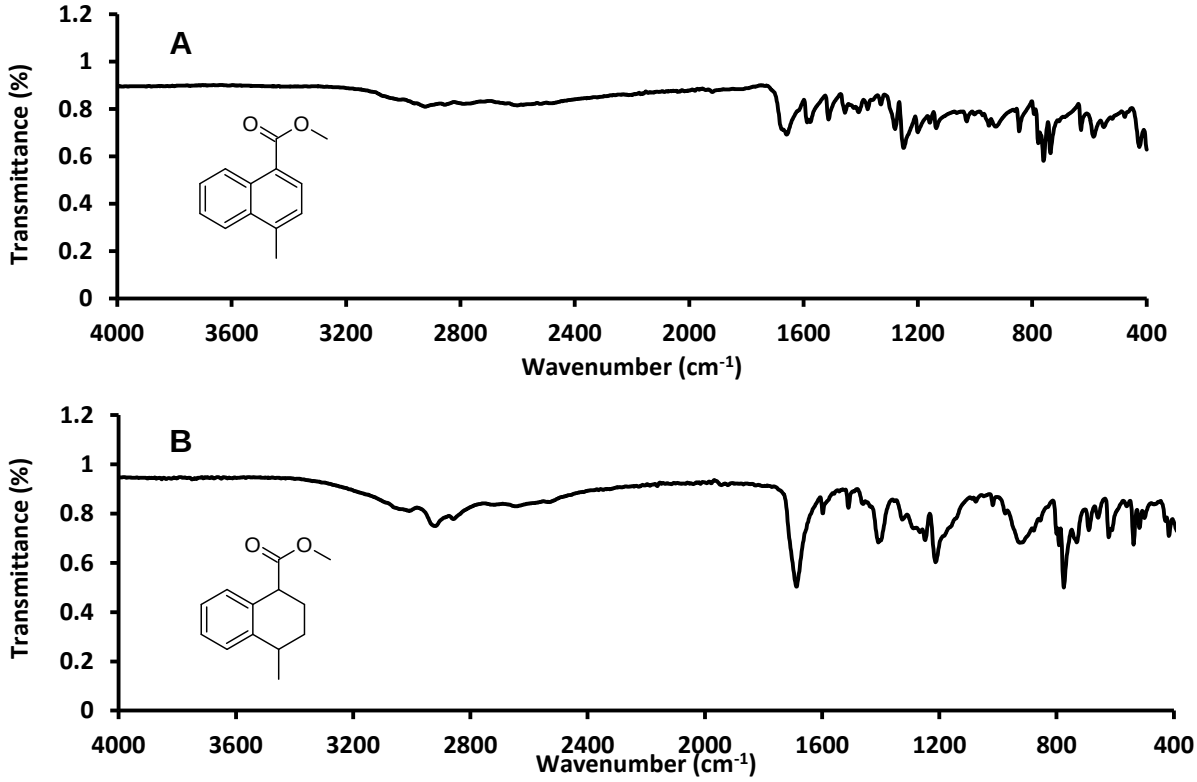

Figure 2.90. Infra-red spectra for (A) 4-methylnaphthalene-1-carboxylic acid methyl ester and (B) isomers of 4-methyltetrahydronaphthalene-1-carboxylic acid methyl ester.

2.3.17. Synthesis of 3,7-dimethyloctanoic acid

An isoprenoid acid (3,7-dimethyloctanoic acid) was attempted to be synthesised. As no authentic reference standard was available commercially an authentic sample of 3,7-dimethyloct-6-enoic acid (citronellic acid) was purchased (Sigma Aldrich; Stated purity >96%) and hydrogenated using the H-Cube® catalytic hydrogenator (Figure 2.91).

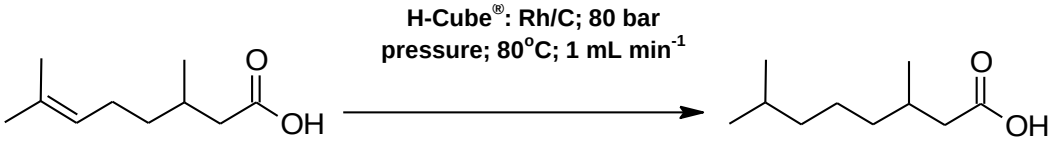

Figure 2.91. Reaction scheme for the catalytic hydrogenation of the reactant (3,7-dimethyloct-6-enoic acid) to the product (3,7-dimethyloctanoic acid); plus hydrogenation conditions.

A small sample was reacted with the BF_3-MeOH complex and assessed with GC-MS for purity (Figure 2.92). It is apparent that there are two distinct peaks displayed in Figure 2.92A, the reactant (RT 11.47) and an unknown peak at RT 9.41 (~30 peak area). Mass spectral analysis confirmed that the chromatographic peak at RT 11.47 was the reactant (Figure 2.92B). The $M^{+\bullet}$ at *m/z* 184 is consistent with the structure and the significant fragment ions at *m/z* 152 (loss of methanol); *m/z* 110 (cleavage of a 2-methyl-hep-2-ene fragment); and m/z 69 (base ion: cleavage of a 2-methylbut-2-ene fragment) indicate that this peak can be assigned to the reactant. A NIST database search for the unknown chromatographic peaks mass spectrum (Figure 2.92C) reveals a 46% match for 2H-indan-2-one-octahydro-3-carboxylic acid methyl ester. This contaminant was postulated to be present due to the BF_3-MeOH esterification process.

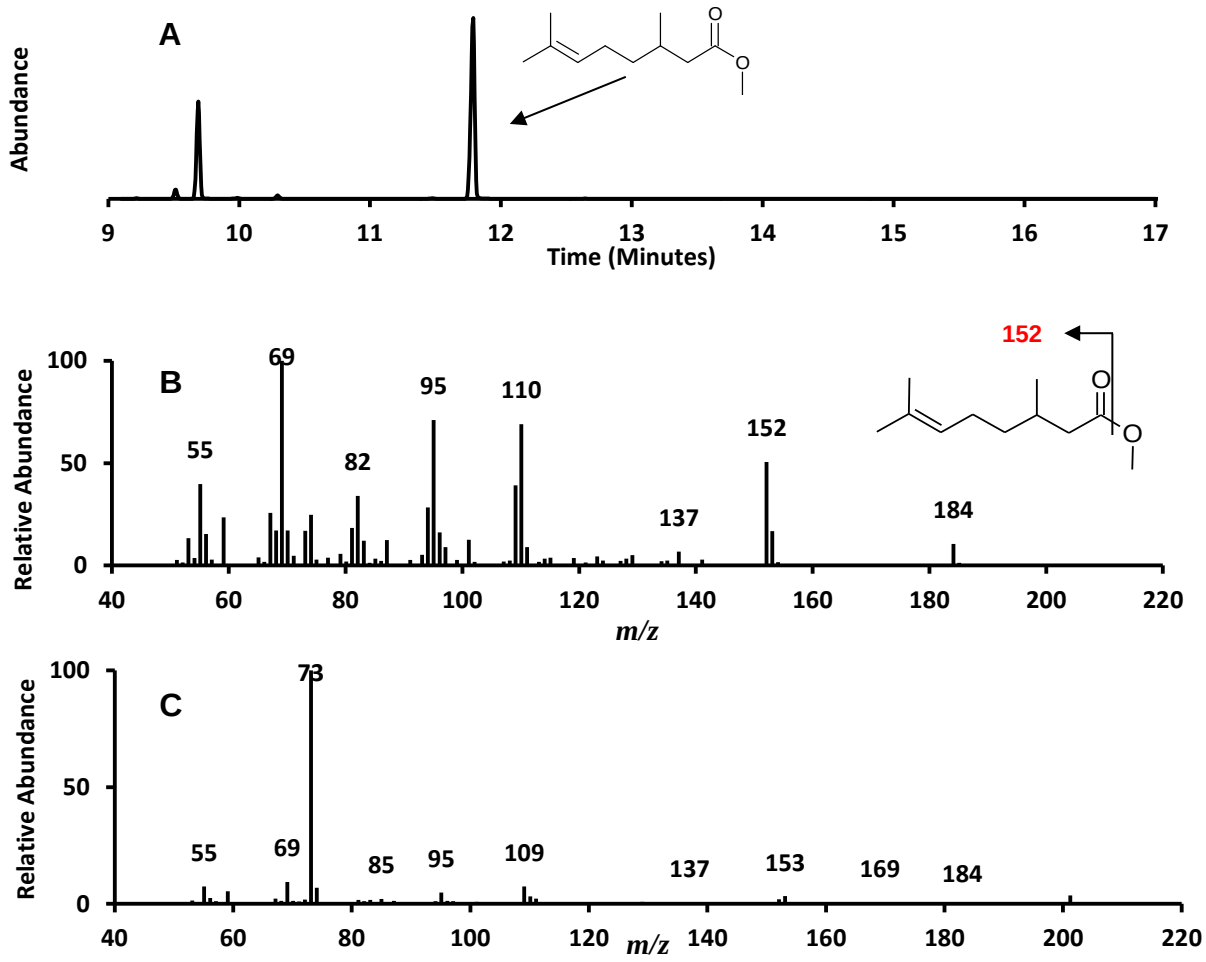

Figure 2.92. (A) Chromatogram of 3,7-dimethyloct-6-enoic acid methyl ester. (B) Mass spectrum of component eluting at RT 11.47 minutes. (C) Mass spectrum for the component eluting at RT 9.41 minutes, GC-MS conditions as described in Figure 2.13.

In order to test this hypothesis a sample of the free acid was analysed with GC-MS (Figure 2.93). This chromatogram displays the very poor chromatography that is associated with free acids when analysed with a GC column and highlights the reasons behind the methylation process carried out on acidic compounds.

The mass spectrum of the free acid has an $M^{+\bullet}$ at *m/z* 170 consistent with a dimethyloctanoic free acid, significant fragment ions exist at *m/z* 152 (loss of

water); *m/z* 110 (cleavage of a 2-methylhep-2-ene fragment) and *m/z* 69 (base ion, cleavage of a 2-methylbut-2-ene fragment). When analysed with the NIST database the mass spectra achieved a 94% match to 3,7-dimethyloct-6-enoic acid confirming the acids purity and the contamination route through the esterification process

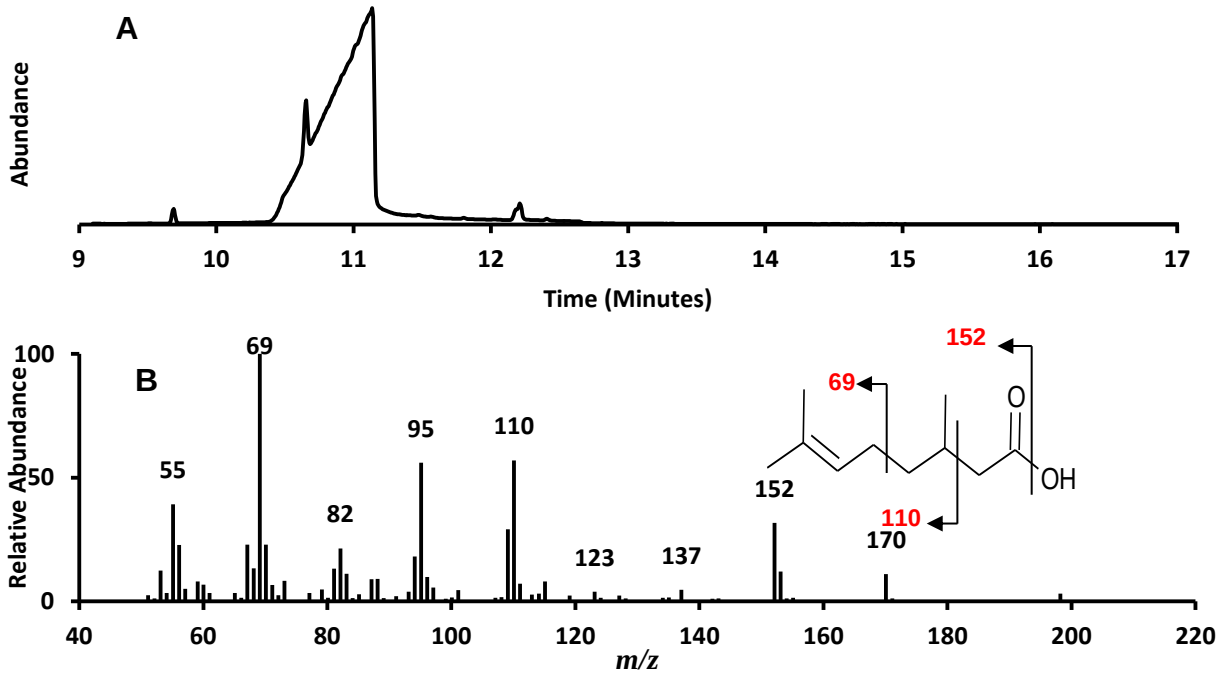

Figure 2.93. (A) Chromatogram of the 3,7-dimethyloct-6-enoic free acid; and (B) mass spectrum for component eluting at RT ~11.00 minutes**,** GC-MS conditions as described previously.

It was decided that hydrogenation of the sample to a 3,7-dimethyl octanoic acid (H-Cube® hydrogenator; Rh/C; 80 bar and 80°C) would alleviate the contamination problem. The subsequent product was reacted with BF_3-MeOH and analysed with GC-MS (Figure 2.94). Only one chromatographic peak is now apparent (RT 9.18 minutes). Mass spectral analysis reveals that the $M^{+\bullet}$ is *m/z*

186, consistent with the addition of two hydrogen atoms increasing the molecular weight by two Daltons. Significant ions exist at *m/z* 171 (loss of methyl); *m/z* 155 (loss of methoxy); *m/z* 143 (loss of propane); *m/z* 129 (loss of 2-methylpropane); *m/z* 101 (cleavage of a methyl butanoate ion); and *m/z* 74 (base ion; cleavage of an ethanoate ion). The $M^{+\bullet}$ alongside the fragmentation pattern confirms the compound as a 3,7-dimethyloctanoic acid methyl ester.

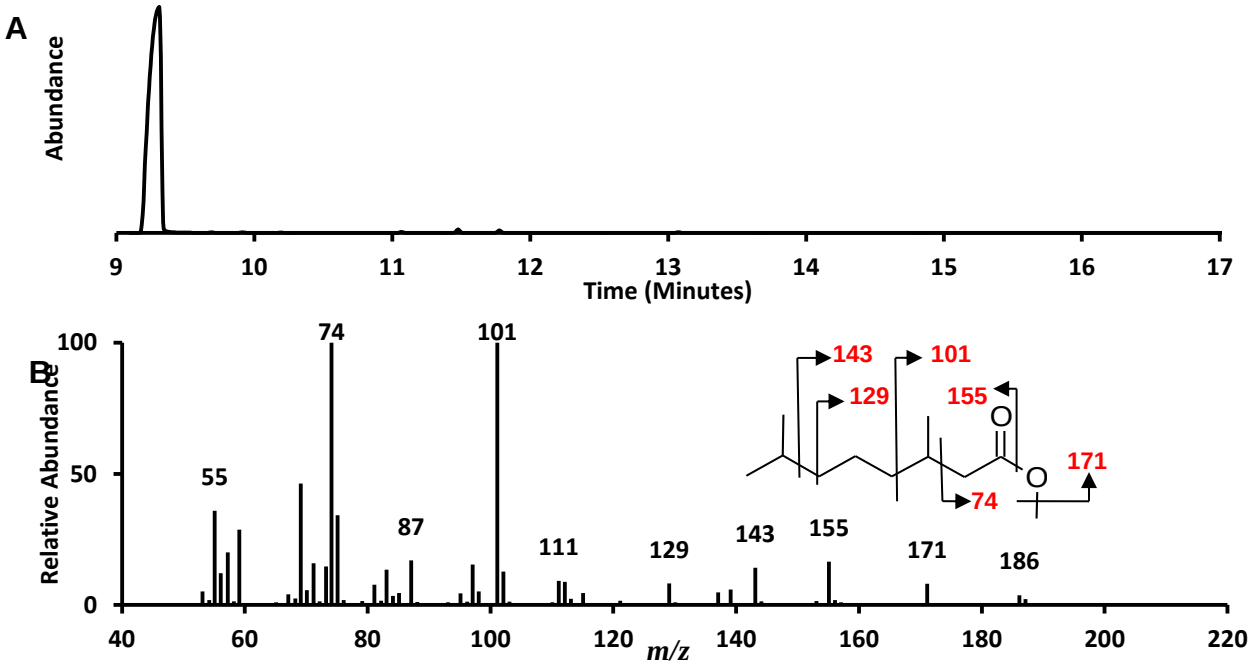

Figure 2.94. (A) Chromatogram) of 3,7-dimethyloctanoic acid methyl ester. (B) Mass spectrum of component eluting at RT 9.18 minutes**,** GC-MS conditions as described in Figure 2.13.

2.3.18. TMS and Methyl Esters of Petroleum Acids

Adamantane type acids were analysed on GC-MS to assess purity and to produce mass spectra that was used for comparison purposes for identification of acids existing within petroleum acid mixtures. These adamantane acids were all reacted with the BF_3-MeOH complex to create the methyl esters (Figure 2.95). Adamantane acids were all authentic standards purchased from Sigma Aldrich with stated purities >98% except Figure 3.83E which was synthesised in house. Reaction with BF_3-MeOH was at 70^{o}C for 30 minutes throughout.

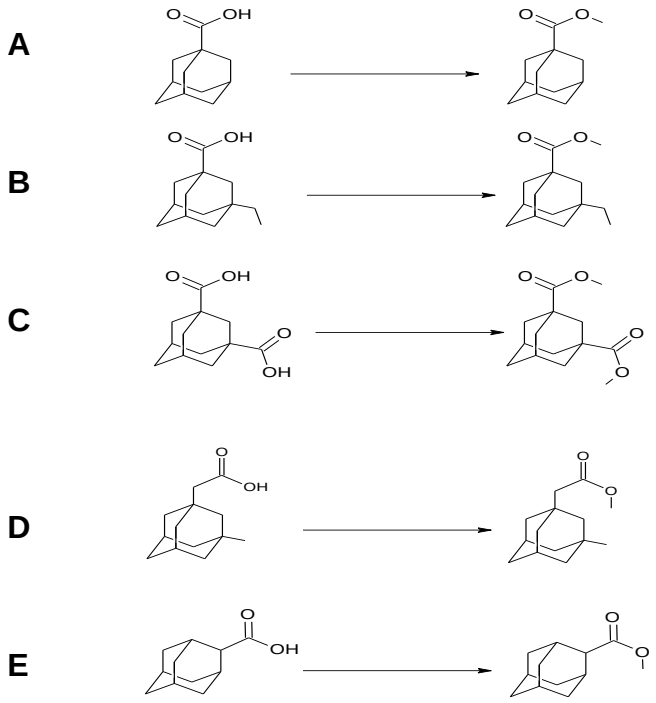

Figure 2.95. Reaction scheme for adamantane acids with BF_3-MeOH**;** (A) adamantane-1-carboxylic acid methyl ester; (B) 3-ethyladamantane-1-carboxylic acid methyl ester; (C) 1,3-adamantane-dicarboxylic acid; (D) 3-methyladamantane-1-carboxylic acid; and (E) adamantane-2-carboxylic acid.

Figure 2.96 displays the chromatogram and mass spectrum for adamantane-1-carboxylic acid methyl ester. It is revealed that there is a single chromatographic peak at a retention time of RT 12.25 minutes (Figure 2.96A). Analysis of the mass spectrum (Fifgure 2.96B) reveals an $M^{+\bullet}$ at *m/z* 194, consistent with an adamantane-1-carboxylic acid methyl ester. There is a significant ion at *m/z* 135 (base ion) which indicates cleavage of the alkanoate side chain.

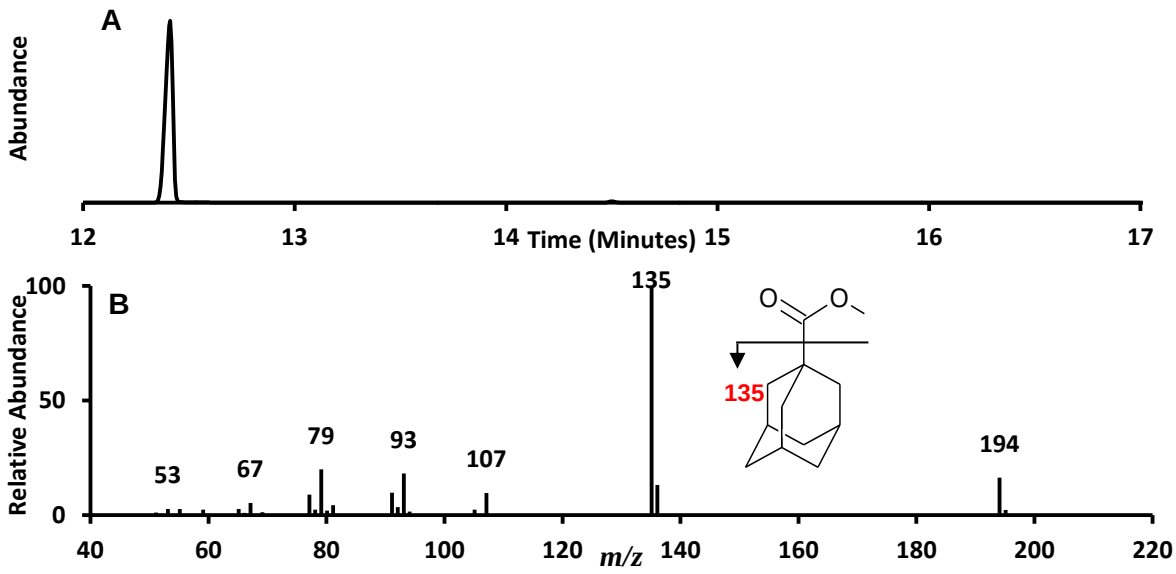

Figure 2.96. (A) Chromatogram for adamantane-1-carboxylic acid methyl ester. (B) Mass spectrum for component eluting at RT 12.25 minutes. GC-MS conditions as described in Figure 2.13.

Figure 2.97 displays the chromatogram and mass spectrum for 3-ethyladamantane-1-carboxylic acid methyl ester. It is revealed that there is a single chromatographic peak at a retention time of RT 14.51 minutes (Figure 2.97A). Analysis of the mass spectrum reveals an $M^{+\bullet}$ at *m/z* 222, consistent with

a 3-ethyladamantane-1-carboxylic acid methyl ester. There are significant ions at *m/z* 163 (base ion) which indicates cleavage of the alkanoate side chain and *m/z* 193 which is consistent with cleavage of the ethyl side chain.

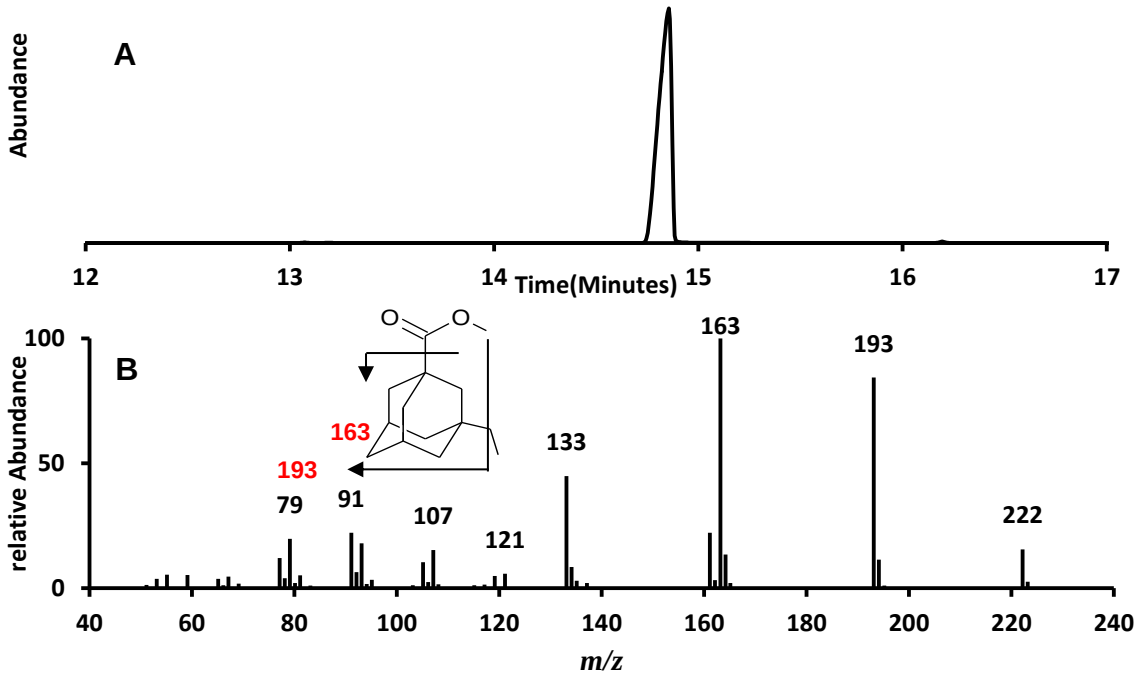

Figure 2.97. (A) Chromatogram for 3-ethyladamantane-1-carboxylic acid methyl ester; and (B) mass spectrum for component eluting at RT 14.51 minutes**,** GC-MS conditions as described previously.

Figure 2.98 displays the chromatogram and mass spectrum for 1,3-adamantane-dicarboxylic acid methyl ester. It is revealed that there is a single chromatographic peak at a retention time of RT 17.10 minutes (Figure 3.86A). Analysis of the mass spectrum reveals an $M^{+\bullet}$ at *m/z* 252, consistent with a 1,3-adamantane-dicarboxylic acid methyl ester. There are significant ions at *m/z* 193

(base ion) which indicates cleavage of the alkanoate side chain and *m/z* 220 which is consistent with cleavage of a methanol group (Figure 2.98B).

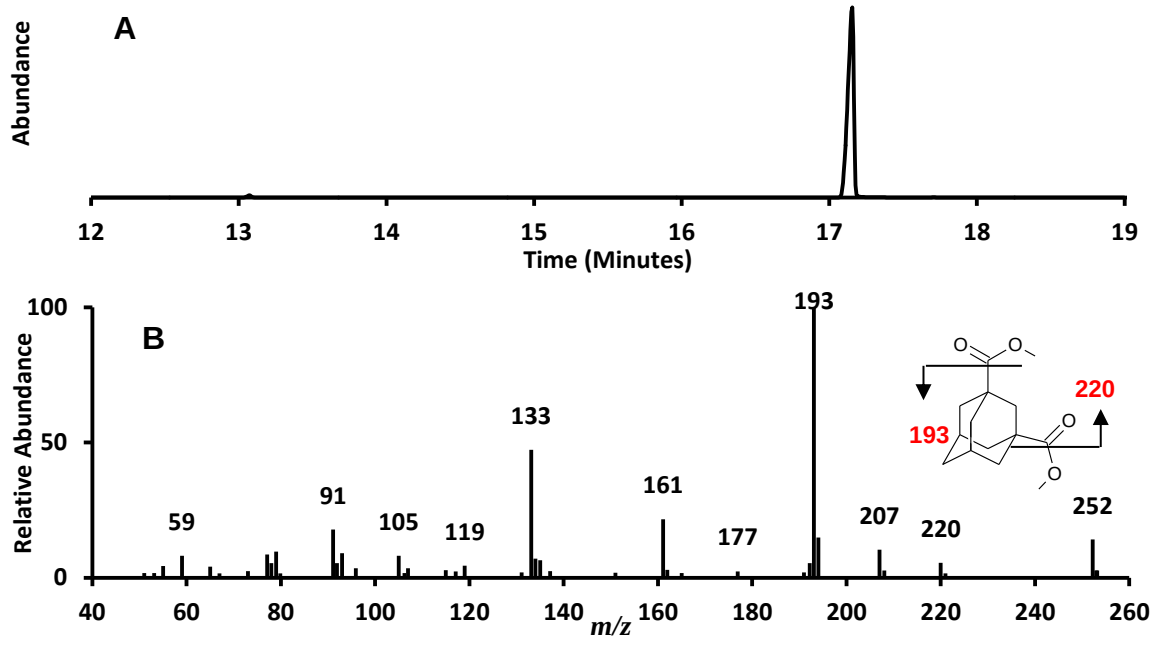

Figure 2.98. (A) Chromatogram for 1, 3-adamantane-dicarboxylic acid methyl ester. (B) Mass spectrum for component eluting at RT 17.10 minutes. GC-MS conditions as described in Figure 2.13.

Figure 2.99 displays the chromatogram and mass spectrum for 3-methyladamantane-1-ethanoic acid methyl ester. It is revealed that there is a single chromatographic peak at a retention time of RT 13.31 minutes (Figure 2.99A). Analysis of the mass spectrum reveals an $M^{+\bullet}$ at *m/z* 222, consistent with a ,3-methyladamantane-1-ethanoic acid methyl ester. There are significant ions at *m/z* 149 (base ion) which indicates cleavage of the alkanoate side chain; *m/z* 162, consistent with the cleavage of a carboxylate group; *m/z* 191, indicating a methoxy fragment ion; and *m/z* 207 which is consistent with cleavage of a methyl

group (Figure 2.99B).

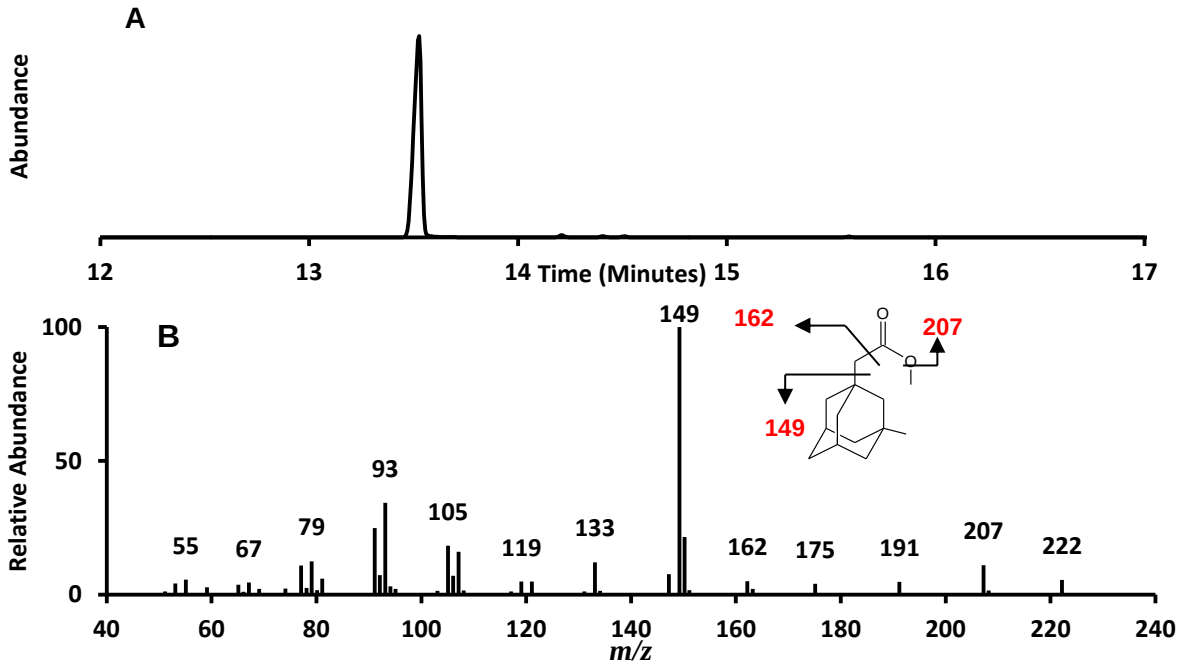

Figure 2.99. (A) Chromatogram for 3-methyladamantane-1-ethanoic acid methyl ester.(B) Mass spectrum for component eluting at RT 13.31 minutes. GC-MS conditions as described in Figure 2.13.

Figure 2.100 displays the chromatogram and mass spectrum for adamantane-2-ethanoic acid methyl ester. It is revealed that there are three chromatographic peaks, with a distinct peak at a retention time of RT 12.40 minutes (Figure 2.100A) and two lesser peaks at RT 12.25 and RT 13.10; the chromatographic peak exhibits a similar RT to adamamtane-1-carboxylic acid. Analysis of the mass spectra in Figure 2.100B and C reveals an $M^{+\bullet}$ at *m/z* 194 consistent with adamantane-carboxylic acid methyl ester. There is a significant ion at *m/z* 135 (base ion) which indicates cleavage of the alkanoate side chain, the similarity of the mass spectra and the retention time allows an assignment of adamantane-1-carboxylic acid to Figure 2.100B. Significant fragment ions are revealed in Figure

3.88C at *m/z* 162, consistent with the cleavage of a carboxylate group; and *m/z* 134 which is consistent with cleavage of the alkanoate side chain, the $M^{+\bullet}$ and fragmentation pattern allows an assignment of adamantane-2-carboxylic acid. The peak at RT13.10 is an unknown contaminant possibly left over from the attempted synthesis.

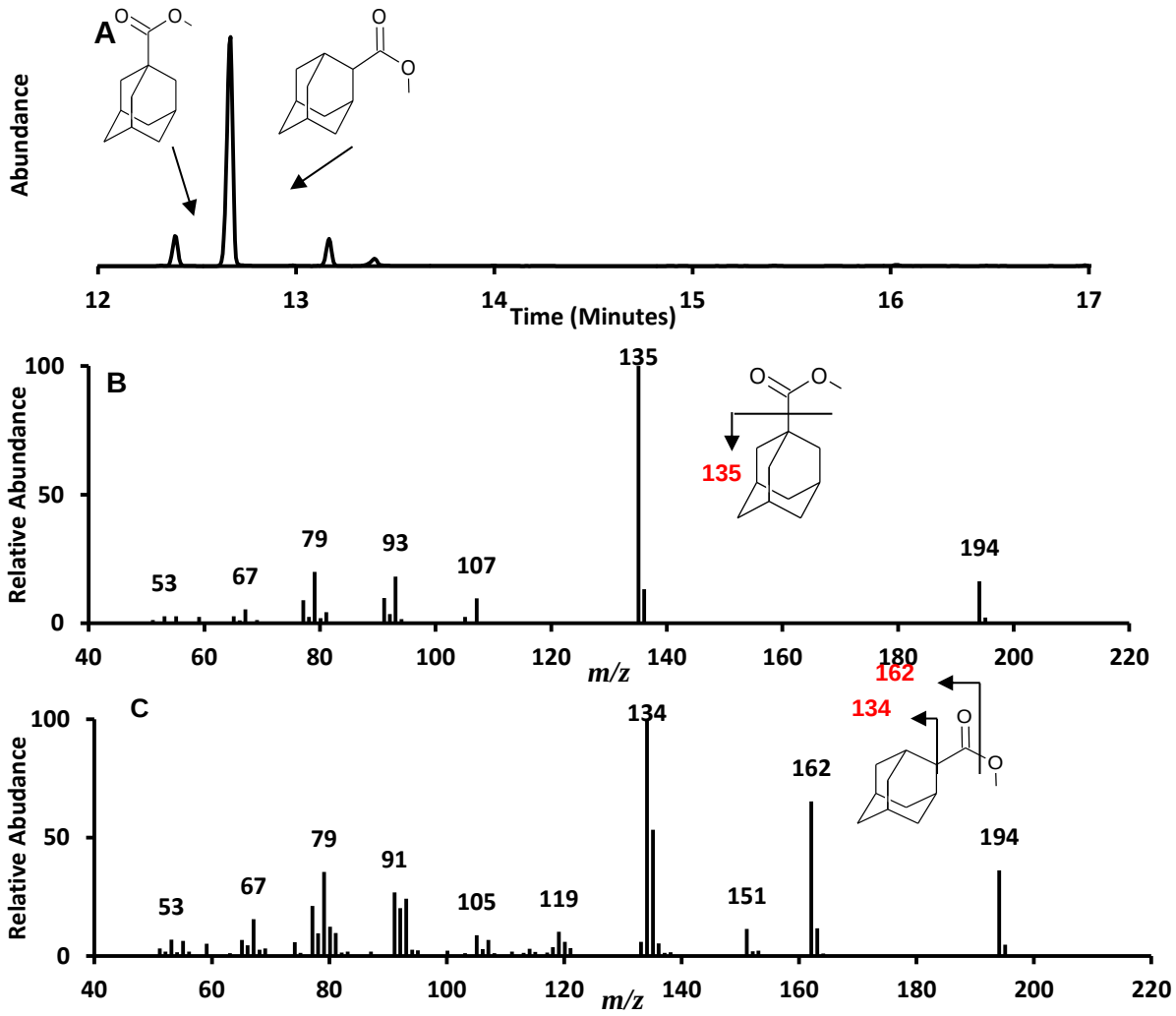

Figure 2.100. (A) Chromatogram for adamantane-2-carboxylic acid methyl ester. (B) Mass spectrum for component eluting at RT 12.25 minutes. (C) Mass spectrum for component eluting at RT 12.40 minutes. GC-MS conditions as described in Figure 2.13.

Noradamantane-3-carboxylic acid was reacted with BF_3-MeOH (30 minutes 70^{o}C) to create the methyl esters (Figure 2.101)

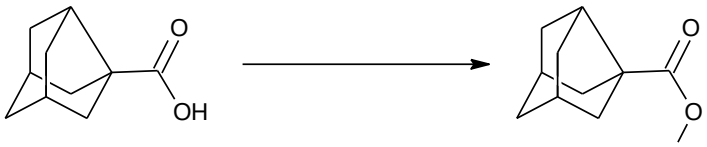

Figure 2.101. Reaction scheme for noradamantane-3-carboxylic acid to the methyl esters

Analysis of the chromatogram and the mass spectra (Figure 2.102) confirms the conversion. Figure 2.102A shows one distinct peak at a retention time of RT 10.46 minutes. Analysis of the mass spectrum (Figure 2.102B) reveals an $M^{+\bullet}$ at *m/z* 180 which is consistent with a noradamantane-3-carboxylic acid methyl ester. Significant fragments exist at *m/z* 165 (loss of methyl); *m/z* 148 (loss of methanol); and *m/z* 121 (loss of the alkanoate side chain).

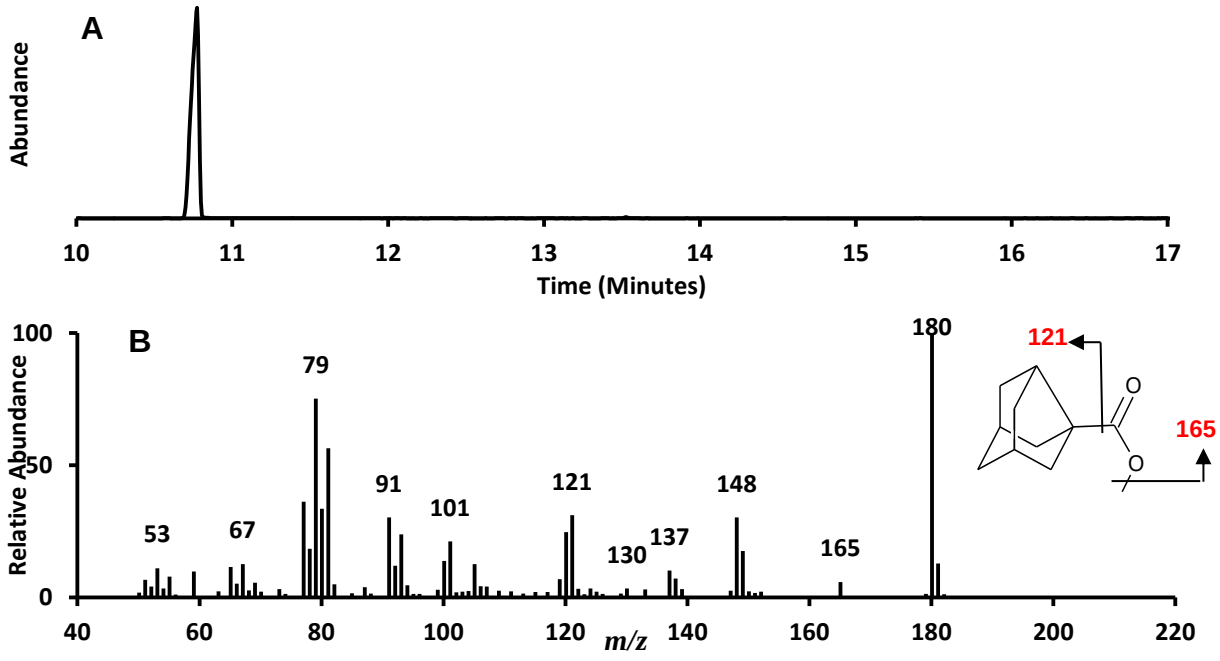

Figure 2.102. (A) Chromatogram for noradamantane-3-carboxylic methyl ester; and (B) mass spectrum for component eluting at RT 10.46 minutes**,** GC-MS conditions as described in Figure 2.13.

Both diamantane-1-carboxylic acid and diamantane-1,6,-dicarboxylic acid were esterified with BF_3-MeOH (70^{o}C, 30 minutes) to test purity on a GC-MS (Figure 2.103).

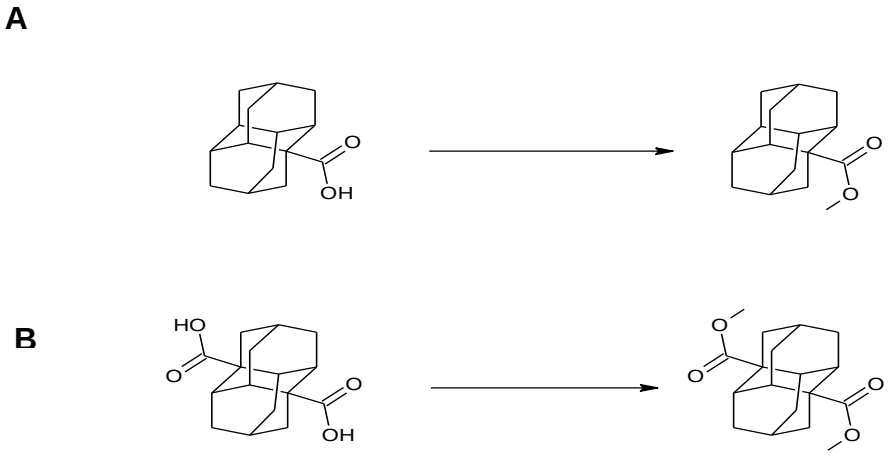

Figure 2.103. Esterification of (A) diamantane-1-carboxylic acid and (B) diamantane-1,6,-dicarboxylic acid

No product was noticeable within the chromatogram of the dicarboxylic moiety (Figure 2.104A), it is postulated that no esterification had taken place so the compound, which did not solubilise in hexane in its di-acid form stayed in the water phase during the extraction

Two distinct peaks and a minor peak are noticeable in Figure 2.104B. The minor pear exists at RT 17.41 minutes whilst the first major peak elutes at RT 18.09 minutes. A free acid peak is noticeable in the chromatogram at RT 18.46 minutes; this chromatographic peak exhibits the large tailing and poor chromatography consistent with free acids.

Analysis of the mass spectrum reveals that Figure 2.104C and D have $M^{+\bullet}$ at *m/z* 246, consistent with the molecular weight of a diamantane carboxylic acid methyl ester. Significant ions exist at *m/z* 187 (base ion, loss of the alkanoate side

chain) in both Figure 2.104C and D and a fragment ion consistent with the loss of methanol is revealed in Figure 2.104C, but is absent from Figure 2.104D, the ion at m/z 207 is likely to indicate column bleed.

Analysis of Figure 2.104E reveals an $M^{+\bullet}$ at m/z 232, consistent with a diamantane carboxylic free acid. Significant ions indicate a loss of water at m/z 214 and loss of the alkanoate side chain at m/z 187.

Figure 2.104 was able to give comparative mass spectra for identification purposes. However as it was decided that neither compound would be soluble enough to assess on the Microtox™ toxicity assay (see chapter 3) and that di-acid moieties had yet to be identified in the acid extracts of an Oil Sands Process Affected Water or the commercially derived mixture of naphthenic acids no further attempts to esterify these compounds were made.

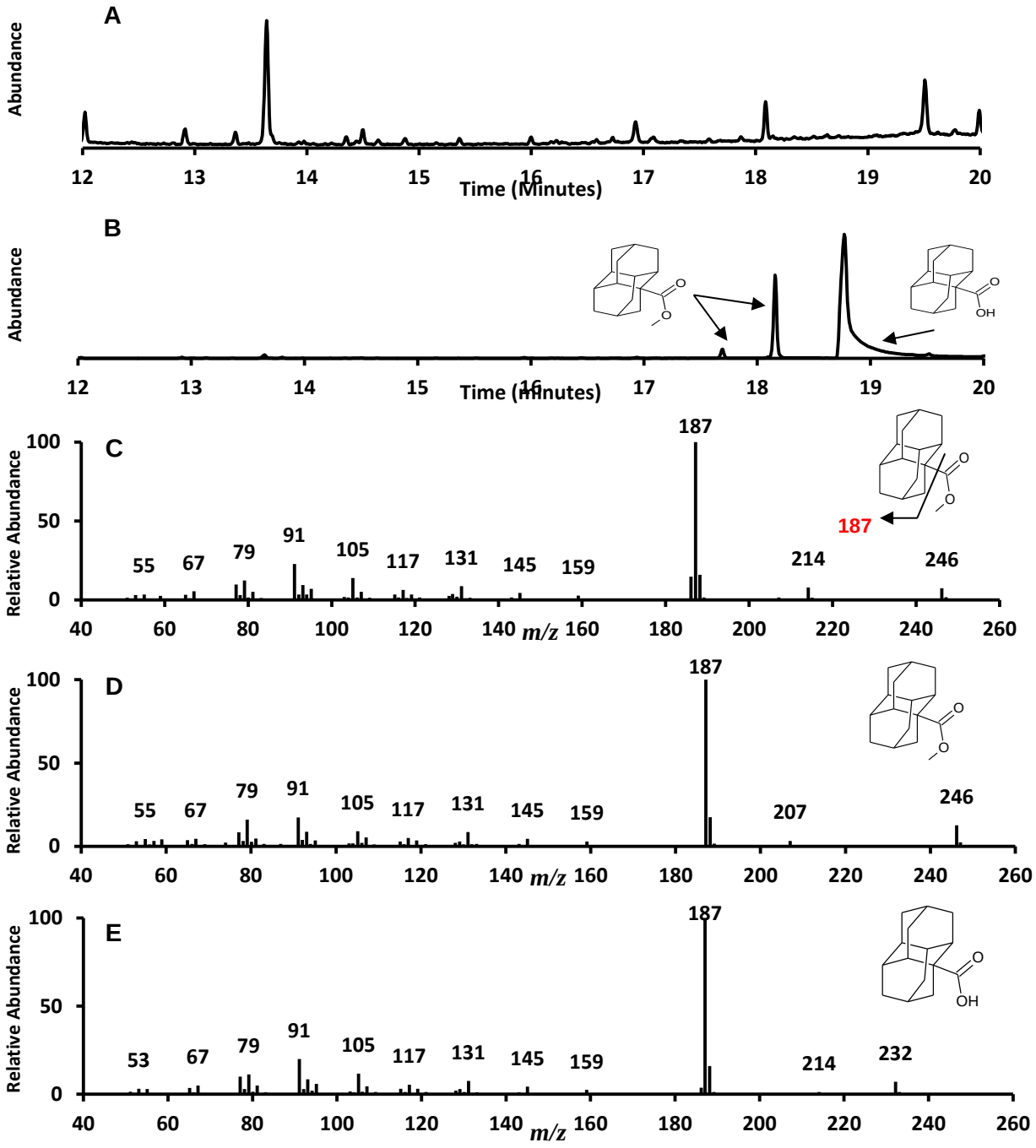

Figure 2.104. (A)Chromatogram for diamantane-1,6-dicarboxylic acid methyl ester. (B) Chromatogram for diamantane-1-carboxylic acid methyl ester. (C) Mass spectrum for component eluting at RT 17.41 minutes. (D) Mass spectrum for component eluting at RT 18.09 minutes. (E) Mass spectrum for component eluting at RT 18.46 minutes. GC-MS conditions as described in Figure 2.13.

Adamantane and diamantane carboxylic acids were chemically adjusted by a colleague to their ‘ring opened’ moieties which were then hydrogenated from saturated moiety (chromatograms and mass spectra not available) via the H-Cube® (Rh/C catalyst; 80 bar; 80^{o}C) and were methylated for a purity check (Figure 2.105 and Figure 2.106).

Figure 2.105. Esterification of ring opened adamantane carboxylic acid

Analysis of Figure 2.106A reveals that a large amount of contamination occurred during the experimental processes and only a small amount of ring opened adamantane carboxylic acid was revealed in the chromatogram (chromatographic peak at RT 11.55 minutes). As only a small amount of product (0.4 mg) was made available the hydrogenation and subsequent esterification was unable to be repeated.

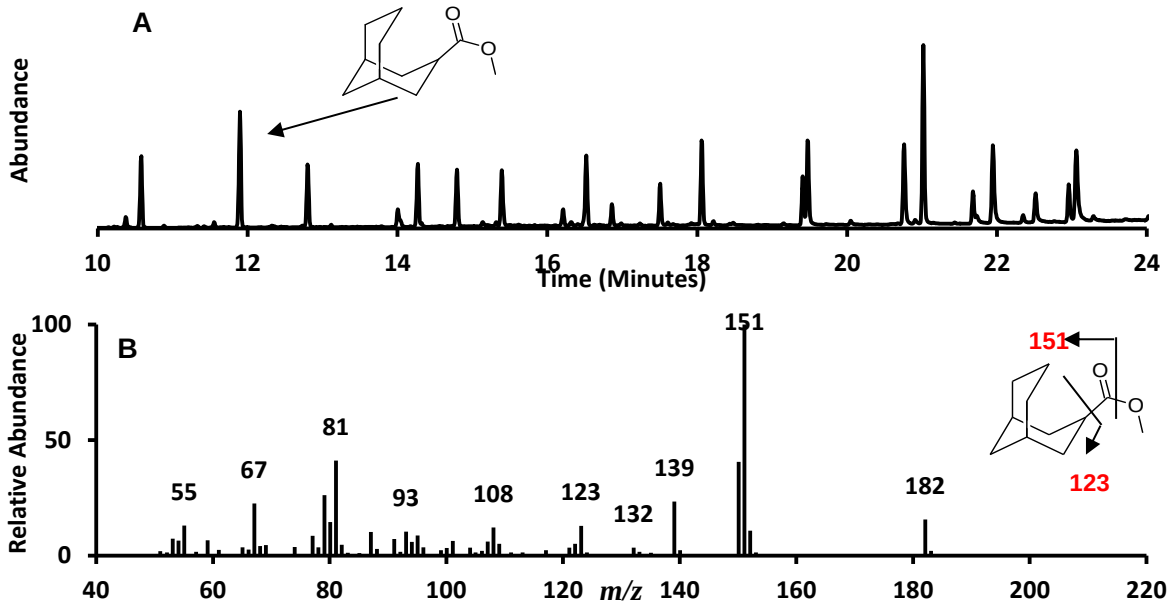

Figure 2.106. (A) Chromatogram of component assigned as the product (ring opened adamantane carboxylic acid methyl ester). (B) Mass spectrum of component eluting at 11.55 minutes. GC-MS conditions as described in Figure 2.13.

Analysis of the mass spectrum (Figure 2.106B) reveals that the $M^{+\bullet}$ exists at *m/z* 182 which is consistent with the analysed moiety. Significant ions exist at *m/z* 151 (loss of methoxy) and *m/z* 123 (loss of the alkanoate side chain.

The diamantane ring opening experiment shows similar results. A small amount of the attempted ring open moiety was hydrogenated (prepared by colleague) under the same conditions as the adamantane moiety and esterified for a purity check (Figure 2.107; Figure 2.108).

Figure 2.107. Esterification of a ring opened diamantane carboxylic acid

Analysis of Figure 2.108A reveals that there was a very small amount of successfully synthesised compound (RT 16.19 minutes <1%) with the main chromatographic peak (RT 17.30 minutes) a possible diamantane carboxylic acid isomer; the position of the carboxylic acid functional group is only postulated as the original mass spectra and chromatograms for the saturated moiety are not available.

Analysis of the mass spectra displayed in Figure 2.104B reveals an $M^{+\bullet}$ at *m/z* 234, consistent with a ring opened diamantane carboxylic acid methyl ester, significant fragment ions exist at *m/z* 202 (loss of methanol) and *m/z* 175 (cleavage of the alkanoate side chain).

Analysis of Figure 2.104C reveals a potential $M^{+\bullet}$ at *m/z* 246, consistent with a diamantane carboxylic acid methyl ester. The fragment ion at *m/z* 187 could be indicative of the cleavage of an alkanoate side chain from the diamantane moiety presenting some evidence for the assignment of a diamantane carboxylic acid methyl ester. However it is more likely that the $M^{+\bullet}$ exists at *m/z* 270 (with the presence of an M^{+1} at *m/z* 271. A NIST database comparison indicates that a 14-methyl pentadecanoic acid methyl ester has a 98% chance of fitting this mass spectrum. It is revealing that the base ion at *m/z* 74 could be the McLafferty rearrangement ion indicative of long chain carboxylic acid methyl esters, the presence of *m/z* 87 could confirm this assignment. (McLafferty and Turecek., 1993). Loss of a methoxy group is indicated by *m/z* 239 and *m/z* 227 indicates

loss of an ethane group. The continued fragmentation in units of 14 Daltons indicates that a long chain acid is the most likely candidate (Figure 2.108C).

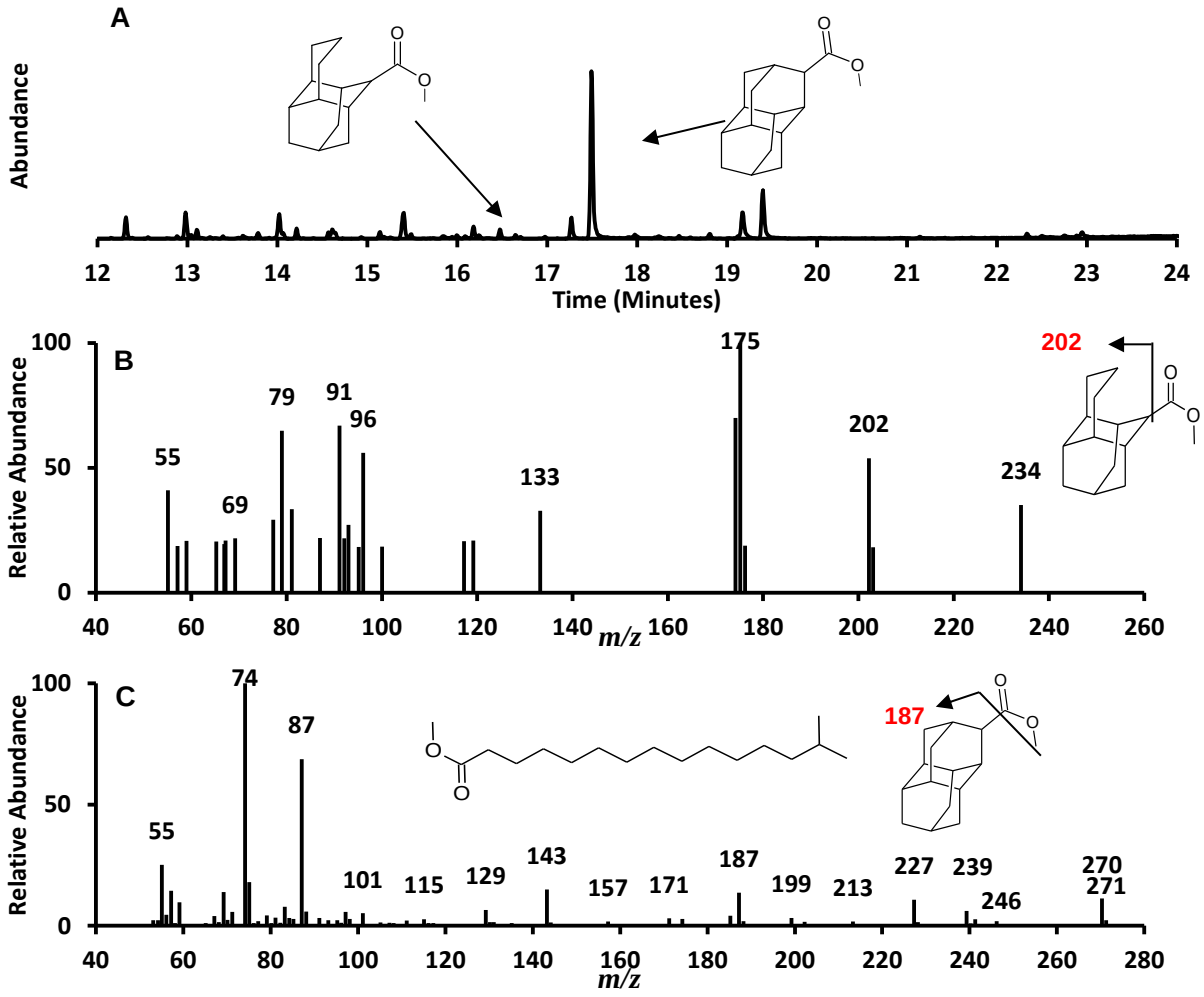

Figure 2.108. (A) Chromatogram for the methyl ester of the attempted ring opening of a diamantane carboxylic acid. (B) Mass spectrum of component eluting at RT 16.19 minutes. (C) Mass spectrum component eluting at RT 17.30 minutes. GC-MS as described in Figure 2.13.

2.3.19. Methyl Esters of Bicyclic Compounds

A few bicyclic acid compounds were purchased (Sigma Aldrich; stated purity >98%) and esterified for mass spectral comparison purposes.

Bicyclo[2,2,2]heptane-2-ethanoic acid was reacted with BF_3-MeOH (30 minutes 70^{o}C; Figure 2.109) and analysed with GC-MS.

Figure 2.109. Esterification of bicyclo[2,2,2]heptane-2-ethanoic acid

Analysis of the chromatogram (Figure 2.110A) displays a single distinct peak at RT 10.10 minutes. The mass spectrum (Figure 2.106B) reveals an $M^{+\bullet}$ at *m/z* 168, consistent with the methyl esters of a bicyclo[2,2,2]heptane-2-ethanoic acid. Significant ions exist at *m/z* 153 (loss of methyl); *m/z* 136 (loss of methanol); *m/z* 108 (loss of a carboxylate ion); and *m/z* 95 (loss of the alkanoate side chain).

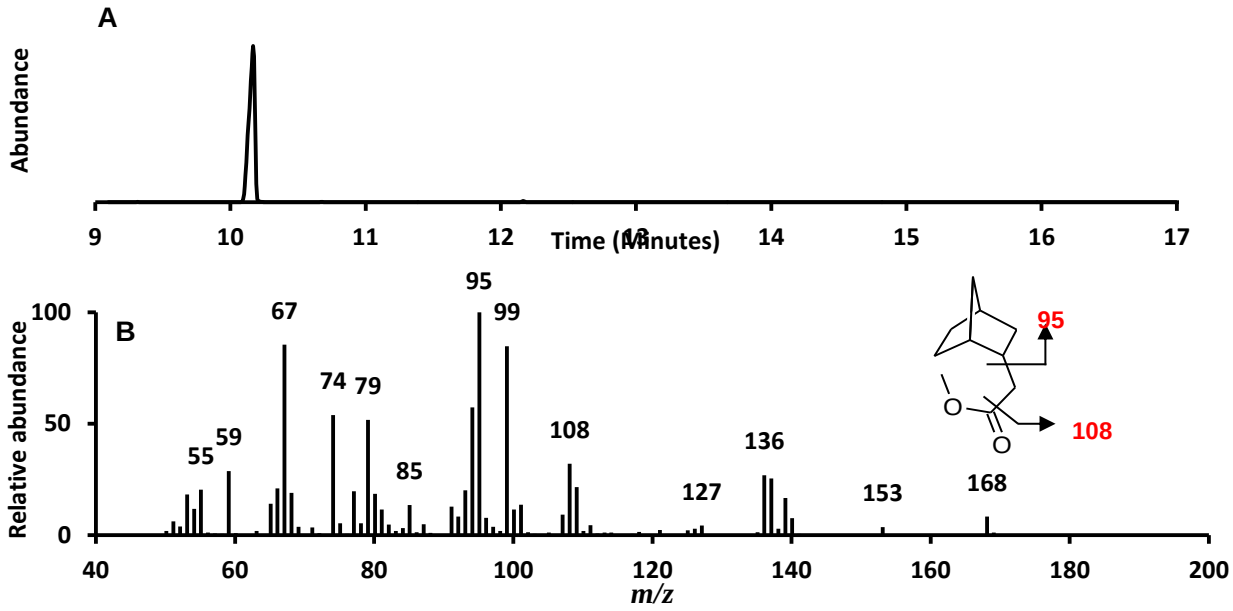

Figure 2.110. (A) Chromatogram for the methyl ester of bicyclo[2,2,2]heptane-2-ethanoic acid. (B) mass spectrum of component eluting at RT 10.10 minutes. GC-MS conditions as described in Figure 2.13.

Bicyclo [3.3.1] nonane-1-carboxylic acid was esterified with BF_3-MeOH (Figure 2.111) (30 minutes, 70^{o}C) and analysed with GC-MS (Figure 2.111).

Figure 2.111. Esterification of bicyclo [3.3.1] nonane-1-carboxylic acid

Analysis of the chromatogram (Figure 2.112A) reveals a single distinct peak at RT 11.23 minutes, analysis of the mass spectrum (Figure 2.112B) shows an $M^{+\bullet}$ at *m/z* 182, characteristic of a bicyclo [3.3.1] nonane-1-carboxylic acid methyl ester. Significant ions exist at *m/z* 150 (loss of methanol) and *m/z* 123 (loss of

the alkanoate side chain).

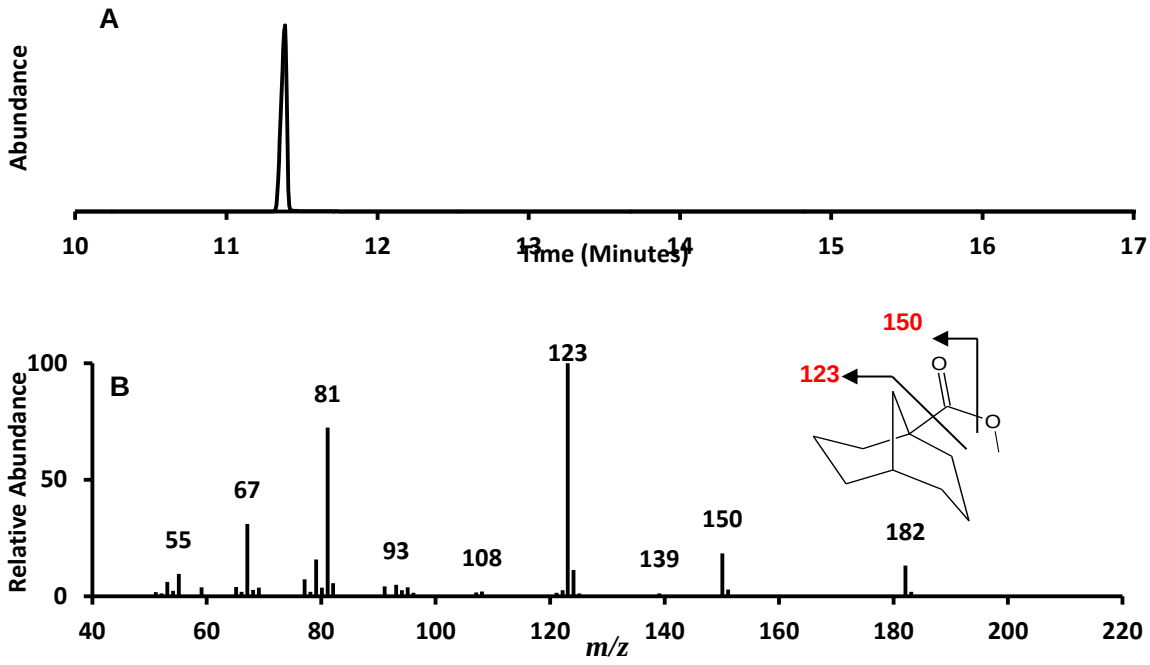

Figure 2.112. (A) Chromatogram for the methyl ester of bicyclo [3.3.1] nonane-1-carboxylic acid. (B) Mass spectrum of the component eluting at 11.23 minutes**.** GC-MS conditions as described in Figure 2.13.

A naturally occurring compound found in pine trees is hypothesised to be able to enter the OSPW and be oxidised to pinane carboxylic acid (2,6,6-trimethylbicyclo[3.1.1]heptane-3-carboxylic acid) by bacteria. To test this hypothesis an authentic sample of 2,6,6-trimethylbicyclo[3.1.1]heptane-3-carboxylic acid (Sigma Aldrich; Stated purity >98%) was purchased and esterified (Figure 2.113) and analysed with GC-MS before being analysed with two dimensional GCxGC MS for mass spectral and two dimensional retention time comparison.

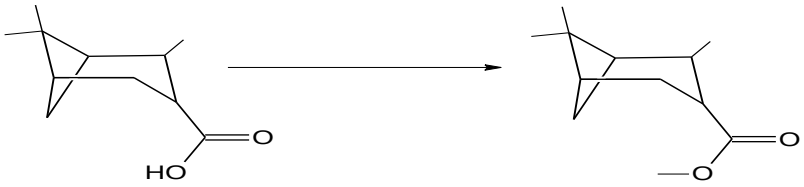

Figure 2.113. Esterification of 2,6,6-trimethylbicyclo[3.1.1]heptane-3-carboxylic acid

Analysis of the chromatogram (Figure 2.114A) reveals one distinct peak at RT 10.49 minutes. The mass spectrum (Figure 2.114B) is shown to have an $M^{+\bullet}$ at *m/z* 196, with significant fragment ions at *m/z* 181 (loss of a methyl group); *m/z* 165 (loss of methoxy); and *m/z* 136 (loss of the alkanoate side chain).

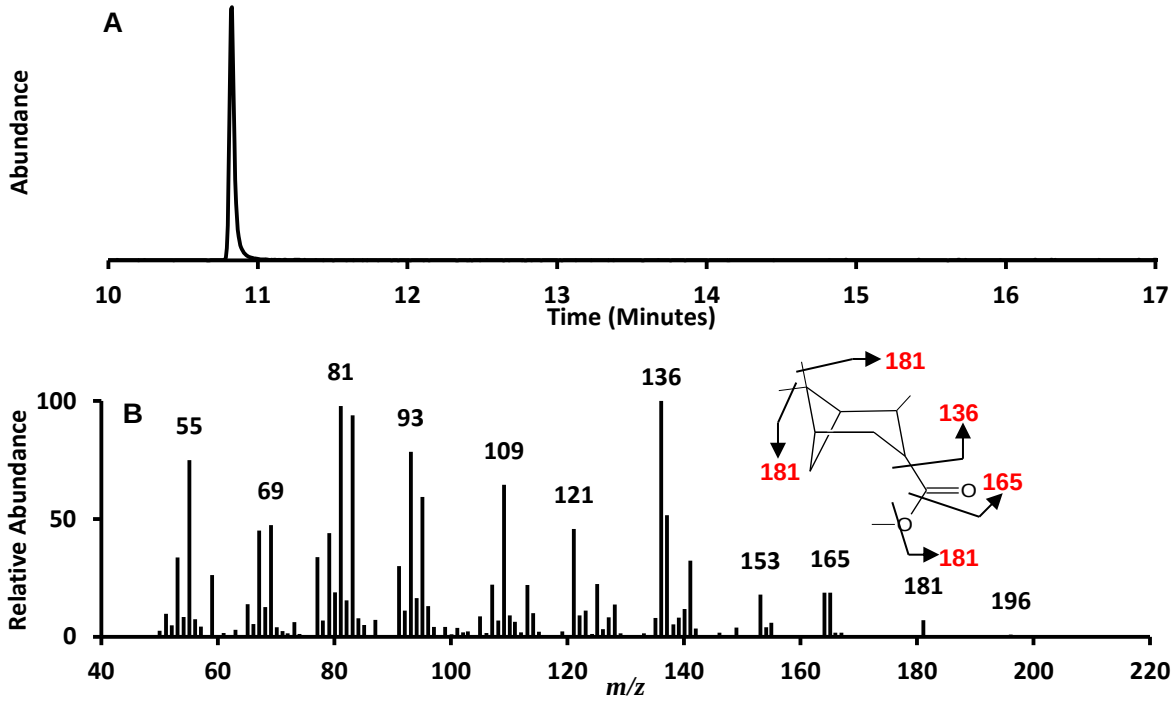

Figure 2.114. (A) Chromatogram for the methyl ester of 2,6,6-trimethylbicyclo[3.1.1]heptane-3-carboxylic acid. (B) mass spectrum of the component eluting at RT 10.49 minutes. GC-MS conditions as described in Figure 2.13.

2.3.20. Methyl Esters of Polycyclic Compounds

A number of polycyclic compounds had been tentatively identified within the naphthenic acid 'super-complex' mixtures. An authentic standard of abietic acid (Sigma Aldrich; stated purity >60%) was purchased and esterified with the BF_3-MeOH complex (Figure 2.115) and analysed with GC-MS.

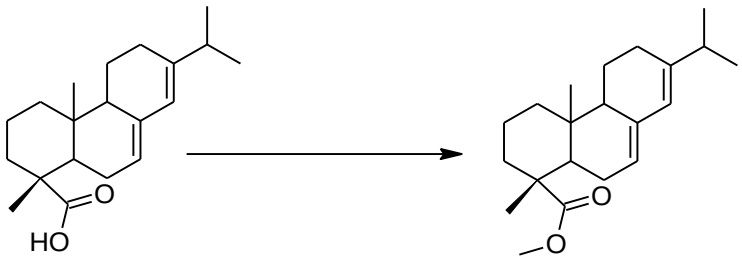

Figure 2.115. Reaction scheme for the esterification of abietic acid

Analysis of the chromatogram (Figure 2.116A) reveals that the abietic acid sample has an amount of contamination, analysis of the mass spectrum (Figure 2.116B) allows an identification of abietic acid methyl ester eluting at RT 21.49 as there is an $M^{+\bullet}$ at *m/z* 316, consistent with abietic acid. Significant ions exist at *m/z* 301 (loss of methyl); *m/z* 273 (loss of the iso-propyl group); and *m/z* 256 (loss of the alkanoate side chain).

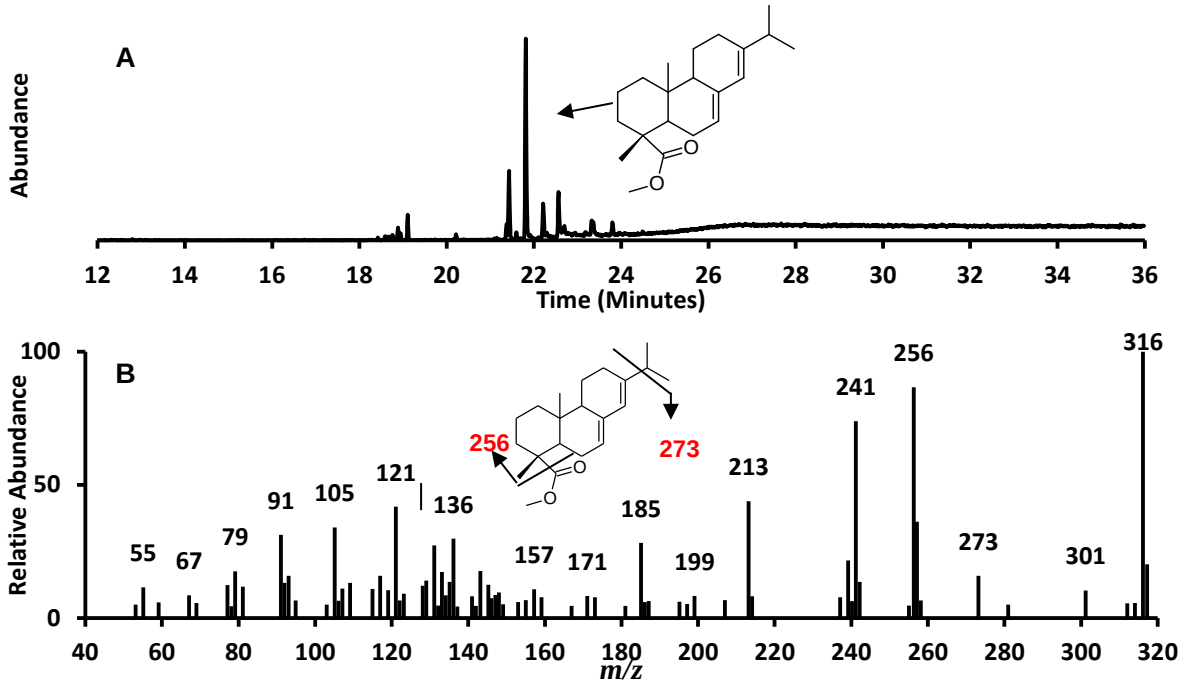

Figure 2.116. (A) Chromatogram for the methyl ester abietic acid. (B) mass spectrum of component eluting at RT 21.49. GC-MS conditions as described in Figure 2.13.

A fresh sample of abietic acid was esterified and analysed with GC-MS (Figure 2.117A), However on this occasion only one chromatographic peak with a low abundance was apparent (RT 21.26 minutes) (Figure 2.117A). Analysis of the mass spectrum (Figure 105B) revealed an M+• at *m/z* 314, which is different to that observed in Figure 2.116B, significant ions at *m/z* 299 and *m/z* 255 describe the losses from the alkanoate side chain cleavage. Identification of a dehydroabietic acid methyl ester was confirmed by comparison with the NIST database (Figure 2.117C). It is postulated that the dehydroabietic acid methyl ester was created during the esterification process.

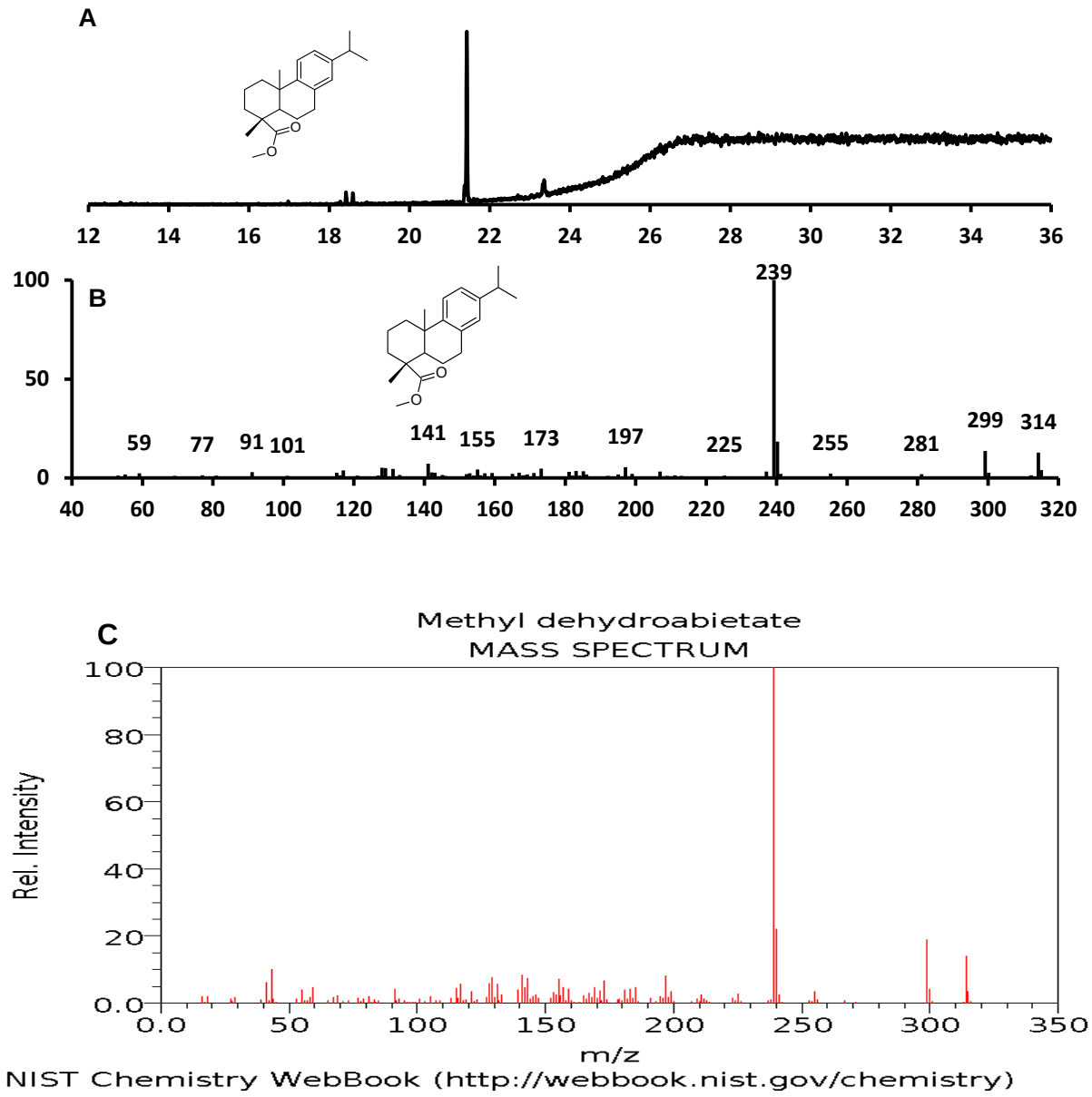

Figure 2.117. (A) Chromatogram for the methyl ester of dehydroabietic acid. (B) Mass spectrum for the component eluting at RT 21.26 minutes. (C) NIST derived mass spectrum for dehydroabietic acid methyl ester**.** GC-MS conditions as described in Figure 2.13.

Aromatic polycylic compounds were tentativley identified within the acid extract of the OSPW. A number of polycyclic poly aromatic compounds (fluorene-1-carboxylic acid; fluorene-4-carboxylic acid and fluorene-9-carboxylic acid) were

purchased from Sigma Aldrich (stated purity >99%), esterified by BF_3 MeOH (Figure 2.118). and analysed with GC-MS and GCxGC MS.

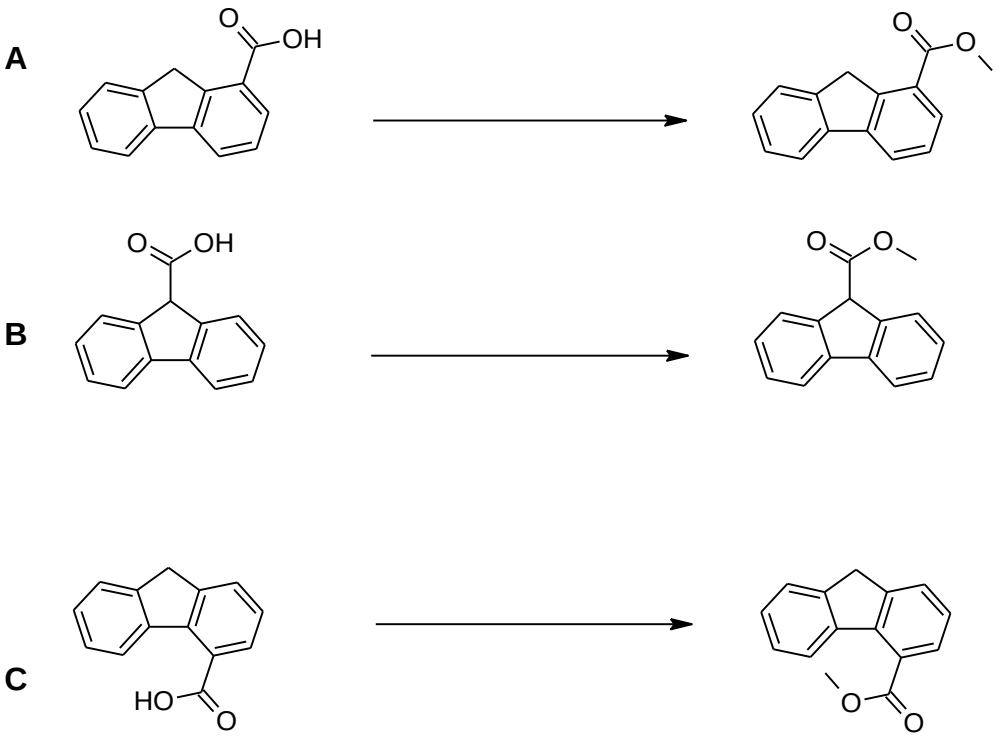

Figure 2.118. Reaction scheme for the esterification of (A) fluorene-1-carboxylic acid; (B) fluorene-9-carboxylic acid; and (C) fluorene-4-carboxylic acid.

Analysis of the chromatograms (Figure 2.119A) revels that each polycyclic compound displays a distinct peak; with fluorene-9-carboxylic acid methyl ester eluting at RT 17.22 minutes; fluorene-1-carboxylic acid methyl ester eluting at RT 18.34 minutes; and fluorene-4-carboxylic acid methyl ester eluting at RT 18.40 minutes.

Analysis of the mass spectra (Figure 2.119 B, C and D) reveals that all three compounds exhibit an $M^{+\bullet}$ at *m/z* 224 which is consistent with the methyl esters of fluorene carboxylic acids.

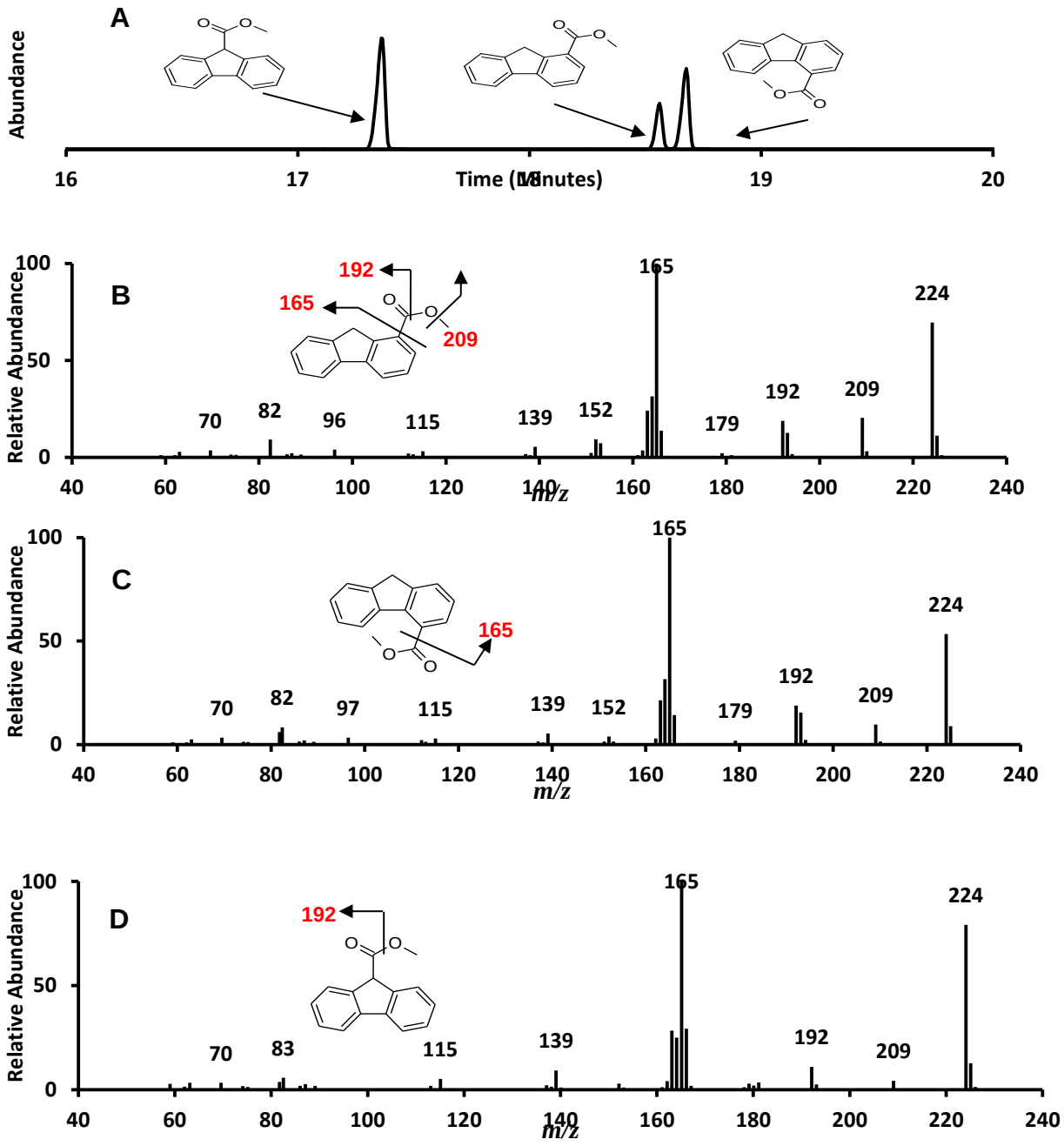

Figure 2.119. Over-laid chromatograms for (A) fluorene-1-carboxylic acid methyl ester, fluorene-4-carboxylic acid methyl ester and fluorene-9-carboxylic acid methyl esters. (B) Mass spectrum for component eluting at 18.34 minutes. (C) Mass spectrum for component eluting at RT 18.40 minutes. (D) Mass spectrum for component eluting at RT 17.22 minutes. GC-MS conditions as described in Figure 2.13.

Significant ions exist at *m/z* 209, 192 and 165 (base ion) which describe the cleavage of the alkanoateside chain. Only small differences in ion abundance exist in these mass spectra with the most noticable being descibed by the $M^{+\bullet}$ of the different isomers; i.e. fluorene-1-carboxylic acid methyl ester $M^{+\bullet}$ abundance is 62%; fluorene-4-carboxylic acid methyl ester $M^{+\bullet}$ abundance is 54%; and fluorene-9-carboxylic acid methyl ester $M^{+\bullet}$ is 79%.

An ethanoic moeity (fluorene-9-ethanoic acid) was aslo purchased from Sigma Aldrich (stated purity >99%), esterified with the BF3-MeOH complex and tested for purity with GC-MS (Figure 2.120)

Figure 2.120. Reaction scheme for the esterification of fluorine-9-ethanoic acid

Analysis of the chromatogram (Figure 2.121A) reveals a distinct chromatographic peak at RT 18.25 minutes. The mass spectrum (Figure 2.121B) displays an $M^{+\bullet}$ at *m/z* 238, which is consistent with a fluorine ethanoic acid methyl ester. Significant ions are revealed at *m/z* 207 (loss of a methoxy ion); *m/z* 178 (loss of a carboxylate ion) and *m/z* 165 (loss of the alkanoate side chain).

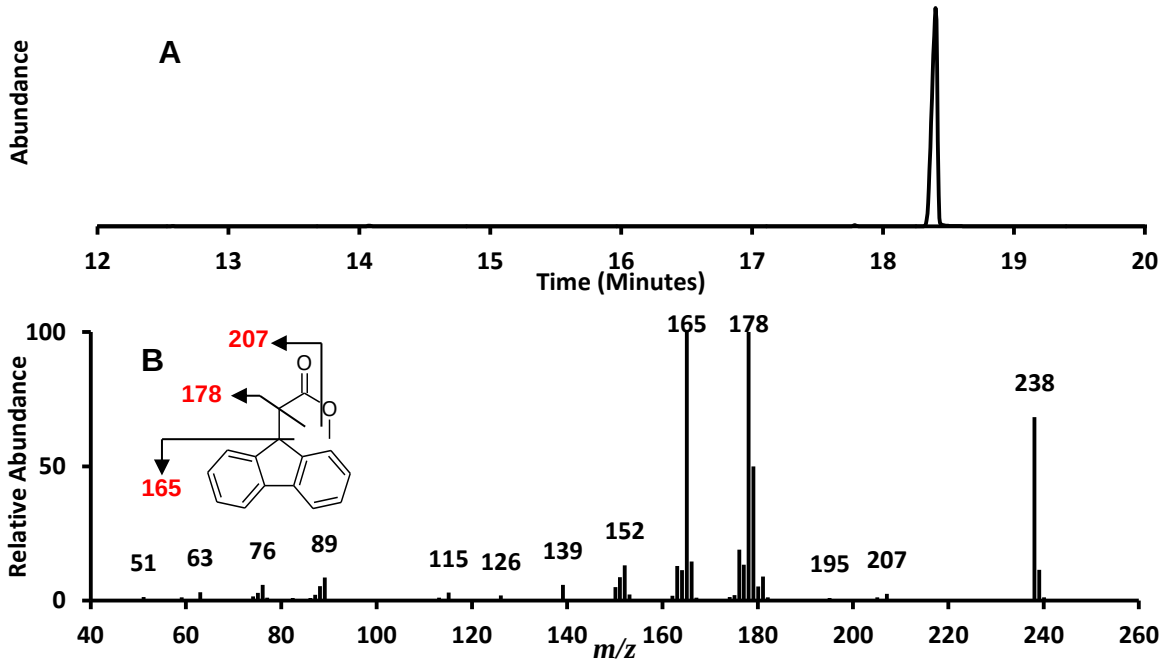

Figure 2.121. (A) Chromatogram for the methyl ester fluorine-9-ethanoic acid. (B) Mass spectrum for component eluting at RT 18.25 minutes. GC-MS conditions as described in Figure 2.13.

2.3.21 Methyl Esters of Hydroxy Acids

Hydroxy type adamantane acids were converted to the methyl esters with the BF_3-MeOH complex, however the first attempt with 3-hydroxyadamantane-1-carboxylic acid methyl esters and 3-hydroxyadamantane-1-ethanoic acid methyl esters (Figure 2.122) showed no trace of the compounds.

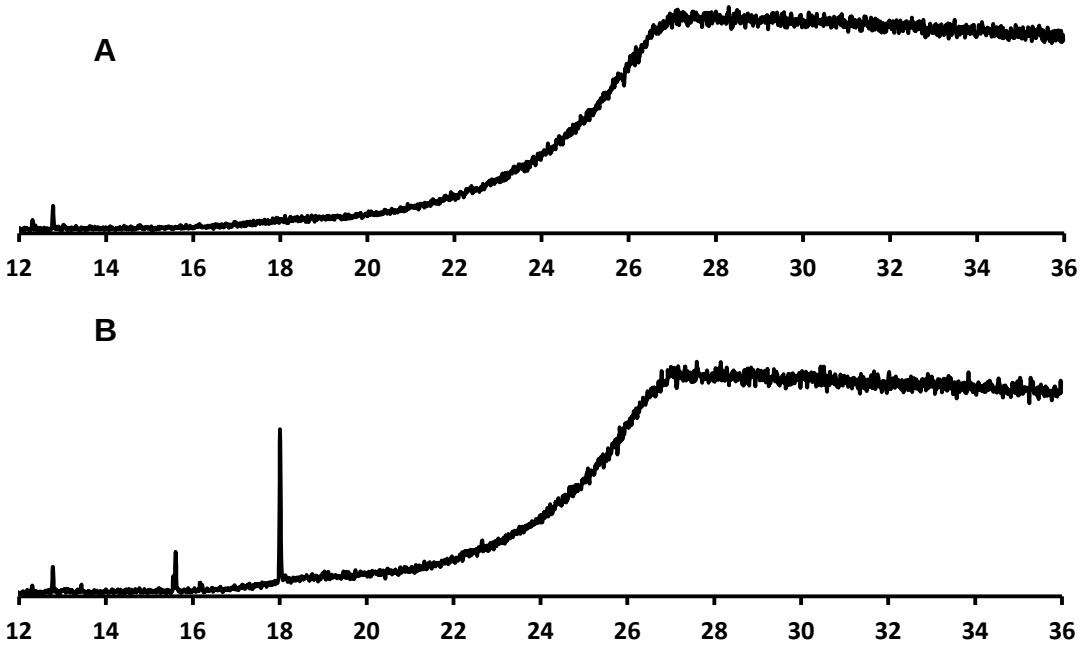

Figure 2.122. Chromatogram of first methylation and extraction of (A) 3-hydroxyadamantane-1-carboxylic acid and (B) 3-hydroxyadamantane-1-ethanoic acid Peak at 18 minutes in chromatogram B has been designated a siloxane bleed ion due to the presence of m/z 207 and m/z 281.

It was postulated that the esterification process was not going to completion and the hydroxy acids were remaining in the hexane phase when the extracting the methyl esters.

In order to test the purity of the hydroxy adamantanes a fresh sample of each was converted to the TMS esters (BSTFA+1%TMCS; 30 minutes, 70^{o}C) (Figure 2.123 and Figure 2.124).

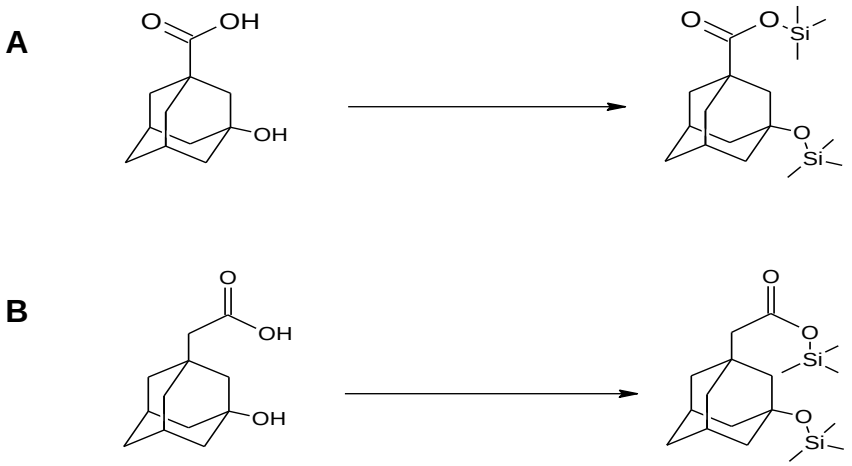

Figure 2.123. Reaction scheme for the TMS esterification of 3-hydroxyadamantane-1-carboxylic acid (A); and 3-hydroxyadamantane-1-ethanoic acid (B).

Analysis of the chromatograms in Figures 3.108A and B reveals that one distinct peak is displayed at a retention time of RT 16.21 minutes in Figure 2.124A and RT 17.29 minutes in Figure 2.124B.

Analysis of the mass spectra reveals an $M^{+\bullet}$ in Figure 2.124C at *m/z* 340, consistent with a 3-hydroxyadamantane-1-carboxylic acid TMS di-ester. Significant fragment ions are revealed at *m/z* 325 (loss of methyl; base ion); *m/z* 267 (loss of TMS ion); *m/z* 251 (loss of oxy-TMS); *m/z* 223 (loss of the carboxylic acid TMS ester) and *m/z* 73 (indicative of TMS esters). The $M^{+\bullet}$ in Figure 2.124D is revealed at *m/z* 354, consistent with a 3-hydroxyadamantane-1-ethanoic acid TMS di-ester.

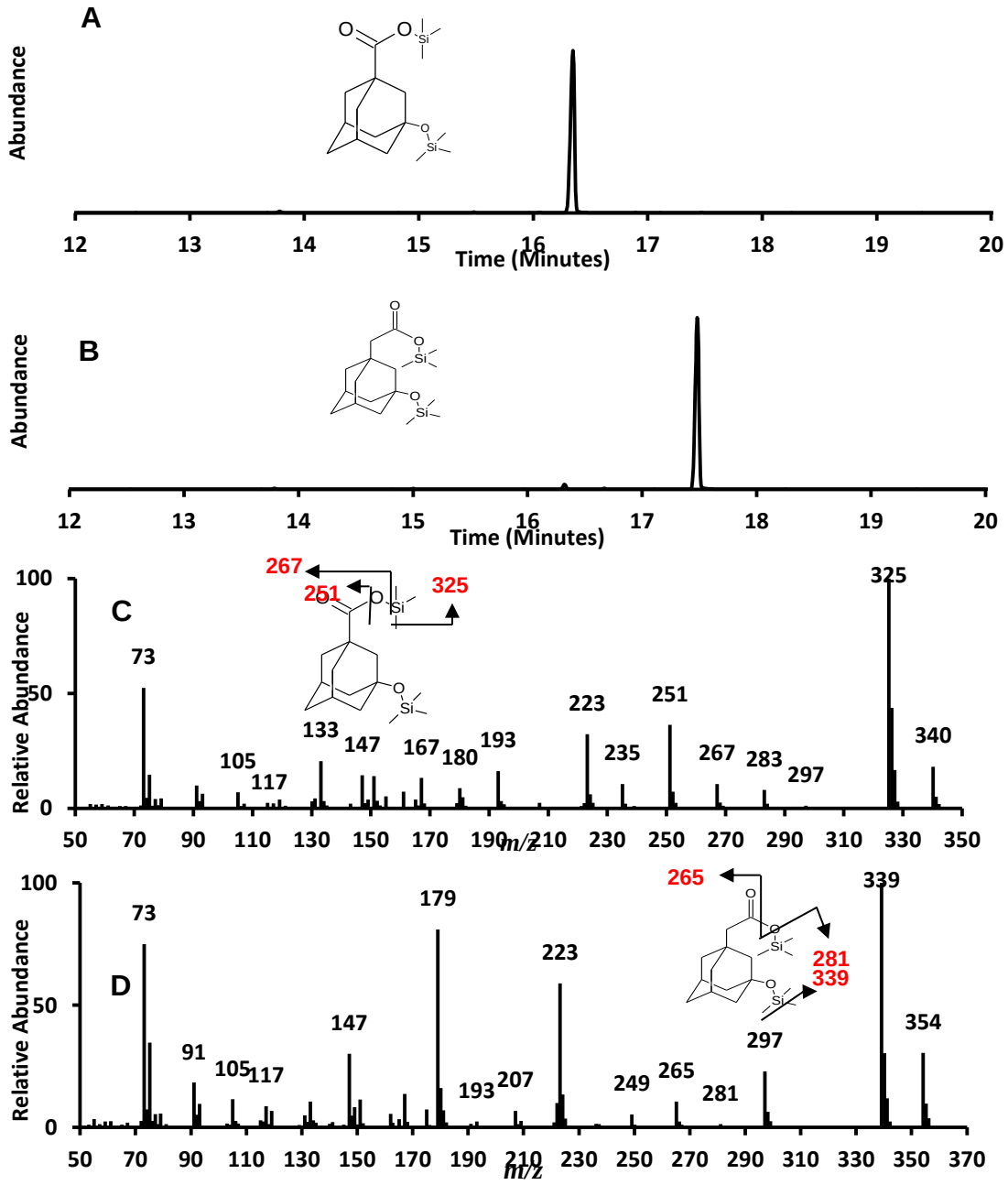

Figure 2.124. (A) Total ion current chromatogram for the TMS esters of 3-hydroxyadamantane-1-carboxylic acid trimethylsilyl di-ester. (B) Chromatogram for the TMS 3-hydroxyadamantane-1-ethanoic acid trimethylsilyl di-ester. (C) Mass spectrum for compound eluting at RT16.21 minutes. (D) Mass spectrum for the compound eluting at RT 17.29 minutes, GC-MS conditions as described in Figure 2.13.

Significant ions are displayed at *m/z* 339 (loss of methyl; base ion); *m/z* 281 (loss of TMS ion); *m/z* 265 (loss of oxy-TMS); *m/z* 223 (loss of the ethanoic acid TMS ester) and *m/z* 73 (indicative of TMS esters). This derivatisation with TMS ester showed that the molecules were pure and that the issue was likely to lay with the BF_3-MeOH esterification processes.

In order to determine whether the hydroxyl moieties were remaining within the water in the BF_3- MeOH extraction it was decided that a re-extraction with ethyl acetate after the hexane extraction and the addition of an internal standard and a non-hydroxy adamantane of the same structural type would test the hypothesis. A 3,5-dimethyl adamantane-1-carboxylic acid (internal standard) and adamantane-1-carboxylic acid were mixed with the 3-hydroxyadamantane-1-carboxylic acid, whilst the internal standard and an ethanoic adamantane acid was mixed with the ethanoic hydroxyl adamantane. It was assumed that the non hydroxyl would be extracted by the hexane and the hydroxyl would be extracted in the ethyl acetate. However, whilst the non hydroxyl adamantanes were extracted by the hexane the hydroxyl acids were not removed from the water phase by the ethyl acetate (Figure 2.125 and 3.110)

Analysis of the chromatogram in Figure 2.125A (BF_3-MeOH hexane extraction) shows two peaks at RT 12.25 minutes and RT 12.38 minutes. Analysis of Figure 2.125B (ethyl-acetate extraction) reveals a chromatogram akin to a hexane blank with no compound eluting throughout. The mass spectra displayed in Figure 2.125C reveals an $M^{+\bullet}$ at *m/z* 194 and a significant fragment ion at *m/z* 135 indicative of the loss of an alkanoate side chain.

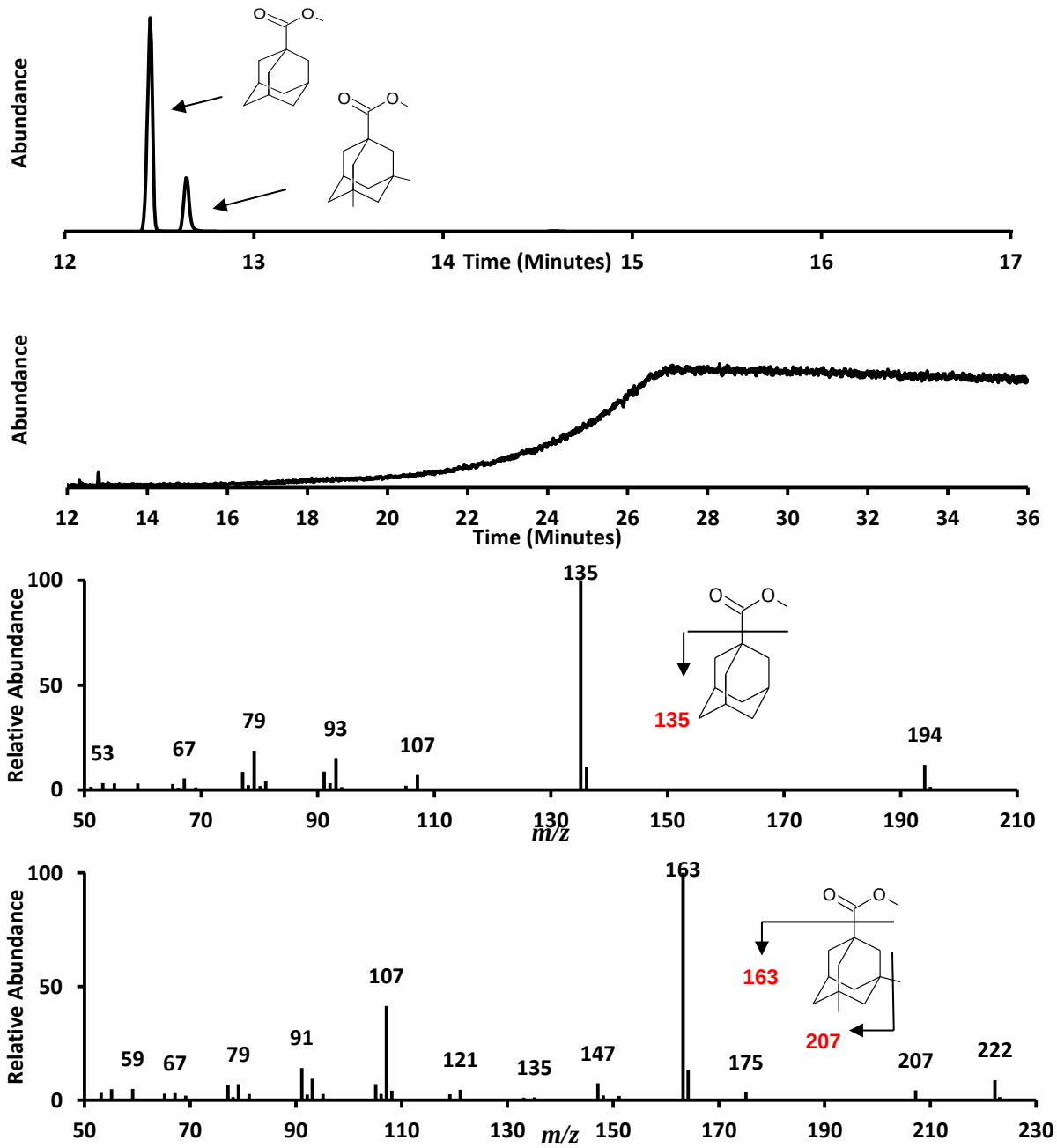

Figure 2.125. Total ion current chromatograms for (A) Hexane extraction from the hydroxyadamantane partitioning experiment. (B) Ethyl acetate extraction from the hydroxyadamantane partitioning experiment. (C) Mass spectrum for the compound eluting at RT 12.25 minutes. (D) Mass spectrum for the compound eluting at RT 12.38 minutes. GC-MS conditions as described in Figure 2.13.

This mass spectra and related retention time are also identical to that displayed in Figure 2.84 confirming the assignment of adamantane-1-carboxylic acid methyl ester. Analysis of Figure 2.125D reveals an $M^{+\bullet}$ at *m/z* 222, consistent with a 3,5-dimethyladamantane-1-carboxylic acid methyl ester. Significant fragments exist at *m/z* 207 indicating loss of a methyl group and *m/z* 163 characteristic of the cleavage of the alkanoate side chain.

Similar results were obtained when examining the ethanoic moieties. Examinations of the chromatograms confirm that the non-hydoxy moieties were extracted by the hexane (Figure 2.126A), but neither hexane nor ethyl-acetate extracted the hydroxyl moieties (Figure 2.126B). Two chromatographic peaks are evident in Figure 2.126A at retention times of RT 12.38 minutes and RT 13.32 minutes. Analysis of the mass spectra (Figure 2.126C) reveals that the chromatographic peak at RT 12.38 has a $M^{+\bullet}$ at *m/z* 222, consistent with a 3,5-dimethyladamantane-1-carboxylic acid methyl ester. Significant fragments exist at *m/z* 207 indicating loss of a methyl group and *m/z* 163 characteristic of the cleavage of the alkanoate side chain. The fragmentation pattern and the identical RT confirms this as a 3,5-dimethyl adamantane-1-carboxylic acid methyl ester.

Analysis of Figure 2.126D reveals a $M^{+\bullet}$ at *m/z* 208, consistent with a adamantane-1-ethanoic acid methyl ester. Significant fragments exist at *m/z* 177 indicating loss of a methoxy group, *m/z* 148, indicating cleavage of a carboxylate group and *m/z* 135 characteristic of the cleavage of the alkanoate side chain.

The fragmentation pattern and the $M^{+\bullet}$ confirms this as a 3,5-dimethyl adamantane-1-carboxylic acid methyl ester.

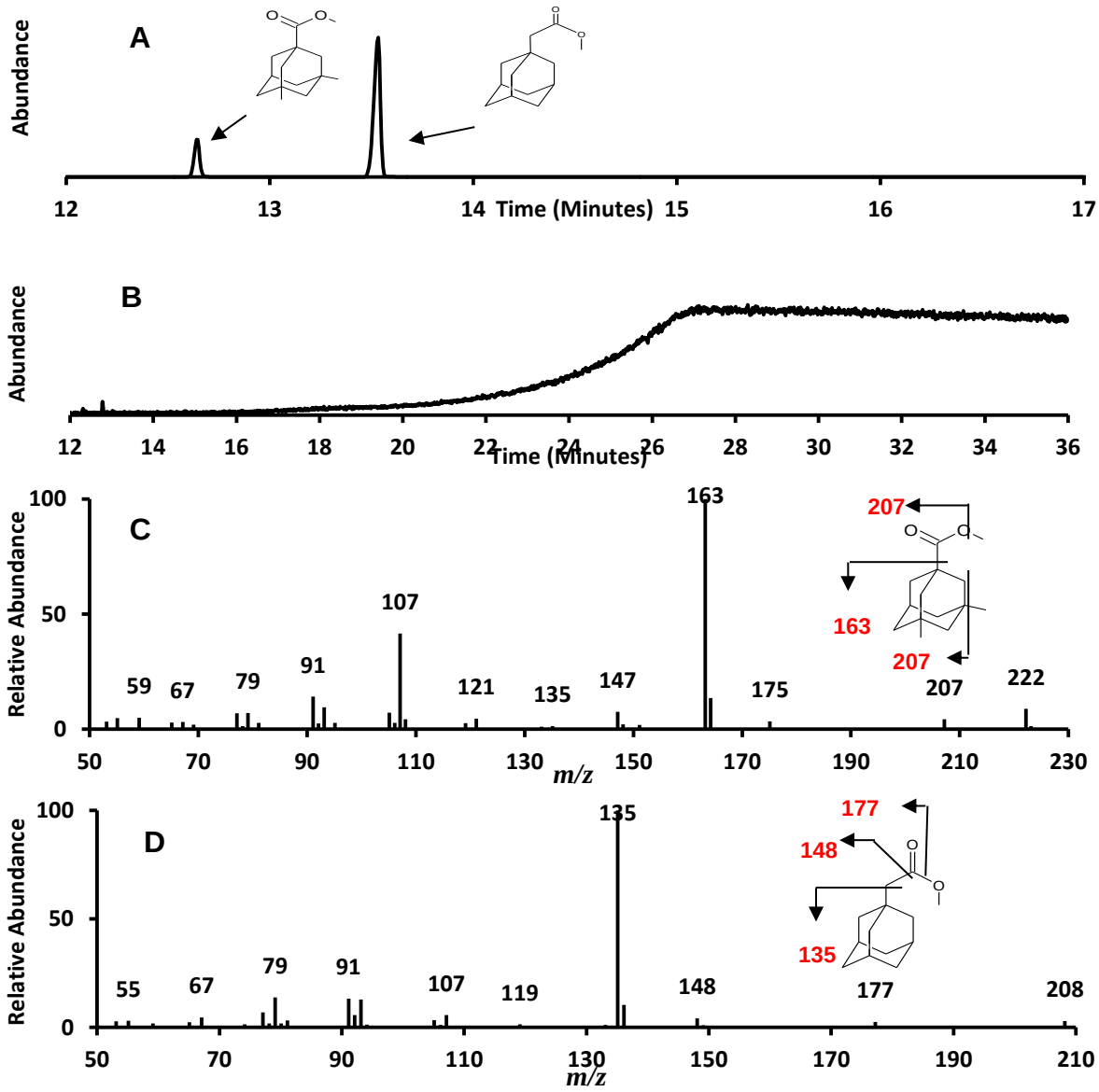

Figure 2.126. Chromatograms for (A) Hexane extraction from the hydroxyadamantane partitioning experiment. (B) Ethyl acetate extraction from the hydroxyadamantane partitioning experiment. (C)Mass spectrum for the compound eluting at RT 12.38 minutes. (D) Mass spectrum for the compound eluting at RT 13.32 minutes**.** GC-MS conditions as described in Figure 2.13.

It was assumed that either the hydroxyl moieties were either too polar to be extracted from the water or were adsorbing onto the drying agent used in the extraction process. The sodium sulphate used in the experiment was sonicated in DCM for 20 minutes and the residue was analysed with GC-MS. No hydroxyadamantane was determined in these fractions only a residue of the non-hydroxyl acids and internal standards (Figure 2.127).

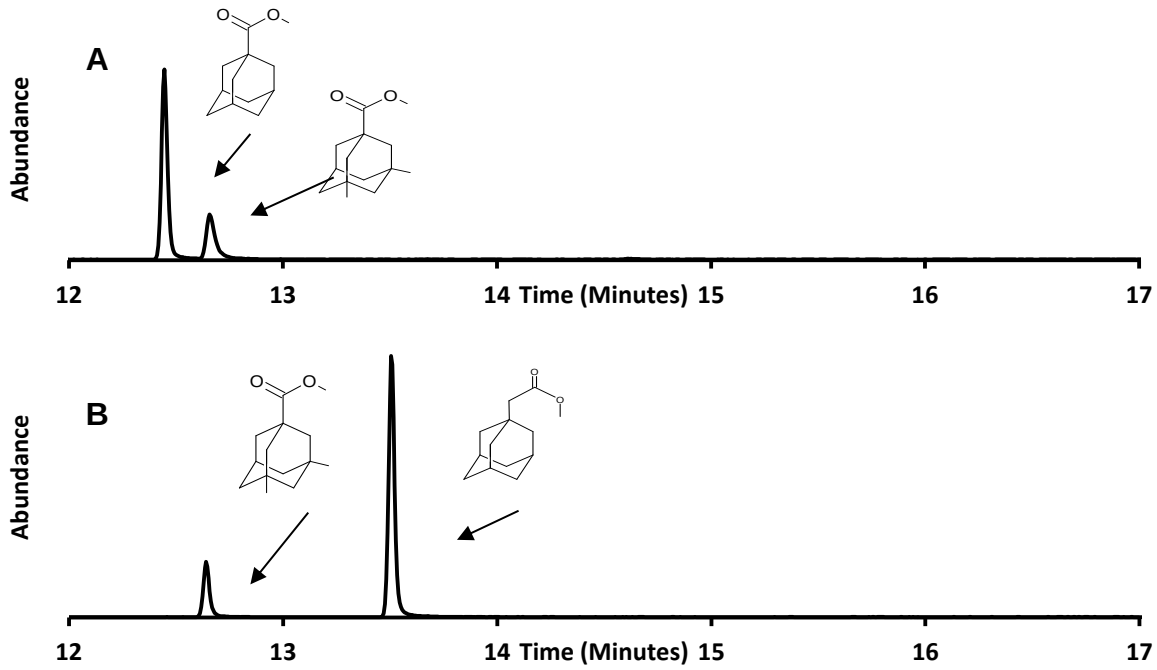

Figure 2.127. Chromatograms of compounds extracted from the sonication of sodium sulphate drying agent used in hydroxyadamantane partitioning experiments, mass spectra are available in Figures 2.109 and 2.110.

It seems then that hydroxyl acids do not perform well under the esterification conditions of BF_3-MeOH as they are unlikely to be extracted from the water phase using two separate solvents. It is recommended that BSTFA+TMCS or other derivatising agents are used for their analysis.

2.3.22 Synthesis of Bicyclo[3.2.1]octane-6-carboxylic Acid

A number of postulated structures are not available commercially so it is important to synthesise them in house so they can be co-chromatographed via GCxGC MS for positive identification. One of the tentatively identified acids was bicyclo [3.2.1] octane-6-carboxylic acid. A commercially available authentic standard, 2-hydroxybicyclo [3.2.1] octane-6-carboxylic acid (Sigma Aldrich; Stated purity >99%)) was purchased and an attempt at dehydration and Hydrogenation to bicyclo [3.2.1] octane-6-carboxylic acid was made (Figure 2.128) .

A sample (50 mg) of 2-hydroxybicyclo[3.2.1]octane-6-carboxylic acid was reacted with dry pyridine and phosphoryl chloride and allowed to stand overnight, the product was subsequently hydrogenated using the H-Cube® hydrogenator, aliquots were reacted with BF_3-MeOH (Figure 2.128) and analysed with GC-MS (Figure 2.129). Because of the issues detailed above no chromatogram or mass spectrum is available for the hydroxyl moiety.

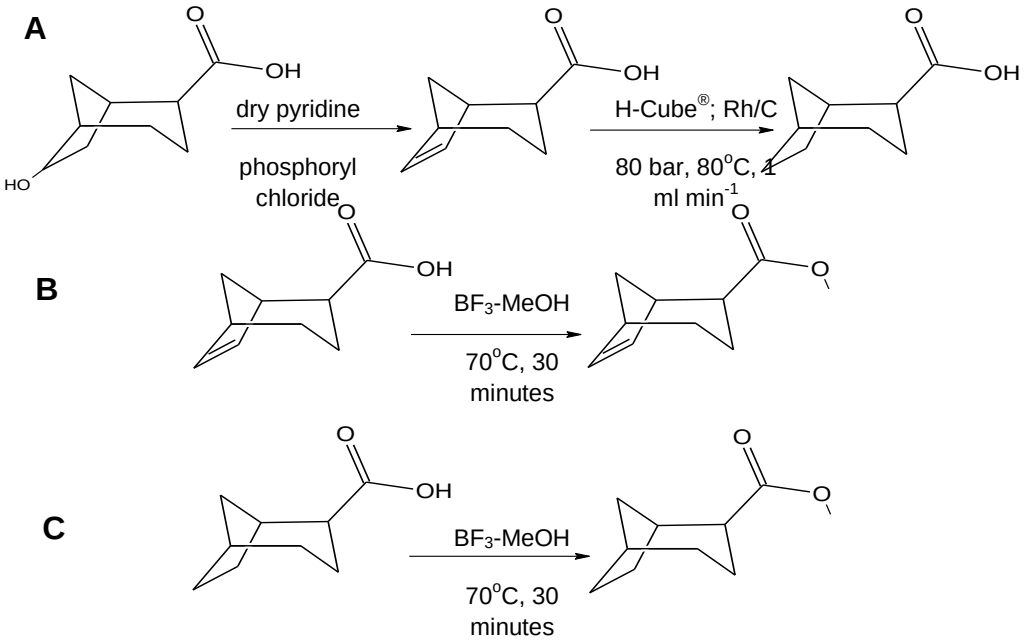

Figure 2.128. (A) Reaction schemes for the dehydration and Hydrogenation of 2-hydroxybicyclo[3.2.1]octane-6-carboxylic acid to produce bicyclo [3.2.1] octane-6-carboxylic acid; plus esterification of (B) bicyclo[3.2.1]oct-6-ene-2-carboxylic acid and (C) bicyclo [3.2.1] octane-6-carboxylic acid.

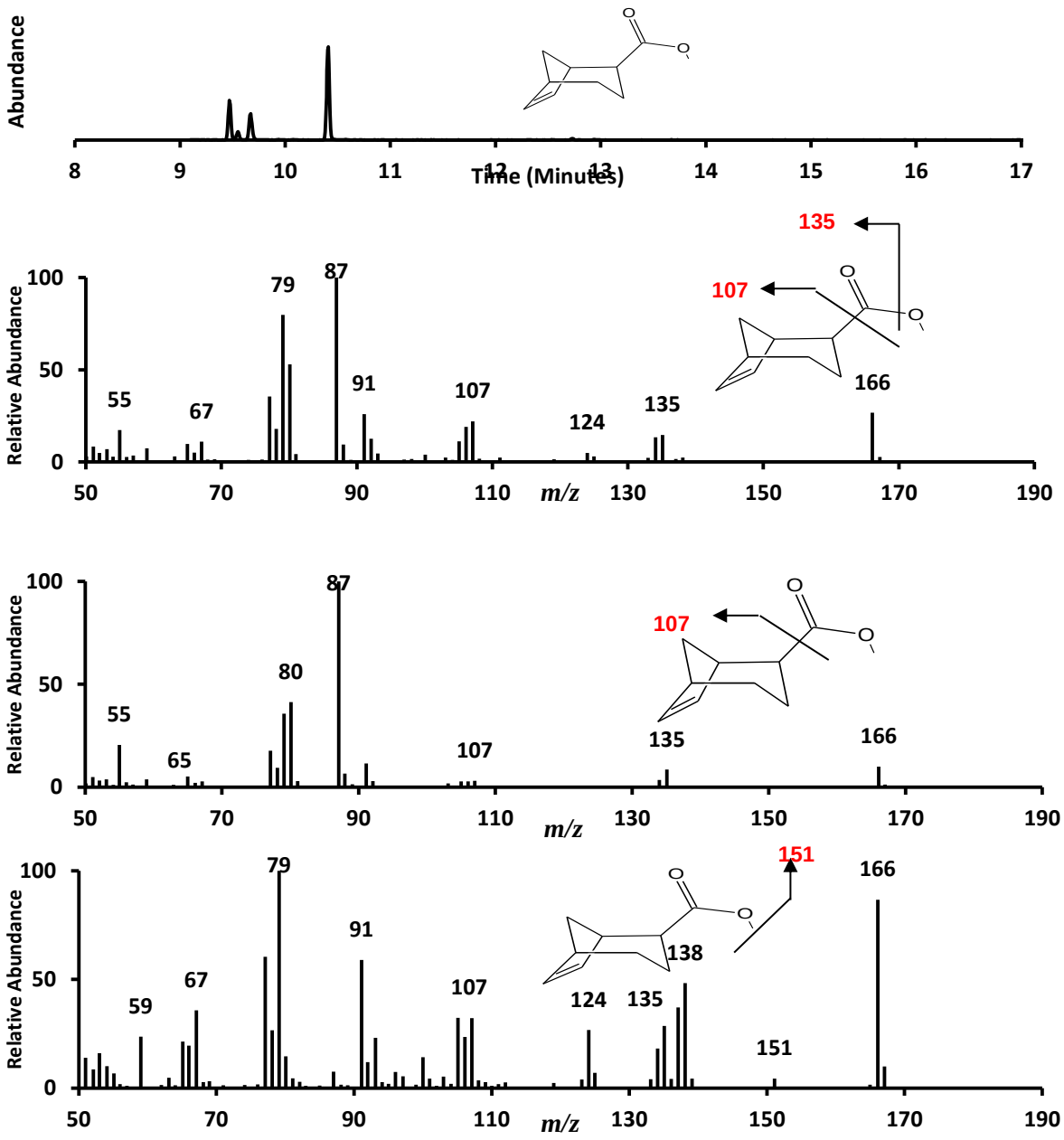

Figure 2.129. (A) Chromatograms for isomers of of bicyclo[3.2.1]oct-2-ene-6-carboxylic acid methyl esters. (B) Mass spectrum for component eluting at RT 9.34 minutes. (C) Mass spectrum for component eluting at RT 9.41 minutes. (D) Mass spectrum for component eluting at RT 9.10.24 minutes. GC-MS conditions as described in Figure 2.13.

Analysis of the chromatogram (Figure 2.129A) reveals one distinct chromatographic peak (RT 10.24 minutes) and three lesser peaks (RT 9.28, 9.34 and 9.41 minutes). Analysis of the mass spectra reveals that all four mass spectra have an $M^{+\bullet}$ at m/z 166 which is consistent with a bicyclo[3.2.1]oct-2-ene-6-carboxylic acid methyl ester and indicating that the four peaks represent four separate isomers.

Significant fragment ions exist in all four spectra. Cleavage of the alkanoate side chain is revealed by the ion at m/z 107 and m/z 135 indicates loss of a methoxy group. Figure 2.129B-D are similar in aspect apart from the ion abundances of the $M^{+\bullet}$, whereas 3.113E displays different ion abundances throughout with an unexplained ion at m/z 138 (M-28) and a fragment ion at m/z 151 indicating loss of a methyl group.

Figure 2.130 displays the chromatogram and mass spectra from the Hydrogenation of bicyclo[3.2.1]oct-2-ene-6-carboxylic acid. The products were reacted with BF3-MeOH and analysed with GC-MS. Figure 2.130A reveals two distinct chromatographic peaks with retention times of RT 9.48 minutes and RT 10.24, the latter being identical to the major peak revealed in Figure 2.129A.

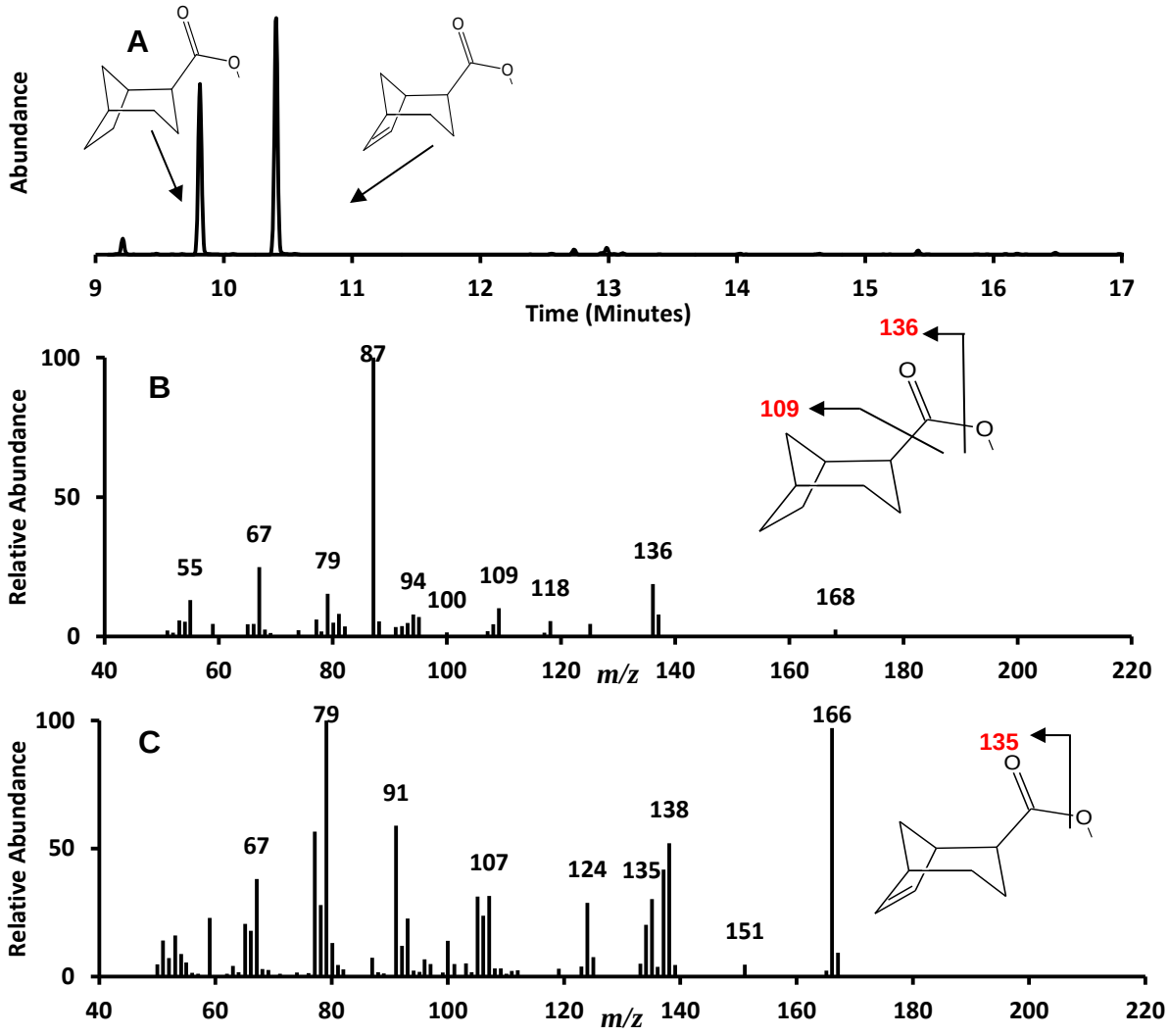

Figure 2.130. (A) Chromatogram for Hydrogenation of bicyclo[3.2.1]oct-2-ene-6-carboxylic acid methyl ester. (B) Mass spectrum for component eluting at RT 9.48 minutes. (C) Mass spectrum for component eluting at RT 10.24 minutes. GC-MS conditions as described in Figure 2.13.

Analysis of the mass spectra in Figure 2.130A reveals a $M^{+\bullet}$ at *m/z* 168, consistent with a bicyclo [3.2.1] octane-6-carboxylic acid methyl ester. Significant fragment ions exist at *m/z* 136 (loss of methanol) and *m/z* 109 (loss of an alkanoate side chain). Analysis of Figure 2.130B reveals a mass spectra identical

to that displayed in Figure 2.129E, with a $M^{+\bullet}$ at *m/z* 166 and significant fragments at *m/z* 151, 135 and 107 characteristic of a bicyclo[3.2.1]oct-2-ene-6-carboxylic acid methyl ester. The chromatogram in Figure 2.130A indicates that ~45% of the reactant was converted to the product, as this was enough for 2D GCxGC MS analysis the experiment was stopped at this point.

2.4. Conclusions

Because of the stability caused by the overlapping π orbitals, aromatic compounds are often difficult to fully saturate, industry (for instance) use high temperatures and pressures to overcome this stability. The use of low pressures and temperatures meant that the full saturation of aromatic compounds is a difficult task that often requires many repetitions.

That complete hydrogenation of aromatic compounds was achieved using both the Buchii reaction chamber and the novel H-Cube® hydrogenator reveals that this challenging undertaking can be overcome.

However only one compound was able to be fully saturated using the Buchii in isolation of the H-Cube® (decahydro-1-carboxylic acid) and this only occurred after a 21 hour experiment. There were specific problems with the Buchii system, which was primarily designed for temperature based reactions rather than hydrogenation, chief amongst these was the pipette being forced from the chamber at pressures > 1 bar, unless the pipette clamp was tightened, which subsequently reduced the hydrogen flow to zero. Other issues concerned the cage that held the reaction vessel being too tall for the 150 mL chamber meaning the magnetic stirrer needed to be clamped to the side of the chamber, causing

sporadic mixing. Using the 300 mL chamber meant that the hydrogen delivery pipette was not fully immersed into the solution. However, using the Buchii did mean that the correct catalyst could be used (Adams catalyst).

The H-Cube® easier and potentially far safer to use than the Buchii (no hydrogen cylinders required) however the success of the first experiment was not easily repeatable and the frequency with which the catalyst was rendered inoperative was concerning, making this system far more expensive to use than the Buchii reaction chamber. It was also found that the recommended 5-10 minute system flush between compounds was not enough to prevent contamination, and it is recommended that a flush with clean solvent is carried out for at least 20 minutes.

Whilst more compounds were brought to full saturation with the H-Cube® it is telling that some of the best results were obtained by an amalgamation of both methods, the H-Cube® to start with (higher pressure and temperature; inappropriate catalyst) and then the Buchii (correct catalyst) to finish.

Table 2.9. Table of recoveries and purities of hydrogenated compounds

Compound	Hydrogenator	Attempts	Reactant (mg)	Stated Purity of Reactant % (Actual purity in parenthesis)	Product (mg)	% Total Recovery	% Aromatic Compound	% Partially Saturated Compound (mg)	% Fully Saturated compound	Purity Assessed by
3,7-dimethyloctanoic acid	HCH	1	99.6	>96	85.4	86	-	< 1	>99	GC-MS
4-n-hexylcyclohexylethanoic acid	RBF	1	100.5	>99	76.7	76	42	-	58	GC-MS
4-n-hexylcyclohexylethanoic acid	HCH	3	76.7	-	34	44	66	-	34	GC-MS
4-methylcyclohexylethanoic acid	HCH	3	75	>99	38	51	< 1	-	>98	GC-MS
Cyclohexyl-6-hexanoic acid	HCH	2	50.1	>99 (98)	48.2	59	20.2	-	78	GC-MS
Cyclohexyl-6-hexanoic acid	BRC	1	48.2	-	41.2	85	< 1	-	>98	GC-MS
4-isopropylcyclohexylethanoic acid	HCH	2	87.1	>99 (98)	71.8	82	79.8	-	20.2	GC-MS
4-n-pentylcyclohexylethanoic acid	HCH	4	101.6	>99	71.6	64	<1	-	>98	GC-MS
4-n-nonylcyclohexylethanoic acid	HCH	1	20.2	>99	17.3	86	48	-	52	GC-MS

4-tert-butylcyclohexylethanoic acid	HCH	2	100.4	>99	67.2	67	11	-	89	GC-MS
4-tert-butylcyclohexylbutanoic acid	HCH	4	101.2	>98	68.4	68	72	-	28	GC-MS
Octahydroindene-2-carboxylic acid	HCH	2	98.8	>99	68.5	69	25.5	3	73	GC-MS
1-methyl-octahydroindene-2-carboxylic acid	HCH	2	100.8	>99	96.6	96	-	35	65	GC-MS
Decahydronaphthalene-1-carboxylic acid	BRC	3	106.3	>99 (88)	67.0	63	-	2.5	>97	GC-MS
Decahydronaphthalene-1-carboxylic acid	HCH	1	85.0	>99 (88)	71.0	84	-	3.5	>96	GC-MS
Decahydronaphthalene-2-carboxylic acid	HCH	2	86.8	>99	74.0	85	< 1	-	>99	GC-MS
Decahydronaphthalene-1-ethanoic acid	BRC	2	106.3	>99	103.5		88	12	-	GC-MS
Decahydronaphthalene-1-ethanoic acid	HCH	2	112.3	>99	85.9	76.5	47	51	1	GC-MS
Decahydronaphthalene-2-ethanoic acid	BRC	2	104.4	>99			0	34	66	GC-MS
Decahydronaphthalene-2-ethanoic acid	HCH	2	109.3	>99	88	80	-	< 1	> 99	GC-MS
Decahydronaphthalene-1-propanoic acid	HCH	3	49	>99 (98)	41		-	16	15 (11)	GC-MS
Decahydronaphthalene-1-propanoic acid	BRC	1	41	>99 (98)			-	< 1	> 99	GC-MS
4-methyldecahydronaphthalene-1-carboxylic acid	HCH	3	107.8	>99	85.8		95	5	-	GC-MS
4-methyldecahydronaphthalene-1-carboxylic acid	BRC	1	85.8	>99			<1	>99	-	GC-MS
Bicyclo[3,2,1]octane-6-carbxylic acid	HCH	1	6	-	2.8	47	-	54	46	GC-MS

Hydrogenator: HCH is H-Cube Hydrogenator; BRC is Buchii Reaction Chamber; RBF is Round Bottomed Flask. Smaller % recoveries indicate more than once on the flow through hydrogenator

As can be seen in Section 2.3.21 BF_3-MeOH esterification of products does not always have the desired results. Hydroxy compounds, for instance, were not able to be extracted from the water phase of the BF_3 MeOH extraction. Plus the BF_3 method can be time consuming and includes a number of steps that have to be carefully carried out to ensure no contamination ensues.

The importance of analysing both the mass spectra and the chromatograms was highlighted by the almost identical mass spectra for adamantane-1-carboxylic acid produced when analysing the methyl esters of the hydrogenated products of 1-methyl-1*H*-indene-2-carboxylic acid (Figures 2.50, 2.51) only a combined analysis of both the retention times of the compounds and the mass spectra allowed an accurate assignment of compounds.

Most of the analysed compounds have been assessed toxicologically both individually and within mixtures (Jones et al., 2011: Chapter 3 and 4) and have been analysed through two dimensional gas chromatography mass spectrometry (Rowland et al., 2011d). These compounds have generally been tentatively identified within a sample of the acid extracts of an Oil Sands Process Water and within a sample of a commercial mixture of naphthenic acids.

Chapter 3
Aquatic Toxicology of Individual Petroleum Acids

3.1. Introduction

The phrase ‘naphthenic acids are described as being amongst the most toxic components in Oil Sands Process Affected Waters (OSPW)’ is prevalent in the scientific literature (e.g. Mackinnon and Boeger, 1986; Rogers et al., 2002; Kannel and Gan, 2012). However, as described in Chapter 1, this statement is open to question. Naphthenic acids (NA) exist within the OSPW and crude oils as unresolved mixtures (Quagraine et al., 2005b) and since NAs have been of scientific interest, identification of the individual compounds or even the compound classes has been fraught with difficulties. Not until pioneering work using two dimensional gas chromatography was any positive identification made (Rowland et al., 2011 a-d).

This causes a problem in understanding the aquatic toxicology of the petroleum acids; that they have an acutely toxic affect is beyond doubt, but just how toxic are they; which, of the many compounds within the complex mixture, cause the toxicity; and is there anything else within the OSPW or even the petroleum acids that could cause similar effects? Are potentially toxic components of the OSPW being ignored because NAs are deemed to be, oftentimes, the only toxic component of note (Nero et al., 2006; Young et al., 2008).

It is quite often the case that researchers who assay the OSPW (not just the acid extracts) conclude that OSPW is toxic and the toxicity is due to naphthenic acids because OSPW contains naphthenic acids. However it is well known that OSPW

contains other potentially toxic components (Allen, 2008; Hrudey et al., 2010) so how is a distinction of toxic effects made?

A way of assessing the actual toxicity of petroleum acids would be to assess their toxicity as individual components. A few authors have attempted this approach (i.e. Frank et al., 2010) but the because of the lack of positively identified compounds the assays were performed on so called ‘surrogate’ naphthenic acids, which were postulated to exist within the OSPW by Brient et al., (1995) (and others). However, the results of these assays showed that NAs were either moderately toxic, compared to other non acid components, or completely non-toxic. Not much can be inferred from these results as only a small number of acids were assayed and quite often research was not followed up, with alternative toxicity assays preferentially performed on individual ‘Z’ groups, distilled fractions, or whole mixtures (Frank et al., 2008; Kavanagh et al., 2011).

Assessment of actual individual components could lead to the knowledge of which acids (or structural classes) are most toxic, whether there is some sort of cut off (i.e. solubility) and whether it is indeed the NAs that are the most toxic components or whether it is the other compounds of concern that create the toxic affects shown by numerous assays (e.g. Kelly et al., 2009; West et al., 2011).

In order to identify individual components an advance in analytical characterisation methods is required. Recent work by Rowland et al., (2011 a-e) was able to set the groundwork to numerous individual toxicity assays by positively identifying numerous compounds (such as aromatic and adamantane type acids) within the OSPW and within a commercial naphthenic acid mixture (Chapter 2, this work; Rowland et al., 2011 a-e). The compounds were identified through use of first principal mass

spectral analysis (to tentatively identify compounds) and use of authentic standards to match both mass spectra and two dimensional retention times.

Herein lay a problem, the identified acids quite often did not match up to the acids postulated by Brient and most research papers since 1995, which meant that some previous research was rendered ineffectual because testing had occurred on compounds that are not present. However (in the current study at least) it also meant that toxicity assays were performed on a number of individual acids for the first time, and that the actual toxicity of petroleum acids could be elucidated.

Speculation also abounds about the toxic ‘mode of action’ of NAs with many authors postulating that NAs act in a baseline (or narcosis) mode of action (MOA) which occurs when the toxicant does not gain access to the cell but interferes with the cell membrane (Frank et al., 2010). Narcosis is a non specific MOA where the compound of interests permeates the cells lipid bilayer and ultimately disrupts the function of the membrane (fluidity, surface tension and thickness) and can eventually lead to the cells death. Hydrophobic compounds with a molecular weight of <1000 Daltons are able to permeate the membrane of a cell and as most (if not all) NAs have a molecular weight of <1000 Daltons it is expected that NAs act through this mode of action (Frank et al., 2009 plus references therein). Being able to identify and assay individual compounds could also lead to a confirmation of this MOA as after individual toxicities are assessed an assay of a mixtures of known compounds can be carried out (Chapter 4).

3.1.1. Toxicity Assays

In the current study initial toxicology on the Microtox™ assays were planned to be basic screening tests, designed to identify the toxic components for further toxicology testing. At this stage a number of carefully chosen, but essentially surrogate acids were tested using authentic commercial standards and ‘in house’ synthesised compounds from previous studies (e.g. Smith, 2006). The groups of assayed acids were *n*-acids, methyl branched *n*-acids, tricyclic acids (Section 3.3.1) isoprenoid acids, monocyclic acids, branched monocyclic acids, decalin acids and mono aromatic acids (Section 3.3.2).

The Microtox™ assay is a proven method to assess acute toxicity with many tests on NAs and other toxicants having been done (e.g. Frank et al., 2009; Altenburger et al., 2000). As is mentioned in Chapter 1, the assay records the reduction in light output from the bioluminescent marine bacterium *Vibrio fisheri.* There is a direct correlation between toxic effect and bioluminescence reduction.

The assay has a pH range of 6-8; any testing outside of this range would show up the stress on the bacterium from the pH rather than the toxicant. Which, in some ways, makes it difficult to directly asses the toxicity of the NAs or OSPW as the oil sands tailing ponds have an average pH of 9.5, however the Athabasca river which flows next to the oil sands development has a pH of 7.5, which is within the Microtox™ range, and as testing should be relevant to the environment at risk this is the pH at which the NAs were assayed.

The Microtox™ assay method was taken from the instruction manual with adjustments made by reference to relative literature. However, as is often the case, methods sections are often brief and sporadically helpful so a new method was

developed for the preparation of these acids. Literature was referred to so that the testing occurred at an environmentally relevant pH (Section 3.2).

Once the characterisation and identification of the acids was underway more compounds were added to the test schedule (Table 1.1), however a number of these were too insoluble to assay, often leaving a large amount of white precipitate and on a few occasions forming a precipitate 'plug'.

As each compound had an essentially unknown toxicity Log K_{ow}, solubility and predictive toxicology was used to elucidate whether the NA in question was made to a 200 mg L^{-1} solution, a 10 mg L^{-1} solution or points in between. The programme used to gain this information was the USENA in house predictive programme ECOSAR.

3.1.2 Predictive Toxicity

3.1.2.1 ECOSAR Model

ECOSAR is a Quantitive Structure Activity Relationship (QSAR) based model used by the United States Environmental Protection Agency to assess chemical substances under the Toxic Substances Control Act. It has been ranked as amongst the best QSAR effect based models (e.g. Frank et al., 2010). By use of the Simplified Molecular Input Line Entry System (SMILES) the ECOSAR programme is able to estimate the toxicity of a given compound to a range of organisms (Fish, Daphnid, Algae) and endpoints (96 hr and 48 hr LC_{50}s) through estimation of the Log K_{ow} and water solubility (Table in Appendix A). This programme was primarily used to assess what the concentrations of NAs should be for effective testing on the Microtox™ assay and for a comparison between the actual and predictive toxicity data. Whilst all of the 'candidate' NAs were assessed via the ECOSAR model, it became apparent

that not all of them would be assayed on the Microtox™ test. This primarily is due to solubility issues, but in many cases it was because it was apparent that they either do not exist with the complex mixture or they have yet to be positively identified. Out of the 145 acids on the list <70 were attempted on the Microtox™ assay and of these <45 produced results that can be utilised. Some NAs were assayed before positive identification and, as yet, are still not shown to be components of the complex mixture. These results will still be discussed here, even though they have little relevance to the current, overall, study.

3.1.2.2 ADMET Model

ADMET predictor, a commercially available programme, was able to be used on a trial for three months. For this reason the isoprenoid, decalin and adamantane acids are not represented in this section, as these were assayed with the Microtox™ after the trial period ended.

ADMET is primarily used by pharmaceutical companies to model whether a molecules structure will have a number of adverse effects on human health, such as liver effects or mutagenicity; however at least two parameters deal with environmental effects. ADMET models effects on the freshwater fish *Pimephales promelas* (Fathead Minnow) (naming authority: *Rafinesque, 1820*).and the ciliate *Tetrahymena pyriformis* (naming authority: unknown (AADC, 2012)). Comparisons were performed on both the modelled data from *P. promelas* and *T. pyriformis* and the Microtox™ assay data (Figure 3.23 and 3.24).

3.2. Materials and Methods

3.2.1 Materials

Solvents were purchased from Rathburn (Scotland, UK) and Fisher Scientific (Loughborough, UK). Authentic acids (including HCL and NaOH) were purchased from Sigma Aldrich (Dorset, UK) (unless where specified below). Titration was carried out using an Metler Toledo FiveEasy pH meter fitted with a micro electrode. The pH meter was calibrated to pH 4.01 and pH 7 before use on a daily basis as only three NAs could be titrated and assayed per day.

Alkylphenylalkanoate and *cis/trans* alkylcyclohexylalkanoate (alkyl=methyl to hexyl, nonyl; alkanoate= ethanoate and butanoate) acids were synthesised by a route based on the Kindler modification of the Willgerodt reaction (Carmack and DeTar, 1946). Other acids were obtained by Freidel-Crafts or Willgerodt chemistry (Gilman and Meals, 1943). Straight chain and methyl branched, phytanic, citronellic, adamantane-1-carboxylic, adamantane-1-ethanoic and 3,5-dimethyl-adamantane-1-carboxylic acids were purchased from Sigma (U.K.) with stated purities ≥97%. Decalin carboxylic, decalin ethanoic and decalin propanoic acids were synthesised from the aromatic analogues by hydrogenation (Ref; Chapter 2). The 2,6-dimethylheptanoic and 2,6,10-trimethylundecanoic acids were synthesised for previous studies and 3,7-dimethyloctanoic acid was obtained by hydrogenation of citronellic acid (PtO_2, 1 bar. H_2). Purity of methyl esters of synthetic acids was assayed by gas chromatography – mass spectrometry and was generally ≥99%.

All glassware was soaked in Decon90 for 24 hours before being rinsed in de-ionised water and dried at 110^{o}C for 24 hours. Vials were rinsed in hexane and MeOH before use and dried under a stream of N_2.

3.2.2 Methods

3.2.2.1. Microtox™ (*Vibrio fischeri*) Bioluminescence assay

Synthesised and commercially available acids were carefully weighed on an Oxford five figure balance and placed into pre weighed and pre rinsed 7 mL vials. The acids (maximum 20 mg) were subsequently dissolved in 1 or 2 mL of 1M NaOH and mixed on an autovortex mixer (Stuart Scientific) until completely dissolved. These solutions were then pH adjusted by drop-wise titration with a pasteur pipette with 1, 0.1 and 0.01M HCL until a pH of between 6 and 8 was achieved. The amount of HCL/NaOH added to the solution by the titration was then calculated (on average 0.04 mL per drop) and a calculated amount was added to 10.0 mL of Microtox™ diluent which was then agitated by an autovortex mixer and titrated using 0.01M HCL/NaOH until a pH of 7.5 ± 0.1 was achieved. The concentrations of these solutions ranged between 5 and 200 mg L^{-1} (± 2%) depending on predicted solubility and toxicity. The acids tested were initially screened on the Microtox™ M500 analyser (SDI Europe) using the 45% basic (15 minute) test as a toxicity screening method.

Briefly: Microtox™ glass cuvettes were placed in the M500 analyser and an amount of diluent was added (either 1000 µL or 500 µL depending on position in analyser). 2500 µL of acid solution was then added and osmotically adjusted, this was mixed and an amount was discarded before a 2x serial dilution was carried out. The subsequent test was performed (in triplicate) according to Microtox™ protocols. Phenol was tested as a positive control and found to be within the parameters set by Microtox™ (viz: IC_{50} between 13 and 26 mg L^{-1}).

3.2.2.2 Qualitative Structural Activity Relationships (QSARs)

The ECOSAR QSAR was utilised by converting the structures of the compounds of interest into the SMILES format and uploading into the software. Predicted physiochemical parameters (e.g. Log K_{ow} , solubility) were recorded as was the predicted toxicity to *Daphnia magna* (LC_{50}, 48 hour test), *D. Magna* was chosen as previous research by Frank et al., (2010) indicated a correlation between these predicted results and the observed toxicity recorded by the Microtox™ assay.

Admet was used by simply uploading an Excel™ file into the Admet database and recording the predicted results for both *P. promelas (*LC_{50}) and *T. pyriformis* (IGC_{50}). Other parameters such as pKa were also recorded as were many other potential toxic effects. These other effects are discussed in Scarlett et al., (2012).

3.3 Results and Discussion

In order to assess the toxicity of the individual compounds it is necessary to analyse them in some sort of logical order. With this in mind the NAs were assessed within compound classes. These were straight chain *n*-acids; methyl branched *n*-acids, isoprenoid type acids, monocyclic, branched monocyclic, bicyclic, tricyclic (the adamantane acids) and mono aromatic. Branched *n*-acids (such as butyl octanoic acid) were also assessed but they have yet to be identified in either the OSPW or the commercial naphthenic acid mixture. Results are displayed as IC_{50}s (in this case the concentration required to produce a 50% decrease in bioluminescence to the bacterium *Vibrio fisheri*). Because the pKa of these petroleum acids at the assayed pH the IC_{50} values will pertain to free acids and/or carboxylate ions. IC_{20} and IC_{10} (20% decrease and 10% decrease in bioluminescence respectively) values are available in the supplementary material. IC values are displayed in mM (rather than the more common mg L^{-1}) for the individual acid assays. This is because mM concentrations takes into account the size of the assayed compound and cellular effects can be more easily extrapolated. Where the complex acid mixtures have been assayed (e.g. Figure 3.1) concentrations are shown in mg L^{-1} as an mM concentration would be based on an average carbon number and as not enough is known about the makeup of these mixtures this could be misleading.

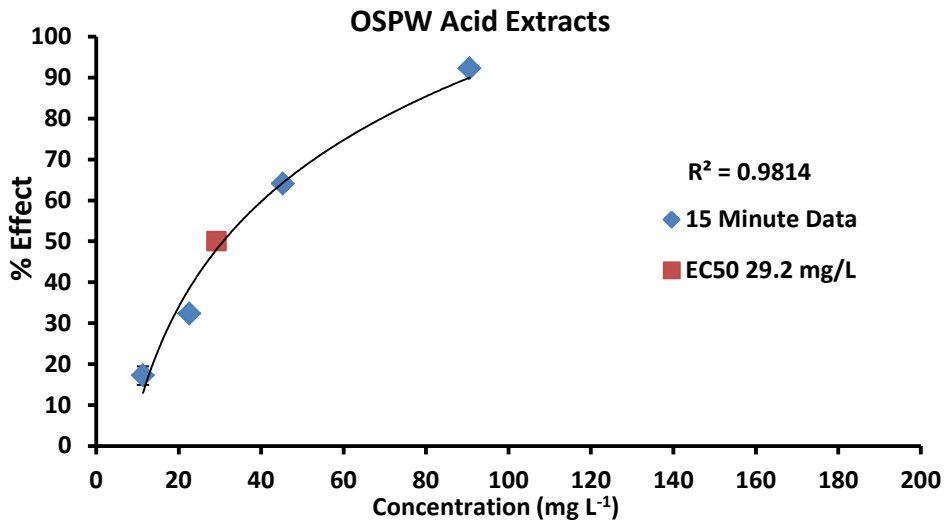

Figure 3.1. IC_{50} of OSPW acid extracts assayed with the Microtox 15 minute 45% basic test

The IC_{50} for the OSPW acid extracts (Figure 3.1) was comparable to other published IC_{50}s on the Microtox™ and other assays (e.g. Frank et al., 2008) but without the knowledge of what makes up the mixture it is difficult to elucidate if there are particular compound classes which dominate the toxicity of the mixtures or whether compound classes act in an equally toxic mode of action. Knowledge of the acid groups which make up these complex mixture can help with determining where the toxicity lies within the mixture and a targeted approached towards removing these compounds can then be utilises which could potentially lessen the overall toxicity.

3.3.1. Petroleum Acids in Oils Sands Process Affected Waters

NAs discussed in this section exist in both the OSPW and the commercial petroleum derived mixture.

3.3.1.1. Straight chain n-acids

As can be seen in Table 3.1 the toxicity of n-acids ranges from 0.7 mM – 0.02 mM, increasing in toxicity with molecular weight (or carbon number). Standard deviations and standard errors were relatively small (as is shown in Figure 3.1). Testing was halted at the C_{13} acid as tridecanoic acid exhibited a solubility cut off and was unable to be assayed.

Table 3.1. *n*-acids assayed by the Microtox™ bioluminescence test

Name	C:N	IC_{50} (mM)	St Dev (mM)	St Error (mM)
Hexanoic	6	0.70	0.065	0.038
Octanoic	8	0.38	0.022	0.013
Nonanoic	9	0.19	0.019	0.011
Decanoic	10	0.12	0.015	0.008
Undecanoic	11	0.04	0.009	0.005
Dodecanoic	12	0.02	0.004	0.002

* C:N is carbon number; mM is millimolar

The average toxicity of the C_6-C_{12} *n*-acids is 0.24 mM (S.D ± 0.25) with a range of 0.68 mM and the median of 0.155 mM, lying between the C_9 and C_{10}. As a comparison a C_9 alkyl-phenol present in the Merichem commercial mixture (West et al., 2011) was assayed in house at 0.00012 mM (Jones., unpublished data), and at a reported value of 0.00007 mM (Choi et al., 2004) a ~2000x increase in toxicity and whilst alkyl-phenols are reported at ca. <0.3 mg L^{-1} (compared to 20-120 mg L^{-1} for NAs) (Hargeshiemer et al., 1984) in OSPW their relative toxicity is likely to be far

higher, which leads to the question just what is causing the acute toxicity shown by these largely unresolved mixtures?

Figure 3.2 shows the toxicity vs. carbon number data plotted as a scatter chart. It can be seen that there is an excellent relationship between the two parameters with an R^2 of 0.9949. The P value of the trend line was calculated by using probability tables available in Fisher and Yates (1963) and shows that the line is statistically relevant with a value of <0.001.

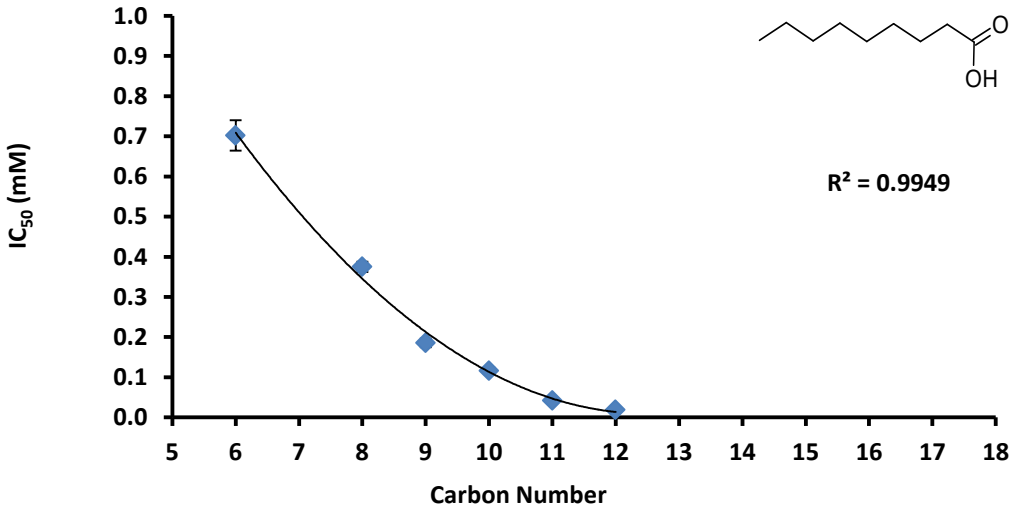

Figure 3.2. Measured IC_{50} values (± standard error (Table 3.1), n=3) for the toxicity of individual n-carboxylic acids to Vibrio fischeri (Microtox™ assay). Where error bars are not apparent the error was smaller than the symbol. R^2 value represents the goodness of fit of the polynomial trend lines. Error bars equal 1x standard error.

A more in-depth statistical test using the Statgraphics statistical programme utilising the individual IC_{50} values from each *n*=3 assay showed that there was a statistical difference when using a Student-Newman-Keuls multiple comparison test between all tested acids apart from undecanoic and dodecanoic acids. However this statistical

analysis failed a Cochran's Variance test and the standard deviations had a more that 3x difference between the largest and the smallest. Because this invalidates most of the results the data was log transformed. The log transformation reduced the size of the standard deviations and the Cochran's variance test was passed with a P value of 0.348, which shows that there is no statistical difference between the standard deviations. The ANOVA P value is <0.0001 and a Student-Newman-Keuls multiple comparison test showed that there were no homogenous groups.

It is noteworthy that the standard error of the hexanoic acid (lowest toxicity) is larger than the other assayed acids. This larger standard error which was apparent when assaying the least toxic compounds was noticed during other assays and is assumed to be a limitation of the Microtox™ assay and could potentially be the reason for the failure of the statistical test on the non-transformed data.

The *n*-acid (so called straight chain or normal) compound class was identified in both the OSPW acid extracts and within the petroleum derived commercial mixtures. However within the OSPW positive identification has occurred on a range of C_9 (nonanoic) to C_{15} (pentadecanoic) which means that neither the C_6 or C_8 assayed acids are postulated to be present, though the C_8 acid has been identified in the commercial mixture.

The extent of these acids within the OSPW is relatively low compared to other compound classes and appears to be dominated with even numbered chains which suggest biogenic origins (S.J. Rowland., 2012 personal communication).

The C_{12} acid (dodecanoic) had the highest reportable toxicity (0.019 ± 0.002), acids with higher carbon numbers (C_{13-19}) that were attempted on the Microtox™ were too insoluble to assay.

Previous work by Frank et al., (2010) reported mM values of 19.1 and 0.33 for hexanoic and decanoic acid respectively however a direct comparison of these results is not able to be performed as preparation methods for the acids before assaying for toxicity are not fully reported.

3.3.1.2. Mono methyl branched n-acids

Table 3.2 shows an IC_{50} range of 0.48-0.012 making the methyl branched moieties of the n-acid compound class slightly more toxic that the n-acid straight chain class. The average toxicity for this class of compounds is 0.185 (±0.180 SD) mM the standard deviation being large because of the extent of the range of toxicity. Toxicity testing included a C_{13} acid (more soluble than the n-acid counterpart) but not a C_{14} acid, where solubility limits were apparent. The median toxicity is 0.143 mM, which matches the measured value for the C_{10} 2-methylnonanoic acid. It can be seen that the 2-methyl and 4-methylnonanoic acids have slightly different IC_{50} values.

The Student-Newman-Keuls multiple comparison test on these two compounds show a statistical difference, but when analysing the median values through a box and whisker plot it shows that the medians (at least) are not statistically different. There is a 5% chance though that the Student-Newman-Keuls test will show a significant difference where, in fact, there is none. An analysis of variance (ANOVA) calculated a P value of <0.0001 showing a difference between the means of the tested acid and a Cochran's variance check had a P value of >0.05 showing no difference between the standard deviations.

Table 3.2. Mono-methyl branched *n*-acids assayed by the Microtox™ bioluminescence test

Name	C:N	IC_{50} (mM)	St Dev (mM)	St Error (mM)
4-Methyloctanoic acid	9	0.483	0.0267	0.0154
2-Methylnonanoic acid	10	0.143	0.0113	0.0065
4-Methylnonanoic acid	10	0.201	0.0284	0.0164
7-Methyldecanoic acid	11	0.085	0.027	0.016
4-Methyldodecanoic acid	13	0.012	0.001	0.001

Figure 3.3 shows an excellent relationship between carbon number and toxicity (R^2 0.9988; $P<0.01$). The 2-methylnonanoic acid is not shown as it is a C_{10} acid (as is 4-methylnonanoic acid) and it was felt that a like for like comparison (there are three other 4-methyl compounds present) would be better and there was not a large enough difference between the IC_{50}s of the two C_{10} compounds for a significant comparison to be shown on the chart. Addition of the other C_{10} compound changes the goodness of fit to an R^2 of 0.9879 (P value <0.01).

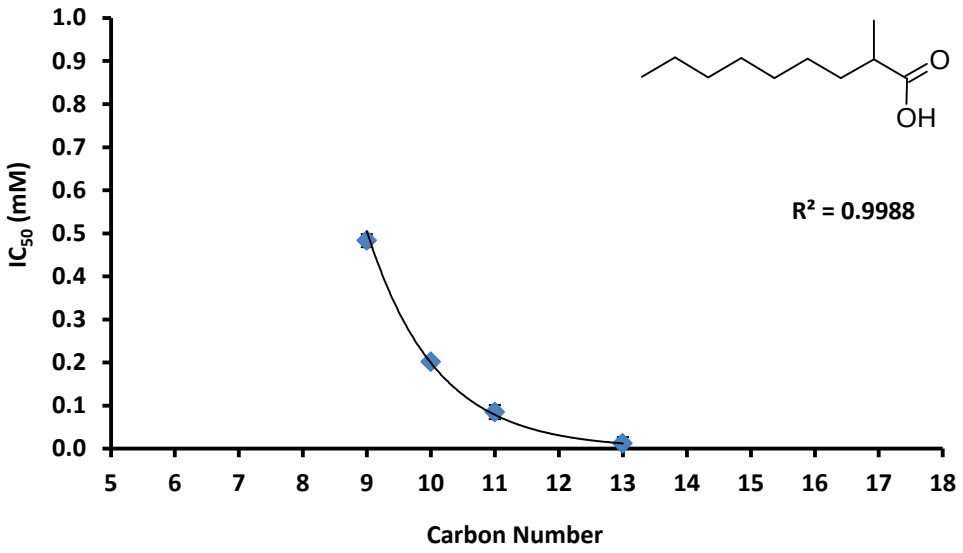

Figure 3.3. Measured IC_{50} values (± standard error (Table 3.2), n=3) for the toxicity of individual methyl branched n-carboxylic acids to Vibrio fischeri (Microtox™ assay). Where error bars are not apparent the error was smaller than the symbol. R^2 value represents the goodness of fit of the polynomial trend lines. Error bars equal 1x standard error.

The slight difference in toxicity between the two C_{10} compounds raises the question about structural based toxicity; does the toxicity change with a differential placement of the methyl group? As yet this question remains largely unanswered for this particular class of acids due to the lack of authentic standards and time constraints placed upon the synthesis of said compounds.

Monomethyl *n*-acids were found with similar carbon numbers and in similar proportions to the n-acids class of compound within the OSPW, however a far more complex group was present in the petroleum derived commercial mixture. The C_{11}-C_{13} acids were the most toxic, again following the trend seen in Figure 3.2, where the higher molecular weight acids are of most concern. However a solubility limit was reached when assessing a C_{14} acid (methyl tridecanoic acid).

3.3.1.3 Tricyclic Acids

Tricyclic acids were amongst the most abundant compound class in the OSPW, with a few structures also present in the petroleum derived acids. Interestingly the tricyclic class of acids indentified were the so-called nano-diamond adamantane type acids.

In previous toxicological screening tests on the Microtox™ the test concentration was limited to ~90 mg L^{-1} as a concentration (as this is 45% of 200 mg L^{-1} and lies within the concentrations found within the tailing ponds) outside of this value was deemed non-environmentally relevant and any acid which did not exhibit toxicity at a value of 90 mg L^{-1} was deemed non toxic. However, in the case of adamantanes when toxicology testing at 90 mg L^{-1} did not produce an IC_{50} it was decided to push the concentrations up to 400 mg L^{-1} (180 mg L^{-1} on the Microtox test) to get a result. This was primarily due to the fact that adamantanes are very abundant within the OSPW so a determining measured (rather than predicted or extrapolated value) was important.

Table 3.3 shows the IC_{50}s for all the concentrations assayed, including those that were extrapolated (marked with an asterisk). Testing was originally carried out at 200 mg L^{-1} on both the adamantane-1-carboxylic acid, 3-ethyladamantane-1-carboxylic acid and 3-methyladamantane-1-ethanoic acid. These acids exhibited reluctance to go into solution at first but through use of a vortex mixer they were eventually persuaded to solubilise. However both assayed acids were relatively non toxic at this concentration with extrapolated values of 0.848 mM (152 mg L^{-1}) 0.46 mM (97.6 mg L^{-1}) and 0.76 mM (159 mg L^{-1}) respectively (Table 3.3) Unfortunately the 3-ethyladamantane carboxylic acid did not solubilise very easily above 200 mg L^{-1} so it was decided to concentrate on the adamantane-1-carboxylic acid. It wasn't until a

concentration of 400 mg L^{-1} (180 mg L^{-1}) on the Microtox™ was assayed that a non extrapolated result was realised (0.784 mM; 141.3 mg L^{-1} Table 3.3).

Table 3.3. Tricyclic adamantane acids assayed with the Microtox™

Name	Concentration (mg L^{-1})	C:N	IC_{50} (mM)	St Dev (mM)	St Error (mM)
Adamantane-1-CA	200* (90)	11	0.848	0.079	0.056
Adamantane-1-CA	300* (135)	11	0.797	0.086	0.012
Adamantane-1-CA	400 (180)	11	0.784	0.185	0.079
Adamantane-1-EA	350 (158)	12	0.667	0.020	0.011
3-methyladamantane-1-EA	200* (90)	13	0.764	0.187	0.108
3-methyladamantane-1-EA	300* (135)	13	0.885	0.188	0.109
3-ethyladamantane-1-CA	200* (90)	13	0.468	0.008	0.005
3,5-dimethyladamantane-1-CA	300 (135)	13	0.565	0.0	0.028
3,5-dimethyladamantane-1-EA	300 (135)		0.33	0.0	0.022

CA is carboxylic acid: EA is ethanoic acid: * denotes extrapolated results. Numbers in brackets are 45% of the starting concentration and is the concentration assayed via the Microtox™.

As the 300 mg L^{-1} extrapolated IC50 (135 mg L^{-1} on Microtox™) was quite close to the top concentration of 141 mg L^{-1} it was decided that further testing on other adamantanes would start at this concentration, if they were soluble enough. Further testing was done on the 3-methyl moiety but the 300 mg L^{-1} solution still exhibited an extrapolated IC_{50} (0.0885; 184 mg L^{-1}), unfortunately this compound was not soluble enough to test at any further concentrations.

Adamantane-1-ethanoic acid did produce a result at 350 mg L^{-1} (158 mg L^{-1} on the Microtox™). An IC_{50} of 0.667 mM (± 0.011) (129 mg L^{-1}) was recorded. Both the dimethyl moieties (carboxylic and ethanoic) also recorded results at 0.565 mM (± 0.049) (117 mg L^{-1}) and 0.337 mM (74 mg L^{-1}) (± 0.022) respectively (Figure 3.4).

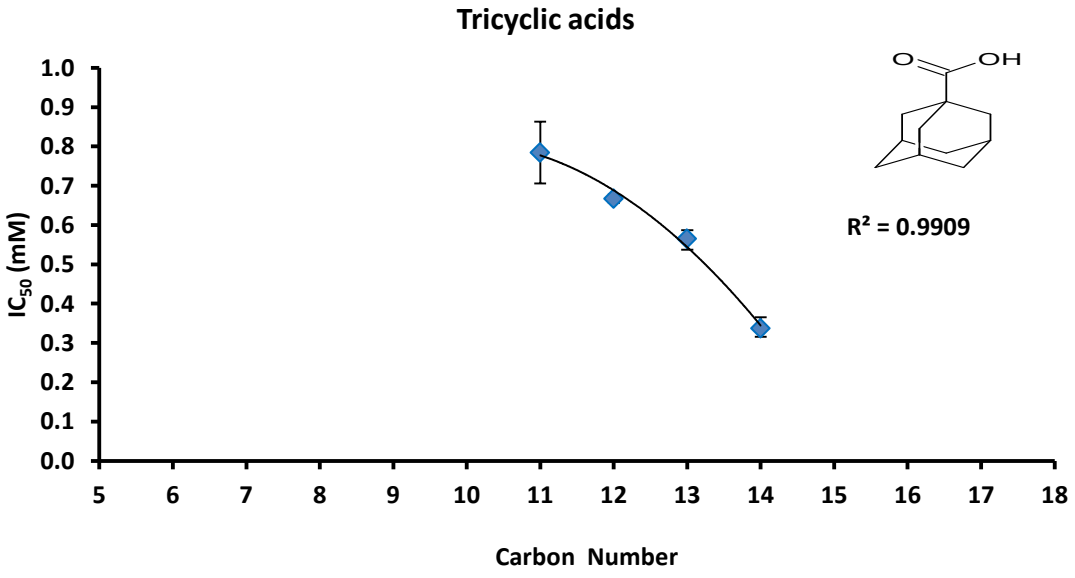

Figure 3.4. Measured IC_{50} values (± standard error (Table 3.3), n=3) for the toxicity of individual tricyclic carboxylic acids (Figure 2.95) to Vibrio fischeri (Microtox™ assay). Where error bars are not apparent the error was smaller than the symbol. R^2 and represents the goodness of fit of the polynomial trend lines. Error bars equal 1x standard error.

Interestingly the profile of the polynomial trend line (whilst statistically significant) was different to the extrapolated trend for the other tested acids. The trend for the adamantanes did not approach asymptotes, as did the other assayed acids, however, as Figure 3.5 shows, a C_{15} adamantane might exhibit similar toxicity to a corresponding C_{15} acid.

Figure 3.5 also shows that compared to the average toxicity of the other tested acids adamantanes were in general far less toxic and if NAs act through a narcosis (or baseline) toxicity do adamantanes act in a 'less than' narcosis mode of action? For instance a C_{14} adamantane displays similar toxicity to a C_9 corresponding acid (0.36 mM ± 0.05) whist a C_{14} corresponding acid has an average IC_{50} of 0.016 mM (± 0.004).

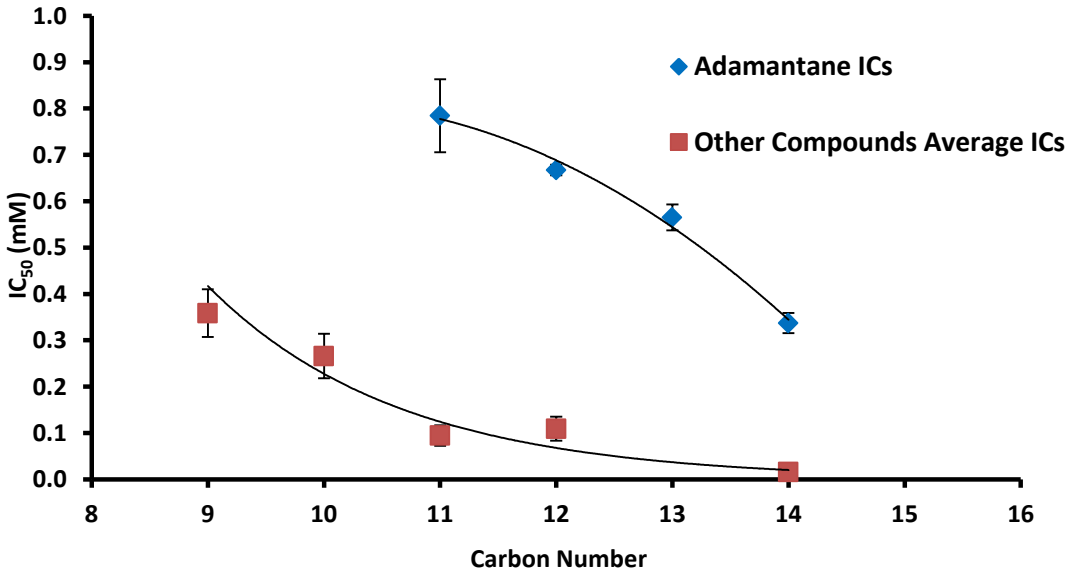

Figure 3.5. Comparison of adamantane IC_{50}s and the average IC_{50}s of acids with corresponding carbon numbers**.**

This lack of toxicity could be due to the adamantanes ‘cage’ type structure which may preclude an interaction with the cellular membrane until a substituted group comes into contact (e.g. carboxylate group, methyl group). Which could lessen the toxicity of the adamantanes compared to the more usual planar structures exhibited by the other tested acids.

When comparing the adamantanes within a statistical test it was found that the standard deviations of each assayed acid had a greater than 3x difference. A follow up Cochran’s variance test produced a P value of <0.05, showing that the standard deviations were statistically different. The data was log transformed and the test was performed again. Although the standard deviations were shown to still have a greater than 3x difference this time the variance test was passed with a P value of 0.08. A subsequent ANOVA had a P value of <0.0001, showing a statistical difference between the means of each compound and the Student-Newman-Keuls multiple comparison test showed that Adamantane-1-carboxylic acid, Adamantane-1-ethanoic acid and 3,5-dimethyladamantane-1-carboxylic acid were all homogenously group with only 3,5-dimethyladamantane-1-ethanoic exhibiting a difference.

3.3.2. Petroleum Acids in Commercial Mixtures of Naphthenic Acids

Acids assayed in this section have been identified in a commercial mixture of petroleum derived acids and although some are postulated to exist in the OSPW acid extracts they have yet to be discovered.

3.3.2.1. Isoprenoid Type Acids

The isoprenoid acids exist in abundance in the commercial mixture because of microbial oxidation of parent type hydrocarbons which are very common in petroleum (e.g. Seifert, 1975); however they have yet to be identified in the OSPW.

Table 3.4. Isoprenoid acids assayed on the Microtox™ assay

Name	C:N	IC_{50} (mM)	St Dev (mM)	St Error (mM)
2,6-dimethylheptanoic acid	9	0.241	0.029	0.017
3,7-dimethyloctanoic acid	10	0.058	0.0118	0.001
2,6,10-trimethylundecanoic acid	14	0.015	0.001	0.007

Only three acids were able to be assayed as none were commercially available (Table 3.4). The 2,6-dimethylheptanoic acid was available from a previous study (E, Teuton) and the 3,7-dimethyloctanoic acid was synthesised by hydrogenating citronellic acid on the H-Cube hydrogenator over a rhodium over carbon catalyst at 80 bar and 80^{o}C (Chapter 2). The trimethyl moiety was sourced from Professor G Dacremont at the University of Ghent. The commercially available C_{20} Phytanic acid (3,7,11,15-tetramethylhexadecanoic acid) was also attempted to be assayed however it was not soluble enough.

IC_{50}s ranged from 0.241 mM (± 0.017 SE) for the C_9 dimethylheptanoic acid to 0.015 mM (± 0.007 SE) for the trimethyl moiety. Interestingly there is a large gap in toxicity between the C_9 and C_{10} acid of 0.18 mM (Table 3.4; Figure 3.6).

Because there are only three points on Figure 3.6 the trend line is unlikely to be statistically significant (R^2 0.9115; P>0.1). Toxicological testing of more isoprenoid acids may have an effect on this non-significant trend, but as yet, this remains to be seen. A Student-Newman-Keuls multiple comparison test however shows a statistical difference between the means of the three individual tests on each acid and an ANOVA test produced a P value of >0.0001. A Cochran's test showed that there was no difference in the standard deviations (at a 95% confidence limit).

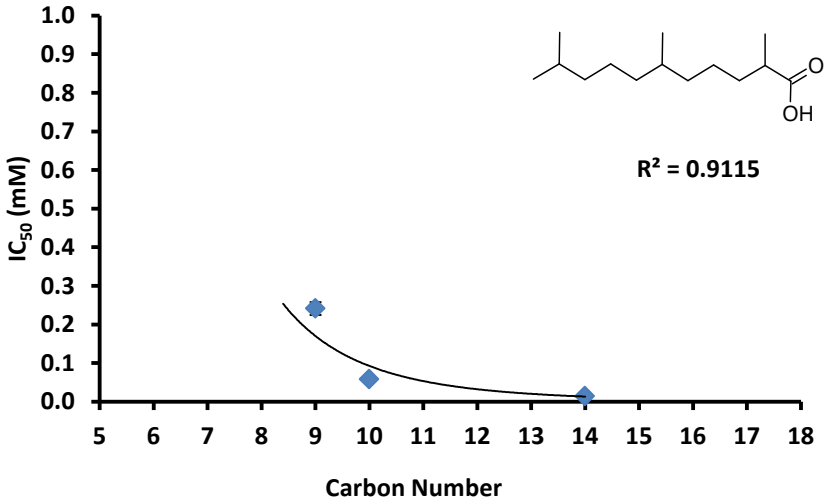

Figure 3.6. Measured IC_{50} values (± standard error (Table 3.4), n=3) for the toxicity of individual isoprenoid carboxylic acids to Vibrio fischeri (Microtox™ assay). Where error bars are not apparent the error was smaller than the symbol. R^2 value represents the goodness of fit of the polynomial trend lines. Error bars equal 1x standard error.

3.3.2.2. Monocyclic acids

Monocyclic acids are present in the petroleum derived commercial mixtures. The toxicity ranged from a non toxic species (C_7 cyclohexylcarboxylic acid: 1.3 mM

extrapolated IC_{50}) to 0.04 mM (± 0.002 SE) (C_{12} cyclohexylhexanoic acid). Cyclohexylcarboxylic acid was not re-assayed as the IC_{50} lay outside of a self-imposed toxicity cut off of 1 mM and was not toxic at the highest concentration tested (90 mg L^{-1} on the Microtox™; 200 mg L^{-1} starting concentration).

Table 3.5. shows that the acids which had a toxic effect at range from a C_9 (0.41 mM ± 0.03 SE) to 0.04 mM (± 0.001 SE) for the C_{12} acid. No solubility limit was reached with this compound class as the cyclohexylhexanoic acid was the compound with the highest molecular weight that was available for testing. The carboxylic, propanoic, butanoic and pentanoic moieties were commercially available, whilst the hexanoic was synthesised in house via hydrogenation using both the Buchii Reaction Chamber and the H-Cube® hydrogenation system (Chapter 2).

Table 3.5. Monocyclic acids assayed with the Microtox™ test

Name	C:N	IC_{50} (mM)	St Dev (mM)	St Error (mM)
Cyclohexylcarboxylic acid	7	1.30*	0.61	0.43
Cyclohexylpropanoic acid	9	0.41	0.03	0.017
Cyclohexylbutanoic acid	10	0.12	0.012	0.007
Cyclohexylpentanoic acid	11	0.05	0.012	0.007
Cyclohexylhexanoic acid	12	0.04	0.002	0.001

* Indicates extrapolated data

Figure 3.7 shows a good correlation between the toxicity and molecular weight (or carbon number) (R^2 0.9091: P<0.02). The errors for the least toxic compound are again far larger than the more toxic compounds.

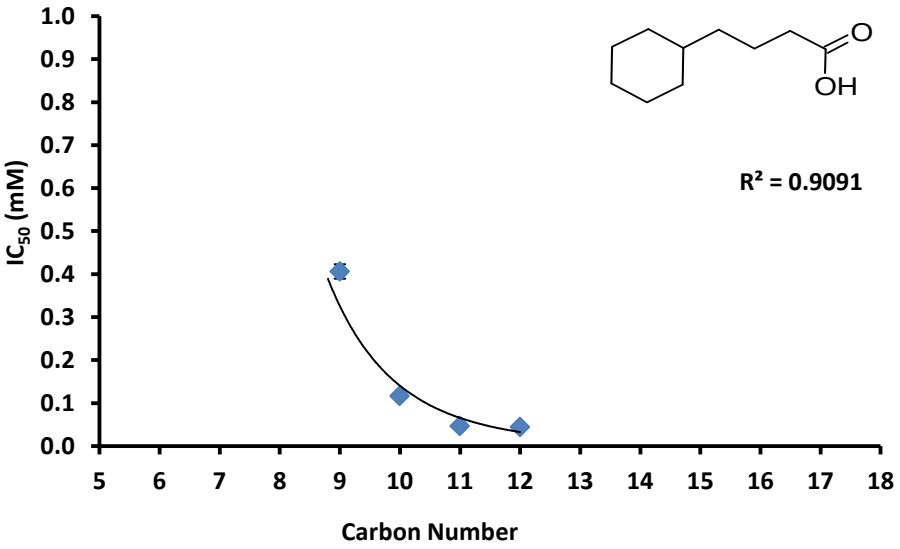

Figure 3.7. Measured IC_{50} values (± standard error (Table 3.5), n=3) for the toxicity of individual monocyclic acids to Vibrio fischeri (Microtox™ assay). Where error bars are not apparent the error was smaller than the symbol. R^2 value represents the goodness of fit of the polynomial trend lines. Error bars equal 1x standard error.

Statistical tests again showed that the standard deviations had a greater than 3x difference and the variance test failed so the data were log transformed however after log transformation the data still failed the variance test, so the data were transformed using square roots.

Although there was still a 3x difference in the standard deviations the Cochran's variance test was passed with a P value of 0.49, showing no statistical difference

in the standard deviations. An ANOVA test produced a P value of >0.0001 showing a difference in the means of the monocyclic acids. The Student-Newman-Keuls multiple comparison test showed that there were two homogenous groups within the ANOVA test, the pentylcyclohexyl moiety and the hexylcyclohexyl moiety. Interestingly the pentylcyclohexyl and the hexylcyclohexyl acids exhibit a similar toxicity (0.05 and 0.04 mM respectively).

3.3.2.3. Branched Monocyclic Acids

The branched type monocyclic are also present in the petroleum derived mixture of NAs. Tested acids ranged from the C_9 methylcyclohexyl ethanoic acid to a C_{14} hexylcyclohexyl ethanoic acid (Table 3.6) the IC_{50}s range from 0.34 mM (± 0.07 SE) to 0.012 mM (± 0.001 SE). Interestingly in this case the methyl branched C_9 moiety exhibits a slightly greater toxicity than the C_{10} ethyl branched moiety. This is counter to all the other available evidence as to the mode of toxicity and the correlation between carbon number and IC_{50}. As yet there is no clear reason for this anomaly and whilst it is possible that a single methyl group in the *para* position on a ring could cause greater toxicity than an equivalent ethyl group it is not very likely. It is more likely that an error occurred in the testing, it is for this reason that the methylcyclohexyl ethanoic acid has been left out of Figure 3.8.

Table 3.6. Branched monocyclic acids assayed on the Microtox™ test.

Name	C:N	IC_{50} (mM)	St Dev (mM)	St Error (mM)
4-methylcyclohexyl EA*	9	0.24	0.04	0.03
4-ethylcyclohexyl EA	10	0.34	0.07	0.04
4-n-propylcyclohexyl EA	11	0.20	0.02	0.01
4-n-butylcyclohexyl EA	12	0.160	0.010	0.006
4-n-pentylcyclohexyl EA	13	0.033	0.008	0.004
4-n-hexylcyclohexyl EA	14	0.012	0.001	0.0004

*EA is ethanoic acid

No solubility limit was reached with these compounds as the C_{14} was the largest compound available for testing. A C_{17} 4-n-nonylcyclohexyl ethanoic acid, synthesised in house, was attempted but was found to be too impure for any elucidation of solubility or toxicity and created a yellow coloured solution which would have interfered with the analysis of light output from the bioluminescent bacterium.

Figure 3.8 displays an good correlation between the C_{10}-C_{14} acids (R2 0.9738 $P<0.01$). The error bars on the lowest molecular weight, lowest toxicity compound are again larger than the error bars for the other (more toxic) compounds.

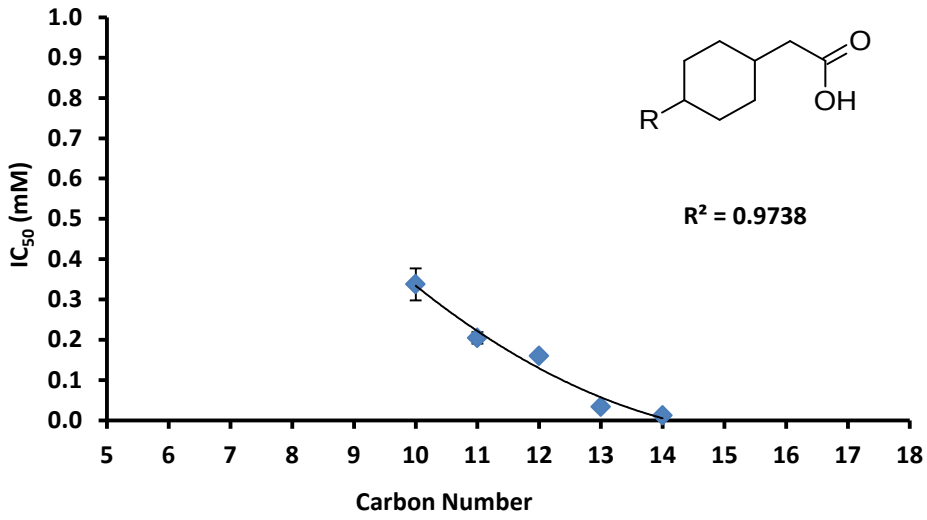

Figure 3.8. Measured IC_{50} values (± standard error (Table 3.6), n=3) for the toxicity of individual branched monocyclic acids to Vibrio fischeri (Microtox™ assay). Where error bars are not apparent the error was smaller than the symbol. R^2 value represents the goodness of fit of the polynomial trend lines. Error bars equal 1x standard error.

Data was log transformed after the Cochran's test was failed on the raw data. After transformation the standard deviations exhibited a 3x difference but the Cochran's test was passed with a P value of 0.354. An ANOVA produced a P value of <0.0001 and a Student-Newman-Keuls multiple comparison test showed that 4-n-propylcyclohexyl and 4-n-butylcyclohexyl ethanoic acid were homogenous groups with no difference between the means. There was no statistical difference in the median values of ethyl, n-propyl and n-butylcyclohexylethanoic acid.

3.3.2.4 Bicyclic acids

Bicyclic decalin (decahydronaphthalene) type acids have yet to be discovered in the OSPW however they are present within the petroleum derived mixtures. No solubility

limits were discovered as these compounds were all synthesised in house via the H-Cube hydrogenation system (Chapter 2). 4-methyl-decahydronaphthalene-1-carboxylic acid was not assayed because of the failure to create a pure compound (Chapter 2). Decahydronaphthalene-1-ethanoic acid was not assessed due to a lack of suitable quantities to assay.

Table 3.7. Bicyclic decalin type acids assayed on the Microtox™ assay.

Name	C:N	IC_{50} (mM)	St Dev (mM)	St Error (mM)
Decalin-1-CA*	11	0.359	0.043	0.025
Decalin-2-CA	11	0.218	0.027	0.016
Decalin-2-EA†	12	0.027	0.003	0.002
Decalin-1-PA‡	13	0.004	0.0002	0.0001

* Carboxylic acid: † Ethanoic acid: ‡ Propanoic acid

Toxicity ranged from the C_{11} decalin-1-carboxylic acid (0.359 mM ±0.02 SE) to the C_{13} 3-decalin-1-yl propanoic acid (0.004 mM ± 0.0001 SE) which was the most toxic of all the tested acids.

Decalin-1-carboxylic acid is not included in Figure 3.9 as it was felt to be more important to compare the two decalin-2 acids, and the inclusion of two C_{11} acids would lead to confusion as to which one was which.

Figure 3.8 shows an excellent correlation between the two parameters (R^2 0.9990 $P<0.02$) even though there are only three data points. It is again noticeable that the standard errors on the least toxic compound are larger than the other two displayed compounds.

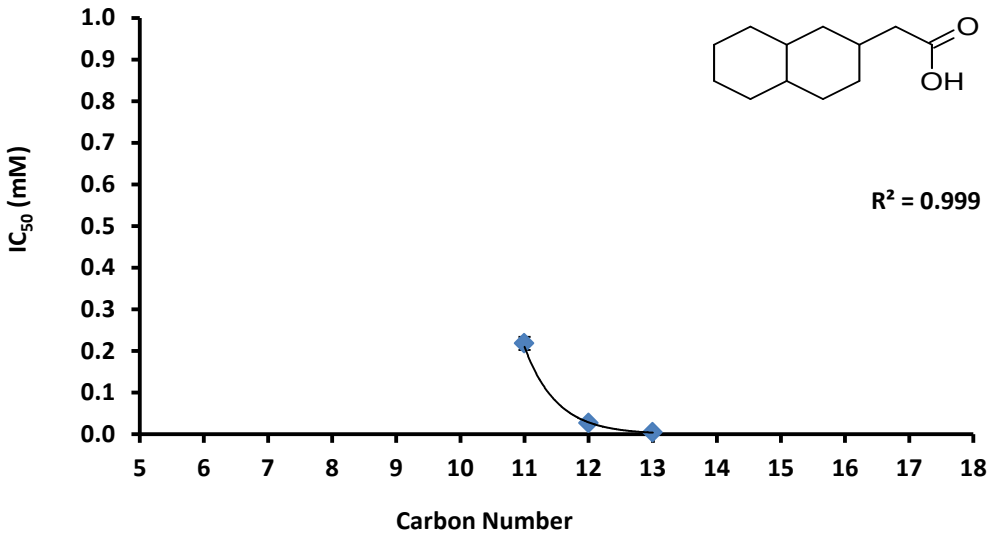

Figure 3.9. Measured IC_{50} values (± standard error (Table 3.7), n=3) for the toxicity of individual decalin acids to Vibrio fischeri (Microtox™ assay). Where error bars are not apparent the error was smaller than the symbol. R^2 value represents the goodness of fit of the polynomial trend lines. Error bars equal 1x standard error.

Decalin acids were also log transformed after the variance test was failed. Once log transformed the variance test had a P value of 0.82 showing no difference in the standard deviations and an ANOVA had a P value of <0.0001. A multiple comparison test showed no homogenous groups.

3.3.2.5 Monoaromatic Acids

The monoaromatic acids are present in the commercial mixture but have yet to be identified in the OSPW. A number of the acids were non-toxic at the imposed concentration cut off and were discarded from further testing (Table 3.8). Toxicity ranges from 0.39 mM (± 0.006 SE) for the C_{11} propylphenyl ethanoic acid to 0.023 mM (± 0.005 SE) for the C_{14} hexylphenylethaoic acid.

Table 3.8. Monoaromatic acids assayed on Microtox™ test

Name	C:N	IC_{50} (m	St Dev (r	St Error (
2-methylphenylethanoic acid	9	3.50*	2.74	1.58
3-methylphenylethanoic acid	9	1.65*	0.20	0.11
4-methylphenylethanoic acid (C)	9	1.93*	0.30	0.17
4-methylphenylethanoic acid (S)	9	2.40*	0.44	0.26
4-ethylphenylethanoic acid	10	0.214	0.015	0.009
4-n-propylphenylethanoic acid	11	0.394	0.011	0.006
4-n-butylphenylethaoic acid	12	0.250	0.038	0.022
4-n-pentylphenylethanoic acid	13	0.044	0.002	0.001
4-n-hexylphenylethanoic acid	14	0.023	0.008	0.005

*Indicates extrapolated data: (C) indicates commercial acid: (S) indicates synthesised acid

It is noticeable that the C_9 acid shows an apparent higher toxicity that the C_{10} and C_{11} acid, it is likely that this is due to an error in the testing regime and therefore has not been included in Figure 3.10. All of the methylphenylethanoic acids were considered to be non toxic as all the IC_{50}s were extrapolated after a 90 mg L^{-1} test on the Microtox™.

Figure 3.10 shows a good relationship between toxicity and molecular weight with an R^2 of 0.9473 ($P<0.02$). A C_{17} nonylphenyl ethanoic acid was found to be too insoluble to assay.

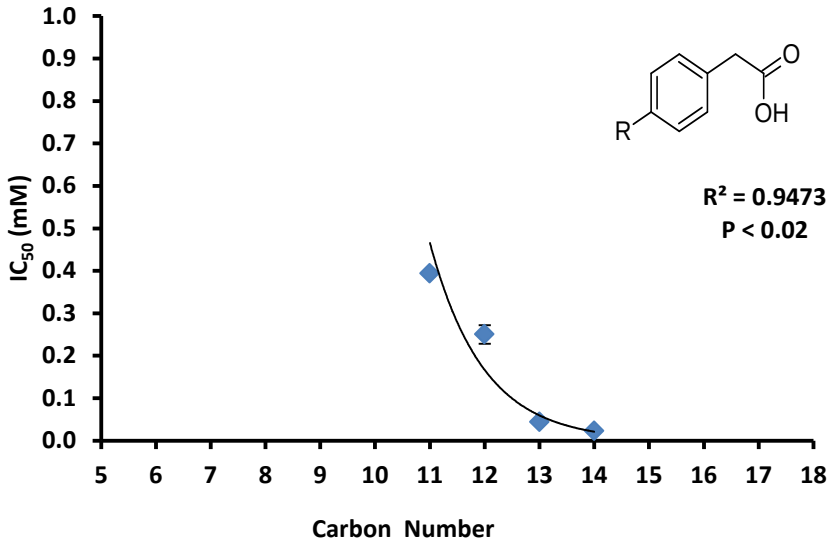

Figure 3.10. Measured IC_{50} values (± standard error (Table 3.8), n=3) for the toxicity of individual mono aromatic acids to Vibrio fischeri (Microtox™ assay). Where error bars are not apparent the error was smaller than the symbol. R^2 value represents the goodness of fit of the polynomial trend lines. Error bars equal 1x standard error.

Data was both log and square root transformed due to a failure of the Cochran's test on the un-transformed data. Log transformed data also failed but the square root transformed data exhibited a P value of 0.208 showing no statistical difference in the standard deviations. An ANOVA produced a P value of <0.0001 and a multiple comparison test confirmed that there were no homogenous groups. However the medians of hexylphenyl and pentylphenyl show no statistical difference.

3.3.3. Other Assayed Petroleum Acids

Other compounds were assayed for their toxicity, these included petroleum derived mixtures (Table 3.9; Figure 3.11); branched n-acids, and acids with either butyl side chains different to the straight chain (or '*n*') configuration or butanoic type acids

previously assayed on different toxicological tests (Smith et al., 2008; Smith., 2006).

3.3.3.1 Petroleum Derived Mixtures

Three petroleum derived acids were assayed at a concentration of 50 mg L^{-1}, because of the lack of knowledge of compounds within these mixtures the results are presented in mg L^{-1} and not mM as has been the case in the previous discussion.

A concentration of 50 mg L^{-1} was chosen as it was felt this was the best concentration to assess toxicity and to have the IC_{50} rest roughly in the middle of the trend as a 50 mg starting concentration would translate to 22.5 mg top concentration on the Microtox™ assay. This would mean that if the results were comparable with literature (10.9 mg L^{-1} on the Merichem mixture at least (Clemente et al., 2004)) then the IC_{50} would be lie the middle of the logarithmic trend.

Table 3.9 shows the IC_{50}s of the three tested mixtures. It can be seen that the Fluka mixture is the most toxic to the Microtox™ followed by the Merichem and the Acros. All of these mixtures have a greater toxicity than the OSPW acid extracts (29.2 mg L^{-1}; Figure 3.1).

Table 3.9. Petroleum derived commercial mixtures assayed by the Microtox™

Name	IC_{50} (mg L^{-1})	St Dev (mg L^{-1})	St Error (mg L^{-1})
Acros	24.76	10.93	6.32
Fluka	7.88	2.20	1.27
Merichem	11.78*	1.41	0.81

*Comparable to literature value of 10.9 mg L^{-1} (Clemente et al., 2004)

Both Fluka and Merichem have observed IC_{50}s that lie within the 22.5 mg L^{-1} limit however the Acros shows extrapolated data. In this case (as the trend is linear and not logarithmic) it was felt that an extrapolation was acceptable. It is also noticeable that there are only three points on the Acros plot. This was because the first point (2.8 mg L^{-1}) was consistently less than zero indicating a completely non toxic response at that concentration.

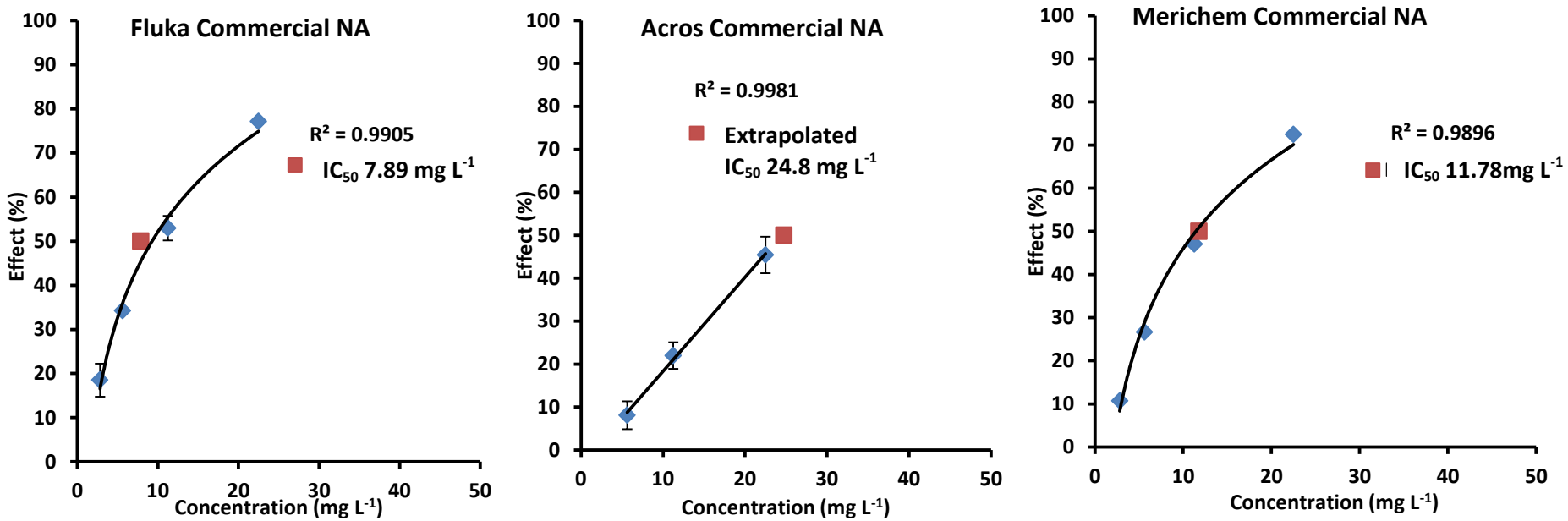

Figure 3.11. Measured IC_{50} values (± standard error (Table 3.9), n=3) for the toxicity of Petroleum derived commercial mixtures assayed to Vibrio fischeri (Microtox™ assay)**.** Where error bars are not apparent the error was smaller than the symbol. R^2 value represents the goodness of fit of the polynomial trend lines. Error bars equal 1x standard error.

3.3.3.2 Branched *n*-acids

Branched n-acids were assayed before the identification of compounds within the mixtures was available, but they were postulated to exist in either the OSPW or the petroleum derived mixtures. As yet none of these moieties has been identified in either mixture.

Only two of the tested acids exhibited toxicities that were not extrapolated from the logarithmic trend given by the Microtox™ assay software (Table 3.10) and in the case of 2-propylpentanoic acid only one result from the three repetitions was recorded by the software, due to a communication error between the software and the controlling laptop computer.

Table 3.10. Branched n-acids assayed on the Microtox™ test

Name	C:N	IC_{50} (mM)	St Dev (mM)	St Error (mM)
2-propylpentanoic acid	8	1.99*	-	-
4-ethyloctanoic acid	10	0.56*	0.0152	0.0091
2-butyloctanoic acid	12	0.15*	0.0221	0.0121
2-butyldecanoic acid	14	0.008	0.0013	0.00077
2-hexyldecanoic acid	16	0.008	0.0012	0.00074

* Indicates extrapolated data

Because only two results were measured no trend in the IC_{50}s can be elucidated and as the IC_{50}s and standard deviations are very similar it is likely that there is no significant difference between the means. A paired two tailed Students T-Test gives

a P value of 0.49 (>0.05) which shows no statistical difference between the means of the two samples.

3.3.3.3 Butyl Substituted Cyclohexyl Acids

Butylcyclohexyl ethanoic acids were tested across isomers to elucidate wether there was a differential effect dependant on the structure of the side chain. As table 3.11 shows the 'n-butyl' isomer is the most toxic (0.16 mM ± 0.006 SE), this is ~2x the toxicity of both the iso and tertiary isomer (which are statistically similar: P value 0.43 (paired two tailed Students T-Test))

Table 3.11. Butylcyclohexylethanoic acids assayed on the Microtox™ test

Name	C:N	IC_{50} (mM	St Dev (mM)	St Error (mM)
4-n-butylcyclohexylethanoic acid	12	0.151	0.015	0.006
4-i-butylcyclohexylethanoic acid	12	0.325	0.080	0.050
4-t-butylcyclohexylethanoic acid	12	0.365	0.013	0.008

Table 3.12 shows the butylcyclohexyl butanoic acids, these acids are ~10x more toxic than the corresponding ethanoic moieties (Table 3.11). Unlike the ethanoic acids there are no clear distinctions between the n acid and the other two tested isomers and there is no statistical differences between the three isomers (ANOVA P value 0.75).

Table 3.12. Butylcyclohexylbutanoic acids assayed on the Microtox™ test

Name	C:N	IC_{50} (mM)	St Dev (mM)	St Error (mM)
4-n-butylcyclohexylbutanoic acid	14	0.029	0.007	0.004
4-s-butylcyclohexylbutanoic acid	14	0.033	0.002	0.001
4-i-butylcyclohexylbutanoic acid	14	0.035	0.004	0.002

It is interesting that the ethanoic moieties seem to exhibit some form of isomer based toxicity yet the butanoic moieties do not. Figure 3.12 highlights the differences with Figure 3.12a showing the butanoic moieties clustered together, whilst 3.12b shows that the n-ethanoic moiety is separated from the other two points on the chart. Figure 3.12b also shows the butanoic moieties as a comparison in relative toxicity, when shown on this scale it can be seen that there is no difference in the toxicity of these compounds on the Microtox™ acute bioluminescence assay.

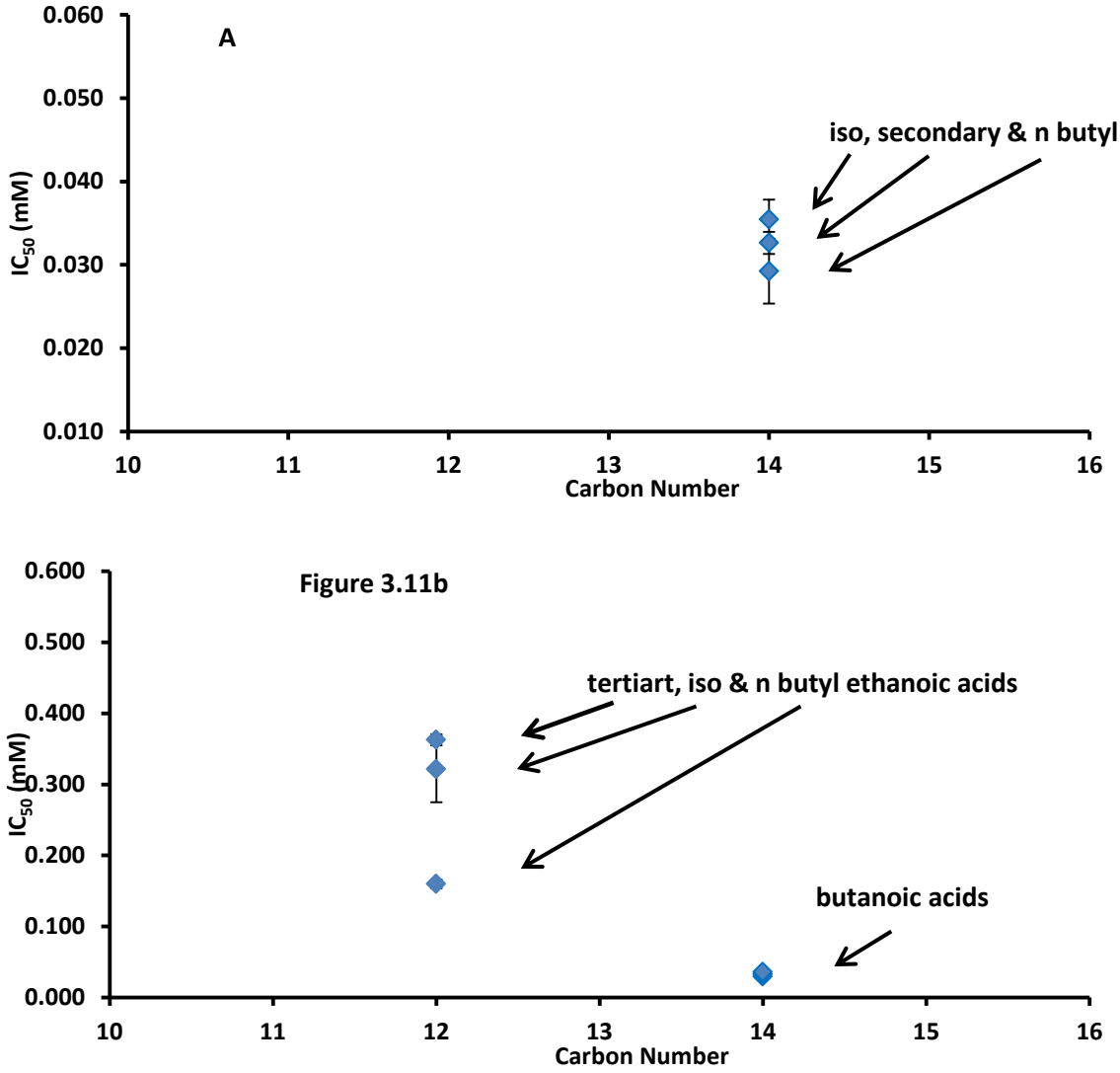

Figure 3.12. Measured IC_{50} values (± standard error (Table 3.1), n=3) for the toxicity of (A) individual isomers of butylcyclohexyl ethanoic acids to Vibrio fischeri (Microtox™ assay); and (B) comparison with butanoic acids. Where error bars are not apparent the error was smaller than the symbol. Error bars equal 1x standard error.

3.3.4 Predictive Toxicology versus Measured Toxicology

Although the ECOSAR predictive toxicology model was initially used to determine the correct concentrations for toxicity testing it became apparent, with the extensive

amount of assays on the Microtox™ assay) that a comparison between the measured and the actual results could be carried out.

This comparison had already been attempted by Frank et al., 2010, (the basis for using ECOSAR) and a good comparison between values, both Microtox™ measured and predicted had been drawn. Because ECOSAR does not assess microbial toxicity the authors utilised the predicted toxicity endpoint to the water flea (*Daphnia Magna*) and recommended that the ECOSAR was fit for purpose when assessing and predicting Microtox™ toxicity. However this assessment was done on a minimal amount of compounds (6) three of which belonged to the same structural family (n-acids). With the 45 measured Microtox™ results from this study a more complete analysis of the ECOSAR model versus the Microtox assay can be performed. When looking at the predicted against measured as a whole no distinct trend is apparent (Figure 3.13) so it is better to assess the data via a structural class basis.

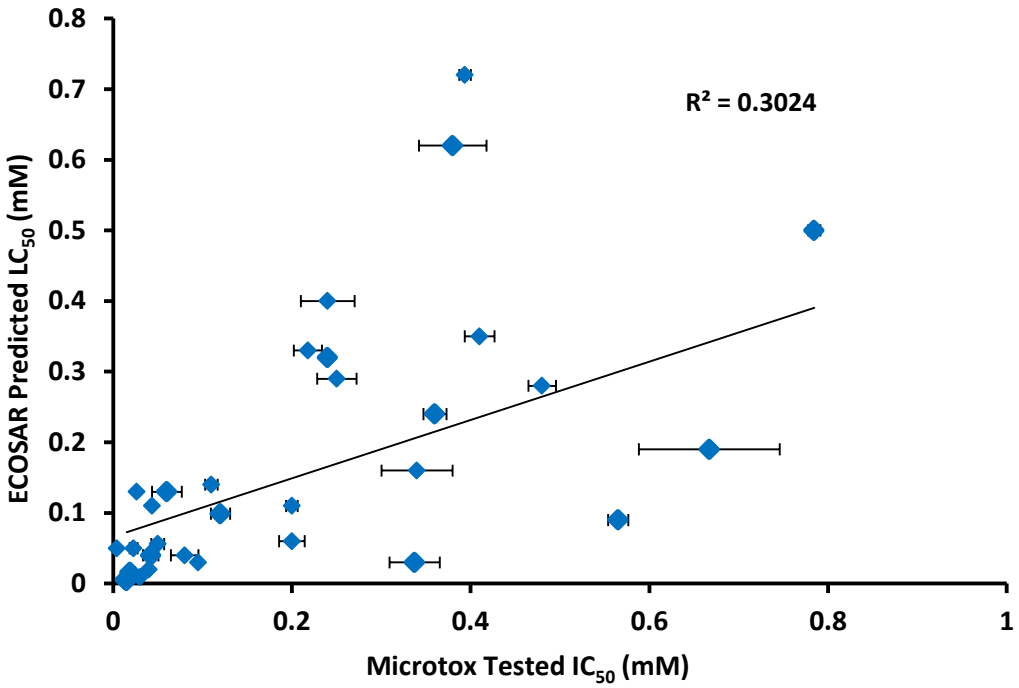

Figure 3.13. Showing the relationship between ECOSAR modelled data and Microtox™ assayed data.

3.3.4.1 *n*-acids

When comparing the predicted and measured values of the *n*-acids it can be seen that (apart from the hexanoic acid) there is a very good relationship. The data in Table 3.13 shows that the endpoints for the C_8-C_{12} acids are very closely correlated, even allowing for the hexanoic and its attendant exponential trend there is an R^2 of 0.952 (Figure 3.14).

Table 3.13. Comparison of ECOSAR predicted and Microtox™ assayed data for *n*-acids

Name	**C:N**	**ECOSAR LC_{50} (mM)***	**Microtox™ IC_{50} (mM)**
Hexanoic acid	6	3.95	0.7
Octanoic acid	8	0.62	0.38
Nonanoic Acid	9	0.24	0.19
Decanoic Acid	10	0.099	0.12
Undecananoic acid	11	0.04	0.042
Dodecanoic acid	12	0.016	0.019

*LC_{50} predicted on the Daphnia Magna 48hr assay

The hexanoic acid prediction seems to be anomalous comNAred to the predictions of the other n-acids, even taking into account the C_6-C_8 gap, a prediction for the heptanoic moiety (C_7; not shown) is 1.5 mM. However even with this anomaly a good fit is still determined.

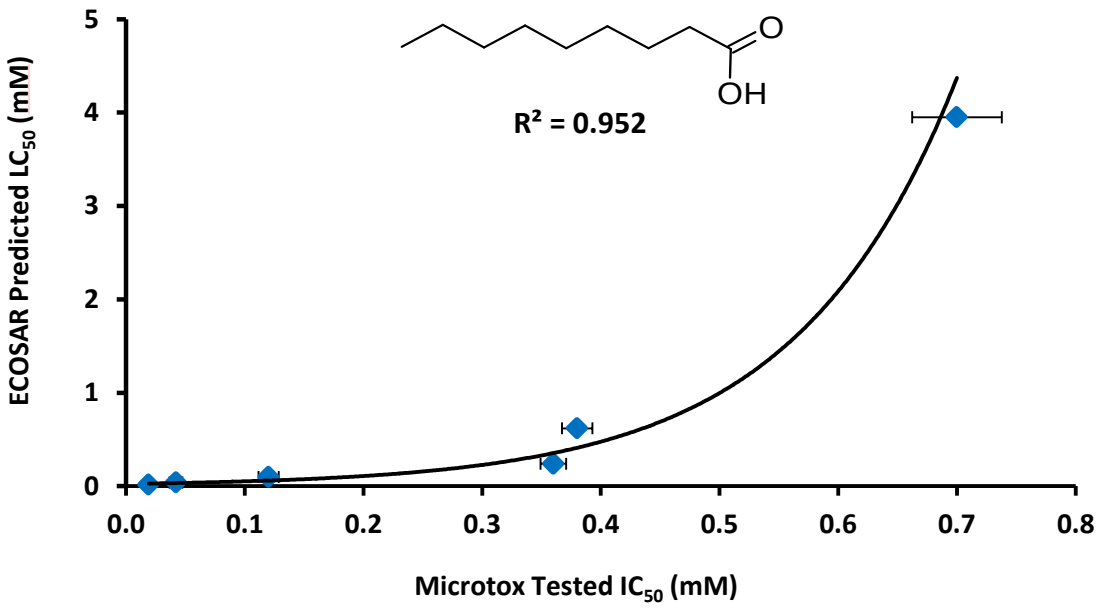

Figure 3.14. Relationship between ECOSAR predicted and Microtox™ assayed data for n-acids. Error bars are 1x standard deviation.

By removing the hexanoic acid (Figure 3.15) it can be seen that there is an excellent linear trend (R^2 0.9752) which does indeed back up the assertions of the previous research and would allow ECOSAR to be used as a stand-alone programme, possibly precluding the need to actual toxicology testing on n-acids. However n-acids make up a small part of the OSPW acid extracts so it is important to assess performance on the other structural groups.

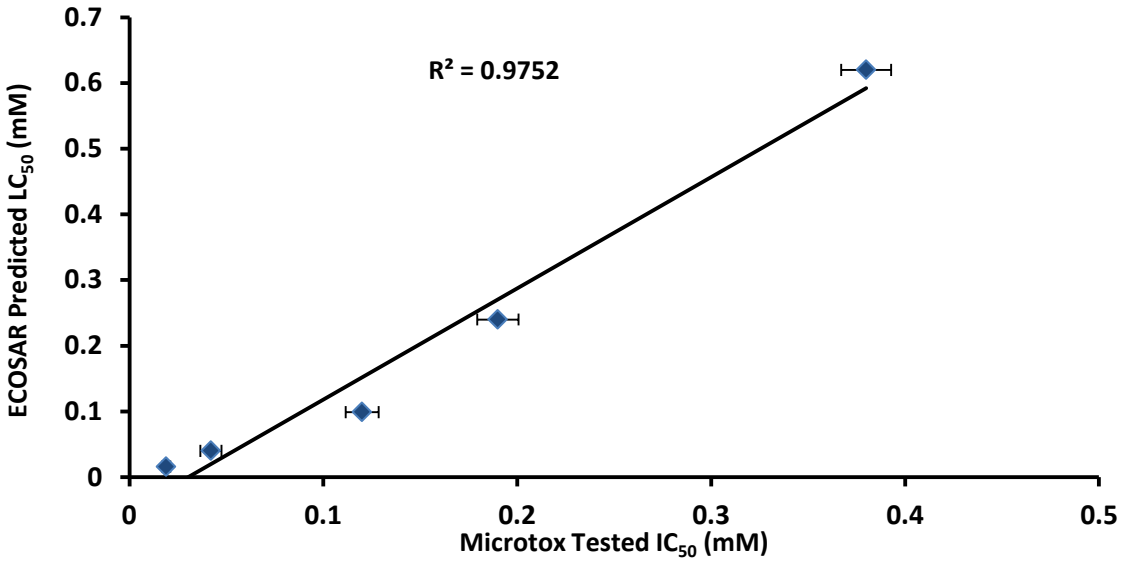

Figure 3.15. Relationship between ECOSAR predicted and Microtox™ assayed data for n-acids, without C6 hexanoic acid data point. Error bars are 1x standard deviation.

3.3.4.2 Methyl branched n-acids

The methyl branched n-acid correlation between the measured and predicted is also excellent, though this time without an anomalous data point. Table 3.14 shows that the ECOSAR and Microtox results are very relevant to each other and that it is likely that ECOSAR could be used as a surrogate test in lieu of actual testing.

Table 3.14. Comparison of ECOSAR predicted and Microtox™ assayed data for methyl branched *n*-acids

Name	C:N	ECOSAR LC_{50} (mM)	Microtox IC_{50} (mM)
4-methyloctanoic acid	9	0.28	0.48
4-methylnonanoic acid	10	0.11	0.20
7-methyldecanoic acid	11	0.04	0.08
4-methyldodecanoic acid	13	0.007	0.012

As figure 3.16 shows there is a strong linear trend to the data (R^2 0.991) which would enable a prediction of the larger, non soluble compounds to be assessed.

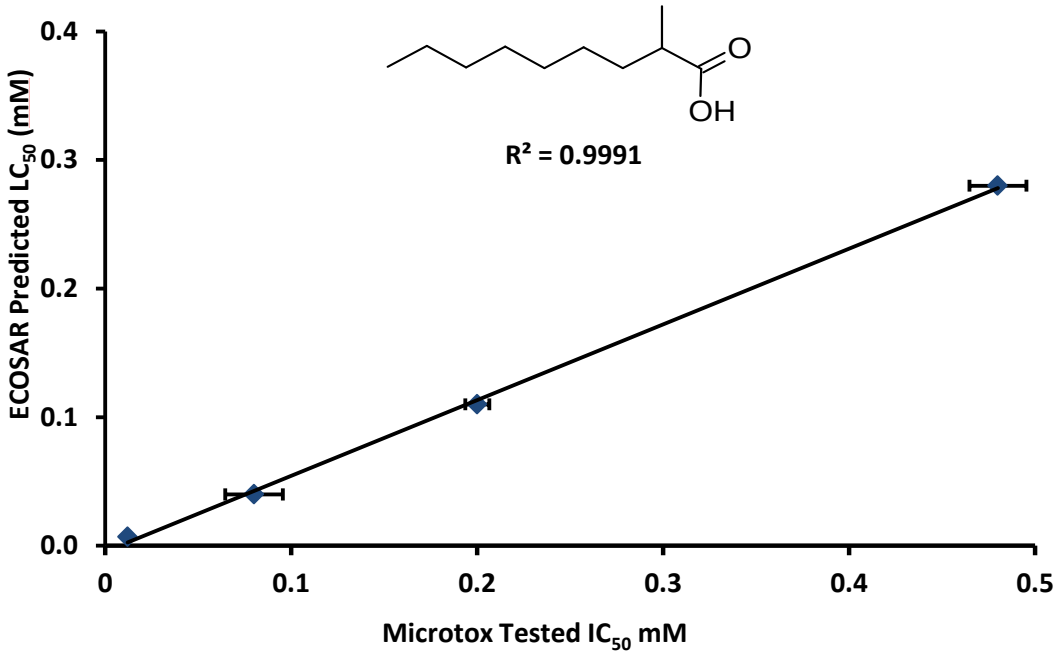

Figure 3.16. Relationship between ECOSAR predicted and Microtox™ assayed data for mono methyl branched n-acids**.** Error bars are 1x standard deviation

3.3.4.3. Isoprenoid Acids

The isoprenoid acids are not so well correlated. Although there may be a discrepancy produced by the amalgamation of dimethyl and trimethyl acids, this is felt to be unlikely as the structures of the acids are essentially similar. Both dimethyl moieties exhibit a better relationship than the single trimethyl moiety (Table 3.15).

Table 3.15. Comparison of ECOSAR predicted and Microtox™ assayed data for isoprenoid-acids

Name	C:N	ECOSAR LC_{50} (mM)	Microtox IC_{50} (mM)
2,6-dimethylheptanoic acid	9	0.32	0.24
3,7 dimethyloctanoic acid	10	0.13	0.06
2,6,10-trimethylundecanoic acid	14	0.004	0.015

Figure 3.17 shows that there is a logarithmic trend has the best fit (R^2 0.9865) a linear trend (although still a good fit) shows an R^2 of 0.9536. It would be interesting to see what would occur if more acids were able to be compared as it seems as if the trimethyl moiety is acting anomalously (like the hexanoic). If more dimethyl acids were available it is likely that a linear trend may be prevalent. Allowing the use of ECOSAR as a surrogate programme, however, as it stands, care must be taken when elucidating toxicity data through ECOSAR alone.

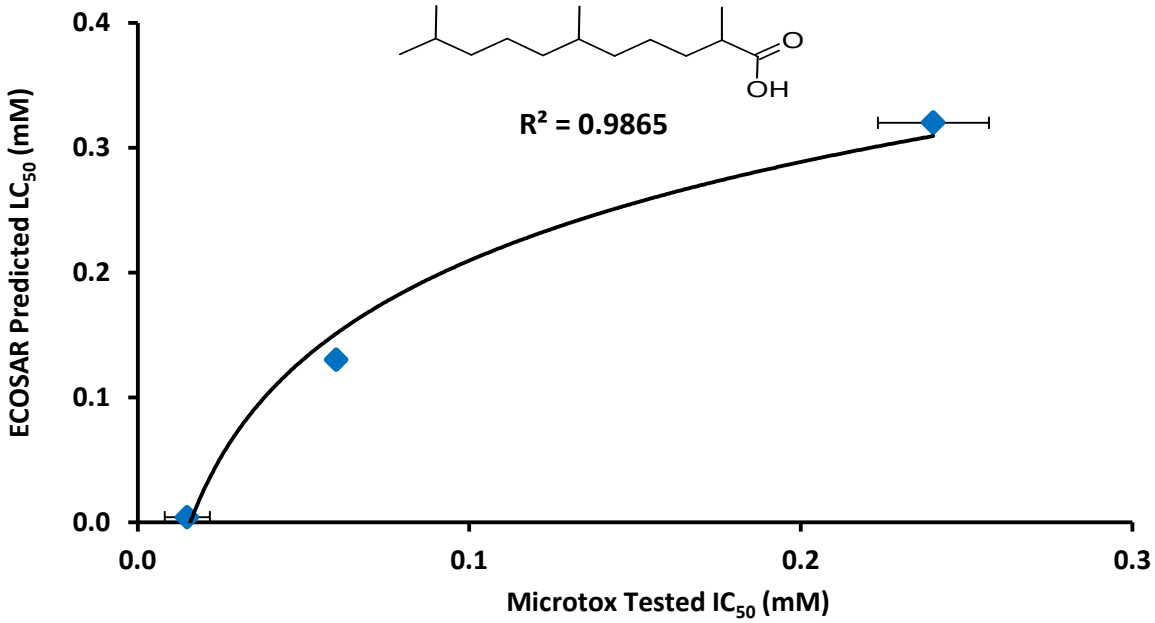

Figure 3.17. Relationship between ECOSAR predicted and Microtox™ assayed data for isoprenoid acids. Error bars are 1x standard deviation.

3.3.4.4. Monocyclic acids

Again there is a good relationship between the data with the model performing adequately on all data points (Table 3.16). However, as Figure 3.18 shows there is a logarithmic trend to the relationship (R^2 0.9929).

Table 3.16. Comparison of ECOSAR predicted and Microtox™ assayed data for monocyclic acids**.**

Name	C:N	ECOSAR LC_{50} (mM)	Microtox IC_{50} (mM)
3-cyclohexylpropanoic acid	9	0.35	0.41
4-cyclohexylbutanoic acid	10	0.14	0.11
5-cyclohexylpentanoic acid	11	0.056	0.05
6-cyclohexylhexanoic acid	12	0.02	0.044

Manipulating the trend to a linear expression does not have such a good relationship (R^2 0.9701) albeit still significant but with a larger margin for error. It is felt that the more significant relationship should be utilised though it is imperative that toxicity assays are carried out to give a significant number of data points so that the trend can be elucidated. It is not recommended that ECOSAR can be used as a surrogate for toxicity testing on these particular acids.

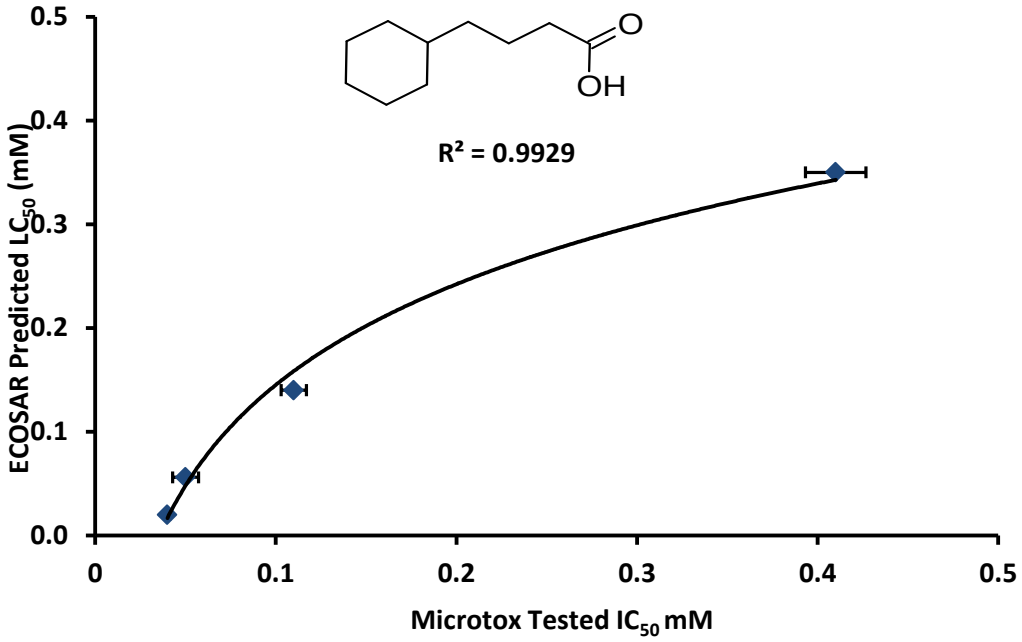

Figure 3.18. Relationship between ECOSAR predicted and Microtox™ assayed data for monocyclic acids. Error bars are 1x standard deviation.

3.3.4.5 Branched Monocyclic Acids

On first glance branched monocyclic acids seem to have a good relationship; however the ECOSAR model consistently overestimates the toxicity of these compounds (Table 3.18)

Table 3.17. Comparison of ECOSAR predicted and Microtox™ assayed data for branched monocyclic acids.

Name	C:N	ECOSAR LC_{50} (mM)	Microtox IC_{50} (mM)
4-ethylcyclohexylethanoic acid	10	0.16	0.34
4-n-propylcyclohexylethanoic acid	11	0.06	0.2
4-n-butylcyclohexylethanoic acid	12	0.03	0.095
4-n- pentylcyclohexylethanoic acid	13	0.009	0.03
4-n- hexylcyclohexylethanoic acid	14	0.004	0.012

Figure 3.19 exhibits a 2nd power polynomial relationship (R^2 0.9948), a corresponding linear relationship gives an R^2 of 0.9523. Although this polynomial trend exhibits an excellent relationship care must be taken when analysing compounds of this structure on the ECOSAR model. With a non linear trend and an overestimation of the toxicity it is not recommended that the ECOSAR model is used as a surrogate test.

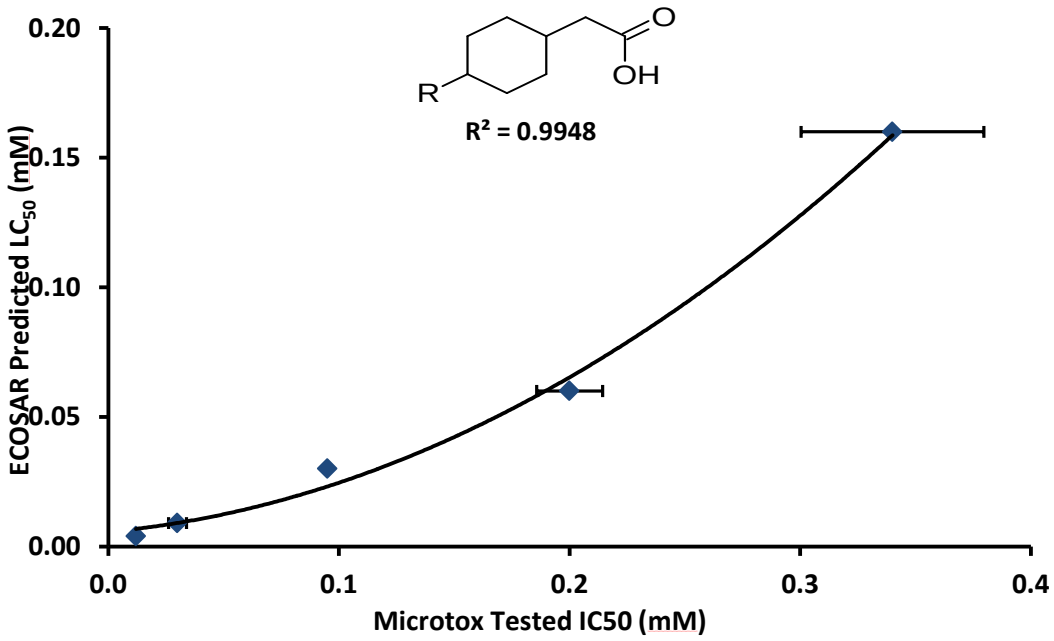

Figure 3.19. Relationship between ECOSAR predicted and Microtox™ assayed data for branched monocyclic acids. Error bars are 1x standard deviation

3.3.4.6 Bicyclic Acids

With the bicyclic acids a good match is achieved in only one of the structures (decalin-1-carboxylic acid (0.33/0.218 for ECOSAR and Microtox™ respectively) however for the remaining two compounds ECOSAR underestimates and overestimates the toxicity (Table 3.19).

Table 3.18. Comparison of ECOSAR predicted and Microtox™ assayed data for bicyclic acids

Name	**C:N**	**ECOSAR LC_{50} (mM)**	**Microtox IC_{50} (mM)**
Decalin-2-carboxylic acid	11	0.33	0.218
Decalin-2-ethanoic acid	12	0.13	0.027
3-Decalin-1-yl-Propanoic acid	13	0.05	0.004

When examining the trend (Figure 3.20) it can be seen that there is a linear regression apparent, though as there are only three data points care must be taken when extrapolating data from this as the trend is not significant.

Testing of more bicyclic acids would firm this trend and determine whether it is indeed linear. At present it is not recommended to use ECOSAR as a surrogate, despite the apparent trend, until more bicyclic compounds can be assayed.

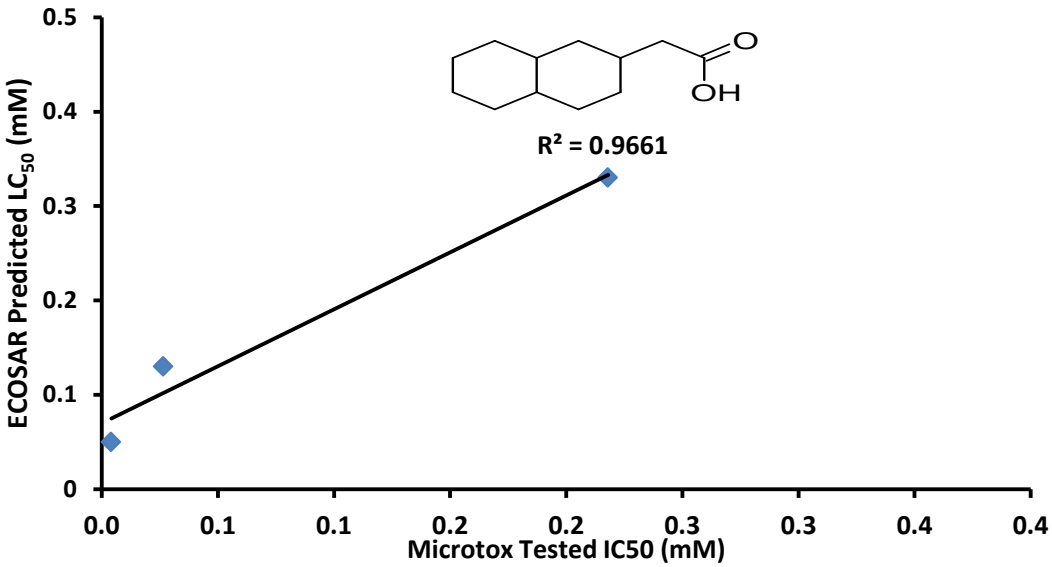

Figure 3.20. Relationship between ECOSAR predicted and Microtox™ assayed data for bicyclic acids. Error bars are 1x standard deviation

3.3.4.7 Tricyclic (Adamantane Type) Acids

Adamantane type acid toxicity is consistently over estimated by the ECOSAR by as much as an order of magnitude (Table 3.20). This is potentially because the SMILES notation used to input the adamantane acids assume a planar rather than a cage type structure, rendering the estimation of Log_{kow} ineffectual and creating an anomalous result.

Table 3.19. Comparison of ECOSAR predicted and Microtox™ assayed data for tricyclic acids

Name	C:N	ECOSAR LC_{50} (mM)	Microtox IC_{50} (mM)
1-Adamantanecarboxylic acid	11	0.50	0.78
1-adamantane ethanoic acid	12	0.19	0.67
3, 5-dimethyl-1-adamantane carboxylic acid	13	0.09	0.57
3, 7-dimethyl-1-adamantane ethanoic acid	14	0.03	0.34

There is an exponential regression in Figure 3.21 that exhibits a relatively good fit, however because the estimation of toxicity is incorrect adamantane type tricyclic acids cannot be determined for toxicity via the ECOSAR model.

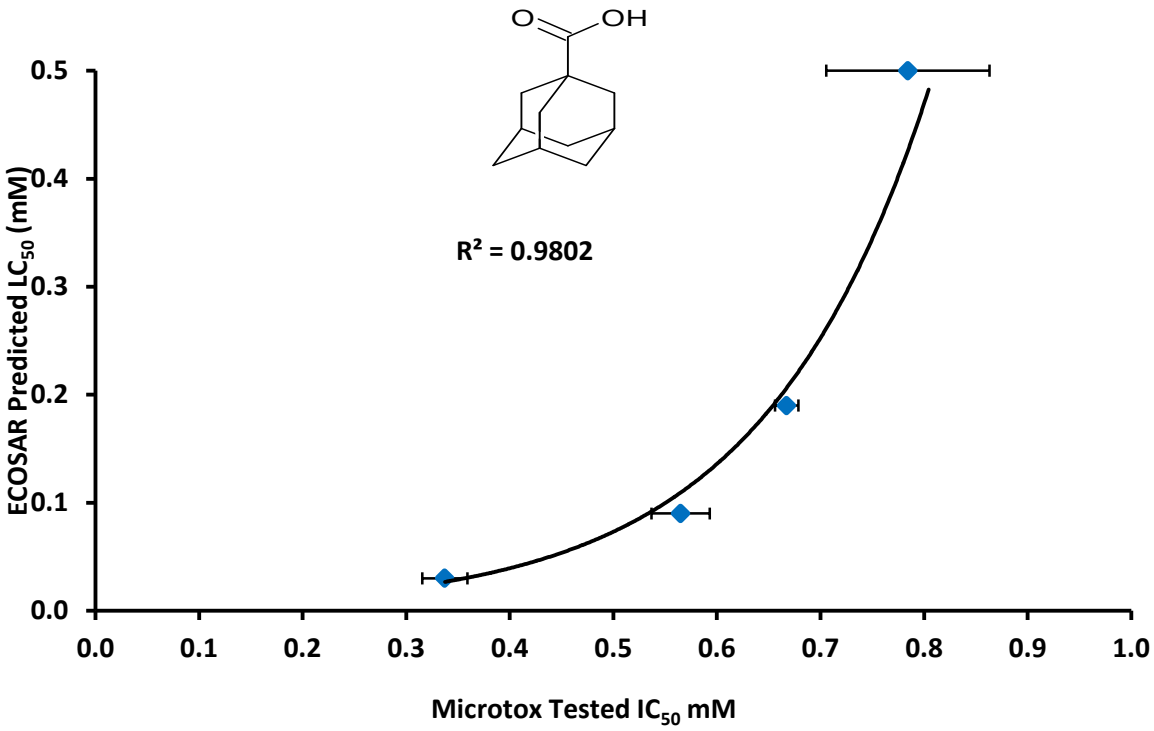

Figure 3.21. Relationship between ECOSAR predicted and Microtox™ assayed data for tricyclic acids. Error bars are 1x standard deviation

3.3.4.8. Branched Monoaromatic Acids

The prediction for the branched mono-aromatic acids slightly underestimates the toxicity (Table 3.21). Apart from the 4-n-butylphenylethanoic acid this underestimation is ~ a factor of 2 less than the measured data.

Table 3.20. Comparison of ECOSAR predicted and Microtox™ assayed data for branched mono-aromatic acids

Name	**C:N**	**ECOSAR LC_{50} (mM)**	**Microtox IC_{50} (mM)**
4-n-propylphenylethanoic acid	11	0.72	0.394
4-n-butylphenylethanoic acid	12	0.29	0.250
4-n-pentylphenylethanoic acid	13	0.11	0.044
4-n-hexylphenylethanoic acid	14	0.05	0.023

The regression shown in Figure 3.22 is a 2nd power polynomial which shows a good fit (R^2 0.9925) however with the underestimation in mind it is not recommended that ECOSAR is used to predict toxicity data for mono aromatic acids unless a number of compounds are first assayed.

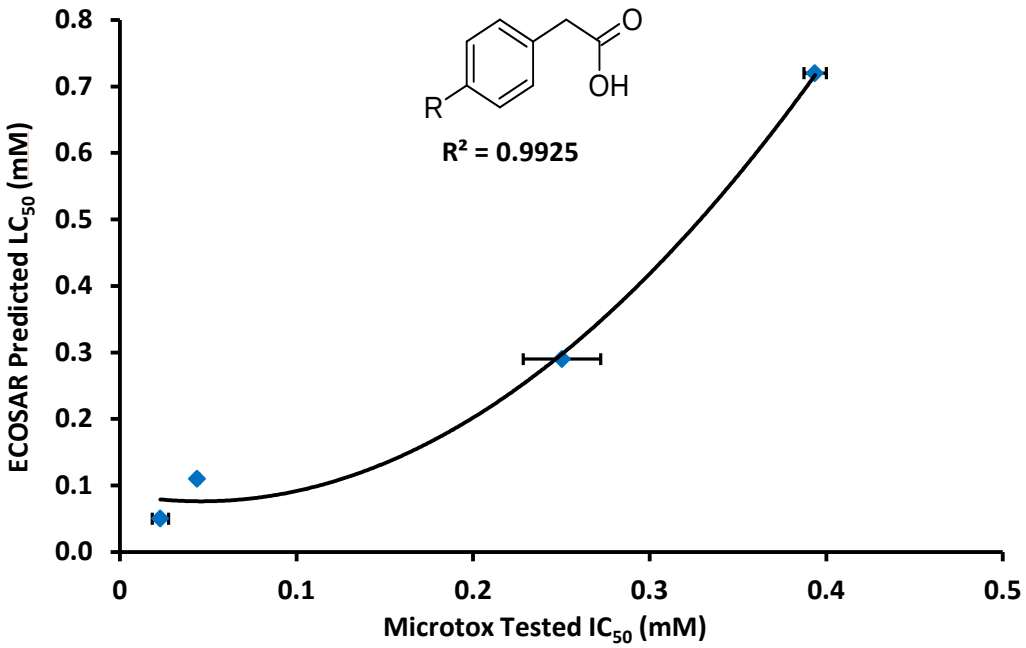

Figure 3.22. Relationship between ECOSAR predicted and Microtox™ assayed data for mono aromatic acids**.** Error bars are 1x standard deviation

3.3.4.9 Isomerism

Because the ECOSAR model bases the toxicity predictions on Log_{kow} isomeric compounds (Figure 3.23) can cause a problem. ECOSAR predicts these compounds to display similar toxicity but when measured by the Microtox™ it was noted that each isomer could exhibit differential toxicity.

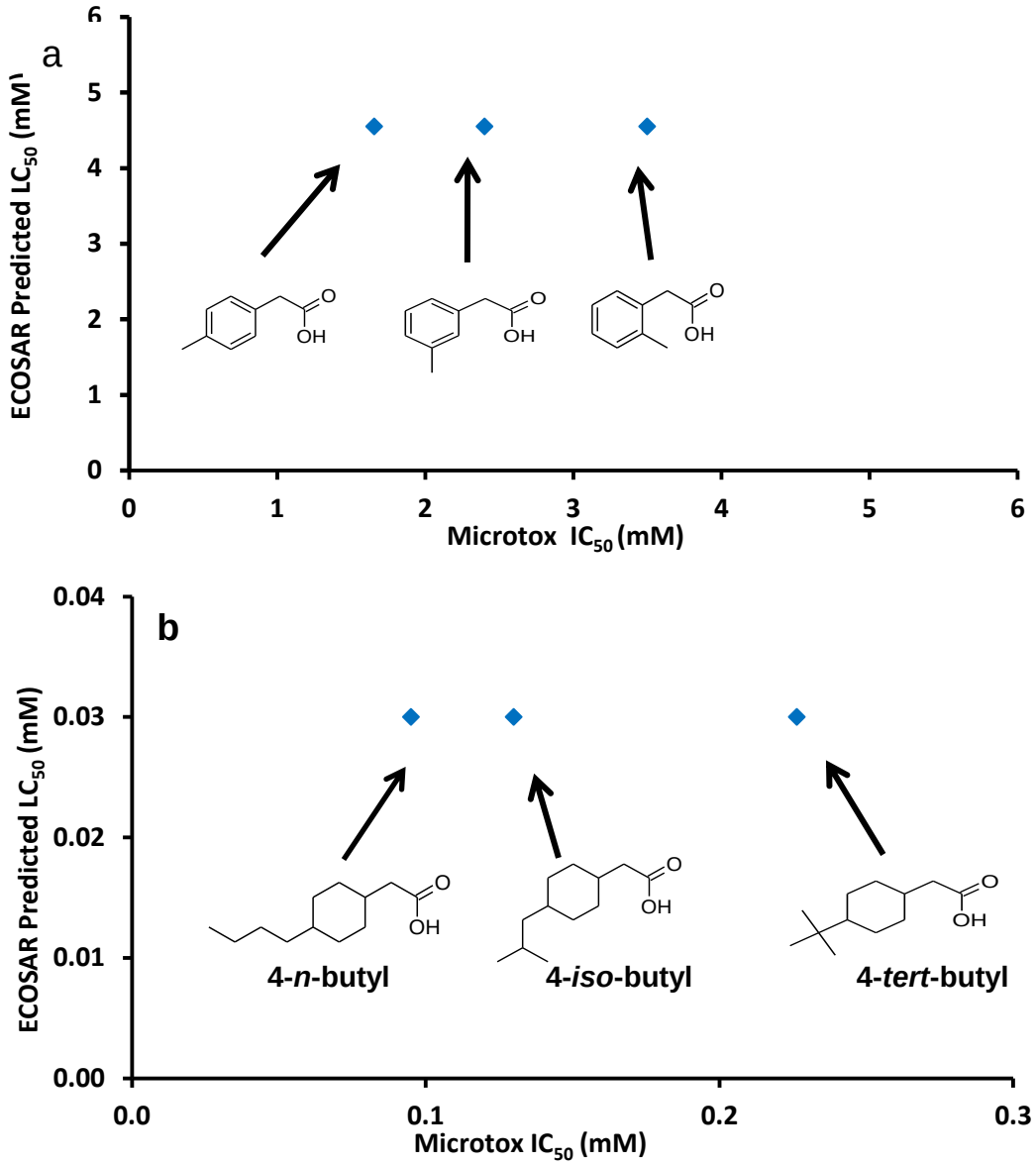

Figure 3.23. Predicted vs. Measured toxicity endpoints for (a) positional isomers of methylphenylethanoic acid and (b) structural isomers of butylcyclohexylethanoic acid**.**

It is also noteworthy that the ECOSAR model overestimates the toxicity of the assessed structural isomers (Figure 3.23b) by an order of magnitude. Great care must be taken or other toxicological models used when assessing the toxicity of isomers on the ECOSAR model.

3.3.5. ADMET Predictor Results

It can be seen that the ADMET predictor performed more or less similarly to the ECOSAR model. When considering the *P. promelas* data it is noticeable that there is a variation in the types of trend that show a best fit. With the *n*-acids displaying a polynomial trend, the methyl branched *n*-acids displaying a linear trend and the remaining three compound classes all displaying exponential trends. There is also a discrepancy with the ADMET model somewhat underestimating the toxicity comNAred to the Microtox™ (n-acids and cyclohexyl acids (Figure 3.25 A and C)), though this could be due to inter-species sensitivity issues and non-comparison of similar species. However the methyl branched *n*-acids (Figure 3.24B) and the branched monoaromatic acids (Figure 3.24E) do display a relatively good fit, as does the first three data points in the branched cyclohexyl data (Figure 3.24D).

When assessing the *T. pyriformis* data it is noticeable that similarities exist with the *P. promelas* data. Both the *n*-acids and cyclohexyl acid modelled data (Figure 3.25 A and C) is underestimating toxicity. Whilst the methyl branched *n*-acids and the mono-aromatic acids display a good fit (Figure 3.25 B and E). Similarly a number of data points in the branched cyclohexyl data also display a relatively good fit though the lower molecular weight (less toxic compounds) are underestimated by the model. In both ADMET datasets it is the cyclohexyl acids that consistently display the worst fit.

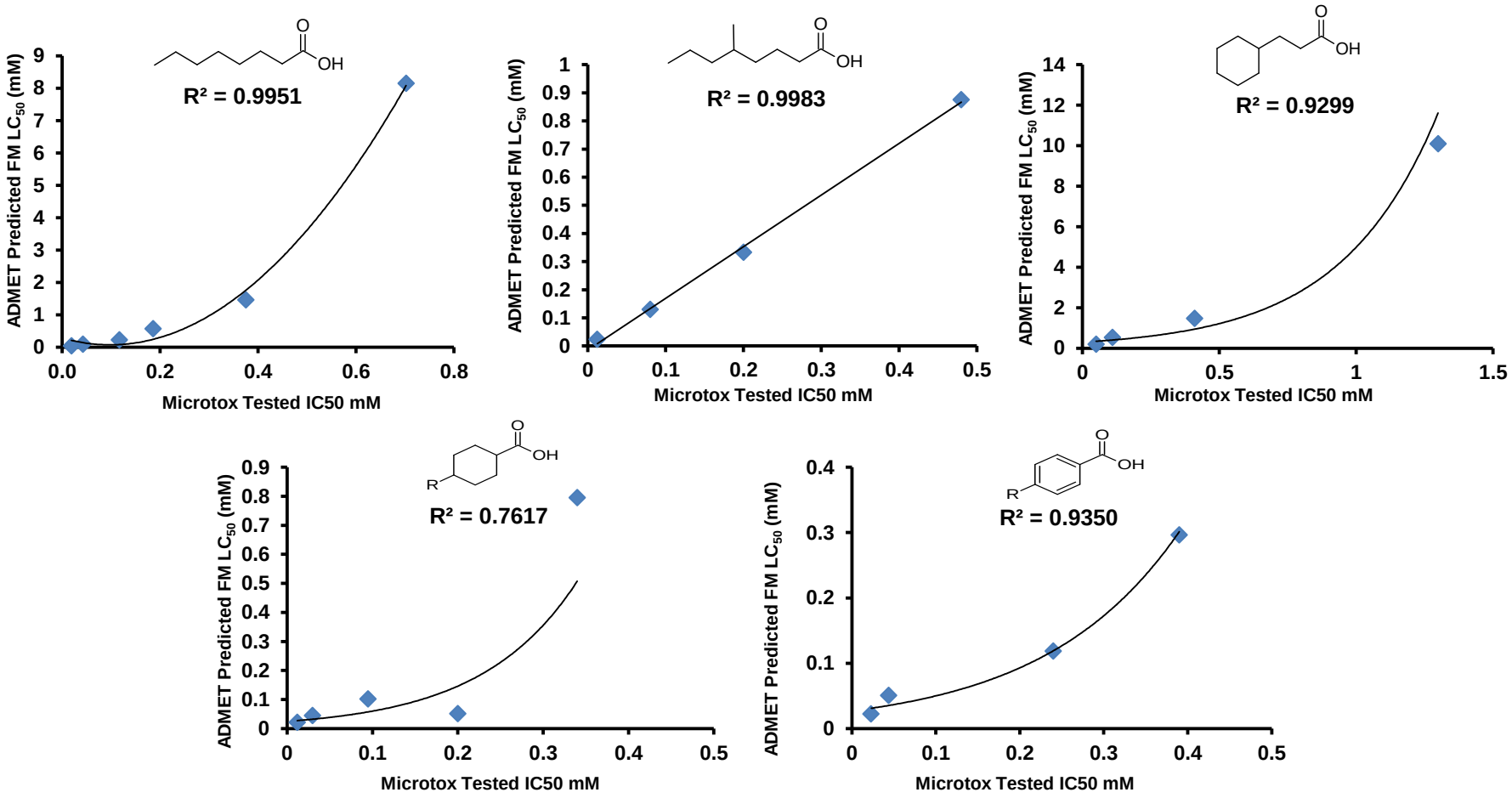

Figure 3.24. ADMET *Pimephales promelas* modelled toxicity data comparison with Microtox™ assayed data with (A) *n*-acids; (B) methyl branched *n*-acids; (C) cycohexyl acids; (D) branched cyclohexyl acids; and (E) branched mono-aromatic acids.

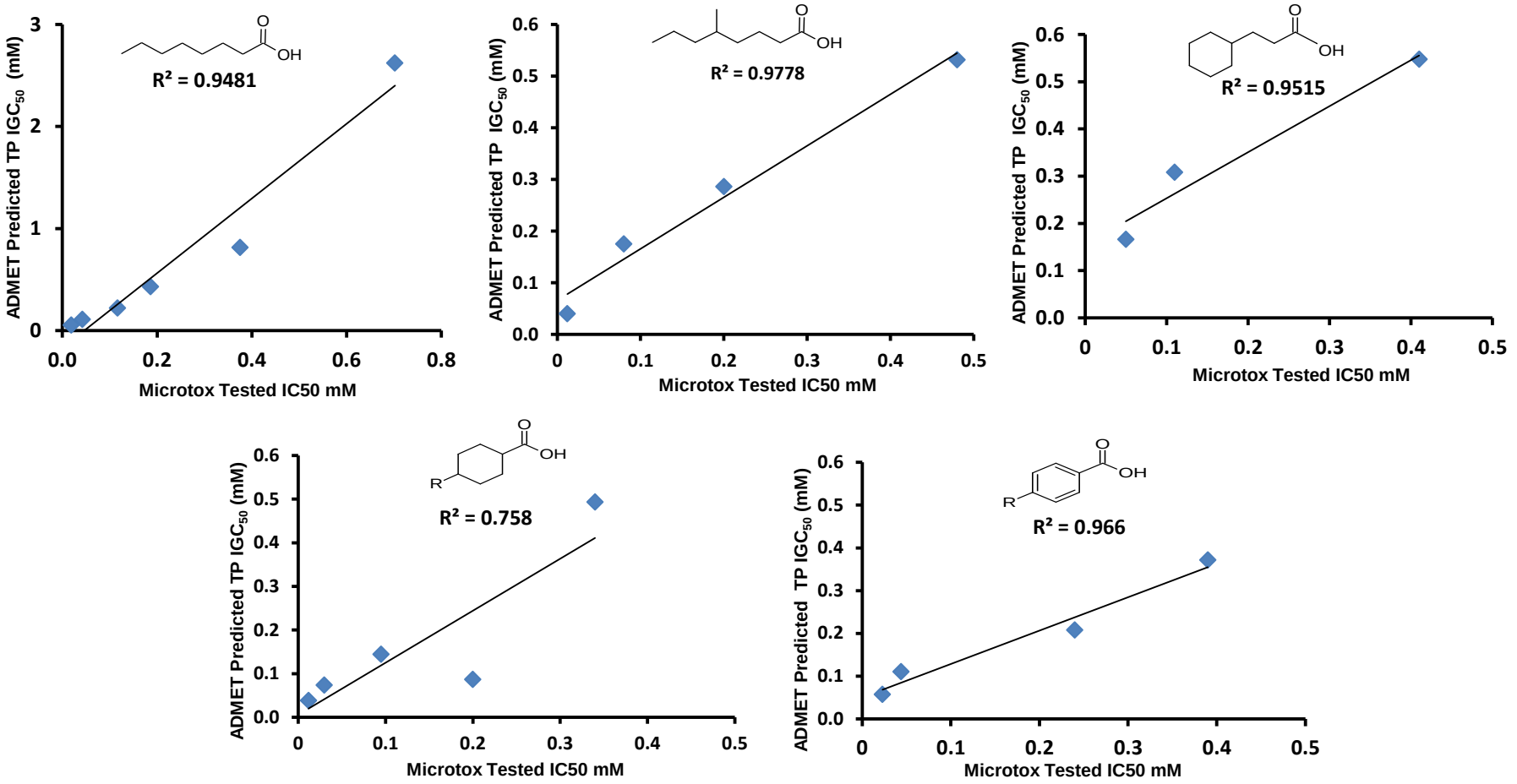

Figure 3.25. ADMET *Tetrahymena pyriformis* modelled toxicity data comparison with Microtox™ assayed data with (A) *n*-acids; (B) methyl branched *n*-acids; (C) cycohexyl acids; (D) branched cyclohexyl acids; and (E) branched mono-aromatic acids.

3.4. Conclusions

The original aim of the toxicity assessment of original compounds was to screen the acids and find those which could then be scaled up to assess via the mussel feeding rate study and the coriphium life cycle study (Scarlet., et al 2007; Booth et al., 2008). However at the end of the study there is little evidence to suggest that NAs are overtly toxic substances when assessed individually with the Microtox™ and generally fail to have large deleterious effects on the bioluminescence of *Vibrio fischeri*. This lack of toxicity precluded additional assessment via more sensitive assays.

Figure 3.35 reveals the similarity in the trends in the dose response curves for all the acid groups except the adamantanes and confirms that there is a definitive relationship between toxicity and carbon number. This result denies the proposed hypothesis by various authors (e.g. Frank et al., 2009; Holowenko et al., 2002) that the opposite effect is observed and indicates that toxicity may be linked to physiochemical parameters such as solubility.

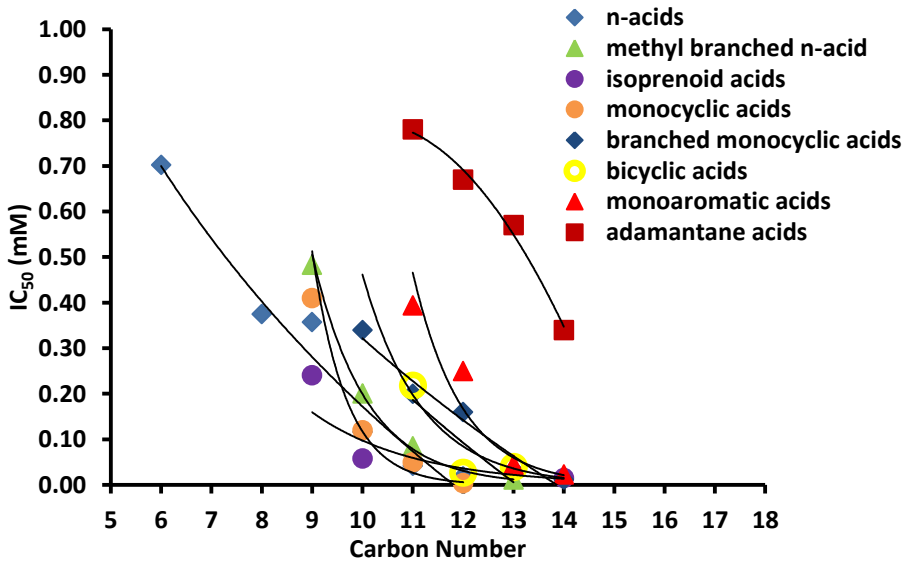

Figure 3.35. Comparison of average IC_{50}s for the assayed acid groups

Comparison with an individual alkylated phenol shows that there are far more toxic compounds existing within both the OSPW and the petroleum derived mixtures. For instance Choi et al., (2004) assayed a number of alkylated phenols with the Microtox™ assay (noted to exist in the commercial acid mixtures by West et al., 2011) and recorded toxicity of four orders of magnitude greater than the most toxic assayed individual acid (decalin-1-propanoic acid: IC_{50} 0.004mM).

However the large concentrations existing within the OSPW (20-120 mg L^{-1}) does make these compounds an environmental threat. Little is known about whether these compounds complex within the mixture as some are able to act as surfactants so could co-solubilise larger, seemingly insoluble compounds, thus increasing their bioavailability and hence their toxicity (Quagraine et al., 2005). It is potentially more correct to state that these particular petroleum acids exhibit a low to medium toxicity because of the solubility limits at this particular pH.

Whether larger (potentially more toxic) acids have an effect on the Microtox™ is open to debate. It is likely that the larger compounds within the super-complex mixtures of OSPW are not soluble so the toxicity is driven by these smaller more soluble acids, even though synergistic or antagonistic co-solubility may occur. A previous study (Frank et al., 2008) was able to distil the OSPW into separate fractions, which were analysed by Microtox™ (see Section 1.2 Figure 1.5 Chapter 1) analysis of these fractions by two dimensional GC enabled calculation of a median carbon number for each of these fractions. IC_{50} values of each fraction was calculated at between 0.14-0.28 mM which lies within the 0.7-0.004 mM concentrations for the individual acids elucidated in this study. This suggests that the higher molecular weight fractions, which should have a larger toxic effect, were in some way de-toxified. A solubility limit would provide a plausible explanation for this. However this does not in any-way suggest that

these fractions or the larger compounds are not toxic, it just suggests that they failed to have an effect on the Microtox™ assay and were just not soluble in the small scale solutions that were created for the toxicity assessment. It is therefore imperative that other un-assessed compounds are tested on other more sensitive assays (such as the Mussel feeding rate assay (e.g. Donkin et al., 1989) alongside the other un-assessed compounds that are not NAs that are known to exist within the OSPW.

When assessed by a more sensitive predictive model (ADMET) these compounds were shown to be potentially non-estrogenic compounds, however some of the compounds tentatively identified within the mixture are predicted to have an effect (Scarlett et al., 2012) which suggests that the OSPW acid extracts may be relatively non-toxic to one assay but still pose a direct toxicological threat because of different modes of action utilised by different structural classes.

With regard to the predictive toxicology model ECOSAR, it was found that in general it was a useful tool, as long as the user was aware of its limitations. Both cage type nano-diamonds and isomers confused the model as it is based upon the compounds Log_{kow}, and, places, it under or overestimated toxicity.

This work has since been published in Environmental Science and Technology and a copy of this research paper has been included in Appendix D.

Chapter 4
The Mixture Toxicity of Naphthenic Acids

4.1. Introduction

How toxicity is altered when compounds are present within a mixture has been investigated in many studies and by numerous methodologies (reviewed in a Report to the European Commission, 2012; Kortencamp et al., 2009; Berenbaum, 1989). The outcome may be that compounds contribute 'equal toxicity', generally due to similar modes of action, normally termed "concentration addition" (CA; Kortencamp et al.,2009). Conversely compounds may contribute unequal toxicity, usually due to operating independently by different modes of action (MOA), normally termed "independent action" (IA; Kortencamp et al., 2009).

By taking the individual toxicity endpoints (IC_{50}s, IC_{20}s etc.) that were calculated in Chapter 3 it is possible to determine whether NAs present as a mixture operate by CA or IA. CA is described as the most effective method for assessing the toxicity of chemicals that act by the so-called baseline (or narcosis) mode of action (MOA) (Kortencamp et al., 2009; European Commission., 2011). As NAs are hypothesised to act via this MOA (e.g. Frank et al., 2008) it seems a prudent assumption to base any subsequent mixture design with this outcome in mind.

There are few studies on the mixture toxicity of NAs, this may be due to the lack of knowledge available as to the toxicity of known individual components of the commercial mixtures or the acid extracts of OSPW. Tollefsen et al., (2012) (also reviewed in Chapter 1.) assessed individual and combined toxicity of 3 isomers of butylphenylbutanoic acid and three isomers of butylcyclohexylbutanoic acid.

Tollefsen et al (2012) noted that the toxicity of the mixture exhibited CA. CA was confirmed by using the concept of a Model Deviation Ratio (MDR) where the predicted toxic response is divided by the observed toxic response. A MDR of 1 is said to describe CA, though a factor of 2 can be applied as a safety factor to reduce the possibility of erroneous classification of synergistic or antagonistic effects (toxicity greater or less than the equivalent molar concentration of the individual compounds) (Drescher and Boedeker., 1995). Tollefsen et al (2012) assessed the six compounds in both binary mixtures and a six compound total mixture for both IA and CA using the trout hepatocyte assay and assessing membrane integrity and metabolic inhibition across a range of µM concentrations (99-1980 µM for the binary mixtures and 99- 943 µM for the 6 compound mix). All of the MDRs generated for CA were within the factor of 2 (range 0.7- 1.8 for the binary mixtures and 1.1-1.5 for the 6 compound mixture. For IA a number of MDRs were within the factor of 2 cut off for the binary mixtures, however a few lay outside of the factor of 2 (MDRs range 0.7-2.6), when assessing the 6 compound mixture only two concentrations lay within the factor 2 with most MDRs lying outside this (range 1.5-3.5). From this Tollefsen et al (2012) deduced that CA described the butanoic naphthenic acid moieties toxicity more effectively than IA. The prediction by Frank et al., (2008) and the recent study by Tollefsen et al., (2012) provide evidence that NAs operate within the concept of CA.

However, to the author's knowledge, no studies exist on the mixture toxicity of NA that utilise live organisms. As limited amounts of pure acids were available assessment of both IA and CA using live organisms was not possible. Therefore

the purpose of this study was simply to confirm or deny that NAs conformed to the concept of CA when using a live organism.

4.1.1. Concentration Addition and Independent Action

The concept of mixture toxicity, in particular CA can be traced back to the work of Loewe and Muischnek (1926) which enabled a mathematical basis to express mixture toxicity. Bliss (1939) was the first researcher to describe the three distinct forms of interactions that can occur within mixture toxicity and was the first to express the mechanisms that each concept follows when assessing the mixture toxicity of nitro-phenol and petroleum oil. Bliss explains that mixture constituents can act in a similar manner; a dissimilar manner or by an interaction between the chemicals within the mixture and was the first author to express IA in a mathematical formula. Hence mixture toxicity concepts are often described as ‘Loewe Additivity’ or ‘Bliss Independence’, experimental deviation from the predicted results can be described as Bliss Synergy/Loewe Synergy (depending on concept) which describes an underestimation of toxicity by the model; or Bliss Antagonism/Loewe Antagonism, which describes an overestimation of the toxicity through the predictive model (Syberg et al., 2008).

A mixture in which the components of the mixture act in a similar way is also known as CA (or dose addition). This occurs if chemicals act via the same mechanism or mode of action and only differ in strength. Methodologies and approaches differ when assessing CA but in general components of the mixture are added after applying a scaling factor which takes into account the potency of each individual chemical (Altenburger et al., 2000; European Commission., 2012)

The Toxicity and Assessment of Chemical Mixtures report prepared by various scientific committees (e.g. Scientific Committee on Health and Environmental Risks) for the European commission in 2011 states that if each individual compound acts in a similar fashion and are in concentrations which are adjusted to a known potency then the effects should be the same no matter which compounds are interacting with a specific target site. In fact CA strictly relies on the assumption that similar types of chemical interact with similar target sites and use the same mechanisms of action (European Commission., 2011). This approach can be modelled effectively using equation 1, described by Kortencamp et al., (2009) as a Toxic Unit Summation (described more effectively by equation 2) (Kortenkamp et al., 2009).

Eq. 1 $$ECx_{mix} = \left(\sum_{i=1}^{n} \frac{Pi}{ECx_1}\right)^{-1}$$ ***Eq. 2*** $$TU_i = ECx_{mix} \times \frac{Pi}{ECx_i}$$

Where ECx_{mix} is the predicted total concentration of a mixture that produces $X\%$ effect; Pi is the relative fraction of component i in the mixture; ECx_i is the concentration of substance i provoking a certain effect if applied alone; and TU_i represents the toxic unit, which in the case of CA would be equal to ~1.

IA occurs if toxicants act independently of each other often utilising different MOAs that do not affect each other. This approach is modelled through the use of Equation 3.

Equ. 3 $$E(C_{mix}) = 1 - \prod_{i=1}^{n}(1 - E(C_i)$$

Where $E(C_{mix})$ is the combined effect at the mixture concentration C_{mix} and $E(C_i)$ is the effect of the individual component i applied at the concentration C_i. Therefore any compound for which C_i is equal to zero does not contribute to the

joint effects of the mixture. Although a few chemicals within the mixture may well pose a risk the majority of chemicals in mixtures of IA acting chemicals tend to pose little or no overall health concerns; as long as the individual components remain below their zero effect level. It is important to mention that the 'zero effect level' in this instance is not the same as the No Observable Adverse Effect Level/Concentration (NOAEC:NOAEL) (European Commission., 2011).

It has been noted that there does not seem to be any general agreement on mixture design for CA so the approach must rely on groupings of structurally similar chemicals. In fact guidance to the Health and Consumer Protectorate of the European Commission states:

> *"…there is currently no general agreement on the scientifically best approach and grouping of chemicals is most often done by expert judgement on a case by case basis…"*

4.2. Methods and Materials

Methods and Materials for the Mixture Toxicity assay were similar to that described in Chapter 3.

4.2.1. Mixture Design

As described in Chapter 3 and Jones et al., (2011) individual NA were assessed for toxicity using the Microtox™ assay. As limited amounts of the synthesised chemicals were available it was decided against a binary mixture approach. Therefore based on the determined toxicity of these 34 compounds mixtures of structurally similar compounds were made for each of seven groups. In addition, a 34 compound mixture composed of each individual toxicant assessed in Chapter 3 was also assessed (Table 4.1 and Table 4.2). The mixture design was based on the hypothesis that NA have a narcosis (or baseline) MOA and should therefore operate by CA (Frank et al., 2008). The CA concept can be modelled through use of Equation 1

As each compound was predicted to have the same effect, components of the mixtures were added according to their relative toxicity. Concentrations of NA were calculated by dividing the previously derived IC_{50} (Jones et al., 2011; Chapter 3) by the number of components in the structural or 34 compound group. The mixtures were adjusted to 10 mM (1 mM for decahydronaphthalene type acids) for use with the Microtox™ assay (Section 4.2.3). Model Deviation Ratios (MDRs) (Deneer, 2000; Tollefsen et al., 2012) were calculated by dividing the predicted concentration by the observed concentration. MDRs of 1 indicate that the mixture acts through CA. An MDR of <1 indicates that the model overestimates the toxicity (i.e. antagonism) and a MDR of >1 indicates

underestimation of the model (i.e. synergism). Deneer (2000) applied a factor of 2 to the MDR to account for variability within the test hence a MDR between 0.5 and 2 was deemed to be not a significant deviation from CA, however, this was based on the observed intra- and inter-laboratory variability and therefore less variability should occur when tests are conducted by a single operator.

4.2.3 Microtox™ Assay

The Microtox™ Assay was performed as described previously (Chapter 3 and Jones et al., 2011).

Table 4.1. Components of the 34 compound mixture with individual IC_{50} values and relative IC_{50} values, relative IC_{50} is defined as the individual IC_{50} divided by the number of compounds in the mixture (IC_{50}/n).

Name	IC_{50} (mM)*	IC_{50}/n (mM)
n-hexanoic acid	0.700	0.0206
Octanoic acid	0.380	0.0112
Nonanoic Acid	0.360	0.0106
Decanoic Acid	0.120	0.0035
undecananoic acid	0.042	0.0012
dodecanoic acid	0.019	0.0006
4-methyloctanoic acid	0.480	0.0141
2-methylnonanoic acid	0.140	0.0041
4-methylnonanoic acid	0.200	0.0059
7-methyldecanoic acid	0.080	0.0024
4-methyldodecanoic acid	0.012	0.0004
2,6-dimethylheptanoic acid	0.240	0.0071
3,7 dimethyloctanoic acid	0.060	0.0018
2,6,10-trimethylundecanoic acid	0.015	0.0004
4-ethylphenylethanoic acid	1.930	0.0568
4-n-propylphenylethanoic acid	0.214	0.0063
4-n-butylphenylethanoic acid	0.394	0.0116
4-n-pentylphenylethanoic acid	0.044	0.0013
4-n-hexylphenylethanoic acid	0.023	0.0007
4-methylcyclohexylethanoic acid	0.240	0.0071
4-ethylcyclohexylethanoic acid	0.340	0.0100
4-n-propylcyclohexylethanoic acid	0.200	0.0059
4-n- pentylcyclohexylethanoic acid	0.030	0.0009
Cyclohexylcarboxylic acid	1.300	0.0382
3-cyclohexylpropanoic acid	0.410	0.0121
4-cyclohexylbutanoic acid	0.110	0.0032
5-cyclohexylpentanoic acid	0.050	0.0015
1-Adamantanecarboxylic acid	0.780	0.0229
1-adamantane ethanoic acid	0.670	0.0197
3, 5-dimethyl-1-adamantane carboxylic acid	0.570	0.0168
3, 7-dimethyl-1-adamantane ethanoic acid	0.340	0.0100
Decalin-2-carboxylic acid	0.218	0.0064
Decalin-2-ethanoic acid	0.027	0.0008
3-Decalin-1-yl-Propanoic acid	0.004	0.0001

*IC_{50}s previously derived, described in chapter 3 and Jones et al., (2011); *n*= 34

Table 4.2. Components of the structural compound mixtures

***n*-acids**	**IC_{50} (mM)**	**IC_{50}/n (mM)**
n-hexanoic acid	0.7	0.117
Octanoic acid	0.38	0.063
Nonanoic Acid	0.36	0.060
Decanoic Acid	0.12	0.020
undecananoic acid	0.042	0.007
dodecanoic acid	0.019	0.003
Methyl branched *n*-acids	**IC_{50} (mM)**	**IC_{50}/n (mM)**
4-methyloctanoic acid	0.48	0.096
2-methylnonanoic acid	0.14	0.028
4-methylnonanoic acid	0.2	0.040
7-methyldecanoic acid	0.08	0.016
4-methyldodecanoic acid	0.012	0.002
Isoprenoid acids	**IC_{50} (mM)**	**IC_{50}/n (mM)**
2,6-dimethylheptanoic acid	0.24	0.080
3,7 dimethyloctanoic acid	0.06	0.020
2,6,10-trimethylundecanoic acid	0.015	0.005
Adamantane acids	**IC_{50} (mM)**	**IC_{50}/n (mM)**
1-Adamantanecarboxylic acid	0.78	0.260
1-adamantane ethanoic acid	0.67	0.223
3, 5-dimethyl-1-adamantane carboxylic acid	0.57	0.190
3, 7-dimethyl-1-adamantane ethanoic acid	0.34	0.113
Branched aromatic acids	**IC_{50} (mM)**	**IC_{50}/n (mM)**
4-ethylphenylethanoic acid	0.214	0.043
4-n-propylphenylethanoic acid	0.394	0.079
4-n-butylphenylethanoic acid	0.250	0.050
4-n-pentylphenylethanoic acid	0.044	0.009
4-n-hexylphenylethanoic acid	0.023	0.005
Cyclohexyl acids	**IC_{50} (mM)**	**IC_{50}/n (mM)**
Cyclohexylcarboxylic acid	1.300	0.325
3-cyclohexylpropanoic acid	0.410	0.103
4-cyclohexylbutanoic acid	0.110	0.028
5-cyclohexylpentanoic acid	0.050	0.013
Decahydronaphthalene Acids	**IC_{50} (mM)**	**IC_{50}/n (mM)**
Decalin-2-carboxylic acid	0.218	0.073
Decalin-2-ethanoic acid	0.027	0.009
3-Decalin-1-yl-Propanoic acid	0.004	0.001

n-acid n=6; methyl branched *n*-acid n=5; isoprenoid acid n=3; adamantane acid n=4; mono-aromatic acid n=5; cyclohexyl acid n=4; decalin acid n=3

4.3 Results and Discussion

4.3.1. Microtox™ Assay

Comparison of the Microtox™ assay results show that, in general, the IC_{50}, IC_{20} and IC_{10} endpoints are all similar with a range of IC_{50} 0.49- 0.83 mM, IC_{20} (0.42-0.21 mM); and IC_{10} (0.1-.24 mM) for all but the aromatic group IC_{50} and the decalin group IC_{20} and IC_{10} which lie outside of these ranges by a factor of ~2 (Table 4.3).

Table 4.3. Inhibition endpoint concentrations for the mixture toxicity assay on the Microtox™.

	IC_{50} (mM)	IC_{20} (mM)	IC_{10} (mM)
Name of NA			
Total Mix	0.77	0.32	0.2
n-acid	0.74	0.3	0.18
m-b n-acid	0.68	0.29	0.17
Isoprenoid	0.75	0.36	0.24
Aromatics	1.45	0.42	0.2
Cyclohexyl	0.82	0.21	0.1
Adamantane	0.64	0.3	0.19
Decalin	0.49	0.14	0.07

m-b n-acid is methyl branched n-acid

A statistical analysis of the IC_{50} data gives an Analysis of Variance (ANOVA) p value of 0.0082 indicating a statistical difference in means of the eight variables at a 95% confidence level (Cochran's variance check p value = 0.07 indicating

no difference in the variance of the eight variables). In order to determine if the individual means show a statistical difference a Student-Newman-Keuls multiple comparison test was carried out. The multiple comparison tests indicated that all groups except the aromatics were homogenous (Figure 4.1).

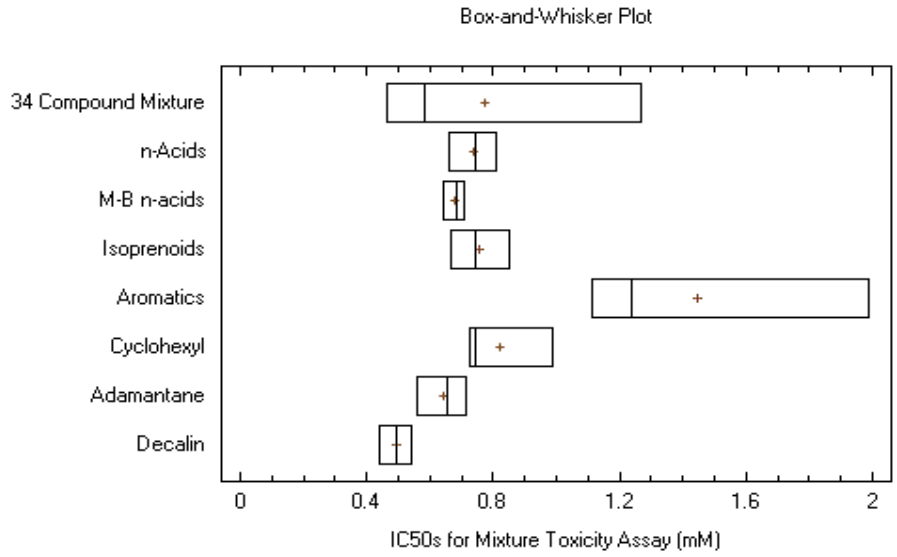

Figure 4.1. Box and Whisker plot for the IC_{50} mixture toxicity data from the Microtox™ assay, boxes represent interquartile ranges, medians are represented by lines across the boxes and the means are shown as a cross**.**

When the IC_{20} values were assessed it was found that there was no statistical difference between the means of the eight variables (p=0.21) however an initial Cochran's Variance test failed with a p value of 0.044 which highlights a statistical difference within the standard deviations at a 95% confidence level, though the Cochran's test has a 5% chance of declaring a difference where there is none.

In the case of the IC_{20}s a –Log transformation of the data was carried out. The –Log transformation revealed that there is no statistical difference between the 8

variables (p-value 0.06). Log transformed data produced a p-value of 0.08 for the Cochran's test indicating that there is no statistical difference in the standard deviations at a 95% confidence level. As the p-value for the ANOVA is close to 0.05 it is possible that an erroneous result has been produced. Checking the multiple comparison test reveals that all but the decalins and aromatic groups are homogenous and a statistical difference is evident between these two groups (Figure 4.2).

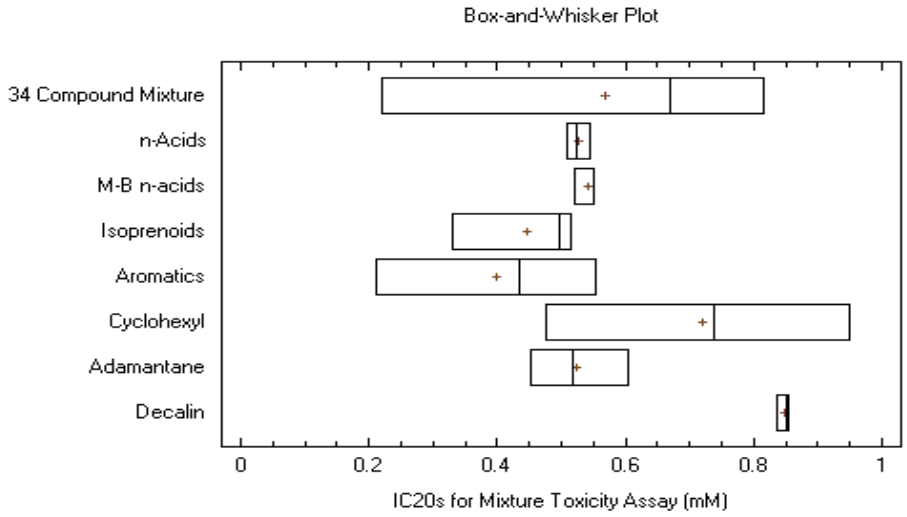

Figure 4.2. Box and Whisker plot for the IC_{20} data from the mixture toxicity assay, boxes represent interquartile ranges, medians are represented by lines across the boxes and the means are depicted as a cross.

Analysis of the EC_{10} values revealed that no statistical difference was apparent in the means of the eight variables at a 95% confidence level (ANOVA p=0.22). However the subsequent Cochran's test failed (p= 0.02) showing a difference in the standard deviations at a 95% confidence level. A –Log transformation of the data was carried out. The –Log transformed data produced a p-value from an ANOVA test of 0.04 (Cochran's variance test p-value 0.18) showing no

statistical difference at a 95% confidence level. Analysis of the Multiple Range Tests showed that at all groups were homogenous (Figure 4.3).

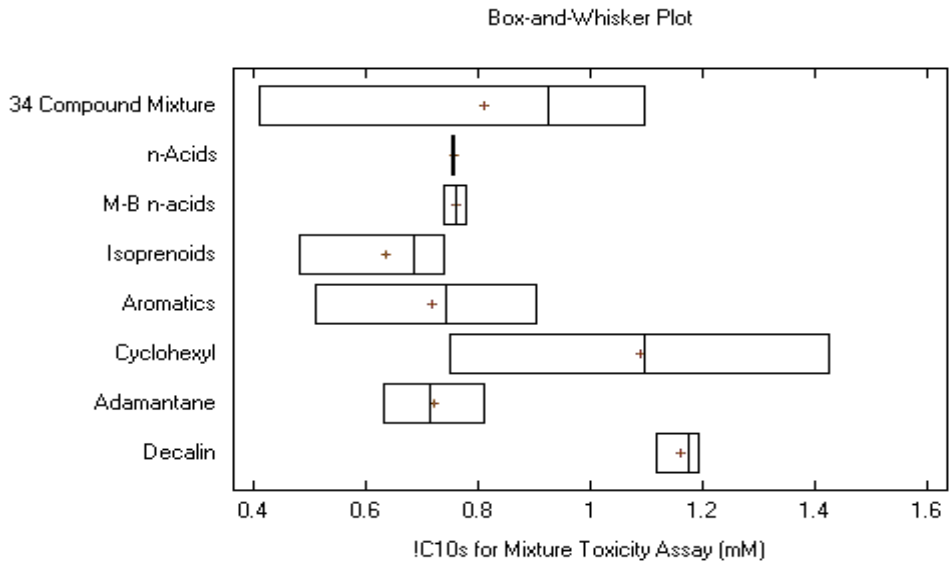

Figure 4.3. Box and Whisker plot for the IC_{10} data from the mixture toxicity assay, boxes represent interquartile ranges, medians are represented by lines across the boxes and the means are depicted by a cross.

Figure 4.4 shows that the aromatic acids are slightly less toxic than the other structural groups (IC_{50} 1.45 mM ± 0.27 SE). The mono-aromatic acids have yet to be identified in the analysed sample of the Syncrude OSPW acid extract, though they are present as a minor component in a commercial preparation of NA (Rowland et al., 2011c). With respect to baseline, or narcosis, toxicity it is not likely that these compounds will have a major acute toxicity based contribution to the overall narcotic toxicity of OSPW derived or commercial NA.

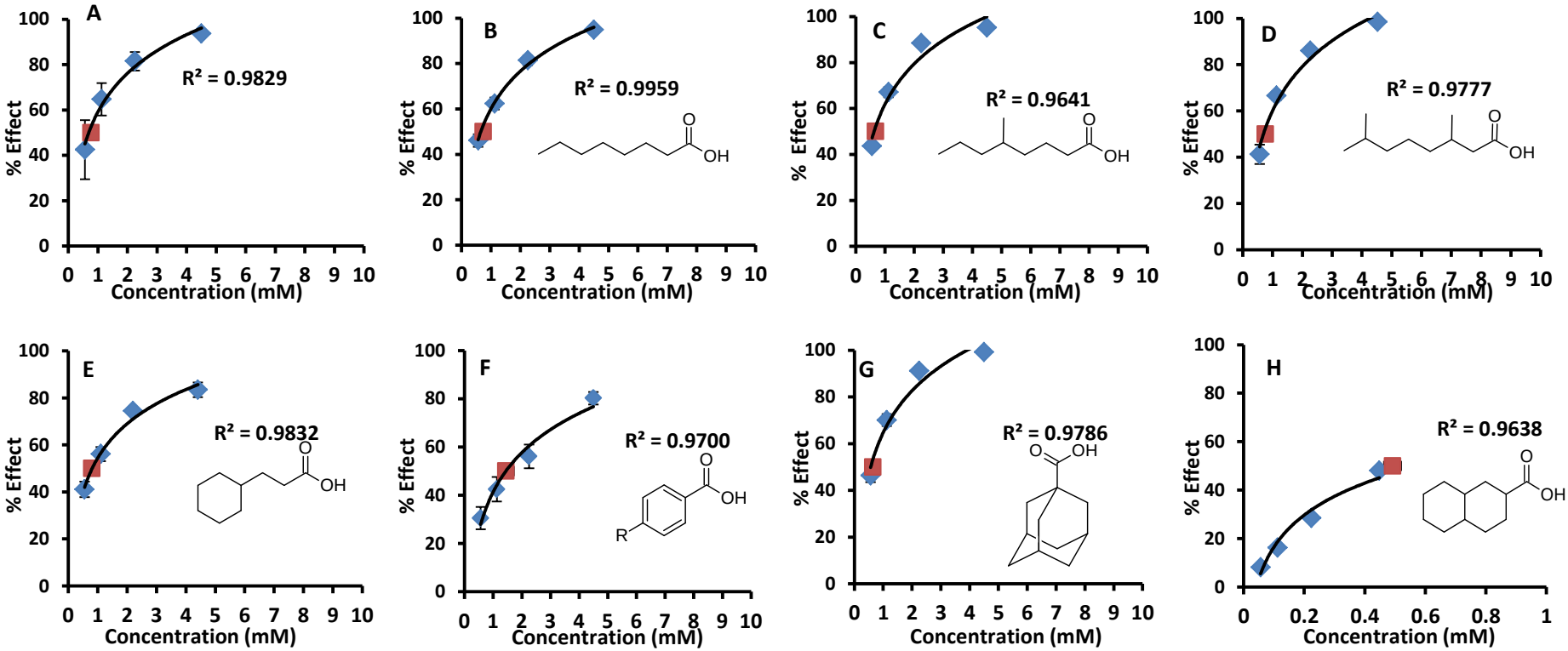

Figure 4.4. Dose-response curves for each of the seven separate structurally classified groups and the 34 compound total mixture; IC_{50}s are indicated with a red square; error bars are 1x standard error. Displaying (A) 34 compound total mixture; (B) *n*-acids; (C) methyl branched *n*-acids; (D) isoprenoid acids; (E) monocyclohexyl acids; (F) branched mono-aromatic acids; (G) adamantane acids; and (H) decalin acids.

Decalin acids exhibited the greatest mixture toxicity (IC_{50} 0.49 mM ± 0.03); this is unsurprising as this mixture also contained the most toxic individual acid (3-decalin-1-yl-propanoic acid) (Table 4.1; Chapter 3, Jones et al., 2011). However, as stated in Chapter 3, bicyclic acids, such as decalin type acids have not yet been identified within the sample of Syncrude OSPW acid extract, (though unidentified bicyclic acids are present (Rowland et al., 2011b)) so these acids will not add to the overall toxicity from the analysed sample of Syncrude OSPW acid extracts. However these acids have been identified in a sample of commercial acids (Rowland et al., 2011c) and may be present in other samples of OSPW.

All the other mixtures have IC_{50} values between 0.64 and 0.82 mM (mean 0.73 mM ± 0.03). Interestingly the adamantane mixture did not behave like the individual acids. When assessed individually the adamantanes were shown to be the least toxic and the least amenable to solubilise in NaOH.

It was apparent that possible co-solubilisation occurred with the adamantane acid mixture. When assessing the adamantane acids individually they were resistant to solubilisation when added to the NaOH and were mixed vigorously, sonicated and heated to 70^{o}C so that solubilisation could occur. When assessed as a mixture the adamantanes solubilised with relative ease. It is also notable that when assessed as a mixture the adamantanes were shown to be the second most toxic group (IC_{50} 0.64 mM ± 0.05).

Overall the toxicity expressed on the Microtox™ assay can be described as low to medium (low aquatic toxicity IC_{50} >100 mg L^{-1}; medium aquatic toxicity IC_{50} 10-100 mg L^{-1}; (USEPA., 2011 available: http://www.epa.gov/dfe/alternatives_assessment_criteria_for_hazard_eval.pdf) however it must be noted that this is one test for narcosis on a marine bacterium and therefore toxicity results should be expressed with care. Comparison of quantitative structure activity relationships between *V. fisheri* and fathead minnows (*Pimephales promelas*) by Dearden et al (1995) suggest that for polar narcotics there are specific modes of action that occur in the fish that are not apparent in the bacterium therefore NA may express additional modes of action not seen in this current study.

4.3.2 Mixture Toxicity

Equation 1 is able to model an endpoint that would agree with the CA concept. Analysis of this data enables a determination of whether the toxicants (in this case NA) are acting in this manner.

Table 4.4 depicts the assayed groups, predicted IC_{50}'s derived from equation 4.1, the observed Microtox™ assay IC_{50}s and the relevant MDRs (Predicted/Observed IC_{50}s). As discussed in section 4.2.2 a MDR of 1 describes CA, an applied factor of two allows an MDR between 0.5 and 2 to describe CA. Values greater than 2 are said to designate a synergistic response and less than 0.5 indicate an antagonistic response. As can be seen only the adamantane and cyclohexyl type acids are acting within the CA concept (MDR 0.92 and 0.57 respectively) whilst remaining groups seem have an antagonistic

response with respect to CA. This result refutes the hypothesis of CA for the bulk of the mixtures and underlines the importance of this work.

Table 4.4. Predicted and observed IC_{50}s derived from equation 4.1 and the Microtox™ assay with calculated MDR values.

Group	Predicted IC_{50} (mM)	Observed IC_{50} (mM)	MDR
Total Mix	0.218	0.770	0.283
n-acids	0.272	0.740	0.368
mb-n-acids	0.183	0.680	0.269
Isoprenoids	0.104	0.750	0.139
Cyclohexyl	0.467	0.820	**0.570***
Aromatics	0.220	1.450	0.152
Adamantanes	0.589	0.640	**0.920***
Decalins	0.084	0.490	0.170

* Bold figures indicate MDRs that are within a factor of 2 of an MDR value of 1 and describe CA effectively.

In the case of cyclohexyl acids the MDR is close to the proposed cut off of an MDR of 0.5. As the MDR is not widely used it is impossible to determine whether an MDR near to the proposed limits of 0.5 or 2 (Deneer., 2000) can actually be said to be indicative of CA or whether an unknown small deviation must be taken into account. In the case of cyclohexyl acids an addition effect is in agreement with Tollefsen et al (2012). Although it is clear that even though the cyclohexyl acids are within the proposed factor of 2 the actual predicted and observed IC_{50}s are quite different (Table 4.4). It is also worth noting again that Tollefsen and colleagues assayed mixtures of mono-aromatics and cyclohexyl type acids on a hepatocyte rather than a living organism assay.

Adamantane acids are therefore the only group of the eight tested mixtures that conform closely to a concentration addition response. When calculated the

MDR was derived as being 0.92, showing that adamantane mixtures potentially act through CA.

It seems then that adamantane acids tend to behave differently to other compound groups both individually and in mixtures (Section 4.3.1). In the case of the mixtures adamantanes are the only group that seem to be acting in accordance with CA. Adamantanes have a low toxicity and have been found to not affect an estrogenicity based bio-assay (Scarlet et al., 2012) these results are not likely to affect the overall toxicity of the super-complex mixture of OSPW derived NA, even though adamantanes have been found in the acid extracts of OSPW in abundance (e.g. Rowland et al., 2011b; Scarlett, (2013) Personal Communication).

When assessing adamantane type acids it would be remiss not to comment on the structural differences compared to the other assayed groups. Whilst the other groups containing rings are planar in structure adamantanes have what is termed a cage type structure (Figure 4.5) which may indicate that adamantanes act via a specific MOA which is not detected when assaying with the Microtox™.

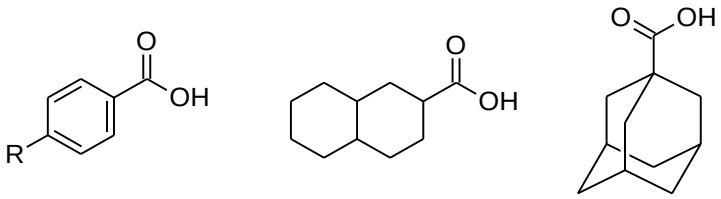

Figure 4.5. Structure comparison of (A) mono aromatic acid, (B) decalin acid and (C) adamantane acid

The smaller individual observed toxicity (Chapter 3) would indicate that a small amount of narcosis is occurring but the principal mode of action possibly remains undetermined. As adamantane acids have only recently been determined in acid extracts of OSPW little work on their toxicology has been carried out, in fact this current study may well be the first analysis of their toxicity in relation to NAs (e.g. Jones et al., 2011; Chapter 3).

A question remains though: why is it only the adamantane acids that seem act in this manner when NAs as a whole are thought to act with a similar MOA (narcosis) (Frank et al., 2008) When assessing the other MDRs it can be seen that they are all very similar (range 0.139-0.368) and act in a somewhat antagonistic manner, however these MDRs are still relatively close to the 0.5 MDR cut off (Figure 4.5) so it is possible that other mechanisms are involved which are reducing the relative toxicity of the mixtures and therefore indicating an antagonistic response erroneously.

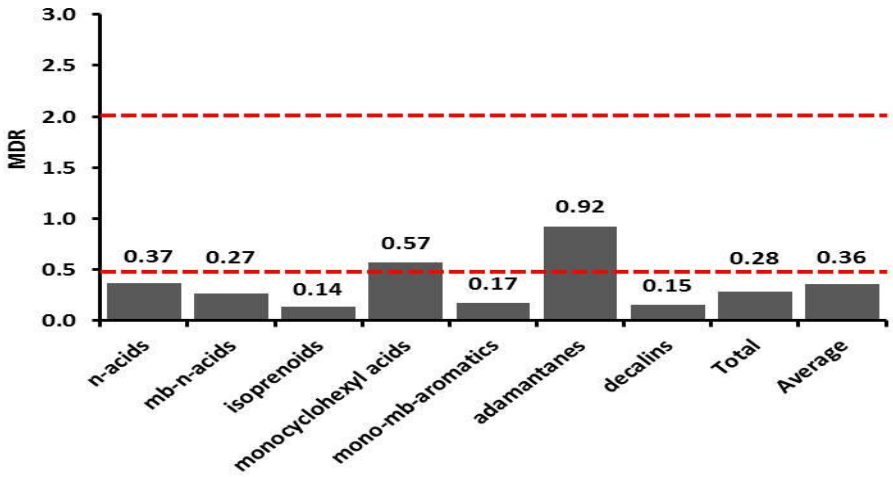

Figure 4.5. Model deviation ratios for the assayed NA mixtures**,** red dotted line indicates factor of 2

However whilst the MDR remains a convenient way to assess the similarities between the predicted and observed toxicity endpoints the factor of 2 cut off remains an arbitrary constant originally applied by one researcher (Deneer, 2000) and used rarely in the study of mixture toxicity. Therefore, whether or not the results are 'close to' the cut off or not the MDRs, apart from the adamantane mixture, still exhibit the characteristics of an antagonistic response with respect to the CA concept.

It is possible that when interaction with the cell membrane occurs that a certain amount of competitive binding to the sites of toxic action occurs (e.g. Hodgson., 2010). This is a well know pharmacological effect and is able to mediate agonistic effects of a toxicant to a cell membrane. It is also able to reduce the effects on the cell membrane from compounds that usually act with a similar MOA (Hodgson, 2010) thus producing an antagonistic result when, in essence, CA is occurring.

This could explain why, when it is generally assumed that NAs act via a similar MOA and the Microtox™ assay assesses this MOA, the acid groups did not act in accordance with the hypothesis of CA. Another test of competitive binding is analysis of the dose response curves from the mixture and how they correspond to the dose response curves from the individual components (Hodgson., 2010). Figure 4.6 shows this relationship between the trends of the individual compounds dose response curves and the dose response curve of the mixture toxicity. Figure 4.6 reveals that it is noticeable that for a number of the mixtures the average individual toxicity (red triangle data points; Chapter 3; Jones et al., 2011) and the IC_{50}s for the mixtures (blue square data points) are relatively close; with only the decalin mixture and the mono-aromatic mixtures exhibiting a distinct difference. This indicates that for some of the mixtures the observed toxicity is not that far off that of the individual compounds.

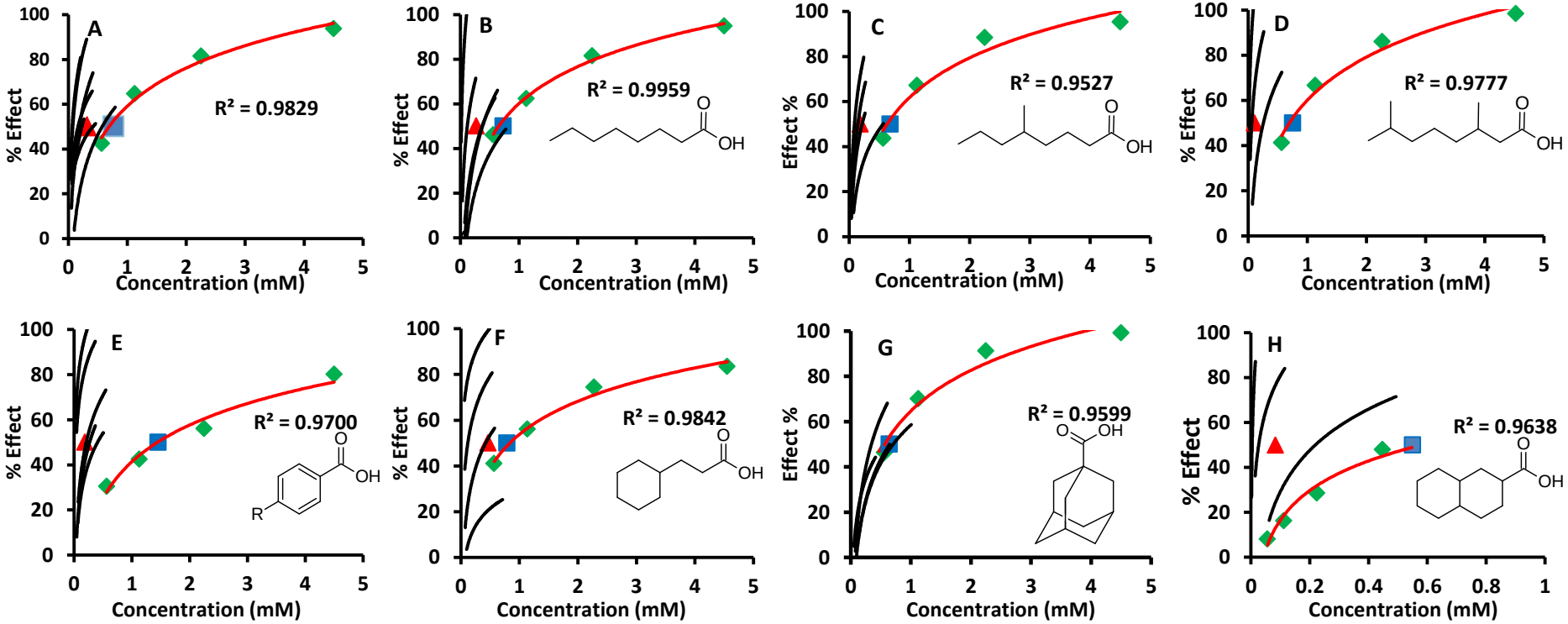

Figure 4.6. Relationship between observed trends for the dose response of the mixture toxicity assay (Red trend line) and the observed trends for each individual component of the mixtures (black trend lines) except for the 34 component mix where the black lines represent the average trend for each structural group. Red triangles represent the average IC_{50} from the individual groups; blue squares indicate the IC_{50} from the mixture assay. Displaying (A) 34 compound total mixture; (B) *n*-acids; (C) methyl branched *n*-acids; (D) isoprenoid acids; (E) monocyclohexyl acids; (F) branched mono-aromatic acids; (G) adamantane acids; and (H) decalin acids. Individual IC_{50} data points for each assayed acid were not displayed for reasons of clarity and are available in Chapter 3.

It is equally and possibly more likely, that the acids in the mixtures act as surfactants and create micelles in the solutions (Personal Communication, Scarlett, 2013), if this is the case then a Critical Micelle Concentration (CMC) is required before a toxic response is evident (Schramm et al., 2000). The reaching of a critical concentration would give an explanation as to why the toxic responses of the bulk of the mixtures are below that expected and would explain the Microtox™ response to the adamantane type acids. The adamantanes, being the least toxic in the individual studies (Section 3.3.1.3, Chapter 3) will therefore have been added to the mixtures in higher concentrations, thus potentially crossing the CMC, hence realising a toxic effect in the predicted range.

Surfactants are well known to create micelles when in an aqueous solution. Micelles are formed when the hydrophobic ‘head’ of the compound interacts with the solvent and the hydrophilic ‘tail’ is sequestered in the centre of the micelles. It has been noted that once the CMC is realised the chemical properties of the micelles, and thus the surfactants change (e.g. Schramm and Maragoni, 2000). It has also been noted that the CMC can change the aqueous solubility of chemical and affect the interfacial tension (amongst other properties) (Schramm and Margoni, 2000). This suggests that far greater co-operative processes are taking place when the CMC is achieved (Schramm and Maragoni., 2000) . The changes in properties may also have an effect on the toxicity of the surfactants.

4.3.3 Limitations of the Study

This mixture assay was performed on a small amount of known compounds existing in both a sample of the OSPW acid extracts and a sample of a commercial mixture, not all of the compounds are present in both so elucidation of these results, to describe the toxicity of the total acid components of the OSPW or commercial mixtures, would not be advised. Both of these complex mixtures include compounds that have only, as yet, had toxicity modelled (Scarlett et al., 2012) or not assessed at all and in some cases are more likely to induce chronic (estrogenic or gene expression effects) rather than acute effects, so assaying via the Microtox™ would not help determine actual toxicity. Both of these mixtures also contain many compounds that have not had any structural properties assigned, so it is unknown how much of the toxicity of the complex mixtures is explained by these unknown components.

The generally observed acute toxicity of these mixtures can be described as low to medium (USEPA., 2011), but this is in respect to the MOA determined by the analysis of the reduction in bioluminescence to *V. fisheri*. It is unknown what, if any, chronic life cycle or estrogenic effects that these mixtures would have. That the adamantanes have been determined not to affect the CALUX bioassay (Scarlett et al., 2012) is reassuring but the other compounds in this mixture assay have not been tested either individually or as mixtures.

It would therefore be prudent for further research to be carried out on the mixtures of naphthenic acids, following both the previously described mixture design and a binary mixture design. A toxicological assay based upon the independent action concept should also be considered.

4.4 Conclusions

This study tested the assumption that NAs act by CA. To test this hypothesis a series of structurally similar and dissimilar mixtures were created and tested with the Microtox ™ assay. It was determined that for most of the mixtures the CA assumption was incorrect. The hypothesis was rejected and antagonism was observed.

However, as noted, it is likely that some form of CMC is needed before a toxic response is noted. Work on the NAs is, at present, on-going to confirm or deny the CMC hypothesis (Personal Communication, Scarlett, 2013).

This study is a timely addition to the knowledge of NA toxicity and to the knowledge of the Microtox™ limitations when assessing toxicity. To the authors knowledge this is this first time that identified (rather than surrogate) naphthenic acids have been used in a mixture toxicity study.

Chapter 5.

Fractionation, Characterisation and Identification of Complex Mixtures of 'Naphthenic Acids'

5.1 Introduction

It would be of use to researchers investigating individual compounds in complex mixtures of naphthenic acids (NAs) if the acids could first be fractionated into less complex mixtures. Previous research by Knoterus (1957) and Seifert (e.g. 1975; discussed in Chapter 2) suggested for instance that aromatic acids, far from being minor components of NA mixtures, could be relatively abundant, but this was difficult to show in such complex mixtures. This view was also upheld somewhat much more recently by research by Kavanagh et al. (2009) who used synchronous fluorescence spectroscopy to suggest the presence of aromatics in NAs. Thus it would seem that a separation of alicyclic from aromatic naphthenic acids might be desirable.

Thin layer chromatography (TLC) with a silver impregnated solid phase (Ag^+TLC) is a conventional method used for separation of saturated from unsaturated lipids and, it was hypothesised herein, may be able to better separate complex NA mixtures into alicyclic and aromatic fractions. Furthermore, if Ag^+TLC was successful, then silver ion open column chromatography might prove useful for separation of larger samples of NAs. Such attempts are described herein.

5.1.1. Silver Ion Chromatography

Much like the processes involved in the interaction of platinum type metals in catalytic hydrogenation (Chapter 2, this work), silver ions (Ag^+) are able to

instigate simple π- complexes with the carbon to carbon double bonds in alkenes, polyunsaturated fatty acids and aromatic moieties (Morris, 1966; Chapter 2, Section 2.1.2). Such complexes are of the 'charge-transfer' type where the alkene (or other unsaturated compound) acts as an electron donor and the transition metal (in this case, silver) acts as an electron acceptor. It is generally accepted that this takes the shape of a σ-bond forming between the occupied 2pπ-orbital of the unsaturated compound and the free 5s and 5p orbitals of the silver ion (Nikolova-Damyanova, 1992). Silver ions (Ag^+) are thereby able to retard the movement of compounds with carbon double bonds (or aromatic π bonds) in chromatographic processes, thus allowing separation in order of increasing saturation. In TLC this means that saturated compounds migrate unrestrained to the top of a TLC plate followed by monoenes, dienes and so on. (Christie, 1989; Figure 5.1).

With respect to alkenes and unsaturated fatty acids, the factors that can inhibit retardation on an Ag^+TLC plate are relatively well known. For instance it is well known that unsaturated acyclic compounds form more stable complexes than aromatic compounds and that stability can decrease with increasing analyte chain length. Conjugated compounds form less stable complexes than those that have methylene interrupted double bonds and stability is increased with greater distance between the double bonds. It has also been noted that stability is affected by isomerism. For example *cis* isomers create more stable complexes than *trans* isomers, with the lower stability of the *trans*-isomers

assigned to steric hindrance caused by ‘R’ groups when they are *trans* position to each other (de Ligny, 1976; reviewed in Nikolova-Damyanova, 1992).

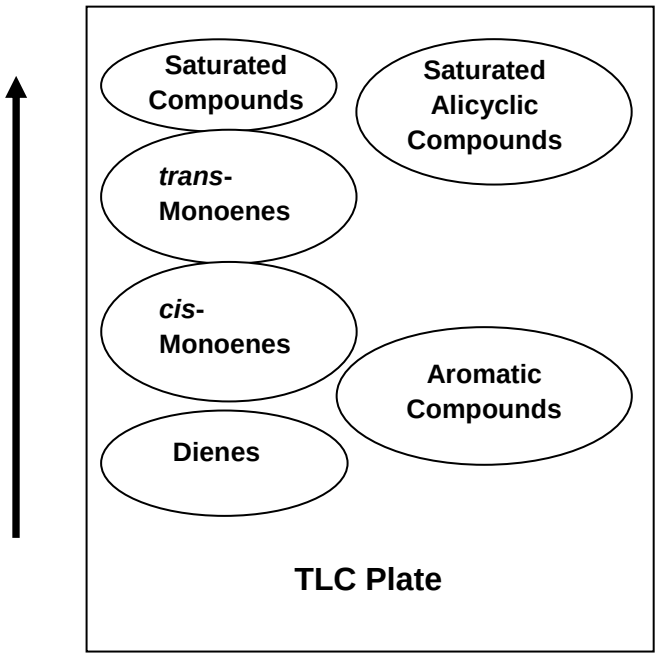

Figure 5.1. Schematic of typical alkane/alkene and alicyclic/aromatic separations on a silver ion stationary phase (e.g. Ag^+ Silica) TLC plate. Arrow indicates direction of travel of the mobile phase.

5.1.1.1. Silver Ion Thin Layer Chromatography

Winstein and Lucas, (1938) published what is generally held to be the first paper discussing complexation of Ag^+ with alkenes in which equilibrium constants for the reaction of Ag^+ with unsaturated compounds (e.g. 2-pentene, 1-hexene and dimethylbutadiene) were obtained and complex ions observed. Combinations of one silver ion and one unsaturated molecule, two silver ions and one unsaturated molecule and one silver ion with two unsaturated molecules, were noted. However it was many years until the benefits of the

silver ion complexes were realised. Working with lipophilic molecules (in essence, lipids) Nichols, (1952) was able measure the argentation constants of methyl *cis*-9 octadecenoate and methyl *trans*-9 octadecenoate and suggested that an adaptation of a paper chromatography method could be used to effect a separation of such compounds (Nichols, 1952).

However, it wasn't until 1962 that the first uses of argentation Thin Layer Chromatography (Ag^+TLC) became apparent (Morris, 1962; reviewed by Morris, 1966; Dobson et al., 1995) where it was demonstrated that Ag^+TLC was a reproducible method for the separation of *cis* and *trans* octadecenoates, and the subsequent separation of these molecules from saturated and polyunsaturated compounds was demonstrated. Since then Ag^+TLC has been generally utilised for the separation of numerous unsaturated lipids (e.g. Carpenter et al., 1976; Conacher, 1976).

Ag^+TLC plates are usually made with a stationary phase comprising silica gel impregnated with silver nitrate. The silver ion content used in TLC plates has varied over the years. Impregnation of between 10 and 20% silver ion was initially considered essential for good resolution (Homburg and Bielefeld, 1979; reviewed by Nikolova-Damyanova, 1992). However such concentrations of silver ions make the plates sensitive to oxidation in daylight, which can then significantly reduce the capabilities of the plates. Plates containing between 5 and 10% silver ions are most commonly used, though there have been occasions where the concentrations have been as low as 0.5% (Chobanov et al., 1975; reviewed by Nikolova-Damyanova, 1992). These can be prepared through an immersion technique, where the prepared plate is immersed in

either methanol, acetone or acetonitrile solutions of silver nitrate. Different ratios of hexane:diethyl ether are often used as mobile phases.

Although it is common for Ag^+TLC separations to be conducted at room temperature, there have been occasions when it has been necessary to perform the experiments at less than ambient temperature. Resolution of the positional isomers of unsaturated fatty acids or of triacylglycerols that contain these fatty acids was only possible when the Ag^+TLC plates were developed at temperatures approaching minus 20^oC (Morris et al., 1966) as the stability of the silver-double bond complex increases as the temperature decreases (Wessels and Rajagopal,1969; reviewed by Nikolova-Damyanova, 1992).

Ag^+TLC is reproducible and relatively easy to use but is somewhat time consuming. Other methods of Ag^+ based separation have thus also been developed.

5.1.1.2. Open Column Ag^+ Chromatography

Silver ion open column chromatography was first developed for use by de Vries (1962). Essentially a new preparative method was reported where glass chromatography columns were packed with silicic acid that had been suspended in a silver nitrate solution. This method was used successfully to separate fatty acid methyl esters from triacylglycerols (de Vries, 1962). The method of column preparation proposed by de Vries was utilised by many subsequent researchers (e.g. Nikolova-Damyanova, 1992). In 1965 it was noted that replacing the silica adsorbent with an acid washed Florisil (typically silicon dioxide mixed with magnesium oxide in a 85:15 ratio (US Silica, 2012)) allowed

greater sample capacity, but inferior separation (Andersen and Hollenbach, 1965; reviewed by Dobson et al., 1995). Large scale preparative separations were performed on commercially available ion exchange resin columns (Amberlyst 1005 and Amberlite XE284) and separations of fatty acid methyl esters with up to four double bonds was achieved to a reasonable purity (e.g. Emken et al., 1967; reviewed by Dobson et al., 1995). Purity and separation were improved with the development of solvent elution methods. However, for small scale separations it was noted that pre-packed columns of benzenesulfonic acid residue bonded to silica could be converted to Ag^+ columns relatively easily by eluting with a silver nitrate solution and subsequent column washes with organic solvents of decreasing polarity (Dobson et al., 1995; Christie, 1989).

In 1989 Christie reported a successful separation of methyl esters of fatty acids with zero to six double bonds using a stepwise elution scheme using commercially available pre-packed columns that he had percolated with a silver nitrate solution (Christie, 1989). Utilisation of this method has allowed separations of fatty acids from soil phospholipids (Zelles and Bai, 1993), fatty acids that can differentiate between yeast strains (Augustyn et al., 1992) and the resolution of plasma cholesterol esters with up to six double bonds (Hoving et al., 1991).

It wasn't until 2008 that pre-packed commercial Ag^+ columns were utilised and discussed in a publication. Writing in the journal *Lipids,* Kramer et al., (2008) used *Supelco Discovery*™ pre-packed Ag^+ columns (in conjunction with GC-FID for detection and monitoring) to determine most of the geometric and positional

isomers of lipids that are present in milk fat (Kramer et al., 2008). It is apparent that Ag^+SPE may have improved the resolution and separation of the fatty acid mixtures in comparison with Ag^+TLC, although this might have been due to the dual temperature programs that were used on the GC-FID; the conclusions in the publication did not make this clear.

Fritsche et al., (2010) analysed one hundred and twenty two food samples from German food markets for their $C_{18:1}$ *trans* fatty acid content. By utilising Ag^+SPE in conjunction with high resolution GC-FID, the authors were able to determine the concentrations of these *trans*-fatty acids, discovering that certain food stuffs had concentrations of up to 27% *trans*-fatty acids (Fritsche et al., 2010).

Dreiucker and Vetter (2011) investigated fatty acid patterns in camel, moose, cow and human milk, using commercially available Ag^+SPE cartridges (Supelco) and a GC-MS program in the selected ion monitoring mode (SIM). The researchers noted that pre-separation with Ag^+SPE followed by GC-MS analysis in SIM generally removed issues concerning the co-elution of fatty acids and methyl branched fatty acids which had previously hampered quantification (Destaillats et al., 2007). However co-elution was still an issue with the *anteiso*-C_{17} fatty acid and phytanic acid (3,7,11,15-tetramethylhexadecanoic acid) and the *iso*-C_{16} fatty acid and pristanic acid (2,6,10,14-tetramethylpentadecanoic acid) This co-elution was somewhat overcome by examination of mass spectral fragment ions but only the more abundant *iso*-C_{16} and *anteiso*-C_{17} acids were able to be quantified. It was also apparent that the *cis* isomer of a $C_{16:1}$ fatty acid (16:1(9)) and the *trans* isomer of a $C_{18:1}$ fatty acid (18:1 (9)) also co-eluted and hampered determination. The

authors stated that this may lead to an overestimation of the *trans* content of the mono-unsaturated fatty acid groups. Dreiucker and Vetter (2011) were able to determine structural information and hence good quantification, on 87 fatty acids in various milk samples, and suggested that Ag^+SPE coupled with GC-MS in SIM mode may well be a reasonably valid method for the determination of fatty acids in milk samples (Dreiucker and Vetter, 2011).

As can be seen from the above brief review, work with Ag^+TLC or AG^+SPE has generally been used for the determination of unsaturated fatty acid profiles. To the present author's knowledge the work detailed below is the first attempt at fractionation of highly complex mixtures of NAs using Ag^+ based chromatographic methods. These results have now been partly published (Rowland et al., 2011; Jones et al., 2012a; Jones et al., 2013) and some, by the author, presented at scientific World Congress, 2012 (Jones et al., 2012b; SETAC 2012, Berlin).

5.2 Methods and Materials

5.2.1. Materials

Solvents and authentic NAs were sourced from Sigma Aldrich (Gillingham, UK); Fisher Scientific (Loughborough, UK) and Rathburn (Walkerburn, Scotland, UK). Oil sand process-affected water (OSPW) acidic extracts were donated by Dr R Frank (Environment Canada). TLC plates were manufactured in house. Silver ion Solid Phase Extraction (Ag^+SPE) columns were *Discovery*™ 750mg/6mL SPE columns from Supelco (Pennsylvania, USA). Glassware was cleaned by the protocols detailed in Chapter 2.

5.2.2. Naphthenic Acid Extraction

A sample of Syncrude OSPW extract (extraction methods described in Frank et al., 2006) was placed in pre-rinsed 30 mL vial and the pH determined (pH 11-12). An amount of HCl was added until the pH was between 1 and 2 and the sample was a cloudy cream colour. The sample was transferred to an ethyl acetate-rinsed separating funnel. The 30 mL glass vial was rinsed with ethyl acetate and this was added to the separating funnel. The funnel was shaken vigorously for two minutes (vapour released at regular intervals) and allowed to settle. The cloudy layer was collected and the remainder extracted twice more. The emulsion that formed was stabilised by adding 3-4 drops HCl and the vial was allowed to stand overnight in the dark. The clear liquid above the emulsion was removed, added to pre-weighed vials and subsequently reduced to dryness under a steady stream of N_2. The extract was derivatised with BF_3-MeOH (Section 5.2.10) and an aliquot was analysed by GC-MS.

5.2.3. Silver Ion Thin Layer Chromatography (Ag^+TLC)

5.2.3.1 Manufacture of Ag^+TLC Plates

Glass plates were arranged in a TLC rack, clamped into position and thoroughly cleaned with acetone. 35g of silica gel (60G) was weighed into a 250mL conical flask and 70 mL of distilled water impregnated with $AgNO_3$ was added (enough to create a 5% w/w $AgNO_3$ TLC plate). The mixture was shaken until the desired consistency was achieved. The mixture was poured into a spreader (with 0.25mm as the trailing edge) which was skimmed across the surface of the glass plates. The side of the rack was beaten to remove any irregularities in the plates. When the plates had dried to a matt finish they were transferred to a holding rack and activated in the oven at 105^oC for at least one hour.

5.2.3.2. Thin Layer Chromatography Protocol

Acid mixtures and authentic acids were derivatised with BF_3-MeOH. A solution of 90:10% hexane:diethyl ether was added to a TLC tank and a paper lining was placed around the edges. Ag^+TLC plates were removed from the oven and allowed to cool; the plates were scored for the spotting of the methylated acid samples. After the addition of the analytes, the plates were placed into the TLC tank. The solvent was allowed to travel up to near the top of the plate before being removed and sprayed with a fluorescent 0.1% Rhodamine in ethanol solution. The plate was then placed under UV light (254nm) and spotting on the plate was marked and the retardation factor (R_f) was calculated.

The areas of the marked spots were then scraped onto aluminium foil which had been pre-cleaned with a DCM rinse. The scrapings were transferred to a Pasteur pipette and eluted with DCM into a pre-weighed 7 mL vial. This was

subsequently reduced to dryness under a steady stream of N_2. The vial was reweighed and made up again in 1 mL of an appropriate solvent. Each sample was analysed by GC-MS.

5.2.4. Silver Ion Open Column Chromatography

Acid mixtures and authentic acids were derivatised with BF_3-MeOH. Solvent ratios were made according to Table 5.1. The methylated acids (methyl esters, ME) and acid extracts were dissolved in hexane and reduced to dryness under a steady stream of N_2. Authentic acids (ME) were made up to 1mg per 100 μL and the acid extracts were made to 5 mg per 300 μL hexane. Ag^+SPE cartridges were prepared by wrapping the lower portion in foil and suspending above pre rinsed glass vials. Four sample cartridges in total and one control cartridge were prepared thus. The cartridges were washed three times with one column volume (6 mL) of hexane before elution. Solvent elutions followed the protocol set out in Table 5.1; SPE cartridges were not allowed to dry. The eluates were collected in separate pre-weighed vials, reduced to dryness and re-weighed before re-elution in 1 mL of hexane and analysis by GC-MS and GCxGC-MS.

Table 5.1. Method development for the solvent ratios for Ag^{+}SPE experiment

Solvent	Standards Ratio	Reps*	1st Sample Ratio	Reps*	2nd Sample Ratio	Reps*
Hexane	100	3	100	3	100	3
Hexane:Diethyl Ether	95:5	-	95:5	4	95:5	4
Hexane:Diethyl Ether	90:10	3	90:10	3	-	-
Hexane:Diethyl Ether	80:20	3	-	-	-	-
Hexane:Diethyl Ether	70:30	3	-	-	-	-
Hexane:Diethyl Ether	60:40	3	-	-	-	-
Hexane:Diethyl Ether	50:50	3	-	-	-	-
Hexane:Diethyl Ether	40:60	3	-	-	-	-
Hexane:Diethyl Ether	30:70	3	-	-	-	-
Hexane:Diethyl Ether	20:80	3	-	-	-	-
Hexane:Diethyl Ether	10:90	3	-	-	-	-
Diethyl Ether	100	3	100	1	100	1
Total Repetitions		33		11		8

*Reps = Repetitions

5.2.5. Infra-Red Spectroscopy

Infrared spectroscopy was carried out using both a Bruker Alpha FT-IR and a Bruker IFS66 Microscope FT-IR spectrometer (Ettlingen, Germany). In brief: a small amount of each fraction was placed onto the FT-IR and analysed with a 32 scan program. The data was initially analysed with Opus Version 6.5 software and Microsoft Excel™.

5.2.6. UV-Vis Spectrophotometry

For UV spectra a small amount of each fraction was dissolved in DCM and added to a 1 cm quartz cuvette. Samples were subsequently analysed on a Perkin Elmer Lambda 35 Spectrophotometer (Massachusetts, USA) with a wavelength range of 190-1100 nm and a slit width of 1 nm. The data were converted for analysis by Microsoft Excel™.

5.2.7. Elemental Analysis

Analysis for carbon, oxygen, nitrogen, hydrogen and sulphur content was carried out by OEA Laboratories, Kelly Bray, Cornwall, UK. Briefly samples were weighed into lightweight tin capsules which were combusted at 1000^{o}C under a constant stream of helium. Prior to combustion the helium stream was dosed with a volume of pure oxygen. Flash combustion at 1800^{o}C occurred and the resultant gases were passed over catalysts to ensure complete oxidation had taken place. The gases were separated on a chromatographic column and quantified by a thermal conductivity detector. The system response was calibrated to known calibration standards. Detailed methods can be found at OEA Laboratories website (http://www.oealabs.com/Services/Analysis/elementalanalysis.html).

5.2.8. Gas Chromatography Mass Spectrometry

Gas chromatography was carried out by the same methods detailed in Section 2.8 Chapter 2. Extracts were analysed using an Agilent GC-MSD (Agilent Technologies, Wilmington, DE, USA). This comprised a 7890A gas chromatograph fitted with a 7683B Series autosampler and a 5975A quadrupole mass selective detector. The column was a HP-5MS fused silica capillary column (30 m x 0.25 mm i.d x 0.25 μm film thickness). The carrier gas was helium at a constant flow of 1.0 mL min^{-1}. A 1.0 μL sample was injected into a 300°C splitless injector. The oven temperature was programmed from 40 to 300 at 10 °C min^{-1} and held for 10 min.

5.2.9. Two Dimensional Gas Chromatography-Time of Flight-Mass Spectrometry

Multidimensional gas chromatography–time of flight-mass spectrometry (GC × GC–MS) analyses were conducted using an Agilent 7890A gas chromatograph (Agilent Technologies, Wilmington, DE) fitted with a Zoex ZX2 GC × GC cryogenic modulator (Houston, TX, USA) interfaced with an Almsco BenchTOFdx™ time-of-flight mass spectrometer (Almsco International, Llantrisant, Wales, UK). The first-dimension column was a 30 m × 0.25 mm × 0.15 µm Carbowax MEGA-Wax HT (MEGA, Italy), and the second-dimension column was a 50% phenyl polysilphenylene siloxane 3 m × 0.25 mm × 0.15 µm BPX50 (SGE, Melbourne, Australia). Helium was used as carrier gas and the flow was kept constant at 0.8 mL min^{-1}. Samples (1 µL) were injected at 280 °C splitless. The oven was programmed from 40 °C (hold for 1 min), then heated to 300 °C at 5 °C min^{-1} and then held for 10 min. The modulation period was 6 s. The MS transfer line temperature was 280 °C and ion source 300 °C. Data processing was conducted using GC Image™ v2.1 (Zoex, Houston, TX, USA).

5.2.10 Accurate Mass Two Dimensional Gas Chromatography-Time of Flight-Mass Spectrometry

Accurate mass GCxGC-MS was conducted (e.g. West et al., 2012) using an Agilent 7890A gas chromatograph fitted with a Zoex ZX1 thermal modulator interfaced with a Jeol AccuTOF GCv (Jeol Inc. USA) time of flight-mass spectrometer operated in positive ion mode. The scan speed was 25 Hz. The first-dimension column was a 100% dimethyl polysiloxane 10 m x 0.25 mm x

0.25 µm DB-1 (Agilent Technologies J & W, Wilmington, DE) and the second dimension column was a 50% phenyl methylpolysiloxane 2 m x 0.1 mm x 0.05 µm DB-17 (Agilent Technologies J & W, Wilmington, DE). Helium was used as carrier gas kept at constant pressure (300 KPa). Samples (1 µL) were injected at 250 °C splitless. The oven was programmed from 40 °C (held for 5 min) and then heated to 300 °C at 2.5 °C min^{-1} (held at 300 °C for 20 min). The modulation period was 12 s. The mass spectrometer transfer line temperature was 270 °C and the ion source temperature 250 °C. The scan range was 40-550 Daltons

5.2.11. Derivatisation Methods

Between 1-10 mg of the sample acid was added to 2 mL of BF_3-MeOH in a glass vial and heated at 70^{o}C for at least 30 minutes. After removal from the heat the vial was allowed to cool and 1 mL of water and 1 mL of hexane was added. The sample was mixed via autovortex and allowed to settle into two distinct phases. The upper layer was removed into a separate vial and more hexane was added, mixed and removed. The extraction was completed between 3 and 5 times and the hexane dried over anhydrous sodium sulphate. Once dry the hexane was carefully removed to a pre-weighed vial and reduced to dryness under a steady stream of N_2. This was re-eluted with the addition of 1 mL of clean hexane and a calculated amount was added to a GC vial and made up to 1 mL to create a ~0.01 mg/mL solution. This was analysed with GC-MS (Section 5.2.8).

5.3. Results and Discussion

The total ion current GC-MS chromatogram shown in Figure 5.2 displays the typical profile of the highly complex mixture of 'naphthenic' acids (as methyl esters) in an oil sands process-affected water extract. The profile of the chromatogram is that of a generally unresolved 'hump' extending from a retention time (RT) of *ca*.10 minutes to *ca.* 32 minutes with two nodes at *ca.* 15.30 and 18.30 minutes. Because of the nature of this unresolved mixture, previous attempts to characterise components in such NA mixtures with GC-MS has often been unsuccessful (e.g. Merlin et al., 2007; Scott et al., 2008; Chapter 1, Section 1.2).

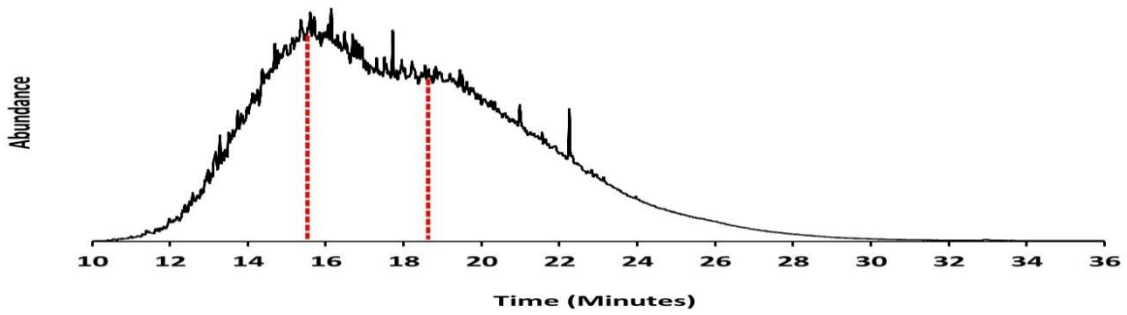

Figure 5.2. Total ion current chromatogram of the methyl esters of an acid extract from a Syncrude Oil Sands Process-Affected Water. Red dotted lines indicate position of the dual nodes within the 'hump'. GC Conditions: Column HP-5MS 30 m x 0.25 mm i.d x 0.25 μm film thickness; Solvent delay 6 minutes; oven programme 40-300^{o}C at 10^{o}C min^{-1}, hold 10 min; injector 300^{o}C); MS conditions: Source 230^{o}C, ionisation energy 70 eV, mass range 50-550 Da.

A few commentators postulated the presence of aromatic acids within such acid mixtures long ago (e.g. Knoterus, 1957) but most workers have subsequently ignored this. It was hypothesised herein that Ag^{+}TLC or Ag^{+}SPE would separate any aromatic acids from alicyclic acids in NA mixtures, and that analysis by GC-

MS might then be more successful and a search for characteristic individual ions may be able to highlight the presence of aromatic acids in one (or more) of the NA fractions. Furthermore, recent experience (e.g. Rowland et al., 2011b) suggested that analysis by GCxGC-MS might then be even more efficient at separating the less complex fractionated mixtures.

5.3.1 Silver Ion Thin Layer Chromatography

5.3.1.1. Thin Layer Chromatography of Aromatic Acids (ME)

The methyl esters of cyclohexylpropanoic and phenylpropanoic acids were combined and analysed by GC-MS to determine the RT and reference mass spectra (Figure 5.3)

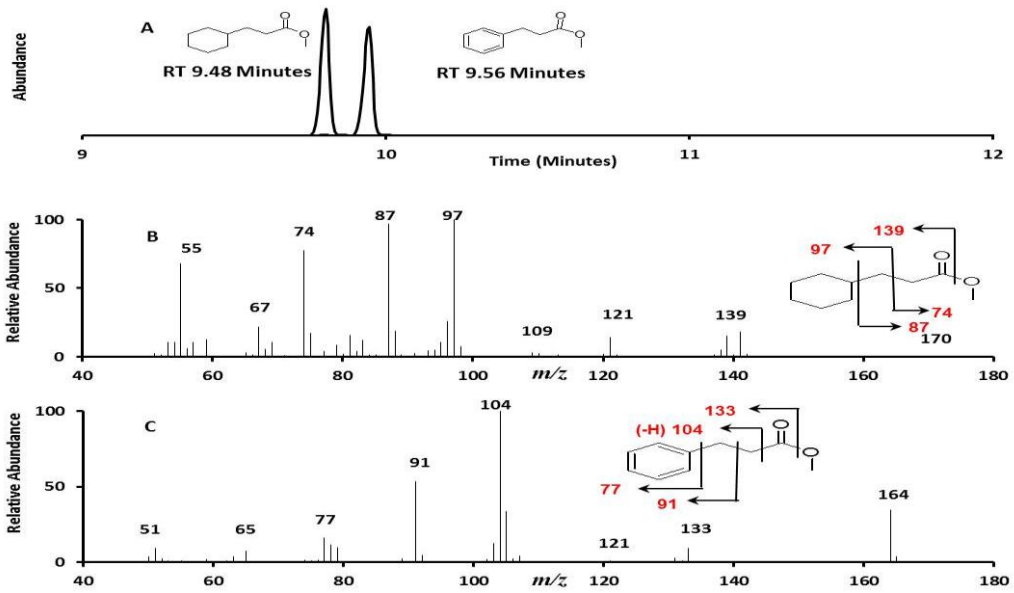

Figure 5.3. (A) Total ion current chromatogram of a mixture of the methyl esters of cyclohexylpropanoic and phenylpropanoic acids. (B) Mass spectrum of the component eluting at RT 9.48 minutes assigned as cyclohexylpropanoic acid methyl ester. (C) Mass spectrum of the component eluting at RT 9.56 minutes assigned as phenylpropanoic acid methyl ester. GC-MS conditions as described in Figure 5.2 .

The chromatogram (Figure 5.3A) displayed two distinct peaks at RT 9.48 and 9.56 minutes. When examining the mass spectra it was revealed that the component at RT 9.48 minutes had a $M^{+\bullet}$ at *m/z* 170, consistent with a cyclohexylpropanoic acid, methyl ester. Significant fragment ions at *m/z* 139 and *m/z* 97 (loss of methoxy and ethanoate moieties respectively) and at *m/z* 87 and 74 which result from and describe cleavage of the alkanoate side chain. A small ion at *m/z* 83 was consistent with the loss of the alkanoate side chain leaving a charged cyclohexyl species ($C_6H_{11}^+$). The spectrum of the component at RT 9.56 minutes had a $M^{+\bullet}$ at *m/z* 164, consistent with a phenylpropanoic acid methyl ester. Significant fragment ions at *m/z* 133 and 104 described the cleavage of a methoxy and a carboxylate ion. Fragment ions at *m/z* 91 and 77 are characteristic of the presence of an aromatic ring due to the formation of the $C_7H_7^+$ tropylium and phenyl $C_6H_5^+$ ions.

The two acids (ME) were spotted just above the baseline of a Ag^+TLC plate and allowed to develop in 90:10 hexane:diethyl ether as the mobile phase. GC-MS of the two resulting TLC bands (Figure 5.4) revealed that the standards were separated with *ca.* 93% of the cyclohexylpropanoic acid (R_f 0.76-0.83) and *ca*. 97% of the phenylpropanoic acid (R_f 0.64-0.72) appearing in different bands (Figure 5.4; Table 5.2).

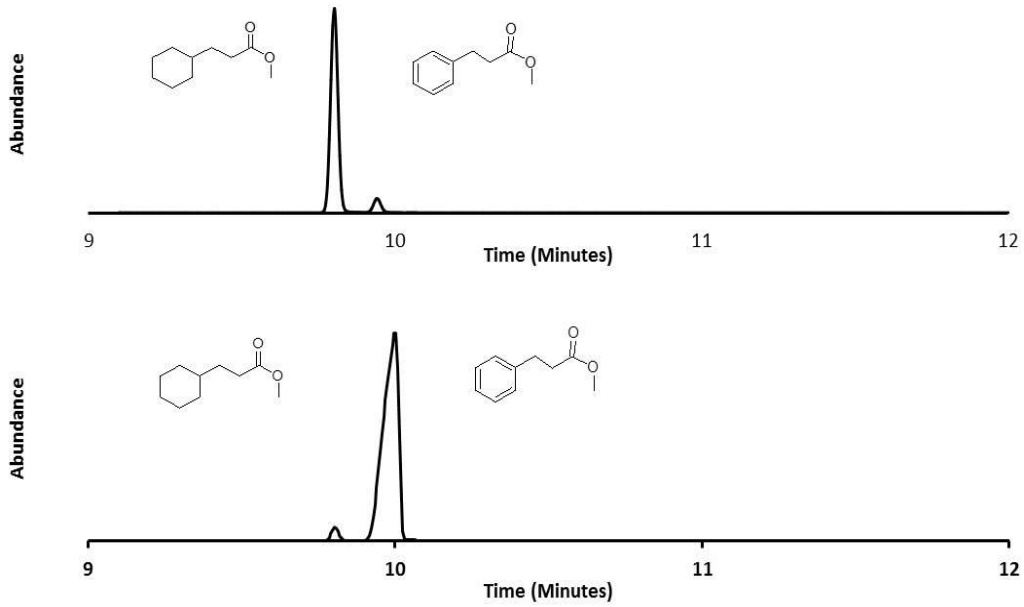

Figure 5.4. Total ion current chromatograms from GC-MS analysis of (A) upper band (R_f 0.76-0.83) of Ag^+TLC plate; and (B) lower band (R_f 0.64-0.72) of Ag^+TLC plate. GC-MS conditions as described in Figure 5.2.

Table 5.2. Percentages and R_f values from the integration of the TIC chromatographic peaks in Figure 5.4 A and B.

Ag^+TLC R_f	Cyclohexylpropanoic acid methyl ester %	Phenylpropanoic acid methyl ester %
0.76-0.83	93	3
0.64-0.72	7	97

5.3.1.2. Ag^+ Thin Layer Chromatography of the Acid Extracts of an Oil Sands Process Water

Since the previous experiment had demonstrated conditions for successful separation of alicyclic from aromatic acids as methyl esters, a small amount (1mg) of an acid extract (again as the methyl esters) from an OSPW was

dissolved in hexane and applied to a fresh Ag^+TLC plate. After development, elution of separated bands and analysis of these by GC-MS, three fractions were obtained (Figure 5.5). The results have been published in part (Rowland et al., 2011c)

Unlike the total ion chromatogram of the esters of the unfractionated OSPW acids (Figure 5.5A) all the Ag^+TLC fractions had single nodes (Figure 5.5B-D). The chromatogram of an Ag^+TLC fraction (R_f 0.74-0.82) revealed an unresolved chromatographic 'hump' maximising at *ca.* RT 16 minutes, with three relatively resolved peaks at *ca.* RT 21, 22 and 23 minutes (Figure 5.5B), whereas that of a further fraction (R_f 0.72-0.74) revealed an unresolved 'hump' maximising at *ca* RT 19 minutes, with two relatively resolved peaks at *ca.* RT 22 and 23 minutes (Figure 5.5C). Finally a further fraction (R_f 0.66-0.72) revealed an unresolved unimodal hump maximising at *ca* RT 22 minutes, with resolved peaks at *ca.* RT 17, 18 and 23 minutes (Figure 5.5D).

The initial and final fractions (R_f 0.74-0.82 and 0.66-0.72) had a similar R_f values to those of the monocyclic and monoaromatic authenic acids (ME; Table 5.2). It was expected that fraction R_f 0.74-0.82 would contain mainly alicyclic acid methyl esters as it was less retained and that fraction R_f 0.64-0.72 might contain esters of aromatic acids more retarded by complexation with Ag^+ . Fraction R_f 0.72-0.74 potentially contained a mixture of both.

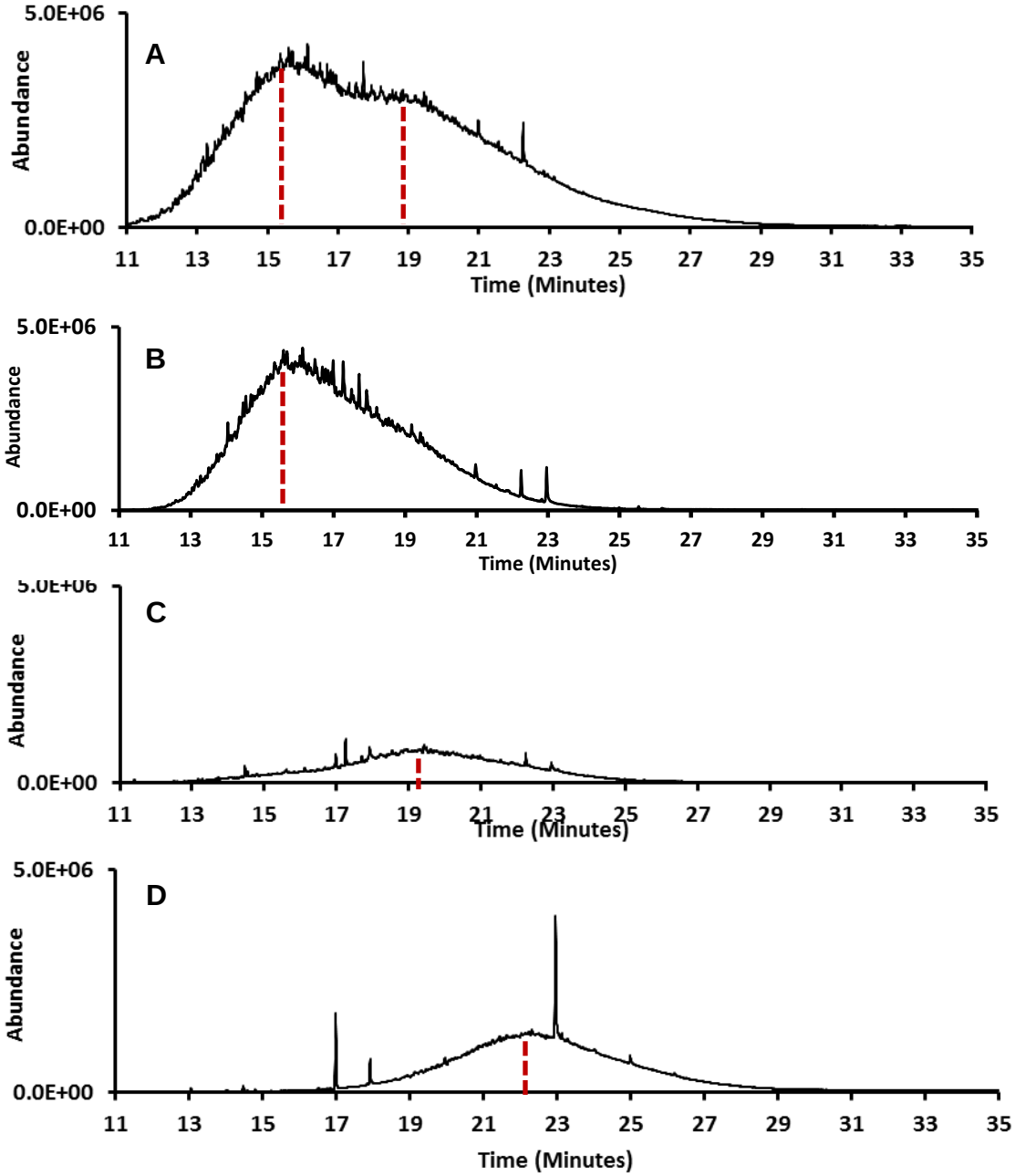

Figure 5.5. Total ion current chromatograms of Ag^{+}TLC fractions, revealing (A) Unfractionated acid extracts as methyl esters. (B) Fraction R_f 0.74-0.82 (node at ca RT 16 minutes). (C) Fraction R_f 0.72-0.74 (node at ca 19 minutes). (D) Fraction R_f 0.66-0.72 (node at ca 22 minutes). GC conditions as described in Figure 5.2. Red dotted lines highlight shifts in node position through the three fractions.

Figure 5.5 also reveals the subdivisions of the initial bi-nodal mixture of acids in the OSPW by Ag^{+}TLC. It can be seen that the node of the 'hump' in the less retained fraction matches the first node in the bi-nodal acid chromatogram of the unfractionated OSPW, whereas the second node of the unfractionated acids matches the single node in Ag^{+}TLC fraction R_f 0.72-0.74. Ag+TLC fraction 0.66-0.72 suggests a third node, not apparent from analysis of the unfractionated acids.

The collected fractions were too small to be accurately weighed with the available micro-balance so in order assess the differences in the amounts present, a manual integration of the total GC-MS peak areas was performed (Figure 5.6). The largest fraction by peak area was fraction R_f 0.74-0.82 (81%), which was the least retarded and assumed to contain principally non-aromatic alicyclic compounds by reference to the similar R_f of cyclohexylpropanoic acid, methyl ester. The next largest fraction was fraction R_f 0.66-0.72 (16%), which had a similar R_f to phenylpropanoic acid, methyl ester, and was assumed to contain esters of aromatic acids. Fraction R_f 0.72-0.74 (3%) was the least abundant fraction and was assumed to contain both alicyclic and aromatic acid methyl esters (Rowland et al., 2011c).

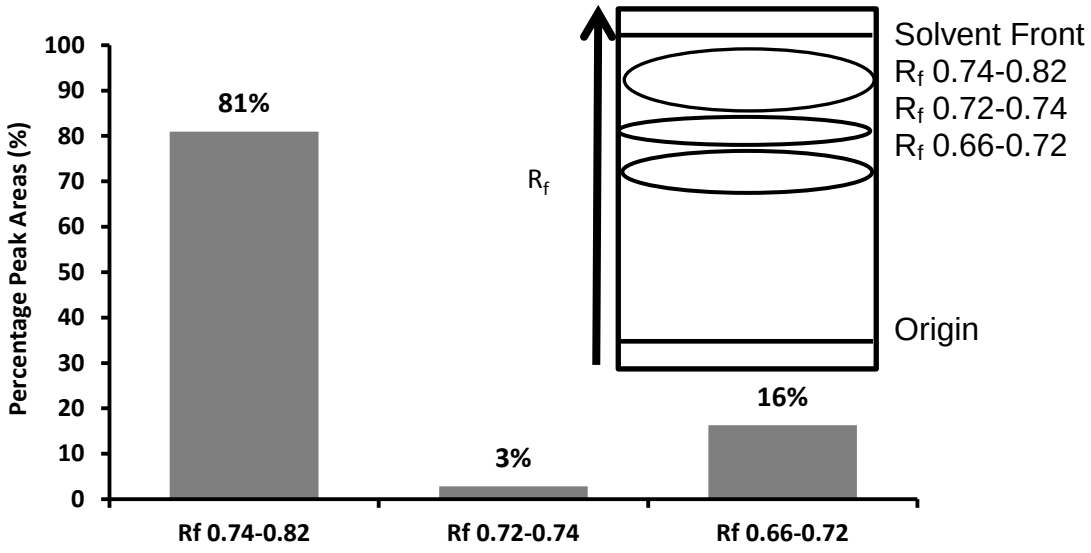

Figure 5.6. Percentage area of each TLC fraction from an integration of the 'humps' revealed by the total ion current chromatograms in Figures 5.5. Box insert reveals a schematic of the Ag^{+}TLC plate with the relative positions of each fraction.

An averaged mass spectrum from the total ion current chromatogram of fraction R_f 0.74-082 was produced (Figure 5.7). The base ion was shown to be *m/z* 95, typical of the mass spectra of many alicyclic acids (ME)(Cason and Khodair, 1966). Mass chromatography of selected ions was used to focus on specific NAs. The fragment ions *m/z* 135 and 163 were profiled as these are key ions within the EI mass spectra of known alicyclic NA MEs (Rowland et al., 2011b). The ion at *m/z* 149 was not used as this ion is abundant in the spectra of alkyl phthalates which are often contaminants from plastics used in sample work up (David et al., 2003). The averaged mass spectrum in Figure 5.7 also revealed several potential even numbered molecular ions ($M^{+\bullet}$; *m/z* 272-328), including the $M^{+\bullet}$ (*m/z* 314) of tentatively identified monoaromatic (A ring opened) steroidal keto acids (Rowland et al., 2011c).

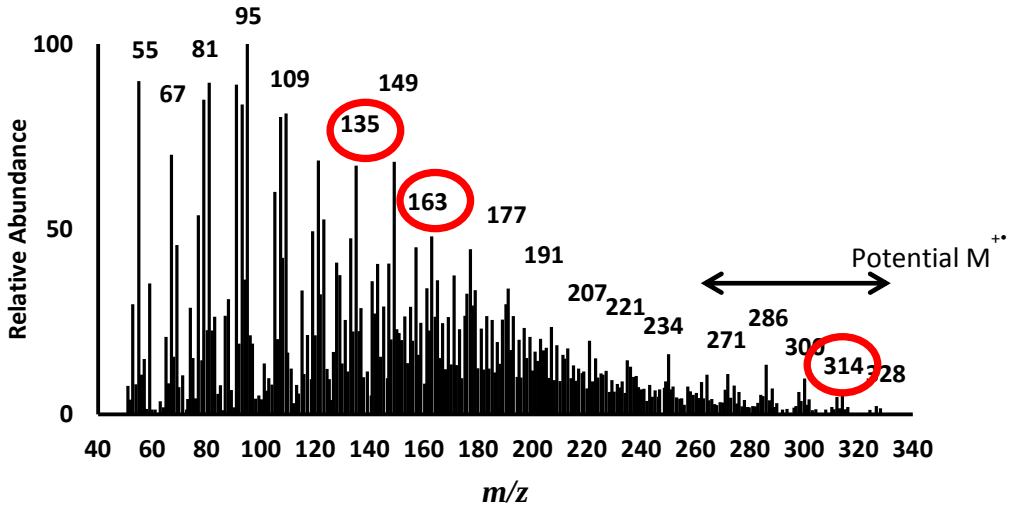

Figure 5.7. Averaged mass spectrum generated from the whole total ion chromatogram of Ag^{+}TLC fraction Rf 0.74-0.82 revealing a region of even numbered *m/z* ions signifying potential $M^{+\bullet}$. Red circles highlight ions chosen for mass chromatography (*m/z* 135, 163 and 314)

Generation of mass chromatograms for *m/z* 135, 163 and 314 (Figure 5.8, Figure 5.9) revealed that the *m/z* 135 and 163 mass chromatograms had relatively similar abundance ($1.2x10^5$ and $1.0x10^5$) whilst the mass chromatogram for *m/z* 314 was less abundant ($3.5x10^4$; Figure 5.10). The *m/z* 135 mass chromatogram contained no resolved peaks and had an unresolved profile (Figure 5.8A).

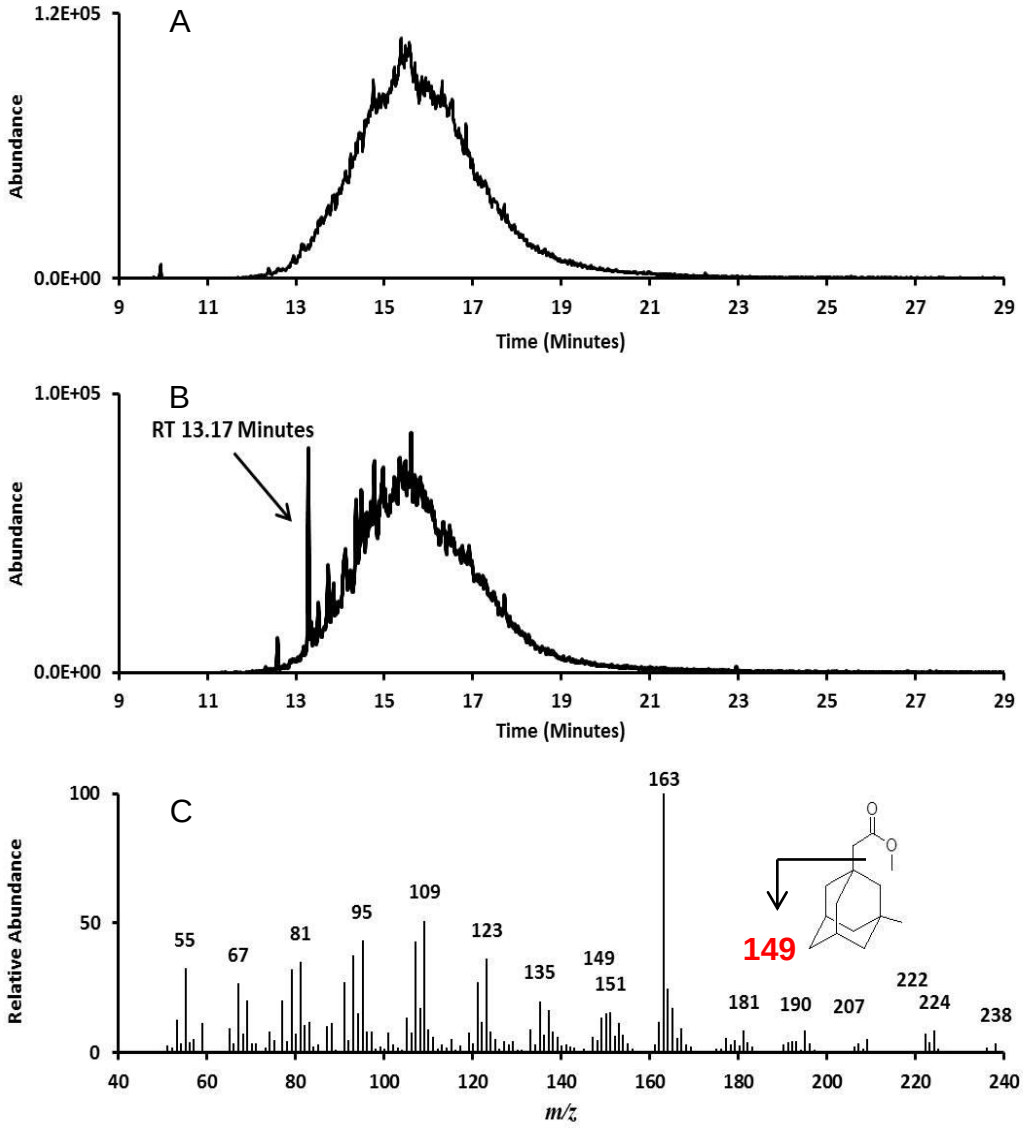

Figure 5.8. Mass chromatograms from the Ag^{+}TLC fraction R_f 0.74-0.82 revealing (A) mass chromatogram of *m/z* 135. (B) Mass chromatogram of *m/z* 163, highlighting resolved peak at RT 13.17 minutes. (C) Mass spectrum of the compound eluting at RT 13.17 minutes within the *m/z* 163 mass chromatogram**.** GC-MS conditions as described in Figure 5.2.

The mass chromatogram for *m/z* 163 (Figure 5.8B) however, contained a relatively resolved peak at RT 13.17 minutes. The mass spectrum (Figure 5.8C) showed a base peak ion at *m/z* 163 and potential $M^{+\bullet}$ at *m/z* 222, 224 and 238. Rowland et al., (2011b) tentatively identified a methyl adamantane ethanoic acid methyl ester with a $M^{+\bullet}$ *m/z* 222 and a base ion at *m/z* 163 which

displayed a spectral profile which was redolent of Figure 5.8C. The retention time (13.17 minutes) was also within a range exhibited by other adamantane acid (MEs) analysed under similar GC-MS conditions (Chapter 2; Section 2.3.18). It is likely that this compound is a methyl adamantane ethanoic acid, methyl ester. However the presence of other potential $M^{+\bullet}$ ions does highlight the need for the better chromatographic resolution achieved by GCxGC-MS (e.g. Rowland et al., 2011b), which reduces such co-elutions and allows a greater certainty of structural elucidation.

Analysis of the mass chromatogram of *m/z* 314 (Figure 5.9A) revealed a 'hump' profile with three relatively resolved peaks at RT 20.59, 21.32 and 22.15 minutes and two peaks that were less resolved (RT 21.50 and 21.52). The mass spectra of each peak revealed that only the peaks at RT 20.59 and 22.15 produced mass spectra that could be tentatively interpreted. The remaining three peaks produced spectra that were extremely complex due to co-elution (not shown).

Examination of the spectra displayed in Figure 5.9B and C revealed that both had potential $M^{+\bullet}$ at either *m/z* 314 or *m/z* 328. Significant fragment ions exist at *m/z* 299 and 282 which may suggest that the likelier candidate for the $M^{+\bullet}$ is *m/z* 314 as *m/z* 299 would then describe cleavage of a CH_3 methyl group (M-15 Da) and *m/z* 282 (M-32 Da) would be characteristic of loss of methanol. Analysis of the relative abundance between the proposed $M^{+\bullet}$ (*m/z* 314) and the M^{+1} (*m/z* 315) suggests that the compound has C_{21}. Adding two oxygen atoms for the

carboxylic acid group leaves a probable empirical formula of $C_{21}H_{30}O_2$ (nominal M/W 314 Da; Double Bond Equivalent (DBE) of 7).

A base ion at *m/z* 145 suggests a $C_{11}H_{13}^+$ fragment most likely from a methyltetrahydronaphthalene or a di-methyl-2, 3-dihydroindan fragment (Figure 5.10) as evidenced by the mass spectrum of 5,6,7,8-tetrahydronaphthalene-ethanoic acid (Chapter 2; Figure 2.72D; reproduced in Figure 5.11A), which had a base ion at *m/z* 145 due to fragmentation of a carboxyl group, which leaves a methyl tetrahydronaphthalene fragment.

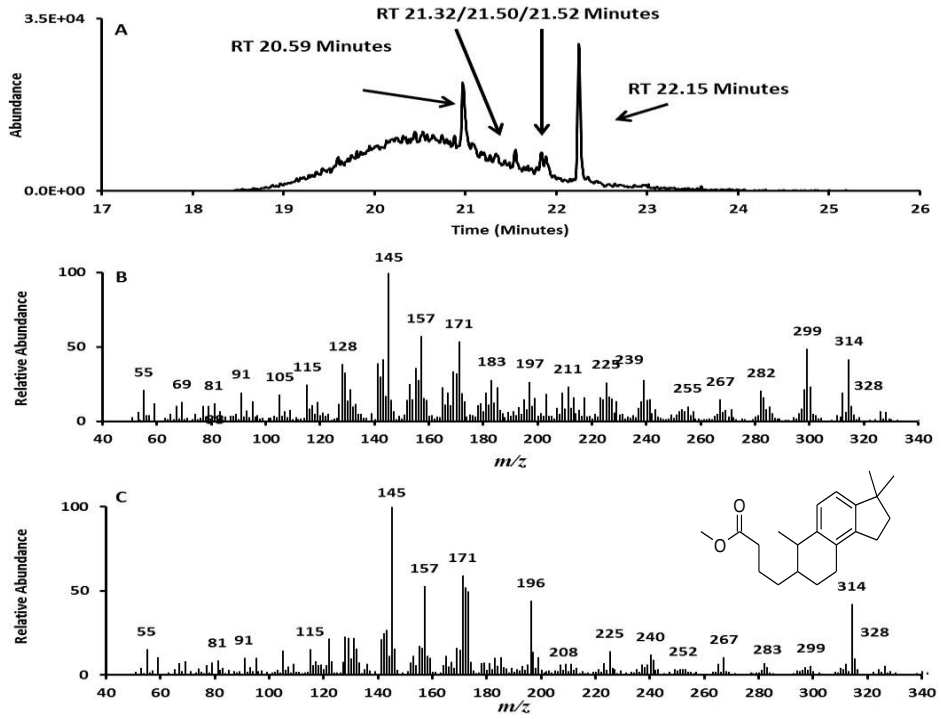

Figure 5.9. Mass chromatograms from the Ag^{+}TLC fraction R_f 0.74-0.82 revealing (A) mass chromatogram of *m/z* 314; (B) mass spectrum of the compound eluting at RT 20.59 minutes within the *m/z* 314 mass chromatogram; and (C) mass spectrum of the compound eluting at RT 22.15 minutes within the m/z 314 mass chromatogram and a tentative structural assignment of a de-A C_3 steroidal acid. GC-MS conditions as described in Figure 5.2.

A base ion at *m/z* 145 suggests a $C_{11}H_{13}^{+}$ fragment most likely from a methyltetrahydronaphthalene or a dimethyl-2, 3-dihydroindene fragment (Figure 5.10).

Figure 5.10. Potential $C_{11}H_{13}^{+}$ structures characteristic of an *m/z* 145 fragment ion with (A) a methyltetrahydronaphthalene ion; and (B) a dimethyl-2, 3-dihydroindene ion

This is evidenced by the mass spectrum of 5,6,7,8-tetrahydronaphthalenethanoic acid (Chapter 2; Figure 2.72D; reproduced in Figure 5.11A), which has a base ion at *m/z* 145 after fragmentation of a carboxyl group, which leaves a tetrahydronaphthalene fragment.

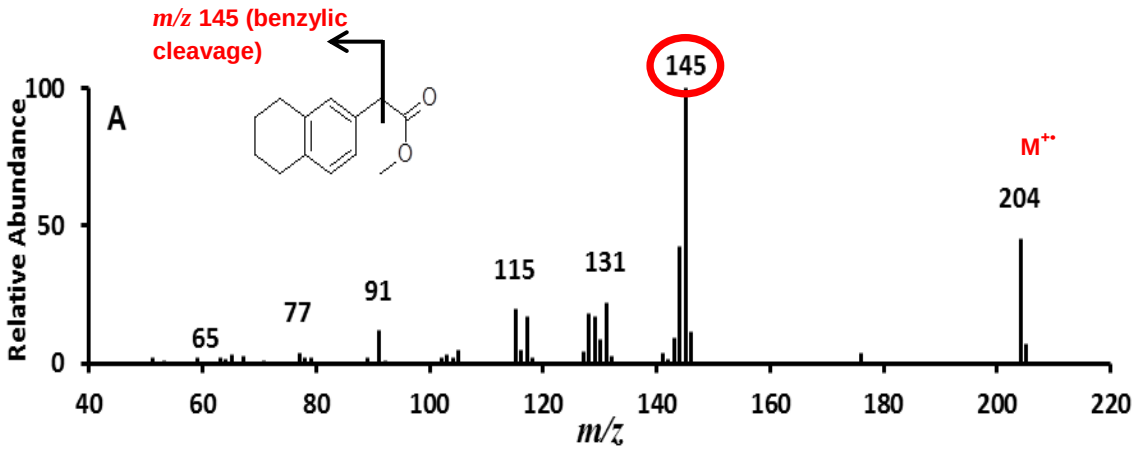

Figure 5.11. Mass spectrum of naphthalene-2-ethanoic acid methyl ester; revealing the key *m/z* 145 ion highlighted by the red circle (reproduced Figure 2.72D; Chapter 2).

An averaged mass spectrum of Ag^{+}TLC fraction R_f 0.72-0.74 was also produced (Figure 5.12). The spectrum revealed that *m/z* 135 and 163 (key alicyclic ions) were not as prevalent in fraction R_f 0.72-0.74, however there is a potential $M^{+\bullet}$ present at *m/z* 314.

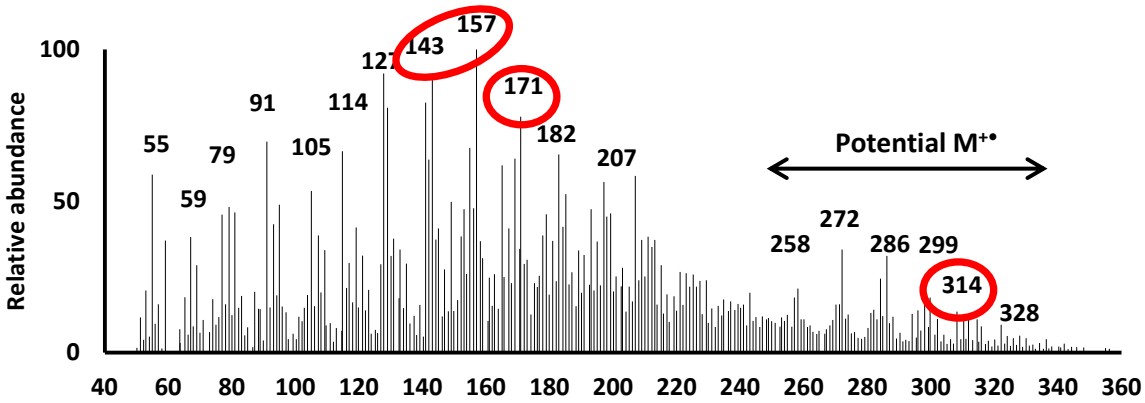

Figure 5.12. Averaged mass spectrum generated from the whole total ion chromatogram of the Ag^{+}TLC fraction R_f 0.72-0.74 revealing a region of potential $M^{+\bullet}$. Red circles highlight ions chosen for mass chromatograms (*m/z* 143, 157, 171 and 314). GC-MS conditions as described in Figure 5.2.

The mass chromatograms of *m/z* 143,157 and 174 revealed an unresolved 'hump' with a resolved peak at RT 22.15 minutes (Figure 5.13 A, B and C). The mass spectrum (Figure 5.13E) revealed that this chromatographic peak was likely the same as that described in Figure 5.9C, with an $M^{+\bullet}$ apparent at *m/z* 314, a base ion at *m/z* 145 and significant fragment ions at *m/z* 299 and 283, which are consistent with the loss of methyl and methoxy groups respectively. However there was also an apparent $M^{+\bullet}$ at *m/z* 328 which again highlights the need for the greater resolving power of GCxGC-MS.

The mass chromatogram of *m/z* 314 (Figure 5.13D) revealed a similar profile to that of Figure 5.9A, mainly comprising an unresolved 'hump' with three or four resolved peaks. However in this instance all but the peak at RT 22.15 produced complex mass spectra which were likely caused by ions due to co-elutions. Only the compound eluting at RT 22.15 minutes produced a mass spectrum

from which some information could be elucidated. This spectrum is similar to the mass spectrum described in Figure 5.9C and has been described previously.

As the m/z 145 ion appears prevalent throughout the analysed mass spectra it seemed be prudent to also generate a mass chromatogram of this particular ion (Figure 5.14). Analysis revealed a 'hump' of low abundance with between five and seven resolved peaks eluting between RT 20.45 and 22.17 minutes, with the most resolved peak at RT 22.15 minutes. Analysis of the mass spectra revealed that these peaks probably belonged to a family of compounds with a base ion at m/z 145. However only the peak at RT 22.15 minutes generated a mass spectrum that was not confused by potentially co-eluting compounds. Analysis by GCxGC-MS has confirmed the assignment of this group of m/z 145 base peak compounds, though identification of these compounds remains tentative (Rowland et al., 2011c).

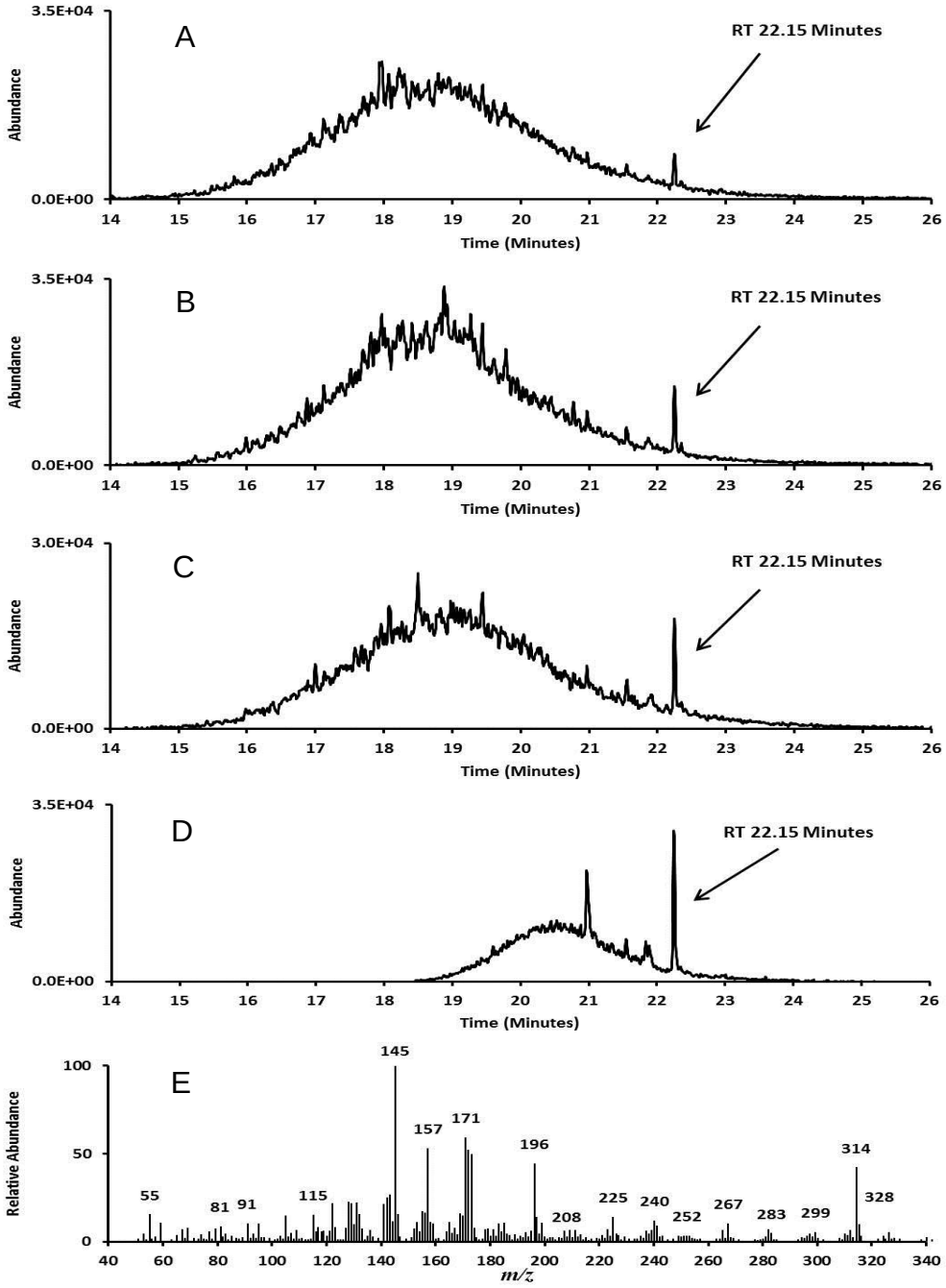

Figure 5.13. Mass chromatograms from Ag^{+}TLC fraction 0.72-0.74 with (A) mass chromatogram of *m/z* 143 showing resolved peak at RT 22.15 minutes; (B) mass chromatogram of *m/z* 157 showing resolved peak at RT 22.15 minutes; (C) mass chromatogram of *m/z* 171 showing resolved peak at RT 22.15 minutes; (D) mass chromatogram of *m/z* 314 showing resolved peaks at RT 20.59 and 22.15 minutes; and (E) mass spectrum of compound eluting at RT 22.15 minutes. GC-MS conditions as described in Figure 5.2.

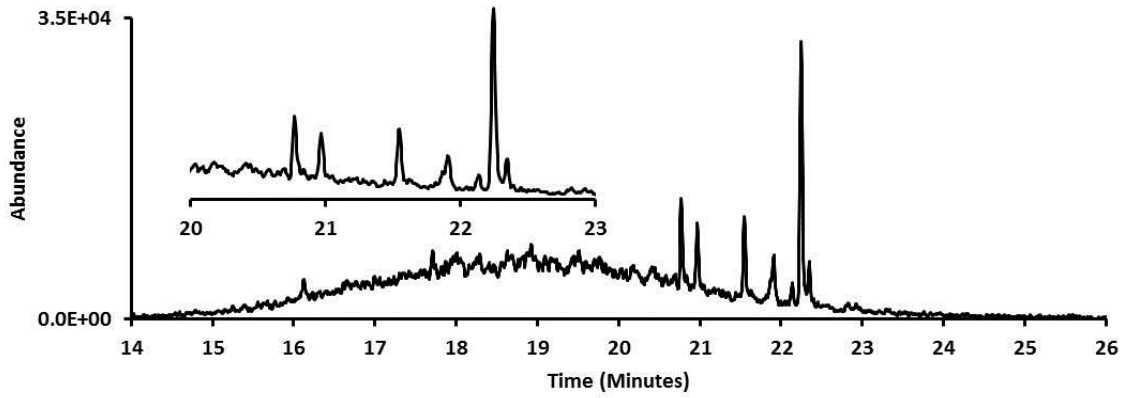

Figure 5.14. Mass chromatograms for *m/z* 145 taken from Ag^+TLC fraction 0.72-0.74, revealing relatively resolved peaks eluting between RT 20.45 and RT 22.17 minutes; inset shows a close up of this region. GC-MS conditions as described in Figure 5.2.

An averaged mass spectrum was also generated for the Ag^+TLC fraction R_f 0.66-0.72 (Figure 5.15). This revealed a spectrum dominated by the *m/z* 149 and *m/z* 207 ions generally indicative of phthalate ester contamination (*m/z* 149) and GC column bleed (*m/z* 207 and 281). Reference to the total ion current chromatogram displayed in Figure 5.5D revealed three resolved peaks at RT 16.58, 17.54 and 22.57 which displayed ions characteristic of phthalates (e.g. base ion at *m/z* 149).

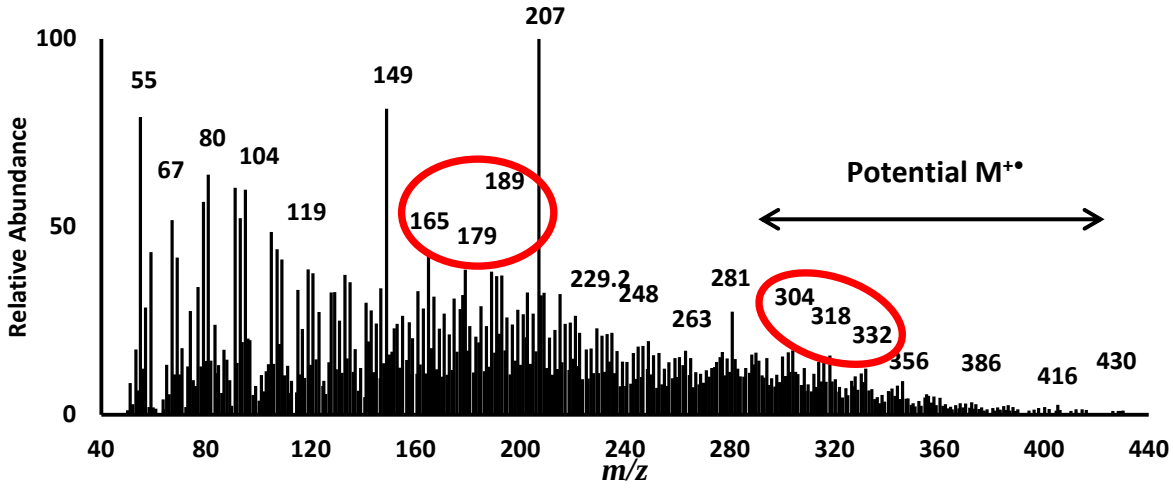

Figure 5.15. Averaged mass spectrum generated from the whole total ion chromatogram of the Ag^+TLC fraction R_f 0.66-0.72; revealing an region of even *m/z* ions signifying potential $M^{+\bullet}$. Red circles highlight ions chosen for mass chromatograms (*m/z* 165, 179, 189, 304, 318 and 332). GC-MS conditions as described in Figure 5.2.

Further analysis of the Ag^+TLC fraction 0.66-0.74 averaged mass spectrum revealed that the key ions considered in fractions R_f 0.74-0.82 and 0.72-0.74 were not as abundant. Instead fragment ions at *m/z* 165, 179 and 189 and potential $M^{+\bullet}$ ions at *m/z* 304, 318 and 332 were investigated (Figure 5.16).

The mass chromatograms of all investigated ions revealed that only unresolved 'humps' of differing abundances were generated and that no resolved peaks were apparent. The peak eluting at RT 21.25 minutes in the *m/z* 165 mass chromatogram (Figure 5.16A) did not generate a mass spectrum which was 'clean' enough to be interpreted. With respect to this fraction, higher resolution chromatography (e.g. GCxGC-MS) may well produce better separations which resolve individual chromatographic peaks. Silver ion open column chromatography (Ag^+SPE) may also help to separate the OSPW acid extracts

(ME) into fractions more amenable for GC-MS and mass chromatographic analysis.

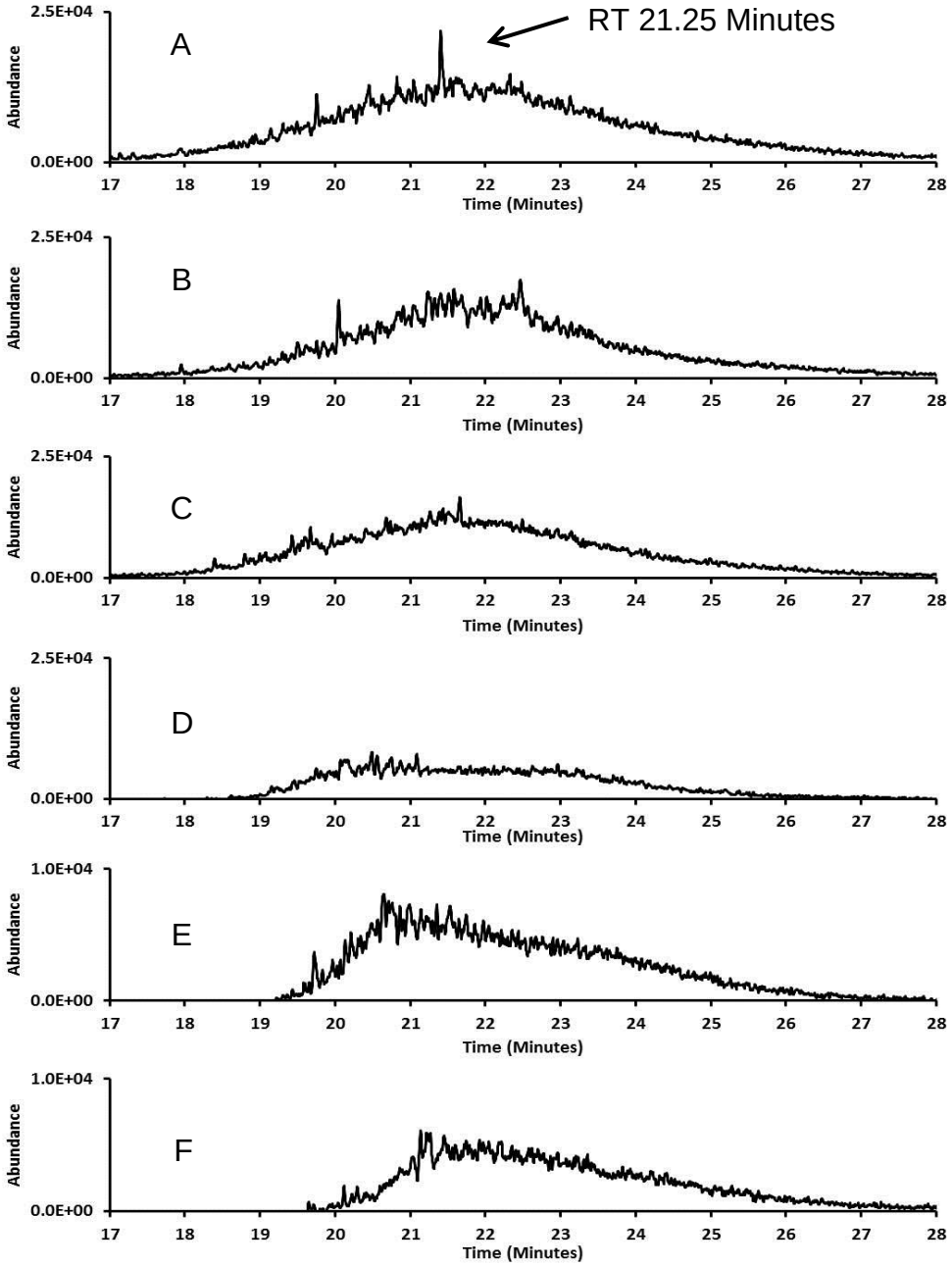

Figure 5.16. Mass chromatograms from Ag^{+}TLC fraction 0.66-0.72 with: (A) Mass chromatogram of *m/z* 165 showing relatively resolved peak at RT 21.25 minutes. (B) Mass chromatogram of *m/z* 179. (C) Mass chromatogram of *m/z* 189. (D) Mass chromatogram of *m/z* 304. (E) Mass chromatogram of *m/z* 318. (F) Mass chromatogram of *m/z* 332. GC-MS conditions as described in Figure 5.2.

5.3.1.3. Ultra Violet-Visible Spectrophotometry of Ag^+TLC Fractions

Ultra Violet-Visible Spectrophotometry (UV-Vis) was performed on the Ag^+TLC fractions and on a sample of unfractionated acid extracts (Figure 5.17). The extent of UV absorption in the unfractionated sample was less than that of the three Ag^+TLC fractions, although a broad absorption was evident in to 230 nm region which indicated that aromatic compounds may be present within the acid extracts. A small absorbance occurred at 263-265 nm consistent with the spectrum published previously by Mohamed et al. (2008) for OSPW free NA.

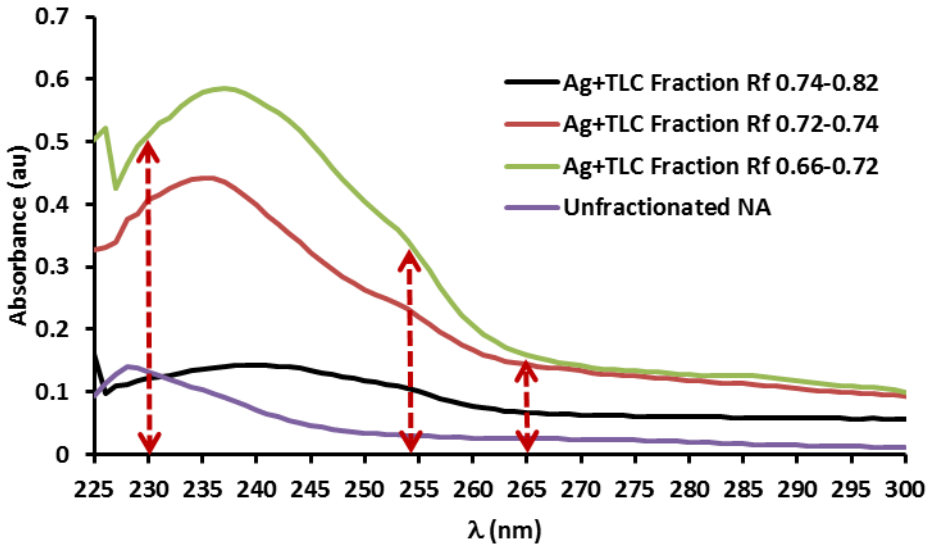

Figure 5.17. Ultraviolet spectra of Ag^+TLC Fractions and unfractionated acid extracts (ME) of an OSPW. Red dashed arrows indicate positions of absorption maxima at 230 nm, 254 nm and 265 nm, typical of aromatic compounds.

Analysis of the spectrum of the Ag^+TLC fraction R_f 0.74-0.82 (the least retarded fraction) revealed no significant absorbance the 230-265 nm region, indicating that whilst some aromaticity may exist in the fraction it was somewhat lower than the more retarded fractions.

Analysis of the remaining Ag^+TLC fractions (R_f 0.72-0.74 and 0.66-0.72) revealed that both fractions exhibited significant UV absorbance in the 230 nm and the 260-280 nm regions, consistent with these fractions being more retarded by the Ag^+ ions and indicating that aromaticity existed in the fractions of the OSPW ME.

5.3.2 Silver Ion Open Column Chromatography

Whilst useful (e.g. Morris et al., 1966; Dobson et al., 1995) Ag^+TLC has a limited loading capacity. In contrast, solid phase extraction (SPE) allows the user to utilise more analyte in an experiment (Nikolova-Damyanova, 1992). It was therefore decided that open column chromatography using commercially prepared silver ion solid phase extraction (Ag^+SPE) cartridges might potentially allow separation of larger amounts of OSPW esters and possibly even afford better resolution than Ag^+TLC by careful adjustment and sequential elution with a range of mobile phases, rather than the one mobile phase used on Ag^+TLC.

5.3.2.1 Ag^+SPE of Authentic Acid Methyl Esters

Three authentic acid methyl esters were chosen for development of the method. The di-aromatic naphthalene-2-carboxylic acid, methyl ester was used in addition to those chosen for the Ag^+TLC experiment (Section 5.3.1.1). The acids were methylated with BF_3-MeOH, mixed in equal proportions (0.01 mg mL^{-1}) and examined by GC-MS (Figure 5.18).

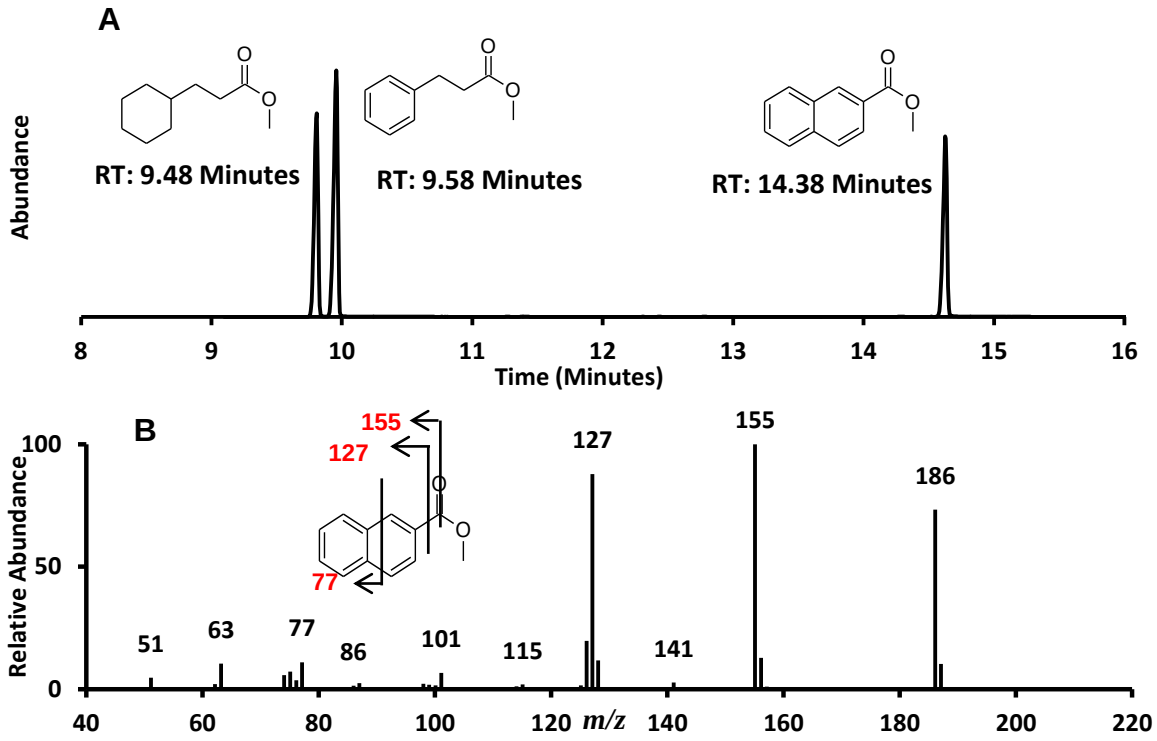

Figure 5.18. (A) Total ion current chromatogram of the acid methyl esters used for the development of a Ag^{+}SPE method. (B) Mass spectrum for the compound eluting at RT14.38 minutes assigned as a naphthalene-2-carboxylic acid, methyl ester**.** Mass spectra for compounds eluting at RT 9.48 and 9.58 are displayed in Figure 5.3. GC-MS conditions were as described in Figure 5.2.

As Figure 5.18 reveals, there were three distinct peaks eluting at RT 9.48, 9.58 minutes and 14.38 minutes in the prepared mixture, as expected. The early eluting peaks (RT 9.48 and 9.58 minutes) had identical retention times and mass spectra to those of cyclohexylpropanoic acid methyl ester and phenylpropanoic acid methyl ester established previously (Figure 5.3). The later eluting peak (RT 14.38 minutes) had a retention time and mass spectrum identical to the authentic diaromatic acid (naphthalene-2-carboxylic acid ME) examined previously (Section 2.3.11).

A small sample (1 mg) of each acid methyl ester was mixed and added to the top of a *Supelco Discovery* Ag^{+}SPE column and eluted with a differing ratio of solvents (Section 5.2.4). Elutions with 100% hexane elution removed the bulk of the alicyclic acid ME and significant amount of the aromatic acids (ME); the 90:10 hexane: diethyl ether elution removed the bulk of the di-aromatic acid; and the 80:20 hexane:diethyl ether elution removed small amounts of the mono-aromatic standard (Figure 5.19).

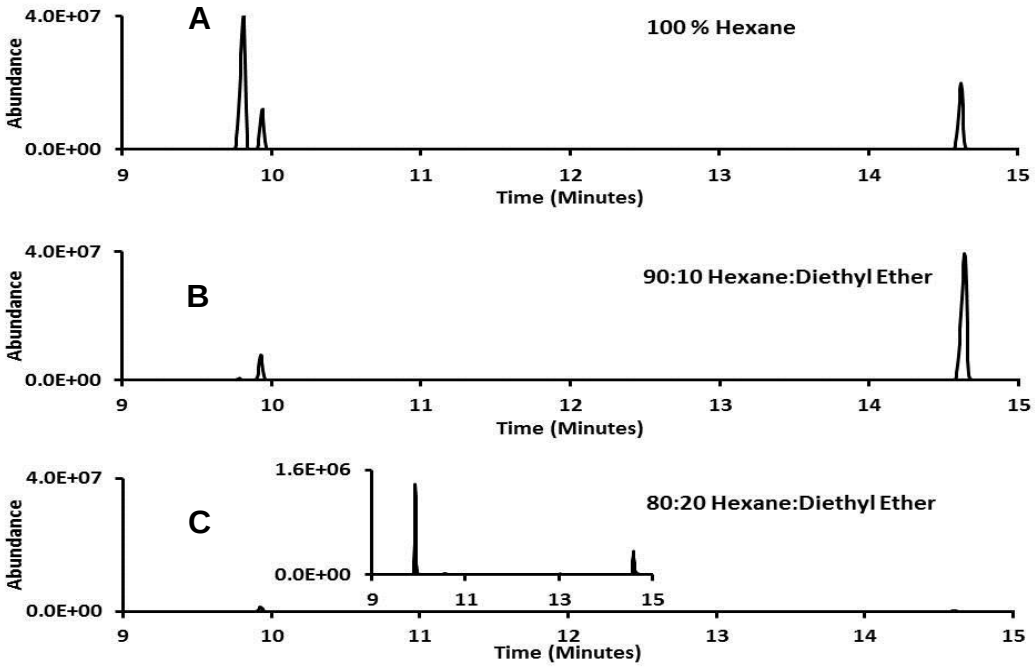

Figure 5.19. Total ion current chromatograms of the Ag+SPE fractions of the three acid methyl ester standards revealing (A) the 100% hexane fraction; (B) the 90:10 hexane:diethyl fraction and (C) the 80:20 hexane:diethyl fraction. Mass spectra and retention times of components were identical to those displayed in Figures 5.3 and 5.11. GC-MS conditions were as described in Figure 5.2.

Figure 5.19 revealed that the alicyclic standard eluted in the early eluting fraction with the two aromatic standards mainly eluting in the later eluting fractions, with the more polar solvent ratios. However only small amounts of the

mono-cyclic and mono-aromatic acids were detected by integration of GC-MS peaks. It was found that (in total) 56% of the components were diaromatic, 36% monocyclic and only 6% mono-aromatic. It was concluded that the bulk of the volatile monocyclic acids (ME) had evaporated during work up procedures. For this reason it was decided that future fractionations would deploy larger, less volatile acids (ME). However, as the bulk of the di-aromatic acid did elute in the 90:10 hexane: diethyl ether fraction, it was decided to proceed with investigating SPE of a small amount of OSPW acid methyl esters, as a further test of the Ag^{+}SPE method.

As only a small amount of acid was apparent in the 80:20 hexane:diethyl ether fraction it was decided that when fractionating the naphthenic acid complex mixture, elutions would be halted after use of the 90:10 solvent ratio. It was also decided that the addition of a 95:5 hexane:diethyl ether solvent mixture might improve the resolution.

5.3.2.2 Ag^{+}SPE of the Acid Extracts of OSPW

A small amount (3 mg) of acid extracts of an OSPW was methylated with BF_3-MeOH and added to the top of an Ag^{+}SPE column. The acid mixture was subsequently eluted with differing solvent ratios (Table 5.1) and fractions analysed by GC-MS (Figure 5.20). In all, eleven fractions were collected and analysed.

Examination of the total ion current chromatograms of each fraction revealed that there was a shift in the retention times of the maxima of each ‘hump’, revealing that each fraction contained slightly more GC-MS retained (possibly

higher boiling point) compounds. The RT of the maxima of the 'humps' ranged from *ca.* RT 15.26 minutes (Fraction 1) to 22.22 minutes (Fraction 7) (Figure 5.20).

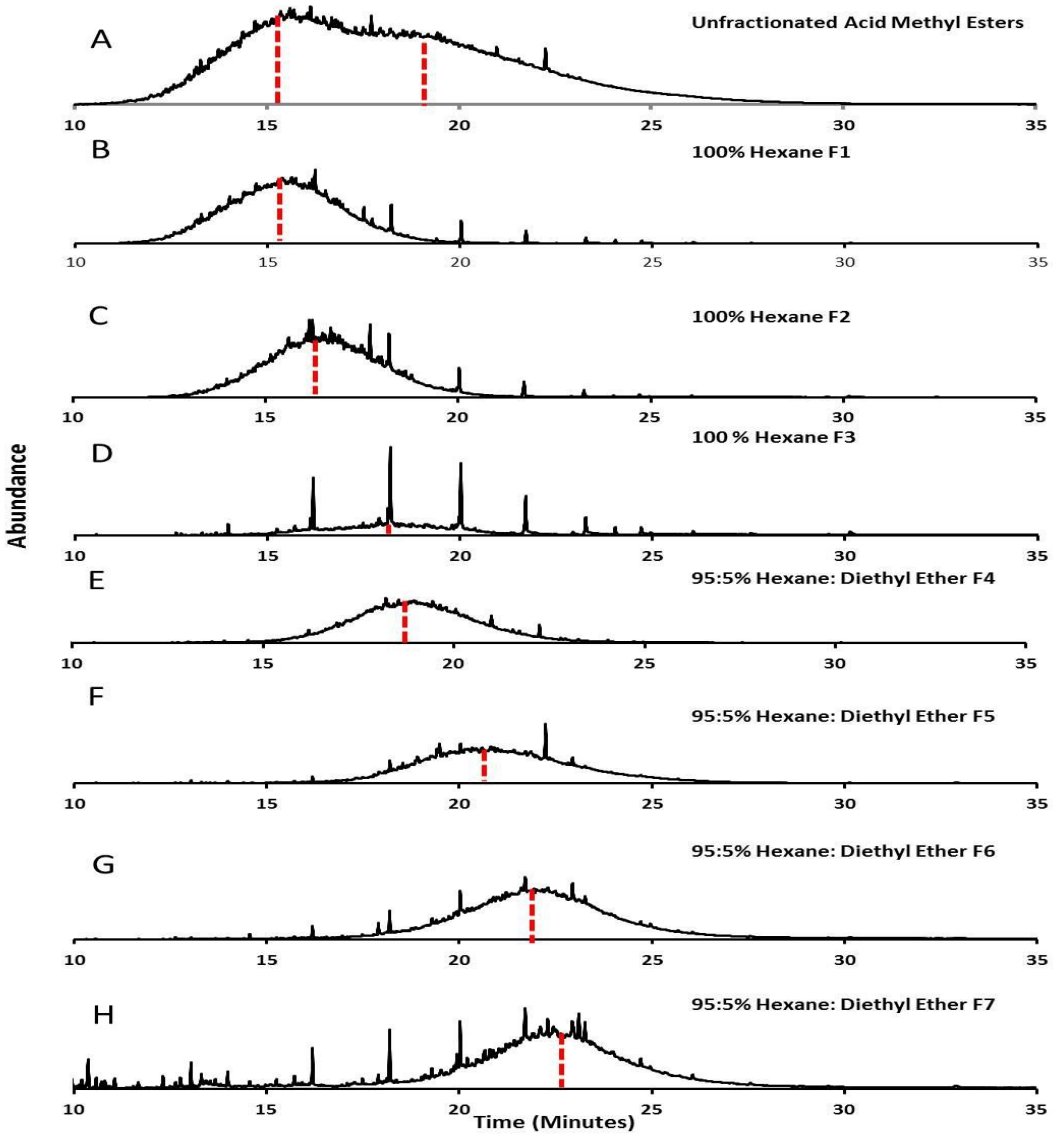

Figure 5.20. Total ion current chromatogram from the Ag^{+}SPE fractionation of the methyl esters of the acid extracts from a sample of OSPW, with (A) total ion chromatogram of the unfractionated OSPW acid methyl esters; (B-D) showing the three 100% hexane fractions; and E-H showing the four 95:5% hexane:diethyl ether fractions Red dotted line highlights the shift in the total ion current chromatogram maxima. GC conditions were as described in Figure 5.2.

Comparison of the total ion current chromatograms of the Ag^{+}SPE fractions with those of the authentic acid methyl esters revealed that three fractions eluted in the same solvent ratio as the bulk of the mono-cyclic acid standard. This also revealed that there were four fractions eluting with the slightly more polar solvent ration (95:5 hexane:diethyl ether), potentially due to a higher degree of aromaticity retarding these fractions on-column (Figure 5.20).

Examination of the total ion current chromatograms (Figure 5.21) of the remaining fractions (3x 90:10% hexane:diethyl ether and 1x 100% diethyl ether) revealed that there was a pronounced double ‘hump’ in the first two 90:10% hexane diethyl ether fractions (Figure 5.21 A and B) possibly indicating a mixture of alicyclic and aromatic compounds was retained. The final two fractions show a less abundant ‘hump’ with somewhat more resolved peaks apparent (Figure 5.21 C and D). Analysis of the system blanks revealed that these peaks were mainly compounds that eluted from the cartridge when exposed to the more polar solvents. It is possible that these later eluting fractions (8-11) also contain some non-esterified compounds.

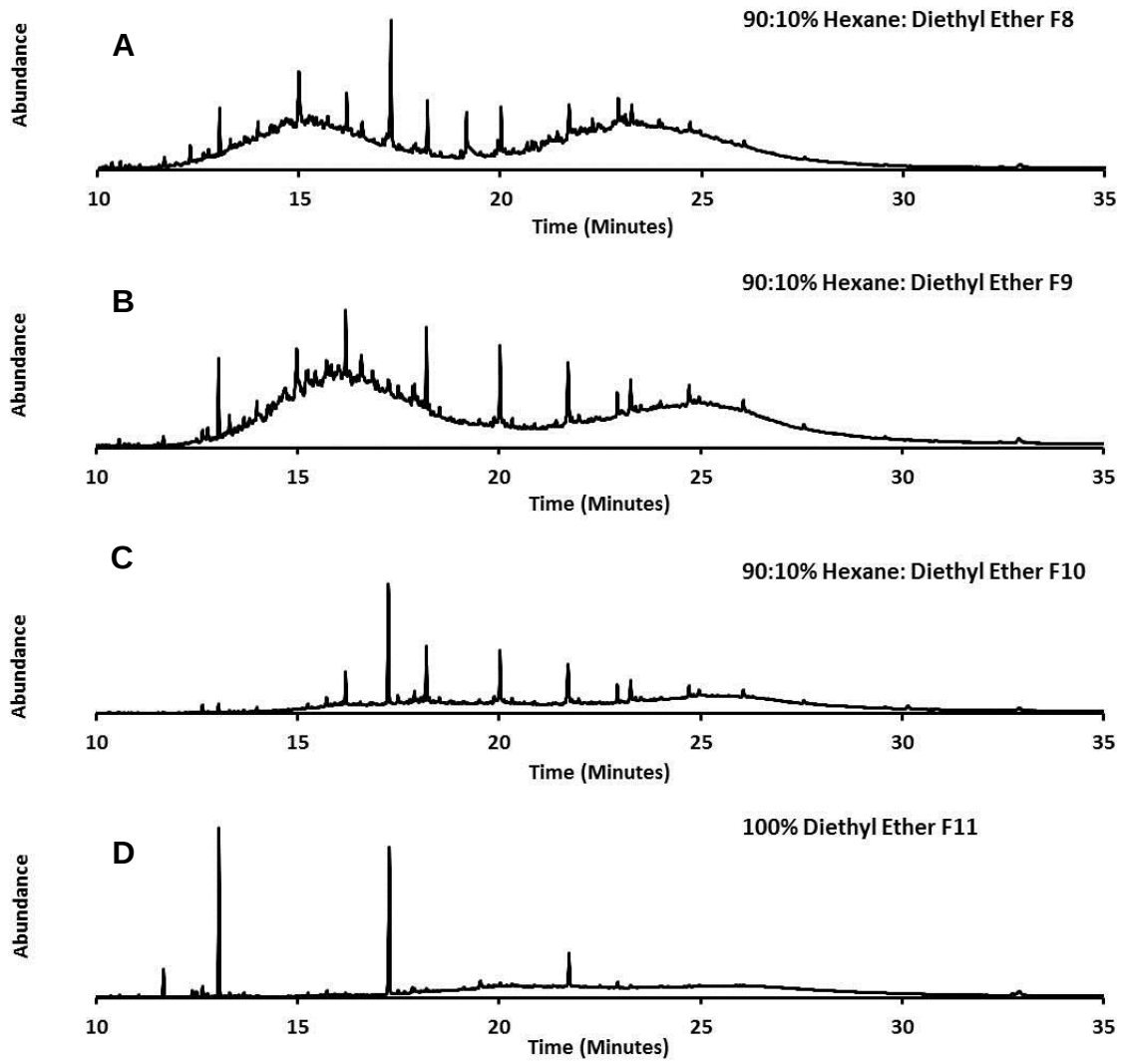

Figure 5.21. Total ion current chromatogram from the Ag+SPE fractionation of the methyl esters of the acid extracts from a sample of OSPW, with (A-C) three 90:10% hexane:diethyl ether fractions and (D) the 100% diethyl ether fraction. GC conditions were as described in Figure 5.2.

Unfortunately Ag^+SPE of 3 mg methyl esters of the acid extracts from the OSPW did not provide enough of any fraction for accurate weights to be obtained. Therefore the peak areas of each total ion current chromatogram were integrated manually and a percentage area for each fraction calculated (Figure 5.22), similar to that achieved previously from Ag^+TLC (Section 5.3.1.2, Figure 5.7)

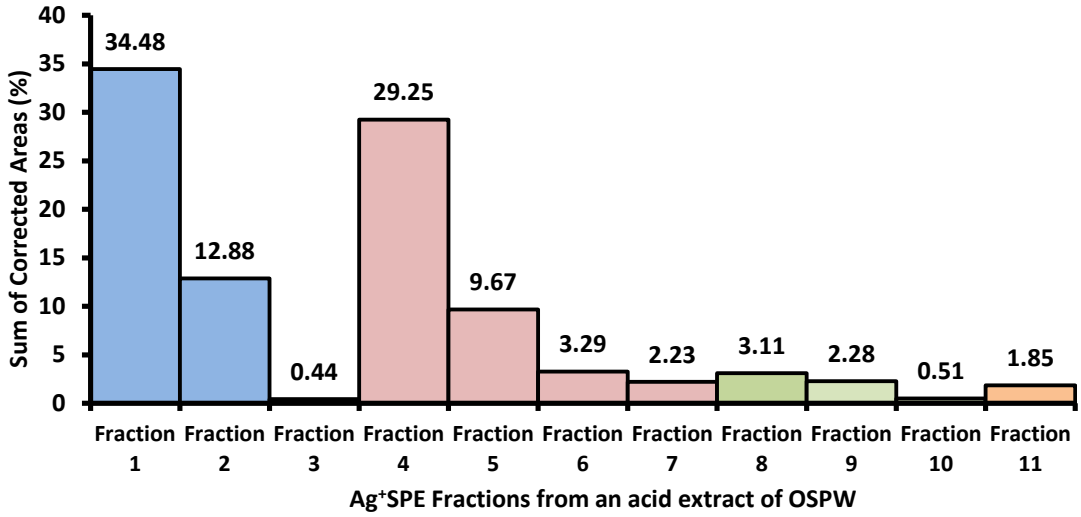

Figure 5.22. Bar chart displaying the corrected percentage areas of a manual integration of each fractions total ion current chromatogram, partly published in Jones et al., (2012a).

As this method integrated essentially a number of unresolved 'humps' in the chromatograms, the method was only approximate. Interestingly the summed percentage areas generally fitted well with the results of previous research (Knoterus, 1957) in which chromatography, infrared and UV analysis, thermal diffusion and dehydrogenation techniques were used to deduce that between 30 and 40% of the NA extracted from a Venezuelan crude oil were likely mono or di-aromatic moieties (discussed in Chapter 2; Section 2.1.2).

An overlay of all the Ag^+SPE fraction chromatographic 'humps' with a chromatogram of an unfractionated acid extract of an OSPW (Figure 5.23) revealed that Ag^+SPE 100% hexane fraction 1 and 95:5% hexane diethyl ether fraction 4 generally explained the bi-nodal nature of the unfractionated acid methyl ester total ion current chromatogram; the chromatogram maxima of each

fraction approximately matching the maxima of each of the unfractionated samples nodes.

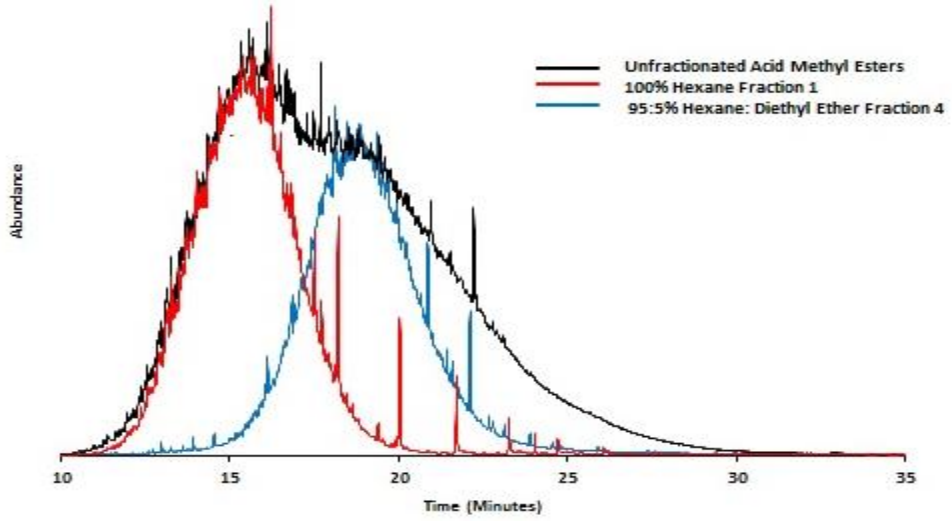

Figure 5.23. Overlay of the total ion current chromatograms of the unfractionated acid methyl esters, 100% hexane fraction 1 and 95:5% hexane diethyl ether fraction 4**.**

5.3.2.3. Mass Chromatographic Analysis

Averaged mass spectra of the total ion chromatograms of two 100% hexane fractions (fractions 1 and 2, RT 10.00-24.00 minutes) and two 95:5% hexane: diethyl ether fractions (fractions 4 and 5, RT 12.00-26.00 minutes and 14.00-28.00 minutes respectively) revealed distinct differences in the spectral profiles between the proposed alicyclic fractions (fractions 1 and 2) and the proposed aromatic fractions (fraction 4 and 5).

Analysis of the averaged mass spectra of fractions 1 and 2 (Figure 5.24) also revealed significant ions that could be used as fingerprint ions for alicyclic/aromatic moieties. For instance, Figure 5.14 A and B revealed the presence of relatively abundant ions at *m/z* 135 and 163. Rowland et al., (2011b) revealed that these were key ions associated with the alicyclic

adamantane type acid methyl esters which have been identified within the acid extracts of OSPW. The fragment ion at *m/z* 149, whilst also associated with the adamantane acid methyl esters (Rowland et al., 2011b; Chapter 2, Section 2.3.18) is also a key ion in phthalate esters, so was not examined further herein.

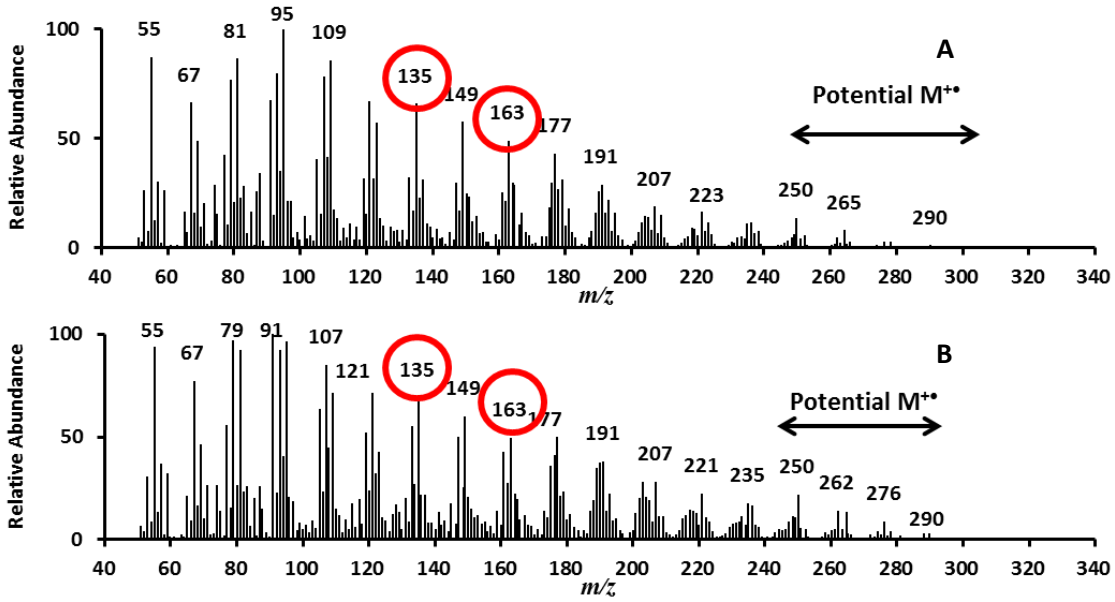

Figure 5.24. Averaged mass spectra of a selection of the unresolved chromatographic 'humps' from the initial Ag^{+}SPE experiment with (A) the average mass spectrum (RT 10 -20 minutes) of Fraction 1; (B) the average mass spectrum of Fraction 2 (RT 11-24 minutes). An area of even *m/z* indicates a potential $M^{+\bullet}$. Red circles highlight significant ions (m/z 135 and 163) used as fingerprints for certain alicyclic acid moieties.

Mass chromatograms were generated from fractions 1 and 2 for *m/z* 135 and 163 (Figure 5.25). Examination of the mass chromatograms revealed that for *m/z* 135 fraction 1 and 2 and *m/z* 163 fraction 2 a smaller unresolved hump was produced. Examination of the mass chromatogram for *m/z* 163 (fraction 1) revealed a relatively resolved peak at RT 13.17 minutes. Examination of the

mass spectrum (Figure 5.25E) revealed that it was the same compound that was noted in the Ag^{+}TLC fraction R_f 0.74-0.86 mass chromatogram for *m/z* 163 (Section 5.3.1.2.; Figure 5.8), *viz* a potential 3-methyl adamantane-1-ethanoic acid methyl ester.

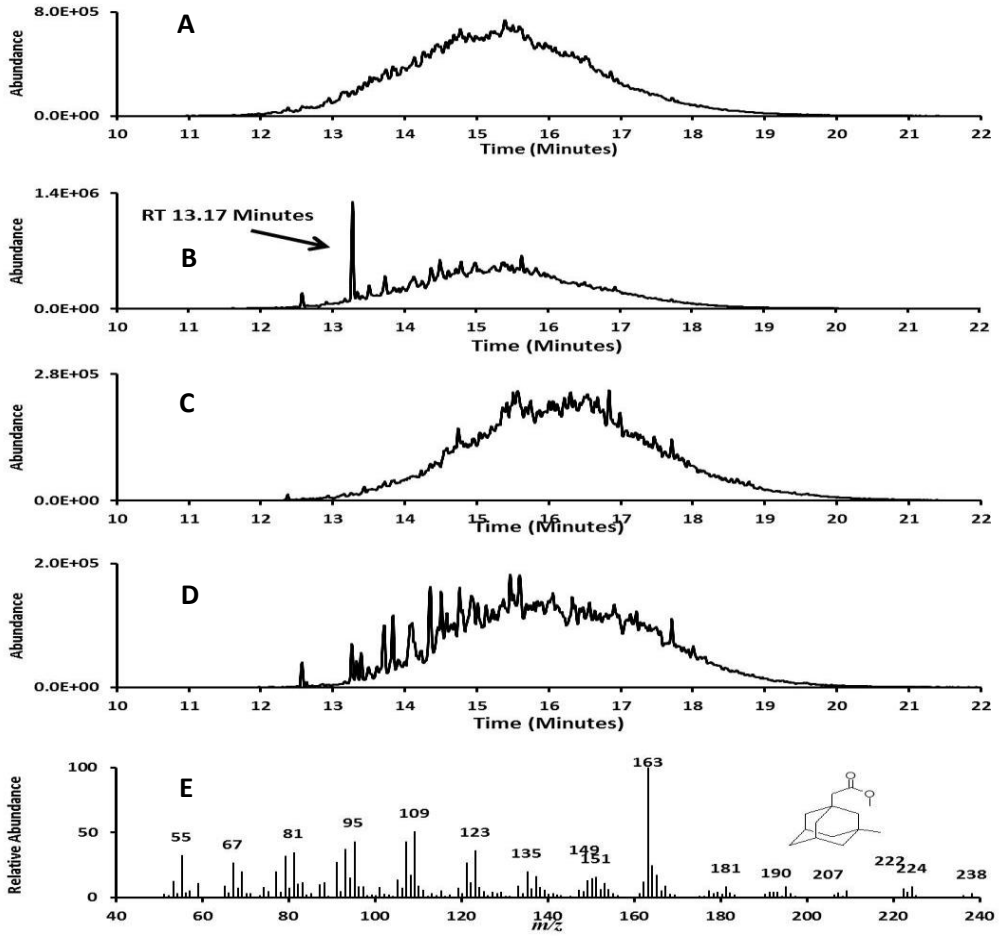

Figure 5.25. Mass chromatograms from fractions 1 and 2 100% hexane revealing (A) mass chromatogram for m/z 135, fraction 1; (B) mass chromatogram for m/z 163, fraction 1 ; (C) mass chromatogram for m/z 135, fraction 2; (D) mass chromatogram for m/z 163, fraction 2; and (E) mass spectrum for the compound eluting at RT 13.17 minutes in the m/z 163 mass chromatogram fraction 1**.** GC-MS conditions as described in Figure 5.2.

In contrast, the mass chromatograms for the 95:5% hexane: diethyl ether fractions (fractions 4 and 5) for *m/z* 135 and 163 (Figure 5.26) revealed generally unresolved humps at lower abundances, indicating that the bulk of the alicyclic compounds were eluting in the earlier 100% hexane fractions.

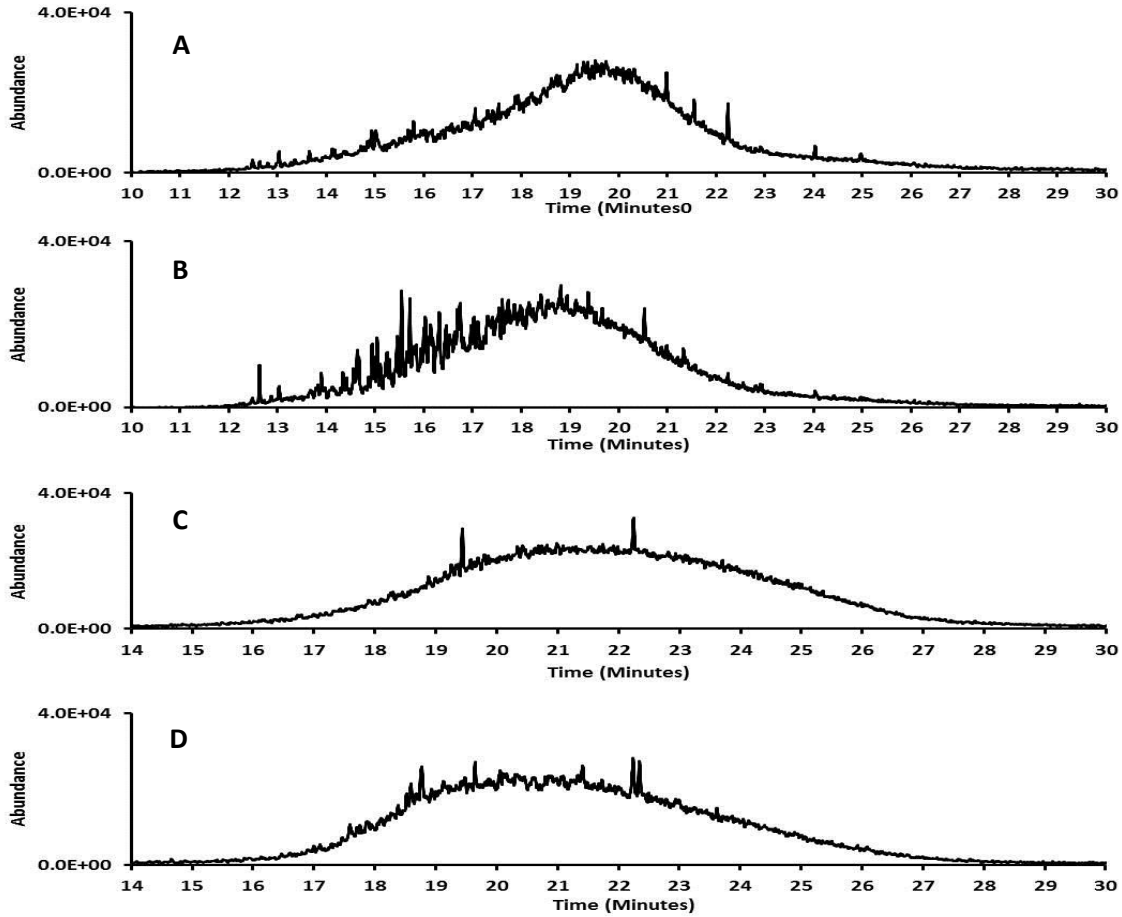

Figure 5.26. Mass chromatograms of fractions 4 and 5 eluted with 95:5% hexane: diethyl ether. (A) Mass chromatogram for m/z 135, fraction 4. (B) Mass chromatogram for m/z 163, fraction 4. (C) Mass chromatogram for m/z 135, fraction 5. (D) Mass chromatogram for m/z 163, fraction 5**.** GC-MS conditions as described in Figure 5.2.

Averaged mass spectra of the 95:5 hexane: diethyl ether fractions 4 and 5 were also generated (RT 12.00-26 minutes and 14-28 minutes respectively; Figure

5.27). The key ions for the alicyclic adamantane compounds (e.g. *m/z* 135, 149 and 163) were far less abundant in fraction 4 which was instead dominated by the fragment ions *m/z* 143, 157 and 171 Figure 5.27A) The mass spectrum also revealed a well defined area of potential $M^{+\bullet}$ from *m/z* 272 to 328. This region includes the $M^{+\bullet}$ of the previously discussed, de-A C_3 steroidal acid (*m/z* 314) (Section 5.3.1.2)

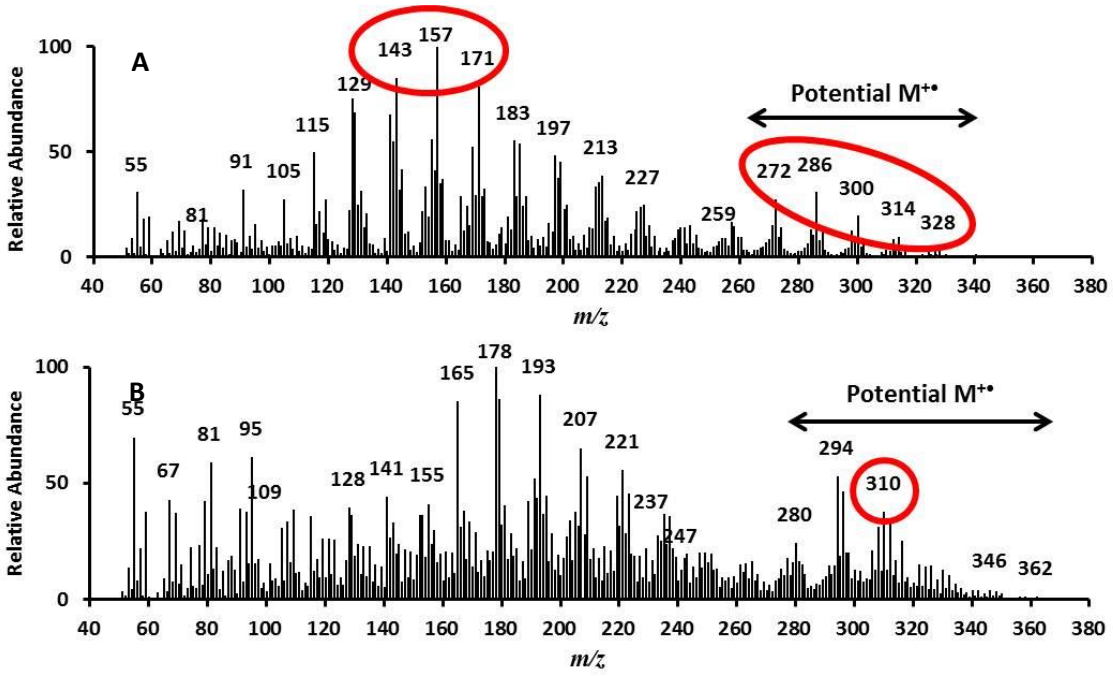

Figure 5.27. Averaged mass spectra of a selection of the unresolved chromatographic 'humps' from the initial Ag^{+}SPE experiment. (A) Averaged mass spectrum (RT 12.00 - 24.00 minutes) of Fraction 4. (B) Averaged mass spectrum of Fraction 2 (RT 14.00 - 26.00 Minutes). Even *m/z* ions (e.g. *m/z* 272-328) indicate potential $M^{+\bullet}$. Red circles highlight significant ions discussed in the text. GC-MS conditions as described in Figure 5.2.

When examining the averaged mass spectrum of fraction 5 (Figure 5.27B) it was noticed that further different ions dominated the spectrum (e.g. *m/z* 165, 178 and 193). Also present was a key ion proposed previously for identification of steroidal type polycyclic mono-aromatic acids (*m/z* 310; e.g. Rowland et al 2011c)

Examination of the mass chromatograms (Figure 5.28) of Ag^+SPE fraction 4 (*m/z* 143, 157, 171 and 314) revealed similar profiles and resolved peaks to the mass chromatograms for the same ions from Ag^+TLC fraction 0.72-0.74 discussed earlier (Section 5.3.1.1.) Analysis of the mass spectra generated from each of the peaks eluting at RT 20.58 and 22.15 minutes revealed similar spectral profiles for compounds eluting from Ag^+TLC with similar GC RT (e.g. $M^{+\bullet}$ *m/z* 314, base ion *m/z* 145; Figures 5.9 and 5.13). As such they can also be tentatively assigned as mono aromatic de-A steroidal type acid methyl esters.

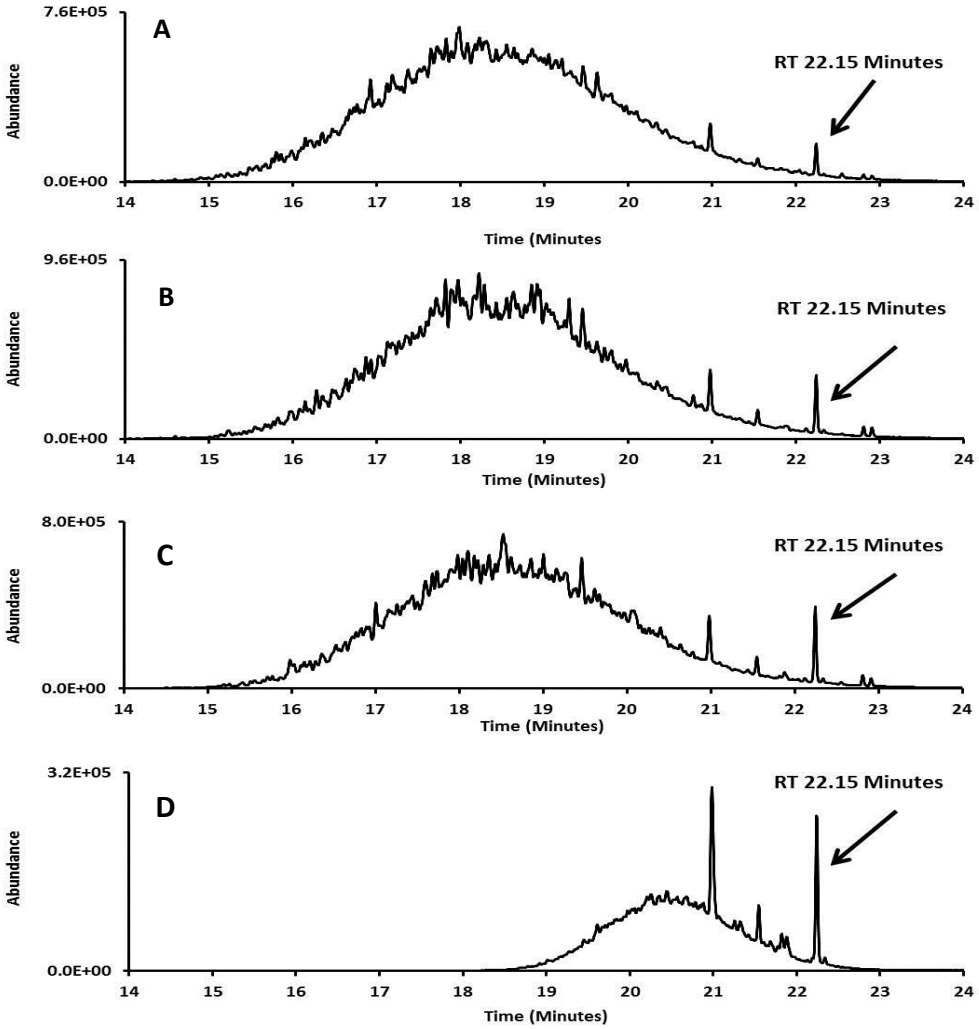

Figure 5.28. Mass chromatograms of fractions 4 and 5 eluted with 95:5% hexane: diethyl ether from Ag^{+}SPE. (A) Mass chromatogram of *m/z* 143, fraction 4. (B) Mass chromatogram of *m/z* 157, fraction 4. (C) Mass chromatogram of *m/z* 171, fraction 4. (D)Mass chromatogram of m/z 314, fraction 4**.** GC-MS conditions as described in Figure 5.2.

When examining the mass chromatograms of *m/z* 165, 178 and 193 from fraction 5 (eluted with 95:5% hexane:diethyl ether) it was apparent that no peaks were resolved and the profiles are that of unresolved 'humps' (Figure 5.29 A-C).

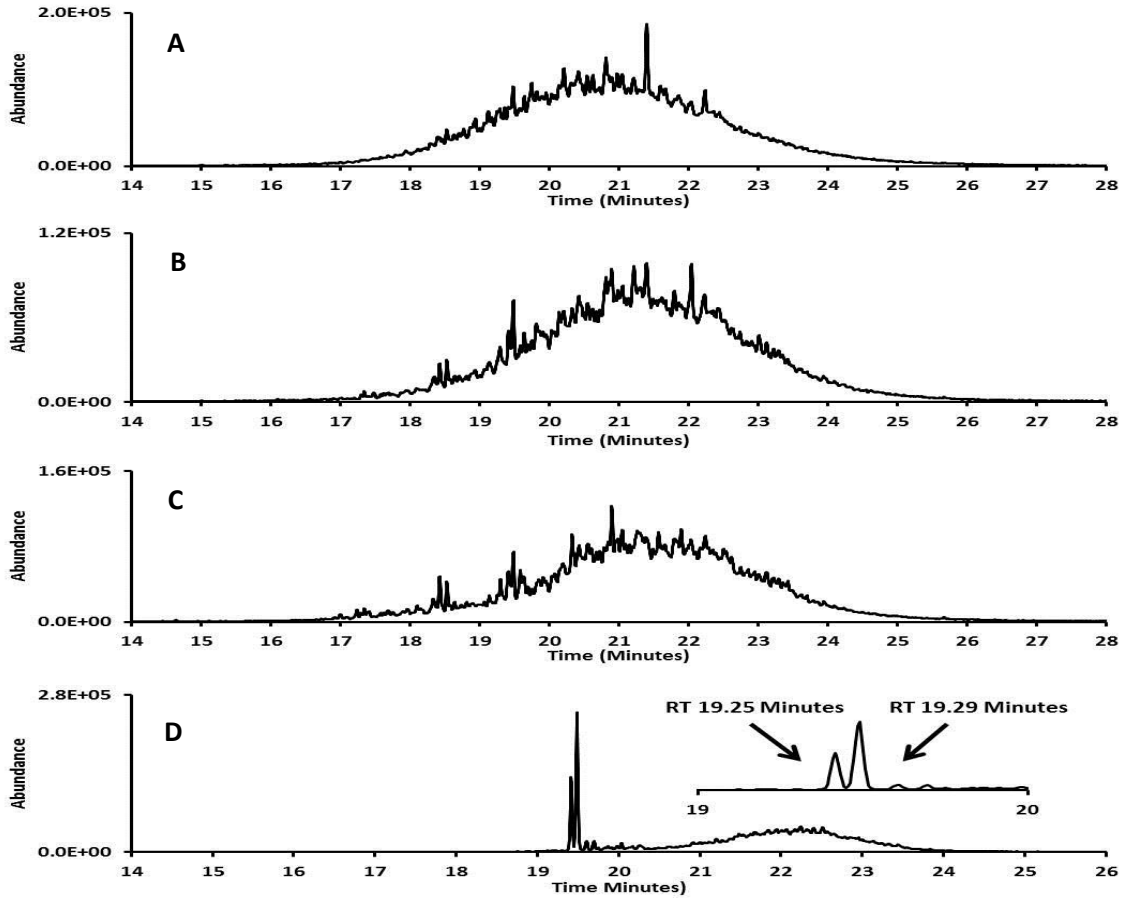

Figure 5.29. Mass chromatograms of Ag^{+}SPE fraction 5 eluted with 95:5% hexane diethyl ether. (A) Mass chromatograms for *m/z* 165. (B) Mass chromatograms for *m/z* 178. (C) Mass chromatograms for *m/z* 193.(D) Mass chromatograms for *m/z* 310. Inset shows peaks eluting at RT 19.25 minutes and 19.29 minutes in *m/z* 310 mass chromatogram**.** GC Conditions as described in Figure 5.2.

However, examination of the mass chromatogram of *m/z* 310 (Figure 5.29D) revealed two resolved peaks eluting at RT 19.25 and 19.29 minutes. The mass spectra (Figure 5.30 B and C) revealed similar characteristics. Both have probable $M^{+\bullet}$ at *m/z* 310 with significant ions at *m/z* 295, 278, 250 and 237 (indicative of an ethanoic acid methyl ester side chain revealing the loss of methyl, methoxy, carboxylate and ethanoate groups respectively). The relative abundance of the M^{+1} (*m/z* 311) to that of the $M^{+\bullet}$ suggested a *ca.* 22% relative

abundance which would correspond with a C_{20} or C_{21} acid methyl ester (McLafferty and Turecek, 1993). Assuming two oxygen atoms are present for the acid group, this gives potential empirical formulae of $C_{20}H_{38}O_2$ or $C_{21}H_{26}O_2$ which generate double bond equivalents (DBE) of 2 and 9 respectively.

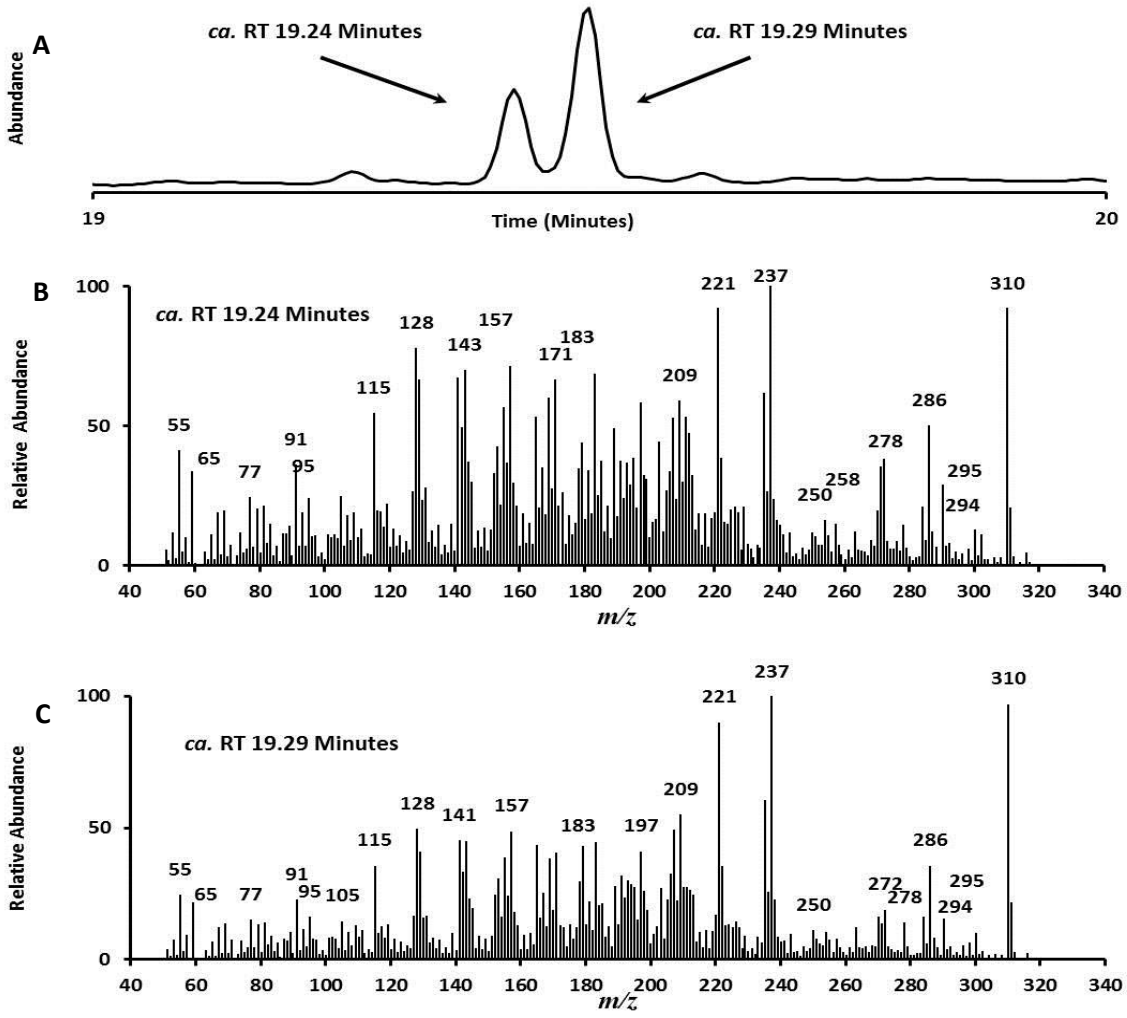

Figure 5.30. (A) Mass chromatogram of m/z 310 from Ag^+SPE Fraction 5 highlighting two resolved peaks. (B) Mass spectrum of the compound eluting at RT 19.24 minutes. (C) Mass spectrum for the compound eluting at RT 19.29 minutes**.** GC-MS conditions as described in Figure 5.2.

A DBE of 2 would only allow one ring or double bond once the carboxyl oxygen was taken into account. A DBE of 9 could possibly describe a steroidal type acid (Figure 5.31 A). The mass spectra may also be describing a $C_{20}H_{22}O_3$ keto acid methyl ester (DBE of 10) (Figure 5.31 B).

Other significant ions that hint towards a mono aromatic polycyclic moiety are m/z 91, 77 and 65, which are can be indicative of a methyl aromatic and an aromatic ring fragment. The lone double bond present in the 'A' ring is purely speculative but is consistent with the presence of an original hydroxy group that has either been dehydrated by the methylation process, or in the hot GC injector (e.g. Johnson et al., 2010)

Two other potential assignments are shown in Figure 5.31. That the structures are of a steroidal nature as based upon literature evidence (e.g. Rowland et al., 2011c) and personal communications (e.g. West., 2012). Moreover it is likely that diaromatic acids (ME) would elute in this SPE fraction (i.e. with 95:5 Hexane:diethyl ether; fraction 5). Figure 5.31C shows a penta-methyl dihydrocyclopentyl naphthalene ethanoic acid methyl ester structure with the empirical formula $C_{21}H_{26}O_2$ (DBE = 9) and a molecular weight of 310 Da, which is consistent with the $M^{+\bullet}$ Figure 5.30. Cleavage of the ethanoate group (73 Da) would leave a nucleus of 237 Da which is highlighted as the base peak in the mass spectra in Figure 5.31 B and C. A cleavage between the cyclopentyl group and the naphthalene group could potentially leave a charged methyl naphthalene fragment at m/z 183 present in Figure 5.31B. Potential methyl groups at the C_8 and C_9 positions of the terpenoid structures proposed in

Figure 5.31 (C and D) might indicate that these structures were originally steroidal type acids that have undergone some form of degradation.

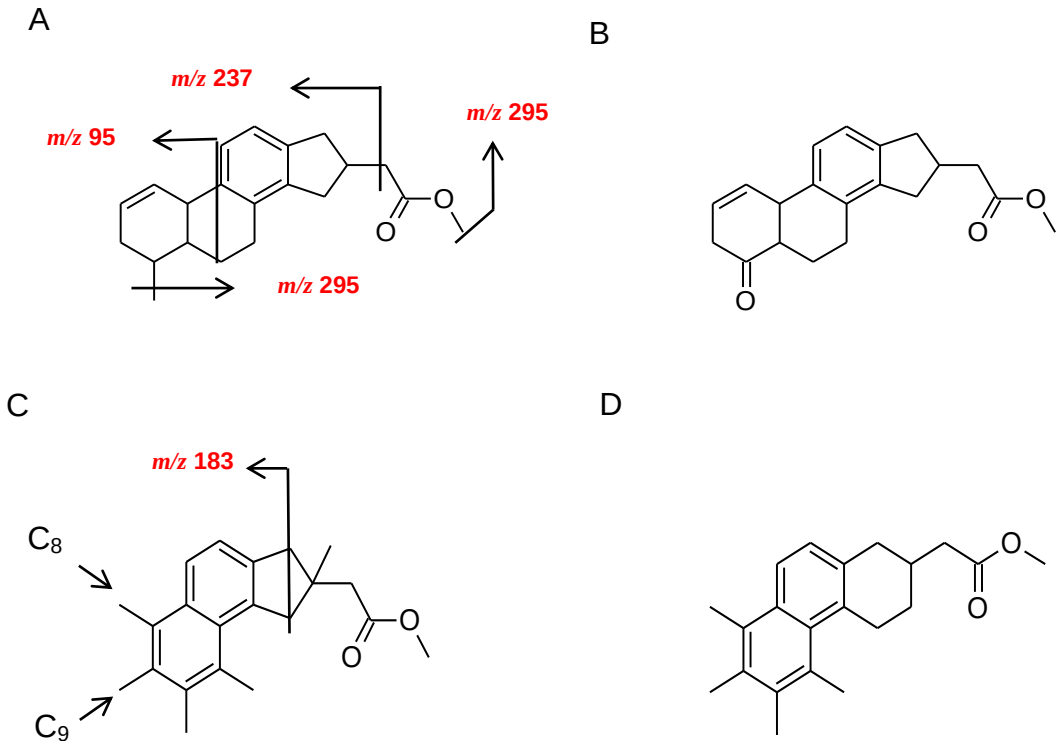

Figure 5.31. Schematic of potential structures and fragmentation patterns for unknowns in Ag+SPE fraction 5. (A) A 4- methyl steroidal ethanoic acid methyl ester. (B)A keto steroidal ethanoic acid methyl ester. (C) A 2,6,7,8,9-pentamethyl-2,3-dihydro-1*H*-cyclopenta[*a*]naphthalen-2-yl ethanoic acid methyl ester. (D) A 2,6,7,8-tetramethyl-1,2,3,4-tetrahydrophenanthren-2-yl ethanoic acid methyl ester .

5.3.2.4. Comprehensive Multi-Dimensional GC-MS of Ag^+SPE Fractions

Selected Ag^+SPE fractions of the OSPW acid extracts were examined by multi-dimensional gas chromatography-mass spectrometry (GCxGC-MS) (Figure 5.32).

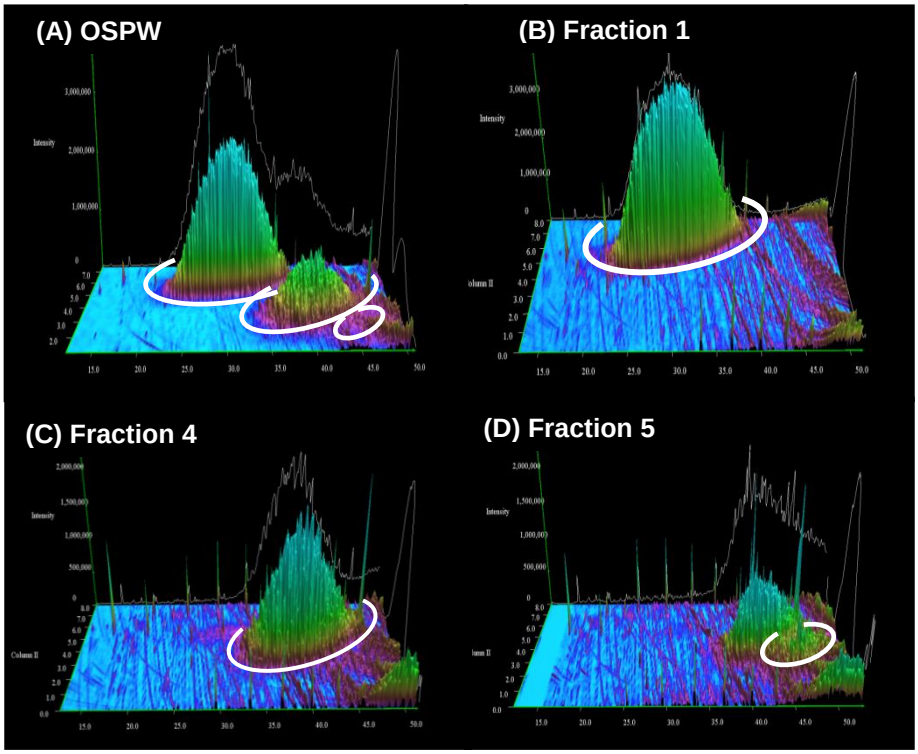

Figure 5.32. Total ion current chromatograms resulting from a GCxGC-MS of (A) methylated acid extracts from an OSPW; (B) Ag^+SPE Fraction 1; (C) Ag^+SPE Fraction 4; and (D) Ag^+SPE Fraction 5. White circles indicate areas of separate fractions. Samples (1 µL) were injected at 280 °C splitless. The oven was programmed from 40 °C (hold for 1 min), then heated to 300 °C at 5 °C min^{-1} and then held for 10 min. The modulation period was 6 s. The first-dimension column was a polar 30 m x 0.25 mm x 0.15 µm Carbowax MEGA-Wax HT and the second-dimension column was an apolar 50% phenyl polysilphenylene siloxane 3 m x 0.25 mm x 0.15 µm BPX50. The MS transfer line temperature was 280 °C and the ion source was 300 °C. Figure originally published in Jones et al., 2012A.

Analysis of the fractions by GCxGC-MS using a polar/apolar GC column configuration confirmed the assignment of fraction 1 as containing mainly alicyclic acid ME and that fractions 4 and 5 contained aromatic acid ME. Thus mass spectra generated from the GCxGC-MS and the dual retention times compared well to those authentic acid methyl esters (e.g. adamantane acids, dehydroabietic acid and fluorene type acids) thus allowing confirmatory assignments of compounds to be made and thus assignment of alicyclic/aromatic groupings within the unresolved humps generated from each Ag^{+}SPE fraction. Methods of characterisation and identification are set out in literature (i.e. Rowland et al., 2011; West et al., 2013). Briefly: tentative identification was achieved through first principal mass spectral analysis. Compounds of interest were either purchased commercially and esterified with the BF_3-MeOH complex or synthesised in house (e.g. Chapter 2). The methyl esters of these commercial or synthetic acids were then examined by GC-MS and GCxGC-MS, using the same chromatographic conditions, and the mass spectra and GC retention times were compared.

Use of different column sets (polar and apolar primary and secondary columns) and further method developments allowed different chromatographic separations than previously (*cf*. Rowland et al., 2011, 2012). These advances in the methodology allowed confirmation that the fractions assignment of alicyclic, aromatic and di-aromatic were generally correct (Figure 5.33; Jones et al., 2012a).

Figure 5.33A indicates that the acid extract of an OSPW was separated in to two or three largely unresolved ‘humps’ when examined by GCxGC-MS with a polar primary and an apolar secondary column. Co-chromatography of authentic acid ME (e.g. 3-methyladamantane-1- carboxylic acid and 3,5-dimethyladamantane-1-carboxylic acid methyl esters; Figure 5.33B) showed that fraction 1 was mainly alicyclic .

Fraction 4 was confirmed to contain acids with a mono aromatic character as shown by the co-chromatography of dehydroabietic acid methyl ester (Figure 5.33 C). Although fluorene-9-carboxylic acid methyl ester eluted outside of the third ‘hump’ revealed in fraction 5 (Figure 5.33D) the elution was within the generally same region indicating, perhaps, some di-aromatic character in the acids within this ‘hump’. The assignments of alicyclic, monoaromatic and diaromatic structures eluting in fractions 1, 4 and 5 generally matched the elution order of the alicyclic, monoaromatic and diaromatic authentic acid ME when eluted through the SPE columns.

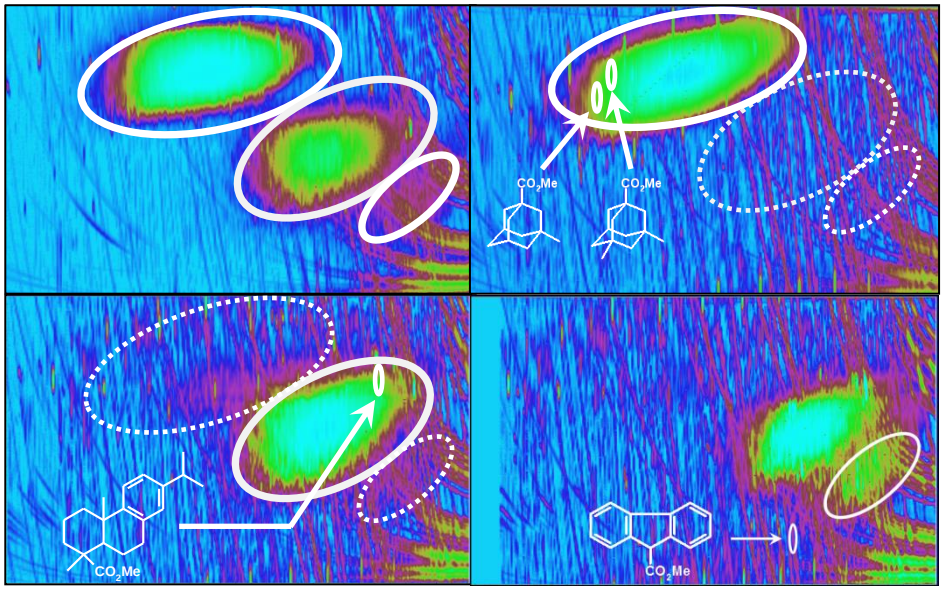

Figure 5.33. Two dimensional total ion current GCxGC-MS chromatograms of (A) acid extracts (ME) of an OSPW. (B) Ag^+SPE Fraction 1. (C) Ag^+SPE Fraction 4. (D) Ag^+SPE Fraction 5**.** White circles indicate approximate areas of individual chromatographic humps observed in the unfractionated (A) and fractionated (B-D) extracts . Figure adjusted from the original, published in Jones et al., 2012a. GCxGC-MS conditions as described in Figure 5.32.

5.3.2.5 Further Ag^+SPE of Authentic Acid Methyl Esters

As the monocyclic and mono-aromatic acid methyl esters used as calibrants for the Ag+SPE fractionation in the previous experiment were apparently evaporating somewhat during work up, it was decided that use of higher molecular weight less volatile, acids would be prudent, in addition to use of the same di-aromatic acid (naphthalene-2-carboxylic acid methyl ester). The mono aromatic and mono cyclic acids were replaced by isobutylphenyl-4-butanoic acid and isobutylcyclohexyl-4-butanoic acid methyl esters (Figure 5.34).

A

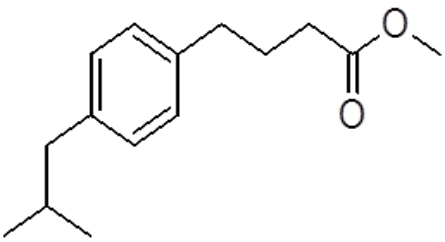

B

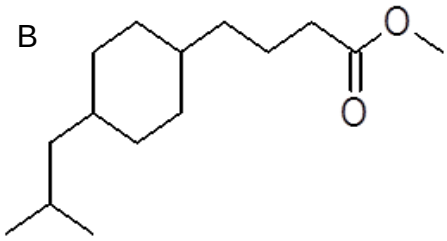

Figure 5.34. Structures of (A) Isobutylphenyl-4-butanoic acid, methyl ester (nominal molecular weight 234 Da). (B) Isobutylcyclohexyl-4-butanoic acid methyl ester (nominal molecular weight 240 Da).

The three acids were mixed (0.01 mg mL^{-1} of each acid methyl ester) and the mixture was examined by GC-MS. As expected, the total ion current chromatogram (Figure 5.35A) showed three peaks at RT 14.38, 15.27 and 15.24 minutes. Analysis of the mass spectra allowed an assignment of each peak.

The component eluting at RT 14.38 minutes had a similar retention time and mass spectrum (e.g. $M^{+\bullet}$ at *m/z* 186, significant fragment ions at *m/z* 155 and 127) to naphthalene-2-carboxylic acid, methyl ester (Figure 5.18) and was assigned thus.

The mass spectrum of the peak at RT15.27 minutes (Figure 5.35B) revealed an $M^{+\bullet}$ at *m/z* 234, consistent with a isobutylphenyl-4-butanoic acid, methyl ester. Significant fragment ions at *m/z* 203, 160 and 147 were characteristic of the fragmentation involving loss of a methoxy group, a methylated ethanoate group and a methylated propanoate group respectively from the butanoate side chain. A fragment ion at *m/z* 191indicates cleavage of the isobutyl group. The presence of *m/z* 91, 77 and 65 were indicative of a potential methyl benzene fragment and may indicate benzylic cleavage.

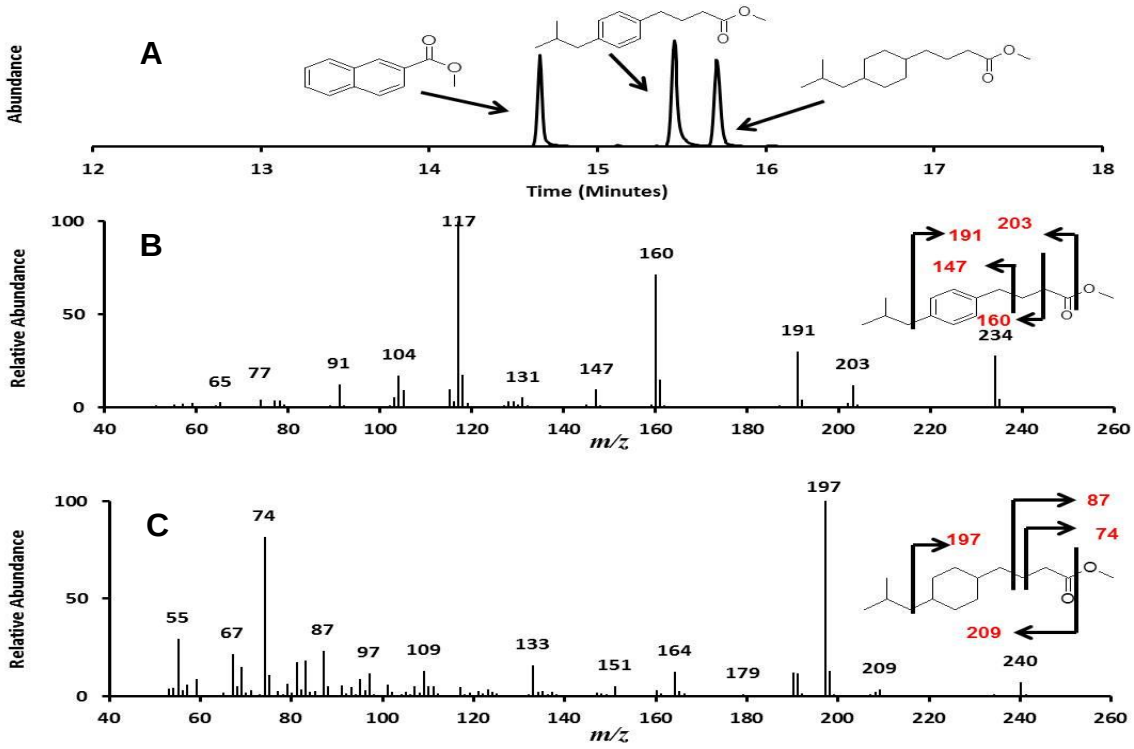

Figure 5.35. (A) Total ion current chromatogram of an acid ME mixture proposed for calibration of Ag+SPE (0.01 mg mL-1). (B) Mass spectrum of the compound eluting at RT 15.27 minutes (isobutylphenyl-4-butanoic acid methyl ester). (C) Mass spectrum for the compound eluting at RT 15.42 minutes (isobutylcyclohexyl-4-butanoic acid, methyl ester). GC-MS conditions as described in Figure 5.2.

The mass spectrum in Figure 5.35C had an $M^{+\bullet}$ at *m/z* 240, which is six Da more than the molecular weight of the butylphenyl butanoic acid, methyl ester and is consistent with the molecular weight expected for butylcyclohexyl butanoic acid, methyl ester. Significant fragments at *m/z* 209, 87 and 74 were consistent with the fragmentation of the butanoic acid, methyl ester group and a fragment ion at *m/z* 197 (base peak) indicated cleavage of the isobutyl group.

Fragments at m/z 97and 83 are consistent with the presence of a methylcyclohexyl fragment. This pattern allows an assignment of an iso-butylcyclohexylbutanoic acid, methyl ester.

A sample of each standard was mixed (1 mg) in 100 μL of hexane and after a thorough column wash was eluted through an Ag^+SPE column. Unlike the initial experiment (Section 5.3.2.1) no acid was apparent in the first eluting hexane fraction. However the isobutylcyclohexyl-4-butanoic acid, methyl ester eluted in fractions 2 and 3 (also with 100% hexane), the isobutylphenyl-4-butanoic acid, methyl ester and naphthalene-2-carboxylic acid methyl ester compounds eluted in fraction 4 (95% hexane; 5% diethyl ether) in approximately equal measures (Figure 5.36) and again in fraction 5 (the di-aromatic being more abundant). No acid methyl esters eluted in the remaining fractions.

These total ion chromatograms (Figure 5.36) revealed poor gas chromatography with each peak displaying a certain amount of tailing. This was due to preceding analysis of hydroxy adamantane acid, methyl esters using a non-standard solvent which adversely affected the GC column. As the desired outcome of the acid standards experiment was to assess the separation of the compounds with Ag^+SPE columns it was decided that, poor chromatography notwithstanding , further Ag^+SPE experiments on the bulk OSPW ME acid extracts could nonetheless proceed.

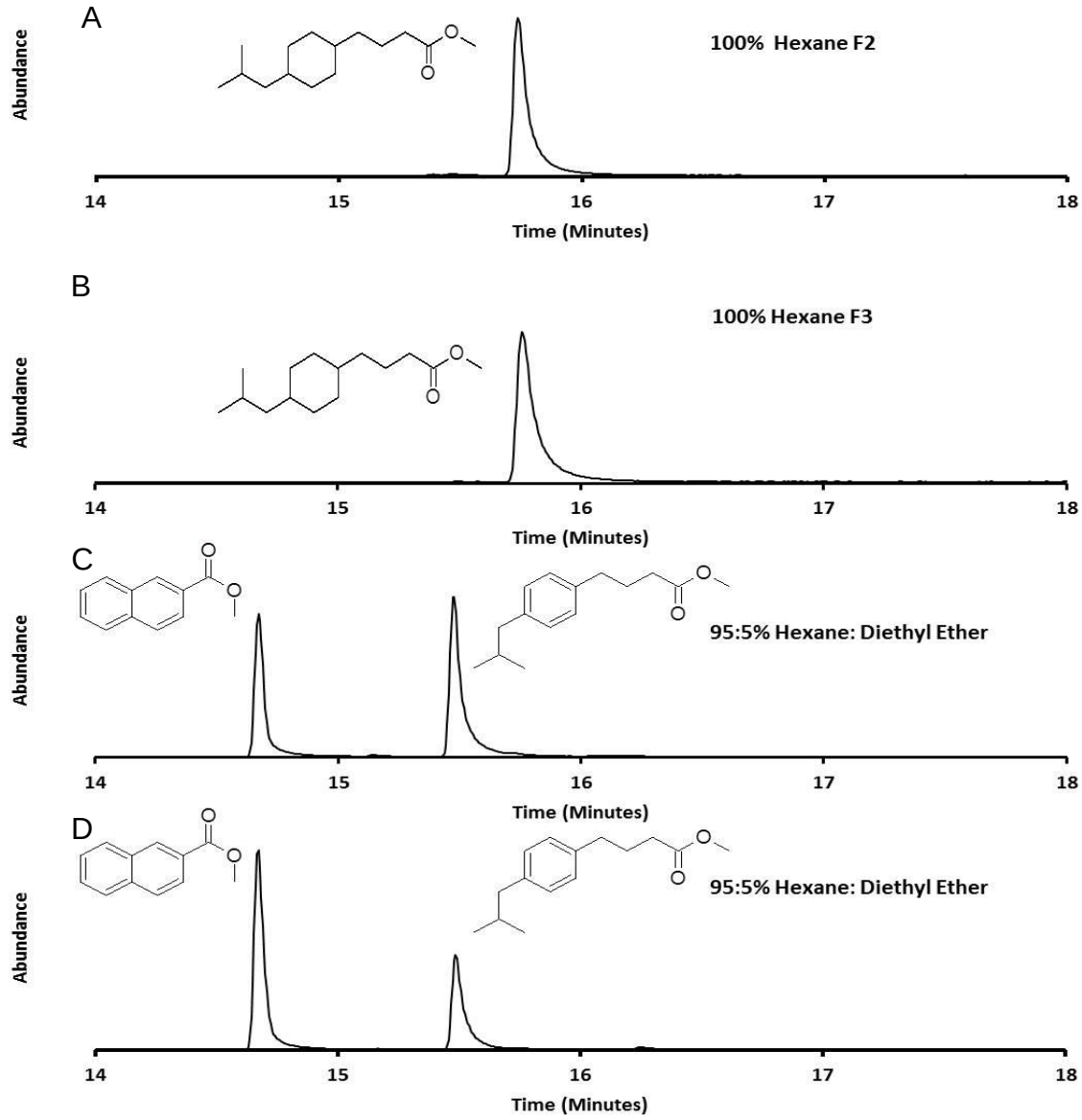

Figure 5.36. Total ion current chromatograms for the Ag^{+}SPE authentic acid ME**.** Chromatograms of the component eluting in fractions 2 (A) and 3 (B) (with 100% hexane) at RT 15.42 minutes , assigned as a isobutlylcyclohexyl-4-butanoic acid, methyl ester. Chromatograms of the components eluting in fractions 4 (C) and 5 (D) (with 95:5% hexane:diethyl ether) at RT 14.38 and 15.24 minutes , assigned as naphthalene-2-carboxylic acid (RT 14.38) and isobutylphenyl-4-butanoic acid (RT 15.24). GC-MS conditions as described in Figure 5.2.

5.3.2.6 Further Ag^+SPE Separations of OSPW Acid Methyl Esters

Since previous Ag^+SPE experiments (section 5.3.2.2) conducted on ≤ 3 mg OSPW acid methyl esters provided un-weighable fractions, a further experiment was conducted on a larger aliquot of OSPW acid esters. This provided fractions which could be weighed and which could be characterised by multiple analytical techniques, including elemental analysis (*vide infra*; Section 5.3.2.8). Thus, 80 mg of OSPW acid extracts was divided into 5 mg aliquots and methylated using the BF_3-MeOH complex. A 5 mg aliquot was analysed by GC-MS and the remaining 75 mg fractionated into eight fractions by Ag^+SPE (3x 100% hexane; 4x 95:5 hexane:diethyl ether; 1x 100% diethyl ether). In total, fifteen Ag^+SPE columns were used to fractionate the 5 mg aliquots over a number of days. For each SPE separation a control SPE cartridge was eluted with clean solvent to the same solvent ratios used for OSPW esters in order to provide some quality control for contaminants entrained in the Ag^+SPE stationary phase and solvents.

Unlike the initial SPE fractionation, the first alicyclic 'hump' of unresolved acids was apparent in the 100% hexane fraction 2 (maxima RT *ca.*15.27 minutes, Figure 5.37). This RT node was the same as that of the components for fraction 1 from the initial fractionation attempt (*ca*. 15.26 minutes; section 5.3.2.2). RT maxima for the mixtures in the remaining hexane fractions and in the four 95:5 hexane:diethyl ether fractions range from *ca.* 16.39 minutes to *ca.* 22.33 minutes (Figure 5.37), the maximum RT for fraction 7 in the initial attempt was *ca.* 22.22 minutes (Section 5.3.2.2).

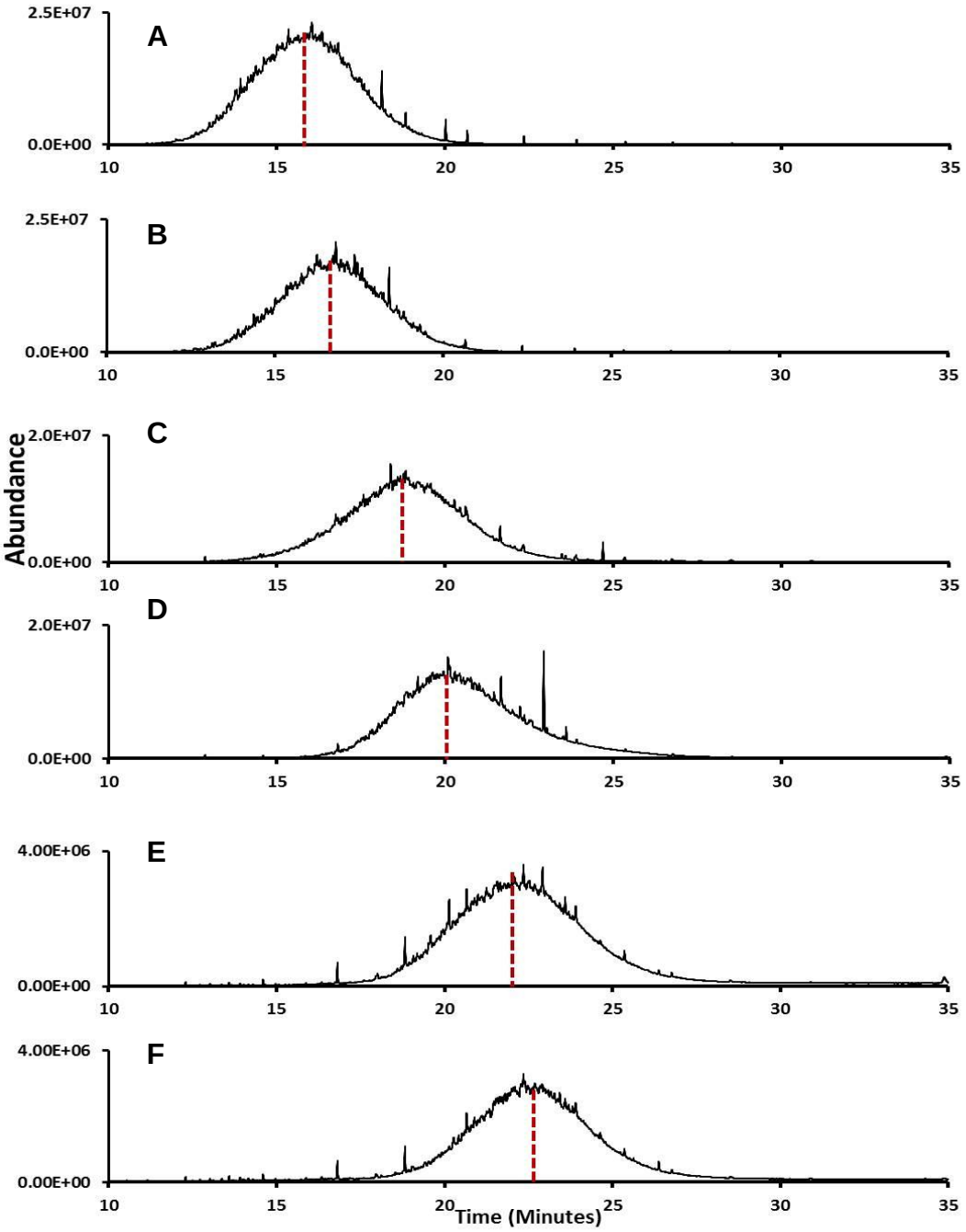

Figure 5.37. Total ion current chromatograms of Ag^{+}SPE fractions 1 to 7 from the larger scale extraction of OSPW derived naphthenic acids. (A) Fraction 2, eluted with 100% hexane. (B) Fraction 3, eluted with 100% hexane. (C) Fraction 4, eluted with 95:5% hexane diethyl ether. (D) Fraction 5, eluted with 95:5% hexane diethyl ether. (E) Fraction 6, eluted with 95:5% hexane diethyl ether. (F) Fraction 7, eluted with 95:5% hexane diethyl ether. Red dotted line highlight shift in maximal retention times. GC conditions as described in Figure 5.2.

When the total ion current chromatograms of each fraction from each repeat Ag^+SPE extraction were overlain, the 'hump' nodal retention times and general chromatogram shape were similar throughout. All seven repeat fractions revealed that the chromatographic separation using Ag^+SPE columns had good reproducibility in both retention time, elution and relative abundance (Figure 5.38).

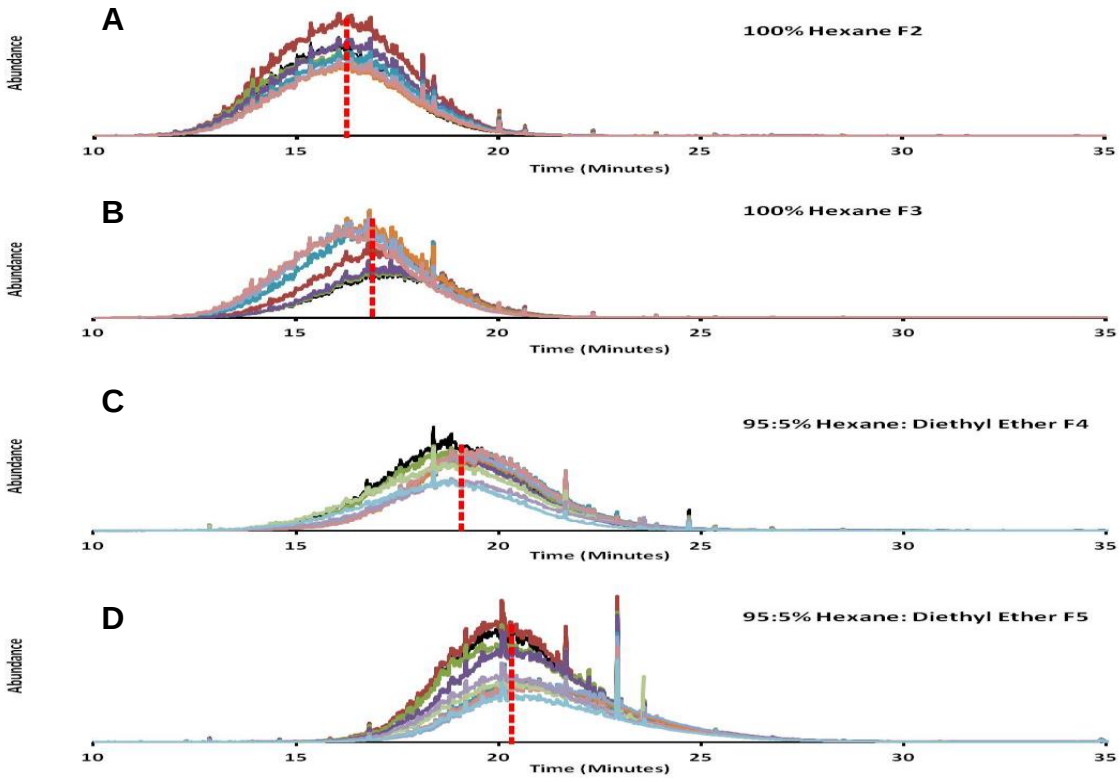

Figure 5.38. Total ion current chromatograms of the Ag^+SPE fractionation of the OSPW acid ME. (A) Overlain Ag^+SPE fraction 2 . (B) Overlain Ag^+SPE fraction 3. (C) Overlain Ag^+SPE fraction 4. (D) Overlain Ag^+SPE fraction 5. Red dotted lines highlight the average maximal retention time for each of the 'humps'. GC conditions as described in Figure 5.2.

As with the previous experiment, an averaged mass spectrum was generated for each of the first four main fractions (fractions 2-5). The mass spectra for Fraction 2 and 3 were very similar to the mass spectra produced by the initial experiment, with the key adamantane acid methyl ester ions (m/z 135, 149 and 163) relatively prominent (Figure 5.39 A and B).

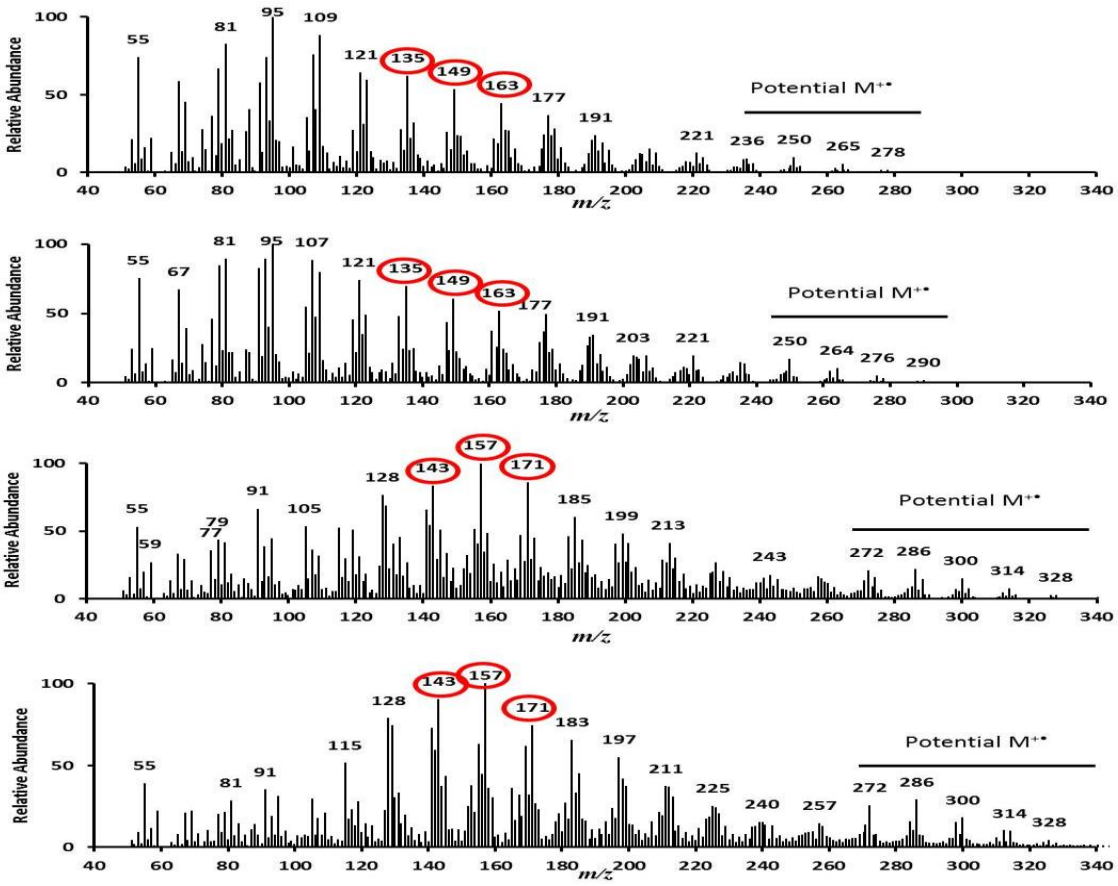

Figure 5.39. Averaged mass spectra of a selection of the unresolved chromatographic 'humps' from the bulk Ag^{+}SPE experiment. (A) Averaged mass spectrum of Fraction 2. (B) Averaged mass spectrum of Fraction 3. (C) Averaged mass spectrum of Fraction 4. (D) Averaged mass spectrum of Fraction 5. Red circles highlight ions chosen for mass chromatographic analysis.

Mass chromatograms of the 100% hexane fractions revealed that they were essentially the same as those produced in the initial experiment (Section

5.3.2.3). Analysis of the 95:5% hexane diethyl ether fractions revealed three distinct ions in both fractions 4 and 5 (*m/z* 143, 157 and 171). For the 95:5% hexane: diethyl ether fraction 4, the mass chromatograms for ions *m/z* 143, 157 and 171 displayed an unresolved hump with three resolved peaks at RT 21.38, 23.29 and 23.35 minutes (Figure 5.40).

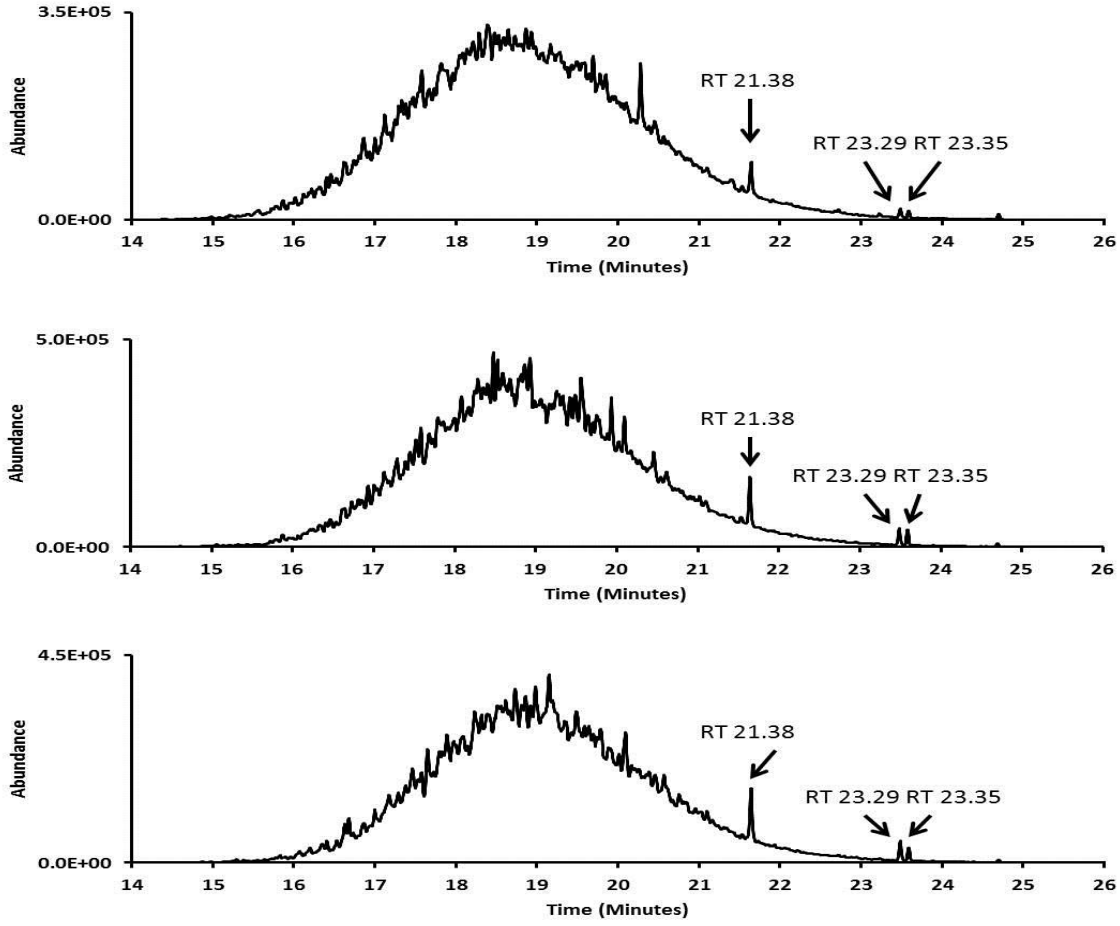

Figure 5.40. Mass chromatograms from the Ag^{+}SPE 95:5% hexane: diethyl ether fraction 4 of the OSPW acid extracts. (A) Mass chromatogram of *m/z* 143. (B) Mass chromatogram of *m/z* 157. (C) Mass chromatogram of *m/z* 171. Figure highlights resolved peaks at RT 21.38, 23.29 and 23.35 minutes. GC conditions as described in Figure 5.2.

The mass spectra of the three resolved peaks (not shown), revealed a base ion at *m/z* 145 . When a mass chromatogram of *m/z* 145 it was evident that the same three peaks (RT 21.38, 23.29 and 23.35) were present, though somewhat more resolved (Figure 5.41A). The mass spectra of these peaks were the same for all four analysed mass chromatograms (Figure 5.40 and Figure 5.41).

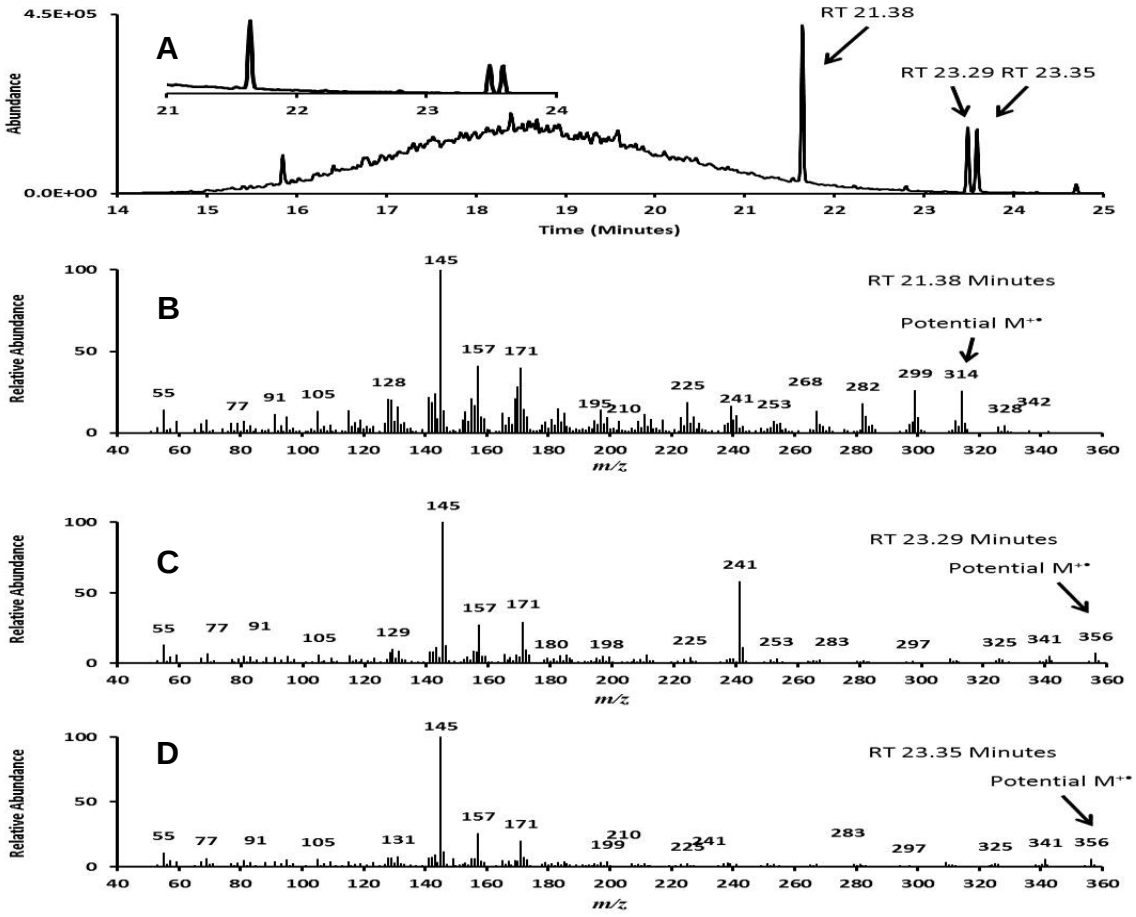

Figure 5.41. (A) Mass chromatogram of *m/z* 145 from the OSPW acid extracts with inset revealing area eluting between 21 and 24 minutes. (B) Mass spectrum for compound eluting at 21.38 minutes. (B) Mass spectrum for compound eluting at 23.29 minutes. (C) Mass spectrum for compound eluting at 23.35 minutes. GC-MS conditions as described in Figure 5.2.

The mass spectrum of the compound eluting at RT 21.38 minutes (Figure 5.41B) revealed two potential $M^{+\bullet}$ (*m/z* 314 and *m/z* 328). When taking significant fragment ions into account it seemed unlikely that *m/z* 328 was the molecular ion of the major component. Assuming an $M^{+\bullet}$ of *m/z* 314 allows for the explanation of *m/z* 299, 282, 267 and 241 ions via the cleavage of a methylated ethanoate side chain. A *m/z* 145 base peak ion coupled with an $M^{+\bullet}$ at *m/z* 314 is consistent with that of a putative de-A steroidal acid (section 5.3.1.2 and Rowland et al., 2011c). However, other assignments may be possible.

Examining the relative abundance of the ion at *m/z* 315 (M^{+1}) with that of the $M^{+\bullet}$ allows a tentative determination of the number of carbons in the compound as the M^{+1} describes compounds with one ^{13}C atom which is at a relative abundance of 1.1% to ^{12}C. The M^{+1} relative abundance (to the base ion) is 6.226% whilst the $M^{+\bullet}$ relative abundance is 25.713%. This means that the relative abundance of the M^{+1} to the $M^{+\bullet}$ is *ca.* 24%. Reference to tables provided by McLafferty and Turecek (1993) reveals that this is roughly equivalent to a C_{22} carbon structure (though C_{21} and C_{23} structures must be considered). Allowing for two oxygen atoms this gives empirical formulae (and double bond equivalents: DBEs of: $C_{21}H_{30}O_2$ (DBE 7); $C_{22}H_{18}O_2$ (DBE 14) and $C_{23}H_6O_2$ (DBE 21). It is unlikely that the compound has a DBE of 21 or a $C_{23}H_6$ formula so these formulae can be dismissed.

If an assignment of $C_{21}H_{30}O_2$ is correct, then allowing for the fragment at *m/z* 241 (loss of an ethanoate side chain) this leaves a $C_{18}H_{23}$ nucleus (DBE 6) which could be described by an octahydrophenanthrene or a hexahydrocyclopentylnaphthalene (Figure 5.42). This classification is confirmed by the base peak ion at *m/z* 145 which is indicative of a methyl-tetrahydronaphthalene fragment (Figures 5.10 and 5.11 Section 5.3.1.2 and Figure 2.72, Chapter 2) or a dimethyl indane fragment, which allows for fragmentation across more than one ring, in both tentative assignments. An assignment of either structure fits the molecular weight, the number of DBEs and the mass spectral fragmentation pattern. Identification of the unknown as a mono-aromatic acid ME also fits with the elution of these compounds within the first 95:5% hexane: diethyl ether fraction from the Ag^+SPE cartridges, since the authenic acid, isobutylphenylbutanoic acid ME, also eluted with the first 95:5% hexane:diethyl ether fraction (Section 5.3.2.5).

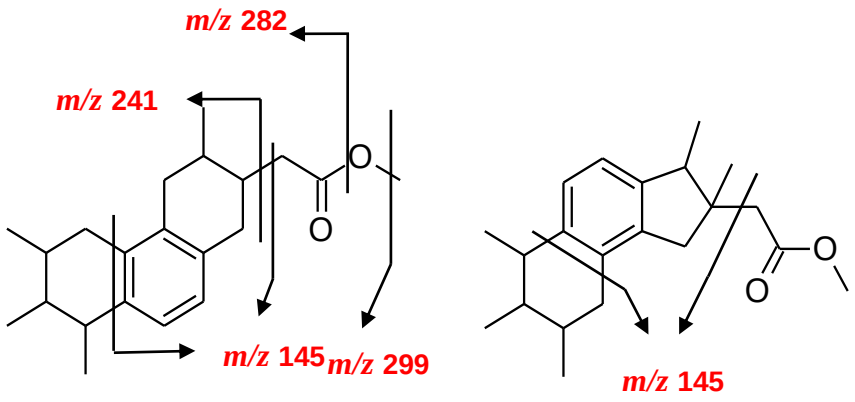

Figure 5.42. Possible structures for the compound eluting at RT 21.38 minutes in the 95:5% hexane:diethyl ether fraction 4 from the Ag+SPE of the OSPW acid extract methyl esters displaying fragmentation of compounds with (A) displaying a tetramethyl octahydrophenathreneethanoic acid methyl ester and (B) displaying a pentylmethyl hexahydrocyclopentylnaphthalene ethanoic acid methyl ester.

Analysis of the two peaks eluting at RT23.29 and 23.35 minutes (Figure 5.42 C and D) revealed that both have a possible $M^{+\bullet}$ at *m/z* 356 (42 Da greater than *m/z* 314, equivalent to three extra carbon atoms and associated hydrogen atoms). Both spectra were alike, with similar significant fragment ions. An ion at *m/z* 269 in both spectra might be characteristic of loss of a propanoic acid methyl ester moiety (M-87). Though the abundance of the *m/z* 241 (M-115) might suggest the loss of a pentanoic methyl ester moeity (Figure 5.41B). Analysis of the relative abundance of the M^{+1} and $M^{+\bullet}$ revealed a relative percentage of *ca.* 28% for which a potential formula of $C_{25}H_{24}O_2$ (DBE 13) is derived, which would indicate a very high degree of unsaturation. A C_{24} structure is more likely (as this is also three carbon atoms more than the *m/z* 314 compound). This would give a $C_{24}H_{36}O_2$ formula, for which a DBE of 7 is derived, equivalent to the *m/z* 314 structure (Figure 5.43).

When examining the mass chromatograms *m/z* 143, 157 and 171 for components eluting with 95:5% hexane: diethyl ether (e.g. fraction 5) a number of relatively resolved peaks were apparent (Figure 5.44). However, all but three produced complex mass spectra, probably due to co-elutions. The three peaks for which some tentative structural information could be determined eluted at RT 22.56 minutes, 23.30 minutes and 23.35 minutes (Figure 5.44), the latter peaks sharing the same retention time as two resolved peaks from Fraction 4 (Figure 5.41A).

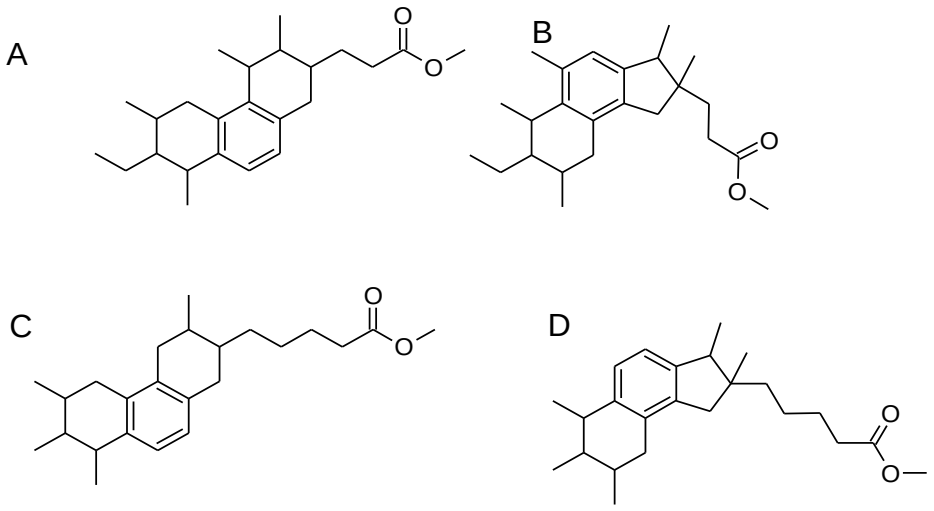

Figure 5.43. Possible structures for the compounds eluting at RT 23.29 and 23.35 minutes in the 95:5% hexane:diethyl ether fraction 4 from the Ag^{+}SPE of the OSPW acid extract methyl esters**.** (A) Displaying an ethyl-tetramethyl octahydrophenathrenepropanoic acid methyl ester. (B)An ethyl-pentylmethyl hexahydro-cyclopentylnaphthalenepropanoic acid methyl ester. (C) Tetramethyl octahydrophenathrenepentanoic acid methyl ester. (D) A pentylmethyl hexahydro-cyclopentylnaphthalenepentanoic acid methyl ester.

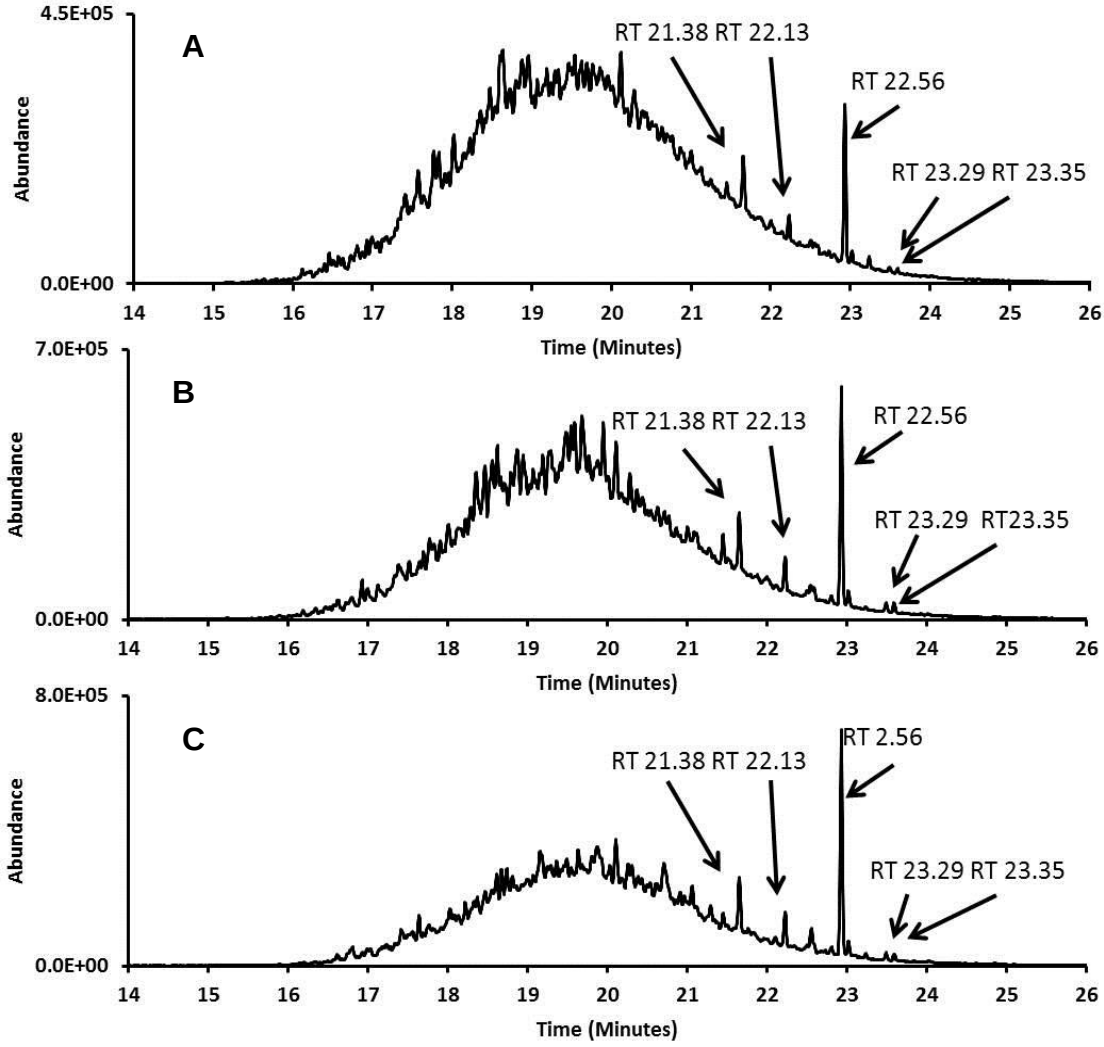

Figure 5.44. Mass chromatograms from the Ag^{+}SPE 95:5% hexane: diethyl ether fraction 5 of the OSPW acid extracts for (A) *m/z* 143; (B) *m/z* 157; and (C) *m/z* 171; highlighting resolved peaks at RT 21.38, 22.13, 22.56, 23.29 and 23.35 minutes. GC conditions as described in Figure 5.2.

As was noted previously for fraction 4, the mass spectra for the peaks eluting at RT 21.38, 22.13, 22.56 and 23.29 in fraction 5, were dominated by an ion at *m/z* 145; therefore a mass chromatogram for this ion was produced (Figure 5.45). The peak eluting at RT 23.35 in fraction 5 had a base ion at *m/z* 149 and was identified by reference to the NIST database (NIST, 2011) as bis-

2ethylhexylphthalate which is a well know contaminant in analytical procedures due to its use as a plasticiser (David et al., 2003).

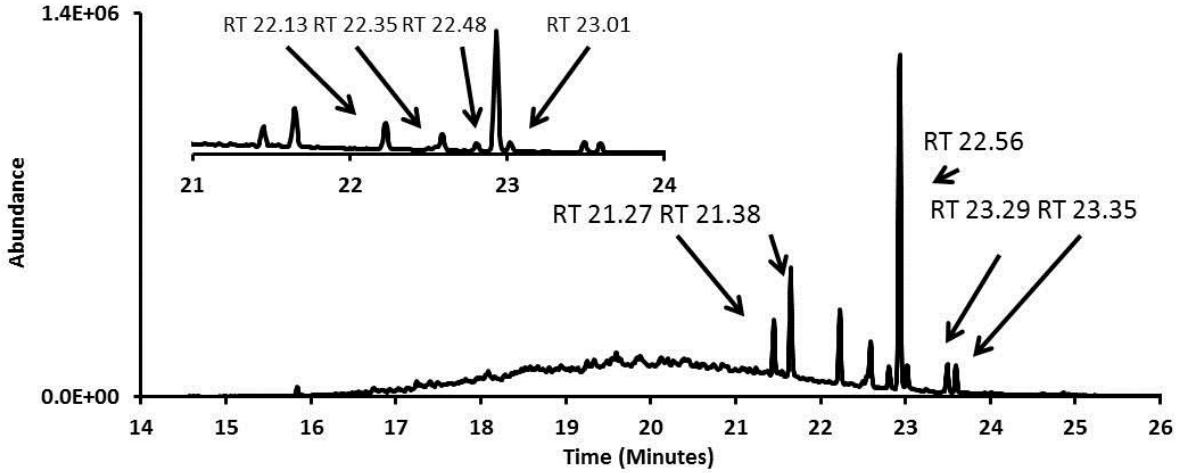

Figure 5.45. Mass chromatogram m/z 145 from the Ag^{+}SPE 95:5 hexane: diethyl ether fraction 5 of the OSPW acid extracts with inset revealing area eluting between 21 and 24 minutes, figure reveals nine resolved chromatographic peaks eluting between RT 21.27 minutes and 23.35 minutes. GC conditions as described in Figure 5.2.

Examination of the mass spectra for the nine other resolved peaks revealed only three peaks with spectra from which some tentative structural information could be determined. These eluted at RT 22.56, 23.29 and 23.35. The peak at RT 21.38 minutes had a similar mass spectrum to the peak eluting at the same time in fraction 4, and is assigned thus. All nine peaks revealed spectra containing a base peak ion at *m/z* 145. Hence they can possibly be described as a 'family' of similar compounds.

The mass spectrum of the compound eluting at RT 22.56 minutes (Figure 5.46B) was similar to that eluting in fraction 4 at RT 21.38 minutes (Figure 5.41B). The $M^{+\bullet}$ was the same (*m/z* 314) as was the relative abundance of the

M^{+1} ion. Significant fragment ions were also similar such as the base peak at *m/z* 145 and fragment ions at *m/z* 157 and 171.

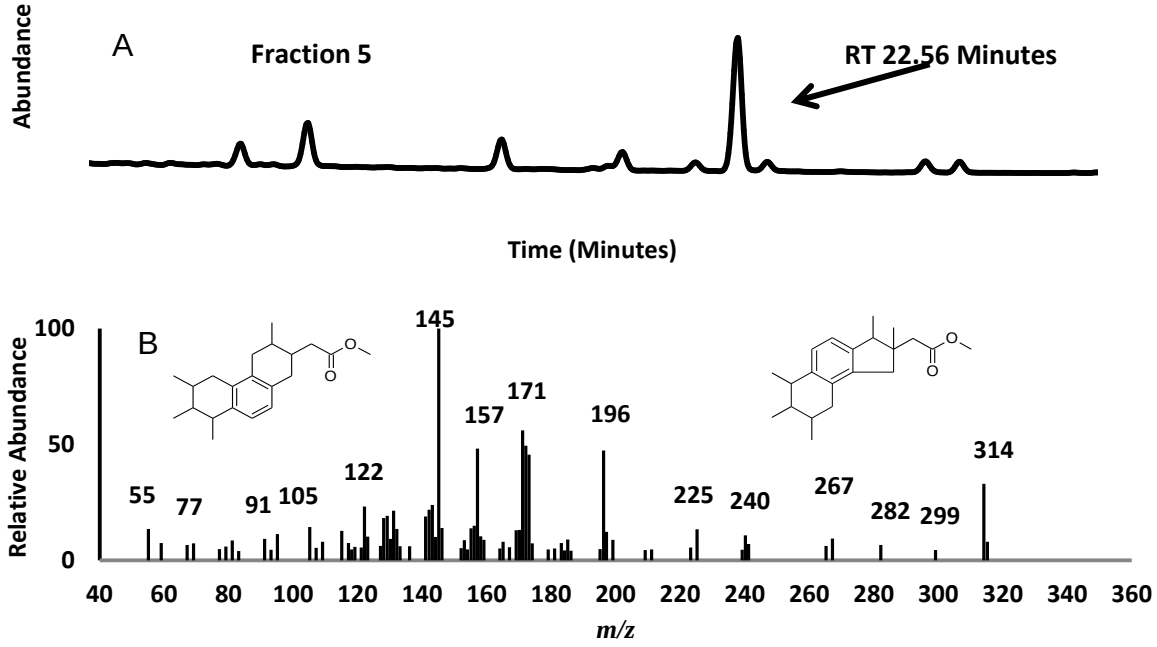

Figure 5.46. (A) Mass chromatogram of m/z 145 for Fraction 5 of the Ag^{+}SPE fractionation; and (B) mass spectrum for the compound eluting at RT 22.56 minutes, assigned as an isomer of either an tetramethyloctahydrophenathrene ethanoic acid methyl ester or a pentamethylhexahydro-cyclopentylnaphthalene ethanoic acid methyl ester. GC-MS conditions as described in Figure 5.2.

The fragmentation of the acid group was characteristic of an ethanoate ion with *m/z* 240, *m/z* 282 and *m/z* 299 consistent with losses of ethanoate radical, a methanol molecule and a methyl radical respectively. It is therefore likely that this compound is an isomer of the compounds described in Figure 5.42.

Examination of the mass spectra of the compounds eluting at RT 23.30 minutes and RT 23.35 minutes (Figure 5.47) showed differences from the mass spectra eluting at the same retention times in fraction 4. Whilst in Figure 5.47B the $M^{+\bullet}$

(*m/z* 356), the propanoate ions (*m/z* 341, 324, 297 and 269) and the base ion (*m/z* 145) were all similar, the ion at *m/z* 241 is absent. This spectrum is also relatively complex with ions which suggests a co-elution of several compounds, though the losses of propanoate radical from the $M^{+\bullet}$ and the base ion at *m/z* 145 were characteristic of the 'tetrahydronaphthalene' ion compounds which suggests an isomer of the compounds described in Figure 5.42.

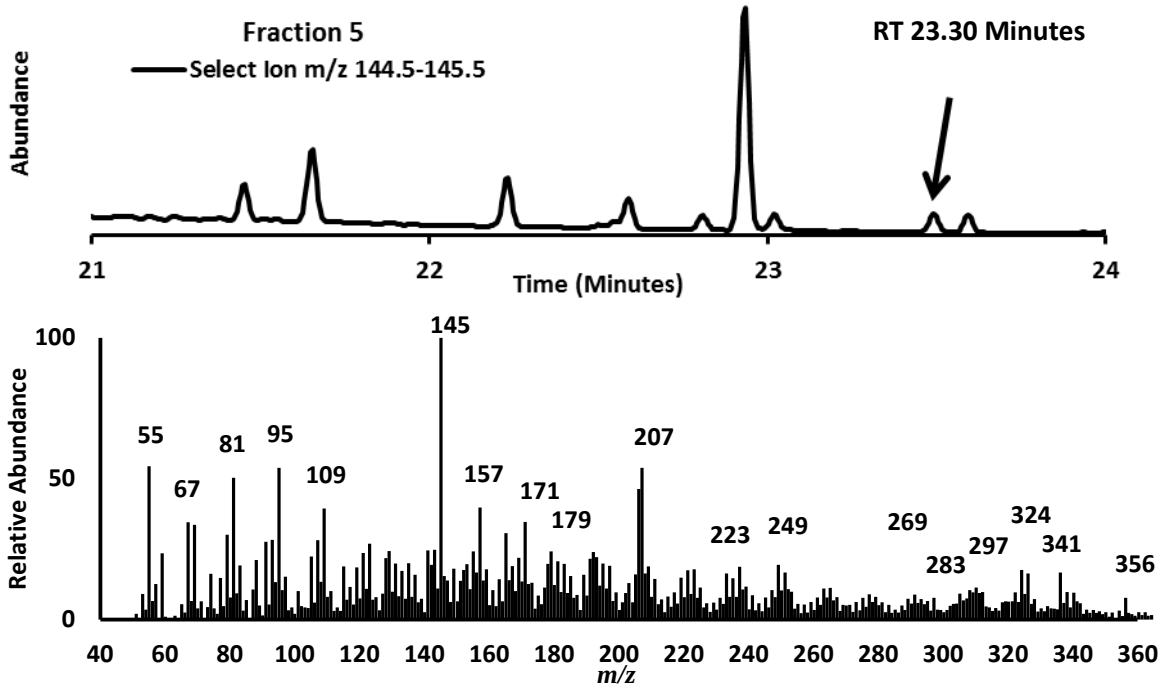

Figure 5.47. (A) Mass chromatogram of *m/z* 145 for Fraction 5 of the Ag^{+}SPE fractionation; and (B) mass spectrum for the compound eluting at RT 23.30 minutes, assigned as either an isomer of a hexamethyloctahydrophenathrene propanoic acid methyl ester or a heptamethylhexahydrocyclopentylnaphthalene propanoic acid methyl ester. GC-MS conditions as described in Figure 5.2.

The mass spectrum of the compound eluting at RT 23.35 minutes in fraction 5 (Figure 5.48) revealed a different base ion (*m/z* 149) and a different

fragmentation pattern to that of the compound eluting at the same RT in fraction 4. Ions were present at *m/z* 356 and *m/z* 341, but this may be due to co-elution. Because of the *m/z* 149 base ion, and reference to the NIST database, this compound has been tentatively identified as di-(ethylhexyl)phthalate contaminant (NIST, 2012; David et al., 2003).

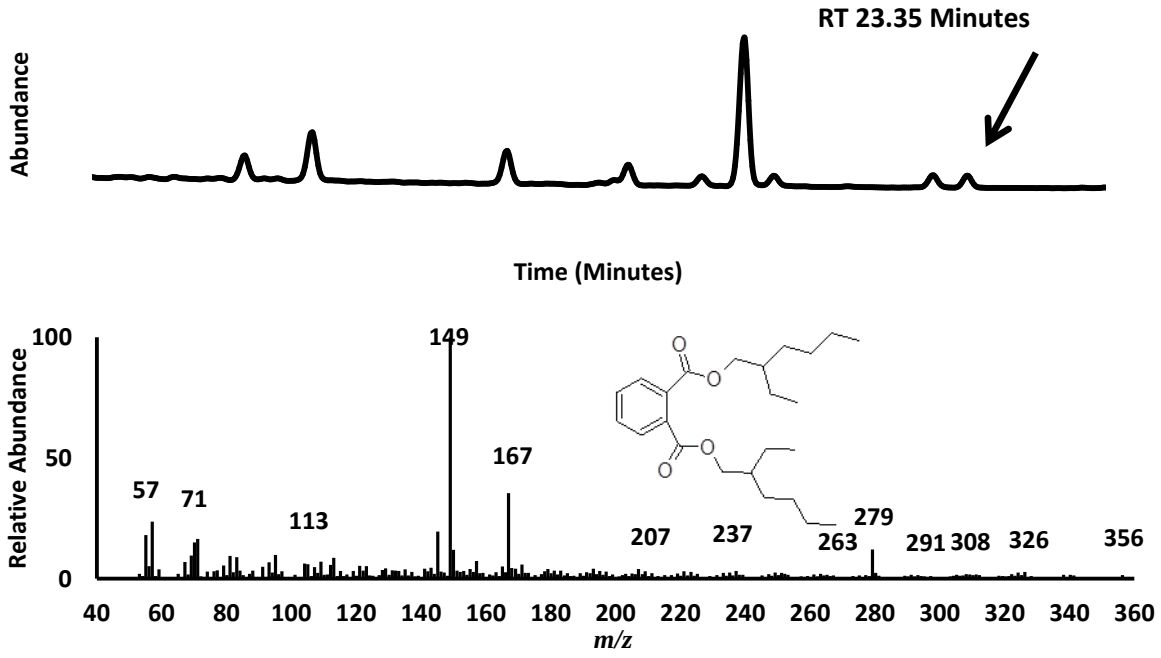

Figure 5.48. (A) Mass chromatogram of m/z 145 for Fraction 5 of the Ag^{+}SPE fractionation; and (B) mass spectrum for the compound eluting at RT 23.35 minutes, assigned as a phthalate ester contaminant (David et al., 2003). GC-MS conditions as described in Figure 5.2.

The differences in the mass spectra for compounds eluting at the same time in different fractions reveals that the preparative chromatographic methods used can have a relatively high degree of resolution and are able to somewhat separate co-eluting compounds for identification purposes without need to analyse the complex mixture by GCxGC-MS.

The chromatogram displayed in Figure 5.49 reveals a bi-nodal complex mixture with a number of seemingly resolved peaks apparent.

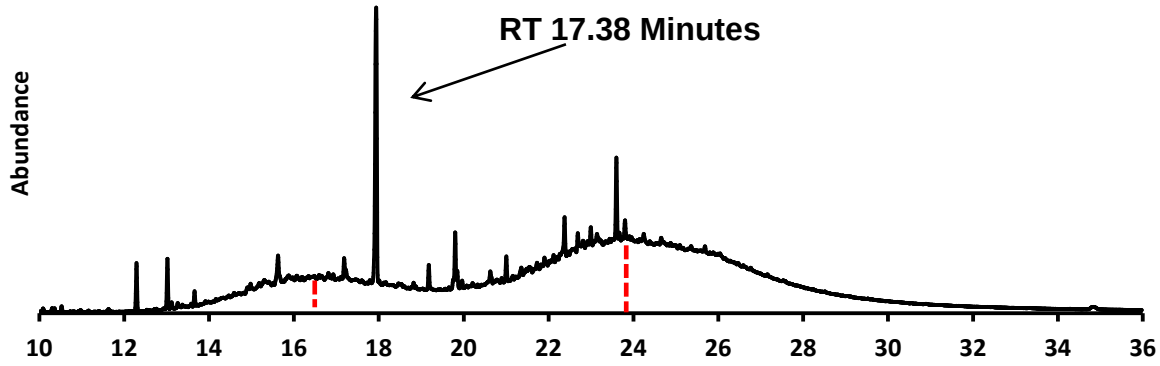

Figure 5.49. Total ion current chromatogram for the Ag^{+}SPE Fraction 8 of the OSPW acid extract ME, highlighted peak identified as phthalate contamination from the SPE column; red dotted lines indicate maximal RTs occurring at *ca*. 16.40 and 23.51 minutes. GC-MS conditions as described in Figure 5.2.

Examination of the mass spectra for the few resolved peaks revealed that some could be assigned to contaminants leaching from the plastic SPE columns used in pre-packed Ag^{+}SPE. For example, the large peak at RT 17.38 minutes (Figure 5.49) had a base peak ion at *m/z* 149 which is often indicative of phthalate esters used as plasticisers (David et al., 2003) However, the spectrum (Figure 5.50) was not similar to that of known phthalates available in library spectra (e.g. NIST) and may represent co-elution of more than one component.

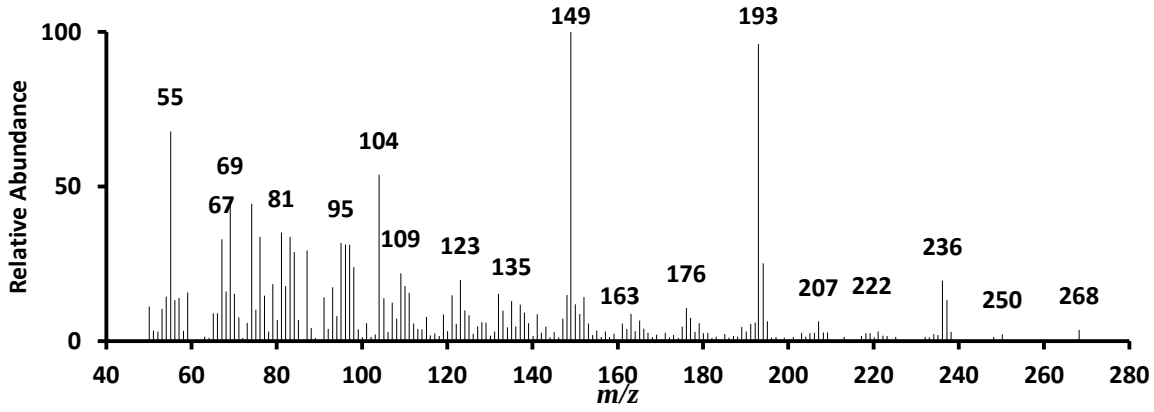

Figure 5.50. Mass spectrum of the compound eluting at RT 17.38 minutes in Ag^+SPE fraction 8**,** assigned as a possible phthalate esters contaminant, possibly leached from the Ag^+SPE column. MS conditions as described in Figure 5.2.

An averaged mass spectrum of fraction 8 was generated (Figure 5.51) and a number of significant ions revealed. Mass chromatograms of *m/z* 215 and *m/z* 225, which appeared significant in the averaged mass spectrum (Figure 5.51) are shown in Figure 5.52.

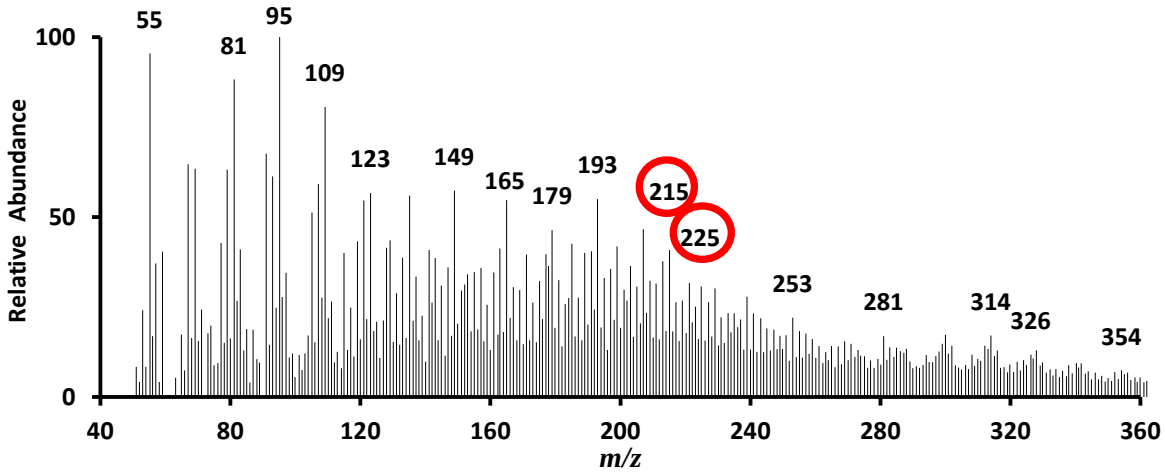

Figure 5.51. Averaged mass spectrum of Ag^+SPE fraction 8 from the OSPW acid extract ME**.** Red circles highlight fragment ions chosen for mass chromatography. MS conditions as described in Figure 5.2 .

The mass chromatogram of *m/z* 225 (Figure 5.52) revealed a small unresolved 'hump' with a number of resolved peaks. Peaks that elute between RT 21 and 22 minutes (Figure 5.52B)) revealed mass spectra with a number of possible $M^{+\bullet}$ (e.g. *m/z* 318, 304 and 288) and a base ion at *m/z* 215.

Fragment ions were present with *m/z* 272, 259, 243 and 229. A $M^{+\bullet}$ at *m/z* 318 would suggest that the ion at *m/z* 259 might describe the loss of a carboxylate ion. However, the presence of a large (*ca.* 30% relative abundance) ion at *m/z* 288 (loss of 30 Da) would not fit a classical fragmentation pattern of an acid methyl ester. This might suggest a co-elution of a number of compounds with *m/z* 316 and *m/z* 288 both being assigned as an $M^{+\bullet}$, with *m/z* 318 (potentially) describing a C_{21} or C_{22} ethanoic acid methyl ester.

Comparison with the NIST database revealed that an $M^{+\bullet}$ at *m/z* 288 with a base ion at *m/z* 215 might be characteristic of a non esterified pyrenebutanoic acid. Examination of the relative abundance of the M^{+1} ion (*m/z* 289) to the $M^{+\bullet}$ reveals that a C_{20} carbon species is most likely. When adding two oxygen atoms the empirical formula becomes $C_{20}H_{16}O_2$ (DBE 13). A characterisation of pyrenepropanoic acid methyl ester might be a more likely assignment (Figure 5.52). Cleavage of a carboxylic acid methyl ester would leave a fragment at *m/z* 259. The base ion fragment at *m/z* 215 might suggest the loss of an ethanoate methyl ester fragment.

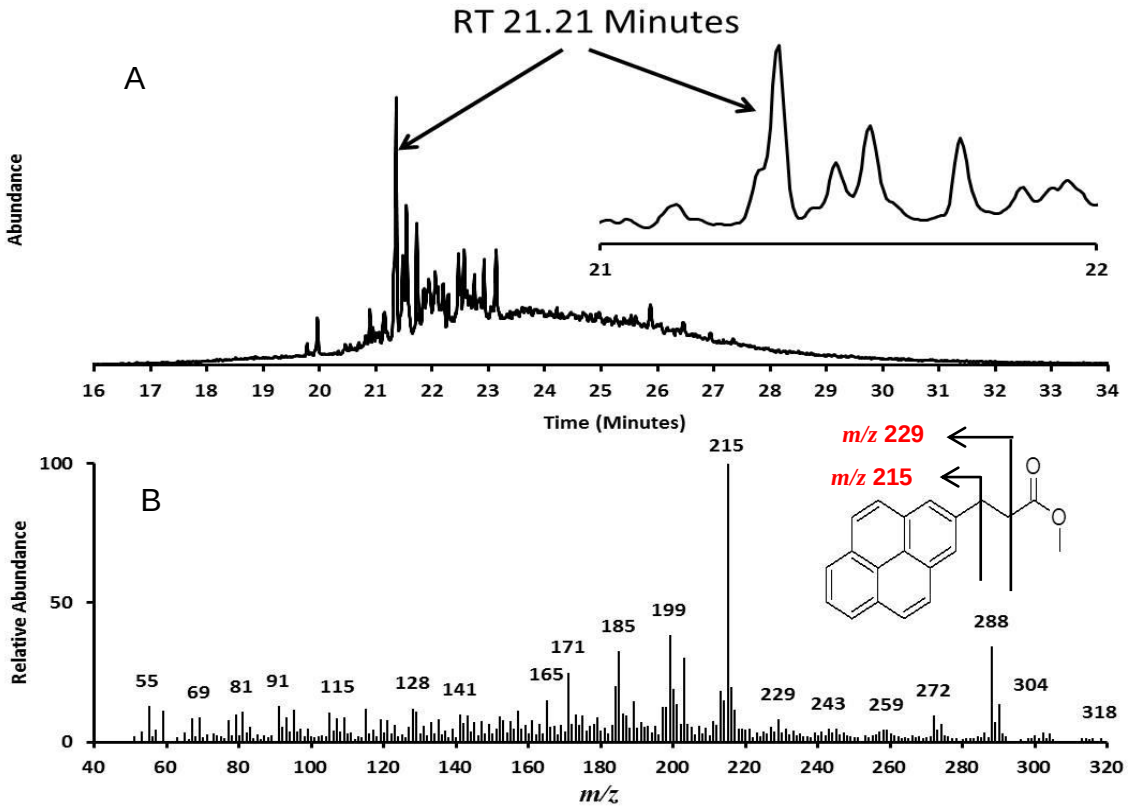

Figure 5.52. (A) Mass chromatogram of m/z 215 from the Ag^{+}SPE Fraction 8. Inset highlights the peaks eluting between RT 21.00 and 22.00 minutes. (B) Mass spectrum for the compound eluting at RT 21.21 minutes, tentatively assigned as an pyrenepropanoic acid methyl ester. GC-MS conditions as described in Figure 5.2.

The highly aromatised pyrene moiety would also form strong complexes with the Ag^{+} ions within the SPE columns and may well be held on column until elution with diethyl ether. Pyrene propanoic acid is commercially available so it would be a prudent step to esterify and co-chromatograph this acid with both GC-MS and GCxGC-MS to either confirm or deny this tentative identification.

However, this assignment does not preclude free acid elution from the Ag^{+}SPE column. BF_3-MeOH complex may not esterify all of the acids (*cf* West et al.,

2013 and references therein) within the complex mixtures of acid fractions, so an amount of free acid may be present.

The mass chromatogram of *m/z* 225 (Figure 5.53) revealed a small unresolved hump and two resolved peaks at RT 23.39 and 23.47 minutes. The mass spectrum of the compound eluting at RT 23.47 revealed a potential $M^{+\bullet}$ at *m/z* 312 (Figure 5.53 C). The mass chromatogram of *m/z* 312 revealed a similar profile to that of *m/z* 225 (Figure 5.59B).

Examination of the relative abundance of the M^{+1} to the $M^{+\bullet}$ hints towards a C_{21} compound. Taking into account the two oxygen atoms this gives an empirical formula of $C_{21}H_{28}O_2$ (DBE 8). The base ion at *m/z* 225 might describe the loss of a propanoic acid methyl ester leaving a nucleus of $C_{17}H_{21}$ (DBE 7), which can be potentially describe a steroidal polycyclic monoaromatic moiety.

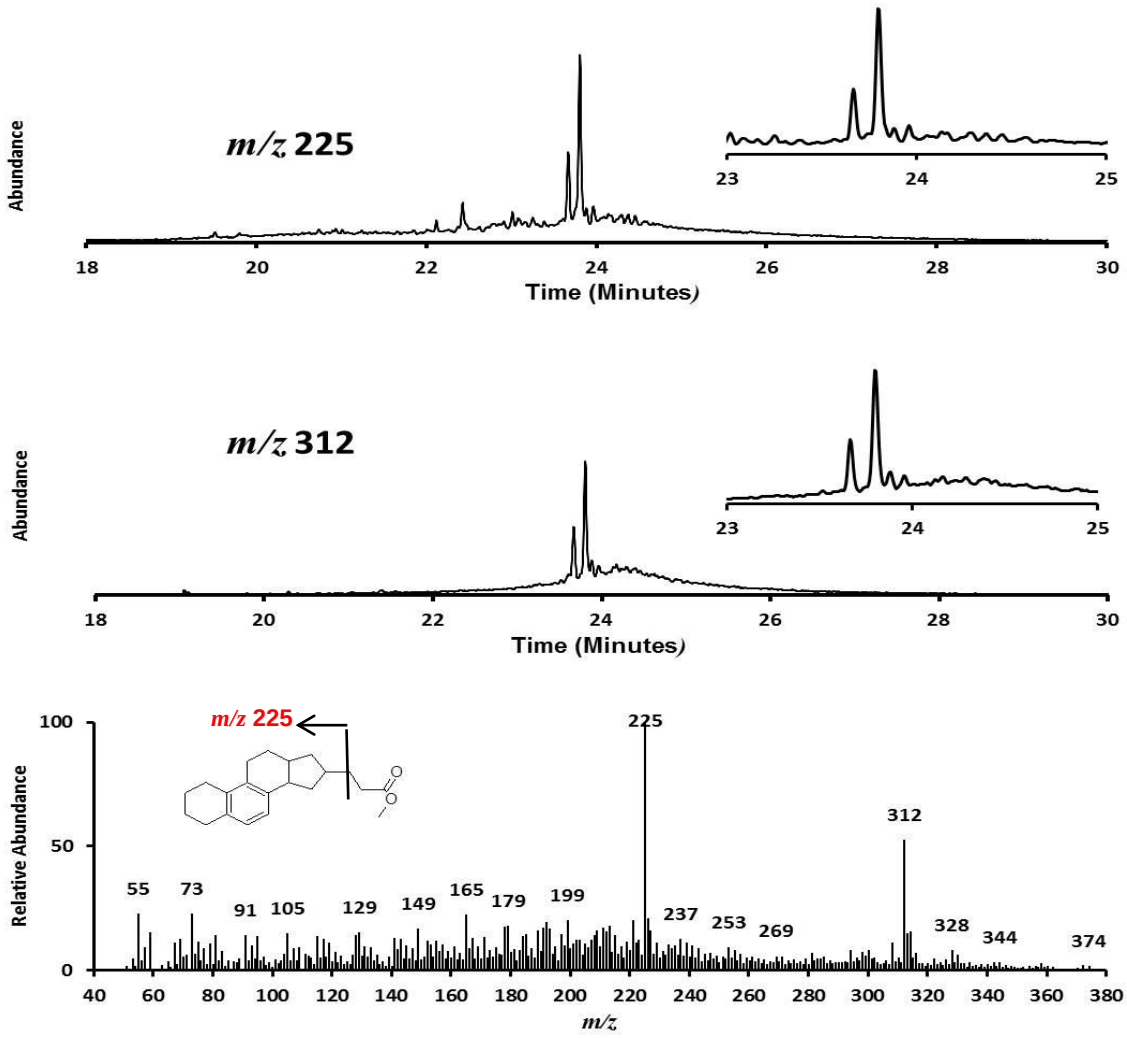

Figure 5.53. (A) Mass chromatogram of m/z 225 from the Ag^{+}SPE Fraction 8. (B) Mass chromatogram of *m/z* 312 from the Ag^{+}SPE Fraction 8. Insets highlight peaks eluting between RT 23.00 and 25.00 minutes. (C) Mass spectrum for the compound eluting at RT 23.47 minutes**.** GC-MS conditions as described in Figure 5.2.

However analysis by GCxGC-MS on the same fraction by revealed a much 'cleaner' mass spectrum with slightly different ion abundances (Figure 5.54). In the GCxGC- MS mass spectrum the relative abundance of the M^{+1} to the $M^{+\bullet}$ suggests a C_{19} moiety and an ion a M^{+2} at 4% relative abundance reveals what may be the presence of one sulphur atom, giving a potential empirical formula

of $C_{19}H_{20}O_2S$ (DBE 10). The base ion at *m/z* 225 is characteristic of the loss of a propanoic acid methyl ester ($C_4H_7O_2$). The relative abundance of the base ion (*m/z* 225) to *m/z* 226 reveals that the nucleus of the compound is potentially a C_{15} species, leaving an empirical formula for the nucleus of $C_{15}H_{14}S$ (DBE 9) which potentially describes a trimethyldibenzothiopene

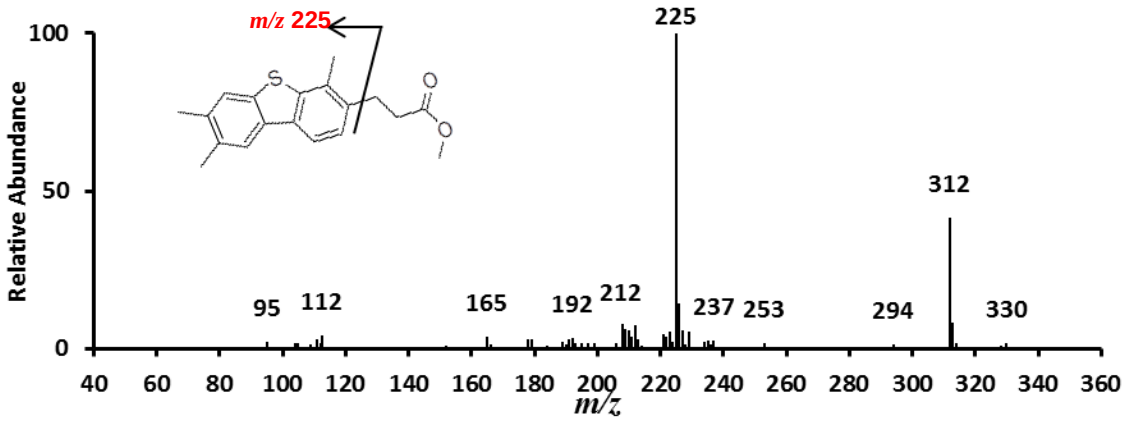

Figure 5.54. Mass spectrum from GCxGC-MS analysis for the compound eluting at RT 23.47 minutes from Ag^+SPE 100% diethyl ether Fraction 8, tentatively assigned as a trimethyldibenzothiopenepropanoic acid methyl ester.

Examination of the methyl esters of fraction 8 on a mass spectrometer with a higher mass accuracy was performed by colleagues in a partner laboratory (e.g. Jones et al., 2013; West et al., 2013; Section 5.2.10) revealed the observed mass of the $M^{+\bullet}$ was 312.1180 Da (Figure 5.55). Calculation of the theoretical mass of $C_{19}H_{21}O_2S$ produces 312.1184 Da. The *m/z* value of the molecular ion (m/z 312.1180) was measured to a mass accuracy of 1.28 ppm. The *m/z* value of the base peak ion (*m/z* 225.0742) was measured to a mass accuracy within 1

ppm of an ion with the composition $C_{15}H_{13}S$. The base peak ion was characteristic of the loss of a propanoic acid methyl ester molecule giving a molecular formula of $C_{19}H_{20}O_2S$, consistent with either a trimethyldibenzothiopenepropanoic acid methyl ester, or a methyldibenzothiopenepentanoic acid methyl ester (Jones et al., 2013), though other dibenzothiopenes moieties are possible.

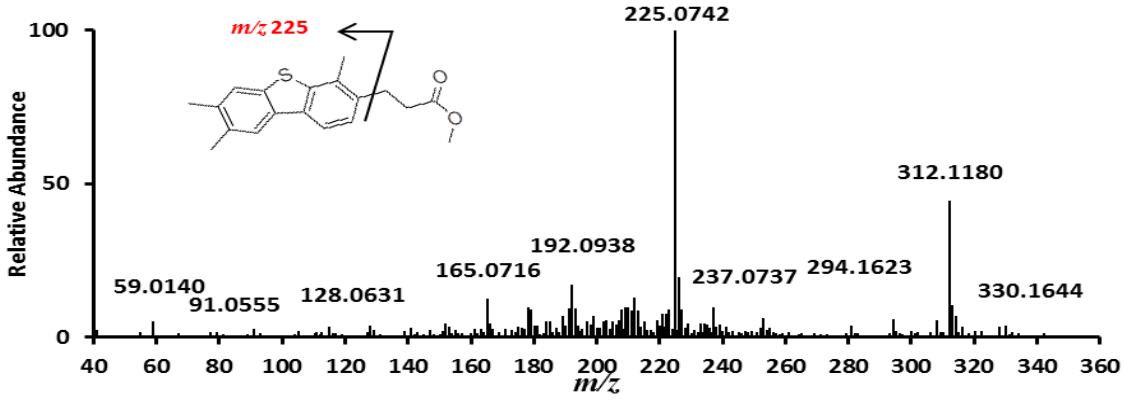

Figure 5.55. Accurate mass spectrum for the compound eluting at RT 23.47 minutes in the mass chromatogram for m/z 312 displayed in Figure 5.56.

Mass chromatographic analysis of the Ag^+SPE fractions was able to reveal a number of resolved peaks from which tentative identifications from mass spectral data have been determined, which is, to the author's knowledge, the first time that compounds have been able to be identified and characterised within these complex OSPW acid extract mixtures.

5.3.2.7 Combined Fractions (1-8) Weights and Elemental Analysis

The results of elemental analyses of the unfractionated methylated OSPW sample and fractions 2-5 and 8 are shown in Table 5.3. Too little of other

fractions (Figure 5.56) was available for weighing for accurate elemental analysis.

The unfractionated, methylated OSPW extract contained virtually no nitrogen (<0.02%) and about 0.5% sulphur. The C/H ratio was 7.4 ± 0.2 (Table 5.3).

Table 5.3. Elemental composition of a representative sample of the Ag^+SPE Fractions from an oil sands derived acid complex mixture.

	Element (%)				
Fraction	C	H	C/H Ratio	N	S
U/F	67.9	9.2	7.4	<0.02	0.5
F2	73.6	10.8	6.8	n.d.	n.d.
F4	74.8	10.0	7.5	0.02	<0.05
F5	76.5	9.6	8.0	n.d.	<0.05
F8	74.6	9.6	8.0	n.d.	1.5

n.d. is 'not detected'

Approximately 35% by weight of the unfractionated acid methyl esters material eluted with hexane (fractions 2 and 3), whilst approximately 45% of the unfractionated methyl esters eluted with 95:5% hexane diethyl ether (fractions 4 to 7), the remainder was eluted in 100% diethyl ether (20%: fraction 8) (Figure 5.49).

Fractions 2 and 3 contained no detectable S or N (<0.02%). The C/H ratio was 6.8 (Table 5.3), which is lower than that of the whole unfractionated sample and consistent with the expectation that fractions eluting with hexane would be dominated by non-aromatic compounds (e.g. esters of alicyclic acids).

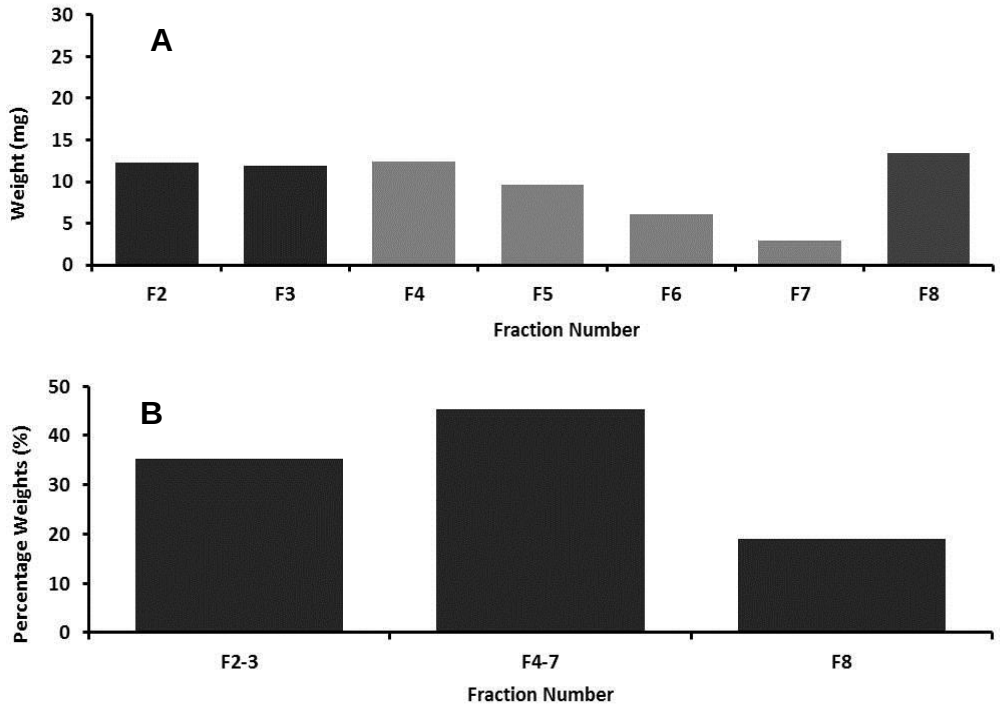

Figure 5.56. (A) Weights (mg) of the sum of each Ag^{+}SPE Fraction (n=15), F2 and F3 were shown by GCxGC-MS to comprise of alicyclic acid MEs; F4-F7 were assigned by GCxGC-MS to comprise of aromatic acid MEs fractions and F8 was the fraction eluted with 100% diethyl ether; and (B) the combined percentage weights of the 100% hexane (alicyclic), 95:5 hexane: diethyl ether (monoaromatic) and 100% diethyl ether fractions.

Fractions 4 and 5 comprised about 45% by weight of the extract recovered (Figure 5.56) and fraction 4 contained about 0.02% N and 0.04% S (Table 5.3) . Fraction 5 contained no detectable N and 0.05% S. From the C/H ratios (Table 5.3), fraction 5 (C/H 8.2) was more aromatic than fraction 4 (C/H 7.5). Both were more aromatic (less H) than fractions 2 and 3 (e.g. C/H 6.8). The data are consistent with increased aromaticity in these fractions as shown by the co-chromatography with authentic aromatic acids by GCxGC-MS (section 5.3.2.4).

Fraction 8 comprised about 20% by weight of the recovered extract (Figure 5.56B). This ether eluate contained no N but about 1.5% S. This is about half of the total S, given the proportion by weight of this fraction (Figure 5.56A).

Therefore half of the S present in the methylated OSPW, seems to be very polar and was mostly unrecovered by elution with an eluotropic series ending in diethyl ether, possibly due to a strong interaction with the Ag^+ phase. The C/H ratio (Table 5.3) of fraction 8 (C/H 7.7), was about the same as that of Fraction 4 (C/H 7.5), also suggesting an, at least partly, naphtheno-monoaromatic composition*.

5.3.2.8. Infra-Red Spectroscopy and Ultra Violet-Visible Spectrophotometry of Ag^+SPE Fractions

The IR spectrum of the unfractionated acid methyl esters (Figure 5.57) contained a relatively weak broad absorption at 3400-2800 cm^{-1} attributed to O-H stretching in free carboxylic acids and possibly some H-bonded O-H stretching in free hydroxyl groups. Absorptions at 2950 and 2869 cm^{-1} were attributed to C-H stretching in CH, CH_2 and CH_3 groups. A distinct absorption (typically observed at *ca* 3000 cm^{-1}) due to aromatic C-H stretch was not clearly observed, but this is often merged with stronger alkyl group absorptions. A strong absorption at 1738 cm^{-1} was attributed to C=O stretch in esters. A small side band was observed, possibly indicating a small proportion of compounds with a different C=O functionality

Absorptions at 1400-1165 cm^{-1} were attributed to bending vibrations in CH_2 and CH_3 groups. A weak absorption at 1020 cm^{-1} was tentatively assigned to S=O stretching in a small proportion of sulfoxides.

---

* Further material containing 6-9% sulphur was eluted with methanol in later experiments (A. Scarlett, Personal Communication)

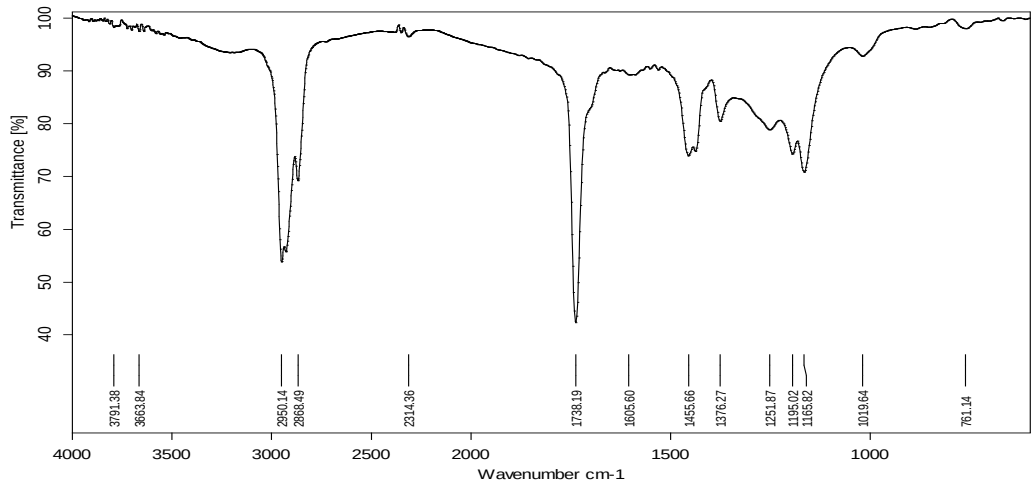

Figure 5.57. Infrared Spectrum of the unfractionated OSPW acid extract methyl esters

The IR spectrum of Fraction 2 (Figure 5.58A) contained no broad absorption at 3400-2800 cm^{-1} attributed to O-H stretching, nor a band due to O-H stretching in free hydroxyl groups. Thus the content of hydroxy acids in this fraction, if any, was undetectable by FTIR. Numerous alicyclic hydroxy acids have been suggested in other OSPW samples previously, on the basis of HPLC-high resolution MS data (e.g. Bataineh et al., 2006), but none have been identified and none were detectable in the present sample. Absorptions at 2950 and 2869 cm^{-1} were attributed to C-H stretching in CH, CH_2 and CH_3 groups. No absorption at *ca* 3000 cm^{-1}, due to aromatic C-H stretch, was observed, again consistent with the expectation that fractions eluting with hexane would be dominated by non-aromatic esters of alicyclic acids as indicated by the GCxGC-MS analysis of the preliminary Ag^{+}SPE fractionation (section 5.3.2.4) with authentic alicyclic acid MEs.

A strong absorption at 1739 cm^{-1} was attributed to C=O stretch in (methyl) esters. A small side band was observed, possibly indicating a small proportion of compounds with a different C=O functionality. Absorptions at 1400-1165 cm^{-1} were attributed to bending vibrations in CH_2 and CH_3 groups. A very weak absorption at 1020 cm^{-1} was tentatively assigned to S=O stretching in sulfoxides (Figure 5.58A) but the low content of sulphur (<0.02%) (Table 5.5) indicated this was very minor. The spectrum of fraction 3 was similar to that of Fraction 2 (Figure 5.58B). The results of these characterisations have been partly published by Jones et al., (2013) (Appendix D).

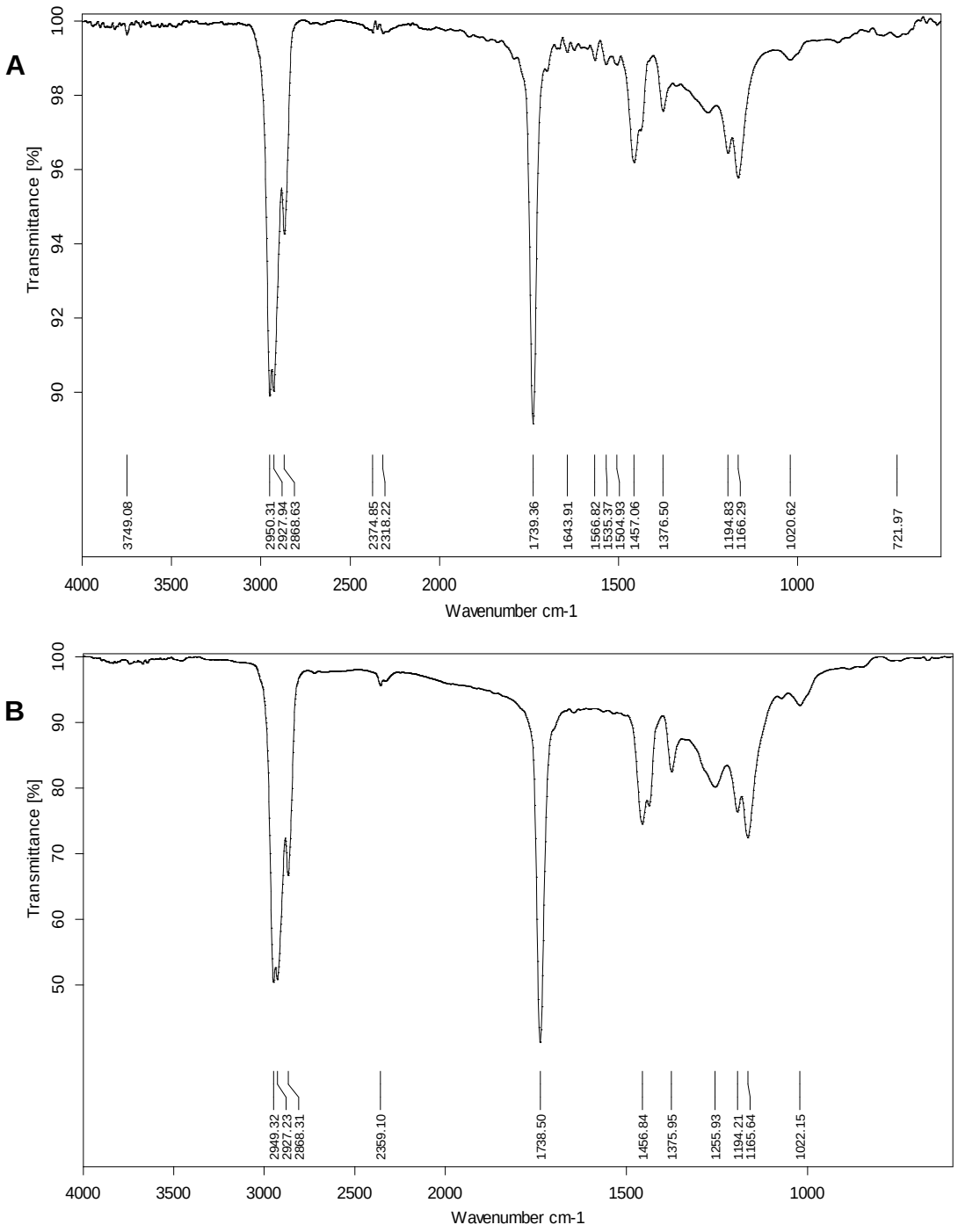

Figure 5.58. (A)Infrared Spectrum of Ag^{+}SPE Fraction 2 from the OSPW acid, extract methyl esters. (B) Infrared Spectrum for Ag^{+}SPE Fraction 3 from the OSPW Acid, extract methyl esters.

The IR spectrum of fraction 5 (Figure 5.59B) contained a very weak broad absorption at 3400-2800 cm^{-1} attributed to O-H stretching in free carboxylic acids and possibly some H-bonded O-H stretching in free hydroxyl groups. Absorptions at 2950 and 2869 cm^{-1} were attributed to C-H stretching in CH, CH_2 and CH_3 groups. A strong absorption at 1739 cm^{-1} was attributed to C=O stretch in (methyl) esters. Absorptions at 1400-1165 cm^{-1} were attributed to bending vibrations in CH_2 and CH_3 groups. A very weak absorption at 1020 cm^{-1} due to S=O stretching in sulfoxides was detected but the low content of sulphur (<0.04%) indicated this was indeed very minor. A weak absorption at 746 cm^{-1} was tentatively attributed to aromatic C-H out of plane bending, consistent with the C/H ratios. The IR spectrum of Fraction 4 (Figure 5.59A), was similar to that of Fraction 5.

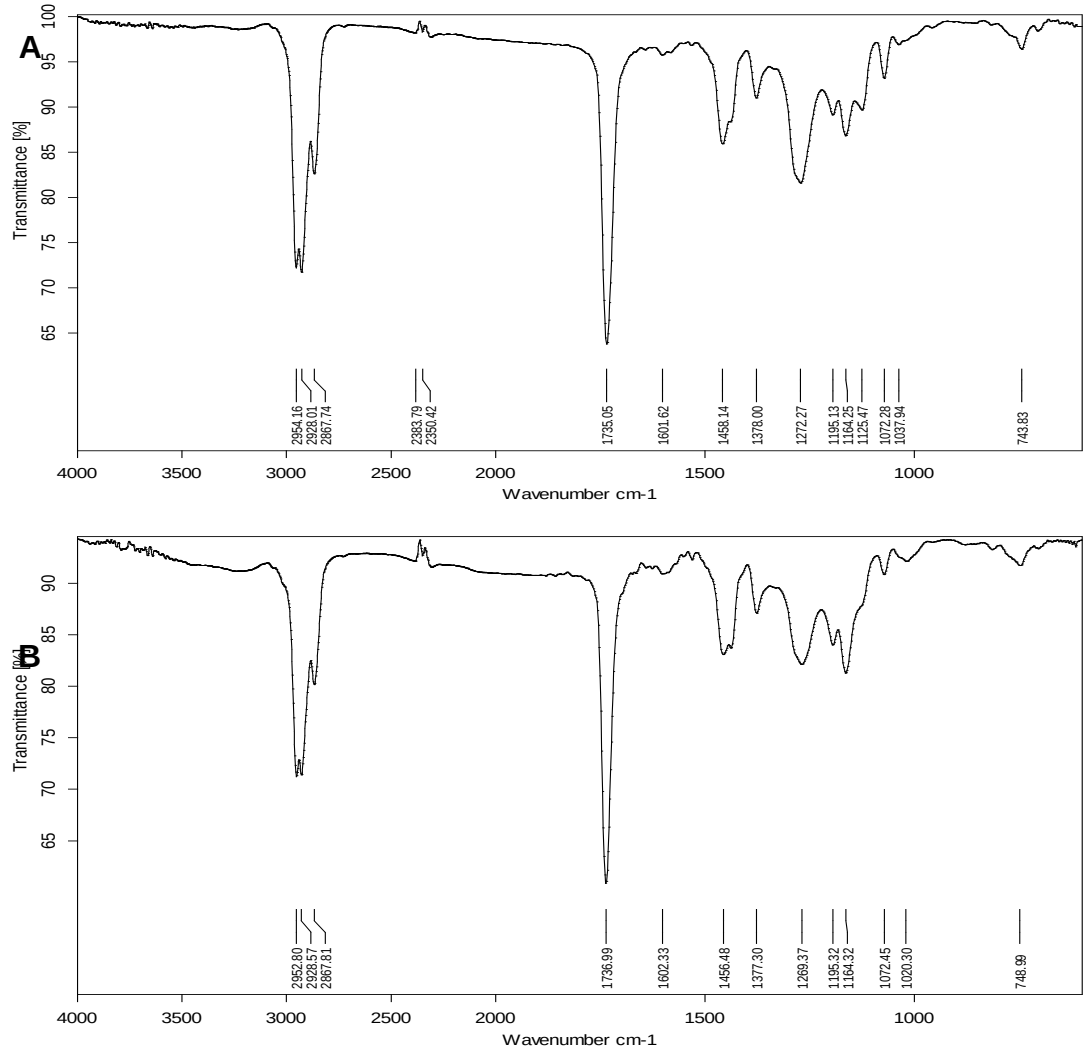

Figure 5.59. Infra red Spectra of (A) Ag^{+}SPE 95:5% hexane:diethyl ether Fraction 4. (B) 95:5% hexane:diethyl ether Fraction 5.

The IR spectrum of fraction 8 (Figure 5.60) contained an apparent absorption at 3400-3200 cm^{-1} attributed to O-H stretching in hydroxyl of free carboxylic acids. Absorptions at 2950 and 2869 cm^{-1} were attributed to C-H stretching in CH, CH_2 and CH_3 groups. A strong absorption at 1735 cm^{-1} was attributed to C=O stretch in (methyl) esters and a second strong absorption at 1700 cm^{-1} was attributed to C=O stretch in free carboxylic acid groups. Absorptions at 1400-1165 cm^{-1} were attributed to bending vibrations in CH_2 and CH_3 groups. A weak absorption

at 744 cm^{-1} was tentatively attributed to aromatic C-H out of plane bending, consistent with the C/H ratio, which also indicated aromaticity (Table 5.5). These data indicate that fraction 8 contained compounds with more than one esterifiable group and at least some components with an esterifiable group plus a free carboxylic group, or some free acids. Candidate compounds may be partial esters of the dicarboxylic acids discussed by Frank et al. (2009) in the unfractionated methylated OSPW by NMR spectroscopy.

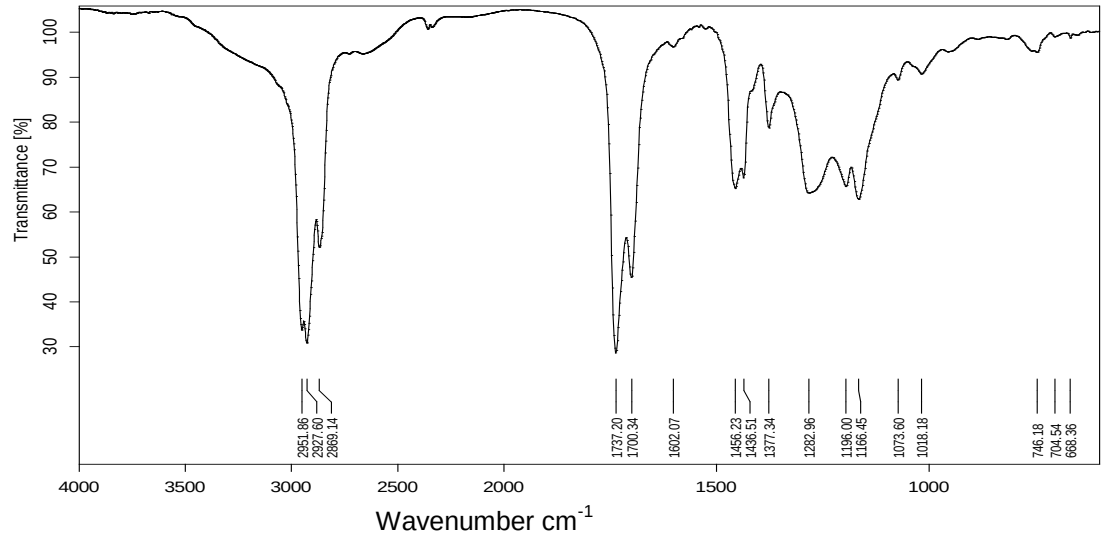

Figure 5.60. IR Spectrum for Ag^{+}SPE Fraction 8; from the OSPW acid extract methyl esters

A weak absorption at 1020 cm^{-1} due to S=O stretching in sulphoxides was detected (Figure 5.60). The higher content of sulphur (ca 1.5%S; ~50% of total S) in this fraction (Table 5.5) therefore suggested that sulphur species other than sulphoxides were present.

The extent of UV absorption (UF) of the unfractionated acid methyl esters (Figure 5.61) was intermediate between those of the fractions. The spectrum exhibited broad absorptions in the 230 and 260-280 nm regions. This indication

of aromaticity is therefore consistent with the elemental C/H ratio (Table 5.5). UV spectra of an unmethylated OSPW extract were published previously (Mohamed et al., 2008) and absorption at 263 nm noted, again consistent with aromaticity.

UV spectra of known concentrations of the esterified fractions 2 and 3 showed no significant UV absorption. (Figure 5.61). However UV spectra of known concentrations of fractions made it clear that on a quantitative basis, Fractions 4, 5 (and 8, *vide infra*), exhibited significant UV absorption, with broad absorptions in the 230 and 260-280 nm regions (Figure 5.61). This indication of aromaticity is consistent with the elemental C/H ratios and inferences from IR data.

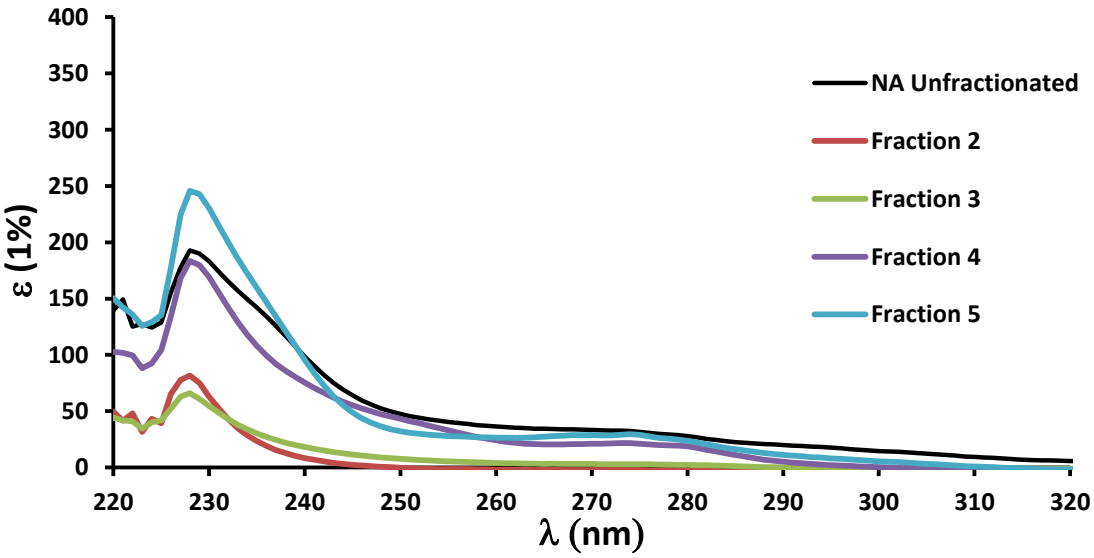

Figure 5.61. Ultra violet visible spectrophotometry spectrum for the Ag+SPE fractions 2-5 and the unfractionated OSPW acid extract methyl esters The y axis shows the extinction coefficient.

Fraction 8 exhibited the strongest UV absorption, indicating greatest aromaticity (Figure 5.62), which is also consistent with the above proposals. In summary,

the data are consistent with the presence of more polar compounds, including monomethyl esters of sulphur-containing naphtheno-aromatic compounds.

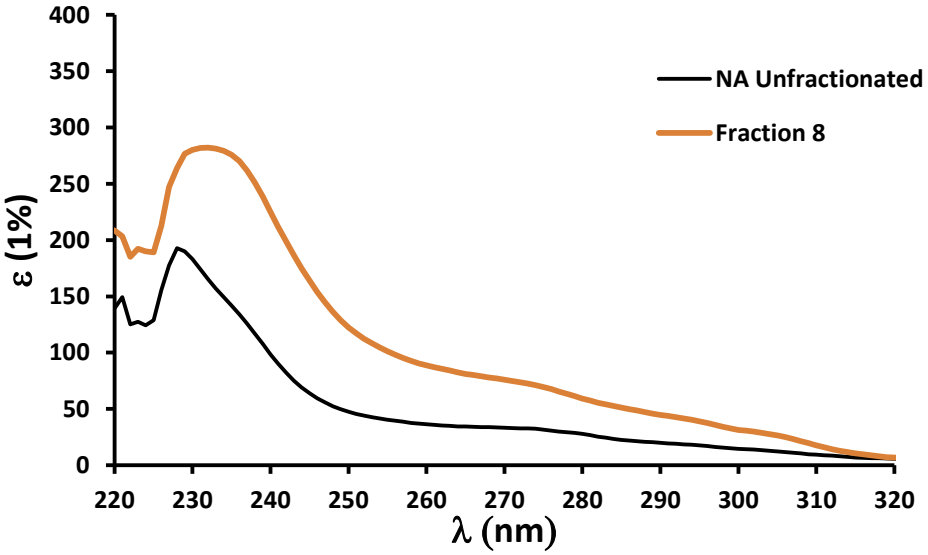

Figure 5.62. Ultra violet visible spectrophotometry spectrum for the Ag+SPE fraction 8 and the unfractionated OSPW acid extract methyl esters**.** The y axis shows the extinction coefficient.

5.3.3 pH Extractions

The oil sands derived acid extracts were also attempted to be separated through use of a pH based extraction technique (Section 5.25), the methods for which were based upon previous work by Grboviv et al., (2012). However, no separation of compounds or structural classes occurred. Only complex mixtures of greater or lesser abundance were apparent in the gas chromatograms. When mass chromatographic analysis was carried out it was apparent that no chromatographic peaks could be resolved and only smaller ‘humps’ were revealed in the chromatograms. All the chromatograms are presented within Appendix C.

5.4 Conclusions

It is shown preparative silver ion TLC or SPE followed by GC-MS and GCxGC-MS can simplify complex mixtures of the OSPW acid extracts into fraction containing naphthenic acid moieties of principally alicyclic structures and fractions containing principally aromatic structures. These assignments were confirmed by elemental analysis, IR and UV-Vis spectroscopy.

Averaging the mass spectra of each of the Ag^+TLC and Ag^+SPE fractions and subsequent GC-MS mass chromatography of key ions was able to produce some resolved chromatographic peaks and to generate associated mass spectra. Tentative characterisation and identification was carried out through first principle mass spectral analysis, co-chromatography and comparison of spectra with those in the NIST library catalogue. The Ag^+TLC and Ag^+SPE methods were shown to be a robust and reproducible way of fractionating complex OSPW acid mixtures.

This study provides evidence that the naphthenic acids within an OSPW acid extract are not just alicyclic in nature, as generally assumed by many authors (e.g. Headley et al., 2009). Ag^+SPE fractions 4 and 5 and the Ag^+TLC fraction (R_f 0.66-0.72) were determined to contain mono-aromatic acid methyl esters. This reinforces the generally ignored work of Knoterus (1957) who determined that aromatic acids were present in petroleum in similar proportions to that revealed by this current study. A key finding within this chapter is 30-40% of the unfractionated methyl esters of naphthenic acids contain some form of aromatic moiety. Tentative evidence is provided for the presence of polyaromatic

structures, such as pyrene type acid methyl esters, alongside sulphur containing species such as possible dibenzothiopene acid methyl esters.

A pH fractionation method failed to separate the acid complex mixture and no resolved peaks or ‘clean’ mass spectra were generated.

To the author’s knowledge this study is the first time in which acid methyl esters have been resolved from an OSPW acid extract complex mixture by using GC-MS following pre-fractionation by Ag^{+} TLC/SPE. Better acid methyl ester structural determinations may have far reaching consequences for the toxicological assessment of naphthenic acid complex mixtures and any subsequent remediation techniques.

Chapter 6 Conclusions and Future Work

6.1 Introduction

Although there has been some concern about the environmental and other effects of naphthenic acids (NAs) for some years, it is only following the production of vast amounts of acids during the processing of oil sands waste (OSPW), mainly in Canada, that large scale debate has really ensued (e.g. Grewer et al., 2010). Occurring in concentrations of up to 120 mg L^{-1} (Frank et al., 2009, Chapter 1, Chapter 3), NAs are often claimed to be the class of compounds responsible for the majority of the observed toxic effects of OSPW (e.g. Kannel and Gan, 2012; Reviewed in Chapter 1, Section 1.3. and Chapter 3, Section 3.1).

However, a detailed review of the literature revealed that very few individual NAs had been identified at the inception of the current study in 2009. Whilst a number of these papers discuss characterisation and identification, generally the research simply describes a classification of NAs by an empirical formula or classification of the so-called 'Z' number in the formula $C_nH_{2n+z}O_2$, which describes a loss of hydrogen presumed to be due to alicyclic ring formation.

In the current and associated work (e.g. Rowland et al., 2011a-f), using GCxGC-MS to study NAs in OSPW (apparently for only the second time; Hao et al., 2004), several alicyclic NA structures were positively assigned by comparison with data for authentic acids. Others were more tentatively identified, such as putative steroidal type acids (e.g. Rowland et al., 2011b, c; Jones et al., 2012, 2013).

Most previous studies have ignored the possibility of mono and polycyclic aromatic acids in NA mixtures, although this was proposed by Knoterus as early as (1957) and later by Seifert (1975). Most researchers have preferred instead to rely on the classifications put forward in the 1920s to the 1950s (summarised by Lochte and Littman, 1955) and the proposed alicyclic structures postulated by Brient et al., (1996).

Whole classes of potential acid toxicants, such as steroidal or terpenoidal, acids have previously been generally ignored, even though the formulae for such compounds would fit the 'classical' NA formula. This trend seems to be lessening in the more recent research (e.g. Hindle et al., 2013). Poor knowledge of the structures of the NA might mean that the determinations of toxicity on whole OSPW and extracted and refined NA mixtures, although valid, will not reveal where, within the mixture, the toxicity lies. There is a likelihood that efforts to remove the 'classical' NAs (through photo or bioremediation (e.g. Mishra et al., 2010a; Scott et al., 2008)) could lead to more concentrated, potentially more toxic acids remaining behind (Quagraine et al., 2005).

A number of authors refer to NAs as being the source or the direct cause of OSPW toxicity (e.g. Rogers et al., 2002; Nero et al., 2006; Kannel and Gan, 2012, reviewed in Chapter 1, Section 1.3.). It is common to discover publications that state the toxicity of the OSPW is attributable to the concentrations of the NAs alone (for example, Rogers et al., 2002; Peters et al., 2007), with the circular argument that NAs are toxic, OSPW contains NAs which are toxic, therefore the toxicity of OSPW can only be attributed to NAs. Further, not just NAs, but only the alicyclic compounds, that are often assumed to be the

sole constituent of NAs. However, that bioremediation techniques do somewhat lessen the toxicity of the OSPW suggests that NAs are responsible for some of the observed effects from exposure.

Although poor research practice, such as assessing organisms for toxic effects outside of the optimum pH range or not stating the pH of the assay (e.g. Mishra et al., 2010a; Martin et al., 2010) and statements that although NAs were severely degraded by ozonation the toxicity of the OSPW was not affected (Martin et al., 2010) do raise some questions as to whether the bioremediation techniques are as successful as stated. A more robust, multidisciplinary, approach to the research could potentially aid in answering these questions. Co-chromatography of fractionated NAs leading to identification of compounds and followed by relatively in-depth toxicity assays (performed on individual compounds and mixtures of compounds) would enable researchers to elucidate what compounds are in the analysed mixtures and whether remediation techniques are have the desired effect. Testing within environmentally relevant parameters (e.g. concentrations or pH) would be critical to the success of the research.

The statement of NA toxicity is often not helped by studies, such as Kamaluddin and Zwiazek (2002) which refer to toxic effects at 300 mg L^{-1}, far outside environmental relevance and at a higher concentration than is found even in tailings ponds; or Hagen et al (2012) which states clearly in the abstract that the study is conducted on OSPW extracted NA, but lists a Merichem commercial NA in the materials section (reviewed Chapter 1; Section 1.3.1). Nor is the

assessment of toxicity aided by the lack of structural assignment or knowledge of other potential toxicants within the OSPW.

That concentrations of NA are routinely measured at ≤ 1 mg L^{-1} in the Athabasca River and Lake Athabasca (e.g. Schramm et al., 2000; Garcia-Garcia et al., 2011) reveals that it is unlikely to be the NAs that are the main cause the observed toxicity evident in fish that exist in Lake Athabasca (Kurek et al., 2013). Toxicity studies generally reveal that NA concentrations of ≤ 1 mg L^{-1} are not acutely toxic, with toxicity thresholds generally existing in the ca. 10-60 mg L^{-1} range for the acid extracted NA (Frank et al., 2008; Jones et al., 2011; Garcia-Garcia et al., 2011; Scarlett et al., 2013).

6.2. Conclusions and Future Work

Until this research (and associated research by colleagues) very little was known about the structures of NAs in OSPW or indeed, commercial NA from refining of petroleum and whether the previously assumed 'classical' structural classes (*viz*; alicyclics) might be able to produce the observed toxic effects. It was the aim of the present project to address this lack of knowledge and to characterise, identify, synthesise and toxicologically assess individual NAs that exist within the complex mixtures. Work alongside other researchers, who were able to initially (tentatively) identify some individual NAs following GCxGC-MS studies of NA from commercial and OSPW samples, (e.g. Rowland et al., 2011b) led the author to synthesise numerous putative NAs for confirmation studies conducted in collaboration (e.g. Rowland et al., 2011a,b). Synthesis of tentatively identified compounds was essential in order, not just to aid positive identifications of groups of acids (as methyl esters) but also was able to limit the

identification process to help ensure that erroneous identifications were minimised.

The identification of some cyclic acids encouraged the method development of (relatively) low temperature and low pressure hydrogenation of mono and bi aromatic compounds to provide alicyclic analogues (Rowland et al., 2011f; Chapter 2).

The reactants and products of the synthesis and especially the hydrogenation experiments and a number of esterification products of commercially available acids, such as the adamantane acid series were all extensively characterised by mass spectrometry and other methods (Chapter 2; Rowland et al., 2011b). This compilation of often previously unpublished mass spectra should serve as an easily accessed database for future comparisons and may aid future identifications of individual NAs (and groups of acids) by researchers focussing on these complex acid mixtures, whether from commercial petroleum or from the acid extracts of the OSPW.

The synthesis and esterification of these acids enabled colleagues to utilise co-chromatographic techniques by GCxGC MS and positively identify further acid compounds (e.g. Rowland et al., 2011c and d). Although the present author was not necessarily directly responsible for the use of the synthetic compounds for co-chromatography, clearly, without synthetic acids little progress might have been made. In particular, use of the cyclic and polycyclic acids enabled a higher degree of certainty to the identification of acids by GCxGC-MS and co-chromatography. This was especially important where the electron ionisation

mass spectra were ambiguous, as revealed by nearly identical mass spectra for adamantane-1-carboxylic acid methyl ester and 1-methyl-2,3,3a,4,5,6-hexahydro-1*H*-indene-2-carboxylic acid methyl ester (Figure 2.50, Chapter 2).

Synthesis and subsequent identification also allowed, for the first time, relevant toxicological assays to be performed on actual, rather than surrogate, NAs (Jones et al., 2011) and should aid assessments of whether these acids pose an environmental threat (*cf.* Rowland et al., 2011f).

The Microtox™ assay was used within the context of the study as a screening test to reveal compounds that were toxic enough to perform other, more in depth, assays. It was apparent from this screening assay that the toxicity of individually assayed acids was in the low to medium range (low aquatic toxicity IC_{50} >100 mg L^{-1}; medium aquatic toxicity IC_{50} 10-100 mg L^{-1}, (USEPA, 2011)). Individual acid compounds were tested at concentrations typical in OSPW to give environmental relevance and allow comparison with tested concentrations by other authors (e.g. Frank et al., 2009; Peters et al., 2007). It was apparent though that these concentrations lie outside of the average environmental NA concentrations (e.g. Garcia-Garcia et al., 2011). For example a recent study by Ross et al., (2012) discovered surface water concentrations of NAs in the Athabsca region ranging from <2- 81 μg L^{-1}. Concentrations in the Athabasca River were measured at <2-19 μg L^{-1} with the higher concentrations occuring in lakes and tributaries (Ross et al., 2012). This indicates that (in terms of mg L^{-1} IC_{50}) not one assayed compound would be predicted to lead to Microtox™

toxicity if discovered within environmental samples at such concentrations (Jones et al., 2011).

The mixtures of acids were also revealed to have IC_{50} values outside of average environmental concentrations.

The assessment of toxicity of the OSPW and the concentrations of NAs is an important parameter. As the OSPW cannot be released into the Athabasca River (Frank et al., 2009), the assessment of detoxification techniques is essential to allow some ecological function to the tailings ponds and to assess whether there is potential for some small release which will not adversely affect the surrounding environment

The low to medium observed acute toxicity for the NAs tested to date, coupled with computer modelling data (this work and Scarlett et al., 2012), indicated that there was likely to be little benefit to be gained from additional assays. However, as is noted in Chapter 4, within OSPW these acid compounds do not exist individually and are in fact part of complex mixtures containing many thousands of compounds, so assessment of mixture toxicities was performed on relatively simple combinations of acids. The toxicity of such simple mixtures did not conform to the proposed hypothesis of concentration addition (CA). The hypothesis that NAs act through CA was denied but as this was the first, in depth study (34 identified compounds) on NA mixtures, more work needs to occur before the CA hypothesis, with respect to NA, can be completely ruled out. It was postulated in Chapter 4 that NAs need to reach a critical micelle concentration (CMC) before acute effects occur and that this could explain the

lower than expected toxicity. The very steep concentration response curves observed for the Microtox™ assay was also seen during acute lethality tests using zebrafish larvae (Scarlett et al., 2013). This further supports the CMC hypothesis and demonstrates also that the steep concentration response curves observed (Chapter 4) were likely not an artefact of the Microtox™ assay.

That the NAs in higher concentrations (the adamantane acids) conformed to CA is an important result, potentially aiding the CMC hypothesis put forward by Scarlett (Personal Communication, 2012; Scarlett et al., 2013). That a CMC needs to be achieved may be a driving force in the toxicity of these acids. Preliminary results in an on-going study has also noted the importance of the CMC, suggesting that even at a potential CMC, NAs still remain in the low to medium region of toxic effects (Scarlett, Personal Communication, 2013).

That these acids can act as surfactants and may need to achieve the CMC before any toxic effect is apparent has not been extensively discussed by many authors, apart from Schramm (2000). Elucidation of the CMCs of NAs (and how the toxic properties change once the CMC is achieved) could be of critical importance in understanding the toxicity of NAs. That this work could potentially take many years does not reduce the possible significance and importance of the results which could either confirm the NAs place as a toxicant of concern, or point towards another, less abundant yet more toxic, component of the OSPW being responsible for the observed toxic effects. The mixture toxicity assays suggested that other factors might be necessary for toxicity to become evident. A proposal of a critical micelle concentration seems to be a logical conclusion.

The present research not only adds to the current knowledge on the toxicity of NAs, as it was the first time that mixtures of identified compounds had been assayed on live organisms, but also proposes an explanation for the observed low toxicity, not just of the assayed mixtures, but for NAs overall.

The toxicity of the individual acids and the mixtures of acids are in agreement with the observed toxicity of the NA complex mixtures. That acute toxicity is occurring is evident: however, toxicity assays suggest (in literature and within this study) that the observed acute toxicity is in the low to medium category denoted by the USEPA (USEPA, 2011).

Some studies have noted that the NA mixtures from petroleum produced water (Thomas et al., 2009) and from the OSPW (He et al., 2011; Reinardy et al., 2013) reveal a weak estrogenic response. Toxicological modelling by Scarlett et al., (2012) of the acids assayed using Microtox™ revealed that the estrogenicity was unlikely to be caused by the compounds synthesised herein (Scarlett et al., 2012). Previous research by Knoterus (1957) suggested that aromatic moieties were more abundant than suggested by the bulk of the research, so in an attempt to isolate these acids, fractionation of NAs was proposed. If the aromatic acid fractions could be separated then it would be more likely that GCxGC-MS could be used to identify the aromatic moieties within the NA matrix which might be responsible for the weak estrogenic effects. Successful fractionation through silver ion chromatography (thin layer and solid phase extraction) allowed tentative identification of steroidal type acids within the mixture (Rowland et al., 2011c; Chapter 5). Subsequent toxicological assays by Scarlett et al., (2013) and Reinardy et al., (2013) revealed that the

aromatic fractions (*ca*. 30-40% of the total naphthenic acid fractions) were indeed responsible for the weak estrogenic effects displayed by the total acid mixtures. This discovery is important for researchers in bioremediation techniques as preferential removal of these acids would be desirable to remove any potential estrogenic toxicity.

Previous 'characterisation' based research (e.g. Merlin et al., 2007; Scott et al., 2008; reviewed in Chapter 1) suggested that GC-MS was not sensitive enough to gain worthwhile information from NA mixtures. However, silver ion chromatography followed by GC-MS was able to somewhat overcome this. Through use of averaged mass spectra and ion (or mass) chromatography, single peaks with interpretable mass spectral data were able to be characterised from the GC-MS data of some NA fractions. This was the first time that GC-MS was able to be used to gain structural data from such complex mixtures of acids.

It was noted however that the Ag^{+}SPE fractionation method had a *ca*. 60% recovery, leaving *ca.* 40% of the methylated acid extracts on-column. Elemental analysis and IR spectroscopy confirmed the presence of sulphur bearing compounds in the latest eluting fraction (fraction 8, 100% diethyl ether) so it is possible that the compounds remaining 'on-column' also contain sulphur by complexation with Ag^{+} . It is equally likely that the retained compounds are far more polar and may require a more polar solvent to remove them (confirmed by a subsequent 100% methanol fractionation by West et al., 2013). It is interesting that these retained polar, potentially sulphur-containing compounds, comprise *ca.* 40% of the acid extracts. This is a similar percentage composition to that

which Grewer et al., (2010) reported as not being NA-type compounds. It is likely that these retained compounds hold different elemental compositions to those eluted by 100% hexane and 95% hexane: 5% diethyl ether, as the latter eluted compounds are the classical, dominant 'O_2' species (Jones et al., 2013). With the observed higher polarity it is likely that the retained compounds are 'O_3'or 'O_4'(potentially) sulphur- containing moieties (possibly hydroxy or di-acids). If so, this would likely reduce their toxicity, as it has been noted (e.g. Frank et al., 2009) that di-acids (O_4 species) reveal a lesser toxic effect due to the increased polarity and that NA toxicity is linked to an increase in hydrophobicity.

It is therefore likely that any subsequent remediation techniques, particularly bioremediation might remove the O_3 and O_4 species, potentially degrading them to O_2 species. This may have an effect of removing the 'non-toxic' acids and concentrating the NAs, which show medium toxicity, and other, unresolved, non-acid species which may hold the key to the OSPW toxic effects. By attempting to remediate the problem, researchers may well exacerbate the toxicity, so elucidation of structural and elemental information for the compounds contained with the retained 40% is critical to ensure that the toxicity of the OSPW is not increased.

As more compounds are identified within the acid extracts of the OSPW more synthesis of these compounds will be required. Most of the tentatively proposed compounds that have yet to be positively identified await synthetic compounds for co-chromatography where no commercially obtainable compounds are available. Once identification is complete, toxicological assays can take place,

both of individual compounds and of mixtures. The identification of one class of compounds can quite often lead researchers to other classes. GC-MS mass chromatograms of Ag^{+}SPE fractions can help screen the complex mixtures of NAs to potentially elucidate whether these structural classes exist in the OSPW or not. If the new classes of compounds are tentatively identified then it is likely that some synthesis of these compounds will be necessary. This approach is illustrated by the work herein, partly published as Rowland et al., (2012) and Jones et al., (2012, 2013).

Before this study, few research papers discussed the importance of the aromatic moieties existing within the OSPW NAs. In fact only one paper of note (Knoterus, 1957) discussed the presence of aromatic NAs in terms of their prevalence; this work was generally been ignored by the wider research community. This current work has shown that the aromatic fractions are broadly in agreement with Knoterus' conclusions that the aromatic fraction comprised 30-40% of the recovered NAs. Alongside the determination of the aromatic fractions a method was developed as a simple screening tool for eliciting structural information from complex mixtures of organic compounds through use of relatively low resolution GC-MS. This method will allow researchers in many fields of organic geochemistry an ability to tentatively identify individual compounds with complex mixtures (not just NAs) and an ability to drive research into the elucidation of toxicity and bio-remediation for, not just the OSPW, but other incidents of ecological concern on a global basis.

This work has enabled confirmation (and rejection) of hypothesised structures for NAs. The often referenced, so-called 'Brient' structures of acids containing

mono- through penta and hexacyclic rings, (Brient et al., 1996) such as the decahydronaphthalenes , which were synthesised in house (Chapter 2) and co-chromatographically assessed with GCxGC-MS, were not found within the available sample of OSPW NA but some were present in a refined petroleum (commercial) NA (Rowland et al., 2011d). Instead other structures that had not been previously discussed were confirmed in OSPW NA. The discovery that diamondoid type acid methyl esters are prevalent in the OSPW NA (e.g. Rowland et al., 2011b) has led to a paradigm shift in the knowledge of the alicyclic structures of OSPW NA.

This study highlights the need for more proactivity in NA research. That questions about the toxicity and composition are easily raised with many of the publications shows that more robust and reproducible methods (such as those detailed in the previous chapters) and a widening of the research focus are required.

Taken as a whole, this research is a multi-disciplinary approach to the problem of characterisation, identification and toxicity of the complex mixtures of NAs. Taken individually, each chapter stands alone as a piece of research that has moved the respective fields of synthesis, toxicology and chromatography forward. This work has contributed towards thirteen separate publications. The degree of this contribution varies from minor to extensive. Where the contribution has been extensive, the manuscript has been published with the present author named first (e.g. Jones et al., 2011, 2012, 2013). Certain chapters (e.g. Chapter 3 and Chapter 5) have been published, almost, in their

entirety (e.g. Jones et al., 2011; Jones et al., 2013). The high degree of published work that this research has produced highlights its originality.

7. References

A.P.I., 2003. Gas Oils catagory, American Petroleum Institute, The Petroleum HPV Testing Group, High Production Volume Chemical Challenge Program, http://www.epa.gov/hpv/pubs/summaries/gasoilct/c14835tp.pdf.

A.P.I., 2005. Kerosene/Jet Fuel Catagory, American Petroleum Institute, High Production Volume (HPV) Chemical Challenge Program for the US EPA, http://www.epa.gov/hpv/pubs/summaries/kerjetfc/c15020rt.pdf.

Aitken, C.M., Jones, D.M., Larter, S.R., 2004. Anaerobic hydrocarbon biodegradation in deep subsurface oil reservoirs. Nature 431, 291-294.

Alexander, M., 1999. Biodegradation and Bioremediation, Second ed. Academic Press, London.

Allen, E.W. (2008). Process water treatment in the oil sands industry: I. Target pollutants and treatment objectives. Journal of Environmental Engineering and Science **7**: 123–138.

Altenburger R, Backhaus T, Boedeker W, Faust M, Scholze M, Grimme LH. 2000.
Predictability of the toxicity of multiple chemical mixtures to Vibrio fischeri: Mixtures composed of similarly acting chemicals. Environmental Toxicology and Chemistry, 19(9):2341–2347

Anderson, J.C., Wiseman, S.B., Wang, N., Moustafa, A., Perez-Estrada, L., Gamal El-Din, M., Martin, J.W., Liber, K., Giesy, J.P., 2011. Effectiveness of Ozonation Treatment in Eliminating Toxicity of Oil Sands Process-Affected Water to Chironomus dilutus. Environmental Science & Technology 46, 486-493.

Aschan, 1892. Ber 25.

Augustyn, O.P.H., Kock, J.L.F., Ferreira, D., 1992. Differentiation between Yeast Species, and Strains within a Species, by Cellular Fatty Acid Analysis 5. A Feasible Technique? Systematic and Applied Microbiology 15, 105-115.

Barnes, H.M., Amburgey, T.L., Sanders, M.G., 2005. Performance of copper naphthenate and its analogs as ground contact wood preservatives. Bioresource Technology 96, 1131-1135.

Barrow, M.P., Headley, J.V., Peru, K.M., Derrick, P.J., 2004. Fourier transform ion cyclotron resonance mass spectrometry of principal components in oilsands Naphthenic acids. Journal of Chromatography A 1058, 51-59.

Barrow, M.P., Witt, M., Headley, J.V., Peru, K.M., 2010. Athabasca Oil Sands Process Water: Characterization by Atmospheric Pressure Photoionization and Electrospray Ionization Fourier Transform Ion Cyclotron Resonance Mass Spectrometry. Analytical Chemistry 82, 3727-3735.

Bataineh, M., Scott, A.C., Fedorak, P.M., Martin, J.W., 2006. Capillary HPLC/QTOF-MS for Characterizing Complex Naphthenic Acid Mixtures and Their Microbial Transformation. Analytical Chemistry 78, 8354-8361.

Berenbaum, M.C., 1989. What is synergy? Pharmacological Reviews 41, 93-141.

Bhuvaneswary, M.G., Thachil, E.T., 2008. Blends of Natural Rubber with Unsaturated Polyester Resin. International Journal of Polymeric Materials 57, 543-554.

Blakley, E.R., 1974. The microbial degradation of cyclohexane carboxylic acid: a pathway involving aromatisation to form p-hydroxybenzoic acid. Canadian Journal of Microbiology 20, 1297-1306.

Blakley, E.R., Papish, B., 1982. The metabolism of cyclohexanecarboxylic acid and 3-cyclohexenecarboxylic acid by Pseudomonas putida. Canadian Journal of Microbiology 28, 1324-1329.

Bliss, C.I., 1939. The toxicity of poisons applied jointly. *Annals of Applied Biology.* 26, 585-615.

Booth, A.M., Scarlett, A.G., Lewis, C.A., Belt, S.T., Rowland, S.J., 2008. Unresolved Complex Mixtures (UCMs) of Aromatic Hydrocarbons: Branched Alkyl Indanes and Branched Alkyl Tetralins are present in UCMs and accumulated by and toxic to, the mussel Mytilus edulis. Environmental Science & Technology 42, 8122-8126.

Booth, A.M., Sutton, P.A., Lewis, C.A., Lewis, A.C., Scarlett, A., Chau, W., Widdows, J., Rowland, S.J., 2007. Unresolved Complex Mixtures of Aromatic Hydrocarbons: Thousands of Overlooked Persistent, Bioaccumulative, and Toxic Contaminants in Mussels. Environmental Science & Technology 41, 457-464.

Brient, J.A., Wessner, P.J., Doyle, M.N., 1995. Naphthenic Acids: Kirk-Othmer Encyclopedia of Chemical Technology John Wiley & Sons, Inc.

Carmack, M., DeTar, D., 1946. The Willgerodt and Kindler Reactions. III. Amides from Acetylenes and Olefins; Studies Relating to the Reaction Mechanisms, Journal of the American Chemical Society 1946 68 (10), 2029-2033

Cason, J., Graham, D.W., 1965. Isolation of isoprenoid acids from a California petroleum. Tetrahedron 21, 471-483.

Cason, J., Khodair, A.I.A., 1966. Separation from a California Petroleum and Characterization of Geometric Isomers of 3-Ethyl-4-methylcyclopentylacetic Acid1. The Journal of Organic Chemistry 31, 3618-3625.

Cason, J., Khodair, A.I.A., 1967a. Isolation of the eleven-carbon acyclic isoprenoid acid from petroleum. Mass spectroscopy of its p-phthalimidophenacyl ester. The Journal of Organic Chemistry 32, 3430-3433.

Cason, J., Khodair, A.I.A., 1967b. Mass spectra of certain cycloalkylacetates and of related unsaturated esters. The Journal of Organic Chemistry 32, 575-581.

Cason, J., Liauw, K.-L., 1965. Characterization and Synthesis of a Monocyclic Eleven-Carbon Acid Isolated from a California Petroleum*,1. The Journal of Organic Chemistry 30, 1763-1769.

Choi, K., Sweet, L.I., Meier, P.G., Kim, P.-G., 2004. Aquatic toxicity of four alkylphenols (3-tert-butylphenol, 2-isopropylphenol, 3-isopropylphenol, and 4-isopropylphenol) and their binary mixtures to microbes, invertebrates, and fish. Environmental Toxicology 19, 45-50.

Christie, W.W., 1989. Silver ion chromatography using solid-phase extraction columns packed with a bonded-sulfonic acid phase. Journal of Lipid Research 30, 1471-1473

Chobanov,D., Tarandjiiska,R., and Chobanova,R. 1976*Journal of the American Oil Chemists Society*., **53**, 48-51 ().

Clemente, J.S., Fedorak, P.M., 2005. A review of the occurrence, analyses, toxicity, and biodegradation of Naphthenic acids. Chemosphere 60, 585-600.

Clemente, J.S., MacKinnon, M.D., Fedorak, P.M., 2004. Aerobic Biodegradation of Two Commercial Naphthenic Acids Preparations. Environmental Science & Technology 38, 1009-1016.

Colavecchia, M.V., Backus, S.M., Hodson, P.V., Parrott, J.L., 2004. Toxicity of oil sands to early life stages of fathead minnows (Pimephales promelas). Environmental Toxicology and Chemistry 23, 1709-1718.

Conley, R.F., 1996. Dispersant funtioality in nonaqueous media, in: Conley, R.F. (Ed.), Practical dispersion:A guide to understanding and formulating slurries. Wiley-VCH, New York, p. 195.

Cronin, M.T.D., Schultz, T.W., 1997. Validation of Vibrio fisheri acute toxicity data: mechanism of action-based QSARs for non-polar narcotics and polar narcotic phenols. Science of The Total Environment 204, 75-88.

Cyr, T.D., Strausz, O.P., 1983. The structures of tricyclic terpenoid carboxylic acids and their parent alkanes in the Alberta oil sands. Journal of the Chemical Society, Chemical Communications, 1028-1030.

Czarnecki, J., Radoev, B., Schramm, L.L., Slavchev, R., 2005. On the nature of Athabasca Oil Sands. Advances in Colloid and Interface Science 114–115, 53-60.

da Cruz, G.F., de Vasconcellos, S.P., Angolini, C.F.F., Dellagnezze, B.M., Garcia, I.N.S., de Oliveira, V.M., dos Santos Neto, E.V., Marsaioli, A.J., 2011. Could petroleum biodegradation be a joint achievement of aerobic and anaerobic microrganisms in deep sea reservoirs? AMB Express 1, doi:10.1186/2191-0855-1181-1147.

David, F., Sandra, P., Teinpont, B., Vanwalleghen, F., Ikonomou, M., 2003, Analytical methods review; In: Phthalate Esters, The Handbook of Environmental Chemistry, Volume 3, Edited: Staples, C.A., Springer Verlag, Berlin.

de Ligny, C.L., 1976. Advances in Chromatography. Marcel Dekker, New York..

de Vries, B., 1963. Quantitative separations of higher fatty acid methyl esters by adsorption chromatography on silica impregnated with silver nitrate. Journal of the American Oil Chemists' Society 40, 184-186.

Deneer, J.W., 2000. Toxicity of mixtures of pesticides in aquatic systems. Pest Management Science 56, 516-520.

Denton DL, Wheelock CE, Murray SA, Deanovic LA, Hammock BD, Hinton DE. 2003. Joint acute toxicity of esfenvalerate and diazinon to larval fathead minnows (Pimephales promelas). Environmental Toxicology and Chemistry 22, 336–341.

Destaillats, F., Golay, P.-A., Joffre, F., de Wispelaere, M., Hug, B., Giuffrida, F., Fauconnot, L., Dionisi, F., 2007. Comparison of available analytical methods to measure trans-octadecenoic acid isomeric profile and content by gas–liquid chromatography in milk fat. Journal of Chromatography A 1145, 222-228.

Dobson, G., Christie, W.W., Nikolova-Damyanova, B., 1995. Silver ion chromatography of lipids and fatty acids. Journal of Chromatography B: Biomedical Sciences and Applications 671, 197-222.

Dokholyan, B.K., Magomedov, A.K., 1984. Effect of sodium naphthenate on survival and some physiological-biochemical parameters of some fishes. Journal of Ichthyology 23, 125-132.

Donkin, P., Widdows, J., Evans, S.V., Worrall, C.M., Carr, M., 1989. Quantitative structure-activity relationships for the effect of hydrophobic organic chemicals on rate of feeding by mussels (Mytilus edulis). Aquatic Toxicology 14, 277-293.

Drescher, K., Boedeker, W., 1995. Assessment of the combined effects of substances: The relationship between concentration addition and independent action. Biometrics 51, 716-730.

Dreiucker, J., Vetter, W., 2011. Fatty acids patterns in camel, moose, cow and human milk as determined with GC/MS after silver ion solid phase extraction. Food Chemistry 126, 762-771.

Eichler, 1874. Bull. Soc. Natur., Moscou 46.

El-Alawi, Y.S., Huang, X.-D., Dixon, D.G., Greenberg, B.M., 2002. Quantitative structure-activity relationship for the photoinduced toxicity of polycyclic aromatic hydrocarbons to the luminescent bacteria Vibrio fischeri. Environmental Toxicology and Chemistry 21, 2225-2232.

Emken, E.A., Scholfield, C.R., Davison, V.L., Frankel, E.N., 1967. Separation of conjugated methyl octadecadienoate and trienoate geometric isomers by silver-resin column and preparative gas-liquid chromatography. Journal of the American Oil Chemists' Society 44, 373-375.

Engler, C., 1913. Die chemie u. Physik des Erdols, Leipzig.

Report to the European Commission., 2012. Toxicity and Assessment of Chemical Mixtures. Directorate General for Health and Consumers, Brussels, http://ec.europa.eu/health/scientific_committees/environmental_risks/docs/scher_o_155.pdf,.

Fisher, R. A., and F. Yates: Statistical tables for biological, agricultural and medical research. 6. Aufl. Oliver & Boyd, London 1963. 146 S. Preis 30 s. Biometrische Zeitschrift 7, 124-125.

Frank, R.A., Fischer, K., Kavanagh, R., Burnison, B.K., Arsenault, G., Headley, J.V., Peru, K.M., Kraak, G.V.D., Solomon, K.R., 2009. Effect of Carboxylic Acid Content on the Acute Toxicity of Oil Sands Naphthenic Acids. Environmental Science & Technology 43, 266-271.

Frank, R.A., Kavanagh, R., Kent Burnison, B., Arsenault, G., Headley, J.V., Peru, K.M., Van Der Kraak, G., Solomon, K.R., 2008. Toxicity assessment of collected fractions from an extracted Naphthenic acid mixture. Chemosphere 72, 1309-1314.

Frank, R.A., Sanderson, H., Kavanagh, R., Burnison, B.K., Headley, J.V., Solomon, K.R., 2010. Use of a (Quantitative) Structure Activity Relationship [(Q)Sar] Model to Predict the Toxicity of Naphthenic Acids. Journal of Toxicology and Environmental Health, Part A: Current Issues 73, 319 - 329.

Frank, R.A., Kavanagh, R., Kent Burniston, B., Headley, J.V., Peru, K,M., Van der Kraak. Solomon, K.R., 2006. Diethylaminoethyl-cellulose clean-up of a large volume naphthenic acid extract. Chemosphere, 64, 1346-1352.

Freeman, M.H., Memphis, T., 1992. Copper Naphthenate: An effective wood pole and crossarm preservative, in: Barnes, H.M., Amburgey, T.L. (Eds.), Proceedings, First Southeastern Pole Conference Mississippi State University, Starkville, MS, Proceedings, pp. 68-77.

Freidlin, L.K., Litvin, E.F., Gurskii, R.N., Istratova, R.V., Vaisman, I.L., 1975. Investigation of the catalytic hydeogenation of disubstituted benzenes and the configurational isomerization of the corresponding cyclohexanes. Bulletin of the Academy of Sciences of the USSR, Division of chemical science 24, 31-35.

Fritsche, J., Petersen, K.D., Jahreis, G., 2010. Trans octadecenoic fatty acid (TFA) isomers in German foods and bakery goods. European Journal of Lipid Science and Technology 112, 1363-1368.

Garcia-Garcia, E., Pun, J., Hodgkinson, J., Perez-Estrada, L.A., El-Din, M.G., Smith, D.W., Martin, J.W., Belosevic, M., 2011. Commercial Naphthenic acids and the organic fraction of oil sands process water induce different effects on pro-inflammatory gene expression and macrophage phagocytosis in mice. Journal of Applied Toxicology, n/a-n/a.

Grbović, L., Pavlović, K., Prekodravac, B., Kuhajda, K., Kevrešan, S., Popsavin, M., Milić, J., Crin-Novta, V., 2012. Fractionation of complex mixtures of Naphthenic acids, their characterization and biological activity. Journal of the Serbian Chemical Society 77, 147-157.

Gilman, H., Meals, R.N., 1943, Rearrangements in the Freidel-Crafts alkylation of benzene, The Journal of Organic Chemistry 1943 08, 126-146

Grewer, D.M., Young, R.F., Whittal, R.M., Fedorak, P.M., 2010. Naphthenic acids and other acid-extractables in water samples from Alberta: What is being measured? Science of The Total Environment 408, 5997-6010.

Hagen, M.O., Garcia-Garcia, E., Oladiran, A., Karpman, M., Mitchell, S., El-Din, M.G., Martin, J.W., Belosevic, M., 2012. The acute and sub-chronic exposures of goldfish to Naphthenic acids induce different host defense responses. Aquatic Toxicology 109, 143-149.

Han, X., Scott, A.C., Fedorak, P.M., Bataineh, M., Martin, J.W., 2008. Influence of Molecular Structure on the Biodegradability of Naphthenic Acids. Environmental Science & Technology 42, 1290-1295.

Hao, C., Headley, J.V., Peru, K.M., Frank, R., Yang, P., Solomon, K.R., 2005. Characterization and pattern recognition of oil-sand Naphthenic acids using comprehensive two-dimensional gas chromatography/time-of-flight mass spectrometry. Journal of Chromatography A 1067, 277-284.

Hargeshiemer, E.E., T., C.R., MacKinnon, M.D., 1984. Characterisation of simple phenols in oil sands extract ion process water. Environmental Technology Letters 5, 433-440.

Haug, P., Schnoes, H.K., Burlingame, A.L., 1971. Studies of the acidic components of the Colorado Green River Formation oil shale: Mass spectrometric identification of the methyl esters of extractable acids. Chemical Geology 7, 213-236.

He, Y., Wiseman, S.B., Hecker, M., Zhang, X., Wang, N., Perez, L.A., Jones, P.D., Gamal El-Din, M., Martin, J.W., Giesy, J.P., 2011. Effect of Ozonation on the Estrogenicity and Androgenicity of Oil Sands Process-Affected Water. Environmental Science & Technology 45, 6268-6274.

Head, I.M., Jones, D.M., Larter, S.R., 2003. Biological activity in the deep subsurface and the origin of heavy oil. Nature 426, 344-352.

Headley, J.V., Armstrong, S.A., Peru, K.M., Mikula, R.J., Germida, J.J., Mapolelo, M.M., Rodgers, R.P., Marshall, A.G., 2010. Ultrahigh-resolution mass spectrometry of simulated runoff from treated oil sands mature fine tailings. Rapid Communications in Mass Spectrometry 24, 2400-2406.

Headley, J.V., Barrow, M.P., Peru, K.M., Derrick, P.J., 2011a. Salting-out effects on the characterization of Naphthenic acids from Athabasca oil sands using electrospray ionization. Journal of Environmental Science and Health, Part A 46, 844-854.

Headley, J.V., Barrow, M.P., Peru, K.M., Fahlman, B., Frank, R.A., Bickerton, G., McMaster, M.E., Parrott, J., Hewitt, L.M., 2011b. Preliminary fingerprinting of Athabasca oil sands polar organics in environmental samples using electrospray ionization Fourier transform ion cyclotron resonance mass spectrometry. Rapid Communications in Mass Spectrometry 25, 1899-1909.

Headley, J.V., McMartin, D.W., 2004. A Review of the Occurrence and Fate of Naphthenic Acids in Aquatic Environments. Journal of Environmental Science and Health, Part A: Toxic/Hazardous Substances and Environmental Engineering 39, 1989 - 2010.

Headley, J.V., Peru, K.M., Barrow, M.P., 2009. Mass spectrometric characterization of Naphthenic acids in environmental samples: A review. Mass Spectrometry Reviews 28, 121-134.

Headley, J.V., Peru, K.M., McMartin, D.W., Winkler, M., 2002. Determination of Dissolved Naphthenic Acids in Natural Waters by Using Negative-Ion Electrospray Mass Spectrometry. Journal of AOAC International 85, 182-187.

Hell, C., Medinger, E., 1874. Ber 7.

Hindle, R., Noestheden, M., Peru, K., Headley, J., (2013), Quantitative Analysis of Naphthenic Acids in Water by Liquid Chromatography–Accurate Mass Time-of-Flight Mass Spectrometry, Journal of Chromatography A, In press.

Homburg,E. and Bielefeld,B. *Fette Seifen Anstrichm*., **81**, 377-381 (1979).

Holowenko, F.M., MacKinnon, M.D., Fedorak, P.M., 2001. Naphthenic acids and surrogate naphthenic acids in methanogenic microcosms. Water Research 35, 2595-2606.

Holowenko, F.M., MacKinnon, M.D., Fedorak, P.M., 2002. Characterization of Naphthenic acids in oil sands wastewaters by gas chromatography-mass spectrometry. Water Research 36, 2843-2855.

Holzmann, E., Pilat, S., 1933. Brennstoff -Chem 14.

Hoving, E.B., Muskiet, F.A.J., Christie, W.W., 1991. Separation of cholesterol esters by silver ion chromatography using high-performance liquid chromatography or solid-phase extraction columns packed with a bonded sulphonic acid phase. Journal of Chromatography B: Biomedical Sciences and Applications 565, 103-110.

Hsu, C.S., Dechert, G.J., Robbins, W.K., Fukuda, E.K., 1999. Naphthenic Acids in Crude Oils Characterized by Mass Spectrometry. Energy & Fuels 14, 217-223.

Hutchinson, T.H., Shillabeer, N., Winter, M.J., Pickford, D.B., 2006. Acute and chronic effects of carrier solvents in aquatic organisms: A critical review. Aquatic Toxicology 76, 69-92.

IUPAC, 1997. Compendium of Chemical Terminology, 2nd ed. Blackwell Science, Oxford.

Johnson, R.D., Lewis, R.J., Angier, M.K. 2010. False carbamazepine positives due to 10,11-dihydro-10-hydroxycarbamazepine breakdown in the GC-MS injector port. Report for the Office of Aerospace Medicine, Washington, DC 20591. Available: https://www.faa.gov/data_research/research/med_humanfacs/oamtechreports/2010s/media/201004.pdf

Johnson, R.J., Smith, B.E., S.J., R., Whitby, C., 2012a. Biodegradation of alkyl branched aromatic alkanoic Naphthenic acids by Pseudomonas putida KT2440. International Journal of Biodeterioration and Biodegradation In Press.

Johnson, R.J., West, C.E., Swaih, A.M., Folwell, B.D., Smith, B.E., Rowland, S.J., Whitby, C., 2012b. Aerobic biotransformation of alkyl branched aromatic alkanoic Naphthenic acids via two different pathways by a new isolate of Mycobacterium. Environmental Microbiology 14, 872-882.

Jones, D., Scarlett, A.G., West, C.E., Rowland, S.J., 2011. The toxicity of indiviual Naphthenic acids to *Vibrio fisheri*. Environmental Science & Technology 45, 9776-9782.

Jones, D., West, C.E., Scarlett, A.G., Frank, R.A., Rowland, S.J., 2012a. Isolation and estimation of the 'aromatic' Naphthenic acid content of an oil sands process-affected water extract. Journal of Chromatography A 1247, 171-175.

Jones, D., Scarlett, A., West, C., Rowland, S., 2012b. Fractionation, Identification and Toxicity of Acid Extracts of Oil Sands Process Affected Water, SETAC, Berlin (Poster Presentation).

Jones, D., Scarlett, A.G., West, C.E., Frank, R.A., Gieleciak, R., Hagar, D., Rowland, S.J., 2013. Elemental and spectroscopic characterisation of sub-fractions of an acidic extract of oil sands process water Chemosphere Submitted.

Kamaluddin, M., Zwiazek, J.J., 2002. Naphthenic acids inhibit root water transport, gas exchange and leaf growth in aspen (Populus tremuloides) seedlings. Tree Physiol 22, 1265-1270.

Kannel, P.R., Gan, T.Y., 2012. Naphthenic acids degradation and toxicity mitigation in tailings wastewater systems and aquatic environments: A review. Journal of Environmental Science and Health, Part A 47, 1-21.

Kaufman, T.S., Gonzalez-Sierra, M., Ruveda, E.A., 1988. Synthesis of an alberta oil sand bitumen C20 tricyclic carboxylic acid bearing a novel diterpenoid skeleton. Journal of the Chemical Society, Perkin Transactions 1, 2323-2327.

Kavanagh, R.J., Burnison, B.K., Frank, R.A., Solomon, K.R., Van Der Kraak, G., 2009. Detecting oil sands process-affected waters in the Alberta oil sands region using synchronous fluorescence spectroscopy. Chemosphere 76, 120-126.

Kavanagh, R.J., Frank, R.A., Oakes, K.D., Servos, M.R., Young, R.F., Fedorak, P.M., MacKinnon, M.D., Solomon, K.R., Dixon, D.G., Van Der Kraak, G., 2011. Fathead minnow (Pimephales promelas) reproduction is impaired in aged oil sands process-affected waters. Aquatic Toxicology 101, 214-220.

Kelly, E.N., Short, J.W., Schindler, D.W., Hodson, P.V., Ma, M., Kwan, A.K., Fortin, B.L., 2009. Oil sands development contributes polycyclic aromatic compounds to the Athabasca River and its tributaries. Proceedings of the National Academy of Sciences 106, 22346-22351.

Knoterus, J., 1957. The chemical constitution of the higher 'Naphthenic acids'. Journal of the Institute of Petroleum 43, 307-312.

Könemann, H., 1980. Structure--activity relationships and additivity in fish toxicities of environmental pollutants. Ecotoxicology and Environmental Safety 4, 415-421.

Kortencamp, A., Backhaus, T., Faust, M., 2009. State of the Art Report on Mixture Toxicity. European Commission http://ec.europa.eu/environment/chemicals/pdf/report_Mixture%20toxicity.pdf.

Kramer, J., Hernandez, M., Cruz-Hernandez, C., Kraft, J., Dugan, M., 2008. Combining Results of Two GC Separations Partly Achieves Determination of All cis and &l trans 16:1, 18:1, 18:2 and 18:3 Except CLA Isomers of Milk Fat as Demonstrated Using Ag-Ion SPE Fractionation. Lipids 43, 259-273.

Kunau, W.-H., Dommes, V., Schulz, H., 1995. β-Oxidation of fatty acids in mitochondria, peroxisomes, and bacteria: A century of continued progress. Progress in Lipid Research 34, 267-342.

Lai, J.W.S., Pinto, L.J., Bendell-Young, L.I., Moore, M.M., Kiehlmann, E., 1996. Factors that affect the degradation of Naphthenic acids in oil sands wastewater by indigenous microbial communities. Environmental Toxicology and Chemistry 15, 1482-1491.

Laredo, G.C., Lopez, C.R., Alvarez, R.E., Cano, J.L., 2004. Naphthenic acids, total acid number and sulfur content profile characterization in Isthmus and Maya crude oils. Fuel 83, 1689-1695.

Lee, K., Neff, J., 2011. Produced Waters, Environmental risks and advances in mitigation technologies. Springer, New York.

Leftley, J., 2000. Marine Bacterial Bioluminescence: Is it a good effects biomarker? A Literaure review. Research and Developement Technical Report E20 Environment Agency Bristol.

Linstead, R.P., Doering, W.E., Davis, S.B., Levine, P., Whetstone, R.R., 1942. The Stereochemistry of Catalytic Hydrogenation. I. The Stereochemistry of the Hydrogenation of Aromatic Rings. Journal of the American Chemical Society 64, 1985-1991.

Lo, C.C., Brownlee, B.G., Bunce, N.J., 2006. Mass spectrometric and toxicological assays of Athabasca oil sands Naphthenic acids. Water Research 40, 655-664.

Lochte, H.L., Littman, E.R., 1955. The Petroleum Acids and Bases. Chemical Publishing Company, New York.

Loewe, S., Muischnek, H., 1926. Effect of combinations: mathematical basis of problem. *N-S. Arch. Ex. Path. Ph.* 114, 313-326.

Lutnaes, B.F., Brandal, O., Sjoblom, J., Krane, J., 2006. Archaeal C80 isoprenoid tetraacids responsible for Naphthenate deposition in crude oil processing. Organic & Biomolecular Chemistry 4, 616-620.

MacKinnon, M.D., Boerger, H., 1986. Description of two treatment methods for detoxifying oil sands tailings pond water. Water Pollution Research Journal of Canada 21, 496-512.

Mahato, S.B., Banerjee, S., 1985. Steroid transformations by microorganisms. Phytochemistry 24, 1403-1421.

Mahato, S.B., Mukherjee, A., 1984. Steroid transformations by microorganisms. Phytochemistry 23, 2131-2154.

Mapolelo, M.M., Rodgers, R.P., Blakney, G.T., Yen, A.T., Asomaning, S., Marshall, A.G., 2011. Characterization of Naphthenic acids in crude oils and Naphthenates by electrospray ionization FT-ICR mass spectrometry. International Journal of Mass Spectrometry 300, 149-157.

Markownikoff, W., Oglobin, W., 1883. Jou. Soc. Russe de Physicochemie 34.

Martin, J.W., Barri, T., Han, X., Fedorak, P.M., El-Din, M.G., Perez, L., Scott, A.C., Jiang, J.T., 2010. Ozonation of Oil Sands Process-Affected Water Accelerates Microbial Bioremediation. Environmental Science & Technology 44, 8350-8356.

McLafferty, F.W., Turecek, F., 1993. Interpretation of Mass Spectra, 4 ed. University Science Books, California, USA.

McMartin, D.W., Headley, J.V., Friesen, D.A., Peru, K.M., Gillies, J.A., 2004. Photolysis of Naphthenic Acids in Natural Surface Water. Journal of Environmental Science and Health, Part A 39, 1361-1383.

Merlin, M., Guigard, S.E., Fedorak, P.M., 2007. Detecting naphthenic acids in waters by gas chromatography–mass spectrometry. Journal of Chromatography A 1140, 225-229

Mishra, S., Meda, S., Dalai, A.K., McMartin, D.W., Headley, J., Peru, K.M., 2010a. Photocatalysis of Naphthenic Acids in Water. Journal of Water Resource and Protection 2, 644-650.

Mishra, S., Meda, V., Dalai, A.K., Headley, J.V., Peru, K.M., McMartin, D.W., 2010b. Microwave treatment of Naphthenic acids in water. Journal of Environmental Science and Health, Part A: Toxic/Hazardous Substances and Environmental Engineering 45, 1240 - 1247.

Mohamed, M., Wilson, L.D., Headley, J.V., Peru, K.M., 2008. Screening of oil sands naphthenic acids by UV-vis absorption and fluorescence emission spectrophotometry. Journal of Environmental Science and Health, Part A 43, 1700-1705.

Morris, L.J., 1966. Separations of lipids by silver ion chromatography. Journal of Lipid Research 7, 717-732.

Moyes, R.B., Wells, P.B., 1973. The Chemisorption of Benzene, in: D.D. Eley, H.P., Paul, B.W. (Eds.), Advances in Catalysis. Academic Press, pp. 121-156.

Muller, J., Pilat, S., 1936. Brennstoff -Chemie 17.

Nero, V., Farwell, A., Lee, L.E.J., Van Meer, T., MacKinnon, M.D., Dixon, D.G., 2006. The effects of salinity on Naphthenic acid toxicity to yellow perch: Gill and liver histopathology. Ecotoxicology and Environmental Safety 65, 252-264.

Neuberg, 1906. Biochem. Z. 1.

Nichols, P.L., 1952. Coördination of Silver Ion with Methyl Esters of Oleic and Elaidic Acids. Journal of the American Chemical Society 74, 1091-1092

Nikolova-Damyanova, B. Silver ion chromatography and lipids. In: *Advances in Lipid Methodology - One.* pp. 181-237 (Ed. W.W. Christie, Oily Press, Ayr) (1992)

OECD, 2000. Guidance document on aquatic toxicity testing of difficult substances and mixtures OECD series on testing and assessment. Organisation for Economic Co-operation and Developement: Joint Meeting of the Chemicals Committee and the Working Party on Chemicals, Pesticides and Biotechnology, Paris, pp. 1-53.

Peters, L.E., MacKinnon, M., Van Meer, T., van den Heuvel, M.R., Dixon, D.G., 2007. Effects of oil sands process-affected waters and naphthenic acids on yellow perch (Perca flavescens) and Japanese medaka (Orizias latipes) embryonic development. Chemosphere 67, 2177-2183.

Pilat, S., Reymann, J., 1932. Ann 499.

Quagraine, E.K., Headley, J.V., Peterson, H.G., 2005a. Is Biodegradation of Bitumen a Source of Recalcitrant Naphthenic Acid Mixtures in Oil Sands Tailing Pond Waters? Journal of Environmental Science and Health, Part A: Toxic/Hazardous Substances and Environmental Engineering 40, 671 - 684.

Quagraine, E.K., Peterson, H.G., Headley, J.V., 2005b. In situ bioremediation of Naphthenic acids contaminated tailing pond waters in the Athabasca Oil Sands Region -demonstrated field studies and plausible options: a review. Journal of Environmental Science and Health, Part A: Toxic/Hazardous Substances and Environmental Engineering 40, 685 - 722.

Reinardy, H.C., Scarlett, A.G**.**, Henry, T.B., West, C.E., Hewitt, L.M., Frank, R.A. and Rowland, S.J. Aromatic naphthenic acids in oil sands process-affected water, fully resolved by GCxGC-MS, weakly induce the gene for vitellogenin production in zebrafish (Danio rerio) larvae. Environmental Science & Technology. (In press).

Rogers, V.V., Wickstrom, M., Liber, K., MacKinnon, M.D., 2002. Acute and Subchronic Mammalian Toxicity of Naphthenic Acids from Oil Sands Tailings. Toxicological Sciences 66, 347-355.

Ross, M.S., dos Santos Pereira, A., Fennell, J., Davies, M., Johnson, J., Sliva, L., Martin, J.W., 2012, Quantitative and Qualitative Analysis of Naphthenic Acids in Natural Waters Surrounding the Canadian Oil Sands Industry, Environmental Science & Technology, 46, 12796-12805

Rowland, S.J., Jones, D., Scarlett, A.G., West, C.E., Hin, L.P., Boberek, M., Tonkin, A., Smith, B.E., Whitby, C., 2011a. Synthesis and toxicity of some metabolites of the microbial degradation of synthetic Naphthenic acids. Science of The Total Environment 409, 2936-2941.

Rowland, S.J., Scarlett, A.G., Jones, D., West, C.E., Frank, R.A., 2011b. Diamonds in the Rough: Identification of Individual Naphthenic Acids in Oil Sands Process Water. Environmental Science & Technology 45, 3154-3159.

Rowland, S.J., West, C.E., Jones, D., Scarlett, A.G., Frank, R.A., Hewitt, L.M., 2011c. Steroidal Aromatic 'Naphthenic Acids' in Oil Sands Process-Affected Water: Structural Comparisons with Environmental Estrogens. Environmental Science & Technology 45, 9806-9815.

Rowland, S.J., West, C.E., Scarlett, A.G., Jones, D., 2011d. Identification of Individual acids in a commercial sample of Naphthenic acids from petroleum by two dimensional comprehensive gas chromatography-mass spectrometry. Rapid Communications in Mass Spectrometry 25, 1741-1751.

Rowland, S.J., West, C.E., Scarlett, A.G., Jones, D., Frank, R.A., 2011e. Identification of individual tetra- and pentacyclic Naphthenic acids in oil sands process water by comprehensive two-dimensional gas chromatography-mass spectrometry. Rapid Communications in Mass Spectrometry 25, 1198-1204.

Rowland, S.J., West, C.E., Scarlett, A.G., Jones, D., Boberek, M., Pan, L., Ng, M., Kwong, L., Tonkin, A., 2011f. Monocyclic and monoaromatic naphthenic acids: Synthesis & characterisation. Environmental Chemistry Letters 9, 525-533. [doi: 10.1007/s10311-011-0314-6].

Rowland, S.J., West, C.E., Scarlett, A.G., Cheuk Ho., Jones, D., 2012. Differentiation of two industrial oil sands process-affected waters by two-dimensional gas chromatography/mass spectrometry of diamondoid acid profiles. Rapid Communications in Mass Spectrometry 26, 572-576. [doi: 10.1002/rcm.6138]]

Russom, C.L., Bradbury, S.P., Broderius, S.J., Hammermeister, D.E., Drummond, R.A., 1997. Predicting modes of toxic action from chemical structure: Acute toxicity in the fathead minnow (Pimephales promelas). Environmental Toxicology and Chemistry 16, 948-967.

Sabatier, P., 1912. Nobel Lectures, Chemistry 1901-1921. Elsevier Publishing, Amsterdam.

Sabatier, P., Espil, L., 1914. Soc. Chim. Fr. Bull 4, 228.

Sabatier, P., Senderens, J.B., 1899. Comptes Rendus Chemie, 1173.

Sabatier, P., Senderens, J.B., 1904. Soc. Chim. Fr. Bull 3, 101.

Sauer, T.C., Costa, H.J., Brown, J.S., Ward, T.J., 1997. Toxicity identification evaluations of produced-water effluents. Environmental Toxicology and Chemistry 16, 2020-2028.

Sauvage, J.-F., Baker, R.H., Hussey, A.S., 1960. The Hydrogenation of Cyclohexenes over Platinum Oxide. Journal of the American Chemical Society 82, 6090-6095.

Scarlett, A., Rowland, S.J., Canty, M., Smith, E.L. and Galloway, T.S. (2007) Method for assessing the chronic toxicity of marine and estuarine sediment-associated contaminants using the amphipod Corophium volutator. *Marine Environmental Research* 63, 457-470. [doi: 10.1016/j.marenvres.2006.12.006].

Scarlett, A., West, C., Jones, D., Galloway, T., Rowland, S., 2012. Predicted Toxicity of Naphthenic Acids Present in Oil Sands Process-Affected Waters to a Range of Environmental and Human Endpoints. Science of The Total Environment, 425, 119-127. [doi: 10.1016/j.scitotenv.2012.02.064].

Scarlett, A. G.; .Reinardy, C. H.; Henry, T. B.; West, C. E.; Frank, R. A.; Hewitt, L. M.; Rowland, S. J., 2013. Acute toxicity of aromatic and non-aromatic fractions of naphthenic acids extracted from oil sands process affected water to larval zebrafish. Chemosphere., in press,

Schramm, L.L., Stasuik, E.N., MacKinnon, M.D., 2000. Surfactants in Athabasca oil sands; slurry conditioning, flotation recovery and tailings processes, in: Schramm, L.L. (Ed.), Surfactants: Fundamentals and applications in the petroleum industry. Cambridge University Press, Cambridge

Schramm, L.L., Stasiuk, E.N., Turner, D., 2003. The influence of interfacial tension in the recovery of bitumen by water-based conditioning and flotation of Athabasca oil sands. Fuel Processing Technology 80, 101-118.

Schultz, T.W., 1987. Relative toxicity of para-substituted phenols: Log K_{OW} and pKa-dependent structure-activity relationships. Bulletin of Environmental Contamination and Toxicology 38, 994-999.

Schultz, T.W., 1989. Nonpolar Narcosis: A review of the mechanism of action for baseline aquatic toxicity. American Society for Testing and Materials, Philadelphia.

Scott, A.C., Mackinnon, M.D., Fedorak, P.M., 2005. Naphthenic Acids in Athabasca Oil Sands Tailings Waters Are Less Biodegradable than Commercial Naphthenic Acids. Environmental Science & Technology 39, 8388-8394.

Scott, A.C., Young, R.F., Fedorak, P.M., 2008a. Comparison of GC-MS and FTIR methods for quantifying Naphthenic acids in water samples. Chemosphere 73, 1258-1264.

Scott, A.C., Zubot, W., MacKinnon, M.D., Smith, D.W., Fedorak, P.M., 2008b. Ozonation of oil sands process water removes Naphthenic acids and toxicity. Chemosphere 71, 156-160.

Seifert, W.K., 1975. Carboxylic acids in petroleum and sediments, in: Herz, W., Grisebach, H., Kirby, G.W. (Eds.), Progress in the Chemistry of Organic Natural Products. Springer-Verlag, Vienna, Austria, pp. 2-49.

Seifert, W.K., Howells, W.G., 1969. Interfacially active acids in a California crude oil. Isolation of carboxylic acids and phenols. Analytical Chemistry 41, 554-562.

Seifert, W.K., Teeter, R.M., 1970a. Identification of polycyclic aromatic and heterocyclic crude oil carboxylic acids. Analytical Chemistry 42, 750-758.

Seifert, W.K., Teeter, R.M., 1970b. Identification of polycyclic Naphthenic, mono-, and diaromatic crude oil carboxylic acids. Analytical Chemistry 42, 180-189.

Seifert, W.K., Teeter, R.M., Howells, W.G., Cantow, M.J.R., 1969. Analysis of crude oil carboxylic acids after conversion to their corresponding hydrocarbons. Analytical Chemistry 41, 1638-1647.

Seward, J.R., Schultz, T.W., 1999. QSAR Analyses of the Toxicity of Aliphatic Carboxylic Acids and Salts to *TetrahymeNA Pyriformis*. SAR and QSAR in Environmental Research 10, 557 - 567.

Shepherd, A.G., van Mispelaar, V., Nowlin, J., Genuit, W., Grutters, M., 2010. Analysis of Naphthenic Acids and Derivatization Agents Using Two-Dimensional Gas Chromatography and Mass Spectrometry: Impact on Flow Assurance Predictionsâ€ Energy & Fuels 24, 2300-2311.

Shipp, 1936. Oil Gas Journal, 56.

Siegel, S., Smith, G.V., 1960a. Stereochemistry and the Mechanism of Hydrogenation of Cycloölefins on a Platinum Catalyst1,2. Journal of the American Chemical Society 82, 6082-6087.

Siegel, S., Smith, G.V., 1960b. The Stereochemistry of the Hydrogenation of Cycloölefins on Supported Palladium Catalysts1,2. Journal of the American Chemical Society 82, 6087-6090.

Singer, M.E., Finnerty, W.R., 1984. Microbial metabolism of straight chain and branced alkanes, in: Atlas, R.M. (Ed.), Petroleum Microbiology. Macmillan, New York.

Smith, B.E., 2006. Naphthenic Acids: Synthesis, characterisation, and factors influencing environmental fate, School of Earth, Ocean and Environmental Sciences. University of Plymouth, Plymouth, p. 252.

Smith, B.E., Lewis, C.A., Belt, S.T., Whitby, C., Rowland, S.J., 2008. Effects of Alkyl Chain Branching on the Biotransformation of Naphthenic Acids. Environmental Science & Technology 42, 9323-9328.

Stanislaus, A., Cooper, B.H., 1994. Aromatic Hydrogenation Catalysis: A Review. Catalysis Reviews 36, 75-123.

Stewart, G.S.A.B., 1990. *In Vivo* bioluminescence: new potentials for microbiology. Letters in Applied Microbiology 10, 1-8.

Sutton, P.A., Smith, B.E., Rowland, S.J., 2010a. Mass spectrometry of polycyclic tetracarboxylic ('ARN') acids and tetramethyl esters. Rapid Communications in Mass Spectrometry 24, 3195-3204.

Sutton, P.A., Smith, B.E., Waters, D., Rowland, S.J., 2010b. Identification of a Novel Ester Obtained during Isolation of C80 (“ARN”) Tetraprotic Acids from an Oilfield Pipeline Deposit. Energy & Fuels 24, 5579-5585.

Syberg, K., Elleby, A., Pedersen, H., Cedergreen, N. and Forbes, V, E., 2008. Mixture Toxicity of Three Toxicants with Similar and Dissimilar Modes of Action to *Daphnia magna*. *Valery Forbes Publications.* Paper 23. http://digitalcommons.unl.edu/biosciforbes/23

Thomas, K.V., Langford, K., Petersen, K., Smith, A.J., Tollefsen, K.E., 2009. Effect-Directed Identification of Naphthenic Acids As Important in Vitro Xeno-Estrogens and Anti-Androgens in North Sea Offshore Produced Water Discharges. Environmental Science & Technology 43, 8066-8071.

Tissot, B.P., Welte, D.H., 1984. Petroleum formation and occurrance, Second ed. Springer-Verlag, Berlin.

Tollefsen, K.E., Petersen, K., Rowland, S.J., 2012. Toxicity of Synthetic Naphthenic Acids and Mixtures of These to Fish Liver Cells. Environmental Science & Technology 46, 5143-5150.

Toor, N.S., Franz, E.D., Fedorak, P.M., MacKinnon, M.D., Liber, K., Degradation and aquatic toxicity of Naphthenic acids in oil sands process-affected waters using simulated wetlands. Chemosphere.

van den Heuvel, M.R., Hogan, N.S., Roloson, S.D., Van Der Kraak, G.J., 2012. Reproductive development of yellow perch (Perca flavescens) exposed to oil sands–affected waters. Environmental Toxicology and Chemistry 31, 654-662.

Veith, G.D., Broderius, S.J., 1990. Rules for Distinguishing Toxicants That Cause Type-I and Type-Ii Narcosis Syndromes. Environmental Health Perspectives 87, 207-211.

Von Braun, J., 1931. Jou. Ann 490.

Von Braun, J., 1938. Ol u, Kohle 14.

Von Braun, J., Wittmeyer, H., 1934. Ber 67B.

Walker, J.D., Cooney, J.J., 1973. pathway of n-alkane oxidation in *Cladosporium resipae*. Journal of Bacteriology 115, 635-639.

Wessels,H. and Rajagopal,N.S. 1969. *Fette Seifen Anstrichm.*, **71**, 543-552

West, C.E., Jones, D., Scarlett, A.G., Rowland, S.J., 2011. Compositional heterogeneity may limit the usefulness of some commercial Naphthenic acids for toxicity assays. Science of The Total Environment 409, 4125-4131. [doi: 10.1016/j.scitotenv.2011.05.061].

West, C.E., Scarlett, A.G., Pureveen, J., Tegelaar, E., Rowland, S.J., 2013. Abundant naphthenic acids in oil sands process-affected water: studies by synthesis, derivatisation and GCxGC–high resolution mass spectrometry. Rapid Communications in Mass Spectrometry 27, 357–365.

Whitby, C., Allen, I.L., Sima, S., Geoffrey, M.G., 2010. Microbial Naphthenic Acid Degradation, Advances in Applied Microbiology. Academic Press, pp. 93-125.

Winstein, S., Lucas, H.J., 1938. The Coördination of Silver Ion with Unsaturated Compounds. Journal of the American Chemical Society 60, 836-847.

Young, R.F., Orr, E.A., Goss, G.G., Fedorak, P.M., 2007. Detection of Naphthenic acids in fish exposed to commercial Naphthenic acids and oil sands process-affected water. Chemosphere 68, 518-527.

Young, R.F., Wismer, W.V., Fedorak, P.M., 2008. Estimating Naphthenic acids concentrations in laboratory-exposed fish and in fish from the wild. Chemosphere 73, 498-505.

Zaikin, V., and Halket, J.M., (2009) A handbook of derivatives for mass spectrometry, IM Publications, Chichester, UK. Page xviii

Zajic, J.E., Cooper, D.G., Marshall, J.A., 1981. Microstructure of Athabasca bituminous sand by freeze-fracture and transmission electron microscopy. Fuel 60, 619-623.

Zelinsky, N., 1924. Ber 57.

Zelles, L. & Bai, Q.Y. 1993. Fractionation of fatty acids derived from soil lipids by solid phase extraction and their quantitative analysis by GC-MS. *Soil Biology and Biochemistry 25*, 495-507.

Zhao, Y.H., Yuan, X., Yang, L.H., Wang, L.S., 1996. Quantitative Structure-Activity Relationships of Organic Acids and Bases. Bulletin of Environmental Contamination and Toxicology 57, 242-249.

Synthesis, Characterisation and Toxicology of Naphthenic Acids from Complex Mixtures

David Jones

Appendices

Appendix A: List of naphthenic acids considered for toxicological testing

Appendix B: Biodegradation Study on adamantane type naphthenic acids

Appendix C: pH based fractionation of the OSPW acid extracts

Appendix D: Presentations and Publications including links to the full text of three first authorship papers

Appendix A

Appendix A

Individual naphthenic acids considered for toxicological testing

Table A1. Individual petroleum acids identified and considered for toxicological testing, with toxicological predictions, source and some physiochemical parameters

			Predicted from Ecosar				
					Daphnia 48 hr test		
Name of Compound	**M/W**	**Carbon Number**	**Log K_{ow}**	**Solubility mg L^{-1}**	**EC_{50} (mg/L)**	**EC_{50} (mM)**	**From**
n-hexanoic acid	116.16	6	2.05	1.03E+04	458.5	3.95	Sigma
n-octanoic acid	144.22	8	3.03	789	89.99	0.62	Sigma
n-nonanoic Acid	158.24	9	3.52	284	39.25	0.24	Sigma
n-decanoic Acid	172.27	10	4.02	61.8	16.99	0.10	Sigma
n-undecanoic acid	186.3	11	4.51	52.2	7.38	0.04	Sigma
n-dodecanoic acid	200.32	12	5	4.81	3.12	0.016	Sigma

n-tridecanoic acid	214.35	13	5.49	33	1.328	0.006	Sigma
n-tetradecanoic acid	228.37	14	5.98	1.07	0.563	0.002	Sigma
n-octadecanoic acid	284.49	18	7.94	0.597	0.018	0.00006	Sigma
2-ethylhexanoic acid	144.22	8	2.96	2000	103.31	0.72	Sigma
2-propylpentanoic acid	144.22	8	2.96	2000	103.31	0.72	Sigma
4-ethyloctanoic acid	172.27	10	3.94	64.05	19.51	0.11	Sigma
2-butyloctanoic acid	200.32	12	4.92	6.746	3.585	0.018	Sigma
2-butyldecanoic acid	228.38	14	5.91	0.6965	0.646	0.002	Sigma
2-hexyldecanoic acid	256.43	16	6.89	0.07	0.115	0.0004	Sigma
4-methyloctanoic acid	158.24	9	3.45	195.5	45.07	0.28	Sigma
2-methylnonanoic acid	172.46	10	3.94	64.05	19.51	0.11	Sigma
3-methylnonanoic acid	172.46	10	3.94	64.05	19.51	0.11	Sigma
4-methylnonanoic acid	172.46	10	3.94	64.05	19.51	0.11	Sigma
8-methylnonanoic acid	172.46	10	3.94	64.05	19.51	0.11	Sigma
7-methyldecanoic acid	186.29	11	4.43	20.85	8.386	0.04	Sigma
4-methyldodecanoic acid	214.34	13	5.43	2.172	1.525	0.007	Sigma
12-methyltridecanoic acid	228.37	14	5.91	0.6965	0.646	0.002	Sigma
13-methyltetradecanoic acid	242.41	15	6.4	0.2225	0.273	0.001	Sigma

2,6-dimethylheptanoic acid	158.24	9	3.38	225.9	51.736	0.32	Synthesised (ET)
3,7 dimethyloctanoic acid	172.27	10	3.87	74.01	22.392	0.13	Synthesised (DJ)
2,6,10-trimethylundecanoic acid	228.38	14	5.76	0.9929	0.851	0.004	Synthesised (BS)
3,7,11,15-tetrahexadecanoic acid	312.54	20	8.63	0.001	0.005	0.00002	Synthesised (GD)
2-methylphenylethanoic acid (commercial)	150.18	9	1.98	3864	683.18	4.55	Sigma
3-methylphenylethanoic acid (Commercial)	150.18	9	1.98	4065	683.18	4.55	Sigma
4-methylphenylethanoic acid (Commercial)	150.18	9	1.98	4851	683.18	4.55	Sigma
4-methylphenylethanoic acid (Synthetic)	150.18	9	1.98	4851	683.18	4.55	Synthesised (BS)
4-ethylphenylethanoic acid	164.21	10	2.47	1947	296.98	1.81	Synthesised (BS)
4-n-propylphenylethanoic acid	178.23	11	2.96	382.3	128.15	0.72	Synthesised (BS)
4-i-propylphenylethanoic acid	178.23	11	2.88	479.9	147.12	0.82	Synthesised (BS)
4-n-butylphenylethanoic acid	192.26	12	3.45	199.4	54.96	0.29	Synthesised (BS)
4-i-butylphenylethanoic acid	192.26	12	3.38	163.8	63.1	0.33	Synthesised (BS)
4-t-butylphenylethanoic acid	192.26	12	3.34	339.1	67.72	0.35	Synthesised (BS)
4-n-pentylphenylethanoic acid	206.29	13	3.94	63.27	23.44	0.11	Synthesised (BS)
4-n-hexylphenylethanoic acid	220.31	14	4.43	19.98	9.95	0.05	Synthesised (BS)
4-n-nonylphenylethanoic acid	262.39	17	5.9	0.4542	0.745	0.003	Sigma
4-phenylbutanoic acid	164.21	10	2.78	1394	165.9	1.01	Synthesised (BS)

6-phenylhexanoic acid	192.26	12	3.76	480	30.702	0.16	Synthesised (BS)
4-n-butylphenylbutanoic acid	220.31	14	4.8	6.81	5	0.02	Synthesised (BS)
4-i-butylphenylbutanoic acid	220.31	14	4.72	7.87	5.75	0.03	Synthesised (BS)
4-s-butylphenylbutanoic acid	220.31	14	4.72	7.87	5.75	0.03	Sigma
4-t-butylphenylbutanoic acid	220.31	14	4.69	8.47	6.17	0.03	Sigma
4-butylbenzoic acid	178.23	11	3.89	22.86	22.046	0.12	Sigma
4-methylcyclohexylethanoic acid	156.23	9	3.27	287.8	63.08	0.4	Synthesised (BS)
4-ethylcyclohexylethanoic acid	170.25	10	3.76	94.37	27.332	0.16	Synthesised (BS)
4-n-propylcyclohexylethanoic acid	184.28	11	4.25	30.74	11.761	0.06	Synthesised (BS)
4-i-butylcyclohexylethanoic acid	198.3	12	4.66	11.5	5.77	0.03	Synthesised (BS)
4-t-butylcyclohexylethanoic acid	198.3	12	4.63	12.39	6.199	0.03	Synthesised (BS)
4-n-butylcyclohexylethanoic acid	198.3	12	4.63	12.39	6.199	0.03	Synthesised (BS)
4-n- pentylcyclohexylethanoic acid	212.33	13	5.23	3.208	2.142	0.009	Synthesised (BS)
4-n- hexylcyclohexylethanoic acid	226.36	14	5.72	1.029	0.908	0.004	Synthesised (DJ)
1-methyl-1-cyclohexanecarboxylic acid	142.2	8	2.81	811	135.009	0.95	Sigma
2-methyl-1-cyclohexanecarboxylic acid	142.2	8	2.77	870.3	144.43	1.02	Sigma
3-methyl-1-cyclohexanecarboxylic acid	142.2	8	2.77	870.3	144.43	1.02	Sigma
4-methyl-1-cyclohexanecarboxylic acid	142.2	8	2.77	870.3	144.43	1.02	Sigma

trans 4-methyl-1-cyclohexanecarboxylic acid	142.2	8	2.77	870.3	144.43	1.02	Sigma
trans 4-pentyl-1-cyclohexanecarboxylic acid	198.3	12	4.74	9.96	5.03	0.03	Sigma
4-n-butylcyclohexylbutanoic acid	226.36	14	5.72	1.029	0.908	0.004	Synthesised (BS)
4-i-butylcyclohexylbutanoic acid	226.36	14	5.65	1.19	1.04	0.005	Synthesised (BS)
4 -s-butylcyclohexylbutanoic acid	226.36	14	5.65	1.19	1.04	0.005	Synthesised (BS)
4-t-butylcyclohexylbutanoic acid	226.36	14	5.61	1.28	1.12	0.005	Sigma
1-Pyrene carboxylic acid	248.28	17	4.31	0.969	14.036	0.057	Sigma
1-Pyreneethanoic acid	262.31	18	4.54	6.708	9.738	0.04	Sigma
1-Pyrenebutanoic acid	290.36	20	5.88	0.327	0.856	0.003	Sigma
Cyclohexylcarboxylic acid	128.17	7	2.36	4600	285.2	2.23	Sigma
3-cyclohexylpronanoic acid	156.23	9	3.34	249	54.95	0.35	Sigma
4-cyclohexylbutanoic acid	170.25	10	3.83	81.67	23.807	0.14	Sigma
5-cyclohexylpentanoic acid	184.28	11	4.32	26.6	10.245	0.056	Sigma
6-cyclohexylhexanoic acid	198.31	12	4.81	8.616	4.38	0.02	Synthesised (DJ)
2-Adamantanone	150.22	10	2.59	463.2	21.49	0.14	Sigma
3-Noradamantane carboxylic acid	166.22	10	2.66	846.7	208.12	1.25	Sigma
1-Adamantanecarboxylic acid	180.25	11	3.15	276.3	89.7	0.50	Sigma
1, 3-Adamantanedicarboxylic acid	224.26	12	1.78	2430	1462.5	6.52	Sigma

1-adamantane ethanoic acid	194.28	12	3.64	89.63	38.446	0.19	Sigma
3, 5-dimethyl-1-adamantane carboxylic acid	208.3	13	4.06	33.53	18.88	0.09	Sigma
3-Ethyl-adamantane-1-carboxylic acid	208.3	13	4.1	31.14	17.59	0.08	Sigma
3-methyl-1-adamantane ethanoic acid	208.3	13	4.1	31.14	17.58	0.08	Sigma
adamantane-1-pronanoic acid	208.3	13	4.1	28.92	16.39	0.08	Sigma
3-carboxyadamantane-1-ethanoic acid	238.29	13	2.28	777.2	617.847	2.6	Sigma
3, 7-dimethyl-1-adamantane ethanoic acid	222.33	14	4.55	10.77	8.01	0.03	Sigma
3,5,7-trimethyl-1-adamantane carboxylic acid	222.33	14	4.51	11.6	8.595	0.04	Sigma
Diamantane-1-carboxylic	232.3	15	4.6	8.99	7.655	0.03	Stanford University
Diamantane-3-carboxylic	232.3	15	4.6	8.99	7.655	0.03	Czech Republic
Diamantane-4-carboxylic	232.3	15	4.6	8.99	7.655	0.03	Czech Republic
Diamantane-1,4-dicarboxylic	276.3	16	3.23	72.9	119.3	0.43	Czech Republic
Diamantane-1,6-dicarboxylic	276.3	16	3.23	72.9	119.3	0.43	Stanford University
Diamantane-4,9-dicarboxylic	276.3	16	3.23	72.9	119.3	0.43	Czech Republic
1-Napthoic acid	172.18	11	3.05	86	104.06	0.6	Sigma
2-Napthoic acid	172.18	11	3.05	47	104.06	0.6	Sigma
1-Napthaleneacetic acid	186.21	12	2.6	420	260.75	1.4	Sigma
2-Napthaleneacetic acid	186.21	12	2.6	507.7	260.75	1.4	Sigma

4-Methyl-1-Napthoic acid	186.21	12	3.6	43.4	40.26	0.21	Sigma
3-naphthalen-1-yl-Pronanoic acid	200.24	13	3.46	119.8	55.89	0.28	Sigma
Decalin-1-carboxylic acid	182.6	11	3.38	174.1	59.62	0.33	Synthesised (DJ)
Decalin-2-carboxylic acid	182.6	11	3.38	174.1	59.62	0.33	Synthesised (DJ)
Decalin-1-ethanoic acid	196.3	12	3.87	56.41	25.53	0.13	Synthesised (DJ)
Decalin-2-ethanoic acid	196.3	12	3.87	56.41	25.53	0.13	Synthesised (DJ)
4-methyl-1-decalin acrboxylic acid	196.3	12	3.79	65.18	29.31	0.15	Synthesised (DJ)
3-Decalin-1-yl-Pronanoic acid	210.32	13	4.36	18.19	10.88	0.05	Synthesised (DJ)
Bicyclo[3.2.1]octane-6-carboxylic acid	154.21	9	2.74	829.8	167.86	1.09	Synthesised (DJ)
4-iso-propylcyclohexylethanoic acid	184.28	11	4.17	35.52	13.5	0.07	Synthesised (DJ)
6-cyclohexylhexanoic acid	198.31	12	4.81	8.62	4.38	0.02	Synthesised (DJ)
4-t-butylcyclohexylethanoic acic	198.31	12	4.63	12.39	6.12	0.03	Synthesised (DJ)
4-t-butylcyclohexylbutanoic acic	226.36	14	5.61	1.28	1.18	0.005	Synthesised (DJ)
4-n-hexylcyclohexylethanoic acid	226.36	14	5.72	1.029	0.908	0.004	Synthesised (DJ)
4-n-nonylcyclohexylethanoic acid	268.44	17	7.19	0.03	0.068*	0.0002*	Synthesised (DJ)
3-Thiophenecarboxylic acid	128.58	5	1.69	4300	454.795	3.54	Sigma
9-Fluorenecarboxylic acid	210.23	14	3.06	30.34	124.15	0.59	Sigma
9-Anthracene carboxylic acid	222.25	15	4.23	85	14.75	0.066	Sigma

4-(3 and 2)-i-butylphenyl-4-pentanoic acid	234.4	15	5.14	2.911	2.789	0.012	Sigma
4-(4-n-butylbiphenyl-4-yl)pentanoic acid	310.44	21	6.98	0.029	0.117	0.0004	Sigma
cyclopentylethanoic acid	114.15	7	1.87	6676	638.9	5.56	Sigma
dicyclohexylethanoic acid	224.35	14	3.15	1.521	1.276	0.006	Sigma
5-(2-decahydroNapthalenel)pentanoic acid	238.37	15	5.34	1.867	1.948	0.008	Sigma
6-heptyldecahydronaphthalen-2-carboxylic acid	266.43	18	6.25	0.2184	0.395	0.0015	Sigma
5β Cholanic acid	304.48	25	5.83	0.2986	0.986	0.003	Sigma
2-norbornane ethanoic acid	154.21	9	2.74	829.28	167.87	1.08	Sigma
bicyclo[3.3.1]nonane-1-carboxylic acid	168.24	10	3.26	235.9	68.06	0.4	Sigma
1,1 cyclohexanediacetic acid	200.24	10	1.97	2257	922.77	4.6	Sigma
(1R,3S)-(+)-Camphoric acid	200.24	10	1.78	3400	1305	6.52	Sigma
1,3,5-Trimethyl-cyclohexane-1,3,5-tricarboxylic acid	258.27	12	0.13	6.90E+04	31410	145.29	Sigma
Tetracosanedioic acid	398.6	24	8.58	0.00045	0.007	0.00002	Sigma
2-cyclohexyllidenebutanoic acid	168.24	10	3.8	88.4	24.85	0.15	Sigma
3-methyl-octahydro-pentalene-1-carboxylic acid	168.24	10	2.81	616.9	158.96	0.94	Sigma
Alpha-propyl-1-cyclopentene-1-ethanoic acid	182.28	11	4.16	37.19	13.65	0.07	Sigma

* BS is Ben Smith; DJ is David Jones: ET is Emma Teuton; GD is Professor G Dacremont from the University of Ghent

Appendix B

Appendix B

Biodegradation of Two Model Naphthenic Acids

B1. Introduction

Two ‘model’ naphthenic acids were biodegraded by a colleague (C. Whitby, University of Essex) using methods set out in Johnston et al., (2012) utilising two bacterial consortia that were sourced from Suncor and Albion Oil Sands Tailing Ponds in Alberta Canada. Both cultures were incubated with two acids (adamantane-1-carboxylic acid and 3-ethyladamantane-1-carboxylic acid) for 35 days; bacteria added to controls were ‘killed’ with the addition of a mercury chloride. Only biodegraded samples and ‘killed’ controls were extracted and analysed.

Briefly the 25 mL solutions, containing the esterified model acids and an internal standard (3, 5-dimethyladamantane-1-carboxylic acid methyl ester), was added to a boiling tube and acidified to pH 2. An amount of ethyl acetate was added to the boiling tube and the mixture was agitated on an auto vortex mixer and shaken by hand for 2 minutes. The ethyl acetate was removed and reduced to dryness under a steady stream of N_2. An amount of hexane was added and the solutions were examined by GC-MS.

However as both biodegraded acids were carboxylic acids an issue as to the veracity of the study was raised. As Smith (2008) showed the biodegradation preferentially occurs on the acid side chain, with butanoic acid (C_4) being degraded to the ethanoic (C_2) moiety. It was unlikely that any change would occur with relation to the acid chain.

It was decided, therefore, that the results from the extractions would be presented as an appendix, rather than a chapter in their own right.

B2. Results

Figure B1.1 reveals a total ion chromatogram and mass spectrums for the mix of standards for the biodegradation experiments.

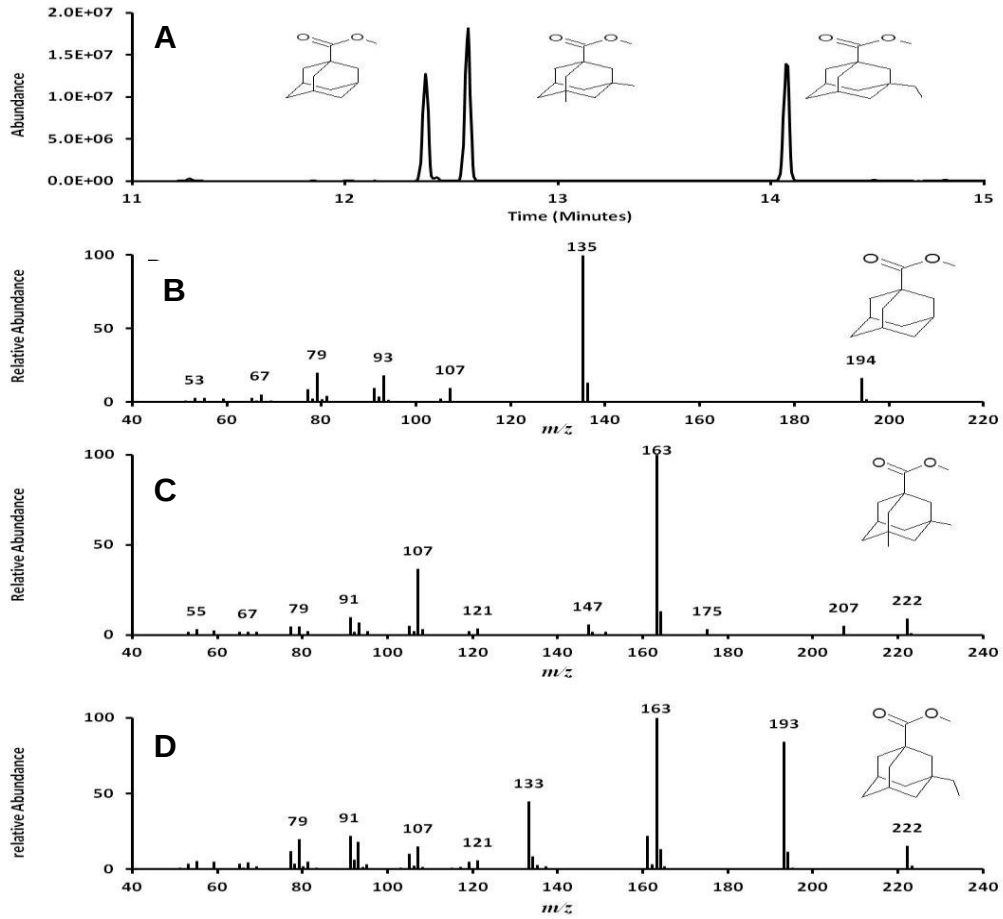

Figure B1.1. (A) total ion chromatogram for the biodegradation standards revealing compounds eluting at retention times 12.25 minutes, 12.34 minutes and 14.04 minutes; (B) mass spectra for the compound eluting at RT 12.25 minutes, assigned as adamantane-1-carboxylic acid methyl ester; (C) mass spectra for the compound eluting at RT 12.34 minutes, assigned as 3,5-dimethyladamantane-1-carboxylic acid methyl ester; and (D) mass spectra for the compound eluting at RT 14.04 minutes, assigned as 3-ethyladamantane-1-carboxylic acid methyl ester. GC Conditions: Column HP-5MS 30 m x 0.25 mm i.d x 0.25 μm film thickness; Solvent delay 9 minutes; oven programme 40-300^{o}C at 10^{o}C min^{-1}, hold 10 min; injector 300^{o}C; MS conditions: Source 230^{o}C, ionisation energy 70 eV, mass range 50-550 Daltons.

Figure B1.2 reveals total ion chromatograms for the biodegradation of adamantane-1-carboxylic acid with a Suncor sourced bacterial consortia over 35 days.

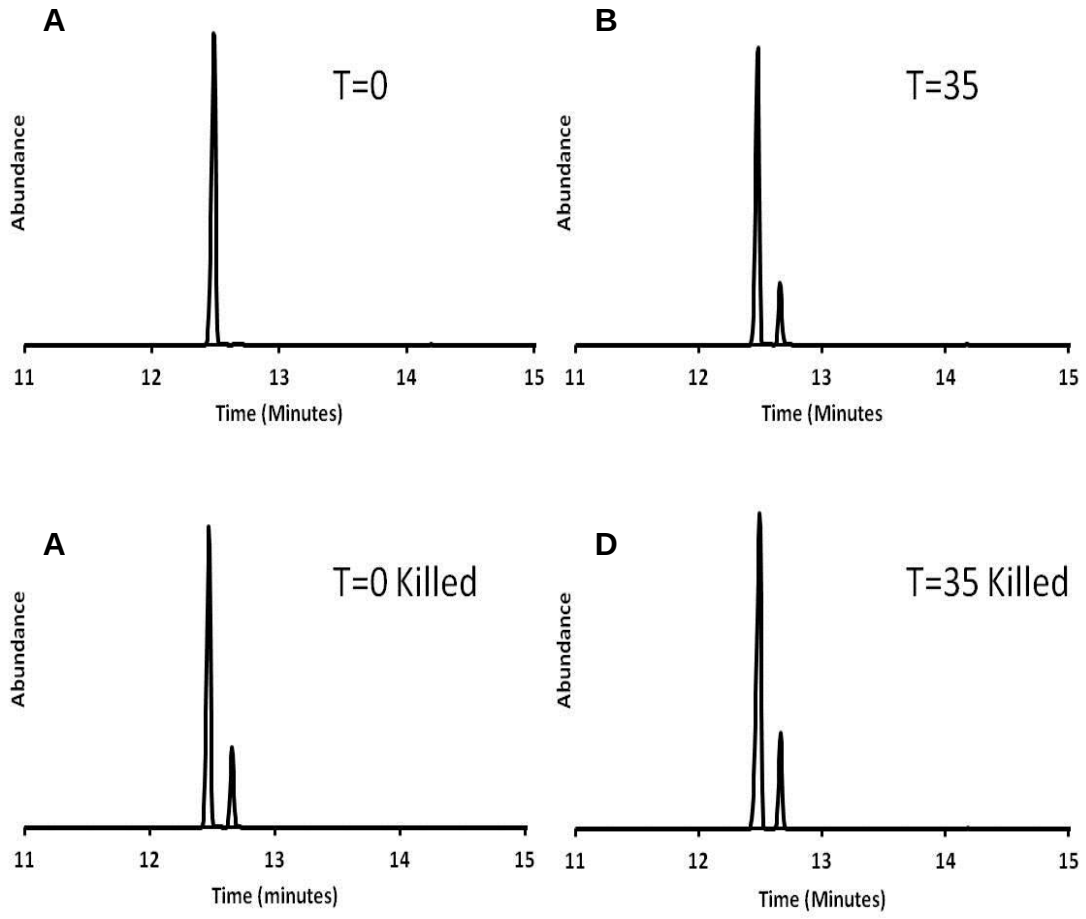

Figure B1.2. Averaged total ion chromatograms (n=3) for the methyl ester of the attempted biodegradation of adamantane-1-carboxylic acid revealing compounds eluting at RT 12.25 minutes and RT 12.34 minutes assigned as adamantane-1-carboxylic acid methyl esters and 3, 5-dimethyl adamantane-1-carboxylic acid methyl ester respectively; (A) adamantane-1-carboxylic acid at time =0 days; (B) adamantane-1-carboxylic acid at time =35 days (C) the 'Killed' control of adamantane-1-carboxylic acid at time =0 days; and (D) the 'Killed' control of adamantane-1-carboxylic acid at time =35 days; GC-MS conditions as described in Figure B1.1.

Figure B1.3 reveals a comparison of the integrated peak areas for the total ion chromatograms displayed in Figure B1.2. Statistical tests (ANOVA and a Student-Newman Keuls Multiple Range Test) reveal that there is no significant difference (to a 95% confidence level) between the T=0 and T=35 samples or between the Killed and non-killed samples, indicating that no biodegradation has taken place.

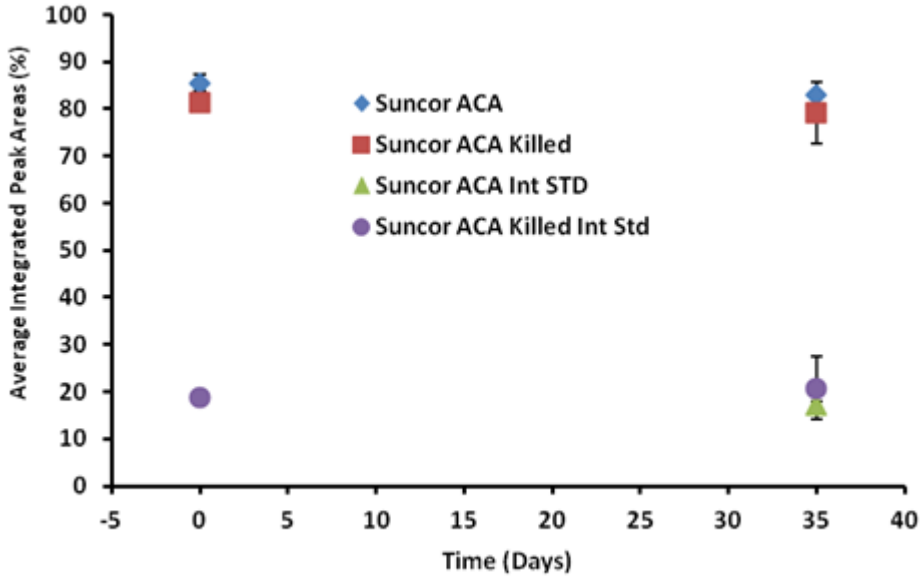

Figure B1.3. Chart revealing the averaged peak areas of the total ion chromatograms produced from the biodegradation of adamantane-1-carboxylic acid with a Suncor Consortia of bacteria; error bars are 1x standard deviation, *n*=3. The abbreviation 'ACA' is adamantane-1-carboxylic acid.

Figure B1.4 reveals total ion chromatograms for the biodegradation of 3-ethyladamantane-1-carboxylic acid with a Suncor sourced bacterial consortia over 35 days.

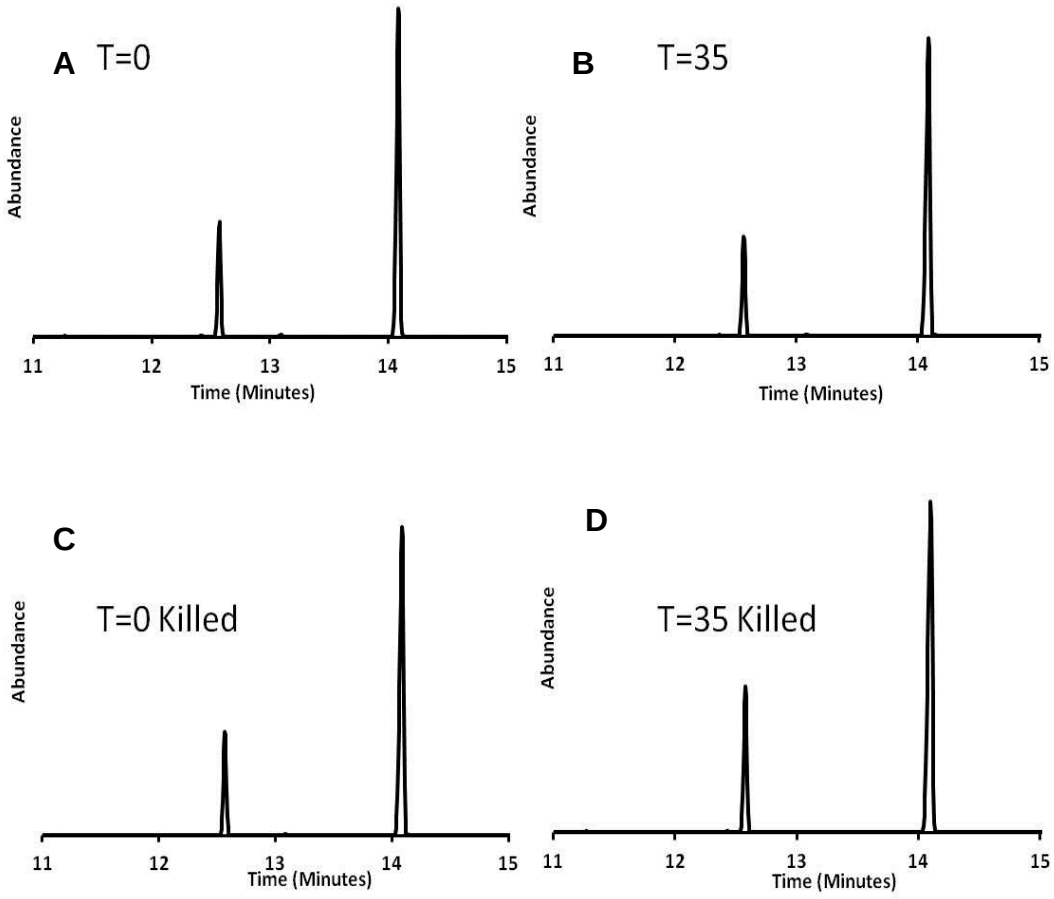

Figure B1.4. Averaged total ion chromatograms for the methyl ester of the attempted biodegradation of 3-ethyladamantane-1-carboxylic acid (*n*=3)revealing compounds eluting at RT 12.34 minutes and RT 14.04 minutes assigned as 3, 5-dimethyl adamantane-1-carboxylic acid methyl esters and 3-ethyladamantane-1-carboxylic acid methyl esters respectively; (A) 3-ethyladamantane-1-carboxylic acid at time =0 days; (B) 3-ethyladamantane-1-carboxylic acid at time =35 days (C) the 'Killed' control of 3-ethyladamantane-1-carboxylic acid at time =0 days; and (D) the 'Killed' control of 3-ethyladamantane-1-carboxylic acid at time =35 days; GC-MS conditions as described in Figure B1.1.

Figure B1.5 reveals a comparison of the integrated peak areas for the total ion chromatograms displayed in Figure B1.4. Statistical tests (ANOVA and a Student-Newman Keuls Multiple Range Test) reveal that there is no significant difference (to a 95% confidence level) between the T=0 and T=35 samples or between the Killed and non-killed samples, indicating that no biodegradation has taken place.

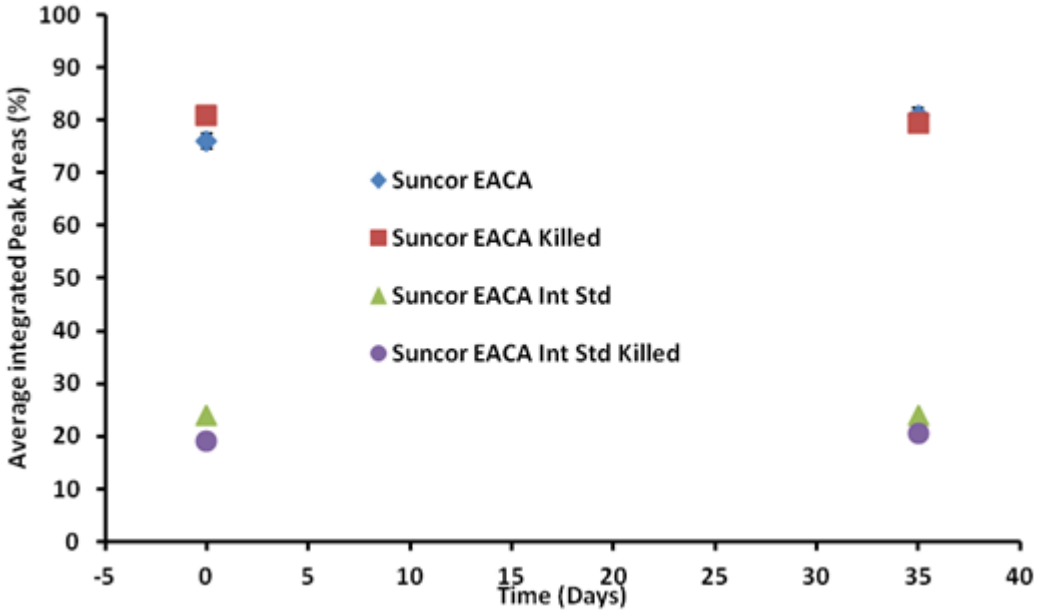

Figure B1.5. Chart revealing the averaged peak areas (%) of the total ion chromatograms produced from the biodegradation of 3-ethyladamantane-1-carboxylic acid with a Suncor Consortia of bacteria; error bars are 1x standard deviation, *n*=3. The abbreviation 'EACA' is ethyladamantane-1-carboxylic acid.

Figure B1.6 reveals total ion chromatograms for the biodegradation of adamantane-1-carboxylic acid with an Albion sourced bacterial consortia over 35 days.

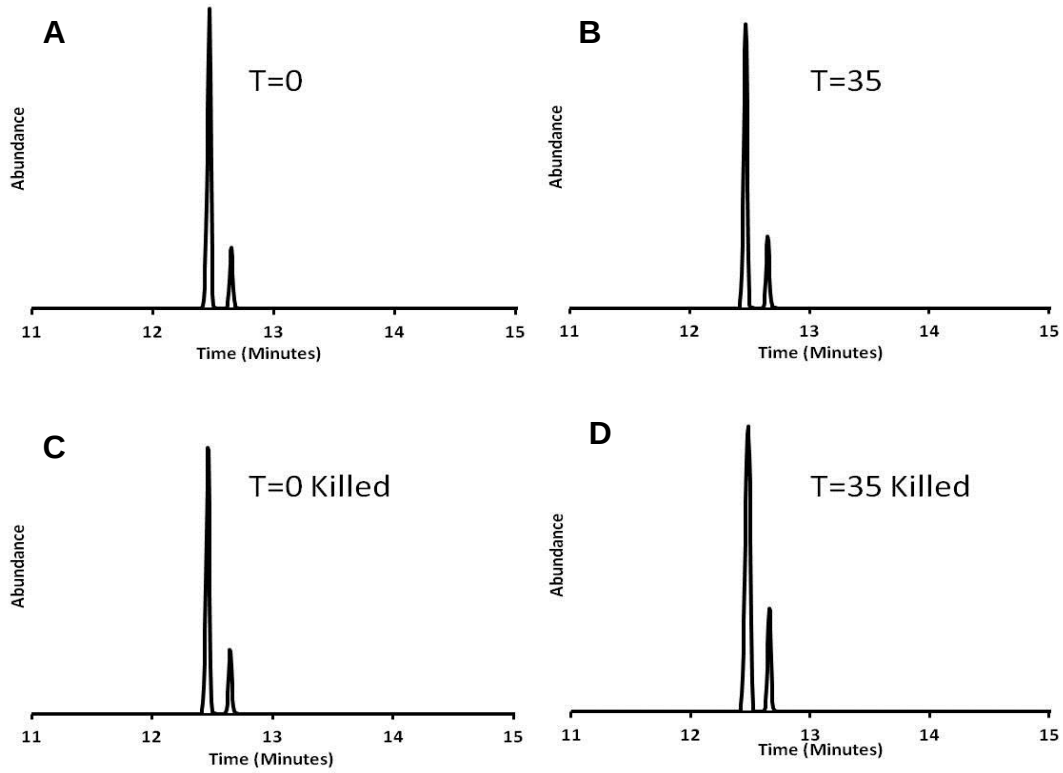

Figure B1.6. Averaged total ion chromatograms (n=3) for the methyl ester of the attempted biodegradation of adamantane-1-carboxylic acid revealing compounds eluting at RT 12.25 minutes and RT 12.34 minutes assigned as adamantane-1-carboxylic acid methyl esters and 3, 5-dimethyl adamantane-1-carboxylic acid methyl ester respectively; (A) adamantane-1-carboxylic acid at time =0 days; (B) adamantane-1-carboxylic acid at time =35 days (C) the 'Killed' control of adamantane-1-carboxylic acid at time =0 days; and (D) the 'Killed' control of adamantane-1-carboxylic acid at time =35 days; GC-MS conditions as described in Figure B1.1.

Figure B1.7 reveals a comparison of the integrated peak areas for the total ion chromatograms displayed in Figure B1.6. Statistical tests (ANOVA and a Student-Newman Keuls Multiple Range Test) reveal that there is no significant difference (to a 95% confidence level) between the T=0 and T=35 samples or between the Killed and non-killed samples, indicating that no biodegradation has taken place.

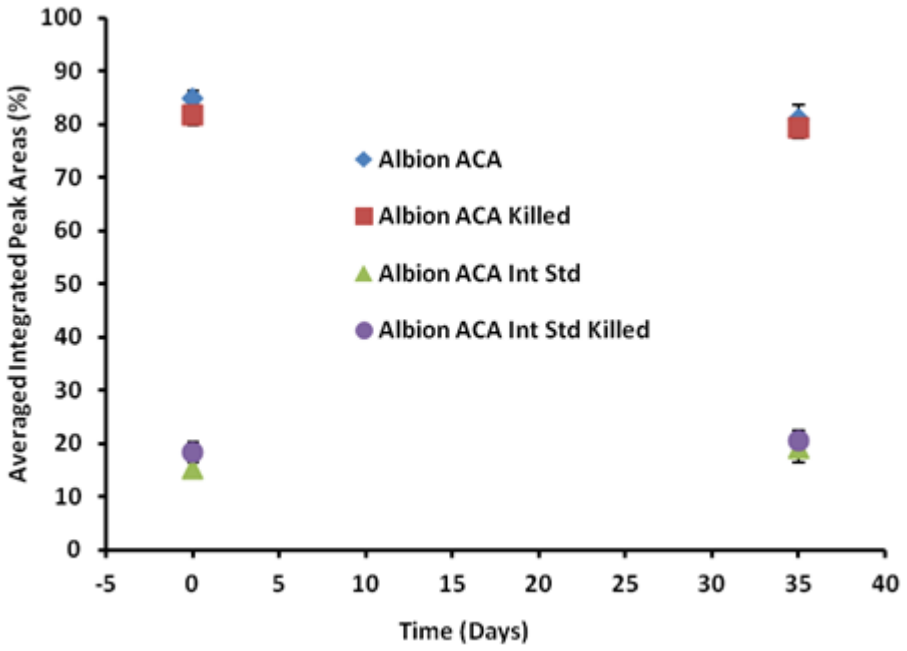

Figure B1.7. Chart revealing the averaged peak areas of the total ion chromatograms produced from the biodegradation of adamantane-1-carboxylic acid with an Albion Consortia of bacteria; error bars are 1x standard deviation, *n*=3. The abbreviation 'ACA' is adamantane-1-carboxylic acid.

Figure B1.8 reveals total ion chromatograms for the biodegradation of 3-ethyladamantane-1-carboxylic acid with an Albion sourced bacterial consortia over 35 days.

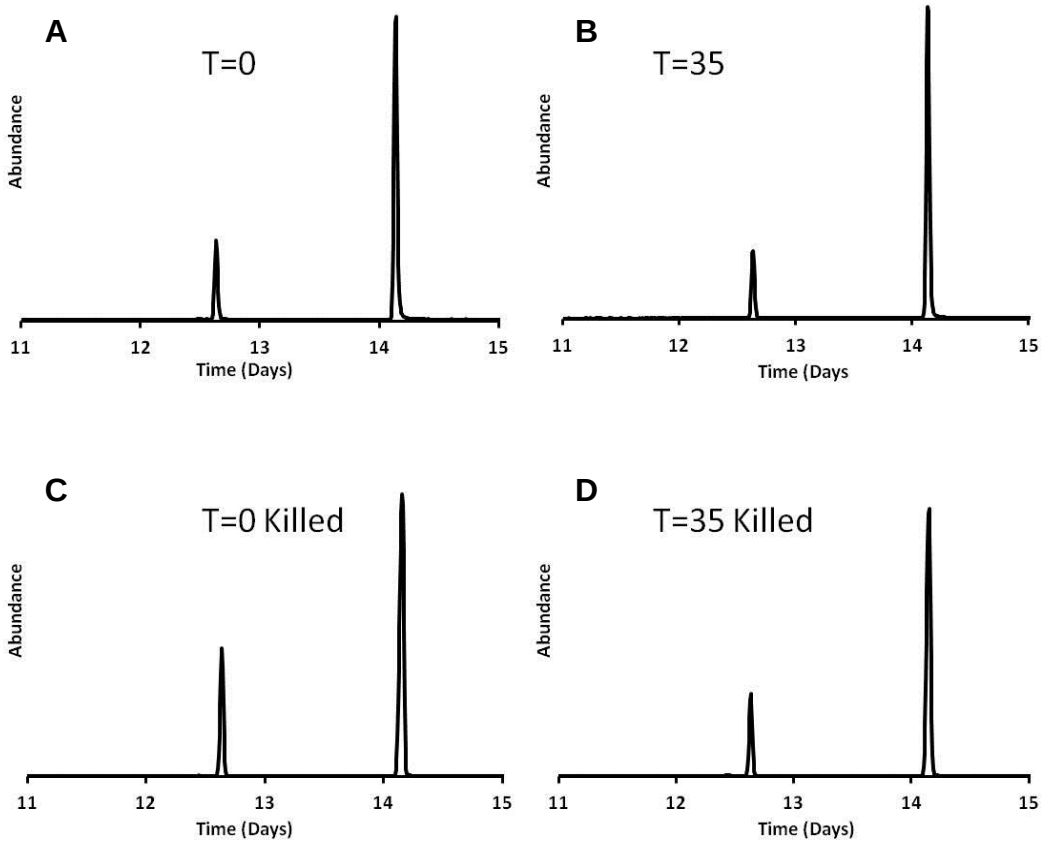

Figure B1.8. Averaged total ion chromatograms for the methyl ester of the attempted biodegradation of 3-ethyladamantane-1-carboxylic acid (*n*=3)revealing compounds eluting at RT 12.34 minutes and RT 14.04 minutes assigned as 3, 5-dimethyl adamantane-1-carboxylic acid methyl esters and 3-ethyladamantane-1-carboxylic acid methyl esters respectively; (A) 3-ethyladamantane-1-carboxylic acid at time =0 days; (B) 3-ethyladamantane-1-carboxylic acid at time =35 days (C) the 'Killed' control of 3-ethyladamantane-1-carboxylic acid at time =0 days; and (D) the 'Killed' control of 3-ethyladamantane-1-carboxylic acid at time =35 days; GC-MS conditions as described in Figure B1.1.

Figure B1.9 reveals a comparison of the integrated peak areas for the total ion chromatograms displayed in Figure B1.8. Statistical tests (ANOVA and a Student-Newman Keuls Multiple Range Test) reveal that there is no significant difference (to a 95% confidence level) between the T=0 and T=35 samples or between the Killed and non-killed samples, indicating that no biodegradation has taken place.

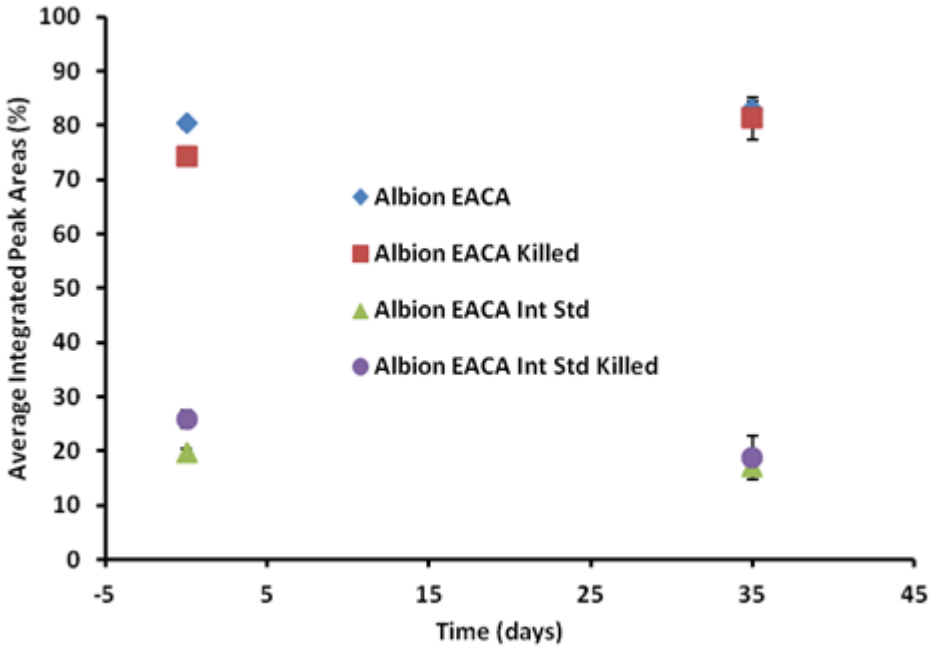

Figure B1.9. Chart revealing the averaged peak areas (%) of the total ion chromatograms produced from the biodegradation of 3-ethyladamantane-1-carboxylic acid with an Albion Consortia of bacteria; error bars are 1x standard deviation, *n*=3. The abbreviation 'EACA' is ethyladamantane-1-carboxylic acid.

B3. Conclusions

It is concluded that no biodegradation has taken place on the 'model' naphthenic acids in either (Suncor and Albion) bacterial consortia

Appendix C

Appendix C

Attempted Fractionation of the Acid Extracts (Methyl Esters) from an Oil Sands Process Affected Water by pH Adjustment.

C1. Introduction

As is evidence by Chapter 5 (this work) both silver ion thin layer chromatography and silver ion open column chromatography were successful in fractionating, and subsequently elucidating structural information, the methyl esters of an acid extract from an Oil Sands Process affected Water (OSPW). Therefore other methods were sought that may have a similar result.

An attempt to fractionate the complex mixture of naphthenic acids via simple pH adjustment was published in the Journal of the Serbian Chemical Society (Grbovic et al., 2012). It was decided to attempt a pH based extraction in order to investigate whether similar information could be elucidated from the separate fractions.

In brief: the acid extracts from an OSPW were added to a separating funnel and the pH was analysed (between pH 12.2 and 12.5). An amount of ethyl acetate was added and the funnel was shaken vigorously for 2 minutes and allowed to settle. The ethyl acetate fraction was collected and the remaining OSPW was acidified with 1 M H_2SO_4 to pH 11, whereupon the experiment was repeated. The pH adjustment continued (in increments of 1 pH point) until a pH of 2 was reached (an adjustment to pH 1 was attempted but was unsuccessful). A control experiment using distilled water in the place of the OSPW was also carried out. The fractions were allowed to settle over a weekend in the dark and were then

reduced to dryness under a steady stream of N_2. The fractions had hexane added and were analysed by GC-FID (as a abundance screen) and GC-MS.

When analysing the results it was noted that a similar fractionation to that previously noted (Chapter 5) did not occur. Instead different pH values extracted different abundances of the same unresolved ‘hump’, until no sample remained. Mass chromatographic analysis revealed no distinct individual peaks in any pH extracted fraction. The results are shown here as it is somewhat interesting that the bulk of the acids were extracted with pH 9, a similar pH to that of the tailings ponds were the original OSPW was collected.

C2. Results

Figure C1.1 reveals the total ion chromatograms for the pH based extractions in the range pH 12-9, revealing the largest abundance within the pH 9 extraction.

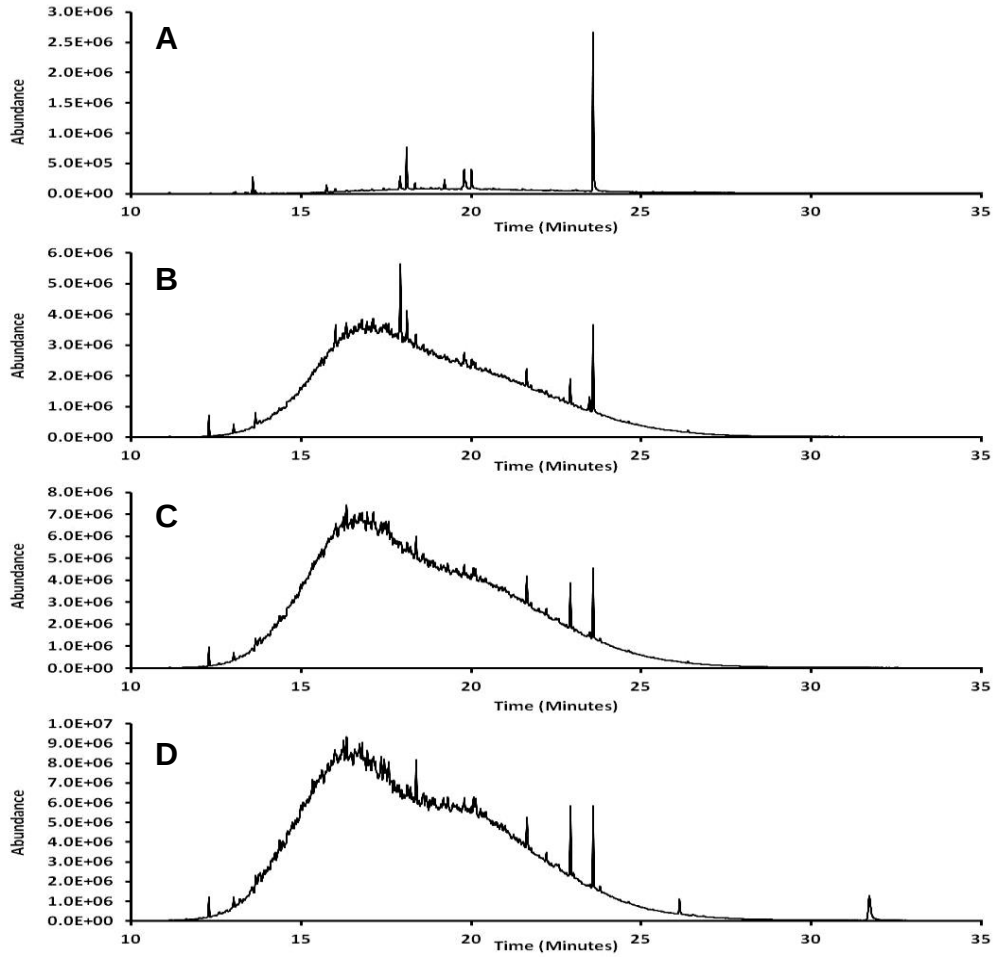

Figure C1.1. Total ion chromatograms from the pH based extractions of the acid extracts of an OSPW (methyl esters) with (A) chromatogram from the pH 12 extraction; (B) chromatogram from the pH 11 extraction; (C) from the pH 10 extraction; and (D) from the pH 9 extraction. GC Conditions: Column HP-5MS 30 m x 0.25 mm i.d x 0.25 μm film thickness; Solvent delay 9 minutes; oven programme 40-300^{o}C at 10^{o}C min^{-1}, hold 10 min; injector 300^{o}C; MS conditions: Source 230^{o}C, ionisation energy 70 eV, mass range 50-550 Daltons.

Figure C1.2 reveals the total ion chromatograms for the pH based extractions in the range pH 8-5.

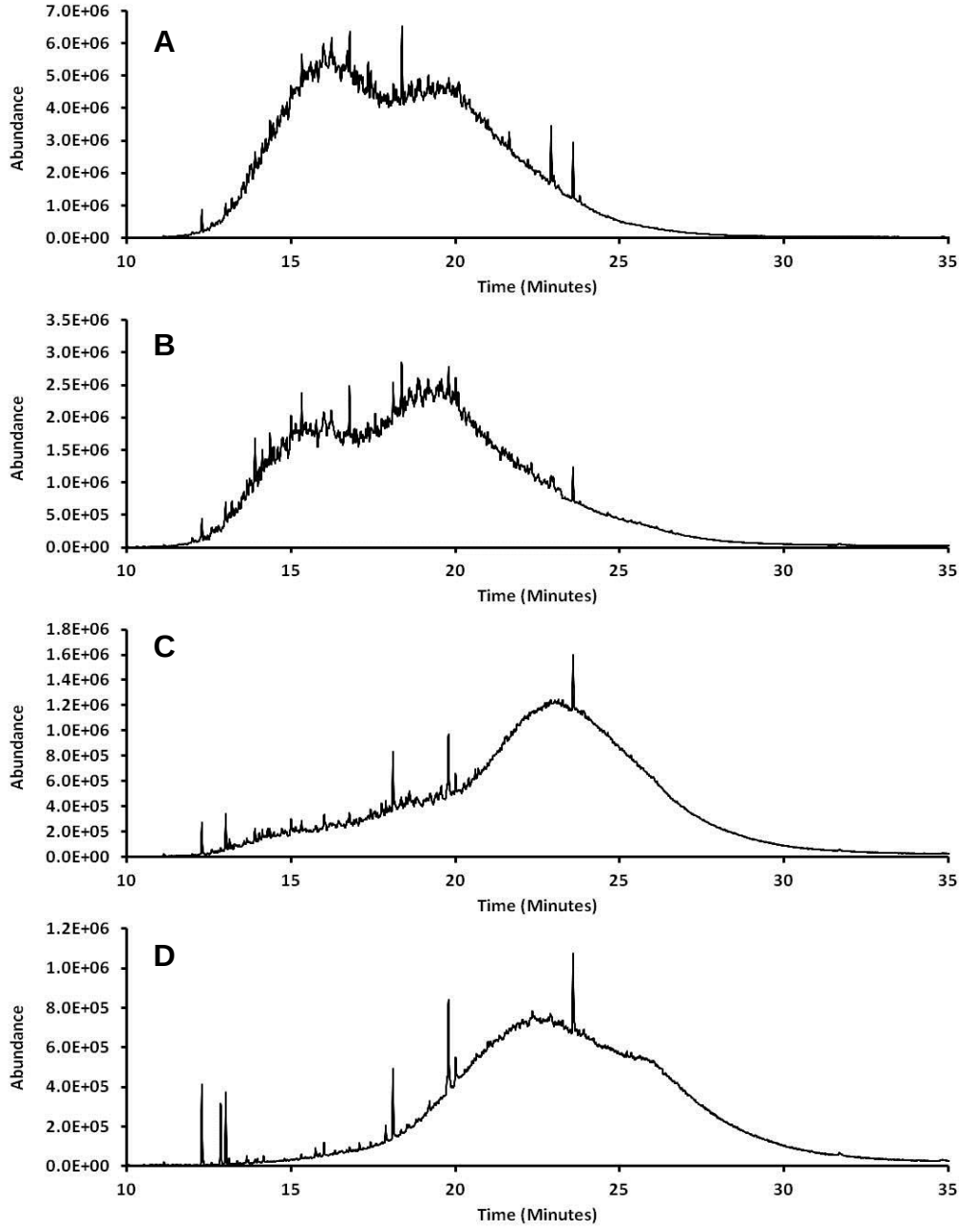

Figure C1.2. Total ion chromatograms from the pH based extractions of the acid extracts of an OSPW (methyl esters) with (A) chromatogram from the pH 8 extraction; (B) chromatogram from the pH 7 extraction; (C) from the pH 6 extraction; and (D) from the pH 5 extraction. GC-MS Conditions as described in Figure C1.1.

Figure C1.3 reveals the total ion chromatograms for the pH based extractions in the range pH 4-2 with a representative control chromatogram from pH 4, highlighting that the abundant peaks are present in the control extractions.

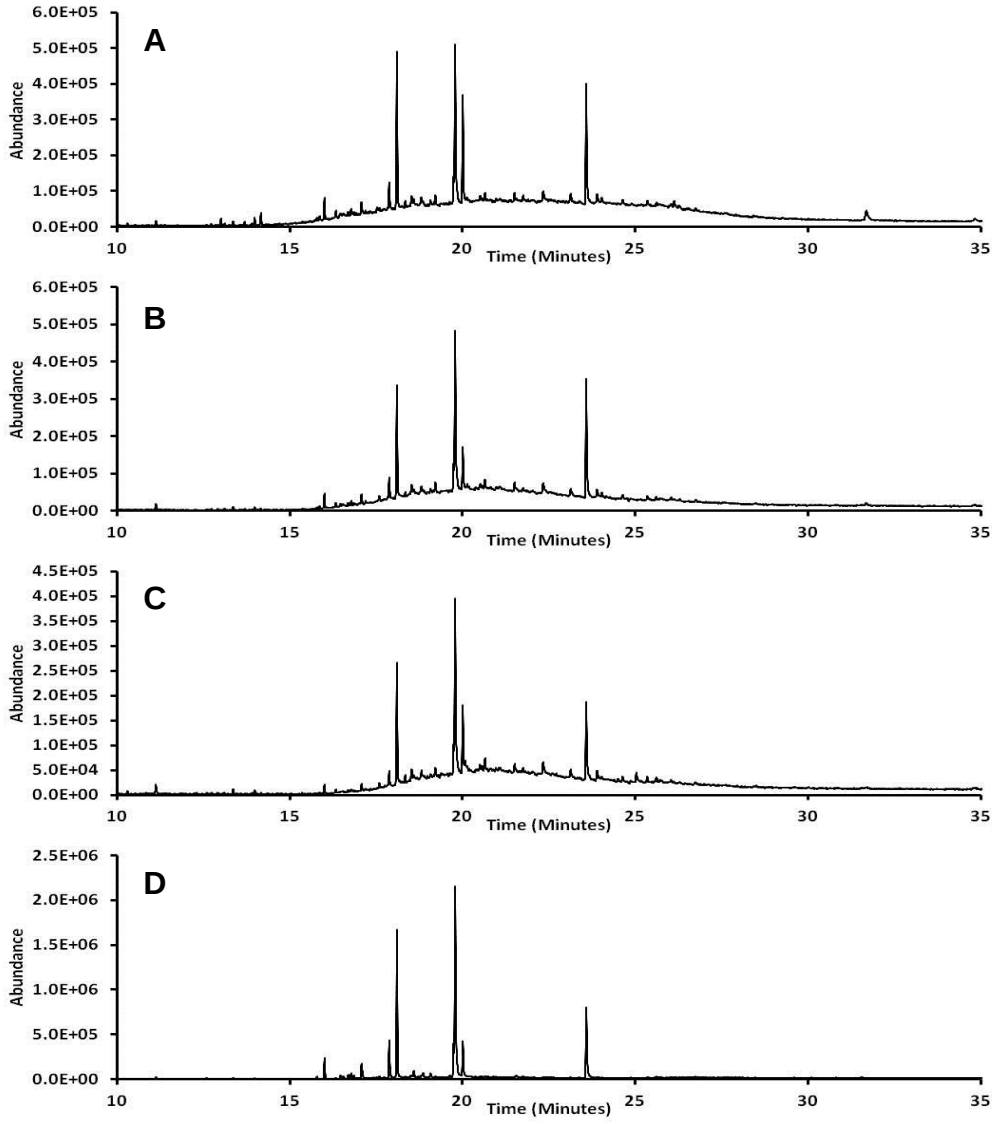

Figure C1.3. Total ion chromatograms from the pH based extractions of the acid extracts of an OSPW (methyl esters) with (A) chromatogram from the pH 4 extraction; (B) chromatogram from the pH 3 extraction; (C) from the pH 2 extraction; and (D) from the pH 4 control extraction. GC-MS Conditions as described in Figure C1.1.

Figure C1.4 reveals the total ion chromatograms for the pH based extractions in the range pH 8 and 9 over-laid with the total ion current chromatogram from the un-fractionated acid extracts from an OSPW. Highlighting a similar (though decreasing in abundance) unresolved ‘hump’.

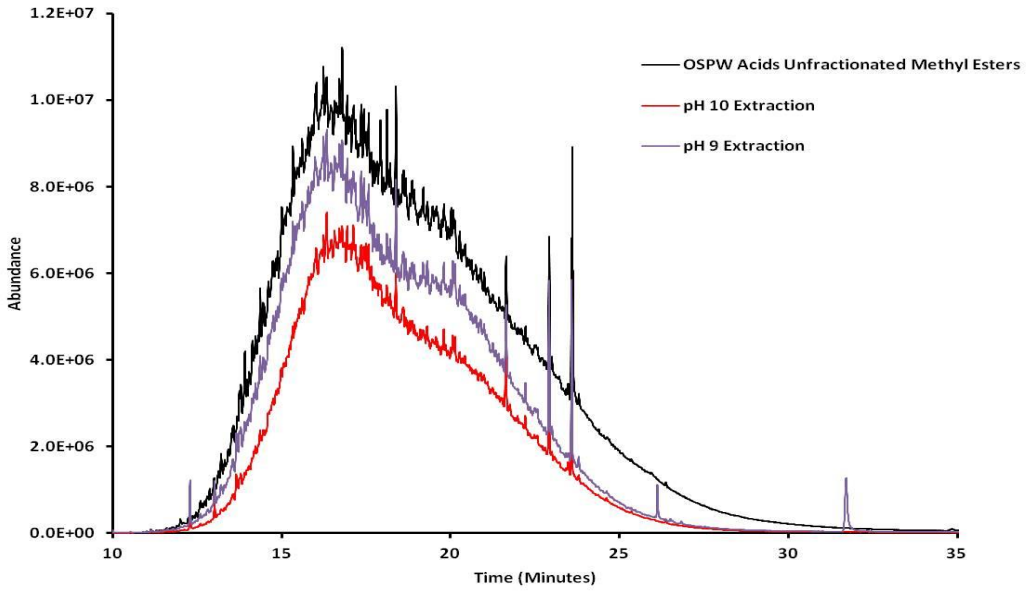

Figure C1.4. Over-laid total ion chromatograms from the pH based extractions of the acid extracts of an OSPW (methyl esters) revealing the chromatograms from the pH 8 and 9 fractions and an un-fractionated sample. GC-MS Conditions as described in Figure C1.1

C3 Conclusions

Although the acid extract was fractionated it was abundance rather than chemical characteristics that were highlighted. That pH 9 is the most abundant is of some interest however this was to be expected as this pH is the same as the tailing ponds in Alberta, Canada. Little structural information could be elucidated from these fractions so this method is not as robust as thin layer or open column silver ion chromatography.

Appendix D

Appendix D

Publications, Oral and Poster Presentations

What follows is a list of articles and presentations published from work produced during the PhD. The full text of the three first authorship papers is included.

D1. Presentations and Posters

- 1st Annual Meeting of the Biogeochemistry Centre, **Plymouth**, **U.K.** 18th December 2009.Oral Presentation: “Toxicity of Carrier Solvents”.
- 21st Annual Meeting of the British Organic Geochemical Society, **Manchester, U.K.**, 6-7 July 2010. Oral presentation: "Toxicity of Naphthenic Acids". Winner of Best Student Prize
- 22nd Annual Meeting of the British Organic Geochemical Society, **Swansea, U.K.**, 6-7 July 2011. Oral presentation: "Using a Model for the Toxicological Assessment of Naphthenic Acids".
- SETAC Europe 21st Annual Meeting, **Milan**, **Italy**, 16-19 May 2011. Oral presentation: "Who Needs Lab Work? An Investigation into Predictive Ecotoxicological Computer Models and Naphthenic Acids".
- 3rd Annual Meeting of the Biogeochemistry Centre, **Plymouth**, **U.K.** 16th December 2011.Oral Presentation: “Fractionation of the Complex Mixture of Naphthenic Acids”.
- SETAC 6th World Congress**, Berlin**, Germany, 20-24th May 2012, Poster Presentation, “Toxicity, Fractionation, Identification and Potential Estrogenic Effects of Acid Extracts of Oil Sands Process Waters

- 4th Annual Meeting of the Biogeochemistry Centre, **Plymouth**, **U.K.** 17 December 2012.Oral Presentation: Who Needs Two Dimensions? Elucidation of Structural Information of Petroleum Acids From One Dimensional GC-MS

D2 Publications

- **Jones, D**., Scarlett, A.G., West, C.E., Frank, R.A. Gieleciak**,** R**.,** Hagar, D. and Rowland, S.J. (2013) Elemental and spectroscopic characterisation of fractions of an acidic extract of oil sands process water, Chemosphere, *In Press.*
- **Jones. D**., West, C.E., Scarlett, A.G. and Rowland, S.J. (2012) Isolation and estimation of the 'aromatic' naphthenic acid content of an oil sands process-affected water extract, Journal of Chromatography A, **1247**, 171-175 [doi: 10.1021/j.chroma.2012.05.073].*
- **Jones, D**., Scarlett, A.G., West, C.E. and Rowland, S.J. (2011) Toxicity of individual naphthenic acids to *Vibrio fisheri*. Environmental Science & Technology, **45**, 9776-9782. [doi: 10.1021/es201948j].*
- Rowland, S.J., West, C.E., Scarlett, A.G. and **Jones, D**. (2011) Differentiation of oil sands process affected water by GCxGC-mass spectrometry of naphthenic acid profiles. Rapid Communications in Mass Spectrometry, **26**, 1–5, [doi: 10.1002/rcm.6138]
- Rowland, S.J., Clough, R., West, C.E., Scarlett, A.G., **Jones, D**. and Thompson, S. (2011) Synthesis and mass spectrometry of some tri- and tetracyclic naphthenic acids. Rapid Communications in Mass Spectrometry **25**, 2573-2578. [doi: 10.1002/rcm.5153].
- Rowland, S.J., **Jones, D**., Scarlett, A.G., West, C.E., Liu Pok Hin, Boberek, M., Tonkin, A., Smith, B.E. and Whitby, C. (2011) Synthesis and toxicity of some

metabolites of the microbial degradation of synthetic naphthenic acids. Science of the Total Environment **409**, 2936-2941. [doi: 10.1016/j.scitotenv.2011.04.012

- Rowland, S.J., Scarlett, A.G., **Jones, D**., West, C.E. and Frank, R.A. (2011) Diamonds in the rough: Identification of individual naphthenic acids in oil sands process water. Environmental Science & Technology **45**, 3154-3159. [doi: 10.1021/es103721b].
- Rowland, S.J., West, C.E., Scarlett, A.G. and **Jones, D**. (2011) Identification of individual acids in a commercial sample of naphthenic acids from petroleum by two dimensional comprehensive gas chromatography-mass spectrometry. Rapid Communications in Mass Spectrometry **25**, 1741-1751. [doi: 10.1002/rcm. 5040].
- Rowland, S.J., West, C.E., Scarlett, A.G., **Jones, D**., Boberek, M., Pan, L., Ng, M., Kwong, L. and Tonkin, A. (2011) Monocyclic and monoaromatic naphthenic acids: Synthesis & characterisation. Environmental Chemistry Letters 9, 525-533. [doi: 10.1007/s10311-011-0314-6].
- Rowland, S.J., West, C.E., Scarlett, A.G., **Jones, D**. and Frank, R.A. (2011) Identification of individual tetra- and pentacyclic naphthenic acids in oil sands process water by comprehensive two-dimensional gas chromatography-mass spectrometry. Rapid Communications in Mass Spectrometry **25**, 1198-1204. [doi: 10.1002/rcm.4977].
- Rowland, S.J., West, C.E., Scarlett, A.G., **Jones, D**., Frank. R. and Hewitt, L.M. (2012) Steroidal aromatic 'naphthenic acids' in oil sands process-affected water: Structural comparisons with environmental estrogens. Environmental Science & Technology **45**, 9806-9815. [doi: 0.1021/es202606d]

- West, C.E., **Jones, D**., Scarlett, A.G. and Rowland, S.J. (2011) Compositional heterogeneity may limit the usefulness of some commercial naphthenic acids for toxicity assays Science of the Total Environment **409**, 4125-4131. [doi: 10.1016/j.scitotenv.2011.05.061].
- Scarlett, A.G., West, C.E., **Jones, D**. Galloway, T.S., and Rowland, S.J. (2012) Predicted toxicity of naphthenic acids present in oil sands process waters to a range of environmental and human endpoints. Science of the Total Environment, **425,** 119-127, [doi: 10.1016/j.scitotenv.2012.02.064].

D3. Full Text of First Authorship Publications

Available here are links to the full text of the three first authorship research papers:

- **Jones, D**., Scarlett, A.G., West, C.E., Frank, R.A. Gieleciak, R., Hagar, D. and Rowland, S.J. (2013) Elemental and spectroscopic characterisation of fractions of an acidic extract of oil sands process water, Chemosphere, *In Press.*
  http://www.sciencedirect.com/science/article/pii/S0045653513004037

- **Jones. D**., West, C.E., Scarlett, A.G. and Rowland, S.J. (2012) Isolation and estimation of the 'aromatic' naphthenic acid content of an oil sands process-affected water extract, Journal of Chromatography A, **1247**, 171-175 [doi: 10.1021/j.chroma.2012.05.073].*
  http://www.sciencedirect.com/science/article/pii/S0021967312008059

- **Jones, D**., Scarlett, A.G., West, C.E. and Rowland, S.J. (2011) Toxicity of individual naphthenic acids to *Vibrio fisheri*. Environmental Science & Technology, **45**, 9776-9782. [doi: 10.1021/es201948j].*
  http://pubs.acs.org/doi/abs/10.1021/es201948j